2018

Synthesis and Medicinal Chemistry of the Antibacterial Cationic Biarylpeptidomimetics

Andrew James Tague
University of Wollongong

Synthesis and Medicinal Chemistry of the Antibacterial Cationic Biarylpeptidomimetics

A thesis submitted in fulfillment of the
requirements for the award of the degree:

DOCTORATE OF PHILOSOPHY

from

by

Andrew James Tague
B.Sc. Honours (Chemistry)
B.Sc. (Chemistry and Pharmacology)

Supervisors:
Prof. Paul A. Keller
Prof. Stephen G. Pyne

School of Chemistry
March 2018

This research has been conducted with the support of an Australian Government Research Training Program Scholarship.

Declaration

I, Andrew James Tague, declare that this thesis is submitted in fulfillment of the requirements for the conferral of the degree Doctorate of Philosophy, from the University of Wollongong, is wholly my own work unless otherwise referenced or acknowledged. This document has not been submitted for qualifications at any other academic institution.

Andrew James Tague

March 27th, 2018

Acknowledgments

I would like to extend my sincere gratitude to all those people whose help and/or guidance were crucial in the completion of this thesis. Most importantly, I would like to thank the following people:

My partner El for her endless support and love throughout this entire endeavor.

Prof. Paul Keller, Prof. Stephen Pyne and Dr. Steven Wales for their continuous support, advice and guidance throughout the entire project. Prof. Thomas Riley, Dr. Katherine Hammer and Dr. Daniel Knight for antibacterial activity testing. Prof. Dena Lyras and Dr. Melanie Hutton for performing the *in vivo* CDI mouse model assays and for allowing me to participate in and learn about the process.

The Keller Research Group for useful input and discussions throughout the project and for help in the laboratory. The entire UOW School of Chemistry for technical, administrative and academic support throughout the project. In particular, Dr. Wilford Lie and Hairrudin Idris for endless NMR-related assistance. Karin Maxwell, Dr. Celine Kelso, and Alan Maccarone for running my countless HRMS samples. The Pyne, Kelso, Hyland and Skropeta Research Groups for generosity with chemicals, equipment and ideas.

The National Health and Medical Research Council for providing funding for the project. The Australian Government for the Australian Government Research Training Program (AGTRP) Award that funded my living expenses for the entire project.

And finally, I would like to thank my family for their constant help and encouragement during the completion of this project – and life in general. I never would have made it this far, without your unwavering help along the way.

Abbreviations

δ	chemical shift in parts per million downfield from TMS signal
μg	microgram(s)
$\overline{\nu}_{max}$	wavenumber of maximum absorption peaks in cm^{-1} (IR data)
+ve	positive (electric charge)
–ve	negative (electric charge)
°C	degrees Celsius
1-D	one-dimensional
2-D	two dimensional
app.	apparent (NMR)
APT	attached proton test
Arg	arginine
amu	atomic mass units
Boc	*t*-butyloxycarbonyl
br	broad (NMR)
calcd	calculated
Cbz	benzyloxycarbonyl
CC_{50}	concentration at 50% cytoxicity
CDC	Centres for Disease Control
CDI	*Clostridium difficile* infection
CFU	colony-forming units
CLogP	calculated partition coefficient (Log P)
cm	centimeter(s)
conc.	concentrated
CuAAC	Cu-catalysed azide alkyne cycloaddition
d	doublet (NMR)
DEPT Q	Distortionless Enhancement by Polarization Transfer with Quaternary carbons present
DBF	dibenzofulvene
DMF	dimethylformamide
DMSO-d_6	deuterated dimethyl sulfoxide
DNA	deoxyribonucleic acid
dt	doublet of triplets (NMR)
EDCI	1-[3-(dimethylamino)propyl]-1-ethylcarbodiimide hydrochloride
em	emission wavelength (fluorescence)
eq	equivalence
ESI	electrospray ionization
ex	excitation wavelength (fluorescence)
FDA	Food and Drug Administration
Fmoc	fluorenylmethyloxycarbonyl

g	gram(s)
gCOSY	gradient correlation spectroscopy
gHMBC	gradient heteronuclear multiple bond correlation
gHSQC	gradient heteronuclear single quantum correlation
GI	gastrointestinal
h	hour(s)
HOBt	1-hydroxy-1*H*-benzotriazole
HPLC	high performance liquid chromatography
HRMS	high resolution mass spectrometry (or spectra)
Hz	Hertz
IR	infrared (spectroscopy)
J	coupling constant (NMR data)
L	litre
LRMS	low resolution mass spectrometry (or spectra)
Lys	lysine
M	molarity (units of concentration = mol/litre)
m	multiplet (NMR)
m/*z*	mass to charge ratio (MS data)
mbar	millibar (unit of pressure)
MBC	minimum bactericidal concentration
mg	milligram(s)
MIC	minimum inhibitory concentration
min	minute(s)
mL	millilitre(s)
mmol	millimole(s)
MRSA	methicillin-resistant *Staphylococcus aureus*
MS	mass spectrometry (or mass spectrum)
NBS	non-binding surface
nm	nanometers
NMR	nuclear magnetic resonance
NOESY	nuclear overhauser effect spectroscopy
OD_{600}	optical density observed at 600 nm
Pbf	pentamethyldihydrobenzofuran-sulfonyl
PBS	phosphate buffered saline
Pd-C	palladium-on-carbon catalyst
PMC	pseudomembranous colitis
ppm	parts per million
q	quartet (NMR)
RNA	ribonucleic acid
rt	room temperature
s	singlet (NMR)
SAR	structure-activity relationship

t	triplet (NMR)
TBAB	tetrabutylammonium bromide
TAEA	tris-(2-aminoethyl)amine
TFA	trifluoroacetic acid
TLC	thin layer chromatography
USD	United States dollars
UV	ultraviolet
v/v	volume-to-volume ratio
VRE	vancomycin-resistant *Enterococcus faecium*
VRSA	vancomycin-resistant *Staphylococcus aureus*
VT-NMR	variable temperature NMR
w/v	weight-to-volume ratio
w/w	weight-to-weight ratio
zTOCSY	z-quantum total correlation spectroscopy

Table of Contents

Abstract

Novel antibiotic chemotherapies are in high demand for the treatment of drug-resistant and hypervirulent bacterial infections. *Clostridium difficile* has been identified as the costliest bacterial pathogen – both in terms of financial burden and human mortality. Furthermore, the current treatments that exist for *C. difficile* infection (CDI) are inadequate and expensive. Therefore, an ongoing collaborative effort has focused on the design and development of novel antibacterial chemotherapeutics for the treatment of CDI. Sixty-two novel biarylpeptide derivatives were synthesized from 17 unique scaffolds and tested for antimicrobial efficacy against a wide range of pathogenic bacteria and fungi at multiple laboratories. An efficient, modular and scalable synthesis that utilized 11 key building block precursors was designed and employed in the realization of the novel biarylpeptide scaffolds. The modular approach allowed for facile diversification and derivatization of the target scaffolds.

One or two peptidomimetic 1,2,3-triazole rings were installed into the peptide backbone of the biarylpeptide derivatives to achieve increased metabolic resistance. Subsequent derivatization of these scaffolds produced a wide array of compounds with structural variation in the following moieties: the hydrophobic aromatic core (biphenyl or binaphthyl), the cationic amino acid residues (lysine and/or arginine) and the hydrophobic termini (mainly aryl or alkyl substituents). All synthesized derivatives exhibited some level of antimicrobial activity – i.e. minimum inhibitory concentration (MIC) values $\leq$ 16 μg/mL against *S. aureus*. The bis-triazole dicationic compound **80b** exhibited the best broad-spectrum antibacterial activity, displaying MIC values of 2 μg/mL against *S. aureus*, 4 μg/mL against MRSA, and 8 μg/mL against both *A. baumannii* and *P. aeruginosa*.

The results of the antimicrobial assays were utilized to explore the structure-activity relationship trends of the compounds so as to aid in the identification of the pharmacophore elements required for *C. difficile* antibacterial selectivity and broad-spectrum antibacterial activity. The structural modifications that were introduced to the biarylpeptide scaffold led to an increase in compound solubility and a substantial increase in antibacterial efficacy against Gram-negative bacteria in the bis-triazole dicationic derivatives. The monocationic derivatives (e.g. compound **77c**) were generally not as potent as their dicationic analogues, but they exhibited strong Gram-positive selectivity, which is beneficial for a CDI chemotherapeutic. The pursuit of novel antibacterial molecules from lead biarylpeptide compounds led to the development of two distinct structural scaffolds (i.e. **80b** and **77c**) that exhibited desirable traits for an antibacterial chemotherapeutic. Compound **77c** exhibited an increase in selectivity for *C. difficile* and Gram-positive bacteria; the molecule was also structurally simple and easier to synthesize, therefore making an ideal candidate for a potential CDI chemotherapeutic. Additionally, compound **80b** exhibited a notable increase in the overall Gram-negative antibacterial efficacy; this could allow the biarylpeptide derivatives to be investigated for use in the treatment of topical and skin-related Gram-negative bacterial infections.

A solubility assay was developed and utilized to allow for solubility comparisons between similar derivatives; this also allowed for correlations to be drawn between a compound's solubility and its *in vitro* and *in vivo* antibacterial activities. Four compounds with varying solubilities were selected based upon their *in vitro* activities against *C. difficile* and subsequently tested in an *in vivo* CDI mouse model. The Gram-positive selective compound **77c** exhibited promising preliminary results and has been selected for testing in further *in*

vivo CDI mouse models. The expected lack of systemic bioavailability following oral administration of the biarylpeptides was proven *via* pharmacokinetics assay on the mouse blood and faeces. A cytotoxicity assay was also employed in conjunction with the *in vitro* antimicrobial testing; compound **80b** exhibited some cytotoxicity (CC_{50} = 16.4 μg/mL) while compound **77c** failed to exhibit any cytotoxic effects at the concentrations tested. Compound **77c** exhibited increased selectivity for *C. difficile* (and other Gram-positive bacteria), structural simplicity and reduced cytotoxicity; these traits make compound **77c** a prime candidate for further biological studies (i.e. *in vitro* and *in vivo* assays) and optimization. Therefore, compound **77c** has been selected for ongoing biological and chemical assays to ascertain its efficacy and potential as a novel CDI chemotherapeutic.

1.0 – Introduction

1.1 – Antibiotic resistance

Bacterial resistance to known antibiotic drugs is a serious threat to modern healthcare and global security.[1-6] Infectious disease is the second leading killer globally (17 million deaths annually) and drug resistant bacterial infections are now considered an "emergent global disease" by the World Health Organization (WHO) and the US Centers for Disease Control and Prevention (CDC).[6-7] The CDC estimates that antibiotic resistance is responsible for more than two million infections and 23,000 deaths each year in the USA.[2] The WHO has initiated a "Global Action Plan" to reduce the prevalence of drug resistance and both organizations have published lists of drug resistant bacteria that are currently considered a major threat.[1, 3, 8] Bacterial strains have emerged that exhibit resistance to our most valued antibiotics and the prevalence of hypervirulent strains only potentiates the problem.[9-10] Thus, the need for novel antibacterial compounds with new modes of action is of utmost importance. The threat of these resistant and/or hypervirulent prokaryotes is a serious concern in today's healthcare sector and this concern is the impetus behind the ongoing need for and development of new antibiotic medications.

In the past eighty years, a plethora of natural and synthetic antibacterial compounds have been discovered and yet, resistant bacterial strains have been reported for virtually all antibiotics.[9] Bacteria can develop resistance to antibiotics rapidly, due to their short regeneration time and their ability to spread resistance to other bacteria *via* horizontal gene transfer.[5, 9] Bacterial resistance to anthropogenic antibiotics has been developing at an alarming rate since the introduction of penicillin in the 1930s; by the end of the 1950s, almost 85% of clinically isolated staphylococci were penicillin-resistant.[9]

Vancomycin was rapidly approved for use as an antibiotic because an effective treatment for penicillin-resistant bacteria was urgently needed.[11] Methicillin, the first semi-synthetic penicillin, was developed in 1959 and it soon became the antibiotic of choice for penicillin-resistant bacteria.[11] The subsequent emergence of methicillin-resistant *Staphylococcus aureus* (MRSA) and its acquired resistance to most other common antibiotics led to vancomycin becoming the 'gold standard' for MRSA treatment.[11] This lead to an increase in vancomycin use in the 1970s – not only for MRSA treatment but also to treat the growing number of severe *Clostridium difficile* infection (CDI) cases.[11] Extensive oral vancomycin use for the treatment of CDI led to the emergence of vancomycin-resistant enterococci (VRE) in 1986,[11] while vancomycin-resistant *S. aureus* (VRSA) also emerged in 2002. In the latter case, the VRSA acquired resistance *via* horizontal gene transfer from VRE in a human patient who had been intermittently treated with vancomycin.[11] Furthermore, some bacteria have developed resistance against multiple drug classes – these multi-drug resistant (MDR) bacteria are a serious concern facing modern healthcare.[4, 7, 12-13] Resistant bacterial isolates, colloquially known as "superbugs", are extremely worrying and they have provided a strong impetus for the discovery of novel antibiotic molecules.

Recent potential vancomycin replacements for treating VRSA, MRSA and other Gram-positive bacterial infections include linezolid, quinupristin/dalfopristin, daptomycin and tigecycline.[10-11] Both daptomycin and linezolid have been used extensively for treating Gram-positive, drug-resistant infections; as a result, resistance to both drugs has already been documented.[11, 14] Gram-negative bacteria are inherently more resistant to antibiotics due to their impermeable outer membrane and their broad-substrate transmembrane efflux pumps (for transporting unwanted molecules out of the cell).[13] Multi-drug resistance

amongst Gram-negative bacteria has been on the increase and there is an unmet need for novel antibiotics capable of treating such infections.[13] Therefore, the research focus has now shifted towards developing new antibiotic molecules for treatment of MDR Gram-negative bacterial infections.[5, 13] The **ESKAPE** pathogens (i.e. ***E****nterococcus faecium*, ***S****taphylococcus aureus*, ***K****lebsiella pneumoniae*, ***A****cinetobacter baumannii*, ***P****seudomonas aeruginosa* and ***E****nterobacter* spp.) are six antibiotic resistant bacterial species that have been identified by multiple agencies (including the Infectious Diseases Society of America) as key pathogens behind the majority of nosocomial infections.[5] These bacteria have been identified due to their virulence, tenacity, propensity for resistance and pathogenicity.[5] Notably, *P. aeruginosa* and *A. baumannii* exhibit a particularly strong ability to resist antibiotic molecules, likely due to their ability to withstand toxic environments.[13] There are limited chemotherapeutic treatments for MDR bacterial infections and pan-drug resistant (PDR) Gram-negative strains have also been identified (i.e. resistant to all known antibiotic treatment options).[13] The lack of viable treatment options for Gram-negative bacterial infections has even led to the reintroduction of polymyxin B and polymyxin E (colistin), despite known toxicity issues – polymyxins are large, cyclic cationic peptides with potent antibacterial activity.[5, 13]

Unfortunately, bacterial resistance is inevitable for almost all antibiotic molecules; bacteria will eventually find a way to negate, destroy, pacify, eliminate or withstand the target antibiotic.[5] Resistance becomes possible as soon as bacteria have been exposed to an antibacterial agent. By increasing the exposure to the antibiotic, there is an increased chance for a resistant bacterial strain to develop. Therefore, the increased use of antibiotics by the agriculture industry (for animal growth – which accounts for > 50% of antibiotics

consumed) and by modern medicine (i.e. misuse and overuse) only serves to exacerbate the problem of resistance by accelerating the process.[7, 15] The overuse of antibiotics is such a big problem that the US White House instituted a 5-year plan in 2015 to reduce the unnecessary use of antibiotics in farm animal growth.[7] Furthermore, the US White House has created the '*National Action Plan for Combating Antibiotic-Resistant Bacteria*' – this plan aims to fund novel antibiotic drug discovery for treating MDR bacterial infections.[7] The antibiotic resistance problem has become so severe that the WHO now warns of a 'post-antibiotic era' where common infections and minor injuries will prove lethal due to the lack of viable antibiotic therapies.[16] Thus, novel antibacterial compounds with unique mechanisms of action are always needed to help combat the constantly evolving threat of bacterial resistance.

1.2 – *Clostridium difficile* infection (CDI)

C. difficile is a Gram-positive, anaerobic bacterium that causes mild to serious infections in the gastrointestinal (GI) tract due to the potent toxins and resilient endospores that are produced by the organism (Figure 1.1).[17-18]

Figure 1.1 - Transmission electron micrograph of *C. difficile* forming an endospore (red).[19]

CDI occurs when the normal GI microbiota is compromised; this allows *C. difficile* to flourish in the GI tract due to the absence of the usual enteric microbiome.[17-18] Most common oral antibiotics, including penicillins, can destroy the normal GI microflora – this unwanted side-effect allows *C. difficile* to infect up to 20% of hospital patients administered oral antibiotics.[17] *C. difficile* produces robust endospores that are spread by the faecal-oral route; these spores are resistant to most antibiotics, alcohol-based hand sanitizers and heat.[20] The hospital setting provides a prime 'breeding ground' for *C. difficile* spores, which can stay viable for months at a time.[17-18] It is often considered a nosocomial infection; the disease is most prevalent in the hospital setting because the main risk factor for CDI is previous antibiotic therapy.[18] Broad spectrum antibiotic therapy indiscriminately destroys the GI microflora, but fails to eradicate *C. difficile* spores.[20] Almost all broad-spectrum antibiotics can instigate CDI by eliminating the commensal GI microflora; however, antibiotics such as ampicillin/amoxicillin, cephalosporins, clindamycin and fluoroquinolones are most commonly associated with CDI.[17]

GI infection from *C. difficile* can result in symptoms such as diarrhoea, abdominal pain and pseudomembranous colitis (PMC – a severe gastric disease). PMC is caused by colonic inflammation due to infection which leads to the appearance of white "pseudomembranes" that inhibit normal colonic function.[17-18, 21] CDI-associated PMC can be so severe as to warrant colectomy (i.e. resection of the colon) for which there is a ~55% mortality rate for patients that undergo such surgery/procedures.[21] Furthermore, toxic megacolon can also result from CDI, wherein the patient suffers from severe colonic inflammation and abdominal distension.[20] CDI exhibits an overall mortality rate of up to 8%[18] and infection

recurrence occurs in up to 20% of cases treated with first-line medications (i.e. vancomycin or metronidazole).[22]

Once the infectious spores have reached the GI tract, the presence of bile salts initiates germination of the spores to produce the vegetative *C. difficile* cells.[20] Disease caused by CDI is primarily the result of two virulence factors (Toxin A and Toxin B) that are excreted by the vegetative *C. difficile* cells; these toxins promote colonic inflammation and epithelial tissue damage which causes fluid loss (i.e. diarrhoea).[20] A third toxin (known as CDT or binary toxin) is found in high levels in hypervirulent *C. difficile* strains, although the role of this toxin in disease has not yet been elucidated.[20]

Recently, both the severity and incidence of CDI cases has increased due to epidemics of hypervirulent *C. difficile* strains, e.g. ribotype 027 – also known as strain B1/NAP1/027.[17-18] The hypervirulent ribotype 027 produces higher levels of toxins than normal *C. difficile* strains – these toxins are thought to be responsible for disease symptoms like diarrhoea and PMC.[18] As a result, ribotype 027 exhibits a mortality rate that is three times higher than normal *C. difficile* isolates.[17]

The prevalence of *C. difficile* infection results in a massive financial burden on the modern healthcare system (>$1 billion/year in the USA);[17, 23] another estimate put CDI-related healthcare costs in 2008 at $4.8 billion.[18] The CDC issued a report in 2013 entitled 'Antibiotic Resistance Threats'; *C. difficile* was listed as the number one bacterial threat facing the healthcare sector and humans in general.[3] A recent update by the CDC reports that CDI is responsible for approximately 500,000 infections and 15,000 deaths annually in the USA – the highest of any of the bacterial threats listed by the CDC.[23] Therefore, the

heightened concern over CDI is understandably justified and the alarm over impending resistance and hypervirulence only complicates the situation. Due to the high levels of infection, recurrence, mortality, cost, and the lack of adequate treatments for CDI, there exists a substantial incentive to pursue novel chemotherapeutics that effectively combat CDI.

Antibacterial selectivity for *C. difficile* is an essential component for a fully effective CDI chemotherapeutic. The elimination of all GI bacteria by broad spectrum antibacterial activity provides an ideal habitat for *C. difficile* spores to grow; therefore, the maintenance and/or restoration of commensal GI microflora is essential for preventing CDI recurrence.[17-18, 20] This explains why CDI is so difficult to eradicate with traditional antibiotics and why CDI recurs in 15-30% of patients treated with vancomycin.[17] Faecal transplantation has thus become a viable method for treating cases of chronic/severe CDI, as it physically replaces the commensal GI microflora.[17-18, 21] The classic chemotherapeutic treatments for CDI (i.e. vancomycin and metronidazole) suffer from efficacy issues, most notably CDI recurrence due to their lack of selectivity for *C. difficile* and inability to prevent sporulation.[17-18] CDI recurrence is also linked with the inability to form a specific antibody response to the toxins released by *C. difficile*; healthy adults normally form an antibody against toxin A.[17] Non-chemotherapeutic treatments (i.e. surgery) are available, but they are generally only used when classic chemotherapeutics fail. Surgical treatments are drastic and permanent – most involve subtotal colectomy in an attempt to physically remove the infection and diseased bowel.[18] Current *C. difficile* treatment options are lacking in completely effective CDI medications. There exists a drastic need for more efficacious *C. difficile* chemotherapeutics for the treatment of CDI; a well-tolerated and

safe medication that could selectively target *C. difficile* (and its spores), while leaving the enteric microbiome intact, would prove invaluable in the treatment of severe and recurrent CDI.

1.3 – Current chemotherapeutic treatments for CDI

There are currently only three medications that are widely-used and accepted as treatments for CDI; vancomycin, metronidazole and fidaxomicin.[17, 20, 22, 24] Vancomycin was the only FDA-approved treatment for CDI until 2011 when fidaxomicin was approved. Metronidazole is widely used off-label as a first-line treatment for mild-to-moderate cases of CDI (despite not being FDA-approved for the aforementioned purpose), whereas oral vancomycin is commonly used for moderate-to-severe or recurrent cases of CDI.

1.3.1 – Vancomycin

Vancomycin (Figure 1.2) is the prototypical glycopeptide antibiotic.[9] The glycopeptides represent a complex class of molecular structures; the main cyclic scaffold is comprised of sugars and amino acids joined *via* peptide bonds. Vancomycin was discovered in 1959 by the Eli Lilly pharmaceutical company – the compound was isolated from a soil sample from the rainforests of Borneo and is now known to be produced by a microorganism named *Amycolatopsis orientalis.*[9] Fermentation of *A. orientalis* yields a broth rich in vancomycin; this production method is economically more viable than synthesis because the drug's structure is so complex.[11] As a result, vancomycin is rather costly (~$31 USD/dose) compared to synthetic, small-molecule medications (e.g. metronidazole).[9, 25]

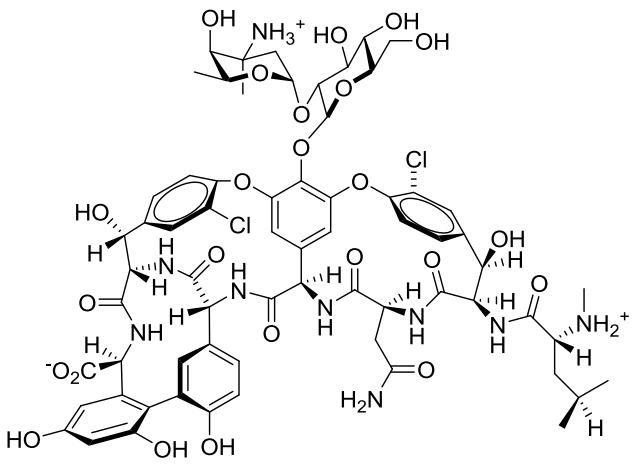

Figure 1.2 – The glycopeptide antibiotic vancomycin.

Vancomycin is known to work by interfering with bacterial manufacture of the peptidoglycan cell wall by binding to the two terminal *D*-alanine residues of the peptidoglycan precursor that participates in enzymatic cross-linking. The binding of vancomycin to the terminal *D*-alanine residues prevents the transglycosylase enzyme from cross-linking the peptide as part of the cell wall manufacture.[9] Vancomycin exhibits potent antibacterial activity against Gram-positive bacteria; minimum inhibitory concentration (MIC) values of ≤ 0.50 μg/mL were observed for 207 *C. difficile* strains that were tested.[26]

Vancomycin exhibits many traits that make it ideal for severe CDI treatment such as a low oral bioavailability and a potent MIC value against *C. difficile*; unfortunately, it has several drawbacks such as production/cost, lack of selectivity for *C. difficile*, and recurrence of CDI following treatment.[9, 11, 25] Vancomycin's broad-spectrum antibacterial activity results in indiscriminate annihilation of the enteric microbiota; this allows the resilient *C. difficile* spores (which are resistant to most antibiotics) to recolonize the colon due to a lack of viable competition, resulting in infection recurrence. Most importantly, because vancomycin fills an important role in treating MRSA and other MDR bacteria, it will never

be given full license for treatment of mild or moderate CDI. The threat of widespread vancomycin resistance limits the compound's use to only the more severe cases.[9, 11]

1.3.2 – Metronidazole

Metronidazole (Figure 1.3) is a nitroimidazole derivative that exhibits antimicrobial activity and has been in use for more than 45 years.[27] The medication was originally used for the treatment of protozoal infections (e.g. *Trichomonas vaginalis* and giardiasis) and was eventually found to be effective against anaerobic bacteria (both Gram-positive and Gram-negative infections).[27-28]

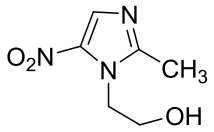

Figure 1.3 – Metronidazole (a nitroimidazole antibiotic).

Metronidazole was renowned for having a very low resistance profile because during the first thirty years of use, there was very little resistance observed.[28] The drug is very versatile because it can be administered intravenously, orally, topically and vaginally; it exhibits ideal pharmacokinetics for a systemic antibiotic.[27-28] The chemical structure of metronidazole is very simple and this allows for cheap production of the drug on a large scale (cost = ~$0.86 USD/dose).[25]

Metronidazole exhibits activity through a free radical mechanism whereby the nitro group is reduced *in vivo* to create an unstable 'nitro radical anion' which rapidly decomposes to give an imidazole radical and a nitrite ion.[20, 28] The imidazole radical and nitrite ion cause oxidative damage to DNA strands, resulting in apoptosis. The intracellular reduction of metronidazole occurs *via* electron capture from a reduced ferredoxin oxidoreductase enzyme.[28] Metronidazole has become a very common-place treatment for mild-to-

moderate CDI, despite not being formally approved by the FDA for CDI treatment.[25, 27-28] Metronidazole has replaced vancomycin as the main treatment for milder cases of CDI as it is much cheaper to manufacture, has a similar efficacy profile in mild cases and its use does not contribute to vancomycin resistance.[25] The majority of oral metronidazole is absorbed systemically which is not ideal for the treatment of a gastric bacterium like *C. difficile*.[27-28] A low oral bioavailability is essential for any oral treatment of CDI as the drug must stay available in the gut and not be absorbed systemically. Metronidazole's usage as a treatment for CDI will wane as newer and more efficacious CDI chemotherapeutics become available.

1.3.3 – Fidaxomicin

Fidaxomicin (Figure 1.4) is the prototypical macrocycle antibiotic and it was approved in 2011 by the FDA specifically for the treatment of CDI.[25] Fidaxomicin is a relatively complex unsaturated macrolide with two sugar derivatives attached; the drug is isolated from the fermentation broth of *Dactylosporangium aurantiacum.*[22] Fidaxomicin is very expensive (~$156 USD/dose) and the molecule is currently under patent.[25]

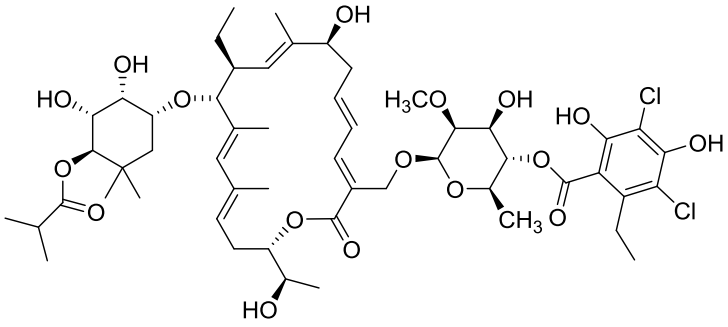

Figure 1.4 – The macrolide antibiotic fidaxomicin.

Importantly, fidaxomicin exhibits narrow-spectrum antibacterial activity; the drug selectively eliminates *C. difficile* and does not harm important commensal GI bacteria.[20, 29]

Fidaxomicin allows the commensal GI microbiome (i.e. *Bacteroides* spp.) to stay intact and it is also known to prevent spore formation.[30] These two combined effects are thought to be responsible for fidaxomicin's reduced recurrence rates.[20, 29] Fidaxomicin exhibits approximately 50% less CDI recurrence when compared to treatment with vancomycin; a recurrence rate of 22.6% was observed for vancomycin versus 11.7% recurrence for fidaxomicin.[30]

Fidaxomicin works by inhibiting bacterial RNA polymerase where it binds to a site distinct from the rifamycin-type antibiotics.[29] Systemic absorption of fidaxomicin is negligible and therefore its notable cytotoxicity is not a problem.[20] The drug is well-tolerated and it exhibited similar tolerability to a comparator medication (i.e. an accepted medication).[29] Fidaxomicin also exhibited an MIC value of 0.008 – 0.25 μg/mL for 90% of *C. difficile* isolates tested and it has given promising results in the treatment of CDI.[22] Fidaxomicin inhibits virulent strains of *C. difficile* better than vancomycin.[25] The lower CDI recurrence rate is likely a result of fidaxomicin's greater ability to leave the intestinal microflora intact while simultaneously inhibiting *C. difficile* (when compared to vancomycin).[25] Fidaxomicin has been shown to lessen the spore load (i.e. the quantity of *C. difficile* spores in the intestine) of a patient following successful CDI treatment and it is thought that this plays a major role in eliminating CDI recurrence. [29] Following treatment cessation with fidaxomicin, there is an extended "post-antibiotic effect" relative to the other common CDI treatments – this period of "sterility" would also help to prevent recolonization by *C. difficile* spores.[25] There are studies currently being conducted to ascertain whether fidaxomicin could function as a prophylactic for CDI or as a post-antibiotic 'chaser' to prevent antibiotic therapy-induced CDI.[25]

1.3.4 – Rifaximin

Rifaximin (Figure 1.5) is a semi-synthetic derivative of the rifamycin antibiotic family which includes such drugs as rifampicin. It has broad-spectrum activity and is extremely potent against *C. difficile*; rifaximin exhibited an MIC value of ≤ 0.015 μg/mL for 110 toxigenic *C. difficile* strains.[25, 31] Rifaximin has poor water solubility and as such, it maintains a high intestinal concentration following oral administration; so high, that 97% of a dose can be reclaimed as unchanged rifaximin in the faeces.[32] The result is a systemic bioavailability of less than 0.4% – this is ideal for the treatment of *C. difficile*.[32]

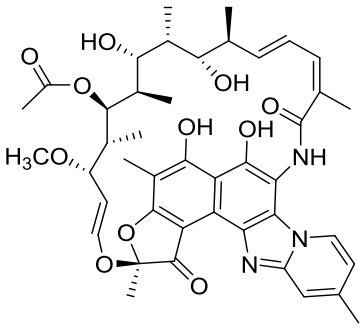

Figure 1.5 – Rifaximin.

Recent studies have shown that rifaximin can be useful in the treatment of resistant CDI – as a "salvage therapy" when the multiple classic treatments have failed.[25, 33] These studies have also shown that rifaximin is well-tolerated by the majority of patients and that it has had some success in treating resilient cases of CDI, including some strains belonging to the NAP1/BI/027 ribotype.[33] Resistance to rifamycins by *C. difficile* is a developing issue with approximately 2% of current strains exhibiting rifaximin resistance; there is growing concern that this number could rise.[33]

Rifaximin's extreme potency against *C. difficile* and its usefulness in treating resilient cases of CDI will result in its continued use in the modern repertoire of CDI treatments –

although concern over rifamycin-resistant *C. difficile* will prevent the drug from becoming the new "standard treatment" for CDI – it will likely remain a useful alternative treatment to utilize when other drugs are ineffective.

1.3.5 – *C. difficile* resistance to the current chemotherapeutics

C. difficile has been shown to exhibit reduced susceptibility to the common chemotherapeutics (vancomycin, metronidazole and fidaxomicin), but the resistance is not widespread. For example, *C. difficile* isolates with reduced susceptibility to metronidazole (MIC > 32 μg/mL) have been documented in recent years.[34] The Anaerobe Research Unit in the UK found that four *C. difficile* isolates, out of 30 tested, showed reduced susceptibility to metronidazole.[34] The reduced susceptibility to metronidazole exhibited by *C. difficile* is not long-lived as it is often lost after freeze-thawing or passaging of the bacteria.[20] Reduced susceptibility to vancomycin and fidaxomicin (MIC values of 4 μg/mL and 16 μg/mL, respectively) has also been observed in *C. difficile* isolates. The reduced susceptibility to metronidazole has clinical significance because concentrations < 32 μg/g faeces are obtained following oral administration of metronidazole (due to the high systemic absorption).[20] The implications of reduced susceptibility to vancomycin and fidaxomicin are less significant, because high concentrations (> 1000 μg/g faeces) of the drugs are obtained in the GI tract due to their low systemic bioavailability following oral administration.[20] The spread of *C. difficile* resistance is a growing concern and multiple new chemotherapeutics are currently being developed to aid in the fight against the *C. difficile* epidemic.

1.4 – Potential CDI chemotherapeutics

There exists a wide array of novel *C. difficile* inhibitors that are currently in various stages of development. Due to the recent high demand for novel CDI chemotherapeutics, a plethora of unique molecules are currently undergoing preclinical and clinical trials for potential application as CDI treatments.[20, 22, 25] Some of the more promising antibiotic compounds will be discussed briefly in terms of their potential for CDI treatment.

Surotomycin

Surotomycin (previously CB-183,315) (Figure 1.5) is a cyclic lipopeptide antibiotic that is structurally related to daptomycin and was developed for CDI treatment by Cubist Pharmaceuticals.[20, 35] Daptomycin is manufactured *via* precursor-directed fermentation of *S. roseosporus* and surotomycin is manufactured through a similar process.[35]

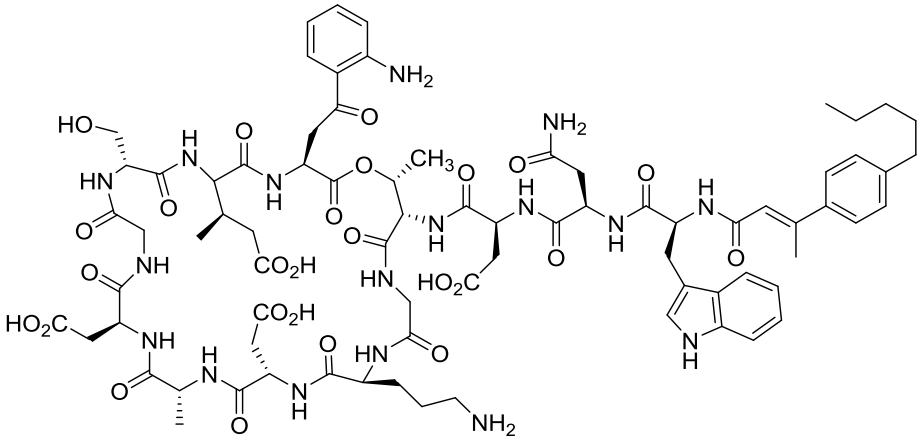

Figure 1.5 – Cyclic lipopeptide surotomycin (previously CB-183,315).

Surotomycin exhibited an MIC value of 0.5 μg/mL against *C. difficile* and exhibited MIC values > 8192 μg/mL for other intestinal bacteria such as "the *Bacteroides fragilis* group, *Prevotella* spp., Gram-negative cocci (*Veillonella* spp. and *Acidaminococcus* spp.), *E. coli*,

Enterobacter spp. and *Klebsiella* spp." – this strong preference for *C. difficile* over other commensal bacteria makes surotomycin a prime candidate for CDI treatment.[36]

A phase II clinical trial evaluated the safety/efficacy of the medication as a CDI treatment; the study concluded that surotomycin was safe and well-tolerated at two doses of 125 mg or 250 mg per day and that the drug "sustained better cure rates" than vancomycin.[37] Surotomycin was then subjected to a similar phase III clinical trial, but the compound failed to meet noninferiority criteria relative to vancomycin.[38] Surotomycin displayed efficacy and tolerability that was on par with vancomycin (clincal cure rates of 79 % and 83.6% for surotomycin and vancomycin, respectively).[38] Overall, surotomycin exhibited potential as a novel CDI chemotherapeutic, but it failed to meet initial phase III criteria for progression into a marketable pharmaceutical.

CRS3123

CRS3123 (Figure 1.6) is a novel diaryldiamine that is currently being developed by the National Institute for Allergy and Infectious Diseases (NIAID); the chemical is active against Gram-positive bacteria like *C. difficile*.[22, 39] CRS3123 works by inhibiting bacterial methionyl-tRNA synthetase and as a result, the chemical exhibits activity against numerous clinically relevant bacteria (e.g. MRSA and *Enterococcus faecium*).[39]

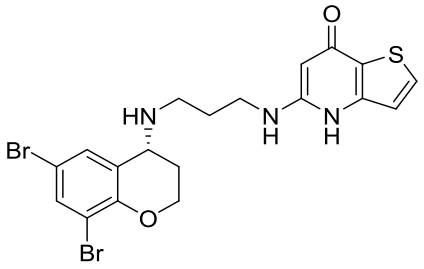

Figure 1.6 – CRS3123 (previously REP3123).

CRS3123 exhibited potent MIC values (1.0 µg/mL) against 108 *C. difficile* clinical isolates.[39] Treatment of lethal CDI in a hamster model by CRS3123 resulted in a substantial increase in survival rate vs. vancomycin. All vancomycin-treated hamsters were dead by day 17, whereas 62% and 75% of the hamsters treated with CRS3123 (at dose rates of 0.5 mg/kg and 5 mg/kg, respectively) were alive at day 35.[22] CRS3123 has recently undergone phase I clinical trials assessing tolerability and safety with positive results.[40]

LFF571

LFF571 (Figure 1.7) is a semi-synthetic thiopeptide that was recently developed as part of an investigation into the activity of 4-aminothiazolyl analogues of GE2270A (a known, natural product antibiotic – see Figure 1.7) for the identification of potential CDI chemotherapetuics.[41]

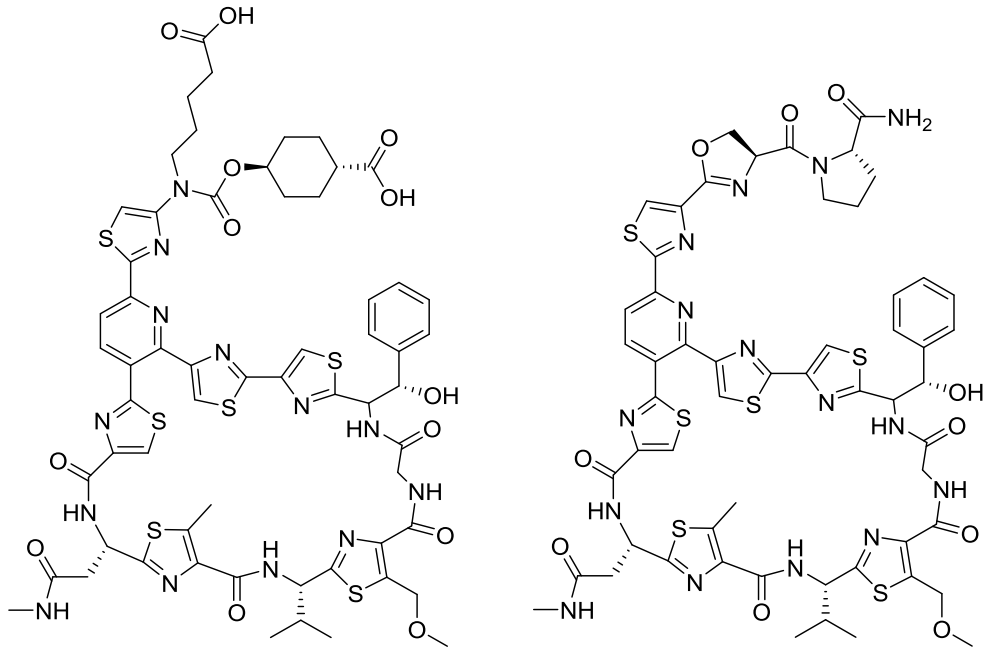

Figure 1.7 – LFF571 (left) and GE2270A (right).

GE2270A was discovered in 1991 by researchers at the Lepetit Research Institute – it was isolated from the fermentation broth of *Planobispora rosea.*[41] The compound was found

to inhibit prokaryotic chaperone elongation factor Tu *via* inhibition of aa-tRNA binding; this translation inhibition mechanism imparts strong antibacterial activity against a broad spectrum of Gram-positive bacteria.[41-43] This novel mechanism of action is important because it prevents the development of cross-resistance to "standard-of-care" antibiotics.[43]

One study indicated that LFF571 exhibits an MIC value of ≤ 0.5 μg/mL for all *C. difficile* isolates tested (whereas vancomycin exhibits an MIC_{90} value ≤ 2.0 μg/mL).[42] In a hamster model of CDI, LFF571 was more effective than vancomycin (at a lower dose and with fewer recurrences of CDI); LFF571 substantially reduced the risk of death when compared to both saline and vancomycin.[42] Novartis Pharmaceuticals has recently performed a phase II clinical trial of LFF571 as a possible treatment for CDI; results showed the drug to be comparable to vancomycin in efficacy and safety.[44]

Nitazoxanide and derivatives

Nitazoxanide (Figure 1.8) is a nitrothiazolide derivative that is licensed by the FDA for use against intestinal parasites like giardiasis and cryptosporidiosis; the medication is now being explored for treatment of CDI.[22, 25, 45]

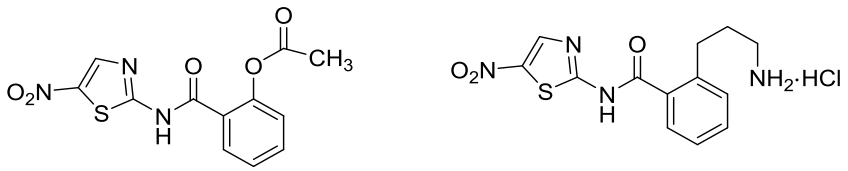

Figure 1.8 – Nitazoxanide (left) and amixicile (right).

Nitazoxanide is known to disrupt cellular metabolism *via* inhibition of the pyruvate:ferredoxin oxidoreductase system.[22, 25] The drug competes with pyruvate for the thiamine pyrophosphate vitamin cofactor of the pyruvate:ferredoxin oxidoreductase complex; by acting upon and inhibiting the co-factor and not the enzyme itself, it is

theorized that nitazoxanide and its derivatives will not be susceptible to the same mutation-based resistance that plagues other enzyme-targeting drugs.[46] The pyruvate:ferredoxin oxidoreductase enzyme system is a semi-selective *C. difficile* target as many beneficial enteric microflora do not utilize pyruvate:ferredoxin oxidoreductase because they make use of pyruvate dehydrogenase.[46]

Nitazoxanide has been shown to exhibit MIC values between 0.3-1.0 µg/mL against *C. difficile* isolates.[22] When the chemical was first trialled against CDI, it was found to be at least as effective as metronidazole and effective in cases where metronidazole was not.[45, 47] Further small studies tested the efficacy of nitazoxanide compared with vancomycin in a double-blind study – the results indicated that nitazoxanide was equally effective against CDI when compared to vancomycin.[47]

Nitazoxanide suffers from poor water solubility and this property makes it accumulate in the intestine following consumption.[46] Amixicile (Figure 1.8) is a chemical derivative of nitazoxanide that was identified amongst 250+ nitazoxanide derivatives as a lead compound with increased solubility and thus increased pyruvate:ferredoxin oxidoreductase inhibitory activity.[46] This new nitazoxanide derivative was tested in an optimized murine model of CDI and the chemical exhibited a greater survival rate (56%) than both vancomycin (15%) and nitazoxanide (22%).[46] CDI recurrence was not observed in mice treated with amixicile and nitazoxanide while the other drugs tested (i.e. vancomycin, fidaxomicin, etc.) exhibited CDI recurrence.[46]

Thus, the nitrothiazolide derivatives represent a promising new class of potential CDI inhibitors. Further pharmacological study into these chemicals is required before they can be relied upon as safe, effective CDI treatments.

NVB302

NVB302 (Figure 1.9) is a chemically modified derivative of the peptide deoxyactagardine B, which is isolated from *Actinoplanes liguriae*.[48] The peptide works by inhibiting cell wall biosynthesis *via* lipid II binding (at a site distinct from that of vancomycin); the drug also exhibits selectivity for *C. difficile* over other intestinal bacteria.[48]

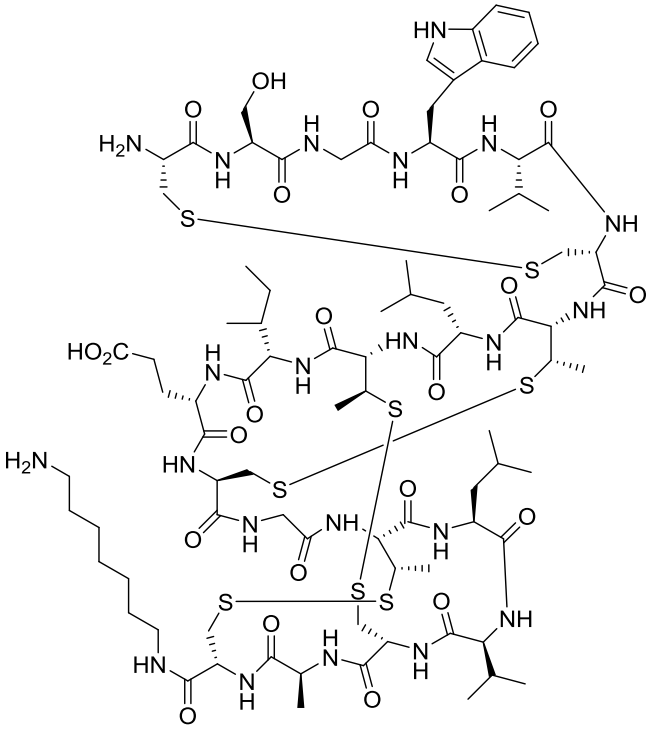

Figure 1.9 – Antibacterial peptide NVB302.

Furthermore, NVB302 has been shown to be stable in the environment of the gut, as up to 60% of the unmetabolized drug is recoverable from the faeces of dosed rats.[22] NVB302 initially exhibited MIC values in the range of 0.5 μg/mL to 2.0 μg/mL against *C. difficile*;

further activity studies against 91 clinical isolates showed an average MIC value of 1.04 µg/mL against *C. difficile*.[22] Furthermore, NVB302 was shown to exhibit MIC values of >256 µg/mL for fusobacteria and *Bacteroides fragilis* – as well as reduced activity against other intestinal microflora (e.g. MIC value of 64 – 256 µg/mL for *Prevotella* spp.).[22] In a comparative study of NVB302 versus vancomycin in a human gut model of CDI, NVB302 was found to be non-inferior to vancomycin and it also exhibited less detrimental effects against intestinal microflora like the *Bacteroides fragilis* group.[48] NVB302 has now completed phase I clinical trials with Novacta Biosystems;[20] unfortunately, the drug has been found to be ineffective at eliminating *C. difficile* spores, much like vancomycin and other common CDI treatments.[22]

Ridinilazole

Ridinilazole (previously known as SMT19969) (Figure 1.10) is a bis-benzimidazole derivative that exhibits strong antibacterial selectivity for *C. difficile* over other bacteria (including *S. aureus* and intestinal microflora).[49-50] Ridinilazole selectively targets specific *Clostridia* spp. without affecting the other commensal GI microflora (both Gram-positive and Gram-negative species); the drug generally shows MIC values of 0.125 – 0.25 µg/mL against most *C. difficile* strains.[50]

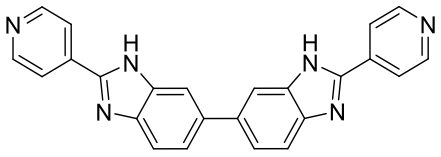

Figure 1.10 – Ridinilazole (formerly SMT19969).

Summit Pharmaceuticals has completed phase I clinical trials with ridinilazole exhibiting good tolerability, low systemic absorption rates and selectivity for *Clostridium* spp.; furthermore, ridinilazole passed superiority criteria against vancomycin in a multicentre

phase II trial of 100 CDI patients.[50] The antibacterial mechanism of action is not completely understood, but studies indicate that ridinilazole is implicated in the inhibition of cell division – the drug is also known to reduce toxin titre levels and spore loads.[50] The company is currently pursuing phase III trials and further development.[50]

Cadazolid

Cadazolid (Figure 1.11) is a oxazolidinone and quinolone antibiotic hybrid that exhibits strong potential as a novel CDI chemotherapeutic.[51] The drug exhibits antibacterial efficacy *via* inhibition of protein synthesis without cross-resistance to the quinolone class or oxazolidinone class of antibiotics.[51-52] Cadazolid also exhibits inhibition of toxin production and sporulation; furthermore, the drug has a low oral bioavailability and it exhibits respectable selectivity for *C. difficile* over intestinal microflora.[51-52]

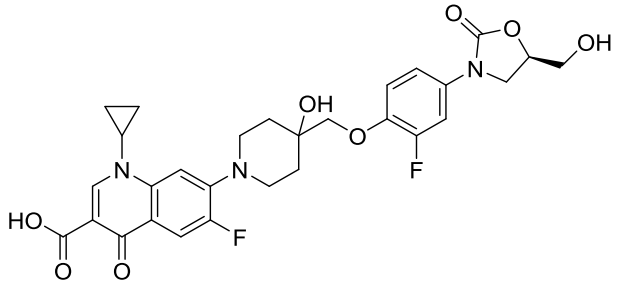

Figure 1.11 – Cadazolid (hybrid quinolone and oxazolidinone antibiotic).

Cadazolid exhibits MIC values ranging from 0.125 – 0.50 μg/mL against *C. difficile* isolates.[51-52] The compound passed initial phase I and II clinical trials, showing similar tolerability and efficacy relative to vancomycin. Recent global phase III clinical trials have been concluded with mixed results (currently unpublished); progression to further phase III trials is currently underway.[53]

Other novel CDI treatments

A plethora of other potential CDI therapies are currently under investigation – these include chemotherapeutics (including small molecules, polymers and larger biological molecules) and non-invasive non-drug therapies (e.g. faecal transplant therapy).[20, 22, 24]

For example, ramoplanin is a lipodepsipeptide antibiotic owned by Nanotherapeutics that is currently undergoing clinical trials for CDI treatment and relapse prevention.[20] Tigecycline is a known antibiotic drug that is also under investigation for potential use as a CDI chemotherapeutic.[20, 25] Furthermore, various synthetic derivatives of purines,[54] macrolides,[55] nitroheterocycles,[56] glycopeptides,[57] tetramic acids,[58] antimicrobial peptidomimetics[59], nylon-3 polymers[60] and bis-indoles[61] have been shown to exhibit significant antibacterial activity against *C. difficile*; these molecular classes are generally under explored and more investigation is certainly warranted as novel, efficacious CDI medications are currently in high demand.

Immunotherapeutic approaches include vaccination and passive antibody therapy; so far, these therapies have all focused on the *C. difficile* toxins. There are three vaccines currently being independently investigated in clinical trials by Sanofi-Pasteur, Pfizer and Intercell.[20] In October 2016, bezlotoxumab (Merck's monoclonal antibody targeting *C. difficile* toxin B) was given FDA approval as an adjunct therapy for patients who are currently undergoing antibiotic therapy for CDI treatment and are at high risk of recurrent infection.[62]

1.5 – Antibacterial binaphthylpeptide derivatives

In our laboratory, there has been an ongoing project focused on the development of novel antibacterial compounds originally based upon a binaphthylpeptide scaffold.[59, 63-69]

The key structural moieties that confer antibacterial activity to this class of compounds are outlined on lead compound **1** (Figure 1.12) as a rudimentary pharmacophore. The essential structural features include a hydrophobic biaryl moiety with an alkyloxy substituent attached to one ring system and a peptide chain attached to the other aromatic ring. The peptide chain comprises one to three amino acid residues; importantly, at least one of the amino acid residues must contain a cationic (i.e. basic) side chain functionality. Lysine (Lys) and arginine (Arg) have been found to be key amino acids for establishing antibacterial activity amongst this class of compounds. A hydrophobic terminus is essential for ensuring potent antibacterial activity, although bifurcation of the terminus does not seem to be vital.[59, 69]

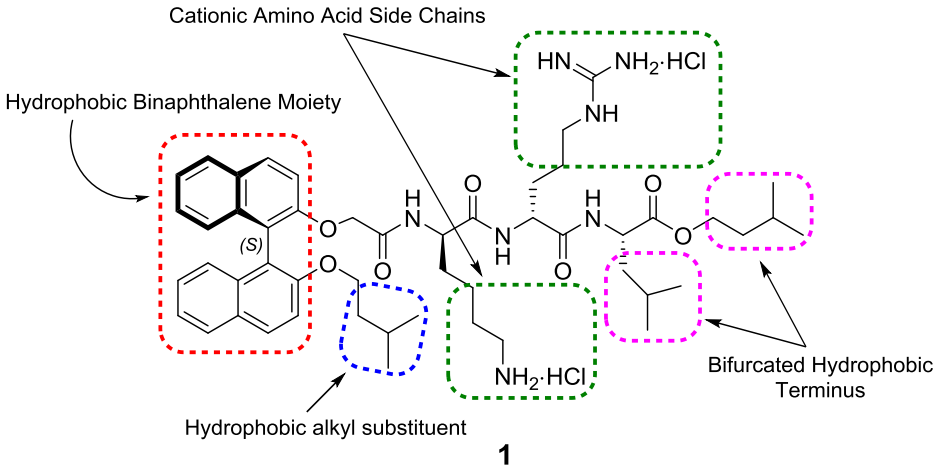

Figure 1.12 – General pharmacophore for binaphthylpeptide compounds (shown on lead compound **1**).

These binaphthylpeptide derivatives generally exhibit broad-spectrum Gram-positive antibacterial activity, e.g. compound **1** exhibits an MIC = 2.0 µg/mL against VRSA and 4.0 µg/mL against VRE.[64] Notably, compound **1** also exhibited potent antibacterial activity against MRSA and *S. aureus* strains that were resistant to linezolid. The compound displayed reduced activity against Gram-negative bacteria, including *E. coli* and *K.*

pneumoniae with MIC values of 16.0 µg/mL and > 32.0 µg/mL, respectively. [64] Compound **1** was licensed to Valevia Pharmaceuticals in 2010 and the company was pursuing topical use of the drug in catheter and wound related infections.[70]

In vitro studies also indicated that resistance to the binaphthylpeptides develops extremely slowly compared to vancomycin; 18 generations of *S. aureus* were required for development of vancomycin resistance, whereas compound **1** required over 50 generations of *S. aureus* for the development of *in vitro* resistance.[64] Bacteria that eventually developed reduced susceptibility to **1** did not exhibit cross-resistance to vancomycin.[64] These data indicate that vancomycin and compound **1** do not share a common mechanism of action.

Recent studies in our laboratory indicated potent antibacterial activity (MIC = 2.0 – 8.0 µg/mL) against *C. difficile* by various oxazole and triazole derivatives of compound **1**.[59, 68] Lead compound **2** was developed as a peptidomimetic derivative of compound **1** and it was found to exhibit notable *in vitro* antibacterial activities against both *S. aureus* and hypervirulent *C. difficile* (Figure 1.13).[69]

Compound **2** was subsequently tested in an *in vivo* murine model of CDI with some promising initial results.[71] Attempts are currently being made to increase antibacterial activity and introduce *C. difficile* selectivity. Notably, these biarylpeptide derivatives are non-drug like as the presence of many heteroatoms and its dicationic nature confers poor membrane permeability to the molecules. This property makes these compounds perfect candidates for a potential new CDI treatment as they are not absorbed systemically; this allows for a high gastrointestinal concentration of the drug to be maintained, which is essential for CDI treatment. Thus, a library of novel derivatives, based upon lead

compound **2,** will be pursued in an attempt to develop a drug that can effectively and safely treat CDI.

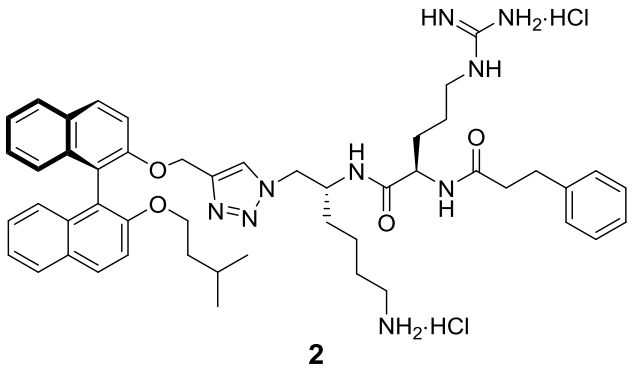

2

MIC Values (μg/mL)		
Bacterial Species	**2**	Vancomycin
S. aureus	4	1
MRSA	4	1
E. faecalis	4	4
S. pneumoniae	4	1
C. difficile	8	0.5
C. difficile (RT027)	8	0.5
E. coli	8	-

Figure 1.13 – Lead compound **2** with a table of antibacterial activities against *S. aureus* (ATCC 29213), *MRSA* (NCTC 10442), *E. faecalis* (ATCC 29212), *S. pneumoniae* (ATCC 49619), *C. difficile* (ATCC 700057, *C. difficile* (RT027 – NSW132) and *E. coli* (ATCC25922).

1.6 – Target design: concepts and synthetic strategy

1.6.1 – Peptidomimetic bioisostere incorporation

The human GI tract is acidic and contains numerous peptidases (i.e. peptide-cleaving enzymes) and other metabolic enzymes; these conditions cause peptide bond degradation *via* acidic hydrolysis or enzymatic cleavage.[72] Peptide bond decomposition can be avoided by replacing an amide moiety (Figure 1.14a – blue circle) in the target molecule with a peptidomimetic bioisostere, such as a 1,4-disubstituted-1,2,3-triazole ring (Figure 1.14c – blue portion).

Studies have shown that the 1,2,3-triazole ring exhibits a similar planarity, dipole (Figure 1.14b and 1.14c) and spatial arrangement (for the 1,4-substituents) to that of a normal peptide moiety.[73-74] Notably, 1,4-disubstituted-1,2,3-triazoles exhibit the same potential to

accept and donate hydrogen bonds as normal amides yet they are considered more resistant to enzymatic cleavage, hydrolysis and oxidation.[74]

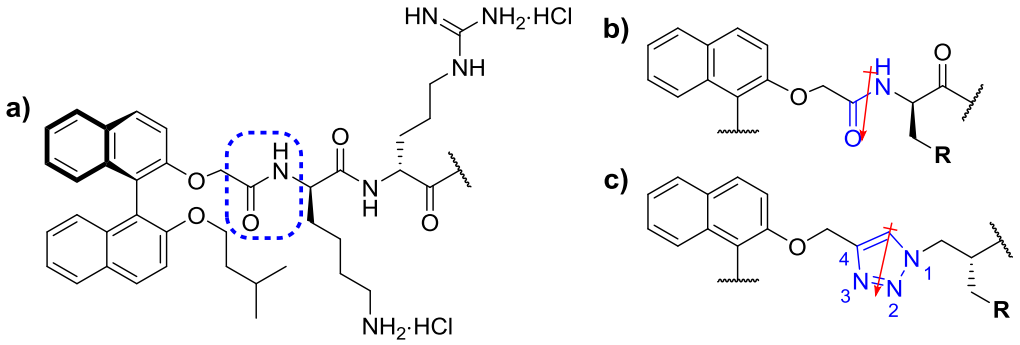

Figure 1.14 – **a)** Portion of lead compound **1** with targeted amide group (blue circle) **b)** Amide moiety (blue) and corresponding dipole moment (red) **c)** 1,2,3-Triazole moiety (blue) and corresponding dipole moment (red).

Peptidomimetic replacement of the first amide (Figure 1.14a – blue circle) in the peptide chain of binaphthylpeptide **1**, by a 1,2,3-triazole moiety, led to derivatives like compound **2**. These triazole moieties were most reliably installed *via* a Cu-catalyzed azide-alkyne [3 + 2]-cycloaddition (CuAAC), i.e. a 'click' reaction.[73-75] The precursors necessary for the formation of the triazole moieties were an alkyne fragment (e.g. compound **4**) and the requisite azido-substituted fragment (e.g. azide **5**), as shown in Scheme 1.1.

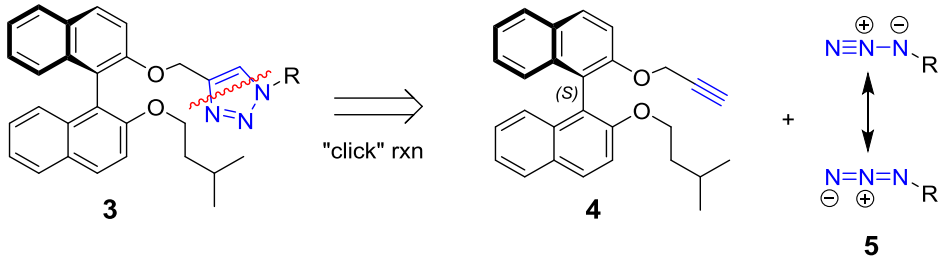

Scheme 1.1 – Retrosynthesis of the internal triazole moiety (compound **3** - blue portion) gives alkyne **4** and azide **5**.

Furthermore, previous research in our laboratory has also led to the development of compounds with terminal 1,2,3-triazole moieties substituted for the amide terminus, e.g. compound **6**[59] (Figure 1.15).

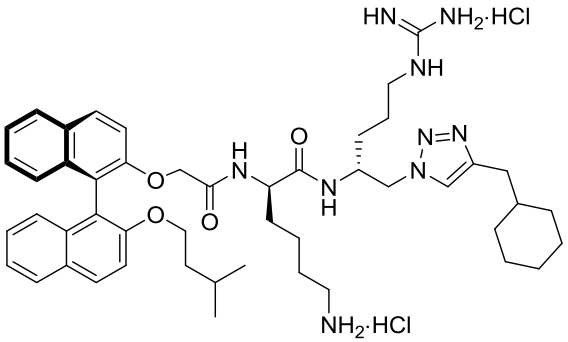

6

MIC Values (μg/mL)		
Bacterial Species	**6**	Vancomycin
S. aureus	2	1
MRSA	2	1
E. faecalis	2	4
S. pneumoniae	4	1
C. difficile	4	0.5
C. difficile (RT027)	4	0.5
E. coli	8	-

Figure 1.15 – Lead compound **6** with a table of antibacterial activities against *S. aureus* (ATCC 29213), *MRSA* (NCTC 10442), *E. faecalis* (ATCC 29212), *S. pneumoniae* (ATCC 49619), *C. difficile* (ATCC 700057, *C. difficile* (RT027 – NSW132) and *E. coli* (ATCC25922).

1.6.2 – Peptide chain orientation

The synthesis of the internal triazole moiety *via* a 'click' reaction allows for two potential peptide chain orientations; the resulting orientation is governed by the placement of the azide precursor functionality on the amino acid starting material (see Scheme 1.2). The amino acid precursor (**7**) can be functionalized in two ways, giving rise to either a β-azido-amine (i.e. compound **8** in Pathway A – Scheme 1.2) or an α-azido-acid (i.e. compound **9** in Pathway B – Scheme 1.2). Subsequent 'click' reactions with these azide derivatives gives either scaffold orientation **A** or scaffold orientation **B**. Both peptide orientations have been utilized in previous research on the biarylpeptides and both orientations are known to produce active compounds.[59, 69, 76] Therefore, it was decided that both scaffold orientations, **A** and **B**, would be pursued and they would be classified into two broad categories, Series A and Series B (respectively).

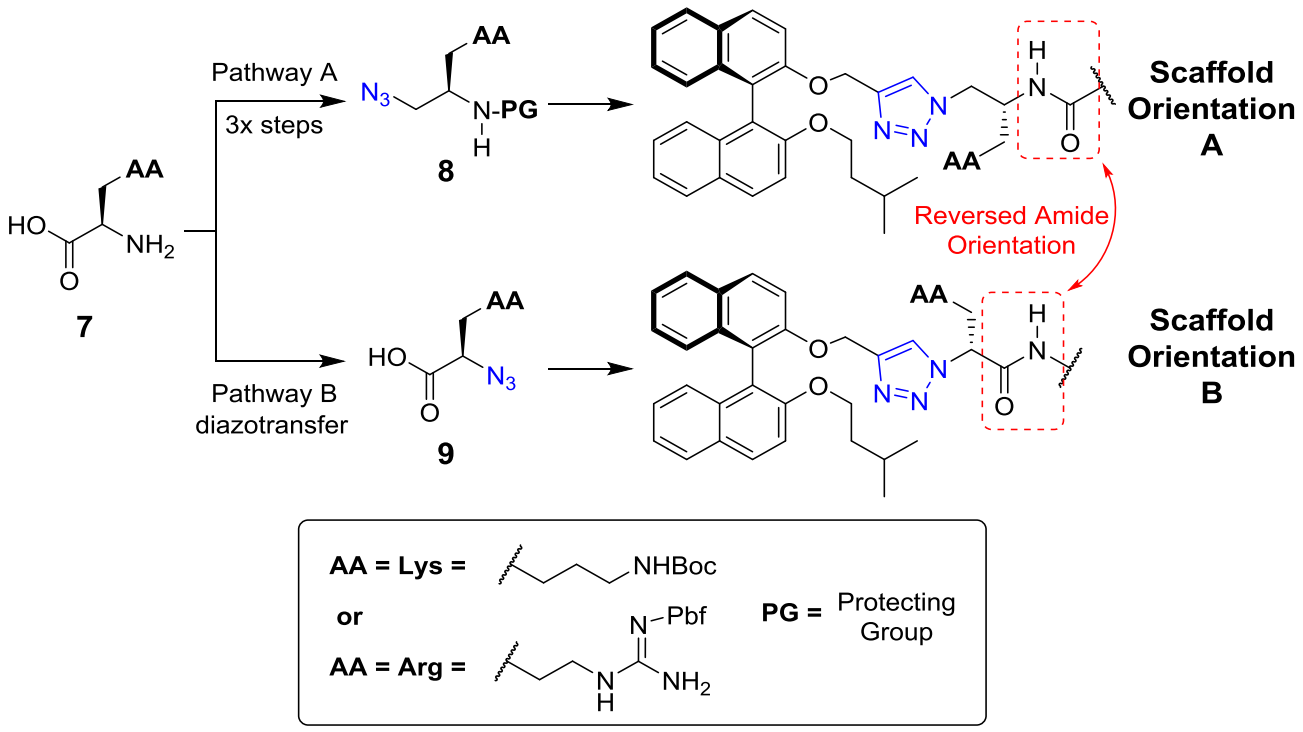

Scheme 1.2 – Effect of azide functionality placement on the resultant scaffold's peptide backbone orientation. Pathway A shows the potential β-azido-amine and the resulting scaffold orientation (**A**). Pathway B shows the potential α-azido-acid and the resulting scaffold orientation (**B**).

1.6.3 – Aromatic core modification

A hydrophobic aromatic core (red circle in Figure 1.12) is essential for the antimicrobial activity of the binaphthylpeptide derivatives. Previous research has shown that the substitution of the binaphthalene moiety (**10**) with an analogous biphenyl core (**11**) (Scheme 1.3) produces compounds with similar antimicrobial efficacy.[65-66]

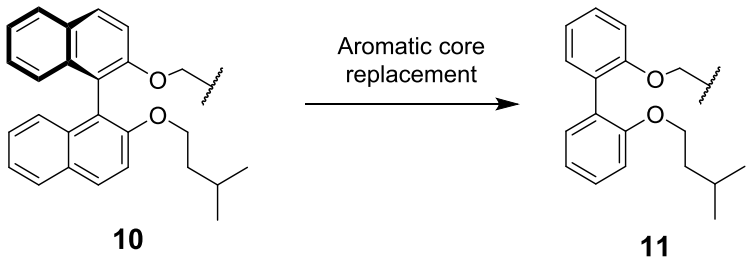

Scheme 1.3 – Aromatic core replacement showing the change from a binaphthalene core (**10**) to a biphenyl core (**11**).

The solubility and structure of the binaphthylpeptide derivatives will be modified by the introduction of a biphenyl aromatic core, which will allow for more variation in the target compound library.

1.6.4 – Target compounds: scaffold variation and derivatization

A large number of structurally different biarylpeptide analogues will be designed and synthesized based upon lead compounds **2** and **6**. A range of unique scaffolds will be synthesized, and each scaffold will be derivatized into a small number of analogues. The following structural scaffold parameters will be varied to give different scaffolds: the number of peptidomimetic 1,2,3-triazoles (Section 1.6.1), the peptide bond orientation (Section 1.6.2), the aromatic core (Section 1.6.3) and amino acid residues (i.e. number, type and orientation). Permutation of these scaffold variations will give rise to a large number of potential scaffold configurations. There are too many possibilities to synthesize them all, so selected scaffold variations will be synthesized to allow for key structure-activity relationship (SAR) comparisons between specific analogues. Examples of the targeted scaffold variations for Series A, B and C are displayed in Figures 1.16, 1.17 and 1.18, respectively. Previous research has shown that monocationic derivatives can display useful antibacterial potency;[59, 69] therefore, simple monocationic derivatives (i.e. scaffold types **12** and **15**) will be targeted as well, because smaller and more synthetically-accessible molecules are always preferable. Each synthesized scaffold will be derivatized by variation of the hydrophobic terminus (**R**); peptide coupling or CuAAC reactions will be utilized for reliable installation of the terminal amide or 1,2,3-triazole moieties, respectively.

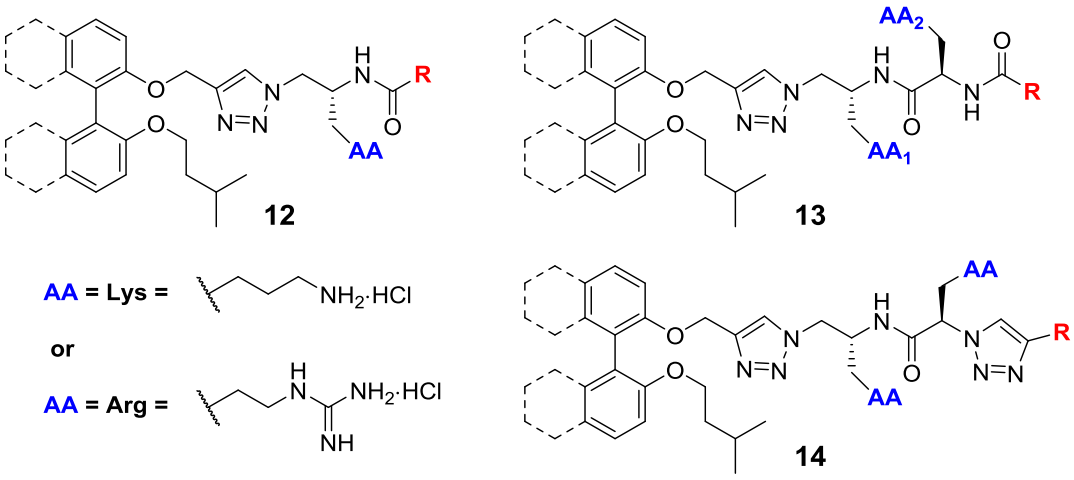

Figure 1.16 – Series A scaffold variations: note the variable structural elements (i.e. amino acid residues (**AA**), hydrophobic terminus (**R**) and the biaryl core).

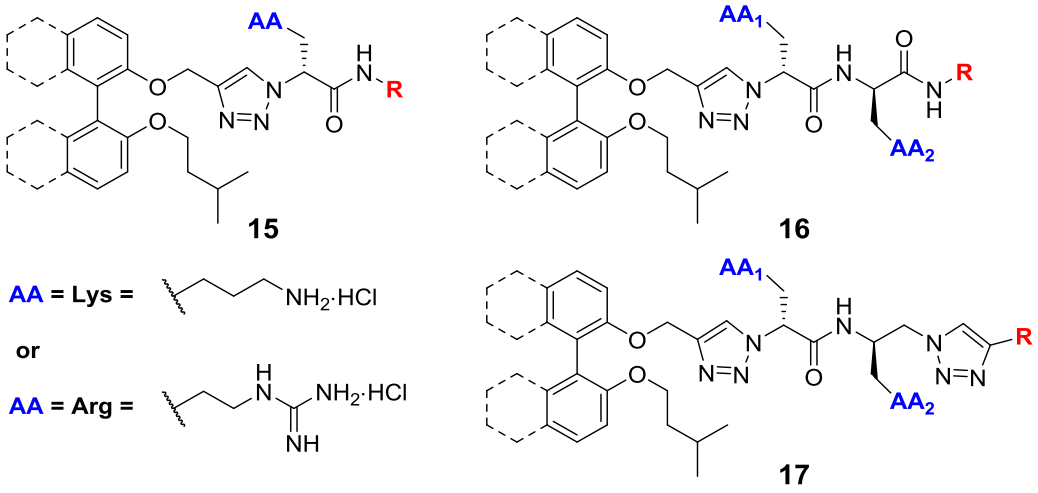

Figure 1.17 – Series B scaffold variations: note the variable structural elements (i.e. amino acid residues (**AA**), hydrophobic terminus (**R**) and the biaryl core).

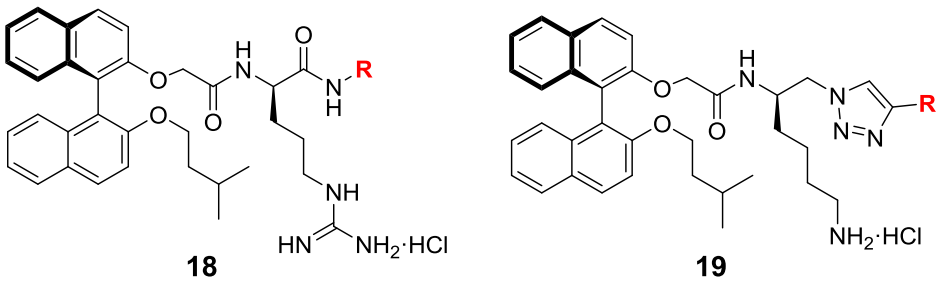

Figure 1.18 – Series C scaffold variations: note the variable hydrophobic terminus (**R**).

Derivatization of the scaffold fragments allows for the synthesis of multiple analogues for each scaffold type, increasing the productivity of the synthetic approach – more molecules translates to an increased number of potential hit compounds. A small number of molecules without an internal triazole moiety (i.e. Series C) will also be synthesized purely for SAR data.

1.6.5 – Modular approach to scaffold synthesis

To allow for easy synthetic access to multiple scaffold variations, a modular approach to scaffold synthesis will be adopted. The variable structural components of the scaffolds in both Series A and B are primarily attached by peptide bonds and 1,2,3-triazole rings; therefore, peptide coupling and CuAAC reactions will allow for the facile and reliable construction of numerous scaffold configurations from a number of primary building blocks (Figure 1.19) that contain these key reactive functionalities: amines ($-NH_2$), acids (-COOH), azides ($-N_3$) and alkynes ($-C{\equiv}CH$). The alkyne building blocks can be combined with the requisite azide building blocks to construct the necessary 1,2,3-triazole moieties. Furthermore, any acid building blocks can be joined to any primary amine functionalities through formation of the required amide bond.

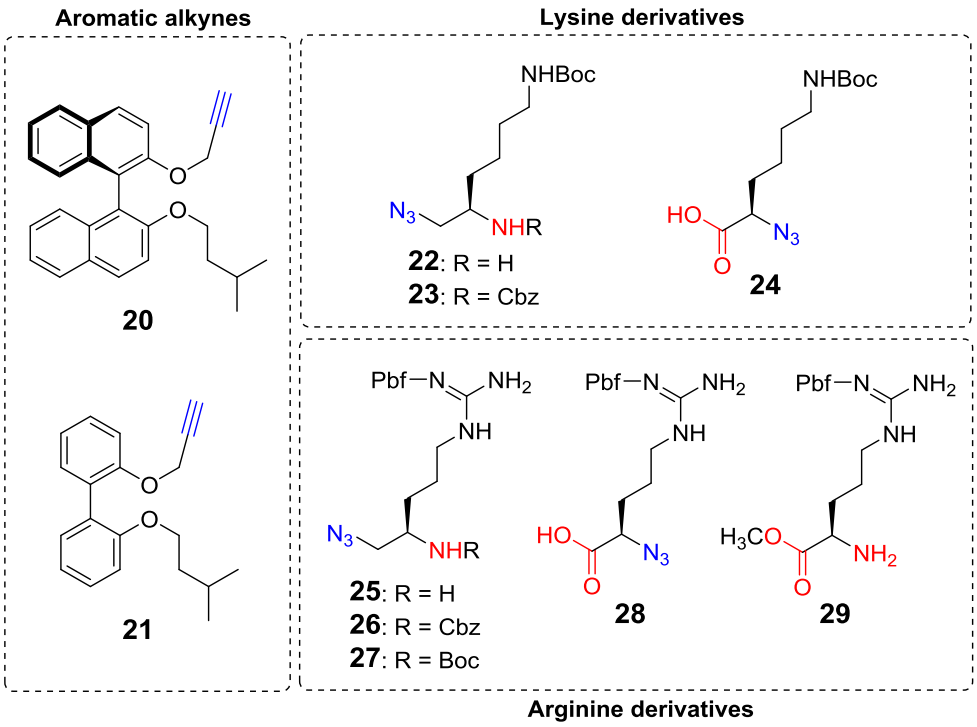

Figure 1.19 – Precursor building blocks for the modular approach to scaffold synthesis: azide and alkyne functionalities (blue) can be readily linked together *via* CuAAC reactions while the amine and acid moieties (red) can also join together *via* peptide coupling methods.

Dual functionalization of the amino acid residues with both an azide and a group capable of peptide coupling (i.e. an amine or carboxylic acid) allows for the combination of multiple precursor building blocks to build the scaffolds; for example, the more complex scaffold types can be constructed from just three modular buildings blocks (Scheme 1.4).

Previous research[69] has shown that CuAAC reactions do not work well with the unprotected β-azido-amines **22** and **25**, so *N*-protected derivatives **23**, **26**, and **27** were utilized for CuAAC reactions that required the β-azido-amine structures.

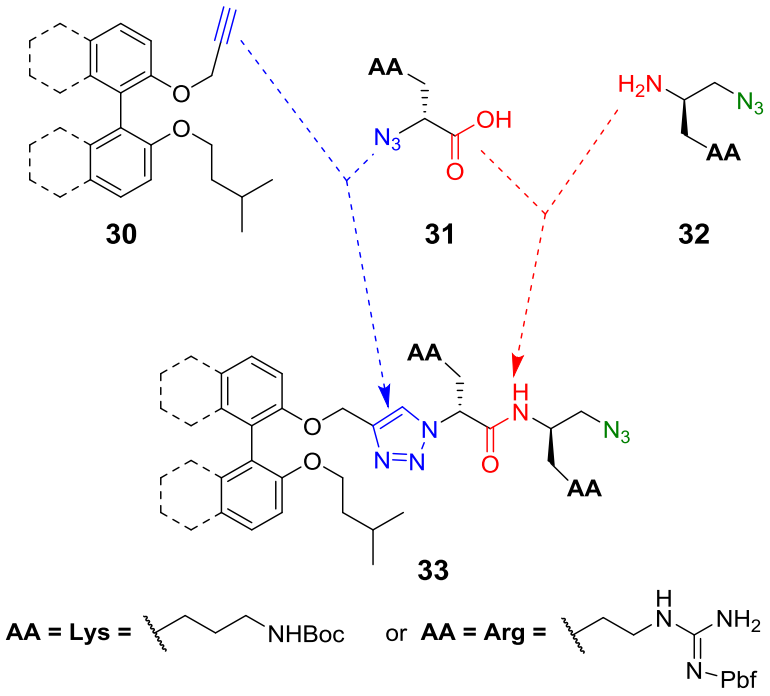

Scheme 1.4 – Modular approach to scaffold synthesis: azide and alkyne functionalities (blue) are combined into a 1,2,3-triazole moiety while the amine and acid moieties (red) are coupled together *via* an amide bond. Note the dual functionalization of the amino acid derivatives that allows for the modular synthesis; the remaining terminal azide handle (green) allows for scaffold derivatization.

1.6.6 – Synthesis: proposed pathway and considerations

The aforementioned precursor building blocks (Figure 1.19) will be achieved through the utilization of known synthetic methodologies; these precursors will be combined through CuAAC and peptide coupling reactions to achieve the aforementioned scaffolds (Section 1.6.4). The various scaffolds will be subsequently derivatized by either CuAAC or peptide coupling reactions followed by side-chain *N*-deprotection and HCl salting; such iterative derivatization of the various scaffold types will allow for the creation of a small library of novel antibacterial compounds.

Importantly, the proposed synthesis requires the use of four protecting groups, i.e. Boc, Cbz, Pbf and Fmoc (Figure 1.20), all of which are utilized for the protection of nucleophilic nitrogens atoms.

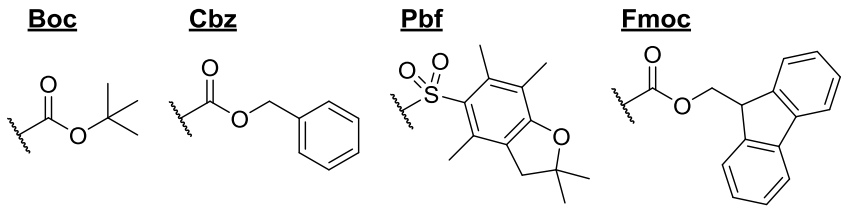

Figure 1.20 – Nitrogen protecting group structures and abbreviations.

Three of the groups (Boc, Cbz, and Fmoc) form carbamates with free amines while the other group (Pbf) protects guanidino residues *via* arylsulfonimide formation. Previous syntheses[64-65] have utilized the Boc and Pbf groups for protection of the lysine and arginine amino acid side-chains, respectively. Importantly, these two groups can be simultaneously cleaved by acidolysis as a final step, which allows the side chains to remain protected throughout the entire synthetic process. In peptide synthesis, the backbone (or α) nitrogen is most commonly protected by the base-labile Fmoc group.[77] The "Boc/Fmoc" orthogonal deprotection strategy (i.e. acid for Boc/Pbf, base for Fmoc) has been employed in the synthesis of previous binaphthylpeptide antibacterials[64-65] and a similar orthogonal protocol will be utilized for the realization of the targeted cationic biarylpeptides. Instead, the Cbz protecting group will be utilized for protection of the α-nitrogen on the amino acid precursors (when required), as this protecting group is stable to the pursuant azidation conditions.[69] Furthermore, the Cbz protecting group is also ideal because it allows for selective deprotection, in the presence of a Boc group, *via* catalytic hydrogenolysis.[78] The Fmoc group will only be utilized in known synthetic procedures for building the unprotected β-azido-amine precursors **22** and **25**, because the *N*-protecting group is not required after azidation for these amine building blocks.

The proposed synthetic pathways (Schemes 1.5, 1.6 and 1.7) allow for the divergent synthesis of multiple scaffold types from simpler scaffold molecules. For example, the

larger scaffold types (e.g. **14**) will be synthesized from the smaller scaffold precursors (e.g. amine scaffold **38** – see Scheme 1.5); this divergent synthetic approach allows for simple diversification of the scaffold types with minimal synthetic labour. This modular synthetic approach will allow for multiple scaffold variations to be synthesized from the same key precursor building blocks. This approach also allows for derivatization of each scaffold type, allowing for the facile synthesis of a large number of antibacterial compounds.

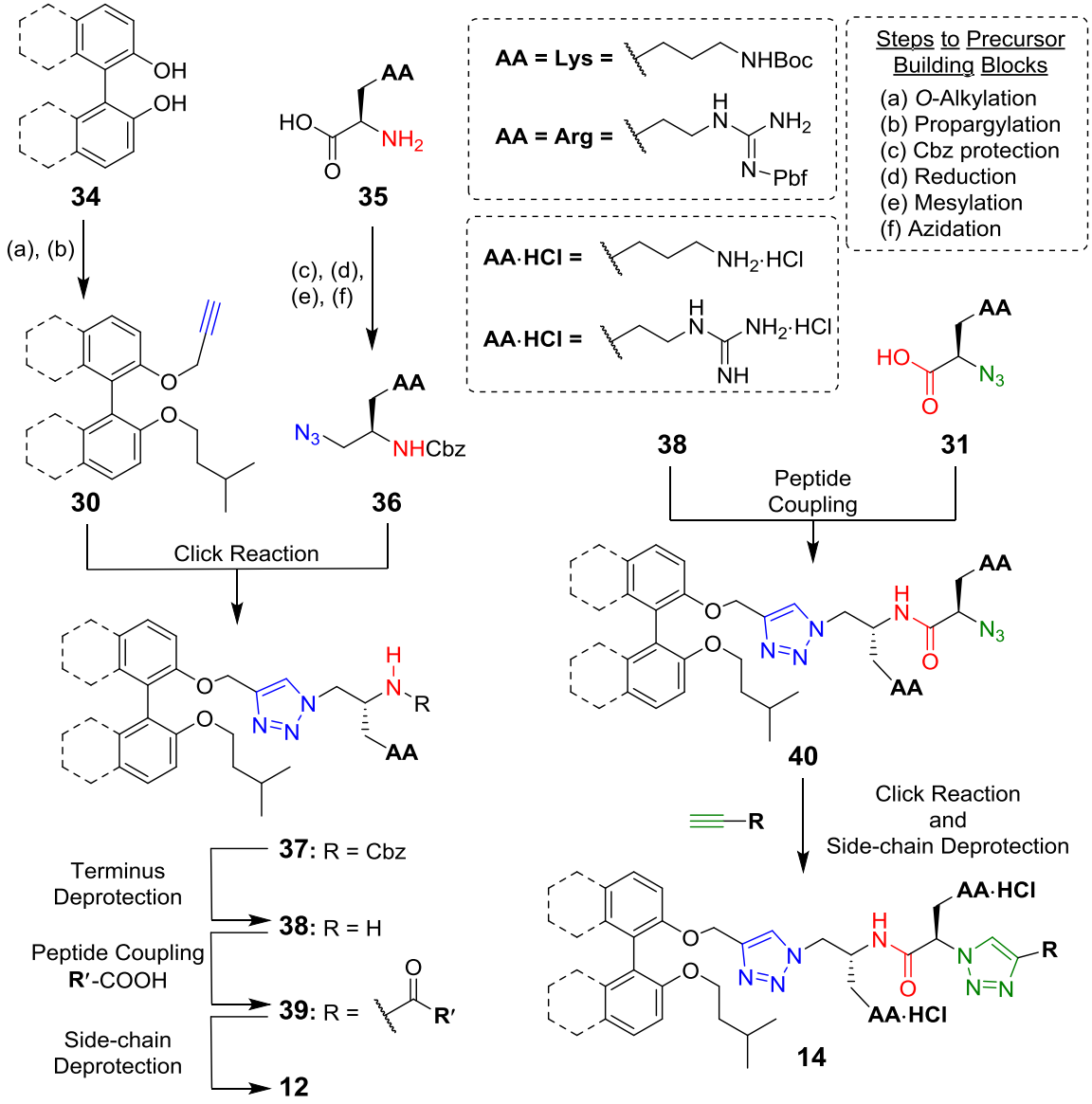

Scheme 1.5 – Potential synthetic pathway to Series A scaffold types **12** and **14**.

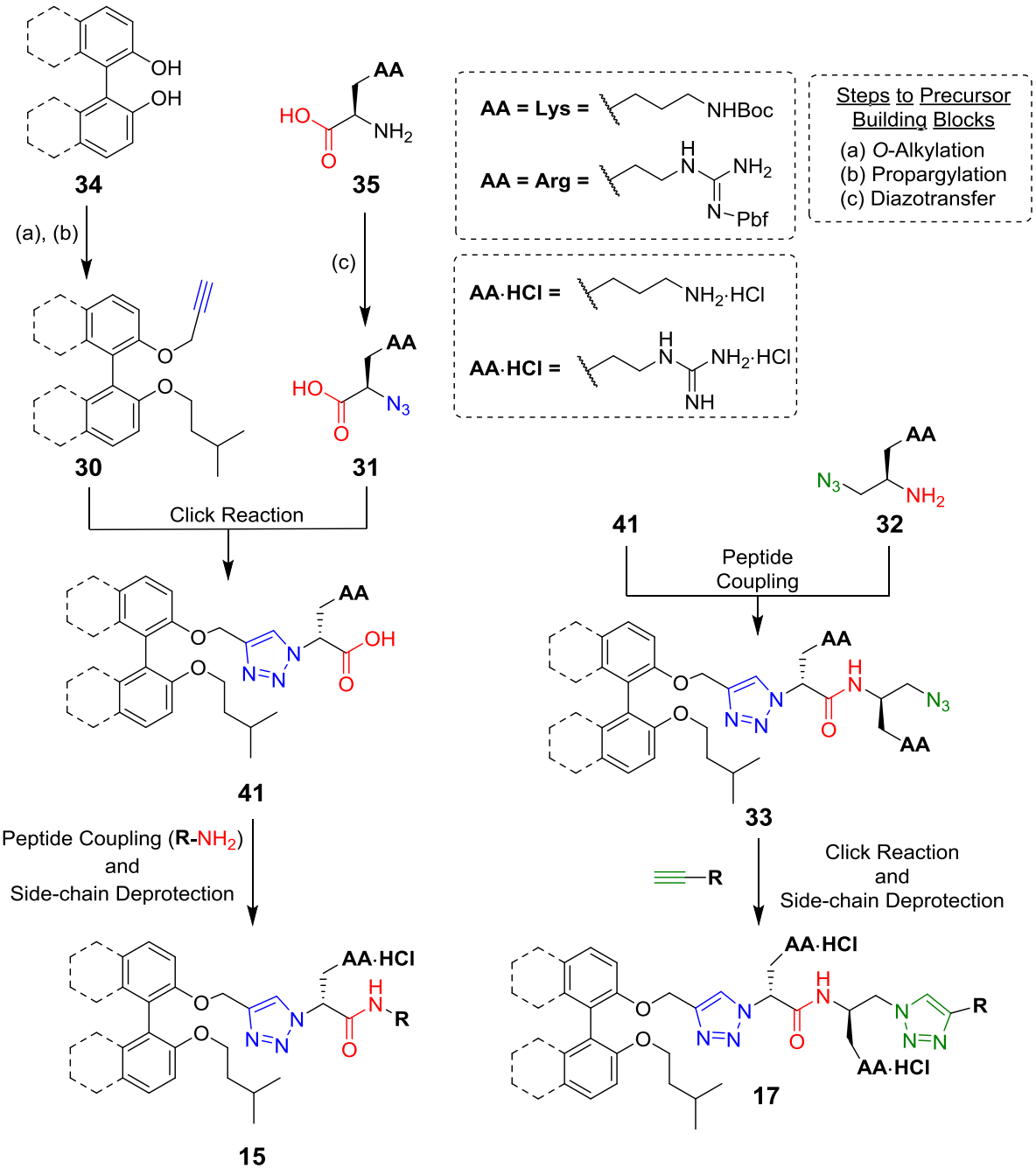

Scheme 1.6 – Potential synthetic pathway to Series B scaffold types **15** and **17**.

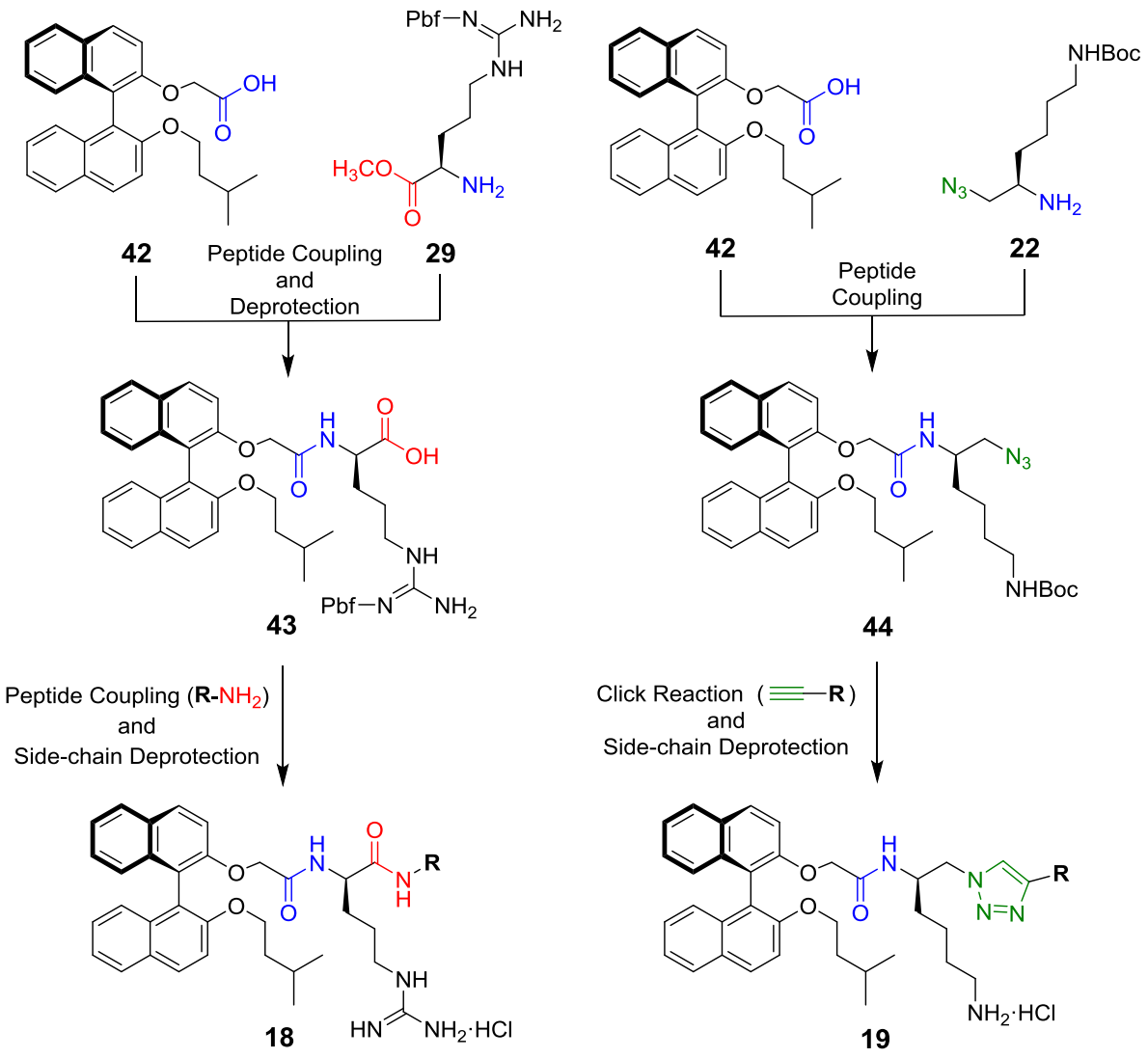

Scheme 1.7 – Potential synthetic pathway to Series C scaffold types **18** and **19**. Precursor compound **42** was gifted from previous researcher (S. Wales). Precursor compound **29** will be synthesized from Fmoc-(D)-Arg(Pbf)-OH *via* methyl esterification followed by *N*-Fmoc deprotection.

1.7 – Project Aims

It is evident that there exists a strong, unmet need for novel antibacterial compounds to effectively treat CDI. Therefore, a joint research project (NHRMC Project Grant# APP1124032) to pursue the synthesis and development of effective CDI chemotherapeutics was established between the University of Wollongong (design and

synthesis), the University of Western Australia (microbiology) and Monash University (pharmacology). The aims of this project are:

- To incorporate an increased number of peptidomimetic bioisosteres (i.e. a 1,2,3-triazole moiety) into the peptide backbone of the lead binaphthylpeptides **2** and **6** – in an attempt to increase gastrointestinal stability by replacing amide moieties with bioisosteres that exhibit increased resistance to enzymatic cleavage;[73]
- To design and establish a viable, multi-gram synthesis of numerous novel triazole-containing scaffolds;
- To simplify the hydrophobic aromatic core in these scaffolds in an attempt to increase compound solubility;
- To vary the number and orientation of cationic amino acid residues embedded in these novel scaffolds;
- To synthesize a small library of novel antibacterial derivatives by installing various hydrophobic termini on the new scaffolds;
- To ascertain the antimicrobial activity of the synthesized derivatives against a range of pathogenic Gram-negative bacteria, Gram-positive bacteria and fungi *via* MIC assays;
- To ascertain the general toxicity of the synthesized compounds *via* cytotoxicity assay;
- To explore the structure-activity relationship of the compounds by utilizing the obtained MIC data;
- To incorporate the structure-activity relationship findings into the target design;

- To design and identify a novel hit compound that could be utilized in the effective treatment of CDI;
- To ascertain the efficacy of the compound as a CDI chemotherapeutic *via* testing in an *in vivo* CDI mouse model;
- To develop and utilize a comparative solubility assay for determining the relative solubilities of the synthesized compounds;

  and
- To perform a rudimentary pharmacokinetics study on the biarylpeptides by testing the blood and faeces of mice from the *in vivo* CDI model.

These goals represent a multi-faceted approach to designing and creating an effective CDI chemotherapeutic based upon the lead binaphthylpeptide scaffolds **2** and **6**. The knowledge gained in this project will also contribute to our overall understanding of the biarylpeptide antibacterial class.

2.0 – Synthesis: results and discussion

2.1 – Synthesis of precursor building blocks

This section describes the synthesis of the scaffold precursor building blocks from commercially available precursors. The known compounds are marked by a reference to the previous literature. All compounds were synthesized with modified literature procedures. Schemes detailing each reaction mechanism can be found in Appendix A – Section A1.

2.1.1 – Synthesis of aromatic cores

2.1.1.1 – Synthesis of alkyne 20

The synthesis of alkyne **20** from precursor **45** was accomplished in two steps: *O*-alkylation followed by *O*-propargylation (Scheme 2.1). The base-promoted mono-*O*-alkylation of (*S*)-BINOL[63] (**45**) (500 mg, 1.75 mmol) with 1-bromo-3-methylbutane was achieved with K_2CO_3 in acetone at reflux (Scheme 2.1) and produced ether **46** in 81% yield. The reaction was also successfully conducted on larger scales with comparable yields – e.g. 10.00 g (34.92 mmol) of (*S*)-BINOL gave a 78% yield of ether **46**.

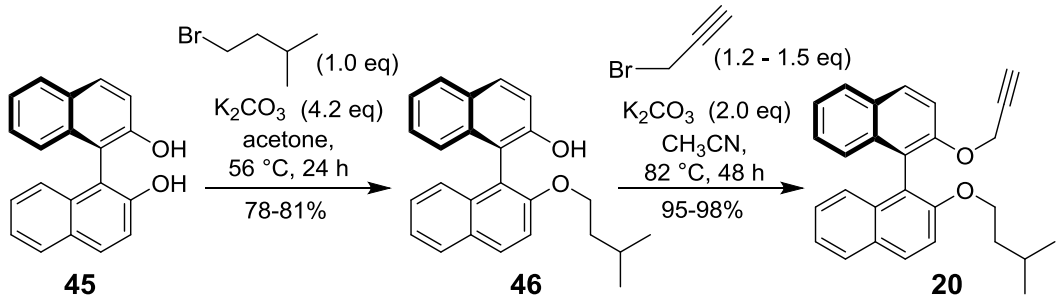

Scheme 2.1 – Two-step synthesis of key alkyne **20**: first, *O*-alkylation of compound **45** to give ether **46** and then *O*-propargylation of **46** to yield target alkyne **20.**

Target alkyne **20** was then realized in 98% yield *via* base-promoted *O*-propargylation of intermediate **46**[79] (1.50 g, 4.21 mmol) with propargyl bromide and K_2CO_3 in acetonitrile at reflux for 48 h. This reaction was also conducive to larger scale as 9.00 g (25.30 mmol) of starting material **46** was reacted to produce alkyne **20** in 95% yield. These compounds (**46**

and **20**) exhibited spectroscopic data that were in agreement with those values reported previously.[63, 69, 79]

2.1.1.2 – Synthesis of alkyne 21

The synthesis of alkyne **21** from precursor **47** was accomplished in two steps: *O*-alkylation followed by *O*-propargylation (Scheme 2.2). The base-promoted mono-*O*-alkylation of 2,2′-biphenol[66] (**47**) (3.00 g, 16.11 mmol) with 1-bromo-3-methylbutane was achieved with K_2CO_3 in acetone at reflux (Scheme 2.2) and produced ether **48** in 89% yield. The reaction was also successfully conducted on larger scales with comparable yields – e.g. 10.00 g (53.70 mmol) of 2,2′-biphenol gave an 81% yield of ether **48**.

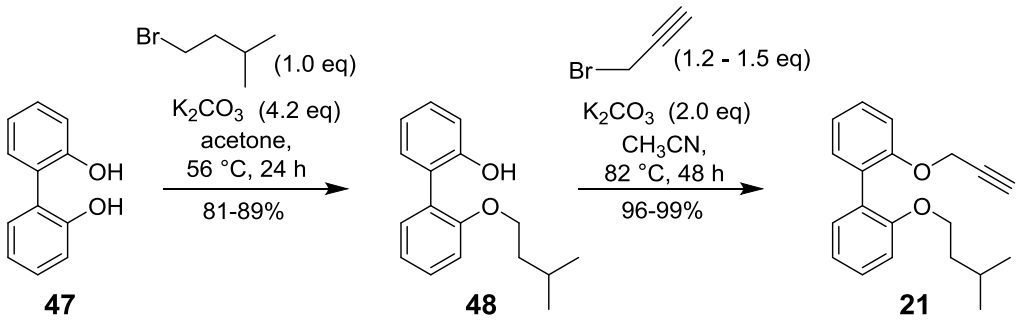

Scheme 2.2 – Two-step synthesis of key alkyne **21**: first, *O*-alkylation of compound **47** to give ether **48** and then *O*-propargylation of **48** to yield target alkyne **21.**

Target alkyne **21** was then realized in 99% yield *via* base-promoted *O*-propargylation of intermediate **48** (1.50 g, 5.85 mmol) with propargyl bromide and K_2CO_3 in acetonitrile at reflux for 48 h. This reaction was also amenable to larger scale as 7.80 g (30.43 mmol) of starting material **48** was reacted to produce alkyne **21** in 96% yield. Ether **48** exhibited spectroscopic data that were in agreement with those values reported previously.[66]

The ^{1}H NMR spectrum for alkyne **21** displayed a characteristic triplet resonance at δ 2.43 that was absent in the ^{1}H NMR spectrum of the starting ether **48** – this resonance exhibited a small coupling constant (J = 2.3 Hz) which is characteristic of long-range propargylic

coupling with the adjacent methylene protons. Therefore, the resonance at δ 2.43 was assigned to the alkyne proton (-CH_2C≡C-H); this assignment was further confirmed by a corresponding gHSQC correlation with a ^{13}C NMR carbon resonance at δ 75.2, which had been assigned as the alkyne methine carbon (-C≡C-H). The ^{13}C NMR spectrum of compound **21** displayed two unique resonances (δ 79.3 and 75.2) that were not present in the ^{13}C NMR spectrum of the starting ether **48**; these ^{13}C NMR resonances were assigned to the quaternary (-C≡C-H) and methine (-C≡C-H) alkyne carbons, respectively. The molecular structure was verified by the presence of a peak at *m/z* 295.1692 in the HRMS that was assigned to the protonated molecular ion $[M + H]^+$ (calcd for $C_{20}H_{23}O_2$ 295.1698).

2.1.2 – Synthesis of lysine derivatives

2.1.2.1 – Synthesis of azide 23

The synthesis of the doubly *N*-protected azide **23** from commercially available H-(D)-Lys(Boc)-OH (**49**) was completed in a three step reaction sequence: Cbz protection,[80] carboxylic acid reduction,[81] and then a two-step, one-pot mesylation/azidation procedure[82] (Scheme 2.3). Installation of the Cbz protecting group on substrate **49** (4.00 g, 16.24 mmol) gave Cbz-Lys(Boc)-OH (**50**) in 95% yield by reaction with benzyl chloroformate and aqueous NaOH solution. This reaction required a substantially modified work-up procedure, due to the solubility of the sodium carboxylate product in organic solvents. A traditional acid/base work-up could not be employed; the product was extracted directly from the reaction mixture into EtOAc as the sodium carboxylate salt followed by back-extraction into distilled H_2O. The intermediate acid **50** (804 mg, 2.11 mmol) was then subjected to a 'mixed anhydride reduction' technique: the acid was converted into a mixed carbonic-carboxylic anhydride by reaction with isobutyl chloroformate in the presence of *N*-methylmorpholine.

The resultant mixed anhydride was then reduced by an aqueous solution of $NaBH_4$ to give the desired alcohol (**51**) in near quantitative yield (98%). This reaction was also implemented on larger scales – 6.81 g (17.90 mmol) of acid **50** produced a 96% yield of alcohol **51**. This intermediate alcohol was then subsequently utilized in the two-step, one-pot synthesis of azide **23**.

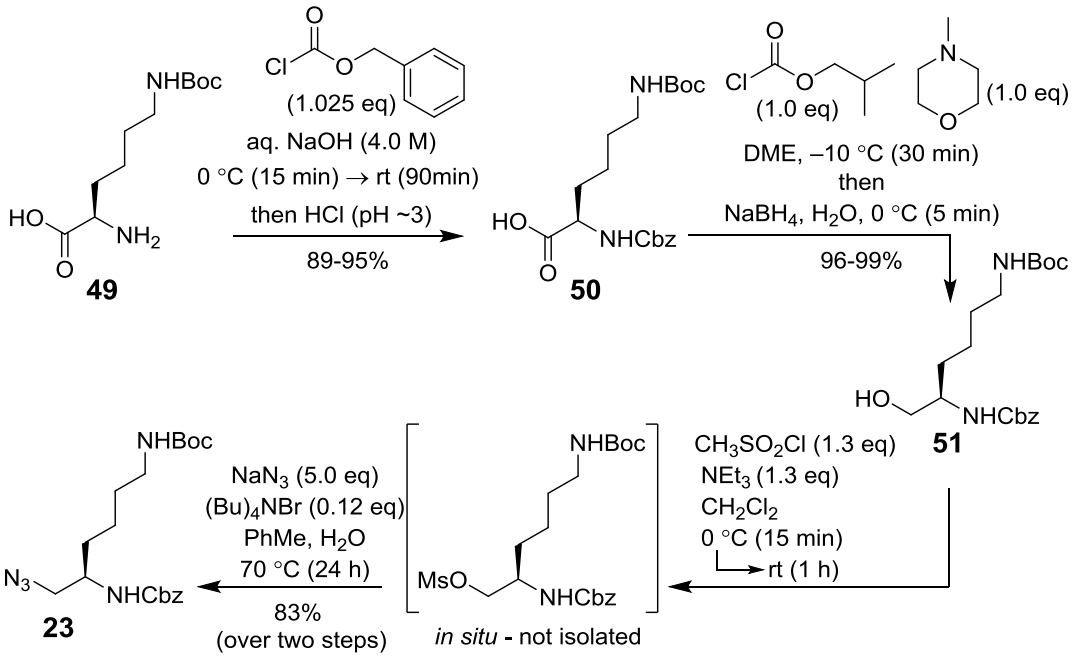

Scheme 2.3 – Synthesis of key azide **23**, from the lysine precursor **49**, in three steps: *N*-Cbz protection to give compound **50**, then reduction of the acid functionality to give alcohol **51**, followed by consecutive mesylation/azidation to furnish the target azide **23**.

The alcohol substrate **51** (6.56 g, 17.90 mmol) was first converted *in situ* to a mesylate *via* $MsCl/NEt_3/CH_2Cl_2$ followed by a biphasic, S_N2-type azidation reaction with NaN_3, toluene, H_2O, and the phase transfer catalyst $(Bu)_4NBr$;[83] azide **23** was thus isolated in 83% yield over the two steps. Compounds **50**, **51** and **23** exhibited spectroscopic data that were in agreement with those values reported previously.[69, 82]

2.1.2.2 – Synthesis of azide 22

The synthesis of azide **22** from commercially available Fmoc-(D)-Lys(Boc)-OH (**52**) was achieved by carboxylic acid reduction[81] followed by mesylation and subsequent azidation/*N*-deprotection[84] (Scheme 2.4). Reduction of the starting acid **52** (4.00 g, 8.54 mmol) *via* a mixed anhydride reduction with isobutyl chloroformate, *N*-methylmorpholine and $NaBH_4$ gave alcohol **53** in 92% yield.

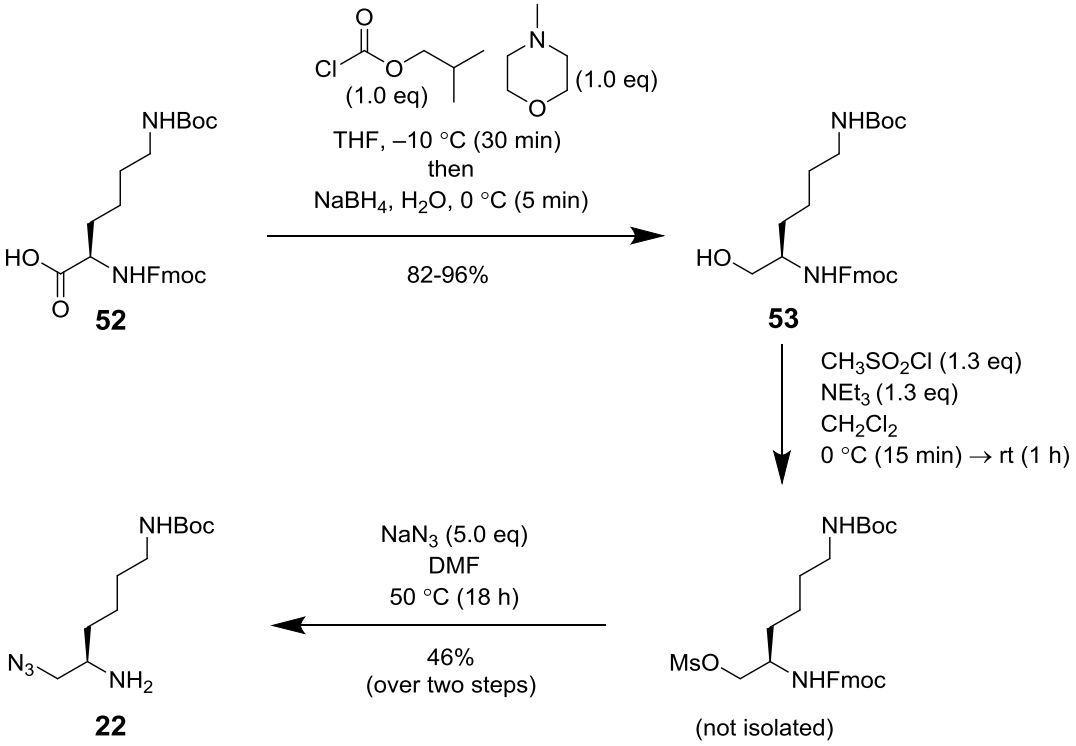

Scheme 2.4 – Synthesis of azide **22** from the lysine precursor **52**: reduction of the carboxylic acid functionality to give alcohol **53**, followed by mesylation and then sequential azidation/*N*-deprotection to furnish target azide **22**.

The intermediate alcohol **53** (100 mg, 0.22 mmol) was then subjected to mesylation with $MsCl/NEt_3/CH_2Cl_2$ followed by azidation and *N*-Fmoc deprotection[84] with NaN_3 in DMF at 50 °C to give the target azide **22** in 46% yield over two steps. It was assumed that the azidation of the mesylate intermediate occured rapidly followed by *N*-Fmoc deprotection with the excess NaN_3 acting as a base to promote the deprotection step (see Appendix A,

Schemes A1.5 and A1.7 for related mechanisms).[84] Compounds **53** and **22** exhibited spectroscopic data that were in agreement with those values reported previously.[59, 85]

2.1.2.3 – Synthesis of azide 24

The synthesis of azide **24** from commercially available H-(D)-Lys(Boc)-OH (**54**) was achieved by copper-catalysed diazotransfer reaction[86] with freshly prepared imidazole-1-sulfonyl azide[87-88] (Scheme 2.5). The diazotransfer reagent (imidazole-1-sulfonyl azide) was prepared in an EtOAc solution as previously described.[87] The EtOAc solution of imidazole-1-sulfonyl azide was stirred with amino acid **54** (2.20 g, 8.93 mmol) in the presence of $CuSO_4 \cdot 5H_2O$ and K_2CO_3 in MeOH at rt; the product α-azido acid **24** was thus furnished in 98% yield utilizing a modified work-up procedure.[87] The purification procedure was modified to eliminate flash chromatography in favour of an acid/base extraction purification with Et_2O. This modification allowed for a faster purification and isolation with less chemical waste. Compound **24** exhibited spectroscopic data that were in agreement with those values reported previously.[89-90]

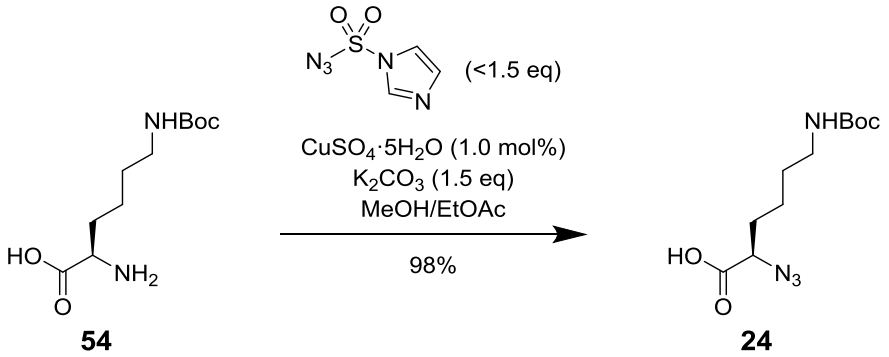

Scheme 2.5 – Synthesis of α-azido acid **24** from the lysine precursor **54** *via* diazotransfer reaction.

2.1.3 – Synthesis of arginine derivatives

2.1.3.1 – Synthesis of azide 26

The synthesis of the doubly *N*-protected azide **26** from commercially available Cbz-(D)-Arg(Pbf)-OH (**55**) was achieved by carboxylic acid reduction[81] followed by a two-step, one-pot mesylation/azidation procedure[82] (Scheme 2.6).

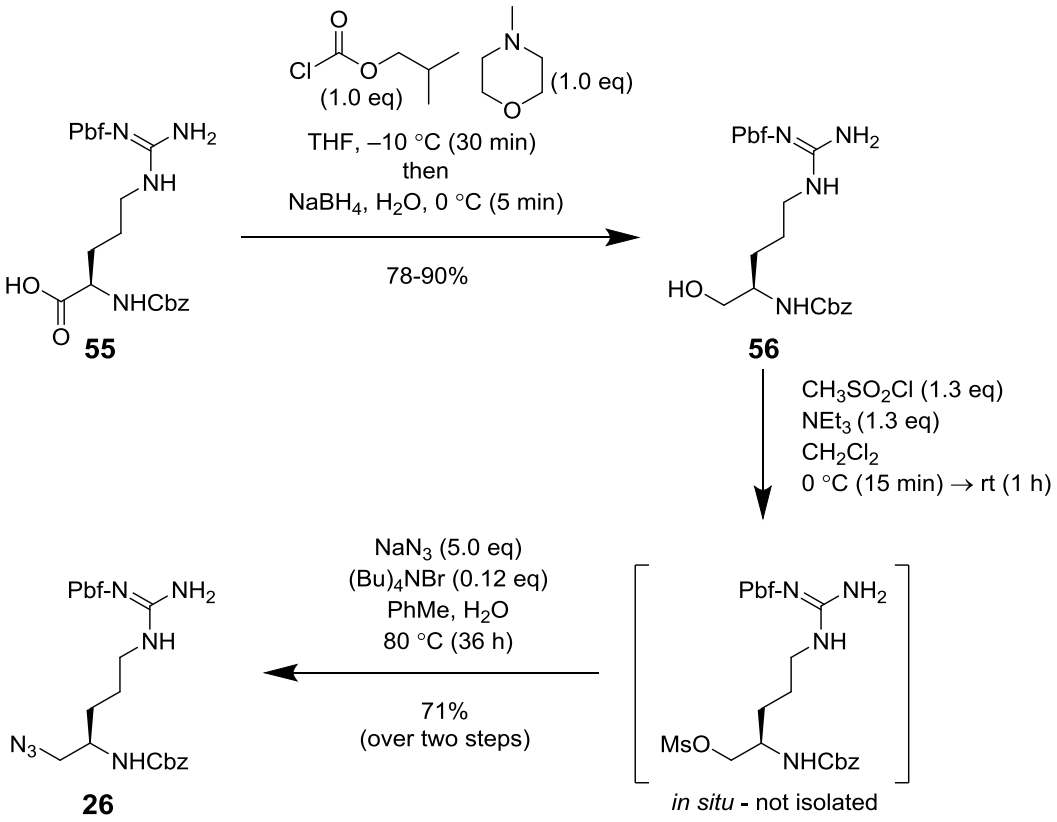

Scheme 2.6 – Synthesis of azide **26** from the arginine precursor **55**: reduction of the carboxylic acid functionality to give alcohol **56** followed by mesylation and then azidation to furnish target azide **26**.

The acid **55** (5.00 g, 8.92 mmol) was converted into a mixed carbonic-carboxylic anhydride by reaction with isobutyl chloroformate in the presence of *N*-methylmorpholine followed by reduction with aqueous $NaBH_4$ to give the desired alcohol (**56**) in 78% yield.

Evidence of the carbonyl reduction was seen in the ^1H NMR spectrum of compound **56** as a new multiplet resonance centred at δ 3.60. This multiplet integrated to three protons and it

was not present in the starting material **55.** Therefore, the multiplet was assigned to the newly installed methylene protons (-C$\underline{H}_2$OH) in conjunction with the adjacent methine proton (-C$\underline{H}$NHCbz). The methine assignment was confirmed by gCOSY correlation to the resonance at δ 5.62 (assigned as the carbamate proton (-N$\underline{H}$Cbz)).

Furthermore, this multiplet resonance displayed gHSQC correlations with two resonances (δ 64.8 and 52.8) in the ^{13}C NMR spectrum of compound **56 –** these resonances were assigned to the corresponding methylene carbon (-$\underline{C}$H$_2$OH) and methine (-$\underline{C}$HNHCbz) carbon, respectively. The molecular structure of compound **56** was verified by the presence of a peak at *m/z* 547.2589 in HRMS that was assigned to the protonated molecular ion $[M + H]^+$ (calculated for $C_{27}H_{39}N_4O_6S$ 547.2590). This intermediate alcohol was then subsequently utilized in the two-step, one-pot synthesis of azide **26**.

The alcohol substrate **56** (3.79 g, 6.94 mmol) was first converted *in situ* to a mesylate *via* MsCl/NEt$_3$/CH$_2$Cl$_2$ followed by a biphasic, S$_N$2-type azidation reaction with NaN$_3$, toluene, H$_2$O, and a phase transfer catalyst;[83] azide **26** was thus isolated in 71% yield over the two steps. The ^{1}H NMR spectrum of azide **26** displayed a 2H multiplet resonance at δ 3.31 which was assigned to the methylene protons (-C$\underline{H}_2$N$_3$) adjacent to the azide moiety; this assignment was confirmed by a gHSQC correlation with a ^{13}C NMR resonance at δ 54.9 (assigned as the corresponding methylene carbon) and by gCOSY correlation with a ^{1}H NMR resonance at δ 3.73 (assigned to the adjacent methine proton (-C$\underline{H}$NHCbz)).

Additionally, the multiplet resonance at δ 3.60 in the ^{1}H NMR spectrum of the starting alcohol **56** (assigned to the corresponding methylene protons (-C$\underline{H}_2$OH)) was no longer visible in the ^{1}H NMR spectrum of the product azide **26**. The resonance at δ 3.31 (assigned

to the methylene protons in the ^{1}H NMR spectrum of the azide) was shifted upfield (i.e. more shielded) relative to the signal at δ 3.60 (assigned to the corresponding methylene protons (-C<u>H</u>$_2$OH)) in the ^{1}H NMR spectrum of the starting alcohol **56** – this upfield shift is to be expected, given the greater deshielding effect of the alcohol group relative to the azide moiety. Analysis of the IR spectrum of azide **26** revealed a characteristic band at 2098 cm^{-1} that was assigned to the newly installed azide moiety. The molecular structure of compound **26** was verified by the presence of a peak at *m/z* 572.2677 in HRMS that was assigned to the protonated molecular ion $[M + H]^+$ (calcd for $C_{27}H_{38}N_7O_5S$ 572.2655).

2.1.3.2 – Synthesis of azide 25

The synthesis of β-azido-amine **25** from commercially available Fmoc-(D)-Arg(Pbf)-OH (**57**) was achieved by carboxylic acid reduction, iodination and subsequent azidation/*N*-deprotection (Scheme 2.7) as previously described.[59] Reduction of the starting acid **57** (4.00 g, 6.17 mmol) *via* a mixed anhydride reduction with isobutyl chloroformate, *N*-methylmorpholine and $NaBH_4$ gave alcohol **58** in 80% yield. The intermediate alcohol **58** (3.10 g, 4.88 mmol) was then subjected to iodination with I_2/PPh_3/imidazole in CH_2Cl_2 at rt followed by azidation and *N*-Fmoc deprotection[84] with NaN_3 in DMF to give the target azide **25** in 80% yield over two steps.

A modified procedure was developed to enhance the yield and reduce the labour required: the azidation and *N*-Fmoc deprotection were carried out independently by allowing the azidation to proceed at rt first before allowing the *N*-Fmoc deprotection reaction to occur by heating the reaction to 50 °C. This modification was introduced to prevent the observed oxazolidinone by-product from forming *via* S_N2 displacement of the iodide leaving group

with the carbamic anion produced during *N*-Fmoc removal (see Scheme A1.6 in Appendix A).

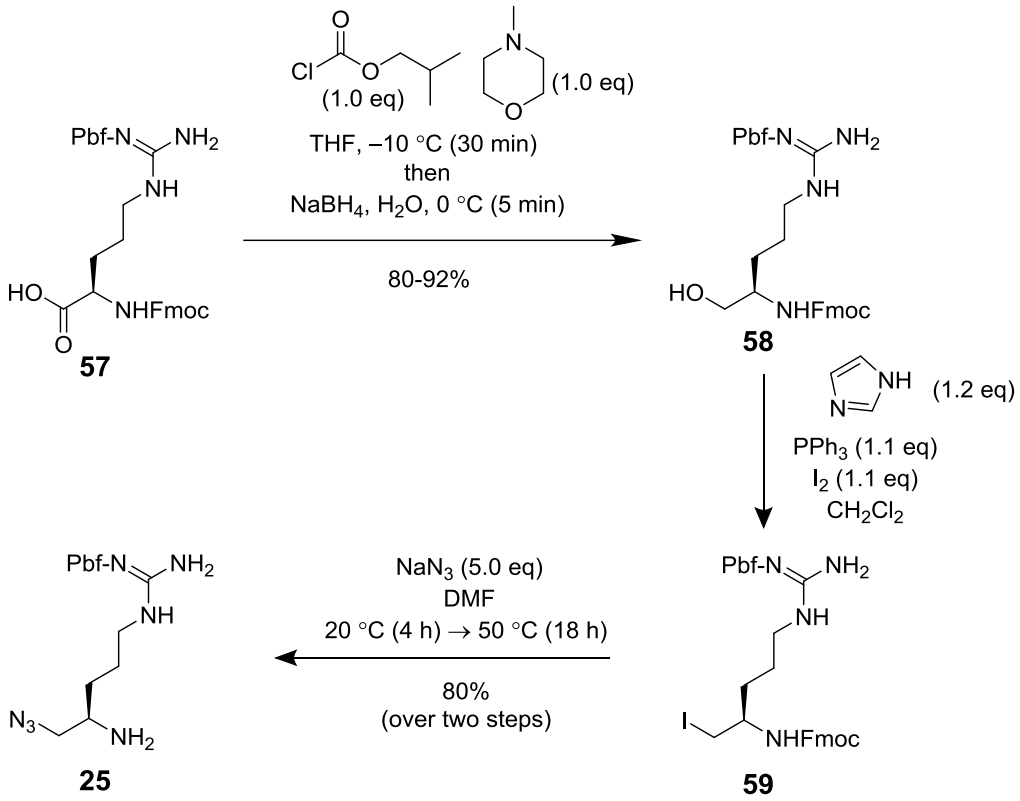

Scheme 2.7 – Synthesis of azide **25** from the arginine precursor **57**: reduction of the carboxylic acid functionality to give alcohol **58**, followed by iodination and then azidation/*N*-deprotection to furnish target azide **26.**

Furthermore, a traditional acid/base work-up procedure was utilized to purify the β-azido-amine product instead of flash chromatography. These modifications led to a substantially increased yield over the literature method (61%[59] to 80%) and significantly easier isolation procedure. Compounds **58** and **25** exhibited spectroscopic data that were in agreement with those values reported previously.[59]

2.1.3.3 – Synthesis of azide 27

The synthesis of azide **27** was achieved by a traditional *N*-Boc protection of β-azido-amine (**26**).[91] The substrate amine **25** (100 mg, 0.23 mmol) was reacted with Boc_2O in CH_2Cl_2 at rt for 2 h to give the target *N*-Boc amine **27** in 98% yield (Scheme 2.8).

The ^{1}H NMR spectrum of compound **27** displayed a prominent singlet resonance at δ 1.43 that was not found in the ^{1}H NMR spectrum of the starting material **25**; this 9H singlet was assigned to the newly introduced *t*-butyl protons (-C(C<u>H</u>$_3$)$_3$).

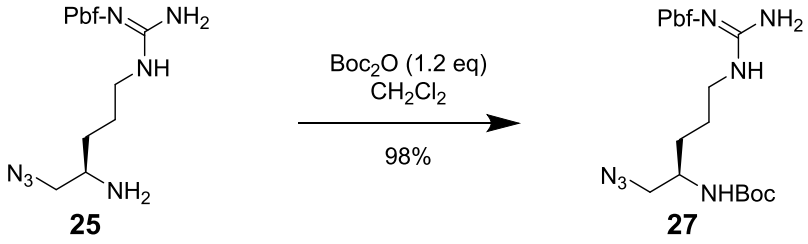

Scheme 2.8 – Synthesis of azide **27** from β-azido-amine **25** *via N*-Boc protection.

The installation of the *N*-Boc protecting group was further confirmed by the appearance of a new ^{13}C NMR resonance at δ 156.1 which was assigned as the new carbamate carbon (C=O). The presence of the *N*-Boc protecting group was further confirmed by the new ^{1}H NMR resonance at δ 4.89 (assigned as the -N<u>H</u>Boc proton) – this broad doublet resonance was not present in the starting β-azido-amine **25** and this resonance displayed coupling by gCOSY correlation with the resonance at δ 3.69 (which was assigned to the adjacent methine proton). The molecular structure of compound **27** was verified by the presence of a peak at *m/z* 538.2811 in the HRMS that was assigned to the protonated molecular ion $[M + H]^+$ (calcd for $C_{24}H_{40}N_7O_5S$ 538.2812).

2.1.3.4 – Synthesis of azide 28

The synthesis of azide **28** from commercially available H-(D)-Arg(Pbf)-OH (**60**) was achieved by copper-catalysed diazotransfer reaction[86] with imidazole-1-sulfonyl azide[87-88] (Scheme 2.9). The EtOAc solution of imidazole-1-sulfonyl azide was then stirred with precursor **60** (2.00 g, 4.69 mmol) in the presence of $CuSO_4 \cdot 5H_2O$ and K_2CO_3 in MeOH at rt; the product α-azido-acid **28** was thus furnished in 83% yield.[87] The purification procedure was modified to eliminate flash chromatography in favour of an acid/base isolation work-up with Et_2O. Compound **28** exhibited spectroscopic data that were in agreement with those values reported previously.[92]

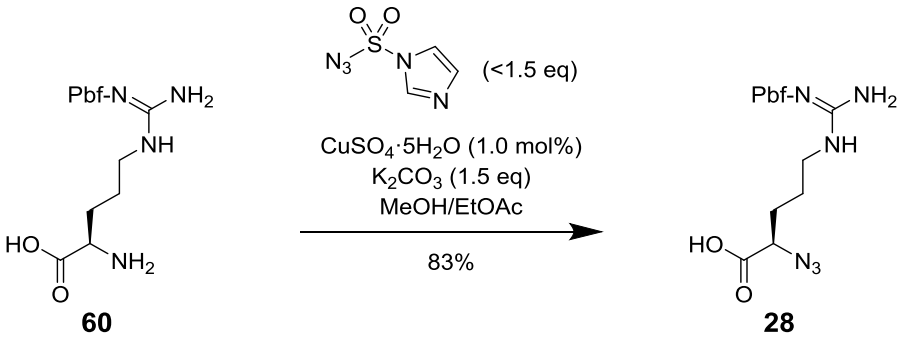

Scheme 2.9 – Synthesis of α-azido-acid **28** from the arginine precursor **60** *via* diazotransfer reaction.

2.1.3.5 – Synthesis of amine 29

The synthesis of amine **29** from commercially available Fmoc-(D)-Arg(Pbf)-OH (**61**) was achieved by esterification followed by base-promoted *N*-Fmoc deprotection (Scheme 2.10).[59, 79, 91] The starting compound **61** (1.00 g, 1.54 mmol) in MeOH was treated with $SOCl_2$ to afford an intermediate methyl ester (i.e. Fmoc-(D)-Arg(Pbf)-OMe) – this ester was then stirred with piperidine in MeOH at rt to furnish the target amine **29** in 80% yield over two steps. Compound **29** exhibited spectroscopic data that were in agreement with those previously reported.[59]

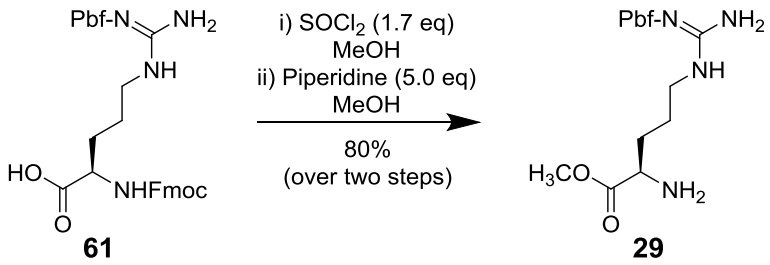

Scheme 2.10 – Synthesis of amine **29** from the arginine precursor **61**: esterification followed by base-promoted *N*-Fmoc deprotection.

2.2 – Series A synthesis: scaffolds and derivatives

2.2.1 – <u>Synthesis of monocationic derivatives (Series A1)</u>

2.2.1.1 – Synthesis of Series A1 scaffolds *via* CuAAC and *N*-deprotection

2.2.1.1.1 – 1,2,3-Triazole formation *via* a 'click reaction'

The synthesis and incorporation of 1,4-disubstituted-1,2,3-triazole rings in novel pharmaceuticals has become an extremely widespread practice and the common 'click reaction' (i.e. a Cu-catalysed azide-alkyne cycloaddition (CuAAC)) has become the most reliable methodology for the formation of these moieties.[73-75, 93-94] Therefore, formation of the key scaffold intermediates **62a-d** (Scheme 2.11) was realized *via* CuAAC reactions.

For example, scaffold **62a** was achieved by following **General Procedure A** (Section 6.2), wherein azide **23** (1.50 g, 3.83 mmol) and alkyne **21** (2.0 eq) were treated with Cu(II)/ascorbate in *t*-BuOH/H_2O[59, 75] for 48 h at rt to give a 75% yield of compound **62a** after purification by flash chromatography. Furthermore, this reaction methodology was effective on a larger scale, as an 88% yield of **62a** was obtained from 2.64 g (6.74 mmol) of precursor azide **23**.

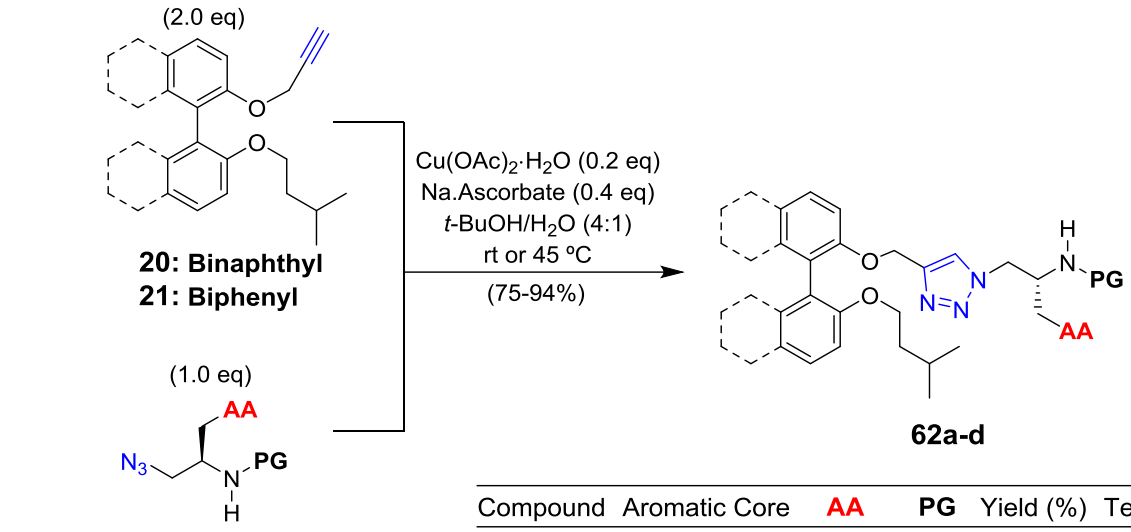

23: **AA** = **Lys(Boc)** = NHBoc
PG = Cbz

26: **AA** = **Arg(Pbf)** =
PG = Cbz

27: **AA** = **Arg(Pbf)** =
PG = Boc

Compound	Aromatic Core	AA	PG	Yield (%)	Temp.
62a	**Biphenyl**	**Lys(Boc)**	**Cbz**	75-88	rt
62b	**Biphenyl**	**Arg(Pbf)**	**Cbz**	82	rt
62c[a]	**Binaphthyl**	**Lys(Boc)**	**Cbz**	84	45 °C
62d	**Binaphthyl**	**Arg(Pbf)**	**Boc**[b]	94	45 °C

[a] Compound **62c** synthesized during previous research.[69]
[b] *N*-Cbz analogue made in 96% yield with same conditions.

Scheme 2.11 - Cu-catalysed [3 + 2] cycloaddition reactions between an alkyne building block (**20** or **21** - blue triple bond) and an azide precursor (**23, 26** or **27** - blue portion) to give the key scaffold intermediates **62a-d** for Series A1.

The ^{1}H NMR spectrum of compound **62a** displayed resonances that corresponded to fragments from both starting materials (alkyne **21** and azide **23**) – see Appendix C (Figures C1.1 and C1.2) for the NMR spectra. The most noteworthy and diagnostic difference was the disappearance of the ^{1}H NMR singlet resonance at δ 2.43 (-C≡C-H) that was seen in the ^{1}H NMR spectrum of alkyne **21** and the appearance of a significantly more downfield resonance at δ 7.17 (triazole CH) in the ^{1}H NMR spectrum of **62a**. This significant difference in chemical shift was indicative of triazole formation; the terminal alkyne proton in compound **21** had now become the lone proton on the newly formed aromatic triazole ring – this results in a strong deshielding of the proton (relative to the alkyne proton) and results in a large

downfield chemical shift. Two unique aromatic ^{13}C NMR resonances at δ 145.2 and 123.3 were present in the ^{13}C NMR spectrum of compound **62a** and they were assigned to the methine and quaternary triazole carbons, respectively. The resonance at δ 145.2 was extremely diagnostic because few other aromatic carbon resonances appear in that region (i.e. δ 141-150). As expected, the ^{13}C NMR resonance at δ 123.3 (triazole CH) displayed a correlation in the gHSQC spectrum with the ^{1}H NMR resonance at δ 7.17 (triazole CH). Furthermore, the appearance of these two unique ^{13}C NMR resonances coincided with the disappearance of the two alkyne (-C≡C-) ^{13}C NMR resonances at δ 79.3 and 75.2 that are evident in the ^{13}C NMR spectrum of starting alkyne **21**. These two alkyne carbons (-C≡C-) had now become the aromatic triazole carbons – this explains the associated large downfield chemical shifts. HRMS analysis confirmed the molecular identity, as a peak was observed at *m*/*z* 708.3755 that was assigned to the sodiated molecular ion, $[M + Na]^+$ (calcd for $C_{39}H_{51}N_5O_6Na$ 708.3737).

Scaffold intermediates **62a-d** (Scheme 2.11) were obtained by implementation of the aforementioned **General Procedure A**. Evidence for the regioselective outcome of the 1,2,3-triazole formation (i.e. solely the 1,4-isomer and not the 1,5-isomer) was established for the scaffold amine (i.e. the N^{α}-deprotected derivative) of **62a** (i.e. compound **63a**) *via* analysis of the relevant gHMBC spectrum; this evidence is discussed in Section 4.2.

The CuAAC reaction requires the presence of a catalytic quantity of Cu(I); this catalyst can be added directly or prepared *in situ* by reduction of a Cu(II) salt with an excess of an antioxidant[75] (e.g. single electron transfer by sodium ascorbate – Scheme 2.12). The latter method is generally preferred, as the presence of an excess amount of reducing agent (relative

to the catalyst) prevents the disproportionation or oxidation of the active catalytic species (i.e. Cu(I)) to the inactive Cu(II) species.[75, 93-94] Most importantly, this allows the reaction to be successfully conducted under open-air conditions without the need for an inert atmosphere.

The regioselective construction of the 1,4-disubstituted-1,2,3-triazole is controlled by the relative binding orientation of the alkyne and azide precursors to the active Cu(I) catalyst complex (Scheme 2.12). The coordination of the primary azide nitrogen to the terminal Cu-acetylide complex restricts the orientation of the resultant [3 + 2]-cycloaddition (Scheme 2.12 – transition state) so that only the 1,4-regioisomer is produced.[75, 93-94] This regioselectivity occurs because the two substituents are forcibly oriented in opposite directions during the catalysed cycloaddition.

The proposed mechanism in Scheme 2.12 represents the currently accepted CuAAC catalysis model, based upon multiple CuAAC studies such as kinetic analysis and DFT calculations.[75, 93-96] Kinetic analysis has found that the reaction is 2nd order with respect to the concentration of Cu(I); this implicates the likely role of a di-nuclear acetylide-bridged Cu(I) complex as the active catalytic species,[93-94] as illustrated in the transition state complex in Scheme 2.12. Furthermore, experimental evidence for the involvement of alkynyl dicopper(I) complexes in the CuAAC reaction has been published.[93, 97] Importantly, the mild catalytic conditions required for the CuAAC reaction allowed for reliable, clean and high-yielding installation of a 1,4-disubstituted-1,2,3-triazoles during scaffold synthesis.

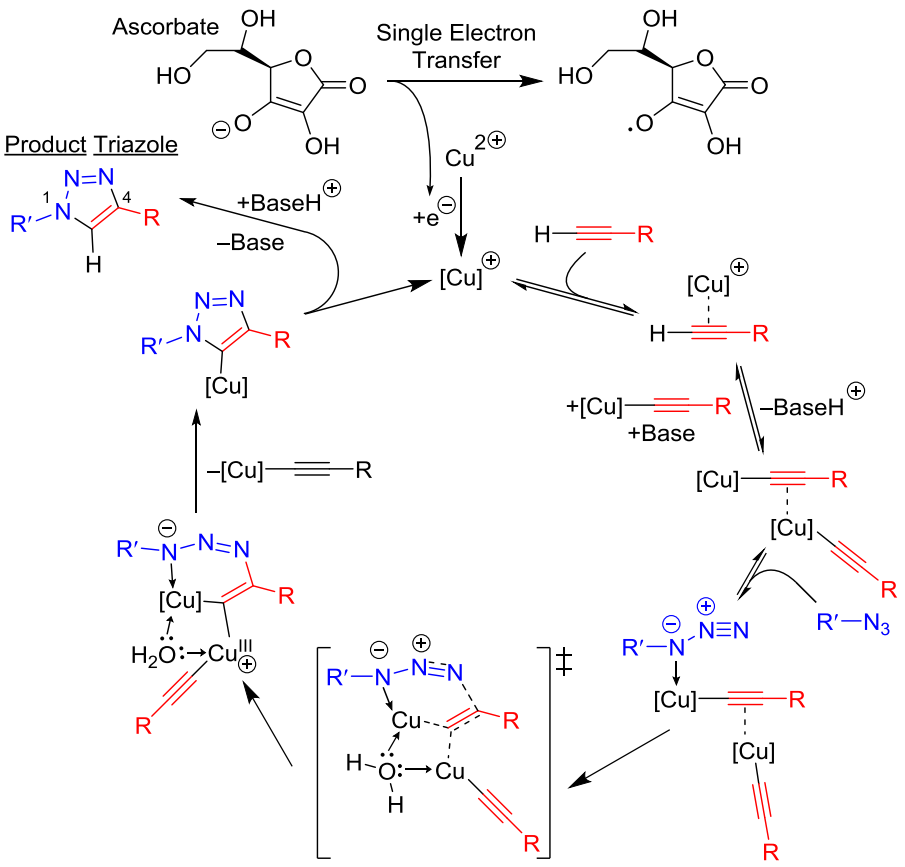

Scheme 2.12 – Proposed catalytic cycle for the CuACC reaction:[75, 93, 95-96] [Cu] represents a Cu(I) complex that is coordinated to the requisite number of ancillary ligands. The mechanism allows for control over the regioselectivity of the cycloaddition by restricting the relative orientation of the 1,4-substituents.

2.2.1.1.2 – *N*-deprotection: Cbz or Boc removal

Removal of the *N*-Cbz protecting group can be achieved through a variety of reaction conditions; the most common methodologies are catalytic hydrogenolysis (e.g. Pd/C and H_2 gas) and acid-promoted nucleophilic cleavage (e.g. HBr/AcOH).[78, 80] To avoid deprotection of the acid-labile Boc group, scaffold intermediate **62a** (1.90 g, 2.77 mmol) was subjected to catalytic hydrogenolysis, by reaction with 10% w/w palladium-on-carbon (Pd-C – 0.15 eq) in a mixture of MeOH/AcOH under an atmosphere of H_2 gas (*via* a balloon attached to the reaction flask), furnishing a 99% yield of scaffold amine **63a** (Scheme 2.13).

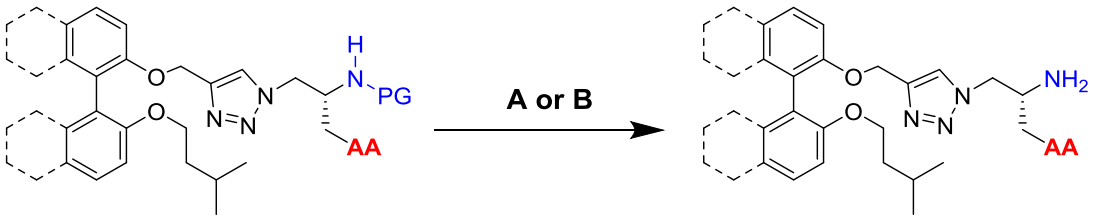

62a-d **63a-d**

Lys(Boc) = NHBoc

Arg(Pbf) = H N NH2 N Pbf

Compound	Aromatic Core	AA	PG (Removed)	Yield (%)	Rxn
63a	**Biphenyl**	**Lys(Boc)**	**Cbz**	99	**A**
63b	**Biphenyl**	**Arg(Pbf)**	**Cbz**	92	**A**
63c[a]	**Binaphthyl**	**Lys(Boc)**	**Cbz**	98	**A**
63d	**Binaphthyl**	**Arg(Pbf)**	**Boc**	95	**B**

A) 10% Pd-C (0.15 eq), H_2 (1 atm), AcOH (20.0 eq), MeOH, rt, 24 h
B) HCl (20.0 eq), MeOH, rt, 18 h

[a] Compound **63c** synthesized during previous research.[69]

Scheme 2.13 – Removal of the *N*-protecting group from intermediates **62a-d** to give scaffold amines **63a-d**: *N*-Cbz removal by catalytic hydrogenolysis (**A**) or *N*-Boc removal by acidolytic cleavage (**B**).

Analysis of the ^{1}H NMR spectrum of amine **63a** revealed the lack of key *N*-Cbz diagnostic resonances at δ 5.06 (-C$\underline{H}_2$Ph) and 7.21 – 7.38 (phenyl) that were present in the spectrum of scaffold intermediate **62a**. The removal of the *N*-Cbz protecting group was further supported by the lack of the characteristic downfield resonance at δ 66.9 (-O$\underline{C}H_2$Ph) normally seen in the ^{13}C NMR spectrum of starting compound **62a**. Furthermore, the disappearance of an additional four aromatic ^{13}C NMR resonances (i.e. the phenyl carbons) provided substantial evidence of *N*-Cbz removal.

TLC analysis of the product compound (**63a**) revealed a more polar compound has been produced and a strong purple colour after staining with ninhydrin confirmed the presence of a free amine. The product identity was confirmed via HRMS analysis; a peak observed at *m*/*z*

552.3564 was assigned to the protonated molecular ion, $[M + H]^+$ (calcd for $C_{31}H_{46}N_5O_4$ 552.3550).

Scaffold amines **63b** and **63c** (Scheme 2.13) were also achieved by implementation of the aforementioned catalytic hydrogenolysis procedure. Attempts to isolate scaffold amine **63d** through the same methodology (i.e. *N*-Cbz removal *via* catalytic hydrogenolysis) failed due to the occurrence of multiple amine by-products (as confirmed by TLC and NMR analysis). The most prevalent by-product exhibited a peak in the LRMS with an *m/z* value that was 28 amu heavier than that of the protonated molecular ion for the desired product (**63d**). With longer reactions times (> 24 h), notably larger quantities of this by-product were observed – these impurities could not be separated by flash chromatography or by recrystallization. In an attempt to solve these issues, the *N*-Boc protecting group was utilized as it would likely allow acidolytic cleavage in the presence of a side-chain *N*-Pbf protecting group. The arginine side-chain protecting group (*N*-Pbf) requires a strong acid for deprotection (e.g. TFA) and hydrogen-bonding solvents like MeOH, EtOH and H_2O are known to suppress the acidolytic *N*-Pbf deprotection reaction.[98-99] Therefore, reaction conditions employing 1.0 M HCl in MeOH/Et_2O were utilized to successfully remove the *N*-Boc group from compound **62d** (113 mg, 0.12 mmol) without cleaving the *N*-Pbf side chain protecting group; a 95% yield of scaffold amine **63d** was realized after 18 h at rt. See Section 2.2.1.2 for more information regarding *N*-Boc deprotection (i.e. mechanism and reaction details).

MeOH is one of the most effective and widely used solvents for catalytic hydrogenolysis of the *N*-Cbz protecting group and the addition of acetic acid is helpful for protonation of the resultant amine product; this prevents coordination of the free amine to the palladium which can cause inactivation of the catalyst.[100-102] Ideally, the only by-products produced are

volatile (i.e. CO_2 and toluene) which makes for an extremely clean reaction and work-up. Benzyl carbamates (i.e. *N*-Cbz groups) are readily cleaved *via* Pd-catalysed hydrogenolysis due to their highly activated benzylic position and their ability to coordinate to the Pd catalyst through either aryl or oxygen coordination.[101] The mechanism for catalytic hydrogenolysis of benzyl carbamates has not been completely elucidated, but certain key steps are understood.[100] The most important and least understood step in the mechanism is the heterolysis of the benzylic C–O bond (Scheme 2.14– red bond scission); this essential step is thought to occur in a manner similar to the deprotection of *O*-benzyl or *N*-benzyl substituents,[100] i.e. through coordination of the Cbz functionality to the Pd surface, followed by hydrogenolytic cleavage of the C–O bond which generates the unstable carbamic acid derivative and toluene (Scheme 2.14).

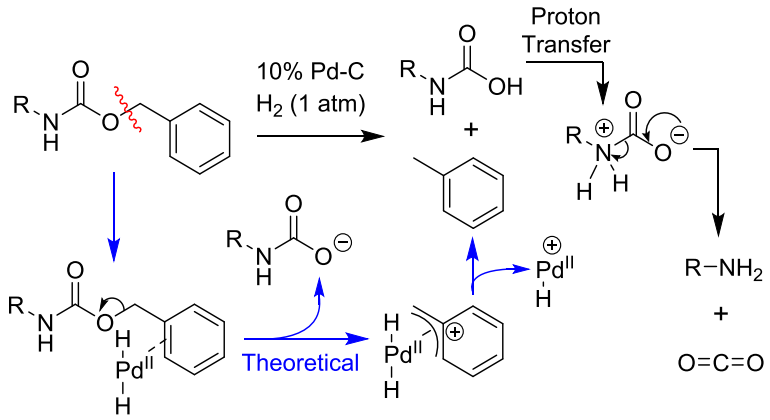

Scheme 2.14 – Known aspects of the Pd-catalysed hydrogenolysis of benzyl carbamates (black arrows) with the theoretical heterolysis mechanism (blue arrows).

Following proton transfer, the carbamic acid derivative readily decomposes to give CO_2 and the desired free amine.[78] One proposed mechanism for the heterolysis step involves Pd^{II}-π aryl electron coordination followed by formation of a η^3-Pd^{II}-benzyl cation complex with concomitant displacement of the carbamate anion (Scheme 2.14 – blue pathway).

2.2.1.2 – Synthesis of Series A1 derivatives *via* amide coupling and *N*-deprotection

The derivatization of mono-amino acid scaffolds required a two-step transformation: installation of the terminal amide moieties followed by side-chain *N*-deprotection to yield the target amines as hydrochloride salts. Previous syntheses of the binaphthylpeptides have utilized the common EDCI/HOBt[†] peptide coupling reagent system to form the necessary peptide bonds while *N*-Boc and/or *N*-Pbf deprotection was previously achieved with TFA/CH_2Cl_2.[59, 64-66, 68-69]

The formation of amide bonds from carboxylic acids and amines (e.g. amino acid derivatives) *via* peptide coupling was an extremely crucial component in the synthesis of the target biarylpeptide derivatives. Therefore, a general amide coupling procedure (**General Procedure B –** Section 6.2) with literature precedent[59] was developed and utilized in all subsequent amide coupling reactions.

The acidolytic cleavage of the *N*-Boc and/or *N*-Pbf protecting groups is easily achieved with a variety of acids – with trifluoroacetic acid (TFA) being used most often.[77, 103] The ability of these two protecting groups to be cleaved independently or simultaneously by relatively mild acidic conditions was an essential feature to this general reaction. As such, a general *N*-deprotection reaction procedure (**General Procedure C –** Section 6.2) was developed by modifying the previously published procedure[59, 66] and employed for the final deprotection of most *N*-Boc and *N*-Pbf protected side chain residues. The mono-lysine derivatives, from both Series A and B, exhibited increased solubility relative to the arginine derivatives and a

[†] Structures for EDCI and HOBt can be found in the amide coupling mechanism in Scheme 2.21 in Section 2.2.2.

modified work-up procedure for the *N*-deprotection reaction (i.e. **General Procedure D**, Section 6.2) was required to enable precipitation of the final hydrochloride salts.

Therefore, for Series A1 derivatives, **General Procedure B** was utilized to install the terminal amide moiety (see Reaction (i) in Schemes 2.15 – 2.17); the resultant *N*-protected amide derivatives were then immediately subjected to acidolytic *N*-Boc or *N*-Pbf cleavage followed by work-up with ethereal HCl (**General Procedure C** or **D**: Reaction (ii) in Schemes 2.15 – 2.17) to achieve the target amine salts (**64a-b**, **65a-b** and **66a-b**).

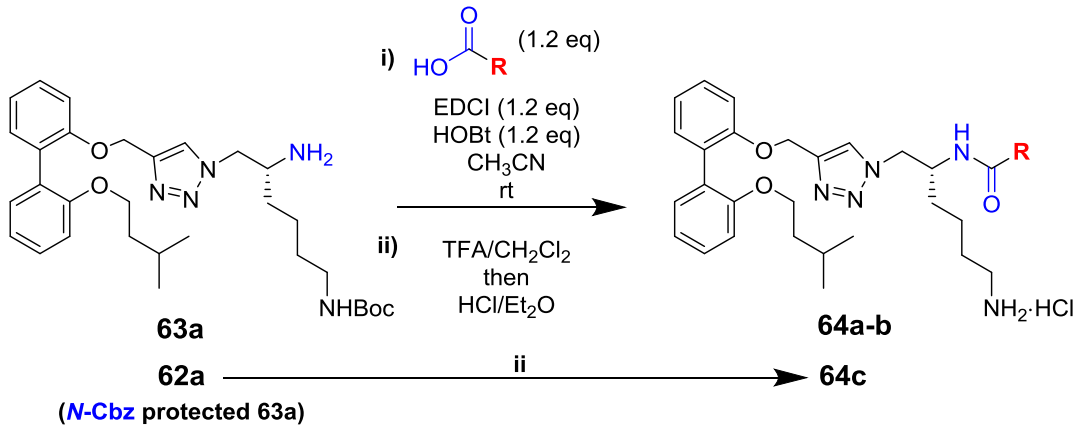

Compound	R	Yield (%)[a]
64a	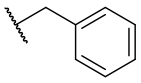	96
64b	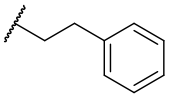	93
64c	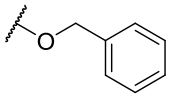	93[b]

[a] Yields are reported over two steps from **63a**
[b] Synthesised in one step from **62a**

Scheme 2.15 – Derivatization of scaffold **63a**: installation of the terminal amide moiety (**R**) followed by removal of the *N*-Boc side chain protecting group to give scaffold derivatives **64a-b** as hydrochloride salts. The synthetic pathway to realize compound **64c** from *N*-Cbz protected scaffold precursor **62a** is also displayed.

Target amines **64c**, **65c** and **66c** were realized directly from scaffold intermediates **62a**, **62b** and the *N*-Cbz analogue of **62d** (respectively) *via N*-Boc or *N*-Pbf deprotection following **General Procedure C** or **General Procedure D**.

Importantly, yields of the final derivatives were undertaken over a two-step process. Reaction completion and product purity of the intermediate *N*-protected amides were monitored by TLC and/or MS analysis prior to subsequent *N*-deprotection. This methodology reduced the number of novel compounds that required extensive characterization, which allowed for facile and efficient derivatization of the scaffolds.

For example, the synthesis of derivative **64a** (Scheme 2.15) was realized in 96% yield over two steps from scaffold amine **63a** (50 mg, 0.09 mmol) by reaction with phenylacetic acid (1.2 eq), EDCI and HOBt in acetonitrile at rt for 24 h to give the corresponding amide which was immediately subjected to *N*-Boc deprotection with TFA in CH_2Cl_2 at rt for 18 h followed by work-up with ethereal HCl.

The ^{1}H NMR spectrum of derivative **64a** displayed a new singlet resonance at δ 3.38 (-C$\underline{H}_2$Ph) and a broad multiplet resonance at δ 7.36 – 7.10 (phenyl). These new ^{1}H NMR resonances support the installation of the terminal benzyl amide in compound **64a**. The presence of the new amide moiety was further confirmed by the following ^{13}C NMR resonances assignments: δ 174.3 (amide $\underline{C}$=O), four resonances in the aromatic region (phenyl carbons) and δ 44.1 (-$\underline{C}H_2$Ph) – these resonances were not seen in the ^{13}C NMR spectrum of the starting amine **63a**. Evidence of *N*-Boc deprotection was clearly seen by the lack of the 9H singlet resonance at δ 1.44 in the ^{1}H NMR spectrum of amine salt **64a** – whereas this *N*-Boc resonance was present in the protected starting amine **63a**. Additionally,

the lack of key *N*-Boc resonances at δ 156.0 (Boc C=O), 79.2 (-C(CH$_3$)$_3$) and 28.5 (-C(CH$_3$)$_3$) in the ^{13}C NMR spectrum of compound **64a** provided further evidence that the *N*-Boc protecting group had been successfully removed. The molecular structure of the product was verified by the appearance of a peak at *m*/*z* 570.3451 in the HRMS that was assigned to the protonated molecular ion, $[M + H]^+$ (calcd for $C_{34}H_{44}N_5O_3$ 570.3444).

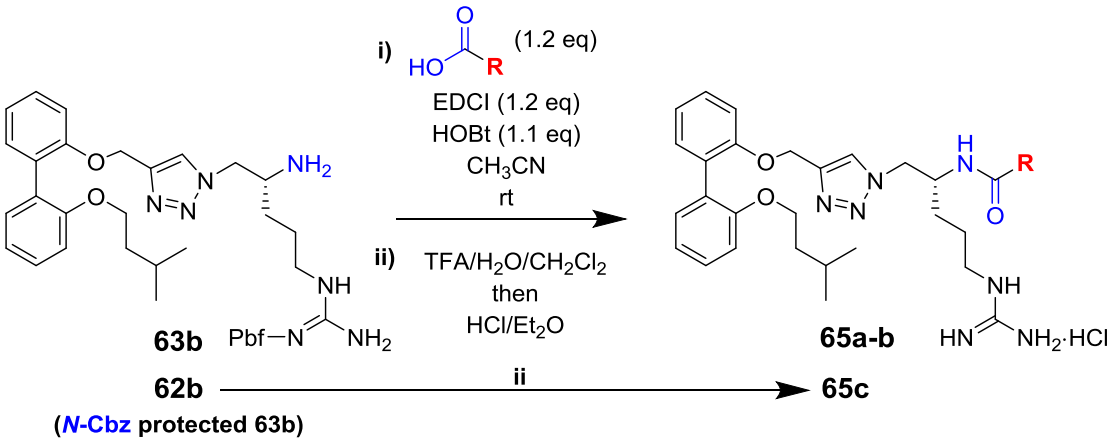

Compound	R	Yield (%)[a]
65a	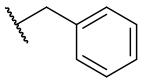	84
65b	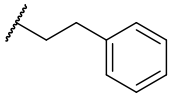	95
65c	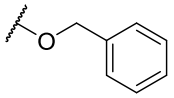	87[b]

[a] Yields are reported over two steps from **63b**
[b] Synthesised in one step from **62b**

Scheme 2.16 – Derivatization of scaffold **63b**: installation of the terminal amide moiety (**R**) followed by removal of the *N*-Pbf side chain protecting group to give scaffold derivatives **65a-b** as hydrochloride salts. The synthetic pathway to realize compound **65c** from the *N*-Cbz protected scaffold precursor **62b** is also displayed.

In another example, the synthesis of derivative **65a** (Scheme 2.16) was realized in 84% yield over two steps from scaffold amine **62b** (50 mg, 0.09 mmol) by a coupling reaction with phenylacetic acid (1.2 eq), EDCI and HOBt in acetonitrile at rt for 24 h to give the

corresponding amide which was immediately subjected to *N*-Pbf deprotection with TFA and H_2O in CH_2Cl_2 at rt for 18 h followed by work-up with ethereal HCl.

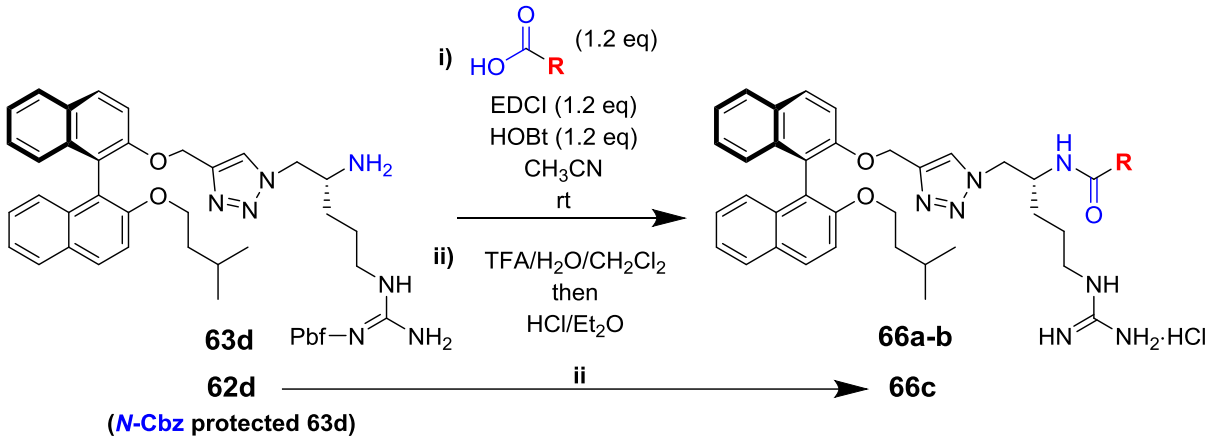

Compound	R	Yield (%)[a]
66a	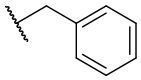	86
66b	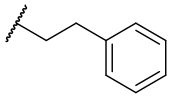	89
66c	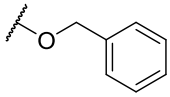	96[b]

[a] Yields are reported over two steps from **63d**
[b] Synthesised in one step from **62d**

Scheme 2.17 – Derivatization of scaffold **63d**: installation of the terminal amide moiety (**R**) followed by removal of the *N*-Pbf side chain protecting group to give scaffold derivatives **66a-b** as hydrochloride salts. The synthetic pathway to realize compound **66c** from the *N*-Cbz protected scaffold precursor **62d** is also displayed.

The ^{1}H NMR spectrum of the final derivative **65a** displayed resonances that were characteristic of the new terminal amide moiety (i.e. δ 3.33 (-C$\underline{H}_2$Ph) and 7.35 – 7.08 (phenyl)). Evidence of *N*-Pbf deprotection was clearly seen by the lack of the five characteristic singlet resonances (δ 2.92, 2.56, 2.47, 2.06 and 1.43) in the ^{1}H NMR spectrum of compound **65a** – these resonances were present in the ^{1}H NMR spectrum of starting amine **63b** and were assigned to the protons of the *N*-Pbf protecting group. Additionally, the lack

of six distinct quaternary aromatic resonances in the ^{13}C NMR spectrum of compound **65a** provided further evidence for the removal of the *N*-Pbf protecting group. Six key non-aromatic *N*-Pbf resonances at δ 86.5 (-$\underline{C}(CH_3)_3$), 43.4 ($ArCH_2$-), 28.7 (-C($\underline{C}H_3)_2$) and 19.4, 18.1 and 12.6 (3 x $ArCH_3$) in the ^{13}C NMR spectrum of starting amine **63b** were also missing from the ^{13}C NMR spectrum of final compound **65a**, further proving the successful removal of the *N*-Pbf protecting group. The molecular structure of the product was verified by the appearance of a peak at *m*/*z* 598.3510 in the HRMS that was assigned to the protonated molecular ion, $[M + H]^+$ (calcd for $C_{34}H_{44}N_7O_3$ 598.3506).

Modifications to the previous published procedure[66] included reporting the synthetic yield over two steps for facile and efficient derivatization and the incorporation of a more recent published extractive aqueous work-up[59] followed by flash chromatography (only when required) for the peptide coupling reaction. This vastly improved derivatization and purification procedure allowed for the rapid turn-over of multiple derivatives simultaneously, obviating the need for extensive flash chromatography for the majority of derivatization reactions.

The most important modification to the *N*-deprotection procedure was the incorporation of 20 equivalents of water to all *N*-Pbf deprotection reactions. This modification was introduced after large quantities of *N*-sulfonation by-products were observed (by NMR and HPLC – See Figures A2.2 and A2.3 in Appendix A) during synthetic scale-up for *in vivo* murine models. During small scale (≤ 0.10 mmol) synthesis, enough H_2O/moisture was present in the TFA and on the flask walls to adequately scavenge the SO_3 by-product produced during *N*-Pbf deprotection (see Scheme 2.19). During larger scale (> 1.00 mmol) synthesis, there was insufficient water present and *N*-sulfonation of the desired deprotected product would

occur.[104] Therefore, it was theorized that a small volume but sufficient molar excess (20.0 eq) of H_2O would prevent *N*-sulfonation by reacting with the SO_3 to produce H_2SO_4; the overall volume percentage of H_2O was kept down to prevent inhibition of the *N*-Pbf deprotection reaction.[98] Thioanisole is traditionally used to scavenge the SO_3[104] and promote deprotection,[105] but H_2O was found to be a cost-effective, clean and safe alternative for these reactions conditions.

The *N*-Boc protecting group is extremely susceptible to acidic conditions; TFA has been observed to fully deprotect the *N*-Boc side chain residue in less than 10 min. Deprotection of the *N*-Boc carbamate gives rise to the amine product (as the TFA salt) and two volatile by-products: CO_2 and isobutene (Scheme 2.18).[78] The acidolytic cleavage mechanism proceeds *via* protonation of the carbamate oxygen followed by heterolytic cleavage of the O–C$(CH_3)_3$ bond to release the carbamic acid intermediate and the stable *t*-butyl carbocation (Scheme 2.18); it is the stability of the resultant carbocation that makes the Boc carbamate susceptible to acidolysis. Proton transfer allows for spontaneous decomposition of the deprotonated carbamic acid derivative to give CO_2 and the free amine product (which rapidly protonates upon reaction with excess TFA); the *t*-butyl carbocation undergoes proton abstraction to give isobutene as a by-product.[78]

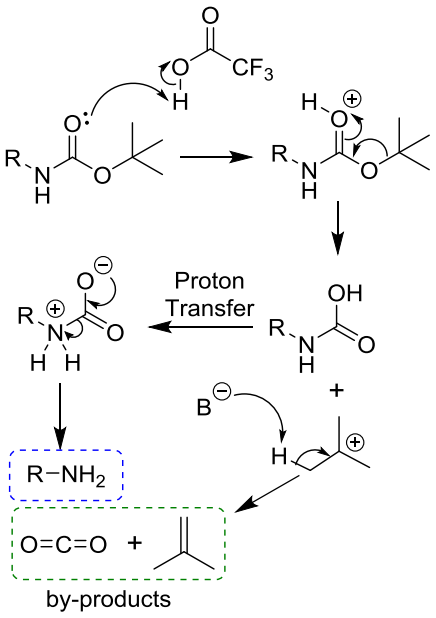

Scheme 2.18 – Mechanism of *t*-butyl carbamate acidolysis by TFA to give the desired amine (blue) and by-products (green).

The *N*-Pbf protecting group is more resistant to acidolytic cleavage than the *N*-Boc group and less amenable to synthesis because it requires notably longer reaction times and side reactions are possible, if a SO_3 scavenger is not utilized.[105] The mechanism for acidolysis (Scheme 2.19) proceeds *via* protonation of the guanidino residue followed by heterolytic cleavage of the N–S bond to give the product guanidine (as its TFA salt) and an arylsulphonyl cation.[103, 105-106]

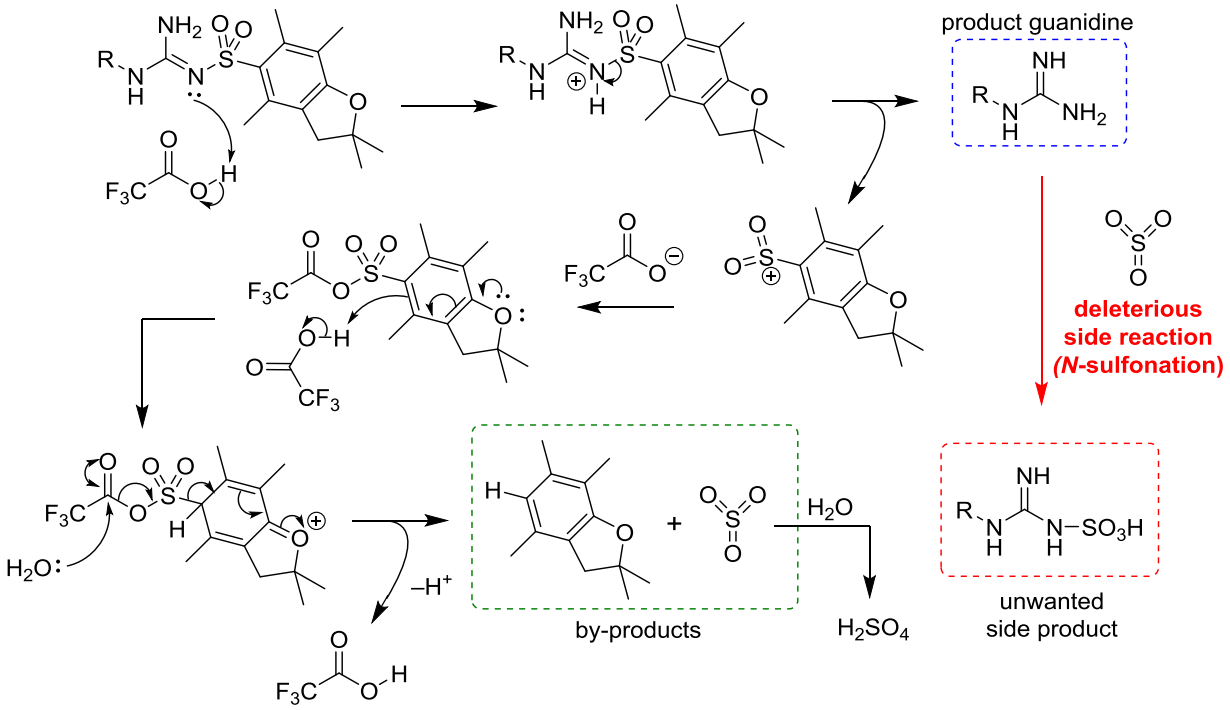

Scheme 2.19 – Mechanism for the acidolysis of an *N*-Pbf group to give the product guanidine (blue) and by-products (green). *N*-Sulfonation of the product guanidine (side reaction - red arrow) and scavenging of the SO_3 (green arrow) are also shown.

The ability of the *N*-Pbf group to undergo acidolysis relies on the ability of the arylsulphonyl group to stabilize the resulting cation.[105-106] The arylsulphonyl cation then combines with the trifluoroacetate anion to generate an intermediate – subsequent protonation and H_2O attack causes decomposition to give 2,2,4,6,7-pentamethyldihydrobenzo[*b*]furan, TFA, and SO_3. The resultant SO_3 by-product is electrophilic and will combine with the free guanidine

product to give sulfamic acid derivative by-products,[104] hence the need for a scavenger (i.e. H_2O or thioanisole).

The simple acidolytic conditions required for both *N*-Boc and *N*-Pbf deprotection allowed for the isolation of the crude TFA-amine salt by simple solvent removal. Solvent-aided anion-exchange with anhydrous HCl in ether then allowed for the simple isolation of the final compounds as the hydrochloride salts by precipitation from Et_2O. The general procedure that was developed allowed for 18 h reaction time to ensure complete deprotection of the *N*-Pbf group, as shorter reaction periods have been observed to give incomplete acidolysis. Due to the volatility of the *N*-Boc deprotection by-products, no resultant impurities were ever observed for *N*-Boc protected derivatives. For *N*-Pbf protected derivatives, the final salt required repeated precipitation and trituration of the final hydrochloride salt to remove the benzofuran by-product. The relative ease, speed and resultant product purity of the acidolytic deprotection and HCl salting allowed for the fast turn-over of multiple derivatives.

2.2.2 – Synthesis of dicationic derivatives (Series A2)

2.2.2.1 – Synthesis of Series A2 scaffolds *via* amide coupling

Traditional peptide coupling[107-108] allowed for the construction of amide bonds from carboxylic acids and amines (e.g. amino acid derivatives) and provided a simple and reliable methodology for the synthesis of dual-amino acid (i.e. Series A2) scaffolds.[59, 68-69] The scaffolds for Series A2 (**67a-c**) were constructed by the formation of a key amide bond between a mono-amino acid scaffold (i.e. Series A1) and a precursor amino acid derivative (Scheme 2.20); this transformation was accomplished by EDCI/HOBt in acetonitrile[59] utilizing the aforementioned **General Procedure B** (Section 6.2).

This procedure was utilized for the formation of all amide bonds (i.e. for both scaffold formation and derivatization). For example, the synthesis of scaffold azide **67a** was realized in 89% yield by reaction of scaffold amine **63a** (300 mg, 0.54 mmol) with precursor α-azido-acid **28** (1.2 eq), EDCI and HOBt in acetonitrile at rt for 48 h followed by purification by flash chromatography.

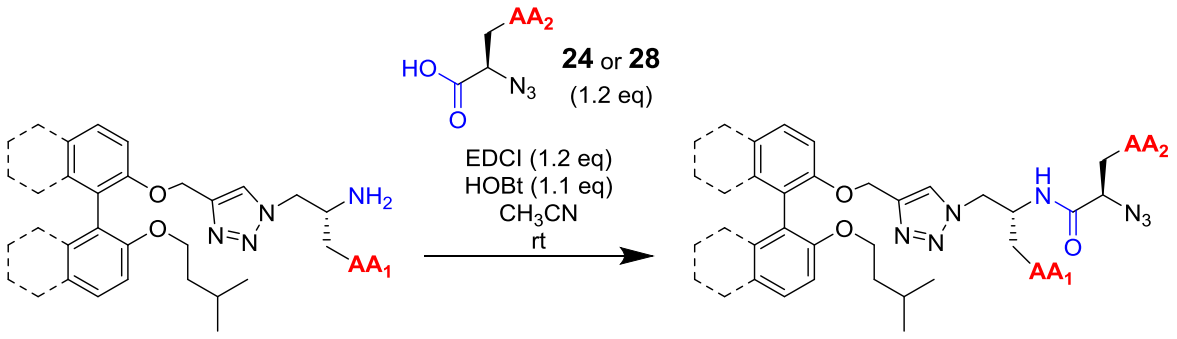

24: AA_2 = Lys(Boc)

= 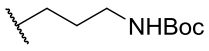

28: AA_2 = Arg(Pbf)

= 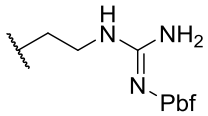

Compound	Aromatic Core	AA_1	AA_2	Yield (%)
67a	**Biphenyl**	**Lys(Boc)**	**Arg(Pbf)**	89
67b	**Biphenyl**	**Arg(Pbf)**	**Lys(Boc)**	77
67c	**Binaphthyl**	**Lys(Boc)**	**Arg(Pbf)**	96

Scheme 2.20 – Synthesis of scaffolds **67a-c**: amide coupling between amine scaffolds **63a-c** and an α-azido-acid precursor (**24** or **28**) to give the scaffold azides **67a-c** for Series A2.

Analysis of the ^{1}H NMR spectrum of compound **67a** confirmed the presence of resonances that were assigned to functionalities from both precursors **63a** and **28**. The broad resonance at δ 3.02 –3.10 (-C<u>H</u>NH$_2$) in the ^{1}H NMR spectrum of starting amine **63a** was no longer observed in the spectrum of **67a**; there was however, a new more deshielded resonance at δ 4.35 that was assigned to the lysine α-methine proton. This evidence indicated that the methine proton, adjacent to the primary amine in precursor **63a**, experienced a downfield chemical shift due to the newly installed amide bond. Furthermore, a gHMBC correlation

was observed between the ^{1}H NMR resonance at δ 4.35 (assigned to the α-lysine methine proton) and the ^{13}C NMR resonance at δ 170.9 (assigned to the new amide carbonyl). The molecular structure of the product was further verified by the appearance of a peak at *m*/*z* 986.5325 in HRMS, that was assigned to the protonated molecular ion, $[M + H]^+$ (calcd for $C_{50}H_{72}N_{11}O_8S$ 986.5286).

The reliable and mild conditions afforded by the amide coupling reagents EDCI and HOBt were essential for the synthesis and derivatization of these multi-functionalized molecules. An uncatalysed reaction between the carboxylic acid and amine components generates an ammonium carboxylate salt; subsequent amide condensation requires intense heat, which would be incompatible with highly functionalized molecules.[108] Therefore, peptide coupling reagents (or 'activators') are utilized to increase the electrophilicity of the acyl moiety; these reagents allow amide bond formation *via* aminolysis of an activated acyl species under much milder conditions.[107-110]

Carbodiimides (e.g. 1-ethyl-3-(3-dimethylaminopropyl)carbodiimide hydrochloride (EDCI)) are employed to generate an active *O*-acylisourea intermediate (Scheme 2.21) by reaction with the carboxylate anion. This intermediate can undergo aminolysis by the precursor amine to give the desired product amide.[107-108] In a possible side reaction, the highly activated *O*-acylisourea intermediate can undergo intramolecular acyl transfer to give an inactive *N*-acylurea by-product (Scheme 2.21 – red pathway),[107-108, 110] thus consuming the precursor acid without formation of the product amide.

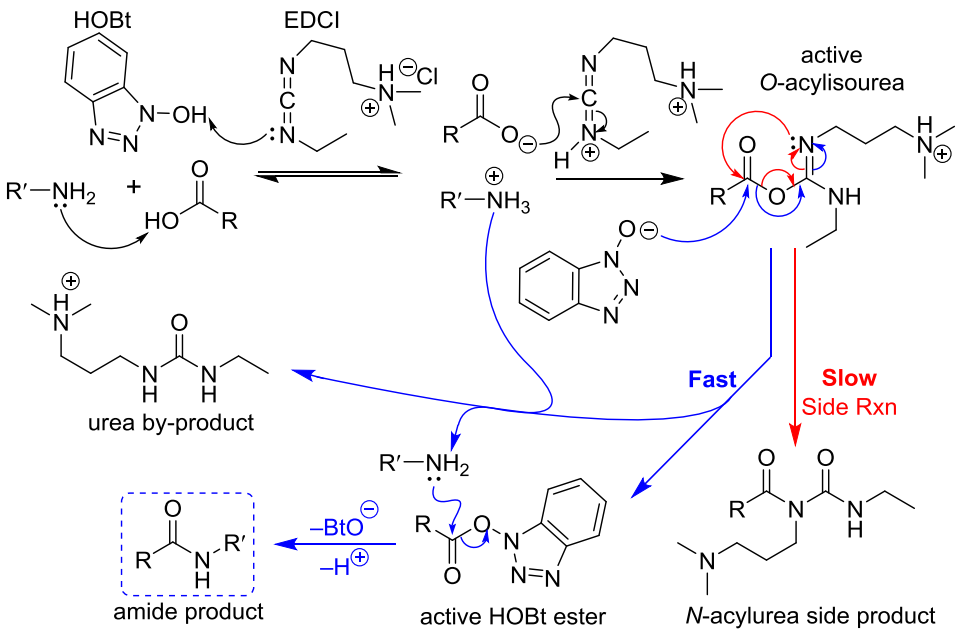

Scheme 2.21 – Mechanism of EDCI/HOBt promoted amide coupling: both the product pathway (blue) and the undesired side reaction (red) are displayed.

To avoid this deleterious side reaction and the possibility of racemization, nucleophilic additives such as HOBt (1-hydroxy-1*H*-benzotriazole) are added to the reaction.[107-110] HOBt reacts with the active *O*-acylisourea intermediate to generate an activated HOBt ester with the key acyl moiety (Scheme 2.21 – blue pathway). Crucially, this reaction occurs faster than the intramolecular acyl transfer, thus preventing the side reaction but still generating an activated acid derivative for subsequent aminolysis to the product amide.[107-108] Epimerization of the stereogenic α-carbon on the *O*-acylisourea intermediate is another possible side reaction and it can occur through two mechanisms – simple enolate formation by deprotonation of the α-hydrogen (resulting in epimerization at the stereogenic centre) or *via* formation of the planar 5(4*H*)-oxazolone intermediate, in which the α-hydrogen is readily deprotonated due the resonance stabilization of the resulting carbanion. HOBt helps to prevent epimerization as the intermediate HOBt ester that is preferentially formed is less activated than the *O*-acylisourea, i.e. the -OBt functionality is less electron-withdrawing than

the corresponding isourea substituent and therefore the adjacent α-hydrogen is less prone to enolization.[107, 110] The lack of epimerization observed during the performed amide coupling reactions was likely a result of the HOBt. Epimerization would result in the formation of diastereomeric products that could be detected by ^{1}H NMR and/or TLC analysis. Based on such analyses, the isolated amide products were obtained as single diastereomers.

2.2.2.2 – Synthesis of Series A2 derivatives *via* CuAAC and *N*-deprotection

The derivatization of the dual-amino acid scaffolds for Series A2 required a two-step transformation: installation of the terminal triazole moieties by CuAAC followed by side-chain *N*-deprotection to yield the target amines as dihydrochloride salts. The derivatization of scaffold azides to achieve terminal triazole biarylpeptides has been accomplished previously *via* CuACC reaction[59] while subsequent *N*-Boc and *N*-Pbf deprotection was previously achieved with TFA/CH_2Cl_2.[59, 69]

Therefore, CuAAC reactions (**General Procedure A**) were employed to derivatize scaffolds **67a-c** and to install the terminal triazole moieties (Reaction (i) in Schemes 2.22 – 2.24); the resultant *N*-protected triazole derivatives were then immediately subjected to acidolytic *N*-Boc and *N*-Pbf cleavage followed by work-up with ethereal HCl (**General Procedure C**: Reaction (ii) in Schemes 2.22 – 2.24) to afford the target amines as their dihydrochloride salts (**68a-d**, **69a-d** and **70a-b**). Much like Series A1, the derivatization of scaffolds **67a-c** for Series A2 was conducted in two consecutive steps; CuAAC reaction completion and product purity was monitored by TLC and/or MS analysis prior to subsequent *N*-deprotection.

For example, the synthesis of compound **68a** (Scheme 2.22) was realized in 86% yield over two steps from scaffold azide **67a** (50 mg, 0.05 mmol) by reaction with 3-phenyl-1-propyne

(3.0 eq), $Cu(OAc)_2 \cdot H_2O$, and sodium ascorbate in *t*-BuOH/H_2O at rt for 20 h to give the intermediate *N*-protected triazole derivative, which was then subjected to *N*-Boc/*N*-Pbf deprotection with TFA and H_2O in CH_2Cl_2 at rt for 18 h followed by treatment with ethereal HCl and purification by precipitation. Scaffold azide **67b** (50 mg, 0.05 mmol) was also directly deprotected with TFA and H_2O in CH_2Cl_2 at rt for 18 h followed by treatment with ethereal HCl and purification by precipitation to give final compound **69d** in 97% yield (Scheme 2.23).

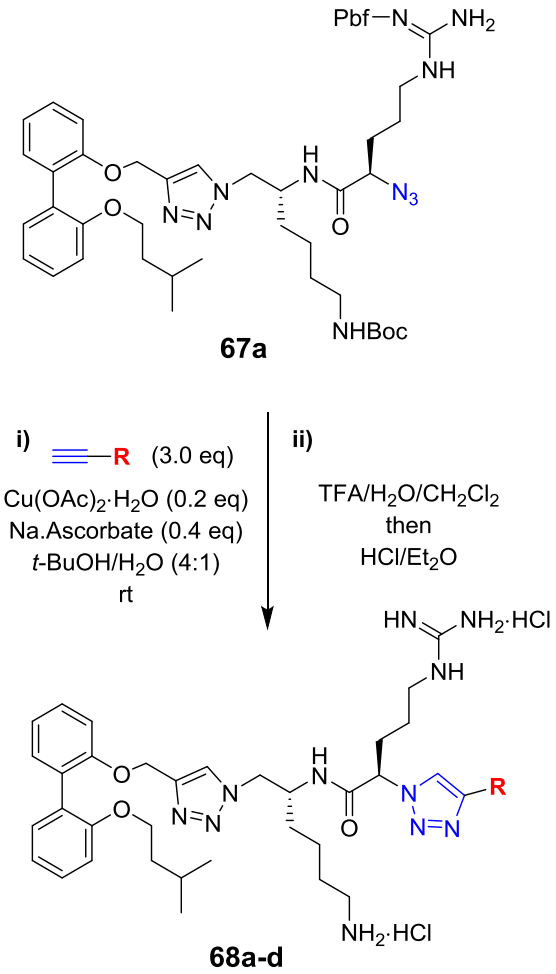

Compound	R	Yield (%)[a]
68a	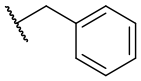	86
68b	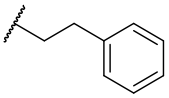	94
68c	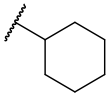	92
68d	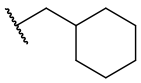	79

[a] Yields are reported over two steps from compound **67a**

Scheme 2.22 – Derivatization of scaffold **67a**: installation of the terminal triazole moiety (with **R** substituent) followed by removal of the side chain *N*-protecting groups to give scaffold derivatives **68a-d** as dihydrochloride salts.

The ^{1}H NMR spectrum of the final derivative **68a** displayed characteristic resonances that were assigned to the terminal benzyl moiety (i.e. a singlet resonance at δ 4.07 (-C<u>H</u>$_2$Ph) and a broad multiplet resonance at δ 7.34 – 7.10 (phenyl)).

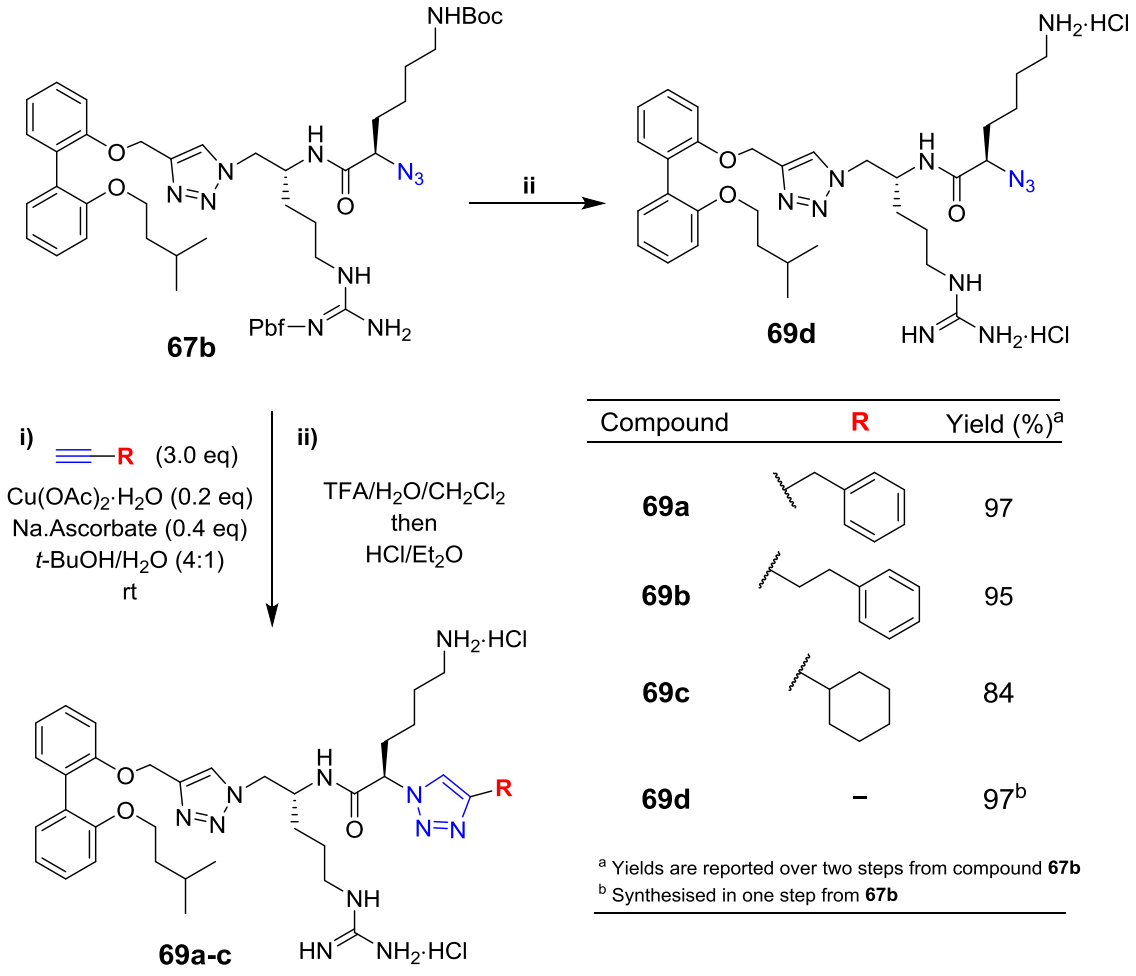

Scheme 2.23 – Derivatization of scaffold **67b**: installation of the terminal triazole moiety (with **R** substituent) followed by removal of the side chain *N*-protecting groups to give scaffold derivatives **69a-c** as dihydrochloride salts. The direct *N*-deprotection of scaffold **67b** to give compound **69d** is also displayed.

Importantly, a new degenerate resonance at δ 7.86 (2H) in the ^{1}H NMR spectrum of compound **68a** was observed and assigned to the protons on both triazole rings. The presence of the new triazole moiety was further confirmed by the ^{13}C NMR resonance assignments: δ 148.4 (quaternary triazole carbon – only observed by gHMBC), four resonances in the

aromatic region (phenyl carbons), δ 124.5 (triazole CH – only observed by gHSQC/gHMBC) and 32.4 (-$\underline{C}H_2Ph$) – these resonances were not seen in the ^{13}C NMR spectrum of the starting azide **67a**. Evidence for successful *N*-Boc deprotection was clearly seen by the lack of the 9H singlet resonance at δ 1.44 (assigned as the *t*-butyl protons (-C(CH_3)$_3$)) in the ^{1}H NMR spectrum of amine salt **68a**. Additionally, the lack of key resonances at δ 156.3 (Boc C=O), 79.2 (-$\underline{C}$(CH_3)$_3$) and 28.5 (-C($\underline{C}H_3$)$_3$) in the ^{13}C NMR spectrum of compound **68a** provided further evidence that the *N*-Boc protecting group had been successfully removed.

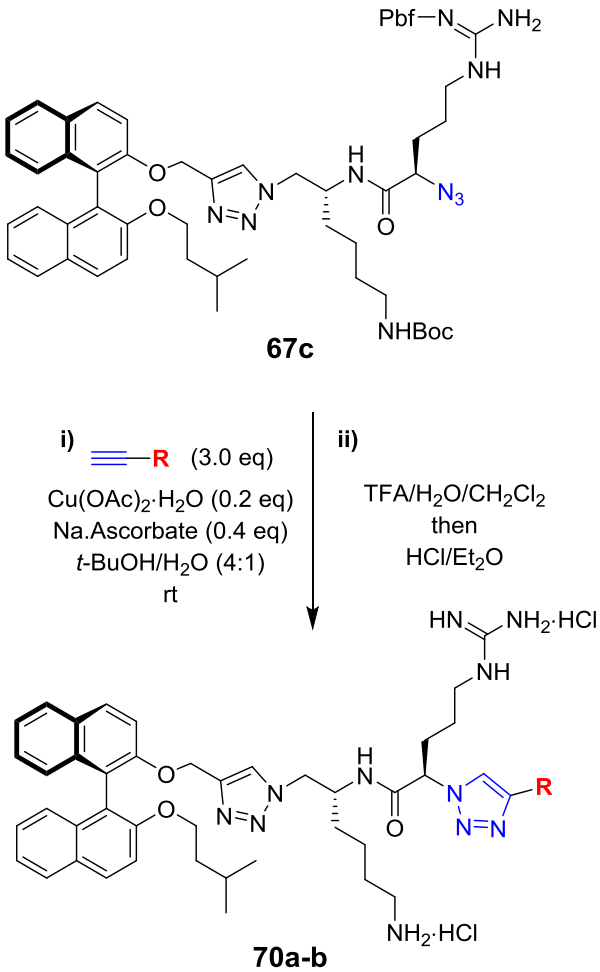

Compound	R	Yield (%)[a]
70a	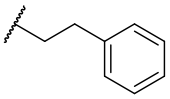	58
70b	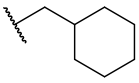	74

[a] Yields are reported over two steps from **67c**

Scheme 2.24 – Derivatization of scaffold **67c**: installation of the terminal triazole moiety (with **R** substituent) followed by removal of the side chain *N*-protecting groups to give scaffold derivatives **70a-b** as dihydrochloride salts.

Conclusive evidence for *N*-Pbf deprotection was clearly seen by the lack of the five characteristic Pbf singlet resonances (δ 2.95, 2.58, 2.51, 2.09 and 1.46) in the ^{1}H NMR spectrum of compound **68a** and the lack of corresponding *N*-Pbf resonances in the ^{13}C NMR spectrum. The molecular structure of the product was verified by the appearance of a peak at *m*/*z* 750.4587 in HRMS that was assigned to the protonated molecular ion, $[M + H]^+$ (calcd for $C_{41}H_{56}N_{11}O_3$ 750.4568).

For more information on both the CuAAC and the *N*-deprotection reactions (e.g. reaction mechanism and details), see Section 2.2.1.1.

2.2.2.3 –Series A2 exceptions

The synthesis of dicationic derivatives with terminal amide moieties for Series A2 was attempted *via* an analogous pathway to those procedures utilized for Series A1 and A2 derivatives. Unfortunately, realization of the required scaffold amine **71** proved difficult. Initial attempts utilized the *N*-Cbz protecting group for the arginine residue; repeated attempts to remove this protecting group *via* catalytic hydrogenolysis resulted in a complex mixture of amine products consisting of the target amine along with at least four other compounds (observed by TLC and MS analysis). MS analysis revealed the major side-product to be 14 amu heavier than the target amine **71**. The target product could not be adequately separated from these side-products, so the *N*-Cbz route was abandoned. Instead, the *N*-Fmoc protecting group was utilized; classic *N*-Fmoc deprotection with piperidine was attempted but a mixture of amine products was also obtained – MS analysis revealed the major side-product to be 40 amu heavier than the target amine **71**. Catalytic hydrogenolysis was then attempted to remove the *N*-Fmoc group,[111] but this methodology also gave a complex mixture of amine products. After extensive trial reactions, the amine scaffold **71**

was isolated and was deemed of sufficient purity (> 90%) for further derivatization (but not characterization). Ultimately, amine **71** was synthesized from scaffold amine **63a** (400 mg, 0.73 mmol) in 58% yield over two steps by reaction with Fmoc-(D)-Arg(Pbf)-OH (1.2 eq), EDCI and HOBt in acetonitrile at rt followed by base-promoted *N*-Fmoc deprotection with tris-(2-aminoethyl)amine (TAEA)[112] in acetonitrile (Scheme 2.25).

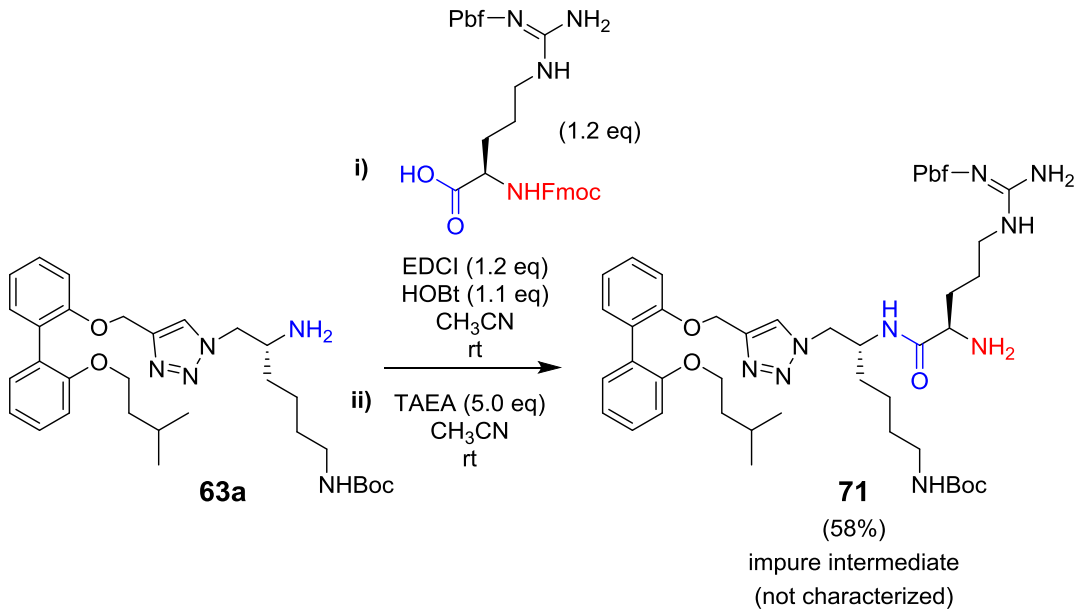

Scheme 2.25 – Synthesis of scaffold **71**: addition of the arginine residue by amide coupling followed by base-promoted removal of the *N*-Fmoc group.

The impure amine **71** (53 mg, 0.06 mmol) was then derivatized in the same manner as Series A1 scaffolds: amide coupling (**General Procedure B**: Reaction (i) in Scheme 2.26) to install the terminal benzyl amide moiety followed by *N*-Boc/*N*-Pbf side chain deprotection (**General Procedure C**: Reaction (ii) in Scheme 2.26) to give final compound **73** as a dihydrochloride salt in 61% yield over two steps. Reaction success for derivatization (i.e. amidation and subsequent *N*-deprotection) was verified in the same manner as Series A1 derivatives; NMR spectral analysis confirmed the installation of the benzyl amide and the removal of the *N*-Boc/*N*-Pbf protecting groups (see Section 2.2.1.2 for specific details).

Furthermore, the molecular identity was confirmed by the appearance of a peak at *m/z* 748.4288 in the HRMS, which was assigned to the sodiated molecular ion $[M + Na]^+$. The derivatization procedures eliminated the side-product impurity that was present in the starting amine **71**; the precipitation and trituration of the final HCl salt helped to remove most impurities that may have been present from previous reactions. Recrystallization of the final HCl salts can also be achieved by slow evaporation of a MeOH/CH_2Cl_2 solvent mixture (see Figure A2.4 in Appendix A).

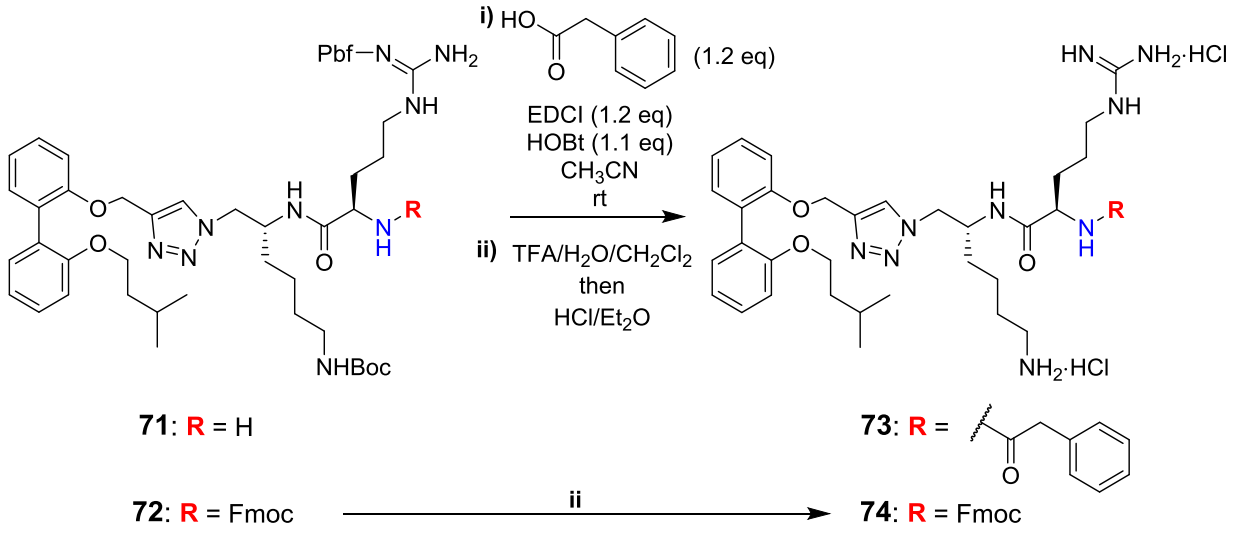

Scheme 2.26 – Derivatization of scaffold **71**: installation of the terminal amide group (**R**) *via* amide coupling followed by side chain *N*-deprotection to give compound **73** as a dihydrochloride salt. The synthetic pathway to realize to compound **74** by side chain *N*-deprotection of the *N*-Fmoc scaffold **72** is also displayed.

Additionally, **General Procedure C** was utilized to realize compound **74** in 95% yield by direct side chain *N*-deprotection of scaffold intermediate **72** (50 mg, 0.04 mmol) (Scheme 2.26).

2.3 – Series B synthesis: scaffolds and derivatives

2.3.1 – Synthesis of monocationic derivatives (Series B1)

2.3.1.1 – Synthesis of Series B1 scaffolds *via* CuAAC

The traditional click reaction (i.e. CuAAC)[75] allowed for the construction of 1,4-disubstituted-1,2,3-triazoles from alkyne and azide precursor components; this provided a simple and reliable methodology for the synthesis of mono-amino acid (i.e. Series B1) scaffolds.[59, 69] The scaffolds for Series B1 (**75a-d**) were constructed from a biaryl alkyne and an α-azido acid precursor by the CuAAC reaction (Scheme 2.27); this transformation was accomplished by utilizing the aforementioned **General Procedure A** (Section 6.2).

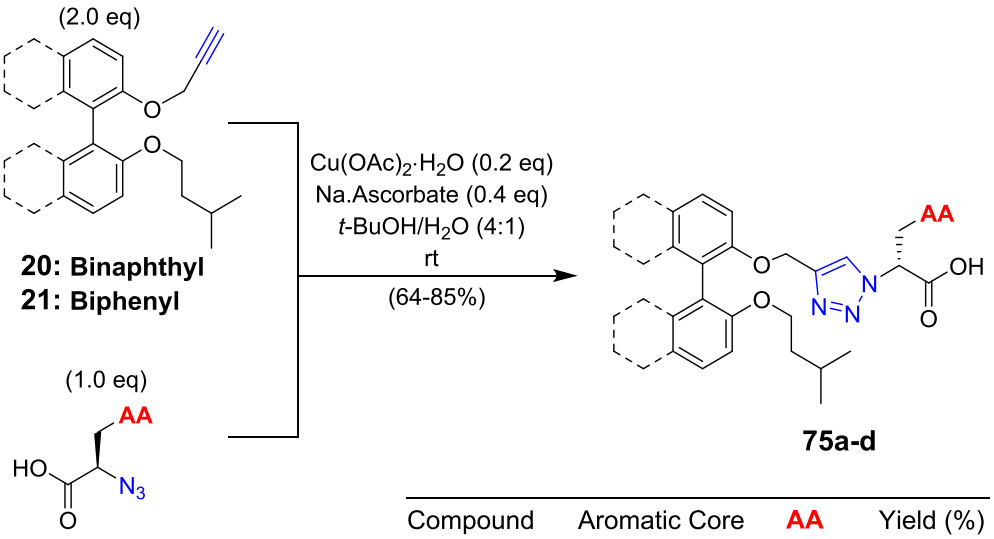

Compound	Aromatic Core	AA	Yield (%)
75a	**Biphenyl**	**Lys(Boc)**	85
75b	**Biphenyl**	**Arg(Pbf)**	82
75c	**Binaphthyl**	**Lys(Boc)**	64
75d	**Binaphthyl**	**Arg(Pbf)**	83

24: AA = Lys(Boc)

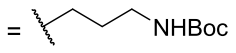

28: AA = Arg(Pbf)

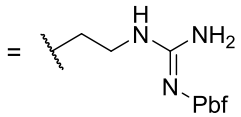

Scheme 2.27 – Cu-catalysed [3 + 2] cycloaddition reaction between an alkyne building block (**20** or **21** - blue triple bond) and an azide precursor (**24** or **28** - blue portion) to give the key scaffold acids **75a-d** for Series B1.

For example, scaffold acid **75a** was achieved in 85% yield by reaction of α-azido acid **24** (400 mg, 1.47 mmol) with alkyne **21** (2.0 eq), $Cu(OAc)_2 \cdot H_2O$ and sodium ascorbate in *t*-BuOH/H_2O at rt for 26 h followed by purification by flash chromatography (Scheme 2.27).

Interestingly, the ^1H and ^{13}C NMR spectra of scaffold acids **75a-d** in CD_3OD were lacking some key resonances; the spectra had to be collected in DMSO-d_6 to ensure all resonances were observed. Despite using DMSO-d_6, the binaphthyl scaffold acids **75c** and **75d** failed to display ^{13}C NMR resonances for the carboxyl carbon (C=O) or the adjacent α-methine carbon (-CHC=O). Furthermore, the resonances assigned to the α-methine proton in the ^1H NMR spectra of compounds **75c** or **75d** exhibited significant broadening. These NMR anomalies are explored in more detail in Section 4.6.

The ^1H NMR spectrum of compound **75a** displayed resonances that corresponded to fragments from both starting materials (alkyne **21** and azide **24**). The most diagnostic difference was the disappearance of the ^1H NMR singlet resonance at δ 2.43 (-C≡C-H) that was seen in the ^1H NMR spectrum of alkyne **21** and the appearance of the significantly downfield resonance at δ 7.89 (triazole CH) in the ^1H NMR spectrum of **75a**. The terminal alkyne proton in compound **21** had now become the lone proton on the newly formed triazole ring in scaffold **75a** – this results in a strong deshielding of the proton (relative to the alkyne proton) and a large downfield chemical shift. Two unique aromatic ^{13}C NMR resonances at δ 142.9 and 123.3 were present in the ^{13}C NMR spectrum of scaffold acid **75a** – these resonances were assigned to the methine and quaternary triazole carbons, respectively. The resonance at δ 142.9 was extremely diagnostic because few other aromatic carbon resonances appear in that region (i.e. δ 141-150). As expected, the ^{13}C NMR resonance at δ 123.3

(triazole CH) displayed a correlation in the gHSQC spectrum with the ^{1}H NMR resonance at δ 7.89 (triazole CH). Furthermore, the appearance of these two unique ^{13}C NMR resonances coincided with the disappearance of the two alkyne (-C≡C-) ^{13}C NMR resonances at δ 79.3 and 75.2 that are evident in the ^{13}C NMR spectrum of starting alkyne **21**. These two alkyne carbons (-C≡C-) had now become the aromatic triazole carbons – this explains the associated large downfield chemical shift. Additionally, the methine proton (adjacent to the acid moiety) was assigned to a downfield resonance at δ 5.19 in the ^{1}H NMR spectrum of compound **75a** – this proton was originally assigned to a resonance at δ 3.95 in the ^{1}H NMR spectrum of starting α-azido acid **24**. This large downfield shift occured due to the formation of the new adjacent triazole ring, which strongly deshielded the nearby methine proton. The molecular identity was confirmed as HRMS analysis displayed a peak at *m*/*z* 589.2993 that was assigned to the sodiated molecular ion, $[M + Na]^{+}$ (calcd for $C_{31}H_{42}N_4O_6Na$ 589.3002).

2.3.1.1 – Synthesis of Series B1 derivatives *via* amide coupling and *N*-deprotection

The derivatization of the mono-amino acid scaffolds for Series B1 required a two-step transformation: installation of the terminal amide moieties followed by side-chain *N*-deprotection to yield the target amines as hydrochloride salts. Previous syntheses of binaphthylpeptides have utilized the common EDCI/HOBt peptide coupling reagent system to form the necessary peptide bonds while *N*-Boc and/or *N*-Pbf deprotection was previously achieved with TFA/CH_2Cl_2.[59, 64-66, 68-69] The derivatization for Series B1 was achieved using the same methodology as Series A1 (see Section 2.2.1.2).

Therefore, for Series B1 derivatives, **General Procedure B** was utilized to install the terminal amide moiety (see Reaction (i) in Schemes 2.28 – 2.30); the resultant *N*-protected

amide derivatives were then immediately subjected to acidolytic *N*-Boc or *N*-Pbf cleavage followed by work-up with ethereal HCl (**General Procedure C** or **D**: Reaction (ii) in Schemes 2.28 – 2.30) to achieve the target amine salts (**76a-f**, **77a-l** and **78a-b**) in high purities.

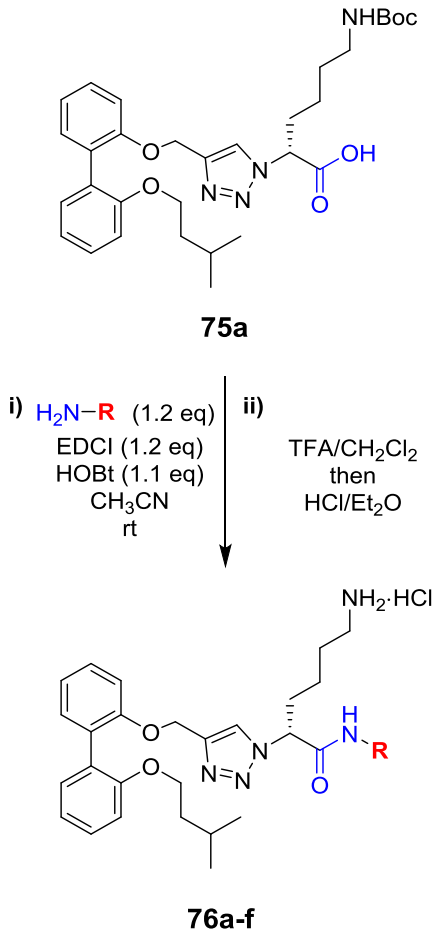

Compound	R	Yield (%)[a]
76a	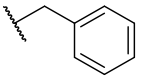	95
76b	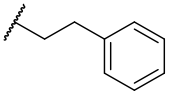	94
76c	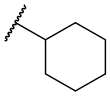	94
76d	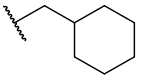	92
76e	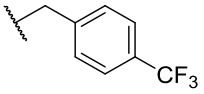	97
76f	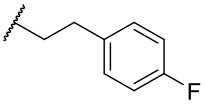	93

[a] Yields are reported over two steps from **75a**

Scheme 2.28 - Derivatization of scaffold **75a**: installation of the terminal amide moiety (**R**) followed by removal of the *N*-Boc side chain protecting group to give scaffold derivatives **76a-f** as hydrochloride salts.

For example, the synthesis of derivative **76a** (Scheme 2.28) was realized in 95% yield over two steps from scaffold amine **75a** (50 mg, 0.09 mmol) by reaction with benzylamine (1.2 eq), EDCI and HOBt in acetonitrile at rt for 24 h to give the corresponding amide which was immediately subjected to *N*-Boc deprotection with TFA in CH_2Cl_2 at rt for 18 h followed by

treatment with ethereal HCl and purification by precipitation. Much like Series A, the derivatization of scaffolds **75a-b** and **75d** for Series B1 was conducted in two consecutive steps; reaction completion and product purity for the amide coupling reactions was monitored by TLC and/or MS analysis prior to subsequent *N*-deprotection.

The ^{1}H NMR spectrum of the final compound **76a** displayed resonances that were assigned to the benzyl amide substituent (i.e. δ 4.37 (-C$\underline{H}_2$Ph) and δ 7.34 – 7.10 (phenyl)). The presence of the new amide moiety was further confirmed by the following ^{13}C NMR resonances: δ 169.8 (amide $\underline{C}$=O), four resonances in the aromatic region (phenyl carbons) and δ 44.6 (-$\underline{C}$H$_2$Ph), which were not seen in the ^{13}C NMR spectrum of the starting acid **75a**. Evidence of *N*-Boc deprotection was seen by the lack of the diagnostic ^{1}H NMR singlet resonance at δ 1.44 (-C(CH$_3$)$_3$) and the lack of key ^{13}C NMR resonances at δ 155.5 (Boc C=O), 77.3 (-$\underline{C}$(CH$_3$)$_3$) and 28.2 (-C($\underline{C}$H$_3$)$_3$) in the spectra of compound **76a**. The molecular structure of the product was verified by the appearance of a peak at *m*/*z* 556.3302 in HRMS that was assigned to the protonated molecular ion, $[M + H]^+$ (calcd for $C_{33}H_{42}N_5O_3$ 556.3288).

In another example, the synthesis of derivative **77a** (Scheme 2.29) was realized in 94% yield over two steps from scaffold acid **75b** (50 mg, 0.07 mmol) by reaction with benzylamine (1.2 eq), EDCI and HOBt in acetonitrile at rt for 22 h to give the intermediate amide which was immediately subjected to *N*-Pbf deprotection with TFA and H_2O in CH_2Cl_2 at rt for 18 h followed by treatment with ethereal HCl and purification by precipitation. NMR spectral analysis confirmed the installation of the benzyl amide and the removal of the *N*-Pbf protecting group as per previous examples (see Section 2.2.1.2). The molecular structure of

the product was verified by the appearance of a peak at *m/z* 584.3373 in HRMS that was assigned to the protonated molecular ion, $[M + H]^+$ (calcd for $C_{33}H_{42}N_7O_3$ 584.3349).

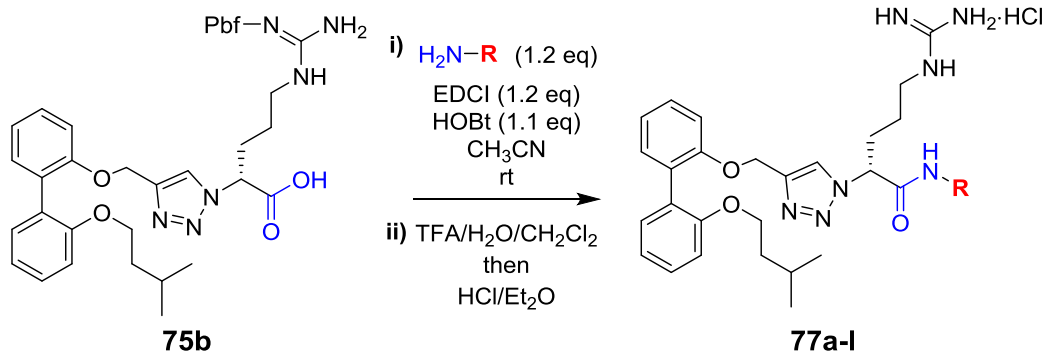

Compound	R	Yield (%)[a]
77a	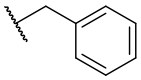	94
77b	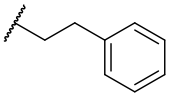	87
77c	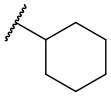	95
77d	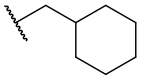	60
77e	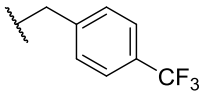	65
77f	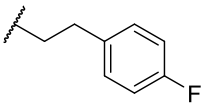	84

[a] Yields are reported over two steps from **75b**

Compound	R	Yield (%)[a]
77g	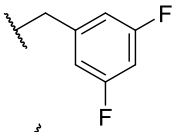	53
77h	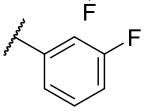	79
77i	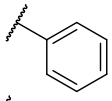	89
77j	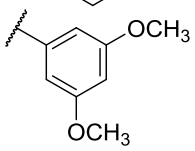	81
77k		89
77l[b]	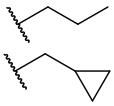	86

[b] *N,N*-disubstituted amide: two **R** groups

Scheme 2.29 – Derivatization of scaffold **75b**: installation of the terminal amide moiety (**R**) followed by removal of the *N*-Pbf side chain protecting group to give scaffold derivatives **77a-l** as hydrochloride salts.

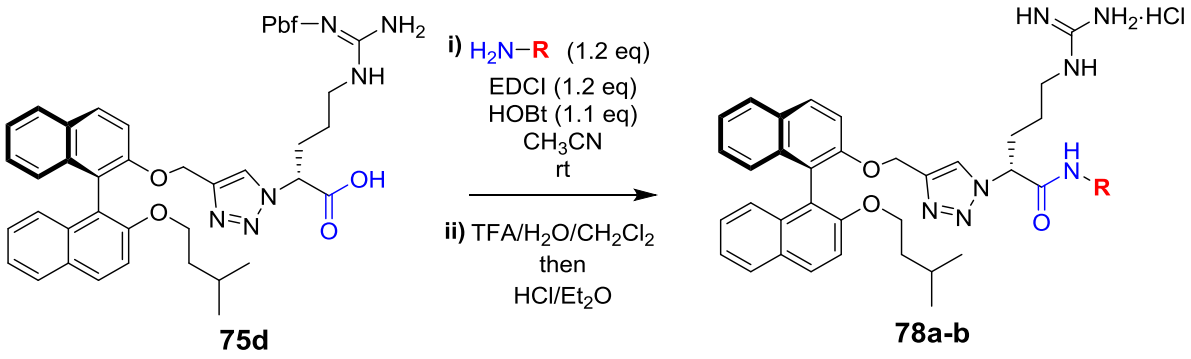

Compound	R	Yield (%)[a]
78a	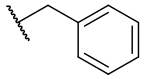	87
78b	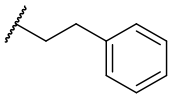	49

[a] Yields are reported over two steps from **75d**

Scheme 2.30 – Derivatization of scaffold **75d**: installation of the terminal amide moiety (**R**) followed by removal of the *N*-Pbf side chain protecting group to give scaffold derivatives **78a-b** as hydrochloride salts.

2.3.2 – Synthesis of dicationic derivatives (Series B2)

2.3.2.1 – Synthesis of Series B2 scaffolds *via* amide coupling

The synthesis of dual-amino acid scaffolds for Series B2 was conducted in a manner analogous to the synthesis of Series A2 scaffolds (Section 2.2.2.1). A second amino acid residue was attached to a scaffold from Series B1 *via* the reliable amide coupling methodology (**General Procedure B**) to generate scaffolds **79a-d** (Scheme 2.31).

For example, scaffold azide **79a** was isolated in 82% yield from starting acid **75a** (176 mg, 0.31 mmol) by treatment with amine **25** (1.2 eq), EDCI and HOBt in acetonitrile at rt for 48 h followed by purification by flash chromatography.

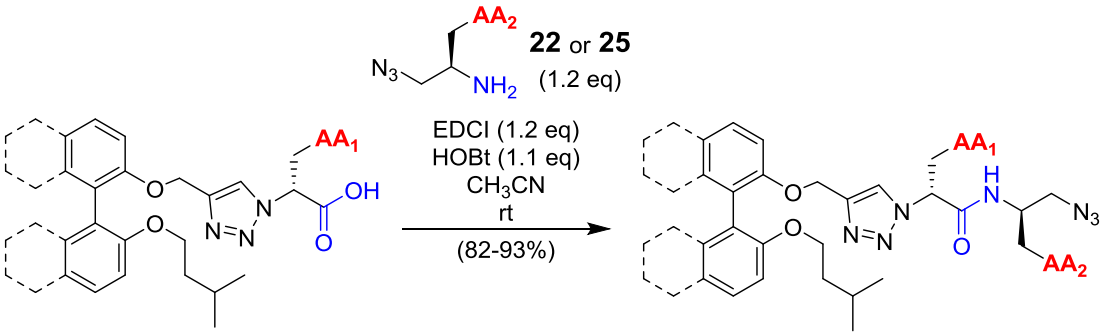

75a-d **79a-d**

22: AA_2 = **Lys(Boc)**

= 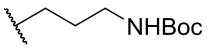

25: AA_2 = **Arg(Pbf)**

= 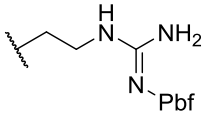

Compound	Aromatic Core	AA_1	AA_2	Yield (%)
79a	**Biphenyl**	**Lys(Boc)**	**Arg(Pbf)**	82
79b	**Biphenyl**	**Arg(Pbf)**	**Lys(Boc)**	91
79c	**Binaphthyl**	**Lys(Boc)**	**Arg(Pbf)**	86
79d	**Binaphthyl**	**Arg(Pbf)**	**Lys(Boc)**	93

Scheme 2.31 – Synthesis of scaffolds **79a-d**: amide coupling between scaffold acids **75a-d** and a β-azido-amine precursor (**22** or **25**) to give the scaffold azides **79a-d** for Series B2.

Analysis of the ^{1}H NMR spectrum of scaffold azide **79a** confirmed the presence of resonances that were assigned to functionalities from both precursors **75a** and **25**. The singlet resonance at δ 2.81 (-C<u>H</u>NH$_2$) in the ^{1}H NMR spectrum of starting acid **75a** was no longer observed in the spectrum of **79a**; however, a new resonance at δ 3.96 (1H) was observed and it was assigned to the arginine α-methine proton. The methine proton, adjacent to the primary amine in precursor amine **25**, had experienced a downfield chemical shift due to the newly installed amide bond. The ^{13}C NMR spectrum of scaffold azide **79a** did not display a resonance at δ 156.6 (assigned to the carboxylic acid carbon, C=O); instead, the spectrum exhibited a new resonance at δ 168.5 that was assigned to the new amide carbonyl (C=O).

Furthermore, a gHMBC correlation was observed between the ^{1}H NMR resonance at δ 3.96 (assigned to the arginine methine proton) and the ^{13}C NMR resonance at δ 168.5 (assigned

to the new amide carbonyl) – providing further evidence of successful amide bond formation. The molecular structure was verified by the appearance of a peak at *m*/*z* 986.5335 in HRMS, that was assigned to the protonated molecular ion, $[M + H]^+$ (calcd for $C_{50}H_{72}N_{11}O_8S$ 986.5286).

2.3.2.2 – Synthesis of Series B2 derivatives *via* CuAAC and *N*-deprotection

The derivatization of the dual-amino acid scaffolds **79a-d** (for Series B2) was accomplished *via* utilization of the same two-step methodology that was employed for the derivatization of Series A2 scaffolds (see Section 2.2.2.2); the terminal triazole moieties were installed *via* CuAAC reactions (**General Procedure A**: Reaction (i) in Schemes 2.32 – 2.35) followed by acidolytic *N*-Boc/*N*-Pbf deprotection and HCl salting (**General Procedure C**: Reaction (ii) in Schemes 2.32 – 2.35) to give the target compounds (**80a-d**, **81a-d**, **82a-b** and **83a-b**) as their dihydrochloride salts. As per Series A2, the derivatization of scaffolds **79a-d** for Series B2 was conducted in two consecutive steps; CuAAC reaction completion and product purity was monitored by TLC and/or MS analysis prior to subsequent *N*-deprotection.

For example, derivative **80a** was afforded in 95% yield over two steps from scaffold azide **79a** (50 mg, 0.05 mmol) by reaction with 3-phenyl-1-propyne (3.0 eq), $Cu(OAc)_2 \cdot H_2O$ and sodium ascorbate in *t*-BuOH/H_2O at rt for 24 h followed by *N*-Boc/*N*-Pbf deprotection with TFA and H_2O in CH_2Cl_2 at rt for 18 h followed by treatment with ethereal HCl and purification by precipitation.

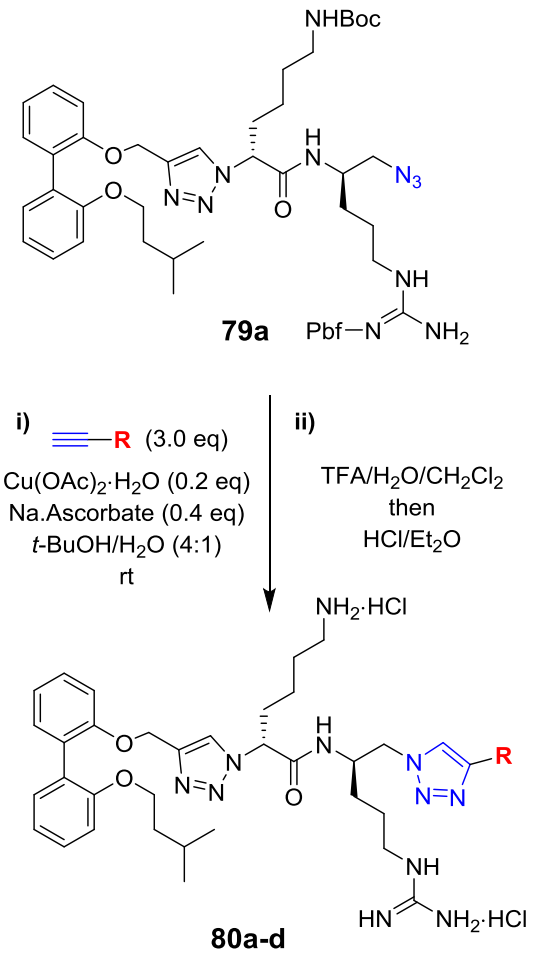

Compound	R	Yield (%)[a]
80a	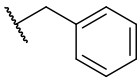	95
80b	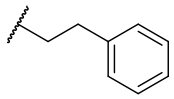	85
80c	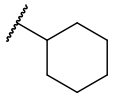	94
80d	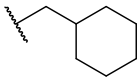	90

[a] Yields are reported over two steps from **79a**

Scheme 2.32 – Derivatization of scaffold **79a**: installation of the terminal triazole moiety (with **R** substituent) followed by removal of the side chain *N*-protecting groups to give scaffold derivatives **80a-d** as dihydrochloride salts.

The ^{1}H NMR spectrum of the final derivative **80a** displayed ^{1}H NMR resonances that were assigned to the new benzyl substituent (i.e. δ 4.08 (-C<u>H</u>$_2$Ph) and δ 7.36 – 7.09 (phenyl)). Furthermore, a new downfield singlet resonance at δ 7.92 (1H) in the ^{1}H NMR spectrum of compound **80a** was observed and assigned to the proton on the newly installed triazole ring. The presence of the new triazole moiety was confirmed by assignment of the ^{13}C NMR resonances: δ 148.3 (quaternary triazole carbon – only observed by gHMBC), four resonances in the aromatic region (phenyl carbons), δ 125.7 (triazole CH) and 32.4 (-<u>C</u>H$_2$Ph), which were not seen in the ^{13}C NMR spectrum of the starting azide **79a**.

NMR spectral analysis of compound **80a** confirmed the removal of the *N*-Boc/*N*-Pbf protecting groups as per previous examples (see Section 2.2.2.2). The molecular structure of the product was verified by the appearance of a peak at *m*/*z* 750.4570 in HRMS that was assigned to the protonated molecular ion, $[M + H]^+$ (calcd for $C_{41}H_{56}N_{11}O_3$ 750.4568).

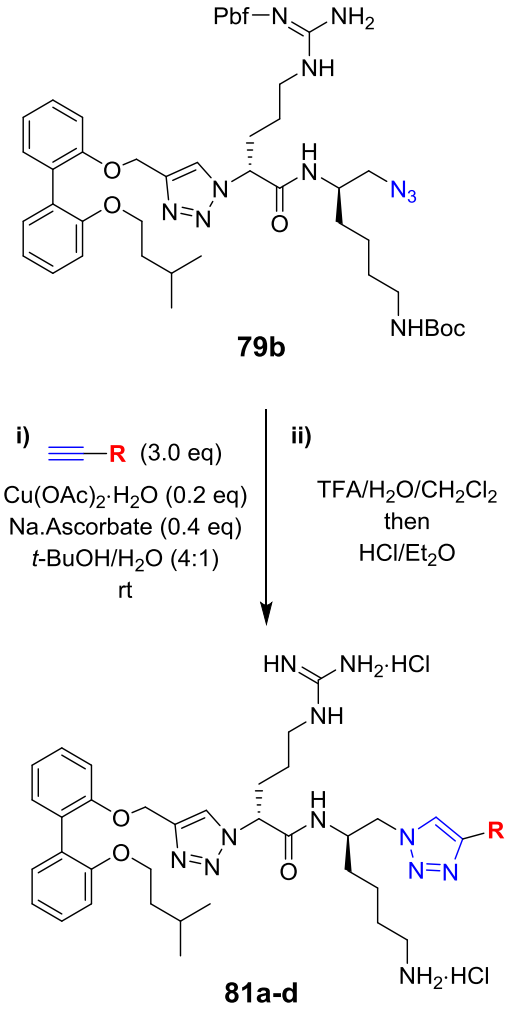

Compound	R	Yield (%)[a]
81a	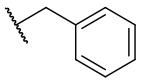	84
81b	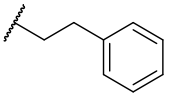	94
81c	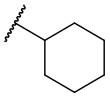	97
81d	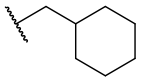	90

[a] Yields are reported over two steps from **79b**

Scheme 2.33 – Derivatization of scaffold **79b**: installation of the terminal triazole moiety (with **R** substituent) followed by removal of the side chain *N*-protecting groups to give scaffold derivatives **81a-d** as dihydrochloride salts.

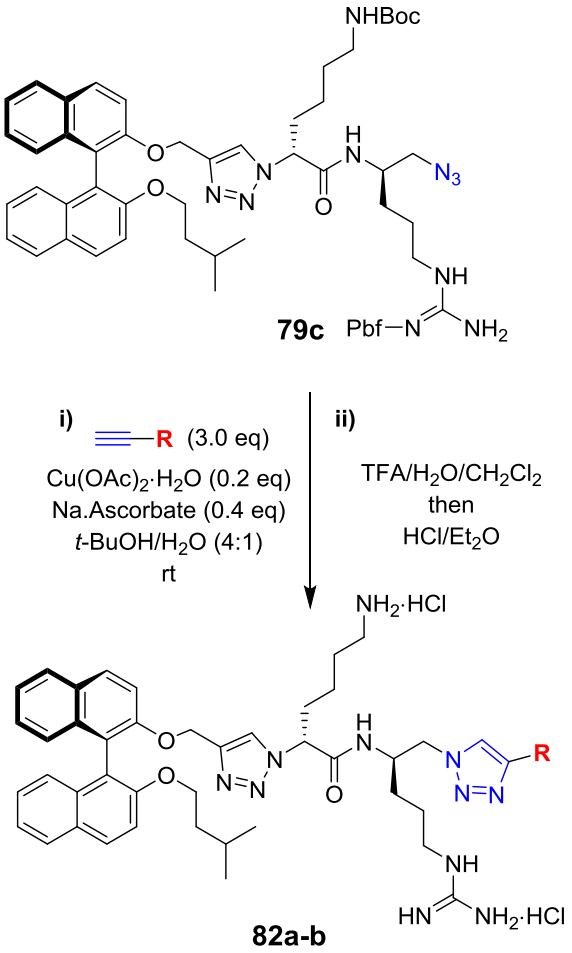

Compound	R	Yield (%)[a]
82a	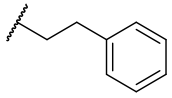	56
82b	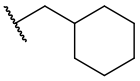	75

[a] Yields are reported over two steps from **79c**

Scheme 2.34 – Derivatization of scaffold **79c**: installation of the terminal triazole moiety (with **R** substituent) followed by removal of the side chain *N*-protecting groups to give scaffold derivatives **82a-b** as dihydrochloride salts.

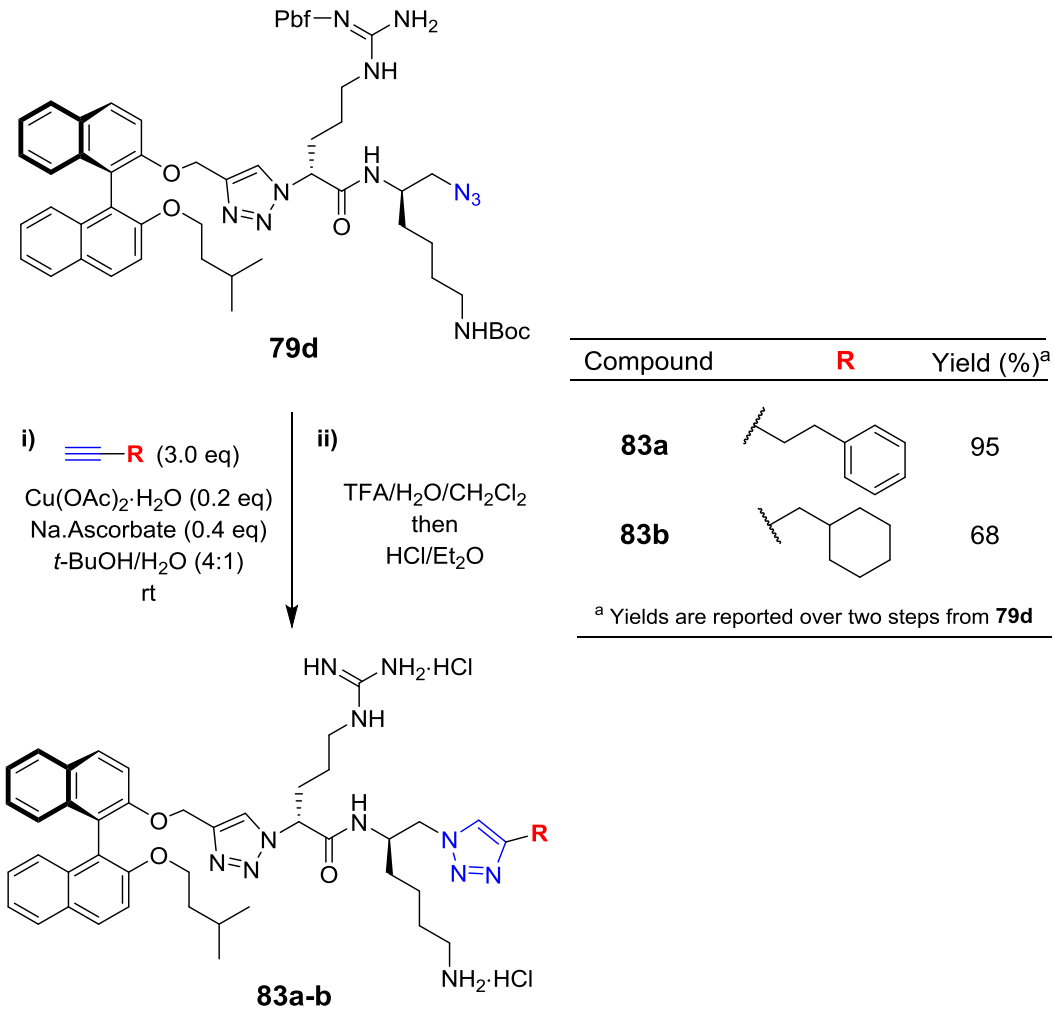

Scheme 2.35 – Derivatization of scaffold **79d**: installation of the terminal triazole moiety (with **R** substituent) followed by removal of the side chain *N*-protecting groups to give scaffold derivatives **83a-b** as dihydrochloride salts.

2.3.2.2 –Series B2 exceptions: terminal amide derivatives

The synthesis of dicationic derivatives with terminal amide moieties for Series B was accomplished *via* the construction of scaffold acid **84** by amide coupling the arginine derivative **29** onto scaffold **75c**[69] followed by base-promoted hydrolysis of the methyl ester group (Scheme 2.36). Scaffold acid **84** was then derivatized to afford compounds **85a-c** as dihydrochloride salts *via* the same two-step methodology employed for Series B1: amide coupling (**General Procedure B**: Reaction (i) in Scheme 2.37) to install the terminal amide

moiety followed by side chain *N*-deprotection and HCl salting (**General Procedure C**: Reaction (ii) in Scheme 2.37).

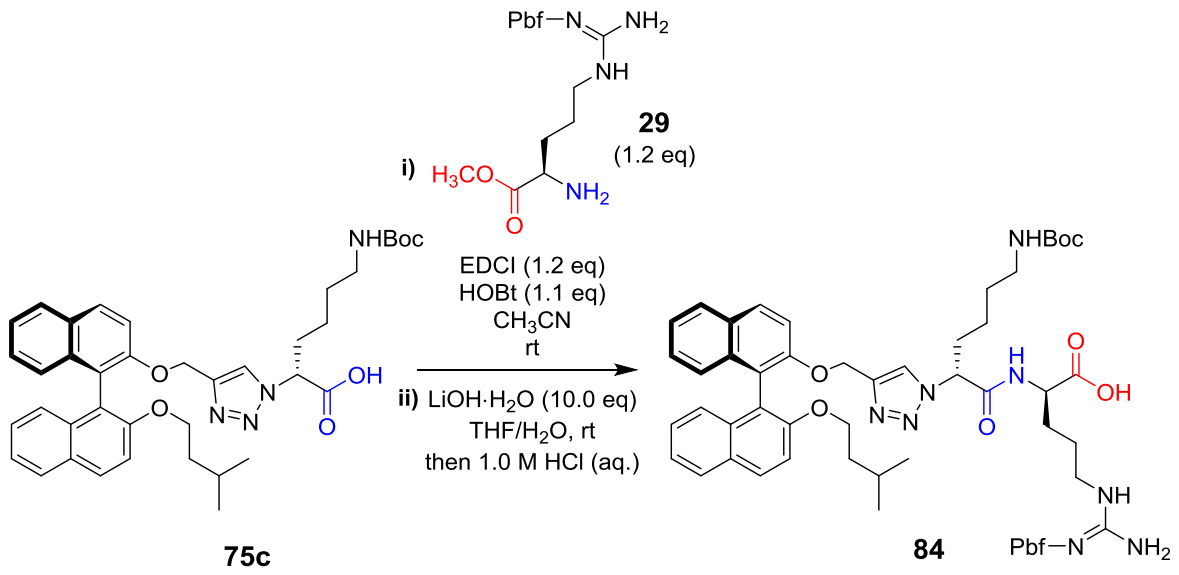

Scheme 2.36 – Synthesis of scaffold **84**: amide coupling between scaffold acid **75c** and amine **29** followed by base-promoted removal of the methyl ester protecting group to give scaffold acid **84**.

Scaffold acid **84** was achieved in 86% yield over steps from scaffold **75c** (150 mg, 0.23 mmol) by reaction with amine **29** (1.2 eq), EDCI and HOBt in acetonitrile at rt for 18 h followed by hydrolysis with LiOH·H_2O in THF/H_2O at rt for 24 h and subsequent acidification with 1.0 M aqueous HCl (Scheme 2.36). Initial examination of the ^{1}H and ^{13}C NMR spectra of scaffold acid **84** suggested the presence of impurities with doubling up of many ^{1}H and ^{13}C NMR resonances (see Figures C1.11 – C1.13 in Appendix C). The compound appeared pure by TLC analysis (one spot) and product identity was confirmed by HRMS analysis (one peak at *m*/*z* 1073.5156 – assigned as the deprotonated molecular ion, $[M - H]^-$ (calcd for $C_{58}H_{73}N_8O_{10}S$ 1073.5170)). The extra resonances in the NMR spectra of scaffold acid **84** were found to be a result of *syn*- and *anti*-carbamate and amide rotamers – this topic is explored in detail in Section 4.3.

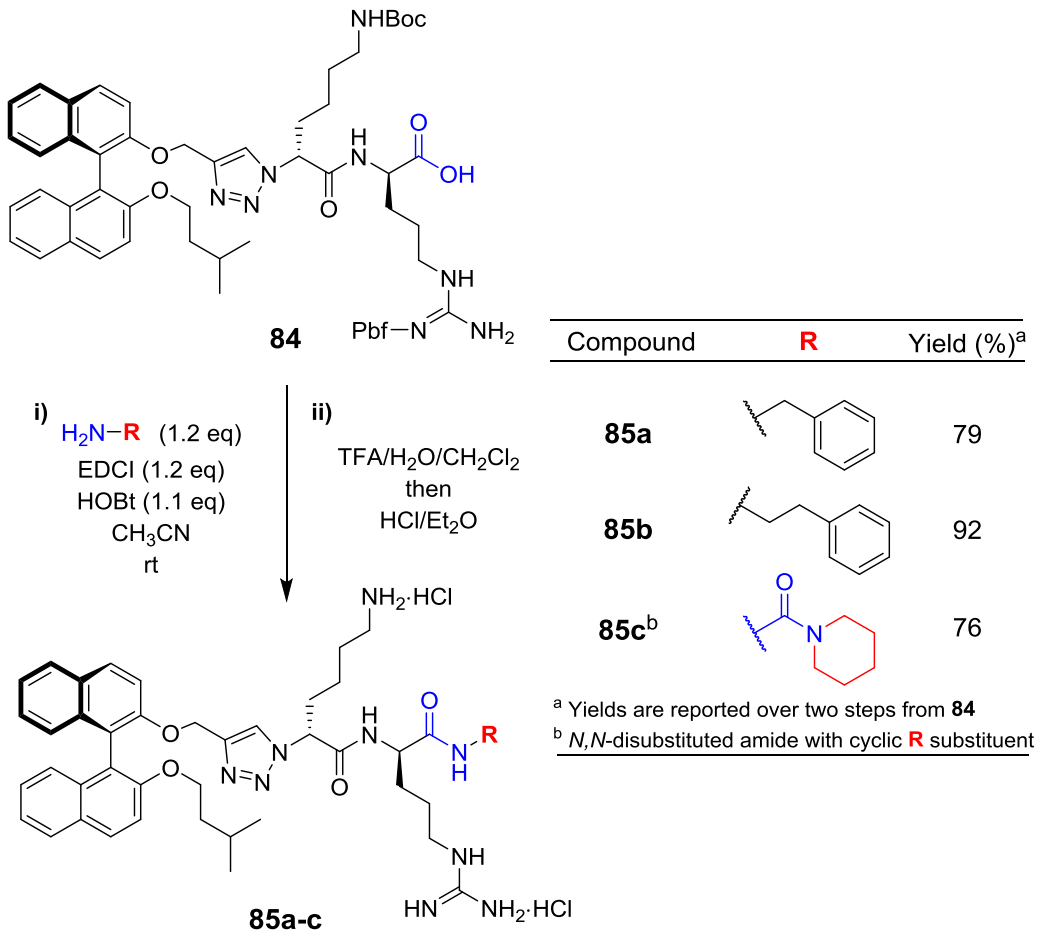

Scheme 2.37 - Derivatization of scaffold **84**: installation of the terminal amide moiety (with **R** substituent) followed by removal of the side chain *N*-protecting groups to give scaffold derivatives **85a-c** as dihydrochloride salts.

In one example of derivatization, compound **85a** was afforded in 79% yield over two steps from scaffold acid **84** (50 mg, 0.05 mmol) by reaction with benzylamine (1.2 eq), EDCI and HOBt in acetonitrile at rt for 24 h followed by side chain *N*-deprotection with TFA and H_2O in CH_2Cl_2 at rt for 18 h – subsequent HCl salting with HCl/Et_2O and purification by precipitation gave the product as a dihydrochloride salt (Scheme 2.37). The derivatization of scaffold **84** was conducted in two consecutive steps without full spectroscopic characterization of the *N*-Boc/*N*-Pbf protected intermediates. Amide coupling reaction

completion and product purity was monitored by TLC and/or MS analysis prior to subsequent *N*-deprotection.

Reaction success for derivatization (i.e. amidation and subsequent *N*-deprotection) was verified in the same manner as Series B1 derivatives; NMR spectral analysis confirmed the installation of the benzyl amide and the removal of the *N*-Boc/*N*-Pbf protecting groups (see Section 2.2.1.2 for specific details). Furthermore, the molecular identity was confirmed by the appearance of a peak at *m/z* 812.4604 in the HRMS, which was assigned to the protonated molecular ion, $[M + H]^+$ (calcd for $C_{47}H_{58}N_9O_4$ 812.4612).

2.4 – Series C synthesis: scaffolds and derivatives

2.4.1 – Synthesis of monocationic derivatives (Series C)

Series C constitutes two biarylpeptide scaffolds (and their derivatives) that did not contain an internal triazole linker in the peptide backbone; one series with no triazoles (Series C1) and one series with terminal triazoles moieties only (Series C2).

2.4.1.1 – Synthesis of Series C1

The scaffold acid **86** for Series C1 was realized in 82% over two steps from aromatic acid **42**[†] (246 mg, 0.59 mmol) from the reaction with amine **29** (1.2 eq), EDCI and HOBt in acetonitrile at rt for 21 h followed by hydrolysis with $LiOH{\cdot}H_2O$ in THF/H_2O at rt for 18 h and subsequent acidification with 1.0 M aqueous HCl (Scheme 2.38).

The ^1H NMR spectrum of acid **86** displayed resonances that were assigned to both the binaphthyl and arginine precursor fragments. Evidence of the newly installed amide bond

[†] Compound gifted from previous researcher (S. Wales).

was seen by the appearance of a broad resonance at δ 7.75 (1H) in the ^{1}H NMR spectrum of scaffold **86**, assigned as the amide proton (N-H).

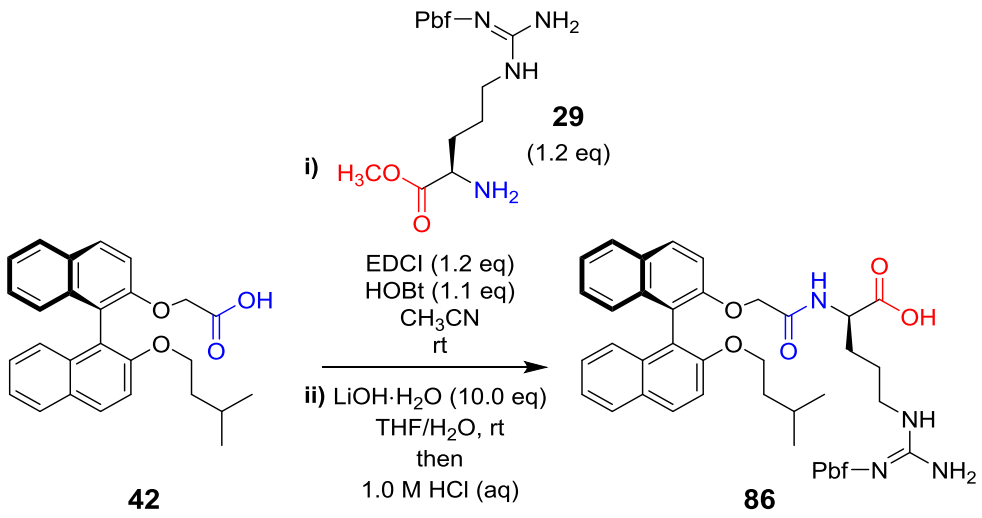

Scheme 2.38 – Synthesis of scaffold **86**: amide coupling of aromatic acid **42** and arginine residue **29** followed by base-promoted removal of the methyl ester protecting group to give scaffold acid **86**.

Notably, the ^{13}C NMR spectrum of compound **86** (in CD_3OD) was missing six *N*-Pbf resonances that were observable only through gHMBC correlations with the protons of the attached -CH_3 groups. The guanidine carbon (C=N) could not be assigned to a resonance in the ^{13}C NMR spectrum but was shown to be present in subsequent derivatives (**87a-c**). It has been observed that carboxylic acid containing derivatives can exhibit weak aromatic *N*-Pbf ^{13}C NMR resonances.

The derivatization of scaffold **86** was conducted in two consecutive steps; amide coupling reaction completion and product purity were monitored by TLC and/or MS analysis prior to subsequent *N*-deprotection. For example, derivative **87a** was isolated in 97% yield over two steps from scaffold acid **86** by reaction with benzylamine (1.2 eq), EDCI, HOBt in acetonitrile at rt for 22 h followed by *N*-Pbf deprotection with TFA and H_2O in CH_2Cl_2 at rt for 18 h with subsequent HCl salting (Scheme 2.39).

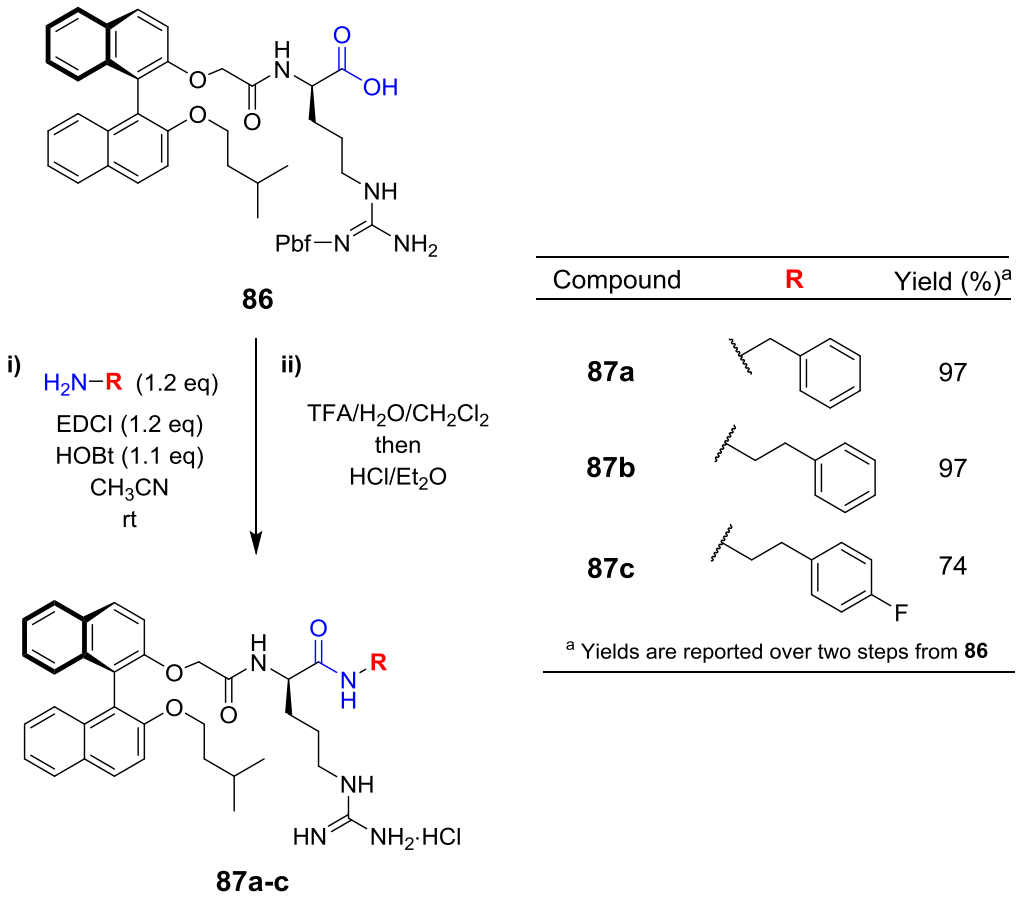

Scheme 2.39 - Derivatization of scaffold **86**: installation of the terminal amide moiety (with **R** substituent) followed by removal of the side chain *N*-Pbf group to give scaffold derivatives **87a-c** (Series C1) as hydrochloride salts.

The ^{1}H NMR spectrum of the final derivative **87a** displayed resonances that were characteristic of the benzyl amide substituent (i.e. δ 4.25 (-C$\underline{H}_2$Ph) and δ 7.39 – 7.15 (phenyl); As seen in previous examples, the lack of key *N*-Pbf resonances in the NMR spectra of compound **87a** provided further evidence for the removal of the *N*-Pbf protecting group. The molecular structure of the product was verified by the appearance of a peak at *m*/*z* 660.3553 in HRMS that was assigned to the protonated molecular ion, $[M + H]^+$ (calcd for $C_{40}H_{46}N_5O_4$ 660.3550).

2.4.1.2 – Synthesis of Series C2 (terminal triazoles)

The scaffold azide **88** for Series C2 was realized in 94% from acid **42** (207 mg, 0.50 mmol) by reaction with amine **22** (1.2 eq), EDCI and HOBt in acetonitrile at rt for 24 h (Scheme 2.40) followed by purification by flash chromatography.

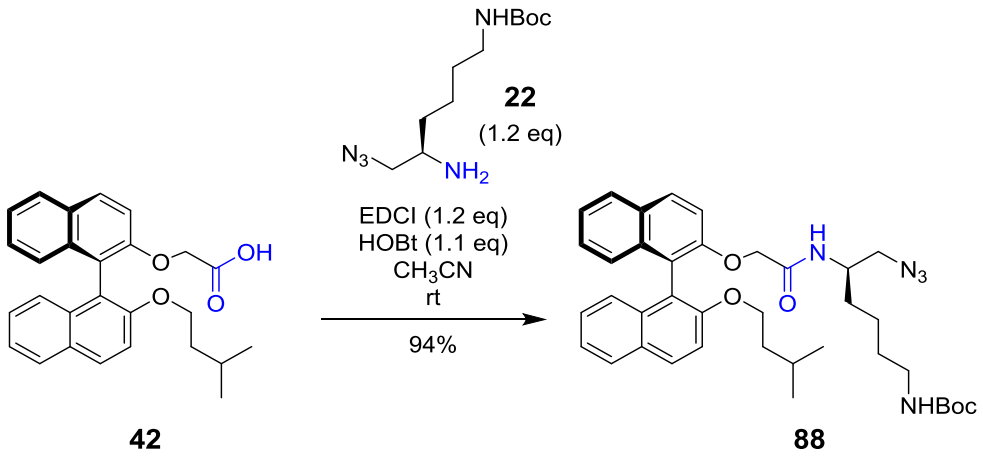

Scheme 2.40 – Synthesis of scaffold azide **88**: amide coupling between aromatic acid **42** and β-azido-amine **22**.

The ^{1}H NMR spectrum of azide **88** displayed resonances that were assigned to both the binaphthyl and lysine precursor fragments. Evidence of the newly installed amide bond was seen by the appearance of a new resonance at δ 5.60 (1H) in the ^{1}H NMR spectrum of scaffold **88** – this broad singlet resonance was assigned as the new amide proton (N-H). Furthermore, the broad singlet at δ 2.89 (-C<u>H</u>NH-) in the ^{1}H NMR spectrum of starting amine **22** was no longer present in the spectrum of scaffold azide **88** – the α-methine proton was assigned to a new downfield resonance at δ 3.75 in the ^{1}H NMR spectrum of target azide **88** and was a direct result of the newly installed amide bond. Additionally, the resonance at δ 167.9 in the ^{13}C NMR spectrum was assigned to the amide carbonyl (C=O) and was confirmed by a heteronuclear gHMBC correlation with the ^{1}H NMR resonance at δ 3.75 (-C<u>H</u>NH-). Analysis of the IR spectrum of azide **88** revealed a strong characteristic band at 2101 cm^{-1} that was assigned to the azide moiety.

The derivatization of scaffold **88** to realize compounds **89a-c** (Scheme 2.41) was conducted in two consecutive steps; CuAAC reaction completion and product purity was monitored by TLC and/or MS analysis prior to subsequent *N*-deprotection.

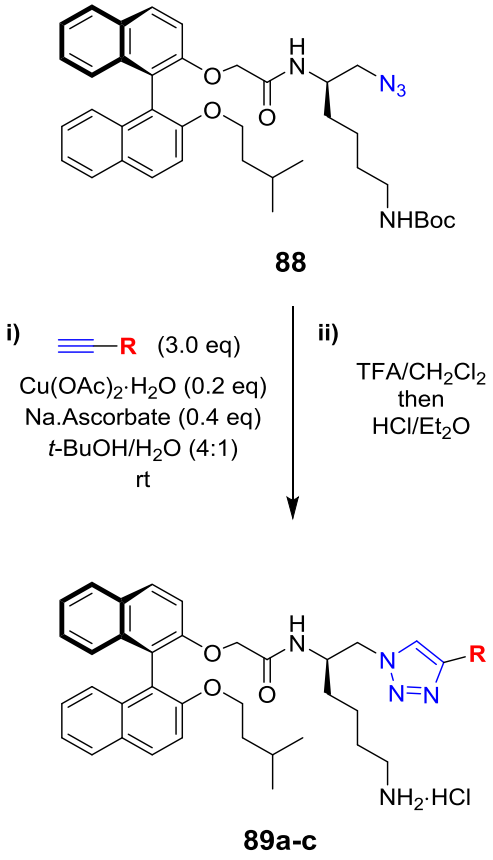

Compound	R	Yield (%)[a]
89a	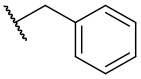	97
89b	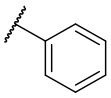	97
89c	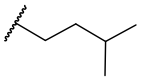	74

[a] Yields are reported over two steps from **88**

Scheme 2.41 – Derivatization of scaffold **88**: installation of the terminal triazole moiety (with **R** substituent) followed by removal of the side chain *N*-Boc group to give scaffold derivatives **89a-c** (Series C2) as hydrochloride salts.

For example, derivative **89a** was isolated in 50% yield over two steps from scaffold azide **88** by reaction with 3-phenyl-1-propyne (3.0 eq), $Cu(OAc)_2 \cdot H_2O$ and sodium ascorbate in *t*-BuOH/H_2O at rt for 20 h followed by *N*-Boc deprotection with TFA in CH_2Cl_2 at rt for 18 h and subsequent treatment with ethereal HCl and purification by precipitation (Scheme 2.41).

The ^{1}H NMR spectrum of the final derivative **89a** displayed resonances that were assigned to the terminal benzyl moiety (i.e. δ 3.95 (-C<u>H</u>$_2$Ph) and δ 7.22 – 7.08 (phenyl)). The presence of the triazole moiety was confirmed by assignment of the following ^{13}C NMR resonances: δ 148.2 (quaternary triazole carbon), 124.3 (methine triazole carbon), four resonances in the aromatic region (phenyl carbons) and δ 32.0 (-<u>C</u>H$_2$Ph), which were not seen in the ^{13}C NMR spectrum of the starting azide **88**. The resonance at δ 7.20 (triazole CH) in the ^{1}H NMR spectrum of derivative **89a** displayed a gHMBC correlation and a gHSQC correlation with the resonances at δ 148.2 and 124.3 (triazole carbons), respectively. As per previous examples, evidence of *N*-Boc deprotection was seen by the lack the characteristic ^{1}H and ^{13}C NMR resonances typical of the *N*-Boc protecting group. The molecular structure of the product was verified by the appearance of a peak at *m*/*z* 692.3611 in HRMS that was assigned to the sodiated molecular ion, $[M + Na]^+$ (calcd for $C_{42}H_{47}N_5O_3Na$ 692.3577).

3.0 – Biological and pharmacological assays: results and discussion

3.1 – Background information

This chapter reports the results of the *in vitro*, *in vivo* and pharmacological assays performed on the library of synthesized biarylpeptide derivatives. All final derivatives were subjected to a multi-phase testing procedure, as outlined in Figure 3.1.

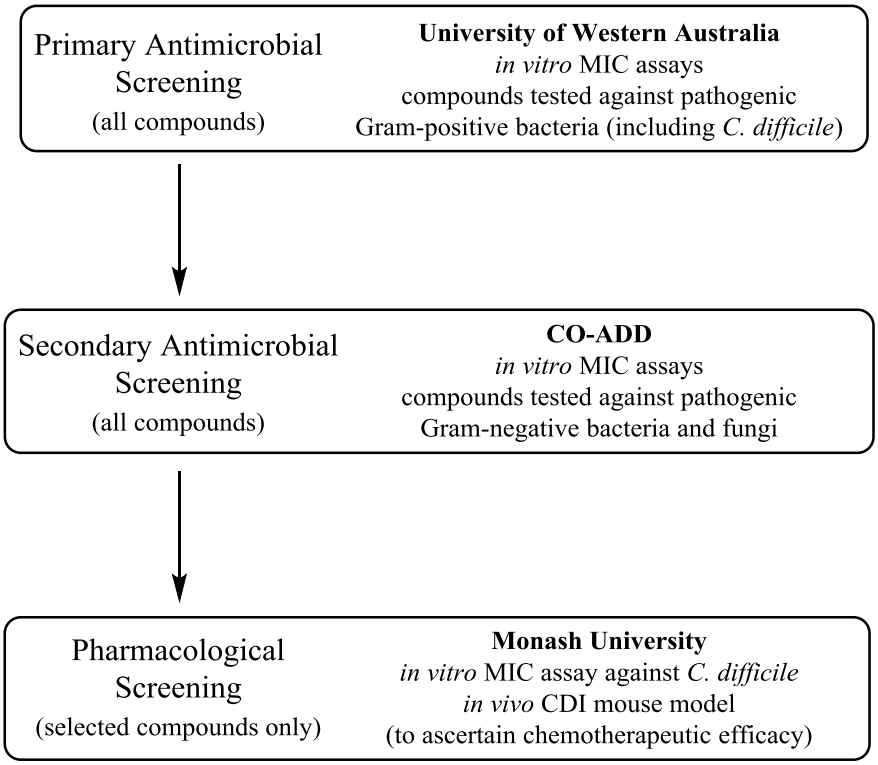

Figure 3.1 – Overview of the three-phase biological testing procedure utilized to determine the antimicrobial activity of the synthesized compounds.

Primary *in vitro* MIC screening (against Gram-positive bacteria including *C. difficile* – see Table 3.1) was performed at the University of Western Australia by project collaborators.† Secondary *in vitro* MIC screening (against Gram-negative bacteria/fungi – see Table 3.1) and

† Prof. Thomas V. Riley, Dr. Katherine A. Hammer and Dr. Dan Knight.

a cytotoxicity assay was performed by CO-ADD.[‡] Compounds that exhibited significant MIC values in the primary and secondary screening phases were then sent to collaborators[§] at Monash University for a third round of *in vitro* MIC testing against the hypervirulent *C. difficile* strain (RT027–M7404); compounds that performed well *in vitro* against the virulent *C. difficile* strain at Monash University were then selected for testing in an *in vivo* murine model of CDI. The *in vivo* murine model of CDI was developed and performed by collaborators[§] at Monash University; this assay was used to ascertain the viability and efficacy of identified hit compounds as potential CDI chemotherapeutics.

In conjunction with the *in vivo* CDI mouse models, a comparative solubility assay was developed and utilized to gauge and compare compound solubilities. Furthermore, a rudimentary pharmacokinetic analysis *via* low resolution ESI-MS was performed at the University of Wollongong on the blood and faeces of the mice from the *in vivo* studies to ensure that the compounds were not being absorbed systemically after oral administration.

3.2 – *In vitro* assays: MIC and cytotoxicity

MIC assays provide a quantitative measurement (in μg/mL) of a compound's ability to inhibit bacterial or fungal growth. The MIC assays were conducted against a range of various pathogenic microbes, including four Gram-positive and four Gram-negative bacterial species (Table 3.1) in total. Furthermore, compounds were also tested against two pathogenic fungal species. The compounds were tested against this wide set of pathogenic bacteria and

‡ Community for Open Antimicrobial Drug Discovery (www.co-add.org) – funded by the Wellcome Trust (UK) and The University of Queensland

§ Prof. Dena Lyras, Dr. Melanie Hutton, Dr. Amy King and Dr. Yogi Srikhanta

fungi to gauge their broad-spectrum activity (i.e. activity against a range of species including five of the six ESKAPE pathogens[5]) and their activity against the various *C. difficile* strains (to identify potential CDI chemotherapeutics or lead compounds).

	Testing Facility		
Gram +ve Bacterial Species	**UWA**	**CO-ADD**	**Monash**
Staphylococcus aureus	ATCC 29213 NCTC 10442 (MRSA)	ATCC 43300 (MRSA)	-
Clostridium difficile	ATCC 700057 NSW132 (RT027)	- -	M7404 (RT027)
Enterococcus faecalis	ATCC 29212	-	-
Streptococcus pneumoniae	ATCC 49619	-	-
Gram −ve Bacterial Species			
Escherichia coli	ATCC 25922	ATCC 25922	-
Klebsiella pneumoniae	-	ATCC 700603 (MDR)	-
Acinetobacter baumannii	-	ATCC 19606	-
Pseudomonas aeruginosa	-	ATCC 27853	-
Fungal Species			
Candida albicans	-	ATCC 90028	-
Cryptococcus neoformans	-	ATCC 208821	-

Table 3.1 – Bacterial and fungal species that were tested against in the various *in vitro* MIC assays.

3.2.1 – General methodology for MIC and cytotoxicity assays

The MIC assays were performed in multi-well micro-titre plates and the wells were filled with inoculated growth medium and varying, incremental concentrations of the compounds to be tested. The plates were then cultured and the resulting bacterial growth inhibition was observed. Compound concentrations ranging from 0.125 μg/mL to 128 μg/mL were typically employed and vancomycin, colistin and fluconazole were utilized as positive controls for Gram-positive bacteria, Gram-negative bacteria and fungi, respectively. For CO-ADD screening, a single point concentration (32 μg/mL) of each compound was first tested to confirm antibacterial activity; compounds that displayed activity at this concentration were then subjected to a comprehensive MIC assay. Compound cytotoxicity

was measured at CO-ADD against human embryonic kidney cells (HEK-293 – ATCC CRL-1573) with tamoxifen as a control and the data is reported as the concentration required to inhibit cell growth by 50% (CC_{50}). The experimental methodologies for the different MIC assays and cytotoxicity assay are reported in Section 6.4.1

3.2.2 – MIC assay results: overview and lead compound identification

The synthesized compounds exhibited antibacterial activities that ranged from inactive (> 128 μg/mL) to potent (2 μg/mL). The results show that some level of antibacterial activity was exhibited by every compound synthesized – see Tables 3.2 – 3.6 for the primary and secondary MIC screening data. For a set of the MIC data with the corresponding compound structures, please see Tables B1.1 – B2.9 in Appendix B.

Most of the compounds exhibited a decreased propensity to inhibit Gram-negative bacteria relative to the Gram-positive bacteria that were tested. These Gram-negative bacteria required concentrations of drug that were approximately two to four times higher than the corresponding Gram-positive MIC values; for example, compound **64a** exhibits an MIC = 8 μg/mL against *S. aureus* but an MIC = 32 μg/mL against *E. coli* (as seen in Table 3.2). The extra membrane inherent to Gram-negative bacteria is known to impede the absorption and therefore the action of various antibiotics.[13] *Klebsiella pneumoniae* was the least susceptible species to the majority of tested compounds and no compound displayed an MIC below 16 μg/mL for this bacterial species. The compounds generally did not exhibit MIC values below 8 μg/mL for the Gram-negative bacteria that were tested (Tables 3.4 – 3.6), whereas activities around 2 – 4 μg/mL were common for the Gram-positive bacterial species (Tables 3.2 and 3.3). Furthermore, *C. difficile* proved to be the most resilient of the Gram-positive bacteria that were tested; the hypervirulent *C. difficile* strain (RT027) also displayed decreased

susceptibility to the tested compounds, when compared with the normal *C. difficile* strain (Tables 3.2 and 3.3).

Out of the 62 antibiotics synthesized and tested, eight structures were identified as potential broad-spectrum lead antibacterial compounds. These novel biphenyl-triazole peptidomimetic compounds (i.e. **68a-d**, **69b**, **80b** and **81c-d**) were found to exhibit broad-spectrum activity against both Gram-positive *and* Gram-negative bacteria; these compounds displayed active MIC values (≤ 16 μg/mL) against all tested bacterial species. Compound **80b** from Series B was the best broad-spectrum lead compound, as it was the only compound to display an MIC value of 8 μg/mL against both *P. aeruginosa* and *A. baumannii* (Figure 3.2 and Table 3.6).

Furthermore, four compounds (i.e. **68c-d**, **77c** and **87a**) were identified as potential CDI chemotherapeutics due to their *in vitro* activities against *C. difficile* (MIC ≤ 8 μg/mL) and solubility profiles; these compounds were then synthesized on larger scale (approximately 500 – 1000 mg) for *in vivo* testing in a murine model of CDI (see Section 3.3.3).

Primary Screening Data							
	S. aureus		*E. faecalis*	*S. pneumoniae*	*E. coli*	*C. difficile*	
Compound	ATCC 29213	NCTC 10442	ATCC 29212	ATCC 49619	ATCC 25922	ATCC 700057	132 (RT027)
64a	8	8	8	8	32	32	32
64b	8	4	8	8	16	8	16
64c	16	16	16	32	32	8	32
65a	16	16	16	16	64	64	16
65b	16	16	16	32	64	128	16
65c	4	4	8	16	32	32	32
66a	4	4	8	8	32	64	64
66b	4	4	8	8	>128	16	16
66c	4	4	8	8	>128	32	32
68a	8	8	16	4	64	16	16
68b	4	4	8	8	64	8	8
68c	8	4	8	4	64	4	8
68d	4	4	4	4	32	4	4
69a	4	4	8	4	32	64	64
69b	4	4	8	4	32	16	16
69c	4	4	8	4	32	32	32
69d	16	16	16	8	64	64	32
70a	4	4	4	4	16	16	16
70b	4	4	4	4	16	8	16
73	8	8	8	8	32	16	16
74	4	4	4	4	64	32	32
76a	8	16	16	8	32	32	32
76b	8	8	8	8	16	32	32
76c	8	16	16	8	32	16	32
76d	8	8	8	8	16	16	32
76e	4	4	4	8	16	32	32
76f	4	8	8	8	16	32	64
77a	4	8	8	4	32	32	64
77b	2	2	4	4	16	8	32
77c	4	4	4	4	16	8	16
77d	4	4	8	8	32	32	64
Vancomycin	1	1	4	1	>16	0.5	0.5

Table 3.2 – Primary antimicrobial screening data for all synthesized compounds reported as the MIC values (μg/mL).

Primary Screening Data (cont.)							
	S. aureus		*E. faecalis*	*S. pneumoniae*	*E. coli*	*C. difficile*	
Compound	ATCC 29213	NCTC 10442	ATCC 29212	ATCC 49619	ATCC 25922	ATCC 700057	132 (RT027)
77e	16	16	16	32	64	128	128
77f	4	4	4	4	32	64	64
77g	8	8	8	16	32	32	32
77h	4	8	8	8	32	32	64
77i	2	2	2	2	16	16	32
77j	4	4	4	4	32	32	32
77k	16	32	32	8	64	64	128
77l	4	4	4	2	32	16	16
78a	4	8	2	8	>128	16	16
78b	8	8	4	16	>128	16	64
80a	4	4	8	4	32	8	16
80b	4	4	8	8	16	16	16
80c	16	16	16	32	64	64	128
80d	4	4	4	8	32	16	16
81a	8	8	8	4	32	32	16
81b	4	8	8	2	16	16	16
81c	8	8	8	2	16	8	16
81d	4	4	4	2	16	8	16
82a	4	4	4	4	16	16	16
82b	4	4	4	4	16	16	16
83a	4	4	4	2	8	16	16
83b	4	4	4	2	8	8	8
85a	8	8	8	8	32	16	16
85b	8	8	4	8	32	16	32
85c	8	8	8	8	16	16	32
87a†	2	2	2	2	>128	8	8
87b	2	2	4	2	>128	32	32
87c	>128	>128	>128	>128	>128	>128	64
89a	4	8	4	32	>128	16	16
89b	4	4	4	32	>128	8	8
89c	8	8	4	32	128	16	16
Vancomycin	1	1	4	1	>16	0.5	0.5

Table 3.3 – Primary antimicrobial screening data for all synthesized compounds reported as the MIC values (μg/mL). † MIC = 2 μg/mL against *C. diff.* (RT027 – M7404).

Secondary Screening - Control Data

Compound	*S. aureus* ATCC 43300 (*MRSA*)	*P. aeruginosa* ATCC 27853	*K. pneumoniae* ATCC 700603	*A. baumannii* ATCC 19606	*E. coli* ATCC 25922	*C. albicans* ATCC 90028	*C. neoformans* ATCC 208821	Cytotoxicity (CC_{50}) (HEK-293) ATCC CRL-1573
Vancomycin	1	>32	>32	>32	>32	-	-	-
Colistin	>32	0.25	0.25	0.25	0.125	-	-	-
Fluconazole	-	-	-	-	-	0.125	8	-
Tamoxifen	-	-	-	-	-	-	-	13.06

Table 3.4 – MIC or CC_{50} values for the various control inhibitors utilized in the secondary antimicrobial screening – reported in μg/mL.

Secondary Screening Data								
Compound	*S. aur.*	*P. aer.*	*K. pneu.*	*A. bau.*	*E. coli*	*C. alb.*	*C. neo.*	CC_{50}
64a	16	32	>32	32	>32	32	32	14.2
64b	16	32	32	>32	32	>32	16	4.8
64c	16	32	>32	32	32	16	32	4.7
65a	16	>32	>32	>32	>32	>32	32	29.0
65b	16	>32	>32	>32	>32	>32	32	>32
65c	8	>32	>32	>32	>32	8	16	>32
66a	4	>32	>32	>32	>32	32	8	16.5
66b	4	>32	>32	>32	>32	32	8	15.9
66c	4	>32	>32	>32	>32	16	4	13.8
68a	4	16	16	8	16	32	32	21.9
68b	2	8	16	16	8	32	4	>32
68c	4	8	16	16	8	32	4	14.2
68d	2	16	16	8	4	>32	4	>32
69a	4	16	32	16	8	32	4	17.8
69b	2	8	16	16	4	32	2	17.4
69c	4	8	32	8	8	32	2	15.3
69d	8	32	32	16	16	>32	4	>32
70a	4	32	>32	32	>32	8	2	>32
70b	2	32	>32	16	32	4	2	>32
73	4	32	32	32	16	32	2	28.7
74	4	>32	>32	>32	>32	>32	8	16.5
76a	16	32	>32	32	>32	>32	>32*	>32
76b	8	>32	>32	32	>32	>32	>32*	>32
76c	8	32	>32	32	>32	32	32*	>32
76d	8	>32	>32	32	>32	32	16*	5.6
76e	8	>32	>32	32	>32	>32	32*	>32
76f	8	>32	>32	16	>32	>32	12*	5.5
77a	8	>32	>32	32	>32	16	16	16.8
77b	8	>32	>32	32	>32	16	32	17.9
77c	4	>32	>32	32	>32	16	16	19.7
77d	4	>32	>32	>32	>32	32	32	16.9

Table 3.5 – Secondary antimicrobial screening data for all synthesized compounds reported as the MIC or CC_{50} values (μg/mL). ***** *Cryptococcus neoformans* data was not consistent with initial screening data – compounds need to be rescreened.

Secondary Screening Data (cont.)

Compound	*S. aur.*	*P. aer.*	*K. pneu.*	*A. bau.*	*E. coli*	*C. alb.*	*C. neo.*	CC_{50}
77e	16	>32	>32	>32	>32	>32	32	>32
77f	16	>32	>32	>32	>32	>32	32	19.1
77g	16	>32	>32	>32	>32	>32	>32	22.9
77h	4	>32	>32	>32	>32	>32	4	>32
77i	8	>32	>32	>32	>32	>32	32	21.6
77j	8	>32	>32	>32	>32	>32	>32	12.2
77k	32	>32	>32	>32	>32	>32	>32	20.0
77l	8	>32	>32	>32	>32	32	32	19.7
78a	8	>32	>32	>32	>32	16	8	16.5
78b	8	>32	>32	>32	>32	32	16	>32
80a	4	16	32	16	8	32	4	17.1
80b	2	8	16	8	8	32	4	16.4
80c	4	16	16	8	8	32	4	19.8
80d	2	32	16	8	8	16	4	19.1
81a	8	16	32	32	>32	32	4*	>32
81b	4	16	16	32	16	32	2*	>32
81c	4	8	16	16	16	32	2*	>32
81d	8	16	16	16	16	32	2*	>32
82a	2	16	>32	8	>32	4	2	>32
82b	2	32	>32	8	>32	4	1	16.6
83a	4	32	>32	32	>32	32	1*	>32
83b	32	32	>32	32	>32	32	1*	>32
85a	4	32	32	32	>32	16	4	17.4
85b	2	32	16	8	>32	16	2	15.2
85c	2	16	16	8	32	16	4	16.8
87a	4	>32	>32	>32	>32	>32	16*	>32
87b	4	>32	>32	>32	>32	32	16*	>32
87c	4	>32	>32	>32	>32	>32	16*	>32

Table 3.6 – Secondary antimicrobial screening data for all synthesized compounds reported as the MIC or CC_{50} values (μg/mL). ***** *Cryptococcus neoformans* data was not consistent with initial screening data – compounds need to be rescreened.

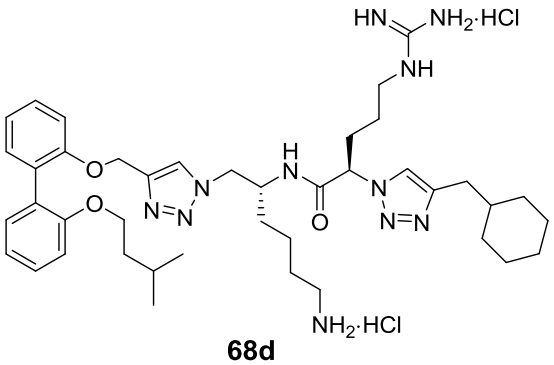

68d

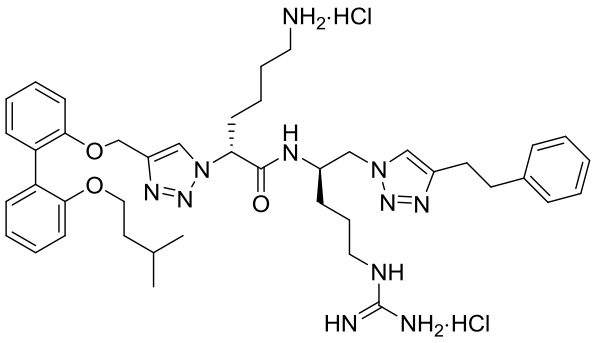

80b

MIC Values (μg/mL)

Bacterial Species	68d	80b	Vancomycin	Colistin
S. aureus	2	2	1	-
MRSA	4	4	1	-
E. faecalis	4	8	4	-
S. pneumoniae	4	8	1	-
C. difficile	4	16	0.5	-
C. difficile (RT027)	4	16	0.5	-
E. coli	4	8	-	0.125
P. aeruginosa	16	8	-	0.25
K. pneumoniae	16	16	-	0.25
A. baumannii	8	8	-	0.25
Cytotoxicity (CC_{50})	>32	16.4	-	-

Figure 3.2 – Structures, MIC and CC_{50} values for lead compounds **68d** and **80b**. See Table 3.1 for the specific bacterial strains that were tested.

The broad-spectrum lead compound **80b** displayed the best antibacterial activity against Gram-negative bacteria of any compound tested; despite this, it did not display the best activity against Gram-positive bacteria (Figure 3.2). Many other compounds displayed better Gram-positive activities, especially against the target species *C. difficile*; therefore, compound **80b** was not chosen for subsequent *in vivo* assay. However, compound **68d** displayed a similar Gram-negative activity profile to compound **80b** while maintaining an excellent Gram-positive activity profile (MIC values ≤ 4 μg/mL – Figure 3.2) with no observable cytotoxicity (unlike compound **80b**). Notably, this compound compared quite favourably with vancomycin, which exhibited MIC values between 1 - 4 μg/mL for the same

Gram-positive bacteria. Thus, both compound **68d** and a similar derivative, **68c**, where chosen for testing in the *in vivo* CDI model.

The other two compounds selected for the *in vivo* CDI mouse model study were compounds **77c** and **87a** (Figure 3.3); both compounds exhibited strong activity against most Gram-positive bacteria (MIC values ≤ 4 μg/mL) with an MIC value of 8 μg/mL against *C. difficile* in preliminary testing. Follow-up testing against the hypervirulent *C. difficile* strain (M7404 – RT027) at the Monash University laboratory revealed an MIC value of 2 μg/mL for compound **87a**.

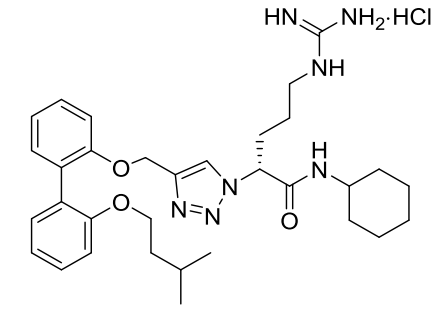

77c

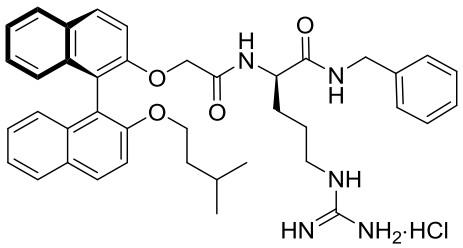

87a

	MIC Values (μg/mL)			
Bacterial Species	**77c**	**87a**	Vancomycin	Colistin
S. aureus	4	2	1	-
MRSA	4	2	1	-
E. faecalis	4	2	4	-
S. pneumoniae	4	2	1	-
C. difficile	8	8†	0.5	-
C. difficile (RT027)	16	8†	0.5	-
E. coli	>32	>128	-	0.125
P. aeruginosa	>32	>32	-	0.25
K. pneumoniae	>32	>32	-	0.25
A. baumannii	32	>32	-	0.25
Cytotoxicity (CC_{50})	>32	>32	-	-

Figure 3.3 – Structures, MIC values and CC50 values for selected compounds **77c** and **87a**. † Compound **87a** exhibited MIC = 2 μg/mL against *C. difficile* (M7404 - RT027) when tested at the Monash University laboratory. See Table 3.1 for the specific bacterial strains that were tested.

3.2.3 – MIC assay results: structure-activity relationship (SAR) trends

Sixty-two antibacterial compounds were synthesized from 17 unique scaffolds; this allowed for a large diversity in compound structure and orientation. There was no observable major difference in the antibacterial activities of the two peptide bonding orientations (blue arrow in Figure 3.4) that were investigated (i.e. Series A vs. Series B) as both series produced highly active derivatives (e.g. **68d** and **80b**) that exhibited broad spectrum activity against both Gram-positive and Gram-negative bacteria (see Figure 3.2). The dicationic derivatives were notably more active than the monocationic compounds and these findings were consistent with previous research.[69] The dicationic derivatives generally exhibited slightly increased antibacterial potency (2 – 4 times more active) against Gram-positive bacterial species – e.g. the activity of dicationic compound **80a** against *S. aureus* (MIC = 4 μg/mL) was notably stronger than the activity of the similar monocationic derivative **76a** (MIC = 8 – 16 μg/mL) – see Tables 3.2 and 3.3. Furthermore, many of the dicationic derivatives (Series A2 and B2) now exhibited significant activity against Gram-negative bacteria, whereas the mono-cationic derivatives (Series A1 and B1) were virtually inactive against Gram-negative bacteria – e.g. the monocationic compounds **65a-c** and the dicationic derivatives **68a-d** in Table 3.5. The introduction of a second cationic amino acid residue conferred a large increase in antimicrobial potency with broad-spectrum activity against both Gram-positive and Gram-negative bacteria. For example, compound **64b** did not exhibit Gram-negative antibacterial activity, but the dicationic analogue (compound **68b**) exhibited activity against all Gram-negative bacteria; it also displayed an MIC = 2 μg/mL against *S. aureus*, whereas the mono-cationic derivative (**64b**) exhibited an MIC = 16 μg/mL (see Tables 3.2 and 3.5). The addition of a second cationic side-chain residue likely allows for strong binding to the outer anionic bacterial membrane. It has been shown previously[69] that arginine residues are slightly more

potent than their corresponding lysine analogues; the current SAR data confirms this finding (e.g. arginine derivative **77a** was generally more potent than the lysine analogue **76a** – see Table 3.2).

While previous dicationic binaphthylpeptide derivatives have been known to exhibit potent antibacterial activity against Gram-positive bacteria, they were not as successful against Gram-negative bacteria. The more soluble biphenyl aromatic core was substituted for the traditional binaphthyl aromatic core (red arrow in Figure 3.4) in an attempt to increase compound solubility without compromising activity; this increase in solubility led to a notable increase in compound activity against Gram-negative bacteria. For example, both binaphthyl dicationic derivatives **70a** and **70b** were effectively inactive against Gram-negative bacteria (Table 3.5); substitution of the biphenyl aromatic core to generate analogues **68b** and **68d** led to observed antibacterial activity against Gram-negative species (MIC values = 4 – 16 μg/mL, see Table 3.5). Interestingly, the biphenyl core did not lead to an increase in Gram-positive antibacterial potency relative to the binaphthyl aromatic core (i.e. the binaphthyl derivative **78a** was more potent against Gram-positive bacteria (e.g. *C. difficile* MIC = 16 μg/mL) than its biphenyl analogue **77a** (*C. difficile* MIC = 32 – 64 μg/mL) – see Tables 3.2 and 3.3. The substitution of a biphenyl aromatic core increased the solubility of the compound (relative to the binaphthyl aromatic core – see Section 3.4.1); this increase in solubility was likely responsible for the increase in antimicrobial efficacy against Gram-negative bacteria. The resilient Gram-negative species are notably impermeable to antibiotics due to their secondary membrane layer; this increase in compound solubility and smaller molecular size may allow for better diffusion into the bacterial cell membrane, hence the increase in antibacterial activity.

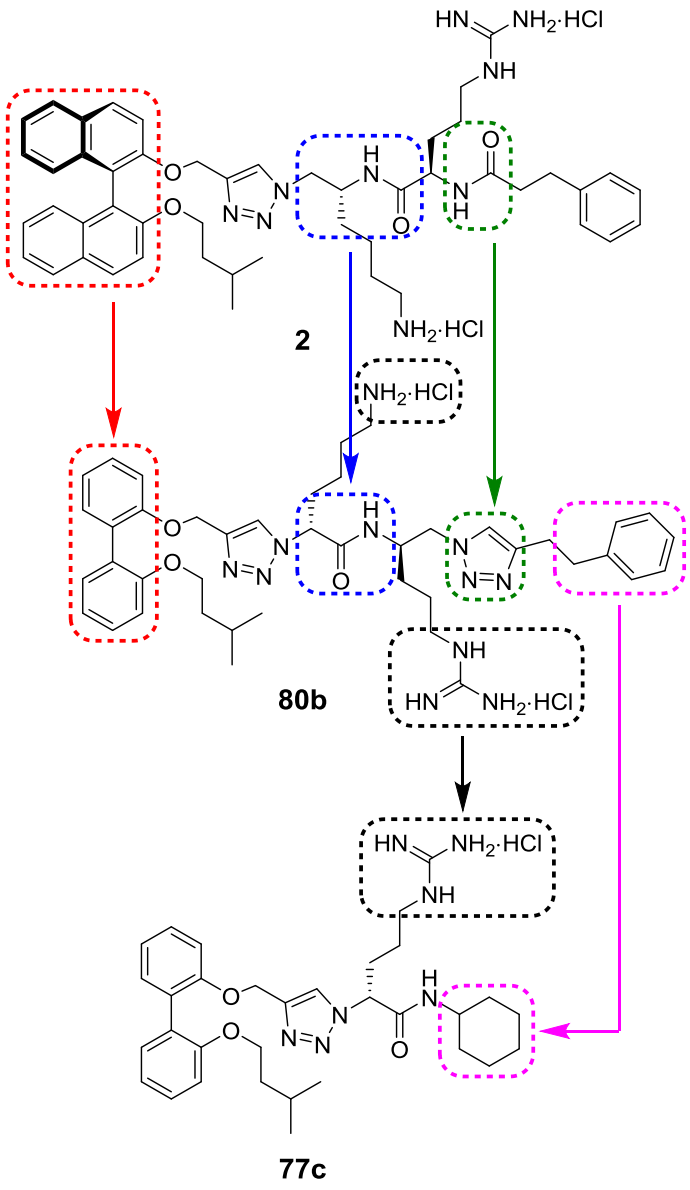

Figure 3.4 – Diagram showing the structural modifications that were investigated: biphenyl core substitution (red), peptide bond orientation (blue), peptidomimetic 1,2,3-triazole incorporation (green), amino acid residue variation (black) and hydrophobic termini variation (magenta).

The addition of a second triazole moiety (green arrow in Figure 3.4) was also key for conferring Gram-negative activity; a biphenyl analogue of lead compound **2** (i.e. compound **73**) was not active against four of the five Gram-negative bacteria tested but the addition of

a second terminal triazole moiety gave a compound (i.e. **68a**) that was active against all the Gram-negative bacteria tested (Tables 3.5 and 3.6).

Interestingly, derivatives **85a-c** did not contain a terminal triazole moiety nor a biphenyl aromatic core, yet these derivatives still exhibited some Gram-negative activity with MIC values ranging from 8 μg/mL to > 32 μg/mL – see Table 3.6.

Compounds that contained the more flexible termini (e.g. phenethyl compared to benzyl derivatives) exhibited slightly better antibacterial activity; for example, compound **68b** (phenethyl derivative) was approximately 2 – 4 times more active than its corresponding benzyl analogue (compound **68a** – Tables 3.2 and 3.5) against most of the bacteria tested. The same was true for the cyclohexyl (Cy) and cyclohexylmethyl (CH_2Cy) derivatives; the more flexible CH_2Cy termini generally gave more active derivatives (e.g. compare compounds **80c** and **80d** in Tables 3.3 and 3.6). This increase in activity is likely due to the flexible termini's ability to adopt more conformations and therefore, there is an increased chance for a more active conformation to be achieved.

The relative positioning of the arginine and lysine amino acid residues in the peptide backbone was found to have a notable influence over the antibacterial efficacy of the molecules. For example, when the order of the two cationic amino acids was switched in compounds **68a-c** to give compounds **69a-c**, there was a loss of antibacterial activity against *C. difficile* (e.g. MIC = 4 μg/mL to 32 μg/mL – see Table 3.2). In the Series B analogues, the same alteration in amino acid order led to an increase in antibacterial efficacy against *C. difficile* for some derivatives (see compounds **80c-d** and **81c-d –** Table 3.3). It was concluded

that the relative orientation of the cationic amino acid residues was important but predicting the result from such structural changes was not possible.

3.2.4 – Mechanism of action

Minimum bactericidal concentration (MBC) values were also recorded for the bacterial species tested at UWA. The MBC data was not included because most compounds exhibited MBC values that were more or less congruent with the observed MIC values; this is indicative of a bactericidal mechanism, as there is little variation between inhibition of cell growth and cell death. Various studies[113-116] have previously implicated membrane depolarization as a likely mechanism for the antibacterial activity of many cationic peptide derivatives. Lysis of the cellular membrane is thought to be achieved by aggregation of the amphipathic compounds on and in the membrane which results in pore formation.[113, 116] The electrochemical gradient that drives cellular biological processes becomes disrupted and this results in cell death.[113] Such a mechanism of action for the biarylpeptide derivatives would explain the lack of disparity between the observed MIC and MBC values. A membrane depolarization mechanism would also explain the increased activity seen with compounds having two cationic amino acid side chains compared to a single cationic side chain, because these moieties are necessary for electrostatic attraction to the anionic bacterial membrane and for amphipathic pore formation *via* molecular aggregation.[115] While the data supports a membrane-based mechanism, it does not rule out the possibility of an intracellular target. Further biological testing (e.g. a membrane depolarization assay) is necessary before any definite conclusions can be made regarding the mechanism of action of these compounds.

3.2.5 – Cytotoxicity assay results

The synthesized compounds were screened for any partial cytotoxicity by testing at the same concentration range that was used for MIC analysis at CO-ADD (≤ 32 μg/mL). Compounds are normally tested for cytotoxicity at much higher concentrations; this low-concentration testing allows for the identification of a CC_{50} value (i.e. the concentration which is cytotoxic to 50% of cells) through curve-fitting and extrapolation of the low-concentration cytotoxicity data. Some compounds did not exhibit significant cytotoxicity at these low concentrations and therefore curve fitting was not possible; a CC_{50} value could not be extrapolated from the data – these compounds have CC_{50} values listed as > 32 μg/mL as they do not exhibit significant cytotoxicity at the tested concentrations. Cytotoxicity assays were completed in duplicate and the lower CC_{50} values are reported in Tables 3.5 and 3.6 (see Tables B2.1 – B2.9 in Appendix B for a set of the cytotoxicity assay data with corresponding structures).

No definitive observable correlations could be drawn between a compound's measured cytotoxicity and its antibacterial efficacy from the data set. The majority of compounds displayed some level of cytotoxicity; only four scaffold types had no cytotoxic derivatives (compounds **70a-b**, **81a-d**, **83a-b** and **85a-c**). Most notably, the mono-cationic derivatives (Series A1 and B1) seemed to exhibit the most significant cytotoxicity; compound **64c** had the strongest observed cytotoxicity with a CC_{50} value of 4.7 μg/mL. Unfortunately, many of the identified lead compounds exhibited some level of cytotoxicity, for example compound **80b** had an observed CC_{50} value of 16.4 μg/mL. Importantly, some of the identified lead compounds (e.g. compound **68d**) failed to exhibit any cytotoxicity at concentrations up to 32 μg/mL (i.e. well above the compound's observed MIC value of 4 μg/mL against *C. difficile*).

Although cytotoxicity is not as important for topical or gastrointestinal (i.e. non-systemic) antibiotic formulations, compounds that exhibited limited or no cytotoxicity were certainly preferred. Previous research[69] has shown a positive correlation between cytotoxicity (as measured by haemolysis) and antibacterial efficacy in the binaphthyltriazole derivatives; compounds with reduced antibacterial efficacy exhibited reduced haemolysis. Such a correlation could be explained if the binaphthylpeptide derivatives exhibit their activity through a membrane depolarization mechanism, like other antimicrobial peptides.[114, 116] In this study, both highly active and less active antibacterial derivatives were found to exhibit CC_{50} values across the range of measured concentrations. While tentative positive correlations were seen when comparing a few individual compounds, there was no consistency amongst the wider set of recorded data. Furthermore, different derivatives of a single scaffold were found to vary in their cytotoxicities; for example, compound set **68a-d** (Series A2) had two derivatives that were non-cytotoxic and two derivatives that exhibited cytotoxic CC_{50} values ($\leq$ 32 μg/mL). A compound's cytotoxicity could not be gauged by the nature of its termini; a particular terminus might cause cytotoxicity in one scaffold, but be non-cytotoxic in another scaffold (e.g. the phenethyl terminus occurs in the cytotoxic compound **69b** and in the non-cytotoxic compound **68b –** Table 3.5).

3.3 – *In vivo* assay: murine model of CDI

3.3.1 – General methodology

The murine model of *C. difficile* infection involved pretreating cohorts of five mice with an antibiotic cocktail prior to infection *via* oral gavage with hypervirulent M7404 *C. difficile* spores; this helped to eliminate the commensal GI microbiota and allowed the *C. difficile* infection to flourish. The infection was allowed to incubate for 12 h before the trial

drugs were administered every 12 h for five days. The mice received a compound dose of 2.5 mg (i.e. 100 mg/kg for an average 25 g mouse) administered in a solvent mixture of DMSO/H_2O (1:9) at each 12 h dosing interval. The mice were weighed daily: if a mouse lost ≥ 10% of its body weight in the first 24 h (or ≥ 15% thereafter), then the infection was obviously proliferating and the mouse was removed from the trial and culled for ethical reasons. The overall survival rate for each drug cohort was used as a measure of drug's effectiveness. The latest murine trial also incorporated the use of physiological parameter scores (like faecal consistency scores and cage appearance scores) as other measures of the drug's efficacy. The full experimental methodology and relevant data for the *in vivo* CDI model can be found in Section 6.4.

3.3.2 – Preliminary trials

Lead compound **2** had been previously synthesized on larger scale[69] (~700 mg) and subjected to an *in vivo* mouse model of CDI at Monash University (with four other binaphthylpeptide derivatives, including lead compound **1**).[71] This initial trial attempted to administer the compounds *via* the drinking water; unfortunately, the mice refused to drink the adulterated water, which ruined the trial results (as the mice were not consuming enough drug and they also became dehydrated and lost weight).

Two compounds were selected (including lead compound **2**) and then subjected to a second CDI mouse model trial wherein oral gavage was utilized for compound administration (*via* a 10% v/v DMSO/H_2O vehicle). These preliminary trials saw a 60% survival rate (three out of five mice) for lead compound **2** compared with a 100% survival rate for the control drug (vancomycin).[71] These results were promising but a new problem was observed; the other tested compound was quite difficult to administer by oral gavage, as it precipitated and

flocculated out of solution almost immediately upon dilution of the compound/DMSO stock solution with water. Despite the initial promising results, it was decided to revisit the CDI murine model after addressing this poor solubility issue (see Section 3.4.1).

3.3.3 – Secondary trial

Four of the synthesized compounds (**68c-d**, **77c** and **87a** – Figure 3.5) were selected for a CDI mouse model trial due to their promising antibacterial activities against *C. difficile* and their varying solubility profiles (see Section 3.4.1).

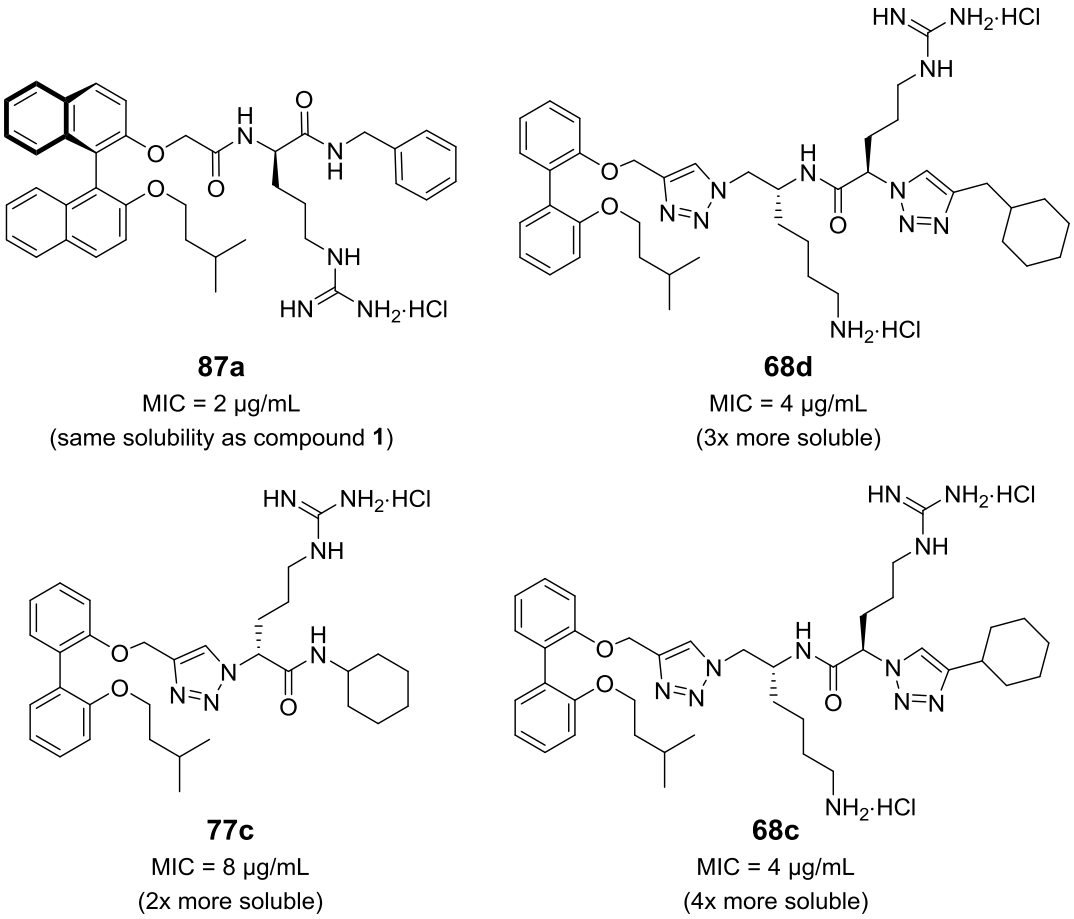

Figure 3.5 – Structures of the four compounds selected for testing in the murine model of CDI. Their MIC values against *C. difficile* and their solubilities (relative to prototypical compound **1**) are displayed.

Due to solubility issues and administration difficulties during previous trials, Andrew Tague attended Monash University to ensure the complete solubilization, proper dilution and administration of the drugs during the CDI murine model.

Unfortunately, none of the compounds fully protected the mice and all mice in the secondary trial had to be culled by 42 h due to disease weight loss (see Figure 3.6). Twenty-four hours after infection with *C. difficile* spores, only one of the four tested compounds (i.e. compound **77c**) displayed signs that it was protecting the mice from disease. The mice that were given compound **77c** lost the least amount of weight by 24 h (Figure 3.7) and they also had the least diarrhoea (as shown by the faecal consistency and cage appearance scores – see Figures 3.8 and 3.9). Furthermore, these mice looked physically healthier than the other three cohorts (as shown by physiological appearance scores – see Figure 3.10). The mice that were given drug **77c** (red line in Figure 3.6) exhibited an 80% (four out of five) survival rate until 42 h, compared with a 40% survival rate in the DMSO control cage group (blue line) until 42 h. Despite being the most active derivative against *C. difficile in vitro*, compound **87a** appeared to make the disease worse; these mice had to be culled by 24 h due to weight loss and disease progression.

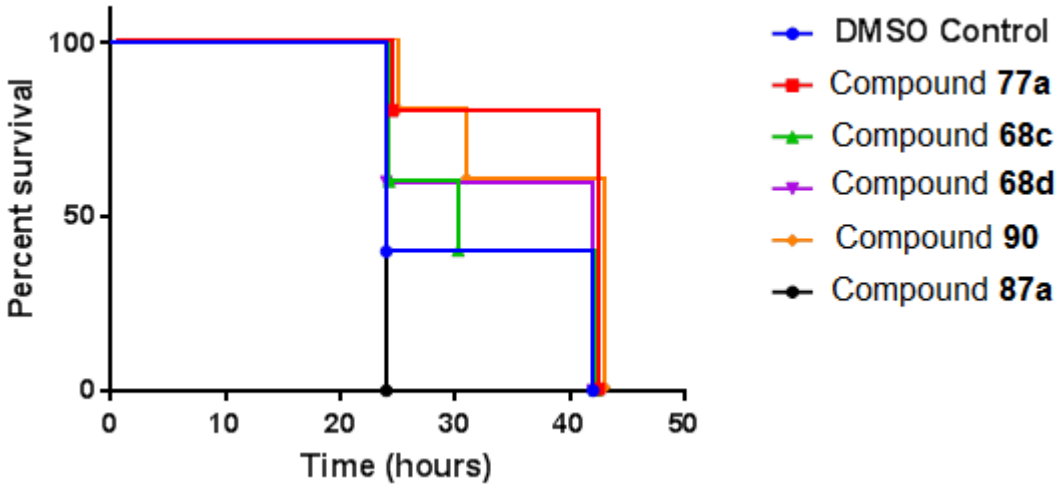

Figure 3.6 – Kaplan-Meier survival curve for the *in vivo* CDI mouse trial. Compound **90** (orange) was made by a current PhD student (Muni Kumar Mahadari) who is continuing the biarylpeptide research.

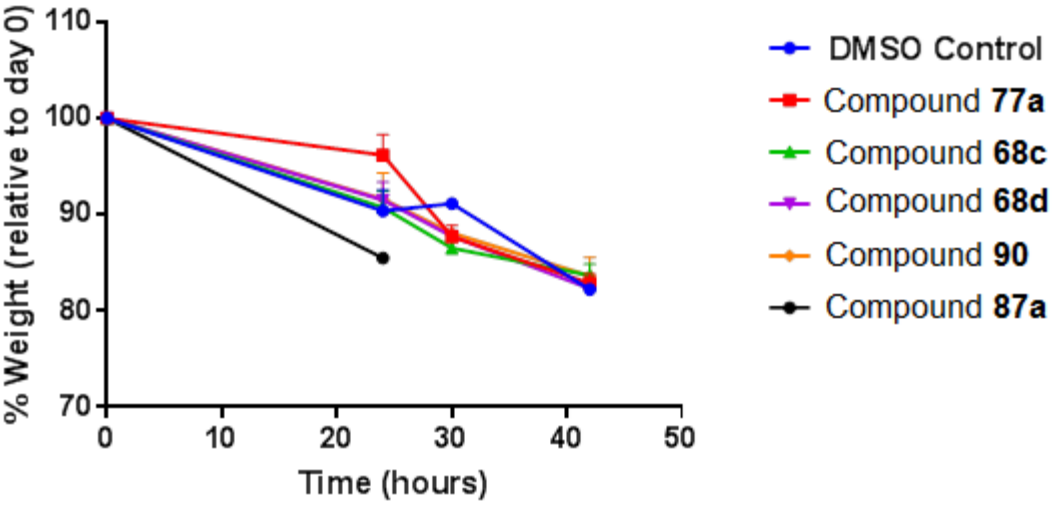

Figure 3.7 – Percentage weight loss for the various compound cohorts in the *in vivo* CDI mouse model.

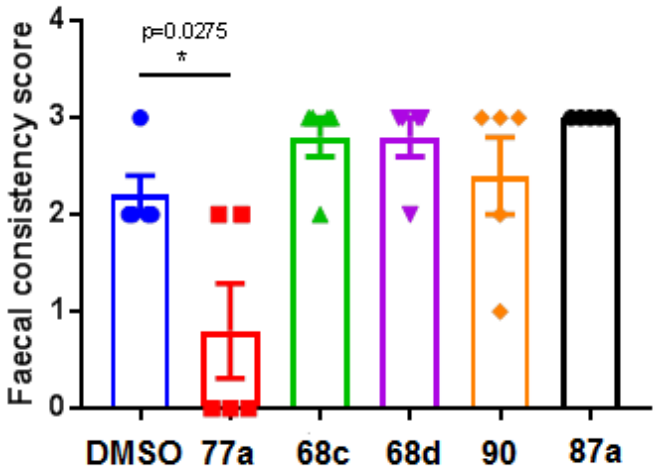

Figure 3.8 – Faecal consistency scores for the various compound cohorts in the *in vivo* CDI mouse model.

Score	Faecal Consistency
0	Normal stool: solid stool that is firm when subjected to pressure with forceps. Mouse has no sign of soiling around the anus and passes the stool quickly and easily.
1	Mildly soft stool: formed stools that appear moist on the outside and have a slightly sticky consistency. Stools will easily submit to pressure applied with forceps. Mouse has no sign of soiling around the anus, but passes faeces quickly and easily.
2	Moderately soft stool: irregularly formed stools that do not hold a normal shape. Stool appears very moist and is difficult to pick up with forceps. Mouse has some signs of soiling around anus and takes a longer than normal time to pass the stool.
3	Diarrhoea: stool has no form and/or has a mucous-like liquid appearance with minimal solid present. Considerable soiling around the anus and the fur around tail. Mouse takes a long time to pass stool if at all.

Table 3.7 – Faecal consistency (stool) scoring system.

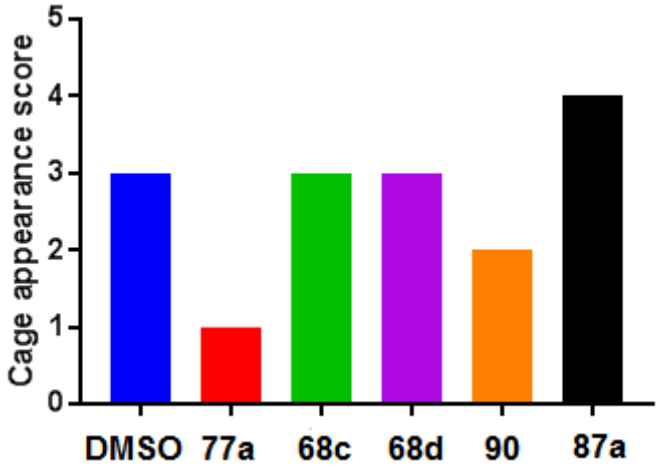

Figure 3.9 – Cage condition scores for the various compound cohorts in the *in vivo* CDI mouse model.

Score	Cage Condition (Diarrhoea)
0	Normal cage
1	Faeces stuck to the side of cage, but clean nest and sawdust.
2	Mildly soiled nest.
3	Moderately soiled nest.
4	Severely soiled nest

Table 3.8 – Cage condition scoring system.

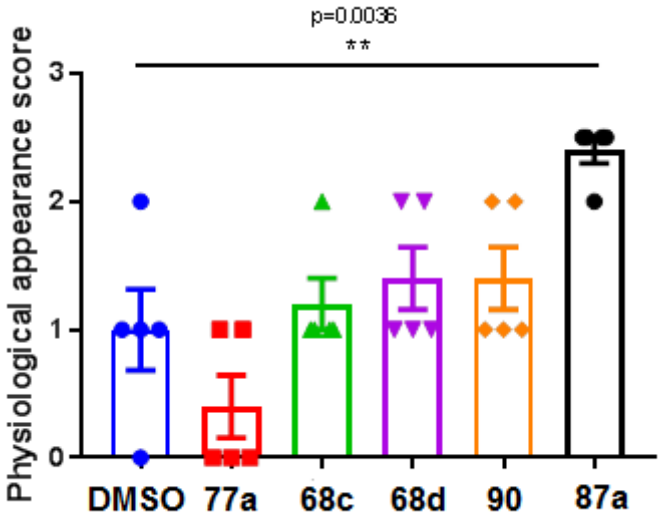

Figure 3.10 – Physiological appearance scores for the various compound cohorts in the *in vivo* CDI mouse model.

Score	Physiological Appearance
0	Normal activity, alertness, breathing and movement/gait.
1	Mouse shows signs of reduced grooming with coat starting to appear rough/scruffy with slight piloerection.
2	Mouse appears slightly hunched with mildly scruffy coat, but moves when the cage is disturbed. Possible diminished alertness, squinted eyes or lethargy.
3	Mouse has isolated itself from cage mates, displays hunched posture and unkempt coat. Mouse does not move when cage is disrupted and has little response to external environment or handling. Possible laboured breathing or eye discharge.

Table 3.9 – Physiological appearance scoring system.

Compound **77c** displayed some promising activity, despite not completely protecting the mice from disease as per the control drug (e.g. vancomycin exhibits a 100% survival rate until trial completion). The compound (**77c**) obviously delayed the onset and severity of the *C. difficile* infection, as measured by multiple physiological parameters. As predicted by their measured solubility parameters, compounds **77c** and **87a** exhibited the least solubility during the *in vivo* CDI mouse trial, rapidly precipitating out of solution after dilution of the DMSO stock solution with water. The insoluble nature of compound **77c** meant that the mice were not receiving the full target dosage (i.e. 100 mg/kg); therefore, compound **77c** will likely be re-trialed with a different drug administration method (possibly in food). By administering the drug in food to each mouse separately, we can ensure the mice will receive a full dose of the drug.

3.4 – Pharmacology experiments

3.4.1 – Comparative solubility assay

Some of the previous binaphthylpeptide derivatives were mostly insoluble in the 10% DMSO/H_2O mixture used in the mouse model of CDI; therefore, a comparative solubility assay was developed to ascertain the relative solubilities of the synthesized compounds. Knowledge of their solubilities was helpful for selecting compounds that would work well in the mouse model of CDI.

Lead compound **1** was used as the prototype molecule and all other compounds were compared to this compound. The compound of interest (5.0 mg) was fully dissolved in DMSO (50 μL) and then H_2O aliquots (5 μL) were added with adequate manual agitation in between additions. Addition of H_2O was continued until a persistent turbidity and cloudiness was apparent that did not fade after agitation. Compound **1** precipitated after the addition of

15 μL H_2O; compounds that required twice as much water (i.e. 30 μL) than compound **1** to precipitate from solution are effectively two times more soluble than compound **1** (i.e. solubility ratio = 2). This comparative solubility ratio was utilized to measure a compound's relative solubility and it thus allowed for comparison between multiple similar compounds.

The solubility assay was performed on a varied sample of the synthesized compounds to ascertain which structural elements are beneficial for solubility (Table 3.10).

Solubility Assay Data

Compound	**H_2O ppt. vol** (μL)	**Solubility Ratio** (Compound : compound **1**)	**CLogP**
1	15	1	7.47
2	45	3	5.76
64a	>300 **(NP)**	>20 **(NP)**	4.97
65c	65	4.33	4.26
66c	20	1.33	6.61
68b	35	2.33	3.89
68c	60	4	4.07
68d	45	3	4.6
69c	30	2	4.07
70a	30	2	6.24
73	15	1	3.02
76d	>200 **(NP)**	>13.3 **(NP)**	5.81
77c	30	2	3.77
80c	30	2	4.07
81d	55	3.67	4.60
83b	15	1	6.94
87a	15	1	5.82

Table 3.10 – Comparative solubility assay data and CLogP values for selected compounds. **NP** = No precipitation observed.

See Tables B3.1 – B3.6 in Appendix B for a set of the solubility assay data with the corresponding compound structures. The CLogP values for the tested compounds are also

included in the solubility tables; unfortunately, no correlation between a compound's CLogP value and its measured solubility was observed.

As expected, the biphenyl derivatives were much more soluble than their corresponding binaphthyl analogues – for example, the Series A1 biphenyl derivative **65c** is over three times more soluble than its binaphthyl analogue **66c** (Table 3.10). This effect is further exemplified by the binaphthyl derivative **83b** from Series B2 – the corresponding biphenyl analogue **81d** is almost four times more soluble (Table 3.10). Compounds that contained a single lysine amino acid side-chain were found to be substantially more soluble than the corresponding arginine containing analogues. Both of the single lysine derivatives (compounds **64a** and **76d**) tested in the solubility assay were so soluble that they failed to precipitate during the experiment. They were shown to be at least five to ten times more soluble than similar mono-arginine derivatives (e.g. compounds **65c** and **77c**). Furthermore, changing the order of the amino acid residues for dicationic derivatives did have an impact on solubility; for example, compound **68c** (Series A2 – Lys-Arg orientation) was two times more soluble than the corresponding Arg-Lys isomer **69c –** see Table 3.10. When this same swap in amino acid order was performed in Series B2, the opposite result occurred; swapping a Lys-Arg orientation for an Arg-Lys pattern resulted in an *increase* in solubility (see Table B3.5 in Appendix B). Therefore, no one particular orientation of amino acid residues was always found to give rise to more soluble compounds than another; this is likely because the solubility was reliant on multiple complex factors (e.g. scaffold shape, internal hydrogen bonding, solvent effects and conformation).

Additionally, the more flexible hydrocarbon termini (i.e. Cy and CH_2Cy) were generally found to be more soluble than the aromatic termini (Bn and PhEt) – as seen in Table 3.10;

the more flexible hydrocarbon derivatives may be able to adopt more soluble conformations than the aromatic derivatives. There was no observable difference in solubility between the Series A and Series B peptide orientations. Both Series A and B derivatives were found to exhibit a range of various solubilities; neither series was generally more soluble than the other.

The solubility ratio data allowed for the selection of compounds for the *in vivo* mouse model of CDI with varying solubilities; compounds with a range of solubilities (Figure 3.5 in Section 3.3.3 and Table 3.11) were chosen so that the effect of solubility on the drug's administration, efficacy and pharmacokinetic parameters could be observed. There was a direct correlation between a compound's solubility ratio and the compound's propensity to precipitate during dilution with H_2O (Table 3.11).

Compound	**Solubility Ratio (Compound / Compound 1)**	**Solubility in DMSO/H_2O (9:1)**
1	**1**	**-**
87a	**1**	**Precipitated**
77c	**2**	**Precipitated**
68d	**3**	**Homogenous suspension**
68c	**4**	**Homogenous solution**

Table 3.11 – The selected compounds for the *in vivo* CDI mouse model are displayed with their corresponding solubility ratio and observed solubility in 10% DMSO/H_2O.

The compound with the worst solubility ratio (i.e. **87a**) was also the compound that exhibited the most precipitation and flocculation (making administration by oral gavage difficult); the compound produced a thick precipitate that stuck to the sides of the vial after dilution with H_2O. Compound **68c** (which had the largest solubility ratio) remained as a homogenous, lightly opaque suspension for the entire 30 min prior to dosing. Compounds required a

solubility ratio of three or greater to prevent immediate precipitation and flocculation of the compound after dilution of the DMSO stock solution with H_2O (Table 3.11).

There did not appear to be a correlation between solubility and compound efficacy in the *in vivo* model; compound **77c** was the second least soluble derivative but it displayed the best efficacy of the compounds tested in the recent *in vivo* model. Mouse blood and faeces from the recent *in vivo* CDI mouse model will be analyzed for the presence of drug (study yet to be performed); by comparing this data to the solubility data, the optimum solubility to avoid systemic absorption may be identified.

3.4.2 – Pharmacokinetics assay

Since CDI chemotherapeutics are required to stay in the GI tract to treat the infection, systemic absorption of the antibiotic is not desirable. Therefore, pharmacokinetic analysis was performed on the blood and faeces of mice that were infected with *C. difficile* and treated with lead compound **2** in the preliminary CDI mouse model trials (see Section 3.3.2).

To ascertain the presence of compound **2** in the blood and faeces, an extraction/analysis procedure employing LRMS was developed and utilized (see Section 6.4.3 for the experimental methodology). The mouse blood was diluted with PBS and then extracted with CH_2Cl_2 (× 2); the faeces was extracted with CH_2Cl_2 (× 1). Concentration of the extracts and LRMS analysis of the residues revealed the presence of the drug (i.e. the doubly-protonated molecular ion, $m/2 = 421 = [M + 2H]^{2+}$) in the faeces; whereas no drug could be found in the blood. To ensure the procedure was viable, mouse blood from an untreated cohort was doped to achieve a final concentration of compound **2** equivalent to an average 25 g mouse absorbing 1% of the total dose into its bloodstream – the drug was readily detected in the doped mouse blood, verifying the validity of the extraction protocol.

These findings confirm that compound **2** was not absorbed systemically into the bloodstream by the mice; following oral administration, the drug clearly stayed in the GI tract (i.e. faeces), as was intended.

3.4.3 – HPLC purity assay

To ensure high sample purity for the *in vivo* CDI murine model, selected compounds **68c-d**, **77c** and **87a** (Figure 3.5, Section 3.3.3) were subjected to reverse-phase HPLC analysis with H_2O and acetonitrile (both with 0.1% v/v TFA) as the polar and non-polar solvents, respectively. A gradient elution from 0:100 → 100:0 (acetonitrile/H_2O) over 30 min was employed and compounds typically eluted between 20 – 25 min. The resultant purities for the four compounds are displayed in Table 3.12; all compounds were shown to be > 95% pure by HPLC (detected at 215 nm). The HPLC traces for compounds **68c-d**, **77c** and **87a** can be found in Section B4 of Appendix B.

Compound	**Purity by HPLC (215 nm)**
87a	**98.3%**
77c	**99.9%**
63c	**99.0%**
63d	**97.3%**

Table 3.12 – Purity of the compounds selected for the *in vivo* CDI mouse model (as measured by HPLC).

4.0 – NMR spectroscopy analysis: regioselectivity, rotamers and anomalies

4.1 – Background information

This chapter contains elaboration on the 1-D and 2-D NMR experiments that were conducted to verify the molecular structures of the synthesized compounds through NMR assignments and [^{1}H – ^{1}H] and [^{1}H – ^{13}C] correlations. During the characterization process, numerous unexpected NMR spectroscopy results (i.e. anomalies) were observed. Due to the volume of spectroscopic data and analysis required for NMR assignment, only the challenging and novel aspects of complete ^{1}H and ^{13}C NMR assignment confirmation and the associated spectroscopic anomalies will be discussed. Protons and carbons will be notated using the same assignment numbers that are given in the Experimental section (Section 6.0).

In particular, this chapter explores the 1,4-disubstitution regioselectivity of the 1,2,3-triazole formation *via* CuAAC and the following anomalous NMR spectroscopy findings: *syn*-rotamers of amides/carbamates/guanidines, guanidine tautomerization, missing ^{13}C NMR resonances (especially in the case of the 1,2,3-triazole-acid systems) and anomalous resonances in the ^{13}C and 2-D NMR spectra of alkynes **20** and **21**.

4.2 - Triazole orientation: proof of 1,4-regioselectivity

The regiochemistry of the installed 1,2,3-triazole moieties were unambiguously established *via* analysis of the gHMBC spectrum of compound **63a** (Figure C1.3 in Appendix C). The key observed [^{1}H – ^{13}C] correlations are depicted in Figure 4.1. Importantly, the ^{1}H NMR resonances

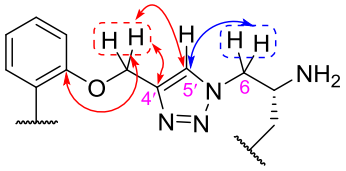

Figure 4.1 – Relevant portion of compound **63a**: significant gHMBC correlations are shown that prove the 1,4-regiochemistry of the 1,2,3-triazole moiety.

assigned to $H6_A$ and $H6_B$ displayed 3-bond gHMBC correlations with the ^{13}C NMR resonance assigned to C5′ (Figure 4.1 – blue arrow) but not with the resonance assigned to C4′. This indicated the orientation of the C(4′)=C(5′) double bond, relative to the H6 proton pair; the 1,4-regioisomer had been selectively formed. If the 1,5-regioisomer had been produced, a correlation between the H6 diastereotopic proton pair and the quaternary triazole carbon (C4′) would have been observed. These findings were congruent with the gHMBC correlations observed between the ^1H NMR resonance at δ 5.17 (-OCH_2-C4′)) and the ^{13}C NMR resonances assigned to both triazole carbons (C4′ and C5′). This evidence conclusively established the expected 1,4-regiochemistry of the 1,2,3-triazole ring.

4.3 – Rotamers

Single C–N bonds that are attached to an adjacent carbon–heteroatom double bond (e.g. C=O or C=N) are known to exhibit partial double bond characteristic due to the delocalization of the nitrogen's lone pair of electrons; this leads to restricted rotation of the C–N bond. If the energy barrier to rotation is high, two distinct rotameric conformations will be generated (i.e. *anti*- and *syn*-rotamers – Figure 4.2), with the *anti*-rotamer generally being preferred in secondary amides, carbamates, and guanidines due to steric considerations.[78, 117]

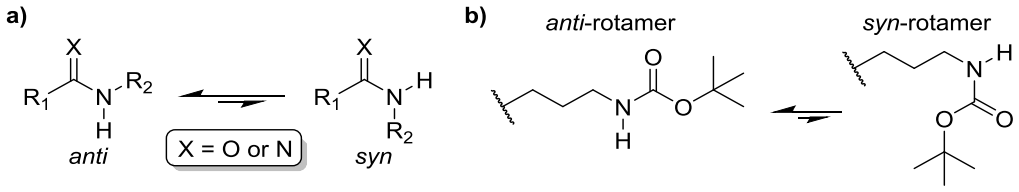

Figure 4.2 – **a)** Generic *anti*- and *syn*-rotamers **b)** *anti*- and *syn*-rotamers of the Boc-carbamate on the lysine side chain

The existence of amide, carbamate and guanidine rotamers (i.e. *anti* and *syn*) was evident by the presence of smaller, additional resonances in the ^1H and ^{13}C NMR spectra of various *N*-protected scaffolds and derivatives. These resonances were observed as additional resonance

"shoulders" or small satellite resonances. For example, compound **64c** displayed some anomalous ^{1}H NMR resonance shouldering and ^{13}C NMR resonance splitting (Figures C1.4 and C1.5 – Appendix C) due to the presence of *anti* and *syn N*-Cbz carbamate rotamers. While an accurate rotamer ratio could not be inferred from this example, one rotamer was most definitely dominant over the other (observed ratio *ca.* 9:1 – presumably *anti* : *syn*).

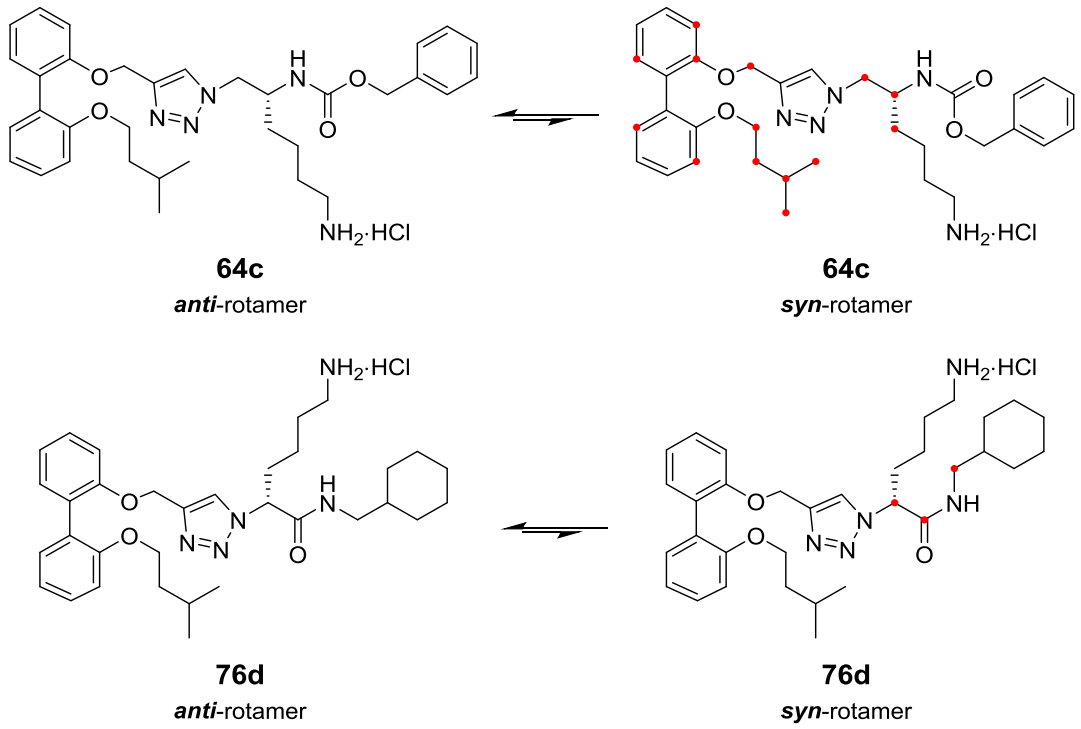

Figure 4.3 – Rotameric forms of compounds **64c** (rotameric carbamate) and **76d** (rotameric amide): carbons assigned to ^{13}C NMR resonances that exhibited splitting or shouldering are marked with red dots (·) on the *syn*-rotamers.

The presence of *syn*-rotamers in compound **64c** (Figure 4.3) was confirmed by utilizing DMSO-d_6 (known to disrupt hydrogen bonding[117]) and variable temperature (VT) NMR experiments (to increase the rate of bond rotation); compound **64c** was dissolved in DMSO-d_6 and subjected to ^{1}H and ^{13}C NMR spectroscopic analysis at both rt and 90 °C. The rotameric shoulder resonances present in the ^{13}C NMR spectrum of compound **64c** (when obtained in CD_3OD – Figure 4.4 – top blue spectrum) were notably reduced when the

spectrum was recorded in DMSO-d_6 at rt (Figure 4.4, middle green spectrum) – the minor *syn*-rotamer resonances became smaller, less apparent and they began to coalesce with the major anti-rotamer resonances. When the temperature was raised to 90 °C, the *syn*-rotamer resonances became virtually non-existent (Figure 4.4, bottom red spectrum).

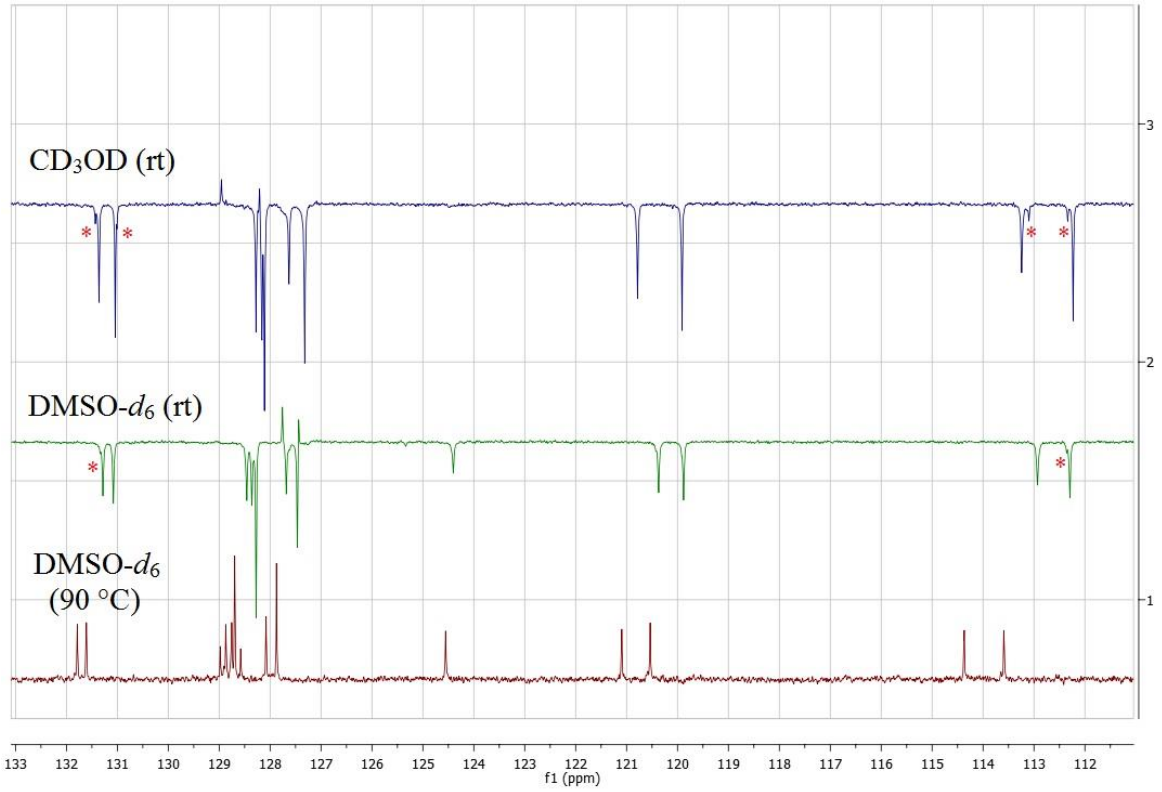

Figure 4.4 – ^{13}C/DEPT Q NMR spectra of compound **64c** recorded in CD_3OD at rt (blue), DMSO-d_6 at rt (green) and DMSO-d_6 at 90 °C (red). Visible rotameric shoulder peaks are marked with a red asterisk (*).

Reduction of the *syn*-rotamer resonances in the ^{13}C NMR spectra of compound **64c** is further exemplified by Figure C1.6 in Appendix C; the use of DMSO-d_6 and VT-NMR can be seen to decrease and almost eliminate the resonances attributed to the *syn*-rotamer. The use of hydrogen bond disruption by DMSO and increased temperature allowed for the positive identification of rotameric entities in the spectra of compound **64c** and various other biarylpeptide derivatives. In another example, compound **76d** was found to exhibit

shouldering and splitting of resonances in the ^{1}H and ^{13}C NMR spectra due to *anti*- and *syn*-amide rotamers (Figures C1.7 and C1.8, Appendix C). The three carbons comprising and adjacent to the terminal amide moiety (see Figure 4.3 – red dots) were assigned to resonances at 170.1 (C=O), 65.0 (-CH-C=O) and 47.2 (-CH_2Cy); these resonances all exhibited a rotameric partner (i.e. the resonance was split into two resonances) due to the presence of a stable *syn*-rotamer (Figure C1.8 in Appendix C).

In a few of the dicationic compounds, the appearance of rotameric resonances in the ^{1}H and ^{13}C NMR spectra was exacerbated by the presence of multiple moieties (e.g. amides, carbamates, guanidines and carboxylic acids) capable of forming or stabilizing rotameric forms. For example, ^{1}H NMR spectrum of scaffold acid **84** showed resonances for multiple rotamers due to the stabilizing influence of a terminal carboxylic acid group[117] – this moiety served to stabilize the s*yn*-rotamer forms of the various rotamer-capable functionalities that were present in the molecule (i.e. amides, carbamates and guanidines). At least two different forms of rotameric splitting were observed; resonances at δ 8.71 (amide NH) and 7.49 (triazole CH) in the ^{1}H NMR spectra of compound **84** exhibited splitting due to *anti*- and *syn*-rotamers at a molar ratio of 54:46 (determined by ^{1}H NMR integration) as seen in Figure C1.9, Appendix C. This splitting pattern (primary rotameric splitting) was also observed in the five resonances assigned to the *N*-Pbf protons (found between δ 3.00 – 1.40); they appeared as apparent doublets in the ^{1}H NMR spectrum of compound **84** (Figure C1.10 in Appendix C). A secondary rotameric splitting of the resonances assigned to the *N*-Pbf protons was also observed in the ^{1}H NMR spectrum of compound **84**; a molar ratio of 86:14 was determined by ^{1}H NMR integration for this secondary rotamer pattern. Interestingly, the small secondary rotameric resonances also exhibited the primary splitting at the molar ratio

of 54:46 (e.g. the secondary rotameric *N*-Pbf resonances appeared as small apparent doublets – see Figure C1.10 in Appendix C). Furthermore, the ^{13}C NMR spectrum of scaffold acid **84** displayed primary rotameric splitting for the majority of resonances observed with some secondary rotameric splitting evident as well (Figures C1.11 and C1.12 in Appendix C). DMSO-d_6 and VT-NMR were utilized to disrupt the rotamer stabilization but the rotameric resonances failed to disappear completely – resonances began to coalesce and move closer together with DMSO-d_6 and increased temperature, but rotamer-free ^{1}H or ^{13}C NMR spectra were not obtained due the strong stabilizing effect of the carboxylic acid moiety. The rotameric nature of compound **84** was proven by the resolution of split resonances in the ^{13}C NMR spectrum by the application of higher temperature; when compound **84** was placed in DMSO-d_6 and then heated to 90 °C, split resonances at approximately δ 157.5 (Pbf C_{Ar}), 153.5 (CAr2), and 18.5 (Pbf Ar$\underline{C}H_3$) were found to coalesce into three individual resonances (Figures C1.13 and C1.14 in Appendix C). Additionally, some of the secondary rotameric resonances in the ^{13}C NMR spectrum of compound **84** were found to resolve and even disappear after the utilization of DMSO-d_6 and VT-NMR (Figure C1.13 in Appendix C). Futhermore, the split resonance at δ 7.5 (triazole CH) in the ^{1}H NMR spectrum of compound **84** was also found to change splitting pattern with the application of DMSO-d_6 and VT-NMR (Figure C1.15 in Appendix C). These spectroscopic experiments were able to show the solvent and temperature dependence of the various ^{1}H and ^{13}C NMR resonances assigned to the rotameric *syn*-conformers in the spectra of the biarylpeptide derivatives.

The stabilization of *syn*-amide and *syn*-carbamate rotamers by carboxylic acids is a well understood phenomenon.[117] Rotamer stabilization can occur through either inter- or intra-molecular hydrogen bonding to any dual hydrogen bond donor-acceptor (e.g. a

carboxylic acid, carbamate or guanidine – see Figure 4.5); the biarylpeptide derivatives exhibit a predilection for such rotameric stabilization due to their flexible scaffold and numerous heteroatoms capable of accepting and donating hydrogen bonds. The ability of a molecule to simultaneously accept and donate hydrogen bonds has been shown to aid stabilization of the normally non-existent *syn*-rotamer in carbamates.[117-118] Therefore, the possible hydrogen bonding arrangements (Figure 4.5) were studied and found to exhibit the correct potential orientation for rotamer stabilization.

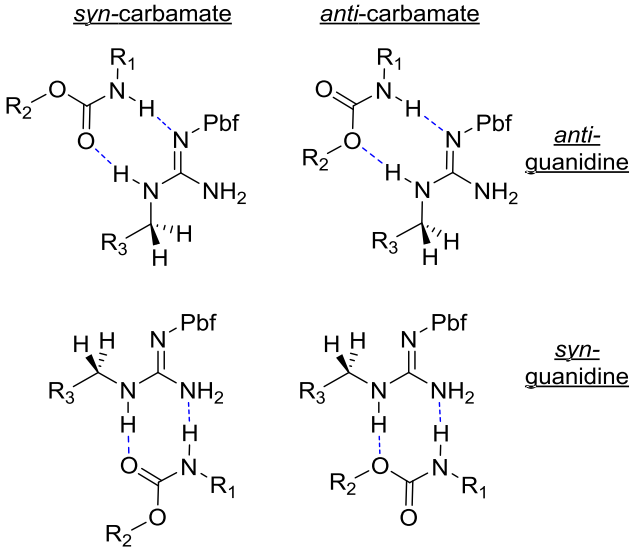

Figure 4.5 – Potential inter- or intra-molecular hydrogen bonding arrangements between the different rotamers (*anti* or *syn*) of the carbamate and guanidine groups.

In summary, the presence of *syn*-rotamers were evident in both the ^{1}H and ^{13}C NMR spectra of various biarylpeptide derivatives. These anomalies were investigated by extensive NMR experiments utilizing DMSO-d_6 and VT-NMR. The results of these experiments indicated the likely stabilization of *syn*-rotamers by hydrogen bonding.

4.4 – Guanidine tautomerization

In the previous published ^{1}H NMR assignments for *N*-Pbf protected binaphthylpeptides,[63-67] the three guanidino protons were always assigned to a single broad resonance around δ 6.50. Analysis of the ^{1}H NMR spectra of *N*-Pbf protected biarylpeptide derivatives found that although a single broad resonance for the guanidine protons (3H) was sometimes observed, it often contained a 'shoulder' adjacent to the main peak. Furthermore, depending on compound concentration (which affects the chemical shifts of exchangeable nitrogen protons[119]) and/or the utilized NMR solvent, the 'shoulder' would resolve completely, resulting in two distinct resonances (i.e. a 1H and 2H resonance – see Figure C1.16 in Appendix C). Reports on the tautomerization of guanidine compounds revealed that guanidine moieties are subject to different tautomeric forms depending on the attached substituents.[120] In the presence of a strongly electron-withdrawing substituent (e.g. a *N*-Pbf group), disubstituted guanidines will tautomerize such that the double-bond is located on the nitrogen to which the electron-withdrawing group is attached (Figure 4.6 – structure **A**).[120]

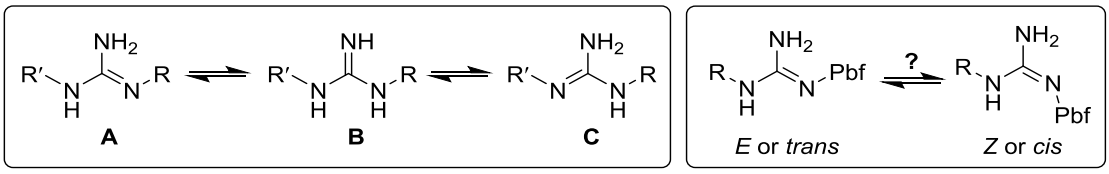

Figure 4.6 – (**Left**) Tautomerization of disubstituted guanidines: if R = electron withdrawing group, then tautomer **A** is preferred.[120] (**Right**) Potential *E* and *Z* isomers of the guanidine double bond.

The electronic preference for structure **A** (Figure 4.6 – left) readily explains the observed 2:1 split seen in the resonances assigned to the guanidino protons. The two resonances are often degenerate, hence the previous published assignments as a single resonance. Additionally, the presence of the *N*-Pbf imine allowed for the possibility of two isomers (*E* or *Z*) as seen in Figure 4.6 (right); it is currently unknown whether the compound exists as one isomer or a

mixture. Steric considerations dictate that the *E*-isomer would be energetically favoured, but there is yet no experimental evidence to support this statement.

4.5 – Missing ^{13}C NMR resonances

4.5.1 – Resonances assigned to the 1,2,3 triazole carbons

Previous research[59, 69] has shown that the final mono- or dihydrochloride salt products do not give adequate NMR spectra (i.e. broad resonances are observed) when $CDCl_3$ is used as the solvent; therefore, the final hydrochloride salts were dissolved in CD_3OD for NMR spectroscopic analysis. Unfortunately, a large number of the synthesized biaryltriazole derivatives exhibited anomalous or missing ^{13}C NMR resonances for the 1,2,3-triazole carbons. Many quaternary triazole carbons were not observed in the ^{13}C NMR spectrum and their presence could only be ascertained by positive gHMBC correlations. The methine triazole carbons were also occasionally afflicted, exhibiting a weak, broad resonance or no observable resonance at all; gHSQC and gHMBC correlations were utilized to detect the presence of the methine triazole carbons.

For example, bis-triazole **68a** failed to display resonances in the ^{13}C NMR spectrum that could be assigned to any of the four triazole carbons (both quaternary and methine) – see Figure C1.17 in Appendix C. A resonance at δ 7.86 (2H) was assigned as the two degenerate triazole proton resonances (H5′ and Hα in Figure 4.8); this resonance exhibited gHSQC correlations with two missing ^{13}C NMR resonances at δ 126.4 (C5′) and 124.5 (Cα) – these correlations allowed for assignment of the triazole methine carbons (Figure C1.18 in Appendix C). ^{1}H NMR resonances at δ 5.11 (-OCH_2-C4') and 4.07 (-C$\underline{H}_2$Ph) were assigned to the two pairs of methylene protons directly attached to the quaternary triazole carbons. gHMBC correlations were observed between these methylene resonances at δ 5.11 and 4.07

and the other two missing ^{13}C NMR resonances at δ 145.7 (C4′) and 148.4 (Cβ), respectively; these correlations allowed for the positive identification of the quaternary triazole carbons (Figure C1.19 in Appendix C). The different gHMBC correlations that allowed for the identification and assignment of the missing ^{13}C NMR triazole resonances are displayed on compounds **68a** and **68b** in Figure 4.8.

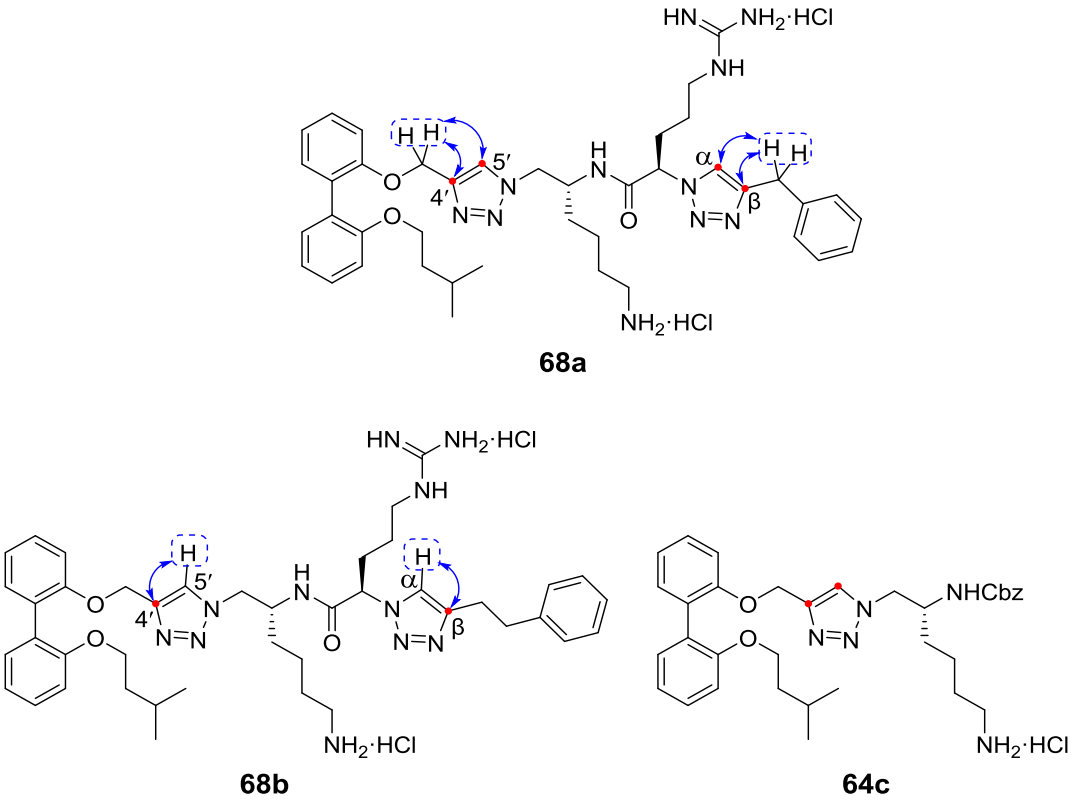

Figure 4.8 - Structures of compounds **68a**, **68b** and **64c**: carbons that could not be assigned to a visible ^{13}C NMR resonance are marked with red dots (·). The key gHMBC correlations that allowed for assignment are displayed with blue arrows. 2-D NMR spectroscopy could not be utilized to assign the triazole carbons in compound **64c** and DMSO-d_6 was ultimately required.

In another example, bis-triazole compound **68b** failed to display any resonances in the ^{13}C NMR spectrum that could be assigned to the two quaternary triazole carbons. Resonances at δ 7.94 and 7.88 in the ^{1}H NMR spectrum of compound **68b** were assigned to the two triazole protons (H5′ and Hα); these resonances displayed gHMBC correlations (Figure C1.20 in

Appendix C) with the two missing ^{13}C NMR resonances at δ 147.2 (Cβ) and 145.6 (C4′) – this evidence allowed for the positive assignment of the two quaternary triazole carbons, despite the lack of visible resonances in the ^{13}C NMR spectrum. Notably, the two methine triazole carbons were positively assigned to two weak, broadened resonances at δ 126.3 (C5′) and 125.0 (Cα) in the ^{13}C NMR spectrum; these assignments were confirmed by gHSQC correlations with the appropriate ^{1}H NMR resonances (Figure C1.21 in Appendix C).

In some derivatives lacking the appropriate ^{13}C NMR triazole resonances, prolonged gHMBC experiments (> 1 h) were not sufficient to detect the desired heterocorrelations. For example, *N*-Cbz analogue **64c** failed to exhibit ^{13}C NMR resonances that could be assigned to either of the triazole carbons (Figure 4.8). Furthermore, no gHMBC or gHSQC correlations could be observed that allowed for the assignment of these triazole carbons; the resonances for these carbons could not be observed when the spectrum was acquired in CD_3OD. When compound **64c** was subjected to ^{13}C NMR experiments in DMSO-d_6, the triazole carbons were easily assigned to resonances that appeared in the expected regions. Figure C1.22 in Appendix C shows how the two distinct ^{13}C NMR resonances assigned to the triazole carbons were not present in the spectrum acquired in CD_3OD, but they can be clearly seen in the spectrum acquired in DMSO-d_6. The use of DMSO-d_6 as an NMR solvent obviated the need for extensive 2-D NMR experiments to determine triazole carbon assignments. Compounds **64c**, **65c** and **66a** all required the use of DMSO-d_6 as a solvent for complete ^{13}C NMR characterization due to missing resonances in other solvents.

It is proposed that hydrogen bonding between the triazole moieties and other capable functionalities was the primary cause of the observed lack of key NMR resonances; for more information regarding this phenomenon, see Section 4.6.

4.5.2 – Trifluoromethyl (CF_3) derivatives

Two final Series B1 derivatives (compounds **76e** and **77e**) contained a terminal 4-CF_3-benzylamide moiety; in both molecules, the strong J_{CF} coupling (caused by the -CF_3 substituent) obscured the ^{13}C NMR resonances attributed to the *ipso* aromatic carbon and the -$\underline{C}F_3$ carbon itself. In the ^{13}C NMR spectrum of compound **76e**, the two expected quartet resonances (assigned as the carbons closest to the fluorine atoms, i.e. -$\underline{C}F_3$ and $\underline{C}$-CF_3) were each missing one of the outer quartet peaks. The strong J_{CF} coupling spread the weak quaternary ^{13}C NMR resonances over multiple lines (as quartets); thus, the resonance became even weaker and buried amongst the background noise. Furthermore, quaternary carbons do not experience the large Overhauser enhancement by proton decoupling that is experienced by protonated carbons, so they exhibit a notably weaker ^{13}C NMR resonance.[119]

Furthermore, the related and expected ^{13}C NMR quartet resonances (assigned to the -$\underline{C}F_3$ and $\underline{C}$-CF_3 carbons) in the spectrum of compound **77e** could not be observed *at all*; the already weak quaternary carbon resonances were distributed across a quartet resonance by the strong J_{CF} coupling – this created extremely weak resonances that were buried amongst the background noise. The presence of these two carbons could not be inferred from relevant 2-D NMR correlations because the quartet splitting and lack of Overhauser enhancement by proton decoupling resulted in correlations that were diffuse and non-observable. The presence of the attached trifluoromethyl moiety was clear from MS analysis and was inferred from the other observed aromatic resonances which displayed distinct J_{CF} coupling constants, multiplicity patterns and chemical shifts.

4.6 – Weak and non-observable NMR resonances in the 1,2,3-triazole-acid system

The triazole acid scaffolds synthesized for Series B1 (i.e. compounds **75a-d**) exhibited a lack of expected NMR resonances normally assigned to the triazole ring and the adjacent methine and carboxylic acid functionalities (Figure 4.9). The ^{1}H and ^{13}C NMR resonances associated with these moieties were observed as broad, weak resonances or not observed when the spectra were acquired in $CDCl_3$ or CD_3OD. The effect was most prominent in the ^{13}C NMR spectra, although some molecules exhibited anomalous resonances in the ^{1}H NMR spectra as well.

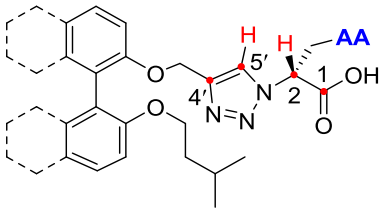

Figure 4.9 – General structure of scaffolds that exhibited weak or non-observable NMR resonances: the affected carbons and protons are marked with red (· or H).

For example, compound **75a** failed to exhibit ^{13}C NMR resonances that could be assigned to the affected carbons (red dots in Figure 4.9) when the spectrum was acquired in CD_3OD. The utilization of DMSO-d_6 and/or 2-D NMR was required for observation of these carbon resonances; when DMSO-d_6 was employed, three resonances appeared in the ^{13}C NMR spectrum of compound **75a** that were assigned to both triazole carbons (C4′ and C5′) and the carboxyl carbon (C1) (Figure C1.23 in Appendix C). The methine carbon (C2) could not be assigned to a resonance in the ^{13}C NMR spectrum of compound **75a**; however, the gHSQC spectrum (acquired in DMSO-d_6) displayed a correlation with a broad ^{1}H NMR resonance assigned as the methine proton (H2) – this allowed for assignment of the methine carbon

(C2). Interestingly, the downfield resonances assigned to the triazole proton (H5′) and methine proton (H2) were substantially broad when the spectrum was acquired in CD_3OD; swapping the solvent to DMSO-d_6 resulted in a sharper resonance that was assigned to the triazole proton (Figure C1.24 in Appendix C).

Additionally, compounds **75b-d** exhibited a similar lack of characteristic NMR resonances for the same moieties as compound **75a** (Figure 4.10); a combination of DMSO-d_6 and 2-D NMR spectroscopy was required for assignment of the missing carbon resonances in these compounds.

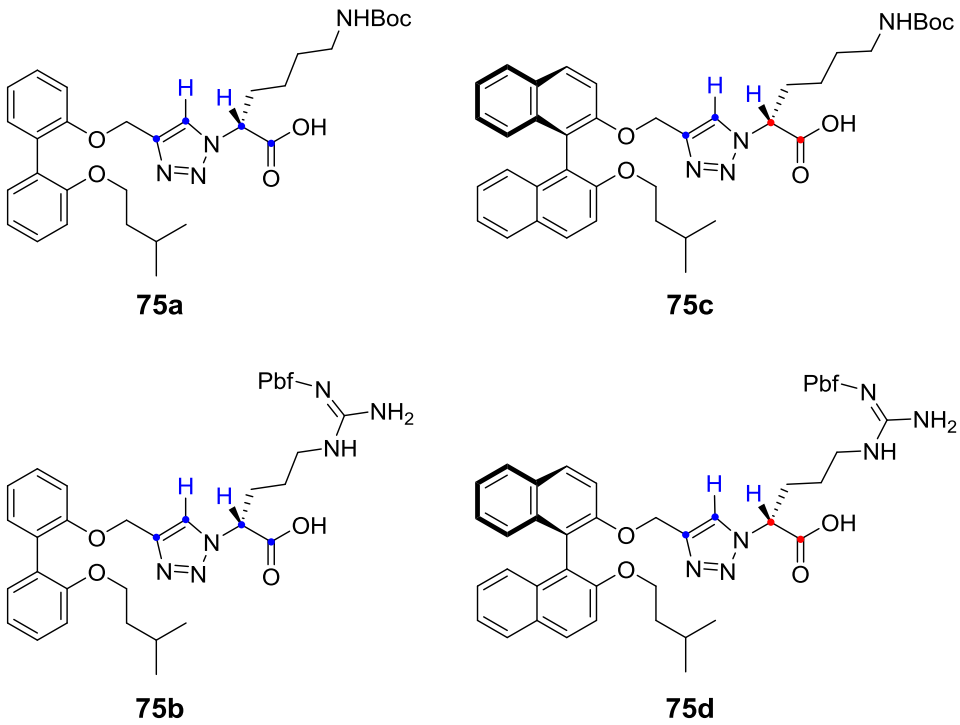

Figure 4.10 – Weak and non-observable NMR resonance assignments for compounds **75a-d**. Carbons that are marked with red (·) could not be assigned to a ^{13}C or 2-D NMR resonance. Carbons that are marked with blue (·) required DMSO-d_6 and/or 2-D NMR for assignment. Protons that are marked with blue (H) exhibited significant NMR resonance broadening.

For the binaphthyl analogues (**75b** and **75d**), the carboxyl (C1) and methine (C2) carbons could not be assigned to any resonances in the ^{13}C NMR spectra of these compounds, despite

the use of DMSO-d_6. Furthermore, these carbons could not be assigned *via* 2-D NMR correlations either.

The weak and non-observable NMR resonances assigned to the triazole-acid systems display parallels with the missing triazole ^{13}C NMR resonances (Section 4.5.1); both anomalies occurred most prominently in the hydrogen bonding solvent CD_3OD and the use of DMSO-d_6 ameliorated or eliminated any observed NMR deactivation phenomena. Therefore, it is proposed that the NMR effects were a result of hydrogen bonding involving the triazole moieties. In the case of missing resonances in simple 1,2,3-triazole systems (i.e. Section 4.5.1), it is likely that the triazole rings were hydrogen bonding to the solvent (or inter-/intra-molecularly with other hydrogen bonding moieties, e.g. amines or guanidines); this bonding resulted in electronic disturbances that influenced the magnetic spin relaxation of the triazole carbons (resulting in weak or non-observable resonances). In the case of the triazole-acid scaffolds **75a-d**, it is theorized that the carboxylic acid was intra-molecularly hydrogen bonding with the triazole moiety (Figure 4.11); this cyclic bonding would also likely result in electronic disturbances that could affect the NMR resonances of the triazole carbons (C4′ and C5′) and the adjacent carbons (C1 and C2). This proposed intramolecular hydrogen bonding could explain the weak and non-observable NMR resonances for scaffolds **75a-d**. The increase in weak/non-observable NMR resonances observed for the binaphthyl analogues **75c** and **75d** could be due to the binaphthyl group having a more extreme electronic effect on the triazole ring than the biphenyl ring system; this could allow for increased hydrogen bonding between the triazole and the carboxylic acid moieties – allowing for the observed increase in weak/non-observable NMR resonances (relative to the biphenyl analogues **75a** and **75b**).

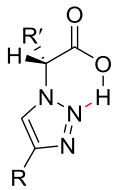

Figure 4.11 – Potential intramolecular hydrogen bonding (----) between the 1,2,3-triazole and the adjacent carboxylic acid moiety.

4.7 – Anomalous gHSQC correlations for alkynes

Precursor alkynes **20** and **21** both displayed anomalous DEPT Q resonances and gHSQC correlations that were assigned to the two alkyne carbons. For alkyne **21**, the DEPT Q ^{13}C NMR resonance and the gHSQC correlation assigned to the methine carbon (-C≡C-H) both exhibited polarities that corresponded to a methylene (CH_2) or quaternary carbon (Figure C1.25 in Appendix C). This unexpected anomalous occurrence was a result of the defined DEPT Q one-bond [^{1}H – ^{13}C] coupling constant frequency (usually set at 145 Hz).[119] Since the methine alkyne carbon exhibited a non-traditional one-bond [^{1}H – ^{13}C] coupling constant (approximately 250 Hz),[119] the parameter values utilized for determining carbon saturation (i.e. the number of C–H bonds) did not apply in this unique case. Furthermore, quaternary alkyne carbons (-C≡C-H) exhibit a two-bond [^{1}H – ^{13}C] coupling constant frequency around 50 Hz; this was sufficiently large to show as a weak correlation in the gHSQC spectrum (Figure C1.25 in Appendix C) but substantially different from the 145 Hz (leading to anomalous resonance/correlation polarities in the DEPT Q and gHSQC spectra).

5.0 – Conclusions and future directions

A diverse set of 62 novel antibacterial biaryl-peptidomimetic derivatives were designed and synthesized as part of an ongoing project into the development of novel antibiotic drugs and *C. difficile* chemotherapeutics. This array of compounds was realized through derivatization of 17 novel scaffolds *via* the installation of various hydrophobic termini. The scaffolds were achieved through implementation of a novel, modular multi-step synthesis that utilized 11 key building block precursors. The modular approach allowed for easy diversification and manipulation of the target scaffolds based upon the resultant SAR data.

The targeted compounds were designed to incorporate additional peptidomimetic 1,2,3-triazole moieties into the peptide backbone of the lead binaphthylpeptide compounds **2** and **6**; this potentially allowed for increased metabolic resistance to the peptidases and acidic conditions found in the GI tract, which is ideal for a CDI chemotherapeutic. Additionally, the binaphthyl aromatic core was replaced with a biphenyl core to attain increased solubility and antibacterial activity. Following synthesis and spectroscopic characterization, the compounds were subjected to antimicrobial and toxicity assays to screen for potential lead or hit compounds. The results of these assays were used to explore the SAR trends of the compounds and thus, to identify pharmacophore elements or other vital structural components necessary for both *C. difficile* antibacterial activity as well as broad-spectrum antibacterial activity.

All of the synthesized compounds exhibited some level of antibacterial activity; the least potent MIC value observed against *S. aureus* was 16 μg/mL, with the majority of compounds having MIC values ranging from 2 – 8 μg/mL. There was a general reduction in the

antibacterial efficacy (2 – 4 times less active) that was observed amongst the monocationic derivatives, relative to the dicationic compounds; this result was in agreement with previous findings.[59, 69] Despite this finding, the simple monocationic compound **77c** (Figure 5.1) was identified as having strong Gram-positive antibacterial potency, especially against *C. difficile*. Interestingly, the biphenyl bis-triazole derivatives (e.g. compound **80b**) were the only compounds that exhibited substantial broad-spectrum antibacterial activity against both Gram-positive and Gram-negative bacteria.

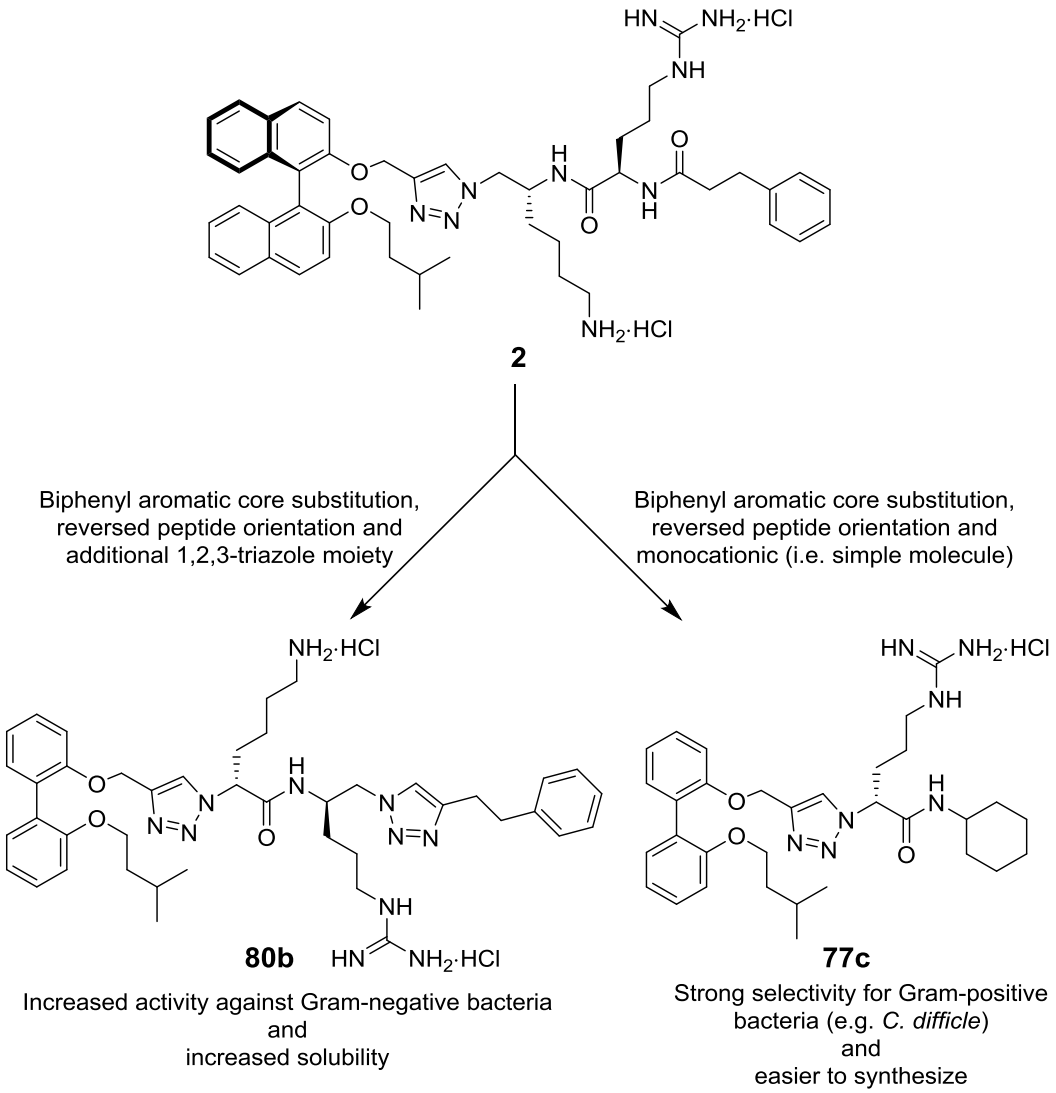

Figure 5.1 – Development of potential hit compounds **80b** and **77c** from lead compound **2**.

The biphenyl bis-triazole compound **80b** exhibited the strongest broad-spectrum antibacterial efficacy, but it did not exhibit strong activity against *C. difficile* – these two spectrums of action were not mutually inclusive. The addition of a biphenyl aromatic moiety led to increased compound solubility which often translated to a decrease in Gram-positive antibacterial activity, but an increase in antibacterial efficacy against Gram-negative bacteria. This increase in solubility and decrease in molecular size may allow the drugs to permeate the extra external membrane exhibited by Gram-negative bacteria.

As seen in Figure 5.1, the pursuit of novel antibacterial molecules from compound **2** led to the development of two distinct structural scaffolds (i.e. **80b** and **77c**) that both exhibited an increase in desirable traits for an antibacterial chemotherapeutic. Compound **80b** exhibited a notable increase in the overall Gram-negative antibacterial efficacy; this could allow the biarylpeptides to be investigated for use in the treatment of Gram-negative bacterial infections. Furthermore, compound **77c** exhibited an increase in selectivity for *C. difficile*; the molecule was also structurally simple and therefore, easier to synthesize.

Four compounds (**68b**, **68d**, **77c** and **87a**) were selected as potential hit compounds based upon their *in vitro* activities against *C. difficile*; they were synthesized on larger scale and used in an *in vivo* CDI mouse model at Monash University. Compound **77c** was identified as the best performer in the *in vivo* CDI mouse model; both mouse weight loss and disease progression were significantly slowed by compound **77c** during the administration of the trial. Compound **77c** has been selected for testing in a further *in vivo* CDI mouse model. Compound **77c** exhibited selectivity for Gram-positive bacteria – it was inactive against all of the Gram-negative bacteria that were tested. This selectivity could be reason for the drug's positive performance in the CDI mouse model; by not eliminating the commensal, Gram-

negative *Bacteroides* spp. and *E. coli*, compound **77c** was likely quite effective at selectively killing *C. difficile* without destroying the entire enteric microflora. The monocationic compound **77c** is a structurally simple molecule; large scale synthesis would be very cost effective, relative to the more complex CDI treatments available (e.g. vancomycin or fidaxomicin). If successful in further trials, the potential hit compound **77c** will be studied and possibly developed as a potential CDI chemotherapeutic. Larger cohort (i.e. sample) sizes are needed to confirm the observed *in vivo* CDI model results; a cohort size of five mice is indicative, but not conclusive. Larger sample sizes are needed to be statistically confident in the *in vivo* CDI model results; unfortunately, the administration of large *in vivo* CDI model is extremely labour intensive and costly, so more preliminary *in vivo* work needs to be done before such a trial could be conducted.

Furthermore, associated pharmacokinetic studies were performed as part of the *in vivo* CDI mouse model; the results confirmed the lack of systemic drug absorption by the mice, as was intended. A solubility assay was also developed and performed on selected compounds to ascertain the role of solubility in the efficacy and administration of the biarylpeptide derivatives. Future pharmacokinetic analysis will be performed on the recently tested derivatives (**68c-d**, **77c**, and **87a**) – i.e. blood and faeces analysis; the relationship between a compound's solubility and its systemic absorption will be investigated.

Numerous anomalies were observed during the analysis of the ^{1}H and ^{13}C NMR spectra of the various biarylpeptide derivatives (e.g. rotamers and some unique NMR properties); these anomalies were investigated in depth so as to ensure the correct characterization (and therefore structures and purities) of the compounds being synthesized. HPLC analysis was also utilized to further ensure compound purity and the lack of any diastereomer formation.

Further experiments are planned that will determine the mechanism of action for the biarylpeptide antibiotics; membrane depolarization assays utilizing permeable and non-permeable fluorescent dyes will be conducted at Monash University to ascertain whether the molecules exhibit bacterial membrane disruption as their mode of action. Determination of the mechanism of the action will allow for a more complete understanding of the antibiotic properties of the biarylpeptides; such knowledge could allow for mechanism-based molecular design. The lack of a formal target is a current limitation in regard to the molecular design. Future drug design and development will likely involve two target streams. One stream will focus on optimizing compound **77c** and other compounds that exhibit selectivity for Gram-positive bacteria, in hopes of achieving a novel CDI chemotherapeutic. The other research stream will likely focus on increasing compound solubility and Gram-negative antibacterial efficacy – this avenue will be pursued because there is a large, unmet medical need for novel medications that work against drug-resistant Gram-negative bacteria.[5, 13]

In summation, a total of 62 novel antibacterial compounds were synthesized and fully characterized as part of this project. The synthesis of these derivatives involved the synthesis of 104 compounds in total, i.e. 88 novel compounds and 16 known compounds A modular synthetic route to various novel biarylpeptide scaffolds was realized and the resultant synthetic derivatives represent a potential new direction for developing novel antibiotics for the treatment of CDI and other bacterial infections. The compounds synthesized and identified in this project are the subject of ongoing studies into the development of a novel CDI treatment. Therefore, the current and future chemical and biological research focused on these biarylpeptide derivatives will aim towards the advancement of an effective and potent CDI chemotherapeutic.

6.0 – Experimental

6.1 – General information

Synthesis

Unless stated otherwise, all solvents and chemicals were laboratory or reagent grade and were purchased from commercial sources. All chemicals were used as received. Water was purified *via* Millipore filtration prior to use. HOBt and propargyl bromide were purchased with added stabilizers (10% w/w H_2O and 20% w/w toluene, respectively); therefore, the quantities required for reactions were adjusted accordingly and are reflected in the reagent masses reported in the experimental (whereas the reported mmol quantities reflect the true quantity of chemical). All reactions were conducted under normal atmosphere and cold reaction temperatures were obtained by an ice bath (0 ºC) or ice/salt bath (–10 ºC). Heating of reactions was performed with a paraffin oil bath. Small quantities of liquid reagents were measured and added to reactions *via* syringe or autopipette. Unless otherwise noted, all filtrations were conducted as vacuum filtration through a sintered glass funnel (medium porosity). Vacuum filtration was achieved with the aid of a water aspirator. Solvent removal *via* concentration was performed on a rotary evaporator under reduced pressure. All solvent mixtures are expressed in terms of volume ratio (i.e. v/v). Thin layer chromatography (TLC) was performed on aluminium-backed SiO_2 gel plates (F_{254} grade - 0.20 mm thickness). Visualization was achieved with UV light, ninhydrin stain or cerium ammonium molybdate stain. Flash chromatography was performed on SiO_2 gel 60 with a positive air pressure. All synthesized compounds were dried under high vacuum (< 1 mbar) before determination of chemical yields and spectroscopic characterization.

Characterization and analysis

All novel precursors, scaffold intermediates and scaffolds were subjected to full spectroscopic characterization and assignment. All final derivatives were subjected to full spectroscopic characterization, but due to the sheer number of final scaffold derivatives, only one example derivative from each scaffold type was fully assigned. ^{1}H NMR spectra were recorded on a Bruker Avance 400 (400 MHz), a Varian VNMRS PS54 500 (500 MHz), a Varian Inova 500 (500 MHz) or a Varian Mercury 300 (300 MHz) NMR spectrometer. Chemical shifts are reported in ppm and were measured relative to the internal standard. Samples were dissolved in $CDCl_3$ (with TMS as the internal standard – 0.00 ppm), CD_3OD (solvent resonance as internal standard – 3.31 ppm) or DMSO-d_6 (solvent resonance as internal standard – 2.50 ppm). The ^{1}H NMR data is reported as follows: chemical shift, multiplicity (s = singlet, d = doublet, t = triplet, q = quartet, dt = doublet of triplets, m = multiplet, br = broad), coupling constants (Hz) and integration. ^{13}C NMR spectra were recorded on a Bruker Avance 400 (101 MHz), a Varian VNMRS PS54 500 (126 MHz), a Varian Inova 500 (126 MHz) or a Varian Mercury 300 (75 MHz) NMR spectrometer with complete ^{1}H decoupling. Chemical shifts are reported in ppm and were measured relative to the internal standard. Samples were dissolved in $CDCl_3$ (solvent resonance as the internal standard – 77.16 ppm), CD_3OD (solvent resonance as the internal standard – 49.20 ppm) or DMSO-d_6 (solvent resonance as internal standard – 39.50 ppm). Variable temperature NMR experiments were performed at 90 °C on the Bruker Avance 400 NMR spectrometer. ^{1}H and ^{13}C NMR signal assignments were confirmed by analysis of NMR experiments: APT, gCOSY, gHSQC, gHMBC, zTOCSY, NOESY and/or gHSQC-TOCSY. The abbreviations section defines all NMR experiment acronyms. Ambiguous degenerate carbon resonances

are marked with a single asterisk * (representing two carbons) or a double asterisk ** (representing three or more carbons) for clarity. Carbon resonances that required 2-D NMR analysis for assignment (i.e. not observed *via* 1-D ^{13}C NMR analysis) are marked with the label "*observed by gHMBC*" or "*observed by gHSQC*". Compounds that exhibited non-observable carbon resonances in both 1-D and 2-D NMR analysis are denoted and explained with footnotes. Unassigned aromatic hydrogens are labelled as "ArH", whereas specific/assigned aromatic hydrogens are labelled with the normal nomenclature (i.e. HAr3 = hydrogen atom attached to aromatic carbon #3). NMR spectra were processed, analysed and prepared with MestReNova (version 6.0) NMR software. Low resolution mass spectra (LRMS) were obtained *via* electrospray ionization (ESI) on a Shimadzu LC-2010 mass spectrometer. LRMS data was recorded as the ion mass/charge ratio (*m*/*z*) with the corresponding relative abundance as a percentage. High resolution mass spectrometry (HRMS) was performed on a Waters Quadrupole-Time of Flight (QTOF) Xevo spectrometer *via* ESI and with Leucine-Enkephalin as an internal standard. All mass spectrometry samples were dissolved in high performance liquid chromatography (HPLC) grade MeOH (containing <1% formic acid for ionization). Optical rotations were measured on a Jasco P-2000 polarimeter with a 10 cm path length; rotation values (α) are expressed in units of "deg cm^3 g^{-1} dm^{-1}" with concentration (*c*) expressed in units of "g/100 mL". Solid-state infrared spectroscopy was performed on a Shimadzu IRAffinity-1 FTIR spectrometer in combination with a MIRacle 10 Single Reflection Attenuated Total Reflectance accessory outfitted with a 1.5 mm round diamond crystal. IR peaks are reported as the wavenumber ($\overline{\nu}_{max}$ in cm^{-1}) of the maximum absorption.

Notes and other considerations

All known compounds are marked with a reference after the compound title; all compounds without a reference are novel. Unless otherwise noted, all rotameric NMR data was expressed with relevant footnotes for clarity. Synthesized compounds that contain the (*S*)-isopentyloxybinaphthalene fragment and some chiral compounds that contain the isopentyloxybiphenyl fragment exhibit a pair of diastereotopic methyl (-CH_3) groups on the terminus of the isopentyl substituent; these carbons are consistently referred to as C4″ and C5″. Importantly, these two carbons (and associated protons) will sometimes exhibit distinct chemical shifts due to the chiral environment imposed by the amino acid residue(s) (for all derivatives) and/or the adjacent (*S*)-BINOL moiety (for binaphthyl derivatives only).

6.2 – General synthetic procedures

General Procedure A: Copper catalyzed azide-alkyne cycloaddition

To a reaction vessel charged with the azide (1.0 eq), alkyne (2.0 – 3.0 eq), $Cu(OAc)_2 \cdot H_2O$ (0.2 eq), and sodium ascorbate (0.4 eq) was added *t*-BuOH (20 mL/mmol azide) and H_2O (5 mL/mmol azide). The mixture was initially sonicated for < 1 min followed by vigorous stirring at rt (unless noted otherwise) for the specified time. The reaction mixture was diluted with EtOAc (20 mL for reactions that contained ≤ 1.0 mmol azide or 20 mL/mmol azide for larger scale reactions) and washed with an equivalent volume of saturated aqueous NH_4Cl solution (e.g. 20 mL). The organic phase was dried ($MgSO_4$), filtered, concentrated and the residue was subjected to flash chromatography over SiO_2 gel to afford the desired 1,4-disubstituted 1,2,3-triazole product.

General Procedure B: Amide coupling

The amine (1.0 eq), carboxylic acid (1.0 eq), EDCI (1.2 eq) and HOBt (1.1 eq) were combined in an acetonitrile solution (10 mL/mmol amine) and stirred at rt for the specified time. The solvent was removed (not required for ≤ 5.0 mL acetonitrile) and the residue was dissolved in EtOAc (25 mL for reactions that contained ≤ 1.0 mmol amine or 25 mL/mmol amine for larger scale reactions). The organic solution was washed successively with aqueous HCl (1.0 M – 2 × 25 mL), saturated aqueous $NaHCO_3$ (3 × 25 mL) and brine (1 × 25 mL). The EtOAc solution was dried ($MgSO_4$), filtered and concentrated. If necessary, the residue was subjected to further purification *via* flash chromatography over SiO_2 gel to furnish the targeted amide product.

General Procedure C: Amine deprotection (*N*-Boc and/or *N*-Pbf removal)

The *N*-protected amine (1.0 eq) was dissolved in a CH_2Cl_2 (30 mL/mmol substrate) with magnetic stirring. If the substrate molecule contained an *N*-Pbf moiety then H_2O (20.0 eq) was also added to the solution. TFA (30.0 mL/mmol substrate) was then added and the reaction mixture was stirred at rt overnight (> 16 h) followed by removal of the solvent. The residue was dissolved in CH_2Cl_2 (30 mL/mmol substrate), an excess amount of anhydrous HCl (2.0 M in Et_2O, 15 mL/mmol substrate, 30.0 eq) was added and the solvent was then removed. The resulting residue was dissolved in a minimal volume of CH_2Cl_2 (or MeOH) and excess Et_2O (25 mL for ≤ 0.1 mmol substrate) was added to precipitate the hydrochloride salt of the amine. The solvent was removed by filtration and the product (both in the filter funnel and in the flask) was triturated with Et_2O (3 × 20 mL). The product was collected by dissolution in MeOH; concentration followed by drying *in vacuo* gave the final mono- or

di-hydrochloride salt as a thin, translucent film that was routinely scratched with a spatula into a fine hygroscopic powder or amorphous gum.

General Procedure D: Modified amine deprotection (*N*-Boc removal)

For the monocationic lysine derivatives, **General Procedure C** was followed with the following modifications: Et_2O (instead of CH_2Cl_2 or MeOH) was utilized to dissolve the residue for final precipitation and petroleum spirits (P.S. – instead of Et_2O) was utilized as the antisolvent for precipitation.

6.3 – Synthesis

6.3.1 – Precursor Building Blocks

Aromatic Cores

(*S*)-2′-(Isopentyloxy)-[1,1′-binaphthalen]-2-ol (46)[63]

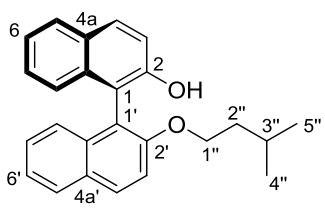

1-Bromo-3-methylbutane (264 mg, 1.75 mmol) was added dropwise to a stirred solution of (*S*)-[1,1′-binaphthalene]-2,2′-diol (**45**) (500 mg, 1.75 mmol) and K_2CO_3 (1.00 g, 7.27 mmol) in acetone (10 mL). The reaction mixture was heated at reflux for 24 h, cooled to rt and filtered. The solid residue was rinsed with acetone (2 × 20 mL), the combined filtrates were concentrated and the resultant residue was subjected to flash chromatography over SiO_2 gel (EtOAc/P.S. – 10:90) to give compound **46** (508 mg, 81%) as a translucent, yellow oil. The spectroscopic data was found to be in agreement with those previously reported.[63] TLC (EtOAc/P.S. – 10:90): R_f = 0.34; ^{1}H NMR (300 MHz, $CDCl_3$) δ 7.80 – 8.01 (m, 4H, H4, H4′, H5, and H5′), 7.01 – 7.44 (m, 8H, H3, H3′, H6, H6′, H7, H7′, H8, and H8′), 4.96 (br s, 1H, -OH), 3.92 – 4.05 (m, 2H, H1′′), 1.21 – 1.37 (m, 3H, H2′′ and H3′′), 0.65 (d, *J* = 5.6 Hz,

3H, H4′′ or H5′′), 0.61 (d, J = 5.6 Hz, 3H, H5′′ or H4′′); ^{13}C NMR (75 MHz, $CDCl_3$) δ 155.8 (C2), 151.5 (C2′), 134.3 (C8a), 134.0 (C8a′), 131.0 (C4), 129.8 (C4′), 129.7 (C4a), 129.3 (C4a′), 128.3 (C5), 128.2 (C5′), 127.4 (C7), 126.4 (C7′), 125.3 (C8), 125.2 (C8′), 124.4 (C6), 123.4 (C6′), 117.6 (C3), 116.5 (C1), 115.8 (C3′), 115.4 (C1′), 68.4 (C1′′), 38.1 (C2′′), 24.9 (C3′′), 22.54 (C4′′ or C5′′), 22.48 (C5′′ or C4′′); MS (ESI +ve) *m/z* 413 ([M + HCOOH + H]$^+$, 100%), 357 ([M+H]$^+$, 58%).

(*S*)-2′-(Isopentyloxy)-2-(propargyloxy)-1,1′-binaphthalene (20)

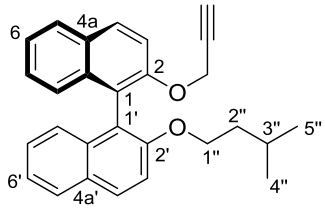

Propargyl bromide (80% w/w in toluene – 750 mg, 6.31 mmol) was added dropwise to a stirred solution of **46** (1.50 g, 4.21 mmol) and K_2CO_3 (1.17 g, 8.40 mmol) in acetonitrile (30 mL). The mixture was heated at reflux for 40 h, cooled to rt and filtered. The solid residue was washed with acetonitrile (2 × 50 mL), the filtrate was concentrated and the resulting residue was subjected to flash chromatography over SiO_2 gel (EtOAc/P.S. – 10:90) to give alkyne **20** (1.65 g, 99%) as a translucent, yellow oil. TLC (EtOAc/P.S. – 10:90): R_f = 0.62; $[\alpha]_D^{23}$ –25.7 (*c* 3.06, MeOH); ^{1}H NMR (500 MHz, $CDCl_3$) δ 7.91 – 7.98 (m, 2H, H4 and H4′), 7.83 – 7.88 (m, 2H, H5 and H5′), 7.56 (d, J = 9.0 Hz, 1H, H3), 7.42 (d, J = 9.0 Hz, 1H, H3′), 7.28 – 7.35 (m, 2H, H6 and H6′), 7.17 – 7.23 (m, 2H, H7 and H7′), 7.15 (d, J = 8.5 Hz, 1H, H8), 7.12 (d, J = 8.5 Hz, 1H, H8′), 4.54 and 4.58 (ABq, 2H, J = 8.5 Hz, -CH_AH_B-C≡C-), 4.01 (dt, J = 9.4, 6.1 Hz, 1H, H1′′$_A$ or H1′′$_B$), 3.91 (dt, J = 9.4, 6.1 Hz, 1H, H1′′$_B$ or H1′′$_A$), 2.37 (s, 1H, -C≡CH), 1.22 – 1.36 (m, 3H, H2′′ and H3′′), 0.63 (d, J = 5.7 Hz, 3H, H4′′ or H5′′), 0.58 (d, J = 5.7 Hz, 3H, H5′′ or H4′′); ^{13}C NMR (126

MHz; $CDCl_3$) δ 154.8 (C2′), 153.4 (C2), 134.3 (C8a), 134.2 (C8a′), 130.0 (C4a), 129.6 (C4), 129.4 (C4a′), 129.2 (C4′), 128.1 (C5), 128.0 (C5′), 126.4 (C7), 126.3 (C7′), 125.8 (C8), 125.7 (C8′), 124.1 (C6), 123.8 (C6′), 121.5 (C1), 120.1 (C1′), 116.3 (C3), 116.0 (C3′), 79.6 (-C≡CH), 75.3 (-C≡CH), 68.4 (C1′′), 57.4 (-CH_2-C≡CH), 38.3 (C2′′), 24.8 (C3′′), 22.6 (C4′′ or C5′′), 22.4 (C5′′ or C4′′); IR (neat) $\overline{\nu}_{max}$ 3288, 3058, 2954, 2868, 2363, 1620, 1590, 1507, 1460, 1429, 1355, 1329, 1270, 1243, 1217, 1146, 1133, 1084, 1050, 1017, 934, 804, 746, 668 cm^{-1}; MS (ESI +ve) *m/z* 417 ($[M + Na]^+$, 100%), 395 ($[M + H]^+$, 40%); HRMS (ESI +ve TOF) calcd for $C_{28}H_{26}O_2Na$ 417.1831, found 417.1841 ($[M + Na]^+$).

2'-(Isopentyloxy)-[1,1'-biphenyl]-2-ol (48)[66]

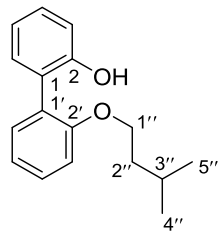

1-Bromo-3-methylbutane (2.43 g, 16.11 mmol) was added dropwise to a stirred solution of 2,2′-biphenol (**47**) (3.00 g, 16.11 mmol) and K_2CO_3 (9.24 g, 66.86 mmol) in acetone (97 mL). The mixture was heated at reflux for 24 h, cooled to rt and filtered. The solid residue was extracted with acetone (2 × 50 mL), the combined filtrates were concentrated and the resulting residue was subjected to flash chromatography over SiO_2 gel (Et_2O/hexanes – 10:90) to give the product ether **48** (3.68 g, 89%) as a translucent, viscous oil that eventually crystallized into a white solid. The spectroscopic data was found to be in agreement with those previously reported.[66] TLC (Et_2O/hexanes – 10:90): R_f = 0.50, (EtOAc/P.S. – 5:95): R_f = 0.34; ^{1}H NMR (300 MHz, $CDCl_3$) δ 7.41 – 7.23 (m, 4H, ArH), 7.16 – 6.96 (m, 4H, ArH), 6.62 (s, 1H, -OH), 4.09 (t, *J* = 6.6 Hz, 2H, H1''), 1.78 – 1.58 (m, 3H, H2'' and H3''), 0.88 (d, *J* = 6.2 Hz, 6H, H4'' and H5''); ^{13}C NMR (101 MHz, $CDCl_3$) δ 155.0 (C2'), 154.0 (C2), 132.7 (C6'), 131.4 (C6), 129.2 (C4 and C4'), 128.1 (C1'), 126.7 (C1), 122.5 (C5'), 121.0 (C5), 117.8 (C3), 113.4 (C3'),

68.5 (C1"), 37.9 (C2"), 25.1 (C3"), 22.6 (C4" and C5"); MS (ESI +ve) *m/z* 279 ($[M + Na]^+$, 100%), 257 ($[M + H]^+$, 16%).

2-(Isopentyloxy)-2'-(prop-2-yn-1-yloxy)-1,1'-biphenyl (21)

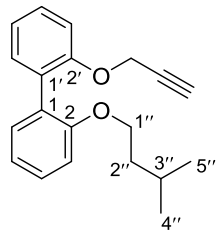

Propargyl bromide (80% w/w in toluene – 1.31 g, 8.78 mmol) was added dropwise to a stirred solution of the ether **48** (1.50 g, 5.85 mmol) and K_2CO_3 (1.62 g, 11.70 mmol) in acetonitrile (41 mL). The mixture was then heated at reflux for 48 h, cooled to rt and filtered. The solid residue was washed with acetonitrile (2 × 50 mL), the combined filtrates were concentrated and the resulting residue was subjected to flash chromatography over SiO_2 gel (EtOAc/P.S. – 5:95) to give alkyne **21** (1.70 g, 99%) as a translucent, yellow oil. TLC (EtOAc/P.S. – 5:95): R_f = 0.46; ^{1}H NMR (400 MHz, $CDCl_3$) δ 7.37 – 7.21 (m, 4H, ArH), 7.10 (d, *J* = 8.1 Hz, 1H, ArH), 7.07 – 6.91 (m, 3H, ArH), 4.60 (d, *J* = 2.3 Hz, 2H, -C<u>H</u>$_2$C≡C-), 3.95 (t, *J* = 6.7 Hz, 2H, H1"), 2.43 (t, *J* = 2.3 Hz, 1H, -C≡CH), 1.71 – 1.44 (m, 3H, H2" and H3"), 0.83 (d, *J* = 6.5 Hz, 6H, H4" and H5"); ^{13}C NMR (101 MHz, $CDCl_3$) δ 156.7 (C2), 155.3 (C2'), 131.9 (C6 or C6'), 131.7 (C6 or C6'), 128.9 (C1'), 128.7 (C4 or C4'), 128.4 (C4 or C4'), 128.0 (C1), 121.3 (C5'), 120.3 (C5), 113.0 (C3'), 112.4 (C3), 79.3 (-<u>C</u>≡CH), 75.2 (-C≡<u>C</u>H), 67.1 (C1"), 56.4 (-<u>C</u>H$_2$C≡C-), 38.1 (C2"), 25.1 (C3"), 22.7 (C4" and C5"); IR (neat) $\bar{\nu}_{max}$ 3292, 2955, 2870, 2362, 2328, 1594, 1502, 1473, 1441, 1384, 1367, 1251, 1212, 1162, 1123, 1110, 1054, 909, 749, 731, 668 cm^{-1}; MS (ESI +ve) *m/z* 317 ($[M + Na]^+$, 100%), 295 ($[M + H]^+$, 22%); HRMS (ESI +ve TOF) calcd for $C_{20}H_{23}O_2$ 295.1698, found 295.1692 ($[M + H]^+$).

Lysine Building Blocks

(*R*)-N^2-(Benzyloxycarbonyl)-N^6-(*tert*-butoxycarbonyl)-2,6-diaminohexanoic acid (50)[69]

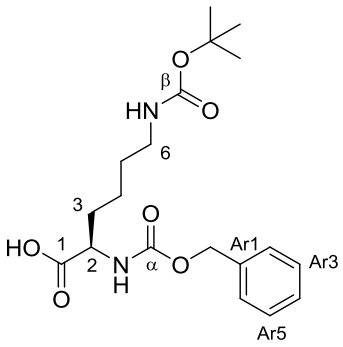

H-(D)-Lys(Boc)-OH (**49**) (4.00 g, 16.24 mmol) was dissolved in 4.0 M NaOH (4.06 mL, 16.24 mmol) and the solution was cooled to 0 ºC in an ice bath. With vigorous stirring at 0 ºC, benzyl chloroformate (2.84 g, 16.65 mmol) and 4.0 M NaOH (4.06 mL, 16.24 mmol) were added portion-wise and alternately over a 15 min period. The mixture was then removed from the ice bath and stirred at rt for 90 min. The reaction mixture was diluted with H_2O (5 mL) and extracted with EtOAc (3 × 20 mL). The combined organic layers were extracted with H_2O (3 × 30 mL); the combined aqueous extracts were then acidified to pH 2-3 with concentrated aqueous HCl (36% w/w) followed by extraction with Et_2O (3 × 40 mL). The combined ethereal extracts were dried ($MgSO_4$), filtered and concentrated to give the acid **50** (5.86 g, 95%) as a light yellow, viscous oil. The spectroscopic data was found to be in agreement those previously reported.[69] TLC (MeOH/CH_2Cl_2 - 10:90): R_f = 0.43; ^{1}H NMR (500 MHz, $CDCl_3$) δ 7.27 – 7.38 (m, 5H, ArH), 5.68 (s, 1H, N^2-H), 5.01 – 5.20 (m, 2H, -C<u>H</u>$_2$Ph), 4.86 (br s, 1H, -OH), 4.70 (s, 1H, N^6-H), 4.34 (s, 1H, H2), 3.08 (br s, 2H, H6), 1.62 – 1.95 (m, 2H, H3), 1.21 – 1.56 (m, 13H, H4, H5 and -C(CH_3)$_3$); ^{13}C NMR (126 MHz; $CDCl_3$) δ 175.8 (C1), 156.6 (Cα), 156.5 (Cβ), 136.5 (CAr1), 128.7 (CAr3 and CAr5), 128.34 (CAr2 and CAr6), 128.27 (CAr4), 79.7 (-<u>C</u>(CH_3)$_3$), 67.2 (-<u>C</u>H$_2$Ph), 54.1 (C2), 40.2 (C6), 32.0 (C3), 29.7 (C5), 28.6 (-C(<u>C</u>H$_3$)$_3$), 22.5 (C4); MS (ESI +ve) *m/z* 403 ([M + Na]$^+$, 100%), 281 ([M – Boc + 2H]$^+$, 28%).

Benzyl ((*R*)-N^6-(*tert*-butoxycarbonyl)-6-amino-1-hydroxyhexan-2-yl)carbamate (51)[82]

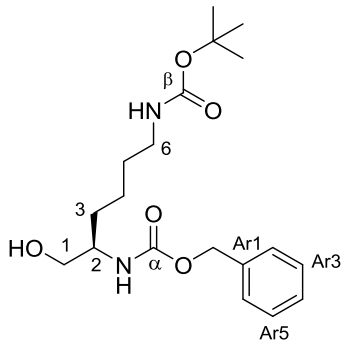

To a stirred solution of the acid **50** (804 mg, 2.11 mmol) in THF (4.3 mL) at −10 ºC was added dropwise *N*-methylmorpholine (243 mg, 2.11 mmol) followed by isobutyl chloroformate (288 mg, 2.11 mmol). The mixture was stirred at –10 ºC for 30 min and then filtered. To the cold filtrate (ice/salt bath) was added a solution of $NaBH_4$ (120 mg, 3.16 mmol) in H_2O (1.1 mL) and then the reaction mixture was manually agitated for 15 s followed by quenching of the reaction with excess H_2O (~65 mL). The reaction mixture was then extracted with EtOAc (3 × 30 mL) and the combined extracts were then washed with H_2O (3 × 30 mL). The organic phase was dried (Na_2SO_4), filtered and concentrated to give alcohol **51** (762 mg, 98%) as a clear, viscous oil. The spectroscopic data was found to be in agreement with those previously reported.[82] TLC ($MeOH/CH_2Cl_2$ – 10:90): R_f = 0.41; ^{1}H NMR (500 MHz, $CDCl_3$) δ 7.29 – 7.41 (m, 5H, ArH), 5.11 (br s, 3H, -C$\underline{H}_2$Ph and N^2-H), 4.61 (s, 1H, N^6-H), 3.54 – 3.73 (m, 3H, H1 and H2), 2.98 – 3.23 (m, 2H, H6), 2.64 (br s, 1H, -OH), 1.75 (br s, 1H, $H3_A$ or $H3_B$), 1.60 (br s, 1H, $H3_B$ or $H3_A$), 1.20 – 1.55 (m, 13H, -C(CH_3)$_3$, H4 and H5); ^{13}C NMR (126 MHz, $CDCl_3$) δ 156.9 (Cα), 156.5 (Cβ), 136.7 (CAr1), 128.7 (CAr3 and CAr5), 128.31 (CAr2 and CAr6), 128.29 (CAr4), 79.5 (-C($\underline{C}H_3$)$_3$), 67.0 (-$\underline{C}H_2$Ph), 65.2 (C1), 53.3 (C2), 40.0 (C6), 30.8 (C3), 30.2 (C5), 28.6 (-C($\underline{C}H_3$)$_3$), 22.9 (C4); MS (ESI +ve) *m/z* 389 ([M + Na]$^+$, 100%), 267 ([M – Boc + 2H]$^+$, 15%).

Benzyl ((*R*)-N^6-(*tert*-butoxycarbonyl)-6-amino-1-azidohexan-2-yl)carbamate (23)[82]

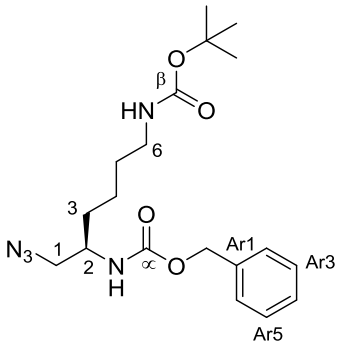

To a stirred solution of the alcohol **51** (6.56 g, 17.90 mmol) in CH_2Cl_2 (54 mL) at 0 ºC was added dropwise triethylamine (2.36 g, 23.27 mmol) followed by the slow, dropwise addition of methanesulfonyl chloride (2.67 g, 23.27 mmol). The reaction mixture was allowed to warm to rt and then stirring was continued for 1 h. Toluene (58 mL) was added and the reaction mixture was concentrated under vacuum (600 mbar) to selectively remove the CH_2Cl_2. To the resulting solution was added sodium azide (5.82 g, 89.50 mmol), tetrabutylammonium bromide (693 mg, 2.15 mmol) and H_2O (5.8 mL) and the mixture was heated at 70 ºC for 18 h with vigorous stirring. A further portion of H_2O (4.0 mL) was added and stirring was continued at 70 ºC for 6 h before the mixture was cooled to rt and partitioned between Et_2O (150 mL) and H_2O (150 mL). The aqueous phase was separated and re-extracted with fresh Et_2O (2 × 75 mL). The combined ethereal extracts were washed with brine (2 × 75 mL), dried ($MgSO_4$), filtered and concentrated. The residue was subjected to flash chromatography over SiO_2 gel (EtOAc/P.S. - 5:95 → 20:80) which gave the azide **23** (5.80 g, 83%) as a clear, viscous oil. The spectroscopic data was found to be in agreement with those previously reported.[82] TLC (EtOAc/P.S. - 40:60): R_f = 0.61; ^{1}H NMR (500 MHz, $CDCl_3$) δ 7.28 – 7.40 (m, 5H, ArH), 5.03 – 5.18 (m, 2H, -C<u>H</u>$_2$Ph), 4.94 (br s, 1H, N^2-H), 4.57 (br s, 1H, N^6-H), 3.77 (br s, 1H, H2), 3.32 – 3.49 (m, 2H, H1), 3.10 (br s, 2H, H6), 1.29 – 1.59 (m, 15H, H3, H4, H5 and -C(CH_3)$_3$); ^{13}C NMR (126 MHz; $CDCl_3$) δ 156.1 (Cα), 156.0 (Cβ), 136.3 (CAr1), 128.5 (CAr3 and CAr5), 128.14 (CAr2 and CAr6), 128.06 (CAr4), 79.1 (-<u>C</u>(CH_3)$_3$), 66.8

(-CH$_2$Ph), 54.7 (C1), 50.8 (C2), 40.0 (C6), 31.6 (C3), 29.7 (C5), 28.4 (-C(CH$_3$)$_3$), 22.8 (C4); MS (ESI +ve) *m/z* 414 ([M + Na]$^+$, 100%), 292 ([M – Boc + 2H]$^+$, 28%).

(9*H*-Fluoren-9-yl)methyl ((*R*)-*N*^{6}-(*tert*-butoxycarbonyl)-6-amino-1-hydroxyhexan-2-yl)carbamate (53)[121]

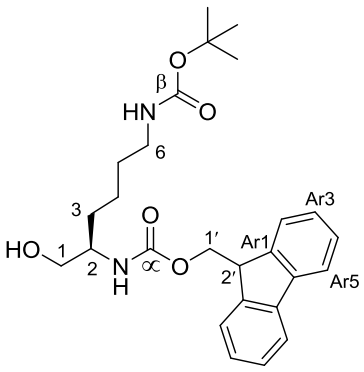

Fmoc-(D)-Lys(Boc)-OH (**52**) (4.00 g, 8.54 mmol) was dissolved in THF (17.1 mL) with magnetic stirring. The solution was brought to −10 °C (ice/salt bath) followed by sequential dropwise addition of isobutyl chloroformate (1.12 g, 8.54 mmol) and then *N*-methylmorpholine (983 mg, 8.54 mmol). The mixture was stirred at −10 °C for 30 min and filtered through a small pad of Celite – the Celite pad was rinsed with fresh, cold THF (5 × 5 mL) and the combined filtrates were kept cold (ice bath). The cold filtrate was added dropwise to a cold aqueous solution of $NaBH_4$ (647 mg, 17.07 mmol in 12.8 mL H_2O) with vigorous stirring. The mixture was stirred for 5 min before being added directly to H_2O (213 mL) with vigorous stirring. The reaction was stirred for 10 min and then the aqueous mixture was extracted with EtOAc (3 × 150 mL). The combined organic extracts were washed with H_2O (2 × 200 mL) and brine (1 × 200 mL). The organic phase was dried ($MgSO_4$), filtered, concentrated and subjected to flash chromatography over SiO_2 gel (EtOAc/P.S. – 50:50) to afford the alcohol **53** (3.57 g, 92%) as a white, amorphous solid. The spectroscopic data was found to be in agreement with those previously reported.[121] TLC (EtOAc/P.S. – 50:50): R_f = 0.35; ^{1}H NMR (400 MHz, $CDCl_3$) δ 7.76 (d, *J* = 7.5 Hz, 2H, HAr5), 7.59 (d, *J* = 7.4 Hz, 2H, HAr2), 7.39 (t, *J* = 7.4 Hz, 2H, HAr3), 7.31 (t, *J* = 7.4 Hz, 2H, HAr4), 5.12 (br s, 1H, N^2-H),

4.61 (br s, 1H, N^6-H), 4.41 (d, *J* = 6.5 Hz, 2H, H1'), 4.20 (t, *J* = 6.7 Hz, 1H, H2'), 3.73 – 3.50 (m, 3H, H1 and H2), 3.24 – 2.97 (m, 2H, H6), 1.68 – 1.19 (m, 15H, H3, H4, H5 and -C(CH_3)$_3$); ^{13}C NMR (101 MHz, $CDCl_3$) δ 156.8 (Cα), 156.5 (Cβ), 144.1 (CAr1), 141.5 (CAr6), 127.8 (CAr4), 127.2 (CAr3), 125.2 (CAr2), 120.1 (CAr5), 79.4 (-<u>C</u>(CH_3)$_3$), 66.7 (C1'), 64.8 (C1), 53.1 (C2), 47.4 (C2'), 39.8 (C6), 30.6 (C3), 30.1 (C5), 28.6 (-C(<u>C</u>H_3)$_3$), 22.7 (C4); MS (ESI +ve) *m/z* 477 ([M + Na]$^+$, 100%).

***Tert*-butyl (*R*)-(5-amino-6-azidohexyl)carbamate (22)**[59]

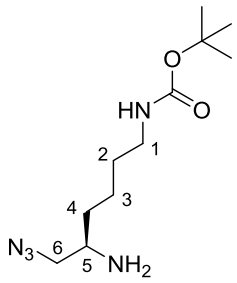

A stirred solution of the alcohol **53** (100 mg, 0.22 mmol) in anhydrous CH_2Cl_2 (2.2 mL) was brought to 0 °C (ice bath). Triethylamine (33 mg, 0.33 mmol) was added followed by the dropwise addition of methanesulfonyl chloride (38 mg, 0.33 mmol). The solution was stirred at 0 °C for 15 min followed by stirring at rt for 60 min. The mixture was diluted with CH_2Cl_2 (30 mL) and washed successively with 1.0 M aqueous citric acid solution (2 × 20 mL) and brine (1 × 20 mL). The organic phase was dried ($MgSO_4$), filtered and concentrated to give the intermediate mesylate as a yellow, translucent gum. The mesylate was dissolved in DMF (1.1 mL) with magnetic stirring. NaN_3 (72 mg, 1.10 mmol) was added and the reaction mixture was stirred vigorously and heated at 45-50 °C for 18 h. After the reaction was complete (as verified by MS/TLC analysis), the DMF was removed from the reaction mixture *via* a rotary evaporator by utilizing the DMF-toluene azeotrope. The residue was subjected to flash chromatography over SiO_2 gel (EtOAc → MeOH/CH_2Cl_2 – 10:90) which afforded the target amine **22** (26 mg, 46%) as a yellow, translucent oil. The spectroscopic data was found to be in agreement with those previously reported.[59] TLC

(MeOH/CH_2Cl_2 – 10:90): R_f = 0.13, (NEt_3/MeOH/CH_2Cl_2 – 2:10:88): R_f = 0.41; ^{1}H NMR (400 MHz, $CDCl_3$) δ 4.85 (br s, 1H, N^1-H), 3.35 (dd, J = 9.3, 4.7 Hz, 1H, $H6_A$ or $H6_B$), 3.18 – 3.04 (m, 3H, $H6_B$ or $H6_A$ and H1), 2.89 (br s, 1H, H5), 1.64 – 1.23 (m, 17H, H2, H3, H4, -$C(CH_3)_3$ and -NH_2); ^{13}C NMR (101 MHz, $CDCl_3$) δ 156.0 (C=O), 78.9 (-$\underline{C}(CH_3)_3$), 58.2 (C6), 50.9 (C5), 40.2 (C1), 34.5 (C4), 30.0 (C2), 28.3 (-$C(\underline{C}H_3)_3$), 23.1 (C3); MS (ESI +ve) *m/z* 258 ($[M + H]^+$, 100%), 280 ($[M + Na]^+$, 10%).

(*R*)-2-Azido-6-((*tert*-butoxycarbonyl)amino)hexanoic acid (24)[90]

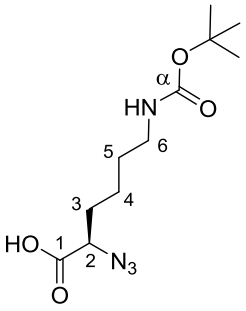

The methyl triflate salt of sulfuryl-diimidazole[87-88] (4.85g, 13.40 mmol) was added to cold (≤ 5 °C) H_2O (16 mL) and the mixture was magnetically stirred over an ice bath until the salt fully dissolved. EtOAc (16 mL) was added to the solution, followed by NaN_3 (1.16 g, 17.86 mmol); the mixture was stirred vigorously at 0 °C for 60 min. The EtOAc layer was separated, dried (Na_2SO_4), filtered and the Na_2SO_4 solids were rinsed with minimal fresh EtOAc. The combined EtOAc filtrate (containing the newly formed diazotransfer reagent) was then added to a reaction vessel containing a solution of H-(D)-Lys(Boc)-OH (**54**) (2.20 g, 8.93 mmol) in MeOH (36 mL), $CuSO_4 \cdot 5H_2O$ (22 mg, 0.09 mmol) and K_2CO_3 (1.85 g, 13.40 mmol). The reaction was stirred vigorously at rt for 24 h, at which point the reaction was shown to be complete by MS analysis. The mixture was diluted with H_2O (50 mL) and a few drops of aqueous NaOH solution (10% w/w) were added to ensure an alkaline mixture (pH > 10). The volatile solvents (EtOAc and MeOH) were removed under reduced pressure at 40 °C. The aqueous reaction mixture was then washed with Et_2O (2 × 50 mL) and made acidic (pH < 3) with concentrated aqueous HCl (36% w/w). The aqueous

phase was extracted with Et_2O (3 × 50 mL) and the combined ethereal extracts were washed with H_2O (3 × 100 mL), brine (1 × 50 mL), dried ($MgSO_4$), filtered and concentrated to afford a residue which was further purified by flash chromatography over SiO_2 gel (EtOAc/P.S. – 0:100 → 40:60) to yield the target α-azido-acid **24** (2.39g, 98%) as a translucent, viscous faint tan oil. The spectroscopic data was found to be in agreement with those previously reported.[90] TLC (EtOAc/P.S. – 40:60): R_f = 0.58; ^{1}H NMR (400 MHz, CD_3OD) δ 4.00 – 3.89 (m, 1H, H2), 3.04 (t, *J* = 6.6 Hz, 2H, H6), 1.90 – 1.79 (m, 1H, $H3_A$ or $H3_B$), 1.79 – 1.67 (m, 1H, $H3_B$ or $H3_A$), 1.56 – 1.35 (m, 14H, H4, H5 and -C$(CH_3)_3$); ^{13}C NMR (101 MHz, CD_3OD) δ 174.0 (C1), 158.7 (Cα), 80.1 (-C$(CH_3)_3$), 63.3 (C2), 41.2 (C6), 32.3 (C3), 30.6 (C5), 29.0 (-C$(CH_3)_3$), 24.3 (C4); MS (ESI −ve) *m/z* 271 ($[M - H]^-$, 100%), (ESI +ve) *m/z* 295 ($[M + Na]^+$, 100%).

Arginine Derivatives

Benzyl (*R*)-(1-hydroxy-5-(2-((2,2,4,6,7-pentamethyl-2,3-dihydrobenzofuran-5-yl)sulfonyl)guanidino)pentan-2-yl)carbamate (56)

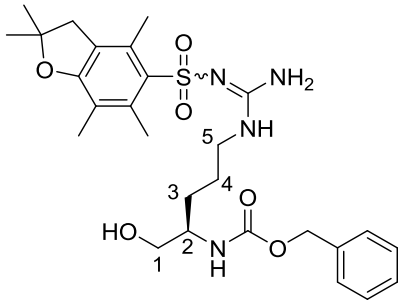

Cbz-(D)-Arg(Pbf)-OH (**55**) (5.00 g, 8.92 mmol) was dissolved in THF (17.8 mL) with magnetic stirring. The solution was brought to −10 °C (ice/salt bath) followed by sequential dropwise addition of isobutyl chloroformate (1.22 g, 8.92 mmol) and *N*-methylmorpholine (1.03 g, 8.92 mmol). The mixture was stirred at −10 °C for 30 min and then filtered through a small pad of Celite – the Celite pad was rinsed with fresh, cold THF (5 × 5 mL) and the combined filtrates were kept cold (ice bath). The cold filtrate was added dropwise to a cold aqueous

solution of $NaBH_4$ (676 mg, 17.84 mmol in 13.4 mL H_2O) with vigorous magnetic stirring. After the addition was complete, the reaction was allowed to react for 5 min and was added to excess H_2O (223 mL) with vigorous stirring. The reaction was stirred for 10 min and the aqueous mixture was extracted with EtOAc (3 × 150 mL). The combined organic extracts were washed with H_2O (2 × 200 mL), brine (1 × 200 mL), dried ($MgSO_4$), filtered and concentrated. The residue was subjected to flash chromatography over SiO_2 gel (EtOAc/P.S. – 80:20 → 100:0) to afford the alcohol **56** (3.82 g, 78%) as a white foam that collapsed into a translucent gum. TLC (EtOAc/P.S. – 80:20): R_f = 0.31; $[\alpha]_D^{23}$ –3.5 (*c* 0.77, MeOH); ^{1}H NMR (400 MHz, $CDCl_3$) δ 7.28 (br s, 5H, ArH), 6.10 – 6.32 (m, 3H, N^5-H/NH_2), 5.62 (d, *J* = 8.5 Hz, 1H, N^2-H), 5.03 (s, 2H, -C$\underline{H}_2$Ph), 3.50 – 3.69 (m, 3H, H1 and H2), 3.17 (br s, 2H, H5), 2.91 (s, 2H, $ArCH_2$-), 2.53 (s, 3H, $ArCH_3$), 2.46 (s, 3H, $ArCH_3$), 2.06 (s, 3H, $ArCH_3$), 1.40 – 1.61 (m, 10H, H3, H4 and -C(CH_3)$_2$); ^{13}C NMR (101 MHz, $CDCl_3$) δ 159.0 (Pbf C_{Ar}), 157.1 (C=O), 156.5 (C=N), 138.5 (Pbf C_{Ar}), 136.6 (Cbz C_{Ar}), 132.7 (Pbf C_{Ar}), 132.4 (Pbf C_{Ar}), 128.6 (Cbz C_{Ar})*, 128.2 (Cbz C_{Ar}), 128.0 (Cbz C_{Ar})*, 124.8 (Pbf C_{Ar}), 117.7 (Pbf C_{Ar}), 86.6 (-$\underline{C}$(CH_3)$_2$), 66.9 (-$\underline{C}H_2$Ph), 64.8 (C1), 52.8 (C2), 43.3 ($ArCH_2$-), 41.1 (C5), 28.7 (-C($\underline{C}H_3$)$_2$), 28.7 (C3), 25.8 (C4), 19.4 ($ArCH_3$), 18.1 ($ArCH_3$), 12.6 ($ArCH_3$); IR (neat) $\bar{\nu}_{max}$ 3431, 3328, 2934, 1696, 1617, 1545, 1454, 1243, 1153, 1088, 1028, 903, 806, 781, 733, 658 cm^{-1}; MS (ESI +ve) *m/z* 569 ($[M + Na]^+$, 100%), 547 ($[M + H]^+$, 56%); HRMS (ESI +ve TOF) calcd for $C_{27}H_{39}N_4O_6S$ 547.2590, found 547.2589 ($[M + H]^+$).

Benzyl (*R*)-(1-azido-5-(2-((2,2,4,6,7-pentamethyl-2,3-dihydrobenzofuran-5-yl)sulfonyl)guanidino)pentan-2-yl)carbamate (26)

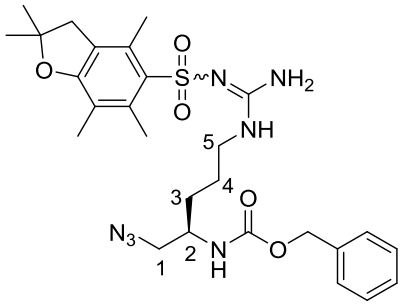

To a stirred solution of the alcohol **56** (3.79 g, 6.94 mmol) in CH_2Cl_2 (21 mL) at 0 ºC was added triethylamine (912 mg, 9.02 mmol) followed by slow, dropwise addition of methanesulfonyl chloride (1.03 g, 9.02 mmol). The reaction was allowed to warm to rt and stirring was continued for 1 h. Toluene (22.5 mL) was added and the mixture was concentrated under vacuum (600 mbar) to selectively remove the CH_2Cl_2. Sodium azide (2.26 g, 34.68 mmol), tetrabutylammonium bromide (268 mg, 0.83 mmol) and H_2O (4.9 mL) were added and the mixture was heated at 80 ºC for 36 h with vigorous stirring before being cooled to rt and partitioned between EtOAc (150 mL) and H_2O (150 mL). The aqueous phase was separated and extracted with EtOAc (2 × 75 mL). The combined organic extracts were washed with H_2O (1 × 100 mL), brine (1 × 100 mL), dried ($MgSO_4$), filtered and concentrated. The residue was subjected to flash chromatography over SiO_2 gel (EtOAc/P.S. – 20:80 → 60:40) which gave the target azide **26** (2.82 g, 71% over two steps) as an off-white foam that collapsed into a translucent gum. TLC (EtOAc/P.S. – 80:20): R_f = 0.69; $[\alpha]_D^{23}$ +4.5 (*c* 13.96, MeOH); ^{1}H NMR (400 MHz, $CDCl_3$) δ 7.31 (br s, 5H, ArH), 6.10 (br s, 3H, N^5-H/NH_2), 5.29 (d, *J* = 9.0 Hz, 1H, N^2-H), 5.13 – 4.99 (m, 2H, -C$\underline{H}_2$Ph), 3.73 (br s, 1H, H2), 3.42 – 3.26 (m, 2H, H1), 3.17 (br s, 2H, H5), 2.93 (s, 2H, $ArCH_2$-), 2.55 (s, 3H, $ArCH_3$), 2.48 (s, 3H, $ArCH_3$), 2.08 (s, 3H, $ArCH_3$), 1.62 – 1.39 (m, 10H, H3, H4 and -$C(CH_3)_2$); ^{13}C NMR (101 MHz, $CDCl_3$) δ 158.8 (Pbf C_{Ar}), 156.4 (C=O), 156.2 (C=N), 138.3 (Pbf C_{Ar}), 136.2 (Cbz C_{Ar}), 132.7 (Pbf C_{Ar}), 132.3 (Pbf C_{Ar}), 128.6 (Cbz C_{Ar})*, 128.2 (Cbz C_{Ar}), 128.0 (Cbz C_{Ar})*, 124.7 (Pbf C_{Ar}),

117.6 (Pbf C_{Ar}), 86.5 (-$\underline{C}(CH_3)_2$), 67.0 (-$\underline{C}H_2Ph$), 54.9 (C1), 50.5 (C2), 43.2 ($ArCH_2$-), 40.8 (C5), 29.6 (C3), 28.6 (-C($\underline{C}H_3)_2$), 25.5 (C4), 19.3 ($ArCH_3$), 17.9 ($ArCH_3$), 12.5 ($ArCH_3$); IR (neat) $\bar{\nu}_{max}$ 3431, 3332, 2930, 2098, 1700, 1616, 1540, 1456, 1242, 1153, 1088, 1028, 908, 807, 781, 732, 658 cm^{-1}; MS (ESI +ve) *m/z* 594 ($[M + Na]^+$, 100%), 572 ($[M + H]^+$, 52%); HRMS (ESI +ve TOF) calcd for $C_{27}H_{38}N_7O_5S$ 572.2655, found 572.2677 ($[M + H]^+$).

(9*H*-Fluoren-9-yl)methyl (*R*)-(1-hydroxy-5-(2-((2,2,4,6,7-pentamethyl-2,3-dihydrobenzofuran-5-yl)sulfonyl)guanidino)pentan-2-yl)carbamate (58)[121]

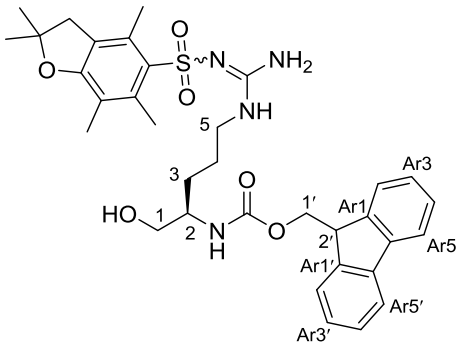

Fmoc-(D)-Arg(Pbf)-OH (**57**) (4.00 g, 6.17 mmol) was dissolved in THF (12.3 mL) with magnetic stirring. The solution was brought to −10 °C (ice/salt bath) followed by sequential dropwise addition of isobutyl chloroformate (842 mg, 6.17 mmol) and *N*-methylmorpholine (710 mg, 6.17 mmol). The mixture was stirred at −10 °C for 30 min and filtered through a small pad of Celite – the Celite pad was rinsed with fresh, cold THF (5 × 5 mL) and the combined filtrates were kept cold (ice bath). The cold filtrate was added dropwise to a cold aqueous solution of $NaBH_4$ (467 mg, 12.33 mmol in 9.3 mL H_2O) with vigorous magnetic stirring. After the addition was complete, the mixture was stirred for 5 min and added to H_2O (154 mL) with vigorous stirring. The reaction was stirred for 10 min and then the aqueous mixture was extracted with EtOAc (3 × 150 mL). The combined organic extracts were washed with H_2O (2 × 200 mL), brine (1 × 200 mL), dried ($MgSO_4$), filtered and concentrated. The residue was subjected to flash chromatography over SiO_2 gel (EtOAc) to afford the alcohol **58** (3.12 g, 80%) as a translucent gum. The spectroscopic data was found

to be in agreement with those previously reported.[121] TLC (EtOAc/P.S. – 60:40): R_f = 0.36; ^{1}H NMR (400 MHz, $CDCl_3$) δ 7.69 (d, *J* = 7.5 Hz, 2H, HAr5), 7.52 (d, *J* = 7.4 Hz, 2H, HAr2), 7.32 (t, *J* = 7.4 Hz, 2H, HAr3), 7.20 (t, *J* = 7.3 Hz, 2H, HAr4), 6.38 – 6.18 (m, 3H, N^5-H/NH_2), 5.72 (d, *J* = 7.9 Hz, 1H, N^2-H), 4.30 (d, *J* = 6.8 Hz, 2H, H1'), 4.09 (t, *J* = 6.7 Hz, 1H, H2'), 3.67 – 3.48 (m, 3H, H1 and H2), 3.18 (s, 2H, H5), 2.86 (s, 2H, $ArCH_2$-), 2.55 (s, 3H, $ArCH_3$), 2.47 (s, 3H, $ArCH_3$), 2.04 (s, 3H, $ArCH_3$), 1.63 – 1.41 (m, 4H, H3 and H4), 1.39 (s, 6H, -$C(CH_3)_2$); ^{13}C NMR (101 MHz, $CDCl_3$) δ 159.0 (Pbf C_{Ar}), 157.1 (C=N), 156.5 (C=O), 144.0 (CAr1 or CAr1') 143.9 (CAr1' or CAr1), 141.3 (CAr6), 138.4 (Pbf C_{Ar}), 132.7 (Pbf C_{Ar}), 132.3 (Pbf C_{Ar}), 127.8 (C4), 127.2 (C3), 125.3 (C2), 124.9 (Pbf C_{Ar}), 120.0 (C5), 117.7 (Pbf C_{Ar}), 86.6 (-$\underline{C}(CH_3)_2$), 66.8 (C1'), 64.8 (C1), 52.8 (C2), 47.3 (C2'), 43.3 ($ArCH_2$-), 41.1 (C5), 28.7 (-$C(\underline{C}H_3)_2$), 28.6 (C3), 25.8 (C4), 19.4 ($ArCH_3$), 18.1 ($ArCH_3$), 12.6 ($ArCH_3$); MS (ESI +ve) *m/z* 657 ($[M + Na]^+$, 100%), 635 ($[M + H]^+$, 86%).

(*R*)-1-Azido-5-(2-((2,2,4,6,7-pentamethyl-2,3-dihydrobenzofuran-5-yl)sulfonyl)guanidino)pentan-2-amine (25)[59]

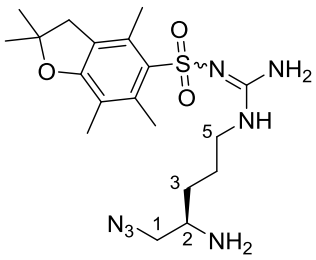

A reaction vessel charged with triphenylphosphine (1.41 g, 5.37 mmol), iodine (1.36 g, 5.37 mmol), imidazole (399 mg, 5.86 mmol) and CH_2Cl_2 (7.0 mL) was stirred at rt for 10 min followed by the addition a solution of the alcohol **58** (3.10g, 4.88 mmol) in CH_2Cl_2 (3.0 mL). The reaction was stirred at rt for 20 h, diluted with CH_2Cl_2 (30 mL) and filtered to remove the white precipitate. The filtrate was concentrated and the residue was subjected to flash chromatography over SiO_2 gel (EtOAc/Et_2O – 50:50) to give a mixture of the intermediate iodide and triphenylphosphine oxide. The mixture was dissolved in DMF

(24.5 mL) and NaN_3 (1.59g, 24.42 mmol) was added to the solution followed by vigorous stirring at rt for 4 h. After the azidation reaction was shown to be complete by TLC analysis (EtOAc/P.S. – 80:20), the reaction was heated to 50 °C (oil bath) overnight (18 h) to remove the *N*-Fmoc protecting group. The reaction mixture was cooled to rt and then partitioned between EtOAc (200 mL) and aqueous HCl (0.5 M – 200 mL) with magnetic stirring for 5 min. The acidic aqueous phase was separated and washed with EtOAc (3 × 100 mL). The aqueous phase was made alkaline (pH > 10) with aqueous NaOH solution (10% w/w) and was extracted with EtOAc (3 × 100 mL). The organic extracts were combined and washed with H_2O (1 × 150 mL), brine (1 × 100 mL), dried (Na_2SO_4), filtered and concentrated to afford the amine **25** (1.71 g, 80% over two steps) as an off-white foam that eventually collapsed into a translucent, pale yellow gum. The spectroscopic data was found to be in agreement with those previously reported.[59] TLC (MeOH/CH_2Cl_2 – 10:90): R_f = 0.21; ^{1}H NMR (400 MHz, $CDCl_3$) δ 6.55 – 6.31 (m, 3H, N^5-H/$NH_{2\ (guanidine)}$), 3.27 (dd, *J* = 12.0, 4.1 Hz, 1H, $H1_A$ or $H1_B$), 3.22 – 3.11 (m, 2H, H5), 3.07 (dd, *J* = 12.0, 7.4 Hz, 1H, $H1_B$ or $H1_A$), 2.95 (s, 2H, $ArCH_2$-), 2.86 – 2.76 (m, 1H, H2), 2.56 (s, 3H, $ArCH_3$), 2.49 (s, 3H, $ArCH_3$), 2.09 (s, 3H, $ArCH_3$), 1.73 (s, 2H, -NH_2), 1.61 – 1.34 (m, 9H, $H3_A$ or $H3_B$, H4 and -$C(CH_3)_2$), 1.31 – 1.19 (m, 1H, $H3_B$ or $H3_A$); ^{13}C NMR (101 MHz, $CDCl_3$) δ 158.8 (Pbf C_{Ar}), 156.4 (C=N), 138.2 (Pbf C_{Ar}), 132.9 (Pbf C_{Ar}), 132.1 (Pbf C_{Ar}), 124.7 (Pbf C_{Ar}), 117.6 (Pbf C_{Ar}), 86.5 (-$\underline{C}(CH_3)_2$), 58.3 (C1), 50.8 (C2), 43.3 ($ArCH_2$-), 40.9 (C5), 31.7 (C3), 28.6 (-$C(\underline{C}H_3)_2$), 25.9 (C4), 19.3 ($ArCH_3$), 18.0 ($ArCH_3$), 12.5 ($ArCH_3$); MS (ESI +ve) *m/z* 438 ($[M + H]^+$, 100%), 460 ($[M + Na]^+$, 53%).

***Tert*-butyl (*R*)-(1-azido-5-(2-((2,2,4,6,7-pentamethyl-2,3-dihydrobenzofuran-5-yl)sulfonyl)guanidino)pentan-2-yl)carbamate (27)**

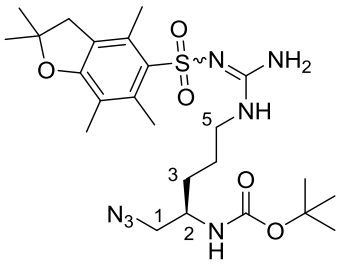

To a stirred solution of amine **25** (100 mg, 0.23 mmol) in CH_2Cl_2 (2.0 mL) was slowly added a solution of Boc_2O (60 mg, 0.27 mmol) in CH_2Cl_2 (0.5 mL) and the resulting mixture was stirred at rt for 2 h. The reaction was then diluted with EtOAc (100 mL) and washed successively with 1.0 M HCl (2 × 50 mL), saturated aqueous $NaHCO_3$ (1 × 50 mL), H_2O (1 × 50 mL) and brine (1 × 50 mL). The organic phase was dried ($MgSO_4$), filtered, concentrated and the resultant residue was subjected to flash chromatography over SiO_2 gel (EtOAc/P.S. – 20:80 → 100:0) to afford the azide **27** (121 mg, 98%) as a light tan, translucent gum. TLC (EtOAc): R_f = 0.67, (MeOH/CH_2Cl_2 – 5:95): R_f = 0.42; $[\alpha]_D^{23}$ –3.3 (*c* 0.70, MeOH); ^{1}H NMR (400 MHz, $CDCl_3$) δ 6.22 (br s, 3H, N^5-H/NH_2), 4.89 (d, *J* = 8.5 Hz, 1H, N^2-H), 3.69 (br s, 1H, H2), 3.38 – 3.12 (m, 4H, H1 and H5), 2.96 (s, 2H, $ArCH_2$-), 2.57 (s, 3H, $ArCH_3$), 2.51 (s, 3H, $ArCH_3$), 2.10 (s, 3H, $ArCH_3$), 1.61 – 1.37 (m, 19H, H3, H4. -$C(CH_3)_3$ and -$C(CH_3)_2$); ^{13}C NMR (101 MHz, $CDCl_3$) δ 158.9 (Pbf C_{Ar}), 156.4 (C=N), 156.1 (C=O), 138.5 (Pbf C_{Ar}), 133.0 (Pbf C_{Ar}), 132.4 (Pbf C_{Ar}), 124.8 (Pbf C_{Ar}), 117.7 (Pbf C_{Ar}), 86.6 (-$\underline{C}(CH_3)_2$), 80.1 (-$\underline{C}(CH_3)_3$), 55.2 (C1), 50.0 (C2), 43.4 ($ArCH_2$-), 41.1 (C5), 30.0 (C3), 28.7 (-$C(\underline{C}H_3)_2$), 28.5 (-$C(\underline{C}H_3)_3$), 25.6 (C4), 19.4 ($ArCH_3$), 18.1 ($ArCH_3$), 12.6 ($ArCH_3$); IR (neat) $\overline{\nu}_{max}$ 3452, 3333, 2975, 2934, 2098, 1684, 1617, 1545, 1456, 1367, 1248, 1163, 1089, 1028, 901, 851, 808, 783, 660 cm^{-1}; MS (ESI +ve) *m/z* 560 ($[M + Na]^+$, 100%), 538 ($[M + H]^+$, 30%); HRMS (ESI +ve TOF) calcd for $C_{24}H_{40}N_7O_5S$ 538.2812, found 538.2811 ($[M + H]^+$).

(*R*)-2-Azido-5-(2-((2,2,4,6,7-pentamethyl-2,3-dihydrobenzofuran-5-yl)sulfonyl)guanidino)pentanoic acid (28)[89]

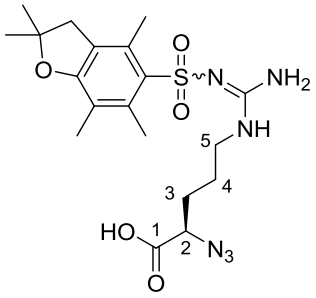

The methyl triflate salt of sulfuryl-diimidazole[87-88] (2.55g, 7.03 mmol) was added to cold (≤ 5 °C) H_2O (8.5 mL) and was stirred over an ice bath until the salt fully dissolved. EtOAc (8.5 mL) was added to the solution, followed by NaN_3 (549 mg, 8.44 mmol) and the mixture was then stirred vigorously at 0 °C for 60 min. The EtOAc layer was separated, dried (Na_2SO_4), filtered and the Na_2SO_4 solids were rinsed with minimal fresh EtOAc. The EtOAc filtrate (containing the newly formed diazotransfer reagent) was then added to reaction vessel charged with a solution of H-(D)-Arg(Pbf)-OH (**60**) (2.00 g, 4.69 mmol) in MeOH (12.7 mL), $CuSO_4 \cdot 5H_2O$ (12 mg, 0.05 mmol) and K_2CO_3 (972 mg, 7.03 mmol). The mixture was stirred vigorously at rt for 24 h, at which point the reaction was shown to be complete by MS analysis; the reaction was diluted with H_2O (50 mL) and a few drops of aqueous NaOH solution (10% w/w) were added to ensure an alkaline mixture (pH > 10). The volatile solvents (EtOAc and MeOH) were removed under reduced pressure at 40 °C. The aqueous reaction mixture was washed with Et_2O (2 × 50 mL) and then made acidic (pH < 3) with concentrated aqueous HCl. The aqueous phase was extracted with Et_2O (3 × 50 mL) and the combined ethereal extracts were washed with H_2O (3 × 100 mL) and brine (1 × 50 mL). The organic phase was dried ($MgSO_4$), filtered and concentrated to afford the α-azido-acid **28** (1.76 g, 83%) as a white foam that collapsed into a translucent gum. The spectroscopic data was found to be in agreement with those previously reported.[89] TLC (EtOAc/P.S. – 80:20): R_f = 0.44, (MeOH/CH_2Cl_2 – 10:90): R_f = 0.37; ^{1}H NMR (400 MHz, $CDCl_3$) δ 6.35 (br s, 4H, N^5-H/NH_2 and -OH), 3.97 (t, J = 6.5 Hz, 1H, H2), 3.25 (s, 2H, H5),

2.95 (s, 2H, $ArCH_2$-), 2.53 (s, 3H, $ArCH_3$), 2.47 (s, 3H, $ArCH_3$), 2.08 (s, 3H, $ArCH_3$), 1.60 – 1.98 (m, 4H, H3 and H4), 1.46 (s, 6H, -$C(CH_3)_2$); ^{13}C NMR (101 MHz, CD_3OD) δ 173.7 (C1), 160.0 (Pbf C_{Ar}), 158.1 (C=N), 139.5 (Pbf C_{Ar}), 134.4 (Pbf C_{Ar}), 133.6 (Pbf C_{Ar}), 126.2 (Pbf C_{Ar}), 118.6 (Pbf C_{Ar}), 87.8 (-$\underline{C}(CH_3)_2$), 63.0 (C2), 44.1 ($ArCH_2$-), 41.4 (C5), 29.7 (C3), 28.9 (-$C(\underline{C}H_3)_2$), 27.1 (C4), 19.7 ($ArCH_3$), 18.6 ($ArCH_3$), 12.7 ($ArCH_3$); MS (ESI −ve) *m/z* 451 ($[M - H]^-$, 100%), MS (ESI +ve) *m/z* 453 ($[M + H]^+$, 100%).

Methyl (*R*)-2-amino-5-(2-((2,2,4,6,7-pentamethyl-2,3-dihydrobenzofuran-5-yl)sulfonyl)guanidinyl)pentanoate (29)[59]

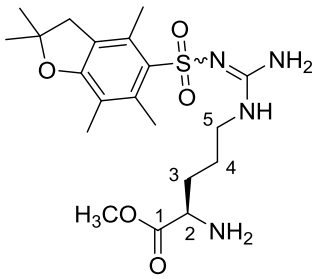

Fmoc-(D)-Arg(Pbf)-OH (**61**) (1.00 g, 1.54 mmol) was dissolved in MeOH (9.3 mL) and the solution was brought to 0 °C (ice bath) with magnetic stirring. Thionyl chloride (312 mg, 2.62 mmol) was added dropwise, the ice bath removed and the reaction solution stirred at rt for 24 h. The solvent was removed and the residue was dissolved in EtOAc (100 mL); the organic phase was washed with aqueous $NaHCO_3$ (5% w/w – 1 × 50 mL), brine (1 × 50 mL), dried ($MgSO_4$), filtered and concentrated to afford the intermediate methyl ester as a translucent gum. The ester was dissolved in MeOH (15.7 mL) with magnetic stirring and piperidine (668 mg, 7.85 mmol) was then added and the mixture was stirred at rt for 24 h. The reaction was diluted with MeOH (80 mL), washed with hexane (5 × 100 mL) and concentrated to afford the target amine **29** (551 mg, 80% over two steps) as a translucent, colourless gum. The spectroscopic data was found to be in agreement with those previously reported.[59] TLC ($MeOH/CH_2Cl_2$ – 10:90): R_f = 0.09, ($NEt_3/MeOH/CH_2Cl_2$ – 2:10:88): R_f = 0.33; ^{1}H NMR (400 MHz, $CDCl_3$) δ 6.57 (br s, 1H, N^5-H), 6.47 (br s, 2H, -$NH_{2\ (guanidine)}$),

3.66 (s, 3H, -OCH_3), 3.40 (br s, 1H, H2), 3.15 (br s, 2H, H5), 2.95 (s, 2H, $ArCH_2$-), 2.55 (s, 3H, $ArCH_3$), 2.48 (s, 3H, $ArCH_3$), 2.06 (s, 3H, $ArCH_3$), 1.74 – 1.63 (m, 1H, $H3_A$ or $H3_B$), 1.61 – 1.39 (m, 9H, $H3_B$ or $H3_A$, H4 and -$C(CH_3)_2$); ^{13}C NMR (101 MHz, $CDCl_3$) δ 176.0 (C1), 158.6 (Pbf C_{Ar}), 156.4 (C=N), 138.1 (Pbf C_{Ar}), 132.9 (Pbf C_{Ar}), 132.0 (Pbf C_{Ar}), 124.6 (Pbf C_{Ar}), 117.4 (Pbf C_{Ar}), 86.3 (-$\underline{C}(CH_3)_2$), 53.8 (C2), 51.9 (-OCH_3), 43.1 ($ArCH_2$-), 40.6 (C5), 31.8 (C3), 28.5 (-$C(\underline{C}H_3)_2$), 25.5 (C4), 19.2 ($ArCH_3$), 17.9 ($ArCH_3$), 12.4 ($ArCH_3$); MS (ESI +ve) *m/z* 441 ($[M + H]^+$, 100%), 463 ($[M + Na]^+$, 95%).

6.3.2 – Series A1

Benzyl ((*R*)-N^6-(*tert*-butoxycarbonyl)-6-amino-1-(4-(((2'-(isopentyloxy)-[1,1'-biphenyl]-2-yl)oxy)methyl)-1*H*-1,2,3-triazol-1-yl)hexan-2-yl)carbamate (62a)

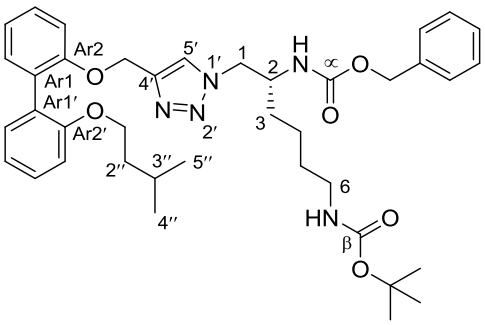

Following **General Procedure A**, azide **23** (1.50 g, 3.83 mmol), alkyne **21** (2.26 g, 7.66 mmol), $Cu(OAc)_2{\cdot}H_2O$ (153 mg, 0.77 mmol) and sodium ascorbate (304 mg, 1.53 mmol) were stirred in *t*-BuOH (77 mL) and H_2O (19 mL) for 48 h to give the triazole **62a** (1.97 g, 75%) as a white foam after flash chromatography over SiO_2 gel (EtOAc/P.S. – 20:80 → 50:50). TLC (EtOAc/P.S. – 50:50): R_f = 0.48; $[\alpha]_D^{23}$ +31.3 (*c* 0.83, MeOH); ^{1}H NMR (400 MHz, $CDCl_3$) δ 7.38 – 7.21 (m, 9H, ArH), 7.17 (s, 1H, H5'), 7.07 – 6.99 (m, 2H, ArH), 6.99 – 6.91 (m, 2H, ArH), 5.14 (s, 2H, -OCH_2-C4'), 5.06 (s, 3H, -C$\underline{H}_2$Ph and N^2-H), 4.55 (br s, 1H, N^6-H), 4.39 (d, *J* = 5.1 Hz, 2H, H1), 3.92 (br s, 1H, H2), 3.88 (t, *J* = 6.6 Hz, 2H, H1"), 3.06 (br s, 2H, H6), 1.62 – 1.52 (m, 1H, H3"), 1.52 – 1.23 (m, 17H, H3, H4, H5, H2" and -$C(CH_3)_3$), 0.79 (d, *J* = 6.6 Hz, 6H, H4" and H5"); ^{13}C NMR (101 MHz,

$CDCl_3$) δ 156.6 (CAr2'), 156.2 (Cβ), 155.9 (Cα), 155.8 (CAr2), 145.2 (C4'), 136.2 (Phenyl C_{Ar}), 131.7 (CAr6 or CAr6'), 131.5 (CAr6' or CAr6), 128.7 (CAr1), 128.54 (Phenyl C_{Ar}* and CAr4 or CAr4'), 128.46 (CAr4′ or CAr4), 128.2 (Phenyl C_{Ar}), 128.1 (Phenyl C_{Ar}* and CAr1'), 123.3 (C5'), 121.1 (CAr5), 120.1 (CAr5'), 113.3 (CAr3), 112.3 (CAr3'), 79.2 (-$\underline{C}(CH_3)_3$), 67.0 (C1"), 66.9 (-$\underline{C}H_2$Ph), 63.4 (-O$\underline{C}H_2$-C4'), 53.1 (C1), 51.2 (C2), 39.8 (C6), 37.9 (C2"), 31.0 (C3), 29.7 (C5), 28.4 (-C($\underline{C}H_3)_3$), 25.0 (C3"), 22.7 (C4), 22.5 (C4" and C5"); IR (neat) $\overline{\nu}_{max}$ 3323, 2952, 2930, 2869, 2358, 2342, 1696, 1506, 1437, 1394, 1364, 1242, 1166, 1052, 1011, 856, 750, 697 cm^{-1}; MS (ESI +ve) *m/z* 708 ($[M + Na]^+$, 100%), 686 ($[M + H]^+$, 22%); HRMS (ESI +ve TOF) calcd for $C_{39}H_{51}N_5O_6Na$ 708.3737, found 708.3755 ($[M + Na]^+$).

Tert-butyl (_R_)-(5-amino-6-(4-(((2'-(isopentyloxy)-[1,1'-biphenyl]-2-yl)oxy)methyl)-1_H_-1,2,3-triazol-1-yl)hexyl)carbamate (63a)

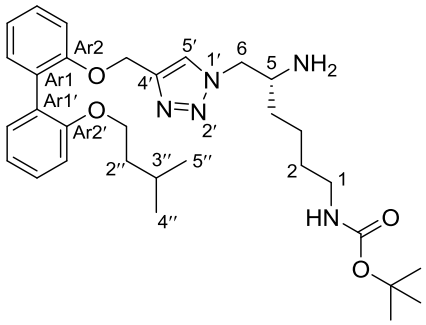

To a reaction vessel charged with carbamate **62a** (1.90 g, 2.77 mmol), acetic acid (3.17 mL, 55.40 mmol) and palladium on charcoal (10% w/w – 442 mg, 0.42 mmol) was added MeOH (27.7 mL) under a flow of N_2 gas. The reaction vessel was then sealed and degassed under high vacuum with magnetic stirring. N_2 gas was allowed into the reaction vessel and the vessel was again degassed; this step was done twice. After the third degassing, the vacuum was maintained and a 2.0 L balloon of H_2 gas was attached and allowed into the reaction vessel. The reaction mixture was then stirred vigorously at rt for 24 h under an atmosphere of H_2 gas. After the reaction was shown to be complete by TLC analysis (EtOAc/P.S. – 50:50), the H_2 source was removed, the reaction vessel was purged with N_2 gas and Celite was added to

the reaction mixture with vigorous magnetic stirring. The mixture was then vacuum filtered through a pad of fresh Celite atop a PTFE membrane, the solids were rinsed thoroughly with MeOH (5 × 20 mL) and the combined filtrates were concentrated until nearly dry. The residue was dissolved in EtOAc (200 mL) and washed successively with saturated aqueous $NaHCO_3$ (3 × 100 mL), H_2O (1 × 100 mL) and finally brine (1 × 100 mL). The organic phase was dried (Na_2SO_4), filtered and concentrated to afford the amine **63a** (1.52 g, 99%) as translucent, light tan gum. TLC (NEt_3/MeOH/CH_2Cl_2 – 2:10:88): R_f = 0.46; $[\alpha]_D^{23}$ +16.5 (*c* 1.67, MeOH); ^{1}H NMR (400 MHz, $CDCl_3$) δ 7.34 – 7.22 (m, 5H, ArH and H5'), 7.08 – 6.92 (m, 4H, ArH), 5.17 (d, *J* = 0.8 Hz, 2H, -OCH_2-C4'), 4.57 (br s, 1H, N^1-H), 4.28 (dd, *J* = 13.6, 4.2 Hz, 1H, $H6_A$ or $H6_B$), 4.07 (dd, *J* = 13.6, 7.9 Hz, 1H, $H6_B$ or $H6_A$), 3.90 (t, *J* = 6.6 Hz, 2H, H1"), 3.21 – 3.02 (m, 3H, H1 and H5), 1.68 – 1.21 (m, 18H, H2, H3, H4, H2", H3" and -$C(CH_3)_3$), 0.80 (d, *J* = 6.6 Hz, 6H, H4" and H5"); ^{13}C NMR (101 MHz, $CDCl_3$) δ 156.6 (CAr2'), 156.0 (C=O), 155.8 (CAr2), 145.2 (C4'), 131.62 (CAr6 or CAr6'), 131.56 (CAr6' or CAr6), 128.7 (CAr1), 128.50 (CAr4 or CAr4'), 128.49 (CAr4' or CAr4), 128.2 (CAr1'), 123.1 (C5'), 121.1 (CAr5), 120.1(CAr5'), 113.2 (CAr3), 112.3 (CAr3'), 79.2 (-$\underline{C}(CH_3)_3$), 67.1 (C1"), 63.54 (-O$\underline{C}H_2$-C4'), 57.0 (C6), 51.5 (C5), 40.2 (C1), 38.0 (C2"), 34.5 (C4), 30.0 (C2), 28.5 (-C($\underline{C}H_3)_3$), 25.0 (C3), 23.0 (C3"), 22.5 (C4" and C5"); IR (neat) $\overline{\nu}_{max}$ 3345, 2955, 2930, 2869, 2362, 2327, 1700, 1506, 1437, 1388, 1364, 1241, 1166, 1125, 1051, 1002, 852, 750, 615 cm^{-1}; MS (ESI +ve) *m/z* 574 ($[M + Na]^+$, 100%), 552 ($[M + H]^+$, 80%); HRMS (ESI +ve TOF) calcd for $C_{31}H_{46}N_5O_4$ 552.3550, found 552.3564 ($[M + H]^+$).

(*R*)-*N*-(6-Amino-1-(4-(((2'-(isopentyloxy)-[1,1'-biphenyl]-2-yl)oxy)methyl)-1*H*-1,2,3-triazol-1-yl)hexan-2-yl)-2-phenylacetamide hydrochloride (64a)

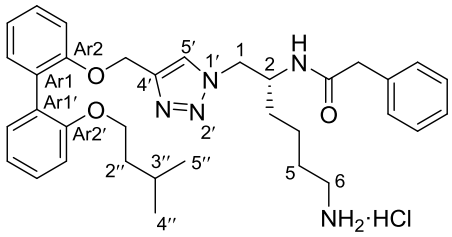

Following **General Procedure B**, amine **63a** (50 mg, 0.09 mmol), phenylacetic acid (15 mg, 0.11 mmol), EDCI (21 mg, 0.11 mmol) and HOBt (15 mg, 0.10 mmol) were stirred in acetonitrile (0.9 mL) for 24 h to give the intermediate amide as a translucent tan gum. Following **General Procedure D**, the amide was dissolved in CH_2Cl_2 (2.7 mL) and treated with CF_3CO_2H (2.7 mL) followed by work-up with ethereal HCl to give the amine salt **64a** (53 mg, 96% over two steps) as a light tan powder that rapidly transitioned to a sticky gum. $[\alpha]_D^{23}$ +22.7 (*c* 1.30, MeOH); ^{1}H NMR (400 MHz, CD_3OD) δ 7.50 (s, 1H, H5'), 7.36 – 7.10 (m, 10H, ArH), 7.06 – 6.91 (m, 3H, ArH), 5.02 (s, 2H, -OCH_2-C4'), 4.51 (dd, *J* = 13.8, 4.3 Hz, 1H, $H1_A$ or $H1_B$), 4.37 (dd, *J* = 13.8, 8.0 Hz, 1H, $H1_B$ or $H1_A$), 4.25 (br s, 1H, H2), 3.90 (t, *J* = 6.4 Hz, 2H, H1''), 3.38 (br s, 2H, -C$\underline{H}_2$Ph), 2.92 – 2.77 (m, 2H, H6), 1.79 – 1.22 (m, 9H, H3, H4, H5, H2'' and H3''), 0.81 (d, *J* = 6.6 Hz, 6H, H4'' and H5''); ^{13}C NMR (101 MHz, CD_3OD) δ 174.3 (C=O), 158.2 (CAr2'), 157.4 (CAr2), 145.4 (C4'), 136.9 (Phenyl C_{Ar}), 133.0 (CAr6 or CAr6'), 132.6 (CAr6' or CAr6), 130.5 (CAr1), 130.3 (Phenyl C_{Ar}*), 129.9 (CAr4 or CAr4'), 129.77 (Phenyl CAr*), 129.75 (CAr1' and CAr4' or CAr4), 128.2 (Phenyl C_{Ar}), 126.0 (C5'), 122.4 (CAr5), 121.5 (CAr5'), 114.8 (CAr3), 113.9 (CAr3'), 68.2 (C1''), 63.6 (-O$\underline{C}H_2$-C4'), 54.6 (C1), 50.8 (C2), 44.1 (-$\underline{C}H_2$Ph), 40.7 (C6), 39.4 (C2''), 32.3 (C3), 28.2 (C5), 26.2 (C3''), 23.9 (C4), 23.1 (C4'' and C5''); IR (neat) $\bar{\nu}_{max}$ 3242, 2955, 2873, 2363, 2337, 1653, 1559, 1539, 1506, 1437, 1261, 1223, 1162, 1124, 1109, 1050, 1003, 876, 849 cm^{-1}; MS (ESI +ve) *m/z* 570 ([M + H]$^+$, 100%),

592 ([M + Na]$^+$, 15%); HRMS (ESI +ve TOF) calcd for $C_{34}H_{44}N_5O_3$ 570.3444, found 570.3451 ([M + H]$^+$).

(*R*)-*N*-(6-Amino-1-(4-(((2'-(isopentyloxy)-[1,1'-biphenyl]-2-yl)oxy)methyl)-1*H*-1,2,3-triazol-1-yl)hexan-2-yl)-3-phenylpropanamide hydrochloride (64b)

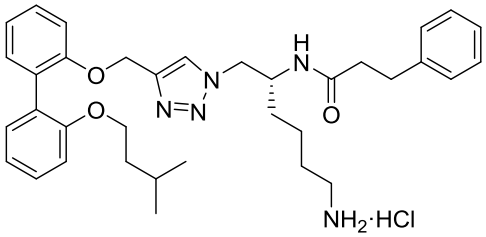

Following **General Procedure B**, amine **63a** (50 mg, 0.09 mmol), 3-phenylpropanoic acid (16 mg, 0.11 mmol), EDCI (21 mg, 0.11 mmol) and HOBt (15 mg, 0.10 mmol) were stirred in acetonitrile (0.9 mL) for 24 h to give the intermediate amide as a translucent tan gum. Following **General Procedure D**, the amide was dissolved in CH_2Cl_2 (2.7 mL) and treated with CF_3CO_2H (2.7 mL) followed by work-up with ethereal HCl to give the amine salt **64b** (52 mg, 93% over two steps) as a light tan powder that rapidly transitioned to a sticky gum. $[\alpha]_D^{23}$ +21.7 (*c* 1.37, MeOH); ^{1}H NMR (400 MHz, CD_3OD) δ 7.53 (s, 1H), 7.36 – 7.08 (m, 10H), 7.06 – 6.89 (m, 3H), 5.09 (s, 2H), 4.45 (dd, *J* = 14.0, 4.4 Hz, 1H), 4.33 (dd, *J* = 13.8, 7.2 Hz, 1H), 4.20 (s, 1H), 3.90 (t, *J* = 6.2 Hz, 2H), 3.00 – 2.75 (m, 4H), 2.50 – 2.29 (m, 2H), 1.80 – 1.18 (m, 9H), 0.81 (d, *J* = 6.5 Hz, 6H); ^{13}C NMR (101 MHz, CD_3OD) δ 175.3, 158.1, 157.4, 145.4, 142.2, 133.0, 132.6, 130.5, 129.9, 129.72, 129.68*, 129.67*, 127.5, 126.1, 122.4, 121.5, 114.8, 113.9, 68.2, 63.6, 54.8, 50.7, 40.7, 39.4, 38.8, 32.8, 32.1, 28.2, 26.2, 23.8, 23.1*; IR (neat) $\overline{\nu}_{max}$ 3242, 2954, 2869, 2358, 2329, 1653, 1559, 1539, 1506, 1437, 1387, 1261, 1225, 1161, 1124, 1109, 1052, 1002, 847, 749, 699 cm^{-1}; MS (ESI +ve) *m/z* 584 ([M + H]$^+$, 100%), 606 ([M + Na]$^+$, 11%); HRMS (ESI +ve TOF) calcd for $C_{35}H_{46}N_5O_3$ 584.3601, found 584.3609 ([M + H]$^+$).

Benzyl (*R*)-(6-amino-1-(4-(((2'-(isopentyloxy)-[1,1'-biphenyl]-2-yl)oxy)methyl)-1*H*-1,2,3-triazol-1-yl)hexan-2-yl)carbamate hydrochloride (64c)

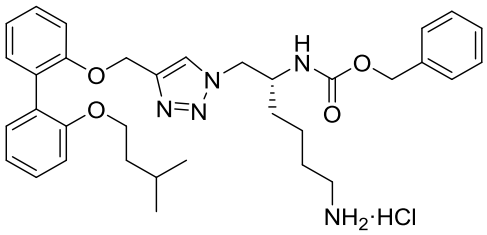

Following **General Procedure D**, carbamate **62a** (50 mg, 0.07 mmol) was dissolved in CH_2Cl_2 (2.1 mL) and treated with CF_3CO_2H (2.1 mL) followed by work-up with ethereal HCl to give the amine salt **64c** (42 mg, 93%) as a light tan powder that rapidly transitioned to a sticky gum. $[\alpha]_D^{23}$ +8.8 (*c* 1.20, MeOH); ^{1}H NMR (400 MHz, DMSO) δ 7.83 (s, 1H), 7.39 – 7.18 (m, 8H), 7.18 – 7.09 (m, 2H), 7.05 – 6.87 (m, 4H), 5.06 (s, 2H), 4.93 (s, 2H), 4.41 (dd, *J* = 13.7, 4.9 Hz, 1H), 4.30 (dd, *J* = 13.6, 7.7 Hz, 1H), 3.94 – 3.77 (m, 3H), 2.78 – 2.66 (m, 2H), 1.60 – 1.24 (m, 9H), 0.78 (d, *J* = 6.6 Hz, 6H); ^{13}C NMR (101 MHz, DMSO) δ 156.0, 155.7, 155.6, 142.8, 137.0, 131.3, 131.1, 128.5*, 128.4, 128.3*, 127.8, 127.7, 127.5, 127.4, 124.4, 120.4, 119.9, 112.9, 112.3, 66.2, 65.2, 61.8, 52.7, 51.0, 38.4, 37.4, 30.9, 26.6, 24.4, 22.3, 22.2*; IR (neat) $\bar{\nu}_{max}$ 2956, 2926, 2873, 2357, 2337, 1700, 1680, 1559, 1539, 1506, 1437, 1339, 1261, 1204, 1125, 1052, 1002, 833, 799, 750, 698 cm^{-1}; MS (ESI +ve) *m/z* 608 ([M + Na]$^+$, 100%), 586 ([M + H]$^+$, 42%); HRMS (ESI +ve TOF) calcd for $C_{34}H_{44}N_5O_4$ 586.3393, found 586.3400 ([M + H]$^+$).

Benzyl (*R*)-(1-(4-(((2'-(isopentyloxy)-[1,1'-biphenyl]-2-yl)oxy)methyl)-1*H*-1,2,3-triazol-1-yl)-5-(2-((2,2,4,6,7-pentamethyl-2,3-dihydrobenzofuran-5-yl)sulfonyl)guanidino)pentan-2-yl)carbamate (62b)

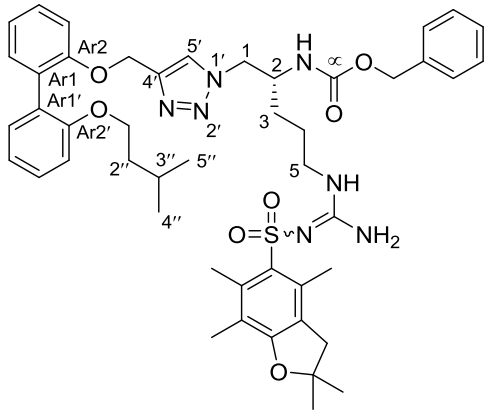

Following **General Procedure A**, azide **26** (1.00 g, 1.75 mmol), alkyne **21** (1.03 g, 3.50 mmol), $Cu(OAc)_2 \cdot H_2O$ (70 mg, 0.35 mmol) and sodium ascorbate (139 mg, 0.70 mmol) were stirred in *t*-BuOH (35 mL) and H_2O (8.8 mL) for 20 h to give the product triazole **62b** (1.24 g, 82%) as a white foam after flash chromatography over SiO_2 gel (EtOAc/P.S. – 10:90 → 80:20). TLC (EtOAc/P.S. – 80:20): R_f = 0.44; $[\alpha]_D^{23}$ +18.3 (*c* 1.53, MeOH); ^{1}H NMR (400 MHz, $CDCl_3$) δ 7.32 – 7.15 (m, 10H, H5' and ArH), 7.04 – 6.96 (m, 2H, ArH), 6.93 – 6.86 (m, 2H, ArH), 6.10 (br s, 2H, -NH_2), 5.92 (br s, 1H, N^5-H), 5.81 (d, *J* = 8.2 Hz, 1H, N^2-H), 5.04 (s, 2H, -OCH_2-C4'), 4.99 (s, 2H, -C$\underline{H}_2$Ph), 4.30 (br s, 2H, H1), 3.97 – 3.88 (m, 1H, H2), 3.84 (t, *J* = 6.6 Hz, 2H, H1"), 3.16 – 3.06 (m, 2H, H5), 2.90 (s, 2H, $ArCH_2$-), 2.54 (s, 3H, $ArCH_3$), 2.46 (s, 3H, $ArCH_3$), 2.06 (s, 3H, $ArCH_3$), 1.60 – 1.33 (m, 13H, H3, H4, H2", H3" and -$C(CH_3)_2$), 0.77 (d, *J* = 6.6 Hz, 6H, H4" and H5"); ^{13}C NMR (101 MHz, $CDCl_3$) δ 158.9 (Pbf C_{Ar}), 156.7 (CAr2'), 156.4 (C=O), 156.3 (C=N), 155.9 (CAr2), 144.8 (C4'), 138.5 (Pbf C_{Ar}), 136.4 (Phenyl C_{Ar}), 132.9 (Pbf C_{Ar}), 132.4 (Pbf C_{Ar}), 131.9 (CAr6 or CAr6'), 131.7 (CAr6 or CAr6'), 128.74 (CAr4 or CAr4'), 128.73 (CAr1), 128.66 (Phenyl C_{Ar})*, 128.6 (CAr1'), 128.3 (Phenyl C_{Ar}), 128.12 (CAr4 or CAr4'), 128.06 (Phenyl C_{Ar})*, 124.8 (Pbf C_{Ar}), 124.1 (C5'), 121.33 (CAr5), 120.30 (CAr5'), 117.7 (Pbf C_{Ar}), 113.6 (CAr3), 112.6 (CAr3'), 86.6 (-$\underline{C}(CH_3)_2$), 67.2 (C1"), 66.9 (-$\underline{C}H_2$Ph), 63.3 (-O$\underline{C}H_2$-C4'), 53.2

(C1), 51.2 (C2), 43.3 ($ArCH_2$-), 40.8 (C5), 38.0 (C2"), 28.9 (C3), 28.7 (-C($\underline{C}H_3)_2$), 25.5 (C4), 25.1 (C3"), 22.6 (C4" and C5"), 19.4 ($ArCH_3$), 18.1 ($ArCH_3$), 12.6 ($ArCH_3$); IR (neat) $\overline{\nu}_{max}$ 3336, 2955, 2927, 2873, 2312, 1715, 1700, 1617, 1559, 1540, 1507, 1457, 1340, 1241, 1154, 1107, 1090, 1052, 1000, 902, 851, 806, 751, 734, 664, 642, 617 cm^{-1}; MS (ESI +ve) *m/z* 888 ($[M + Na]^+$, 100%), 866 ($[M + H]^+$, 9%); HRMS (ESI +ve TOF) calcd for $C_{47}H_{59}N_7O_7SNa$ 888.4094, found 888.4136 ($[M + Na]^+$).

(*R*)-(1-(4-(((2'-(isopentyloxy)-[1,1'-biphenyl]-2-yl)oxy)methyl)-1*H*-1,2,3-triazol-1-yl)-5-(2-((2,2,4,6,7-pentamethyl-2,3-dihydrobenzofuran-5-yl)sulfonyl)guanidino)pentan-2-yl)amine (63b)

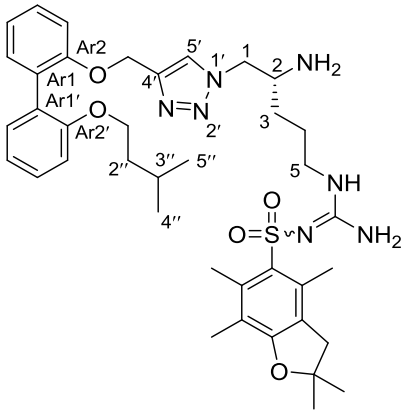

To a reaction vessel charged with carbamate **62b** (1.11 g, 1.29 mmol), acetic acid (1.5 mL, 25.70 mmol) and palladium on charcoal (10% w/w – 205 mg, 0.19 mmol) was added MeOH (13.0 mL) under a flow of N_2 gas. The reaction vessel was then sealed and degassed under high vacuum with magnetic stirring. N_2 gas was allowed into the reaction vessel and the vessel was again degassed; this step was done twice. After the third degassing, the vacuum was maintained and a 2.0 L balloon of H_2 gas was attached and allowed into reaction vessel. The reaction mixture was stirred vigorously at rt for 18 h under an atmosphere of H_2 gas. After the reaction was shown to be complete by TLC analysis (EtOAc), the H_2 source was removed, the reaction vessel was purged with N_2 gas and Celite was added to the reaction mixture with vigorous magnetic stirring. The reaction mixture was vacuum filtered through a pad of fresh Celite atop a PTFE membrane, the solids were rinsed

thoroughly with MeOH (5 × 20 mL) and the combined filtrates were concentrated until nearly dry. The residue was dissolved in CH_2Cl_2 (100 mL) and washed successively with saturated aqueous $NaHCO_3$ (3 × 50 mL), H_2O (1 × 50 mL) and brine (1 × 50 mL). The organic phase was dried (Na_2SO_4), filtered and concentrated to afford the amine **63b** (864 mg, 92%) as translucent, light tan gum. TLC (NEt_3/MeOH/CH_2Cl_2 – 2:10:88): R_f = 0.47; $[\alpha]_D^{23}$ +7.0 (*c* 4.27, MeOH); ^{1}H NMR (400 MHz, $CDCl_3$) δ 7.33 – 7.19 (m, 5H, H5' and ArH), 7.08 – 6.97 (m, 2H, ArH), 6.96 – 6.89 (m, 2H, ArH), 6.29 – 6.13 (m, 3H, -NH/$NH_{2\ (guanidine)}$), 5.10 (s, 2H, -OC$\underline{H}_2$-C4'), 4.22 (dd, *J* = 13.8, 4.2 Hz, 1H, $H1_A$ or $H1_B$), 4.09 (dd, *J* = 13.8, 7.4 Hz, 1H, $H1_B$ or $H1_A$), 3.88 (t, *J* = 6.6 Hz, 2H, H1"), 3.14 (br s, 3H, H2 and H5), 2.92 (s, 2H, $ArCH_2$-), 2.56 (s, 3H, $ArCH_3$), 2.47 (s, 3H, $ArCH_3$), 2.06 (s, 3H, $ArCH_3$), 1.66 – 1.18 (m, 13H, H3, H4, H2", H3" and -C(CH_3)$_2$), 0.78 (d, *J* = 6.6 Hz, 6H, H4" and H5"); ^{13}C NMR (101 MHz, $CDCl_3$) δ 158.9 (Pbf C_{Ar}), 156.7 (CAr2'), 156.3 (C=N), 155.9 (CAr2), 145.0 (C4'), 138.4 (Pbf C_{Ar}), 133.1 (Pbf C_{Ar}), 132.3 (Pbf C_{Ar}), 131.9 (CAr6 or CAr6'), 131.7 (CAr6' or CAr6), 128.8 (CAr1), 128.70 (CAr4 or CAr4'), 128.67 (CAr4' or CAr4), 128.2 (CAr1'), 124.8 (Pbf C_{Ar}), 123.9 (C5'), 121.4 (CAr5), 120.3 (CAr5'), 117.6 (Pbf C_{Ar}), 113.5 (CAr3), 112.6 (CAr3'), 86.5 (-$\underline{C}$(CH_3)$_2$), 67.2 (C1"), 63.4 (-O$\underline{C}H_2$-C4'), 56.6 (C1), 51.3 (C2), 43.4 ($ArCH_2$-), 40.9 (C5), 38.1 (C2"), 31.4 (C3), 28.7 (-C($\underline{C}H_3$)$_2$), 25.6 (C4), 25.1 (C3") 22.6 (C4" and C5"), 19.4 ($ArCH_3$), 18.1 ($ArCH_3$), 12.6 ($ArCH_3$); IR (neat) $\overline{\nu}_{max}$ 3337, 2956, 2870, 2358, 2321, 1715, 1700, 1559, 1539, 1507, 1457, 1340, 1240, 1156, 1106, 1090, 1048, 906, 852, 804, 783, 751, 734, 668, 639, 614 cm^{-1}; MS (ESI +ve) *m/z* 754 ([M + Na]$^+$, 100%), 732 ([M + H]$^+$, 38%); HRMS (ESI +ve TOF) calcd for $C_{39}H_{54}N_7O_5S$ 732.3907, found 732.3931 ([M + H]$^+$).

(*R*)-*N*-(5-Guanidino-1-(4-(((2'-(isopentyloxy)-[1,1'-biphenyl]-2-yl)oxy)methyl)-1*H*-1,2,3-triazol-1-yl)pentan-2-yl)-2-phenylacetamide hydrochloride (65a)

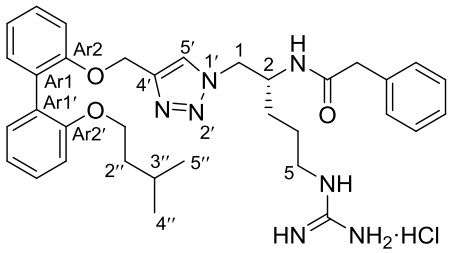

Following **General Procedure B**, amine **63b** (50 mg, 0.07 mmol), phenylacetic acid (11 mg, 0.08 mmol), EDCI (16 mg, 0.08 mmol) and HOBt (11 mg, 0.07 mmol) were stirred in acetonitrile (0.7 mL) for 18 h to give the intermediate amide as a translucent tan gum. Following **General Procedure C**, the amide was dissolved in CH_2Cl_2 (2.0 mL) and treated with H_2O (25 mg, 1.37 mmol) and CF_3CO_2H (2.0 mL) followed by work-up with ethereal HCl to give the amine salt **65a** (36 mg, 84% over two steps) as a light tan powder that rapidly transitioned to a sticky gum. $[\alpha]_D^{23}$ +28.2 (*c* 1.03, MeOH); ^{1}H NMR (400 MHz, CD_3OD) δ 7.48 (d, *J* = 8.0 Hz, 1H, H5'), 7.35 – 7.08 (m, 10H, ArH), 7.05 – 6.86 (m, 3H, ArH), 5.01 (d, *J* = 4.0 Hz, 2H, -OC<u>H</u>$_2$-C4'), 4.55 – 4.14 (m, 3H, H1 and H2), 3.94 – 3.84 (m, 2H, H1''), 3.33 (s, 2H, -C<u>H</u>$_2$Ph), 3.15 (br s, 2H, H6), 1.69 – 1.27 (m, 7H, H3, H4, H2'' and H3''), 0.80 (d, *J* = 6.6 Hz, 6H, H4'' and H5''); ^{13}C NMR (101 MHz, CD_3OD) δ 174.4 (C=O), 158.7 (C=N), 158.1 (CAr2'), 157.4 (CAr2), 144.1 (C4' – observed by gHMBC), 136.8 (Phenyl C_{Ar}), 133.0 (CAr6 or CAr6'), 132.6 (CAr6 or CAr6'), 130.5 (CAr1), 130.3 (Phenyl C_{Ar})*, 129.84 (CAr4 or CAr4'), 129.78 (Phenyl C_{Ar})*, 129.7 (CAr4 or CAr4' and CAr1'), 128.2 (Phenyl C_{Ar}), 125.9 (C5'), 122.4 (CAr5), 121.5 (CAr5'), 114.7 (CAr3), 113.8 (CAr3'), 68.2 (C1''), 63.7 (-O<u>C</u>H$_2$-C4'), 54.5 (C1), 50.7 (C2), 44.1 (-<u>C</u>H$_2$Ph), 42.1 (C5), 39.4 (C2''), 30.1 (C3), 26.4 (C4), 26.2 (C3''), 23.1 (C4'' and C5''); IR (neat) $\bar{\nu}_{max}$ 3336, 2957, 2873, 2362, 2327, 1715, 1700, 1653, 1559, 1540, 1507, 1457, 1437, 1340, 1218, 1162, 1109, 1051, 1003, 914, 852, 751, 729, 668 cm^{-1}; MS (ESI +ve) *m/z*

598 ([M + H]$^+$, 100%), 620 ([M + Na]$^+$, 21%); HRMS (ESI +ve TOF) calcd for $C_{34}H_{44}N_7O_3$ 598.3506, found 598.3510 ([M + H]$^+$).

(*R*)-*N*-(5-Guanidino-1-(4-(((2'-(isopentyloxy)-[1,1'-biphenyl]-2-yl)oxy)methyl)-1*H*-1,2,3-triazol-1-yl)pentan-2-yl)-3-phenylpropanamide hydrochloride (65b)

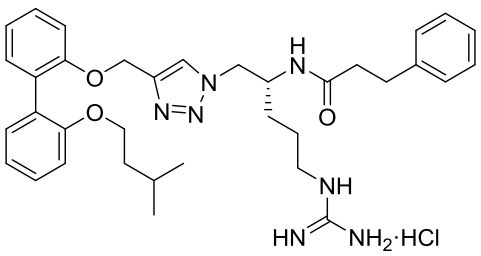

Following **General Procedure B**, amine **63b** (50 mg, 0.07 mmol), 3-phenylpropanoic acid (12 mg, 0.08 mmol), EDCI (16 mg, 0.08 mmol) and HOBt (11 mg, 0.07 mmol) were stirred in acetonitrile (0.7 mL) for 18 h to give the intermediate amide as a translucent tan gum. Following **General Procedure C**, the amide was dissolved in CH_2Cl_2 (2.0 mL) and treated with H_2O (25 mg, 1.37 mmol) and CF_3CO_2H (2.0 mL) followed by work-up with ethereal HCl to give the amine salt **65b** (42 mg, 95% over two steps) as a light tan powder that rapidly transitioned to a sticky gum. $[\alpha]_D^{23}$ +55.1 (*c* 0.53, MeOH); ^{1}H NMR (400 MHz, CD_3OD) δ 7.47 (d, *J* = 3.7 Hz, 1H), 7.34 – 7.05 (m, 10H), 7.03 – 6.84 (m, 3H), 5.07 (d, *J* = 3.8 Hz, 2H), 4.45 – 4.08 (m, 3H), 3.93 – 3.82 (m, 2H), 3.08 (br s, 2H), 2.84 – 2.74 (m, 2H), 2.44 – 2.28 (m, 2H), 1.63 – 1.22 (m, 7H), 0.78 (d, *J* = 6.5 Hz, 6H); ^{13}C NMR (101 MHz, CD_3OD) δ 175.5, 158.7, 158.1, 157.5, 145.5, 142.1, 133.0, 132.6, 130.5, 129.9, 129.74, 129.68*, 129.66**, 127.5, 125.9, 122.4, 121.5, 114.7, 113.9, 113.8, 68.2, 63.7, 54.6, 50.5, 42.1, 39.4, 38.8, 32.8, 29.8, 26.3, 26.2, 23.1*; IR (neat) $\bar{\nu}_{max}$ 3330, 2955, 2873, 2331, 1684, 1653, 1559, 1539, 1507, 1457, 1219, 1162, 1109, 1043, 1003, 913, 880, 852, 750, 698, 668 cm^{-1}; MS (ESI +ve) *m/z* 612 ([M + H]$^+$, 100%), 634 ([M + Na]$^+$, 14%); HRMS (ESI +ve TOF) calcd for $C_{35}H_{46}N_7O_3$ 612.3662, found 612.3676 ([M + H]$^+$).

Benzyl (*R*)-(5-guanidino-1-(4-(((2'-(isopentyloxy)-[1,1'-biphenyl]-2-yl)oxy)methyl)-1*H*-1,2,3-triazol-1-yl)pentan-2-yl)carbamate hydrochloride (65c)

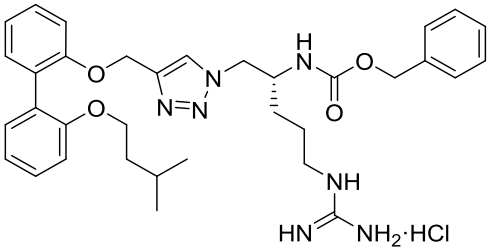

Following **General Procedure C**, carbamate **62b** (50 mg, 0.06 mmol) was dissolved in CH_2Cl_2 (1.9 mL) and treated with H_2O (18 mg, 1.00 mmol) and CF_3CO_2H (1.9 mL) followed by work-up with ethereal HCl to give the amine salt **65c** (33 mg, 87%) as a light tan powder that rapidly transitioned to a sticky gum. $[\alpha]_D^{23}$ +82.0 (*c* 0.37, MeOH); ^{1}H NMR (500 MHz, DMSO) δ 7.83 (s, 1H), 7.53 (br s, 1H), 7.42 – 7.18 (m, 9H), 7.17 – 7.09 (m, 2H), 7.06 – 6.81 (m, 5H), 5.06 (s, 2H), 4.95 (s, 2H), 4.41 (dd, *J* = 13.5, 4.3 Hz, 1H), 4.31 (dd, *J* = 13.5, 8.1 Hz, 1H), 3.92 – 3.80 (m, 3H), 3.05 (br s, 2H), 1.61 – 1.21 (m, 7H), 0.78 (d, *J* = 6.6 Hz, 6H); ^{13}C NMR (126 MHz, DMSO) δ 156.6, 156.1, 155.8, 155.6, 142.9, 137.0, 131.3, 131.1, 128.5, 128.4, 128.3*, 127.8, 127.5*, 127.4*, 124.4, 120.4, 119.9, 112.9, 112.3, 66.2, 65.2, 61.8, 52.6, 50.9, 40.4, 37.5, 28.7, 25.0, 24.5, 22.4*; IR (neat) $\bar{\nu}_{max}$ 3337 3198, 2956, 2930, 2873, 2362, 2323, 1683, 1653, 1559, 1539, 1507, 1457, 1340, 1212, 1162, 1109, 1040, 1003, 913, 852, 749, 697, 668 cm^{-1}; MS (ESI +ve) *m/z* 614 ($[M + H]^+$, 100%), 636 ($[M + Na]^+$, 8%); HRMS (ESI +ve TOF) calcd for $C_{34}H_{44}N_7O_4$ 614.3455, found 614.3438 ($[M + H]^+$).

***Tert*-butyl ((*R*)-1-(4-((((*S*)-2'-(isopentyloxy)-[1,1'-binaphthalen]-2-yl)oxy)methyl)-1*H*-1,2,3-triazol-1-yl)-5-(2-((2,2,4,6,7-pentamethyl-2,3-dihydrobenzofuran-5-yl)sulfonyl)guanidino)pentan-2-yl)carbamate (62d)**

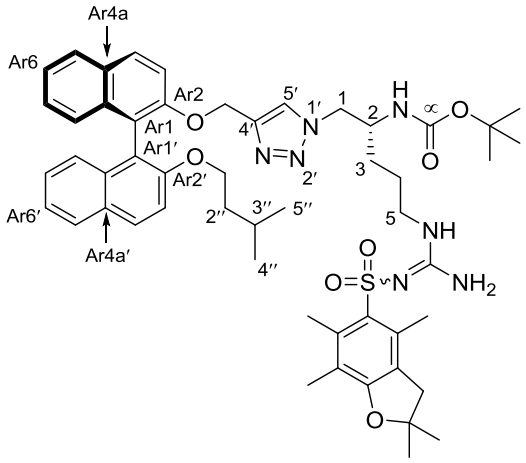

Following **General Procedure A**, azide **27** (94 mg, 0.17 mmol), alkyne **20** (138 mg, 0.35 mmol), $Cu(OAc)_2 \cdot H_2O$ (7 mg, 0.035 mmol) and sodium ascorbate (14 mg, 0.07 mmol) were stirred in *t*-BuOH (3.5 mL) and H_2O (0.9 mL) at 45 °C for 20 h to give the triazole **62d** (153 mg, 94%) as a light tan gum after flash chromatography over SiO_2 gel (EtOAc/P.S. – 10:90 → 100:0). TLC (EtOAc): $R_f = 0.74$; $[\alpha]_D^{23}$ −6.5 (*c* 0.50, MeOH); ^{1}H NMR (400 MHz, $CDCl_3$) δ 7.94 – 7.87 (m, 2H, ArH), 7.87 – 7.79 (m, 2H, ArH), 7.49 (d, *J* = 9.0 Hz, 1H, ArH), 7.39 (d, *J* = 9.0 Hz, 1H, ArH), 7.32 (t, *J* = 7.4 Hz, 1H, ArH), 7.29 – 7.18 (m, 2H, ArH), 7.18 – 7.06 (m, 3H, ArH), 6.66 (s, 1H, H5'), 6.11 (br s, 2H, -NH_2), 5.88 (br s, 1H, N^5-H), 5.16 (d, *J* = 8.5 Hz, 1H, N^2-H), 5.08 (s, 2H, -OCH_2-C4'), 4.23 – 4.06 (m, 2H, H1), 4.01 – 3.92 (m, 1H, H1"$_A$ or H1"$_B$), 3.90 – 3.82 (m, 1H, H1"$_B$ or H1"$_A$), 3.77 (br s, 1H, H2), 3.14 – 3.03 (m, 2H, H5), 2.91 (s, 2H, $ArCH_2$-), 2.57 (s, 3H, $ArCH_3$), 2.49 (s, 3H, $ArCH_3$), 2.07 (s, 3H, $ArCH_3$), 1.59 – 1.10 (m, 22H, H3, H4, H2", H3", -$C(CH_3)_2$ and -$C(CH_3)_3$), 0.57 (d, *J* = 6.3 Hz, 3H, H4" or H5"), 0.52 (d, *J* = 6.3 Hz, 3H, H5" or H4"); ^{13}C NMR (101 MHz, $CDCl_3$) δ 158.9 (Pbf C_{Ar}), 156.2 (C=N), 155.8 (C=O), 154.7 (CAr2'), 153.9 (CAr2), 144.9 (C4'), 138.5 (Pbf C_{Ar}), 134.1 (CAr8a and CAr8a'), 133.1 (Pbf C_{Ar}), 132.4 (Pbf C_{Ar}), 129.9 (CAr4a), 129.6 (CAr4), 129.5 (CAr4'), 129.3 (CAr4a'), 128.1 (CAr5), 128.0 (CAr5'), 126.43 (CAr7), 126.39 (CAr7'), 125.7 (CAr8), 125.5 (CAr8'), 124.7 (Pbf C_{Ar}), 124.1

(CAr6), 124.0 (C5'), 123.7 (CAr6'), 121.5 (CAr1), 120.4 (CAr1'), 117.6 (Pbf C_{Ar}), 116.5 (CAr3), 116.0 (CAr3'), 86.5 (-$\underline{C}(CH_3)_2$), 80.0 (-$\underline{C}(CH_3)_3$), 68.4 (C1''), 64.4 (-O$\underline{C}H_2$-C4'), 53.3 (C1), 50.2 (C2), 43.4 ($ArCH_2$-), 40.8 (C5), 38.2 (C2''), 29.1 (C3), 28.7 (-C($\underline{C}H_3)_2$), 28.4 (-C($\underline{C}H_3)_3$), 25.4 (C4), 24.7 (C3''), 22.5 (C4'' or C5''), 22.2 (C5'' or C4''), 19.4 ($ArCH_3$), 18.1 ($ArCH_3$), 12.6 ($ArCH_3$); IR (neat) $\bar{\nu}_{max}$ 3345, 2967, 2930, 2873, 2537, 2331, 1700, 1683, 1653, 1559, 1539, 1507, 1457, 1362, 1244, 1163, 1088, 1047, 1015, 904, 852, 807, 782, 748, 668, 640, 618 cm^{-1}; MS (ESI +ve) *m/z* 932 ($[M + H]^+$, 100%), 954 ($[M + Na]^+$, 90%); HRMS (ESI +ve TOF) calcd for $C_{52}H_{66}N_7O_7S$ 932.4744, found 932.4790 ($[M + H]^+$).

(*R*)-(1-(4-((((*S*)-2'-(Isopentyloxy)-[1,1'-binaphthalen]-2-yl)oxy)methyl)-1*H*-1,2,3-triazol-1-yl)-5-(2-((2,2,4,6,7-pentamethyl-2,3-dihydrobenzofuran-5-yl)sulfonyl)guanidino)pentan-2-yl)amine (63d)

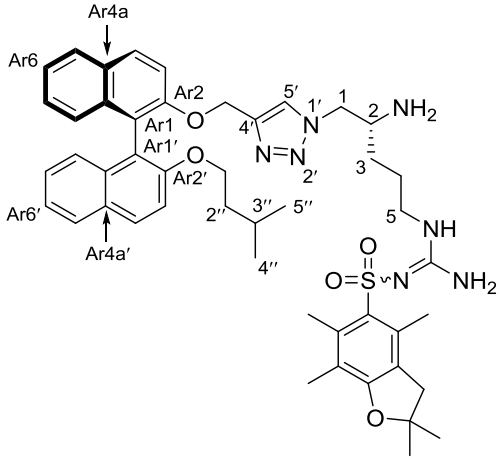

To a stirred solution of carbamate **62d** (113 mg, 0.12 mmol) in MeOH (1.2 mL) was added HCl (2.0 M in Et_2O – 1.2 mL, 2.40 mmol) and the resulting reaction mixture was stirred at room temperature for 18 h. The reaction mixture was concentrated, the residue was dissolved in CH_2Cl_2 (100 mL) and the organic solution was washed with saturated aqueous $NaHCO_3$ (3 × 50 mL) and brine (1 × 50 mL). The organic phase was dried (Na_2SO_4), filtered and concentrated to afford the amine **63d** (104 mg, 95%) as a light tan gum. TLC (NEt_3/MeOH/CH_2Cl_2 – 2:10:88): R_f = 0.46; $[\alpha]_D^{23}$ +64.2 (*c* 0.37, MeOH); ^{1}H NMR (400 MHz, $CDCl_3$) δ 7.95 – 7.87 (m, 2H, ArH), 7.87 – 7.79 (m, 2H, ArH), 7.48 (d, *J* = 9.0 Hz, 1H,

HAr3), 7.39 (d, *J* = 9.0 Hz, 1H, HAr3'), 7.36 – 7.30 (m, 1H, ArH), 7.30 – 7.09 (m, 5H, ArH), 6.58 (s, 1H, H5'), 6.24 (br s, 2H, -NH_2), 6.18 (br s, 1H, N^5-H), 5.12 (s, 2H, -OCH_2-C4'), 4.05 – 3.82 (m, 4H, H1 and H1''), 3.10 (br s, 2H, H5), 2.94 (br s, 1H, H2), 2.89 (s, 2H, $ArCH_2$-), 2.57 (s, 3H, $ArCH_3$), 2.48 (s, 3H, $ArCH_3$), 2.07 (s, 3H, $ArCH_3$), 1.61 – 1.46 (m, 2H, H3), 1.41 (s, 6H, -$C(CH_3)_2$), 1.31 – 1.08 (m, 5H, H4, H2'' and H3''), 0.57 (d, *J* = 6.3 Hz, 3H, H4'' or H5''), 0.52 (d, *J* = 6.3 Hz, 3H, H5'' or H4''); ^{13}C NMR (101 MHz, $CDCl_3$) δ 158.9 (Pbf C_{Ar}), 156.3 (C=N), 154.8 (CAr2'), 153.9 (CAr2), 145.0 (C4'), 138.4 (Pbf C_{Ar}), 134.2 (CAr8a or CAr8a'), 134.1 (CAr8a' or CAr8a), 133.2 (Pbf C_{Ar}), 132.3 (Pbf C_{Ar}), 129.9 (CAr4a), 129.6 (CAr4), 129.4 (CAr4'), 129.3 (CAr4a'), 128.0 (CAr5 and CAr5'), 126.4 (CAr7 and CAr7'), 125.7 (CAr8), 125.5 (CAr8'), 124.8 (Pbf C_{Ar}), 124.1 (CAr6), 123.7 (CAr6' and C5'), 121.3 (CAr1), 120.4 (CAr1'), 117.6 (Pbf C_{Ar}), 116.3 (CAr3), 116.0 (CAr3'), 86.5 (-$\underline{C}(CH_3)_2$), 68.4 (C1''), 64.5 (-O$\underline{C}H_2$-C4'), 56.5 (C1), 51.2 (C2), 43.3 ($ArCH_2$-), 40.9 (C5), 38.2 (C2''), 31.3 (C3), 28.7 (-C($\underline{C}H_3)_2$), 25.6 (C4), 24.7 (C3''), 22.5 (C4'' or C5''), 22.3 (C5'' or C4''), 19.4 ($ArCH_3$), 18.1 ($ArCH_3$), 12.6 ($ArCH_3$); IR (neat) $\bar{\nu}_{max}$ 3336, 2966, 2927, 2871, 2356, 2331, 1700, 1653, 1617, 1559, 1539, 1507, 1457, 1340, 1261, 1243, 1146, 1087, 1046, 1016, 906, 880, 852, 808, 783, 748, 668, 640 cm^{-1}; MS (ESI +ve) *m/z* 854 ($[M + Na]^+$, 100%), 832 ($[M + H]^+$, 64%); HRMS (ESI +ve TOF) calcd for $C_{47}H_{58}N_7O_5S$ 832.4220, found 832.4261 ($[M + H]^+$).

***N*-((*R*)-5-Guanidino-1-(4-((((*S*)-2'-(isopentyloxy)-[1,1'-binaphthalen]-2-yl)oxy)methyl)-1*H*-1,2,3-triazol-1-yl)pentan-2-yl)-2-phenylacetamide hydrochloride (66a)**

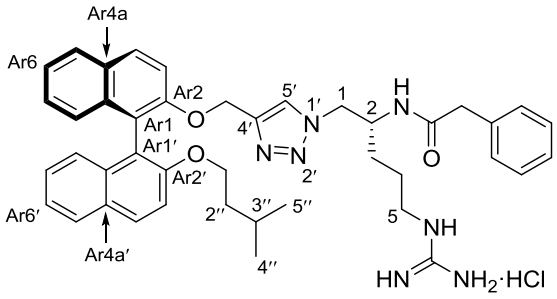

Following **General Procedure B**, amine **63d** (40 mg, 0.05 mmol), phenylacetic acid (8 mg, 0.06 mmol), EDCI (11 mg, 0.06 mmol) and HOBt (8 mg, 0.06 mmol) were stirred in acetonitrile (1.0 mL) for 18 h to give the intermediate amide as a translucent tan gum. Following **General Procedure C**, the amide was dissolved in CH_2Cl_2 (1.5 mL) and treated with H_2O (17 mg, 0.96 mmol) and CF_3CO_2H (1.5 mL) followed by work-up with ethereal HCl to give the amine salt **66a** (30 mg, 86% over two steps) as a light tan powder that rapidly transitioned to a sticky gum. $[\alpha]_D^{23}$ +38.0 (*c* 0.77, MeOH); ^{1}H NMR (400 MHz, DMSO) δ 8.11 (d, *J* = 8.4 Hz, 1H, N^2-H), 8.07 – 7.99 (m, 2H, ArH), 7.96 – 7.89 (m, 2H, ArH), 7.73 (d, *J* = 9.1 Hz, 1H, HAr3), 7.66 (t, *J* = 5.3 Hz, 1H, N^5-H), 7.57 (d, *J* = 9.1 Hz, 1H, HAr3'), 7.41 (s, 1H, H5'), 7.36 – 7.27 (m, 2H, ArH), 7.24 – 7.08 (m, 7H, ArH), 6.94 – 6.86 (m, 2H, ArH), 5.02 and 5.09 (ABq, 2H, *J* = 12.7 Hz, -OCH_2-C4'), 4.33 (dd, *J* = 13.8, 5.1 Hz, 1H, $H1_A$ or $H1_B$), 4.24 (dd, *J* = 13.8, 7.5 Hz, 1H, $H1_B$ or $H1_A$), 4.06 – 3.88 (m, 3H, H2 and H1"), 3.37 – 3.21 (m, 2H, -C$\underline{H}_2$Ph), 3.11 – 2.93 (m, 2H, H5), 1.53 – 1.13 (m, 7H, H3, H4, H2" and H3"), 0.57 (d, *J* = 6.3 Hz, 3H, H4" or H5"), 0.54 (d, *J* = 6.3 Hz, 3H, H5" or H4"); ^{13}C NMR (101 MHz, DMSO) δ 170.2 (C=O), 156.8 (C=N), 154.2 (CAr2'), 153.7 (CAr2), 142.9 (C4'), 136.1 (Phenyl C_{Ar}), 133.42 (CAr8a or CAr8a'), 133.37 (CAr8a' or CAr8a), 129.3 (CAr4), 129.1 (CAr4'), 129.0 (CAr4a), 128.8 (Phenyl C_{Ar})*, 128.7 (CAr4a'), 128.1 (Phenyl C_{Ar})*, 127.93 (CAr5 or CAr5'), 127.89 (CAr5' or CAr5), 126.24 (Phenyl C_{Ar}), 126.17 (CAr7 or CAr7'), 126.1 (CAr7' or CAr7), 124.7

(CAr8), 124.6 (CAr8'), 124.2 (C5'), 123.5 (CAr6), 123.3 (CAr6'), 119.8 (CAr1), 119.2 (CAr1'), 116.2 (CAr3), 115.7 (CAr3'), 67.3 (C1''), 62.7 (-O<u>C</u>H$_2$-C4'), 52.4 (C1), 48.6 (C2), 42.3 (-<u>C</u>H$_2$Ph), 40.1 (C5 – observed by gHMBC), 37.6 (C2''), 28.4 (C3), 24.9 (C4), 24.1 (C3''), 22.2 (C4'' and C5''), 22.1 (C4'' and C5''); IR (neat) $\bar{\nu}_{max}$ 3172, 2954, 2873, 2363, 2331, 1683, 1647, 1636, 1559, 1539, 1507, 1457, 1340, 1261, 1241, 1212, 1146, 1083, 1046, 1013, 908, 865, 808, 746, 727, 694, 668, 625, 615, 609 cm^{-1}; MS (ESI +ve) *m/z* 698 ([M + H]$^+$, 100%), 720 ([M + Na]$^+$, 23%); HRMS (ESI +ve TOF) calcd for $C_{42}H_{48}N_7O_3$ 698.3819, found 698.3806 ([M + H]$^+$).

_N_-((_R_)-5-Guanidino-1-(4-((((_S_)-2'-(isopentyloxy)-[1,1'-binaphthalen]-2-yl)oxy)methyl)-1_H_-1,2,3-triazol-1-yl)pentan-2-yl)-3-phenylpropanamide hydrochloride (66b)

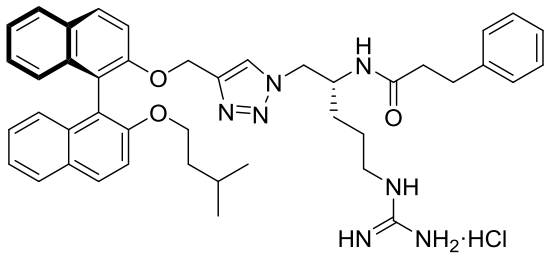

Following **General Procedure B**, amine **63d** (40 mg, 0.05 mmol), 3-phenylpropanoic acid (9 mg, 0.06 mmol), EDCI (11 mg, 0.06 mmol) and HOBt (8 mg, 0.06 mmol) were stirred in acetonitrile (1.0 mL) for 18 h to give the intermediate amide as a translucent tan gum. Following **General Procedure C**, the amide was dissolved in CH_2Cl_2 (1.5 mL) and treated with H_2O (17 mg, 0.96 mmol) and CF_3CO_2H (1.5 mL) followed by work-up with ethereal HCl to give the amine salt **66b** (32 mg, 89% over two steps) as a light tan powder that rapidly transitioned to a sticky gum. $[\alpha]_D^{23}$ +43.0 (*c* 0.67, MeOH); ^{1}H NMR (400 MHz, CD_3OD) δ 8.00 – 7.94 (m, 2H), 7.89 – 7.84 (m, 2H), 7.58 (d, *J* = 9.0 Hz, 1H), 7.48 (d, *J* = 9.0 Hz, 1H), 7.33 – 7.25 (m, 2H), 7.21 – 7.06 (m, 7H), 7.03 (d, *J* = 8.5 Hz, 1H), 6.98 (d, *J* = 8.9 Hz, 1H), 6.96 (s, 1H), 5.15 – 5.01 (m, 2H), 4.27 – 4.14 (m, 2H), 4.07 (br s, 1H), 4.03 – 3.96 (m, 1H),

3.93 – 3.85 (m, 1H), 3.11 – 2.97 (m, 2H), 2.77 (t, *J* = 7.5 Hz, 2H), 2.41 – 2.24 (m, 2H), 1.48 – 1.11 (m, 7H), 0.56 (d, *J* = 6.4 Hz, 3H), 0.51 (d, *J* = 6.3 Hz, 3H); ^{13}C NMR (101 MHz, CD_3OD) δ 175.4, 158.7, 156.2, 155.5, 146.0 (observed by gHMBC), 142.1, 135.60, 135.58, 131.5, 130.9, 130.8, 130.7, 129.7**, 129.3, 129.2, 127.5, 127.42, 127.39, 126.7, 126.4, 125.6, 125.2, 124.8, 122.9, 121.5, 117.9, 117.0, 69.2, 64.9, 54.4, 50.4, 42.1, 39.5, 38.8, 32.8, 29.7, 26.2, 25.8, 23.0, 22.7; IR (neat) $\overline{\nu}_{max}$ 3297, 2954, 2869, 2362, 2320, 1683, 1668, 1647, 1636, 1559, 1539, 1507, 1457, 1340, 1269, 1213, 1150, 1084, 1044, 1016, 990, 953, 867, 807, 776, 747, 703, 668 cm^{-1}; MS (ESI +ve) *m/z* 712 ([M + H]$^+$, 100%), 734 ([M + Na]$^+$, 12%); HRMS (ESI +ve TOF) calcd for $C_{43}H_{50}N_7O_3$ 712.3975, found 712.3991 ([M + H]$^+$).

Benzyl ((*R*)-5-guanidino-1-(4-((((*S*)-2'-(isopentyloxy)-[1,1'-binaphthalen]-2-yl)oxy)methyl)-1*H*-1,2,3-triazol-1-yl)pentan-2-yl)carbamate hydrochloride (66c)

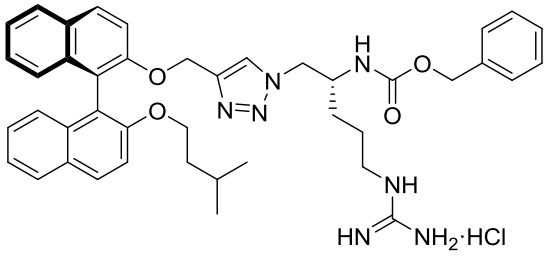

Following **General Procedure A**, azide **26** (310 mg, 0.54 mmol), alkyne **20** (428 mg, 1.08 mmol), $Cu(OAc)_2{\cdot}H_2O$ (22 mg, 0.11 mmol) and sodium ascorbate (43 mg, 0.22 mmol) were stirred in *t*-BuOH (10.8 mL) and H_2O (2.7 mL) at 45 °C for 48 h to give the intermediate triazole (524 mg, 96%) as a light tan gum after flash chromatography over SiO_2 gel (EtOAc/P.S. – 10:90 → 100:0). Following **General Procedure C**, the intermediate triazole (45 mg, 0.05 mmol) was dissolved in CH_2Cl_2 (1.4 mL) and treated with H_2O (17 mg, 0.93 mmol) and CF_3CO_2H (1.4 mL) followed by work-up with ethereal HCl to give the amine salt **66c** (33 mg, 94%) as a light tan powder that rapidly transitioned to a sticky gum. $[\alpha]_D^{23}$ +37.5 (*c* 0.70, MeOH); ^{1}H NMR (400 MHz, CD_3OD) δ 8.00 – 7.91 (m, 2H), 7.90 – 7.81 (m, 2H),

7.55 (d, *J* = 9.0 Hz, 1H), 7.45 (d, *J* = 9.0 Hz, 1H), 7.34 – 6.96 (m, 12H), 5.04 (s, 2H), 4.90 (s, 2H), 4.31 (dd, *J* = 13.9, 4.9 Hz, 1H), 4.20 (dd, *J* = 13.9, 7.8 Hz, 1H), 4.03 – 3.92 (m, 1H), 3.92 – 3.81 (m, 2H), 3.21 – 3.02 (m, 2H), 1.75 – 1.35 (m, 4H), 1.34 – 1.08 (m, 3H), 0.55 (d, *J* = 6.3 Hz, 3H), 0.51 (d, *J* = 6.3 Hz, 3H); ^{13}C NMR (101 MHz, CD_3OD) δ 158.7, 158.5, 156.1, 155.4, 146.0 (observed by gHMBC) 138.3, 135.6, 135.5, 131.5, 130.9, 130.8, 130.7, 129.7*, 129.3, 129.21, 129.17, 128.8*, 127.5, 127.4, 126.7, 126.4, 125.6, 125.2, 124.8, 122.9, 121.5, 117.8, 117.0, 69.2, 67.6, 64.9, 54.8, 52.6, 42.1, 39.5, 30.1, 26.4, 25.8, 23.0, 22.7; IR (neat) $\overline{\nu}_{max}$ 3191, 2953, 2873, 2362, 2331, 1700, 1684, 1669, 1653, 1559, 1539, 1507, 1457, 1340, 1260, 1212, 1146, 1083, 1044, 1016, 903, 860, 807, 774, 746, 697, 668 cm^{-1}; MS (ESI +ve) *m/z* 714 ([M + H]$^+$, 100%), 736 ([M + Na]$^+$, 23%); HRMS (ESI +ve TOF) calcd for $C_{42}H_{48}N_7O_4$ 714.3768, found 714.3799 ([M + H]$^+$).

6.3.3 – Series A2

***Tert*-butyl ((*R*)-5-((*R*)-2-azido-5-(2-((2,2,4,6,7-pentamethyl-2,3-dihydrobenzofuran-5-yl)sulfonyl)guanidino)pentanamido)-6-(4-(((2'-(isopentyloxy)-[1,1'-biphenyl]-2-yl)oxy)methyl)-1*H*-1,2,3-triazol-1-yl)hexyl)carbamate (67a)**

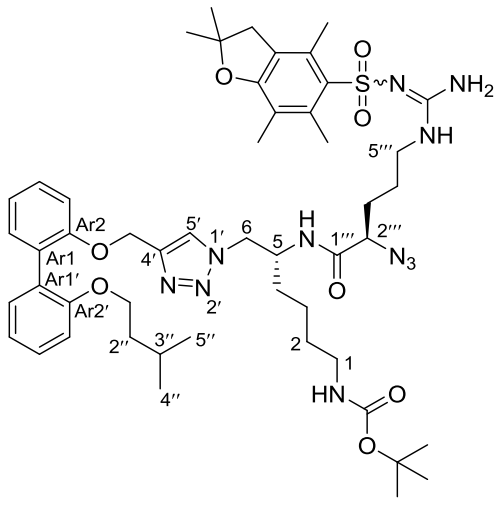

Following **General Procedure B**, amine **63a** (300 mg, 0.54 mmol), acid **28** (271 mg, 0.60 mmol), EDCI (125 mg, 0.65 mmol) and HOBt (88 mg, 0.60 mmol) were stirred in acetonitrile (5.4 mL) for 48 h to give the amide **67a** (479 mg, 89%) as a translucent tan gum after flash chromatography over SiO_2 gel (EtOAc/P.S. – 30:70 → 80:20). TLC

(EtOAc/P.S. – 80:20): R_f = 0.53; $[\alpha]_D^{23}$ −14.7 (*c* 2.97, MeOH); ^{1}H NMR (400 MHz, $CDCl_3$) δ 7.48 (br s, 2H, H5' and N^5-H), 7.33 – 7.19 (m, 4H, ArH), 7.09 (d, *J* = 8.0 Hz, 1H, ArH), 7.05 – 6.92 (m, 3H, ArH), 6.26 (br s, 2H, -$NH_{2\ (guanidine)}$), 5.90 (br s, 1H, $N^{5'''}$-H), 5.11 (s, 2H, -OCH_2-C4'), 4.70 (br s, 1H, N^1-H), 4.49 – 4.32 (m, 3H, H5 and H6), 3.97 – 3.82 (m, 3H, H1" and H2'"), 3.35 (br s, 1H, H5'"$_A$ or H5'"$_B$), 3.06 (br s, 2H, H1), 2.95 (s, 2H, $ArCH_2$-), 2.89 (br s, 1H, H5'"$_B$ or H5'"$_A$), 2.58 (s, 3H, $ArCH_3$), 2.51 (s, 3H, $ArCH_3$), 2.09 (s, 3H, $ArCH_3$), 1.63 – 1.19 (m, 28H, H2, H3, H4, H2", H3", H3'", H4'", -$C(CH_3)_2$, and -$C(CH_3)_3$), 0.80 (d, *J* = 6.5 Hz, 6H, H4" and H5"); ^{13}C NMR (101 MHz, $CDCl_3$) δ 170.9 (C1'"), 159.0 (Pbf C_{Ar}), 156.5 (C=N), 156.4 (CAr2'), 156.3 (C=O), 156.1 (CAr2), 144.6 (C4'), 138.4 (Pbf C_{Ar}), 132.7 (Pbf C_{Ar}), 132.3 (Pbf C_{Ar}), 131.9 (CAr6 or CAr6'), 131.8 (CAr6' or CAr6), 128.9 (CAr4 and CAr4'), 128.4 (CAr1), 128.0 (CAr1'), 124.8 (Pbf C_{Ar}), 124.0 (C5'), 121.5 (CAr5), 120.5 (CAr5'), 117.7 (Pbf C_{Ar}), 114.2 (CAr3), 112.8 (CAr3'), 86.6 (-$\underline{C}(CH_3)_2$), 79.2 (-$\underline{C}(CH_3)_3$), 67.3 (C1"), 63.7 (-O$\underline{C}H_2$-C4'), 61.0 (C2'"), 53.7 (C6), 49.4 (C5), 43.4 ($ArCH_2$-), 40.3 (C1), 38.5 (C5'"), 38.0 (C2"), 31.6 (C4), 29.6 (C3'"), 28.7 (-C($\underline{C}H_3)_2$), 28.5 (-C($\underline{C}H_3)_3$), 27.6 (C2), 25.6 (C4'"), 25.1 (C3"), 23.1 (C3), 22.6 (C4" or C5"), 22.5 (C5" or C4"), 19.5 ($ArCH_3$), 18.1 ($ArCH_3$), 12.6 ($ArCH_3$); IR (neat) $\bar{\nu}_{max}$ 3455, 3335, 2954, 2933, 2875, 2375, 2331, 2104, 1689, 1653, 1559, 1540, 1512, 1457, 1437, 1368, 1243, 1162, 1107, 1091, 1053, 1031, 1003, 903, 853, 807, 784, 751, 734, 663, 641, 617 cm^{-1}; MS (ESI +ve) *m/z* 1009 ($[M + Na]^+$, 100%), 987 ($[M + H]^+$, 17%); HRMS (ESI +ve TOF) calcd for $C_{50}H_{72}N_{11}O_8S$ 986.5286, found 986.5305 ($[M + H]^+$).

(*R*)-*N*-((*R*)-6-Amino-1-(4-(((2'-(isopentyloxy)-[1,1'-biphenyl]-2-yl)oxy)methyl)-1*H*-1,2,3-triazol-1-yl)hexan-2-yl)-2-(4-benzyl-1*H*-1,2,3-triazol-1-yl)-5-guanidinopentanamide dihydrochloride (68a)

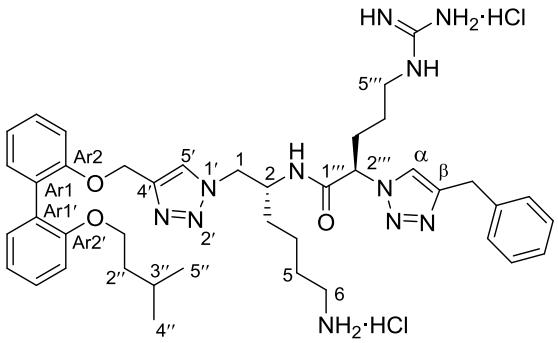

Following **General Procedure A**, azide **67a** (50 mg, 0.05 mmol), 3-phenyl-1-propyne (18 mg, 0.15 mmol), $Cu(OAc)_2 \cdot H_2O$ (2 mg, 0.01 mmol) and sodium ascorbate (4 mg, 0.02 mmol) were stirred in *t*-BuOH (1.0 mL) and H_2O (0.25 mL) for 20 h to give the intermediate triazole as a light tan gum after flash chromatography over SiO_2 gel (EtOAc/P.S. – 10:90 → 100:0). Following **General Procedure C**, the triazole was dissolved in CH_2Cl_2 (1.5 mL) and treated with H_2O (18 mg, 1.00 mmol) and CF_3CO_2H (1.5 mL) followed by work-up with ethereal HCl to give the amine salt **68a** (36 mg, 86% over two steps) as a light tan powder that rapidly transitioned to a sticky gum. $[\alpha]_D^{23}$ −44.2 (*c* 1.07, MeOH); ^{1}H NMR (400 MHz, CD_3OD) δ 7.86 (br s, 2H, H5' and Hα), 7.34 – 7.10 (m, 10H, ArH), 7.04 – 6.87 (m, 3H, ArH), 5.27 (br s, 1H, H2'''), 5.11 (s, 2H, -OCH_2-C4'), 4.62 – 4.51 (m, 1H, $H1_A$ or $H1_B$), 4.50 – 4.36 (m, 1H, $H1_B$ or $H1_A$), 4.28 (br s, 1H, H2), 4.07 (s, 2H, -C$\underline{H}_2$Ph), 3.90 (t, *J* = 6.1 Hz, 2H, H1''), 3.07 (br s, 2H, H5'''), 2.89 (br s, 2H, H6), 2.08 – 1.81 (m, 2H, H3'''), 1.74 – 1.17 (m, 11H, H3, H4, H5, H2'', H3'' and H4'''), 0.80 (d, *J* = 6.5 Hz, 6H, H4'' and H5''); ^{13}C NMR (101 MHz, CD_3OD) δ 169.8 (C1'''), 158.7 (C=N), 158.1 (CAr2'), 157.5 (CAr2), 148.4 (Cβ – observed by gHMBC), 145.7 (C4' – observed by gHMBC), 139.8 (Phenyl C_{Ar}), 133.1 (CAr6 or CAr6'),

132.6 (CAr6' or CAr6), 130.4 (CAr1), 130.0 (Phenyl C_{Ar})*, 129.9 (Phenyl C_{Ar}* and CAr4 or CAr4'), 129.8 (CAr4' or CAr4), 129.7 (CAr1'), 128.0 (Phenyl C_{Ar}), 126.4 (C5' – observed by gHSQC/gHMBC), 124.5 (Cα – observed by gHSQC/gHMBC), 122.5 (CAr5), 121.5 (CAr5'), 115.0 (CAr3), 113.9 (CAr3'), 68.3 (C1"), 65.1 (C2'"), 63.7 (-O<u>C</u>H_2-C4'), 54.8 (C1), 51.4 (C2), 41.6 (C5'"), 40.7 (C6), 39.4 (C2"), 32.4 (-<u>C</u>H_2Ph), 32.3 (C3), 30.4 (C3'"), 28.2 (C5), 26.3 (C3"), 26.1 (C4'"), 23.9 (C4), 23.1 (C4" and C5"); IR (neat) $\bar{\nu}_{max}$ 3159, 3065, 2954, 2926, 2868, 2379, 2314, 1734, 1700, 1684, 1653, 1636, 1559, 1540, 1521, 1507, 1473, 1457, 1437, 1419, 1340, 1212, 1161, 1125, 1049, 1002, 853, 752, 731, 698, 668, 610 cm^{-1}; MS (ESI +ve) *m*/2 376 ($[M + 2H]^{2+}$, 100%), *m/z* 772 ($[M + Na]^+$, 16%), 750 ($[M + H]^+$, 14%); HRMS (ESI +ve TOF) calcd for $C_{41}H_{56}N_{11}O_3$ 750.4568, found 750.4587 ($[M + H]^+$).

(*R*)-*N*-((*R*)-6-Amino-1-(4-(((2'-(isopentyloxy)-[1,1'-biphenyl]-2-yl)oxy)methyl)-1*H*-1,2,3-triazol-1-yl)hexan-2-yl)-5-guanidino-2-(4-phenethyl-1*H*-1,2,3-triazol-1-yl)pentanamide dihydrochloride (68b)

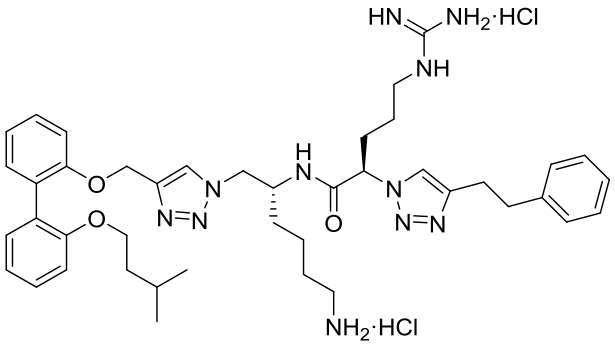

Following **General Procedure A**, azide **67a** (50 mg, 0.05 mmol), 4-phenyl-1-butyne (20 mg, 0.15 mmol), $Cu(OAc)_2 \cdot H_2O$ (2 mg, 0.01 mmol) and sodium ascorbate (4 mg, 0.02 mmol) were stirred in *t*-BuOH (1.0 mL) and H_2O (0.25 mL) for 20 h to give the intermediate triazole as a light tan gum after flash chromatography over SiO_2 gel ($MeOH/CH_2Cl_2$. – 0:100 →

10:90). Following **General Procedure C**, the triazole was dissolved in CH_2Cl_2 (1.5 mL) and treated with H_2O (18 mg, 1.00 mmol) and CF_3CO_2H (1.5 mL) followed by work-up with ethereal HCl to give the amine salt **68b** (40 mg, 94% over two steps) as a light tan powder that rapidly transitioned to a sticky gum. $[\alpha]_D^{23}$ −37.3 (*c* 1.03, MeOH); ^{1}H NMR (400 MHz, CD_3OD) δ 7.91 (s, 1H), 7.84 (s, 1H), 7.36 – 7.08 (m, 10H), 7.06 – 6.88 (m, 3H), 5.36 – 5.24 (m, 1H), 5.12 (s, 2H), 4.62 – 4.54 (m, 1H), 4.44 (dd, *J* = 13.6, 8.9 Hz, 1H), 4.28 (br s, 1H), 3.91 (t, *J* = 6.4 Hz, 2H), 3.15 – 2.93 (m, 6H), 2.89 (t, *J* = 7.1 Hz, 2H), 2.10 – 1.86 (m, 2H), 1.73 – 1.19 (m, 11H), 0.80 (d, *J* = 6.6 Hz, 6H); ^{13}C NMR (101 MHz, CD_3OD) δ 169.5, 158.7, 158.1, 157.5, 147.2 (observed by gHMBC), 145.6 (observed by gHMBC), 141.9, 133.1, 132.6, 130.5, 129.9, 129.8, 129.74, 129.72**, 127.6, 126.3, 125.0, 122.5, 121.5, 115.0, 113.9, 68.3, 65.4, 63.7, 54.7, 51.4, 41.6, 40.7, 39.4, 36.3, 32.2, 30.4, 28.2, 27.9, 26.3, 26.0, 23.9, 23.1*; IR (neat) $\bar{\nu}_{max}$ 3159, 3065, 2954, 2928, 2868, 2379, 2350, 2314, 1734, 1718, 1700, 1684, 1653, 1636, 1559, 1540, 1521, 1507, 1473, 1457, 1437, 1419, 1363, 1340, 1260, 1212, 1161, 1124, 1109, 1049, 1002, 854, 751, 732, 700, 669, 609 cm^{-1}; MS (ESI +ve) *m*/2 383 ($[M + 2H]^{2+}$, 100%), *m/z* 764 ($[M + H]^+$, 12%), 786 ($[M + Na]^+$, 9%); HRMS (ESI +ve TOF) calcd for $C_{42}H_{58}N_{11}O_3$ 764.4724, found 764.4761 ($[M + H]^+$).

(*R*)-*N*-((*R*)-6-Amino-1-(4-(((2'-(isopentyloxy)-[1,1'-biphenyl]-2-yl)oxy)methyl)-1*H*-1,2,3-triazol-1-yl)hexan-2-yl)-5-guanidino-2-(4-cyclohexyl-1*H*-1,2,3-triazol-1-yl)pentanamide dihydrochloride (68c)

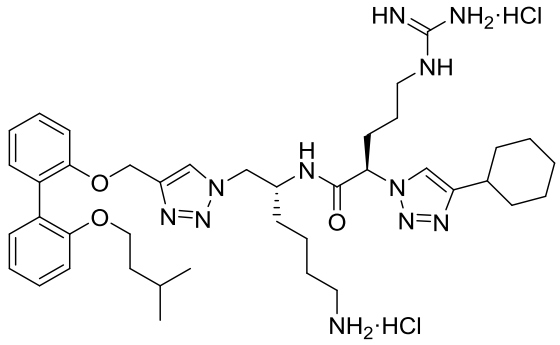

Following **General Procedure A**, azide **67a** (50 mg, 0.05 mmol), cyclohexylacetylene (18 mg, 0.15 mmol), $Cu(OAc)_2 \cdot H_2O$ (2 mg, 0.01 mmol) and sodium ascorbate (4 mg, 0.02 mmol) were stirred in *t*-BuOH (1.0 mL) and H_2O (0.25 mL) for 20 h to give the intermediate triazole as a light tan gum after flash chromatography over SiO_2 gel ($MeOH/CH_2Cl_2$. – 0:100 → 10:90). Following **General Procedure C**, the triazole was dissolved in CH_2Cl_2 (1.5 mL) and treated with H_2O (18 mg, 1.00 mmol) and CF_3CO_2H (1.5 mL) followed by work-up with ethereal HCl to give the amine salt **68c** (38 mg, 92% over two steps) as a light tan powder that rapidly transitioned to a sticky gum. $[\alpha]_D^{23}$ −27.2 (*c* 1.03, MeOH); ^{1}H NMR (400 MHz, CD_3OD) δ 8.11 (s, 1H), 7.85 (s, 1H), 7.37 – 7.23 (m, 2H), 7.23 – 7.12 (m, 3H), 7.07 – 6.88 (m, 3H), 5.36 (t, *J* = 7.2 Hz, 1H), 5.13 (s, 2H), 4.59 (dd, *J* = 13.7, 3.3 Hz, 1H), 4.45 (dd, *J* = 13.6, 8.8 Hz, 1H), 4.28 (br s, 1H), 3.92 (t, *J* = 6.3 Hz, 2H), 3.12 (t, *J* = 6.5 Hz, 2H), 2.90 (t, *J* = 6.8 Hz, 2H), 2.85 – 2.76 (m, 1H), 2.14 – 1.93 (m, 4H), 1.90 – 1.23 (m, 19H), 0.81 (d, *J* = 6.6 Hz, 6H); ^{13}C NMR (101 MHz, CD_3OD) δ 169.3, 158.7, 158.2, 157.5, 153.0 (observed by gHMBC), 145.6 (observed by gHMBC), 133.1, 132.7, 130.5, 129.9, 129.8, 129.7, 126.3, 124.1, 122.5, 121.5, 115.0, 113.9, 68.3, 65.8, 63.7, 54.7, 51.5, 41.7, 40.7, 39.4, 35.9, 33.70,

33.67, 32.2, 30.3, 28.2, 27.1*, 27.0, 26.3, 26.1, 23.9, 23.1*; IR (neat) $\bar{\nu}_{max}$ 3158, 3065, 2950, 2928, 2870, 2380, 2349, 2312, 1734, 1718, 1700, 1684, 1653, 1636, 1559, 1540, 1521, 1507, 1473, 1457, 1437, 1419, 1363, 1340, 1260, 1212, 1162, 1123, 1109, 1040, 1003, 855, 750, 735, 701, 669, 608 cm^{-1}; MS (ESI +ve) *m*/2 372 ($[M + 2H]^{2+}$, 100%), *m/z* 742 ($[M + H]^+$, 11%), 764 ($[M + Na]^+$, 8%); HRMS (ESI +ve TOF) calcd for $C_{40}H_{60}N_{11}O_3$ 742.4881, found 742.4911 ($[M + H]^+$).

(*R*)-*N*-((*R*)-6-Amino-1-(4-(((2'-(isopentyloxy)-[1,1'-biphenyl]-2-yl)oxy)methyl)-1*H*-1,2,3-triazol-1-yl)hexan-2-yl)-5-guanidino-2-(4-(cyclohexylmethyl)-1*H*-1,2,3-triazol-1-yl)pentanamide dihydrochloride (68d)

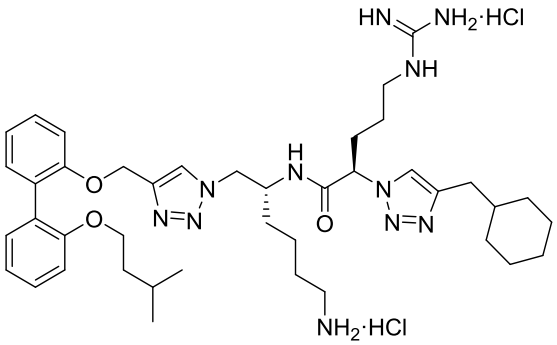

Following **General Procedure A**, azide **67a** (50 mg, 0.05 mmol), 3-cyclohexyl-1-propyne (19 mg, 0.15 mmol), $Cu(OAc)_2 \cdot H_2O$ (2 mg, 0.01 mmol) and sodium ascorbate (4 mg, 0.02 mmol) were stirred in *t*-BuOH (1.0 mL) and H_2O (0.25 mL) for 20 h to give the intermediate triazole as a light tan gum after flash chromatography over SiO_2 gel ($MeOH/CH_2Cl_2$. – 0:100 → 10:90). Following **General Procedure C**, the triazole was dissolved in CH_2Cl_2 (1.5 mL) and treated with H_2O (18 mg, 1.00 mmol) and CF_3CO_2H (1.5 mL) followed by work-up with ethereal HCl to give the amine salt **68d** (33 mg, 79% over two steps) as a light tan powder that rapidly transitioned to a sticky gum. $[\alpha]_D^{23}$ −23.4 (*c* 0.80, MeOH); ^1H NMR (400 MHz,

CD_3OD) δ 7.93 (s, 1H), 7.84 (s, 1H), 7.36 – 7.24 (m, 2H), 7.23 – 7.13 (m, 3H), 7.06 – 6.91 (m, 3H), 5.34 – 5.26 (m, 1H), 5.13 (s, 2H), 4.59 (dd, *J* = 13.9, 3.8 Hz, 1H), 4.44 (dd, *J* = 13.9, 8.9 Hz, 1H), 4.27 (br s, 1H), 3.92 (t, *J* = 6.2 Hz, 2H), 3.10 (t, *J* = 6.8 Hz, 2H), 2.89 (t, *J* = 7.1 Hz, 2H), 2.61 (d, *J* = 6.8 Hz, 2H), 2.11 – 1.89 (m, 2H), 1.77 – 1.13 (m, 20H), 1.04 – 0.91 (m, 2H), 0.81 (d, *J* = 6.2 Hz, 6H); ^{13}C NMR (101 MHz, CD_3OD) δ 169.7, 158.7, 158.2, 157.5, 147.0 (observed by gHMBC), 145.5 (observed by gHMBC), 133.1, 132.7, 130.5, 129.9, 129.82, 129.76, 126.2, 124.8, 122.5, 121.5, 115.0, 113.9, 68.3, 65.2, 63.7, 54.7, 51.4, 41.7, 40.7, 39.44, 39.41, 34.2*, 33.7, 32.3, 30.4, 28.2, 27.6, 27.4*, 26.3, 26.1, 23.9, 23.1*; IR (neat) $\overline{\nu}_{max}$ 3158, 3065, 2950, 2926, 2869, 2380, 2350, 2312, 1734, 1718, 1700, 1684, 1653, 1636, 1559, 1540, 1521, 1507, 1473, 1457, 1437, 1419, 1363, 1340, 1260, 1213, 1161, 1125, 1109, 1040, 1003, 855, 750, 735, 701, 669, 608 cm^{-1}; MS (ESI +ve) *m*/2 379 $([M + 2H]^{2+}$, 100%), *m/z* 756 $([M + H]^+$, 19%), 778 $([M + Na]^+$, 16%); HRMS (ESI +ve TOF) calcd for $C_{41}H_{62}N_{11}O_3$ 756.5037, found 756.5072 $([M + H]^+)$.

***Tert*-butyl ((*R*)-5-azido-6-(((*R*)-1-(4-(((2'-(isopentyloxy)-[1,1'-biphenyl]-2-yl)oxy)methyl)-1*H*-1,2,3-triazol-1-yl)-5-(2-((2,2,4,6,7-pentamethyl-2,3-dihydrobenzofuran-5-yl)sulfonyl)guanidino)pentan-2-yl)amino)-6-oxohexyl)carbamate (67b)**

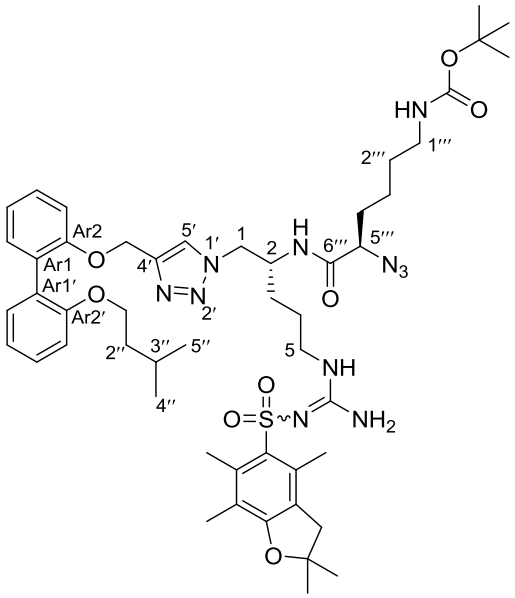

Following **General Procedure B**, amine **63b** (200 mg, 0.27 mmol), acid **24** (82 mg, 0.30 mmol), EDCI (63 mg, 0.33 mmol) and HOBt (44 mg, 0.30 mmol) were stirred in acetonitrile (2.7 mL) for 18 h to give the product amide **67b** (207 mg, 77%) as a translucent tan gum after flash chromatography over SiO_2 gel (MeOH/EtOAc – 0.5:99.5). TLC (MeOH/EtOAc. – 0.5:99.5): R_f = 0.51, (EtOAc/P.S. – 80:20): R_f = 0.38; $[\alpha]_D^{23}$ −5.9 (*c* 0.70, MeOH); ^{1}H NMR (400 MHz, $CDCl_3$) δ 7.34 – 7.19 (m, 5H, H5' and ArH), 7.11 – 6.97 (m, 3H, N^2-H and ArH), 6.98 – 6.90 (m, 2H, ArH), 6.20 (br s, 2H, -NH_2), 5.94 (br s, 1H, N^5-H), 5.13 (s, 2H, -CH_2-C4'), 4.72 (br s, 1H, $N^{1'''}$-H), 4.44 – 4.25 (m, 3H, H1 and H2), 3.88 (t, *J* = 6.6 Hz, 2H, H1''), 3.83 (br s, 1H, H5'''), 3.27 – 2.99 (m, 4H, H5 and H1'''), 2.94 (s, 2H, ArCH_2-), 2.58 (s, 3H, ArCH_3), 2.50 (s, 3H, ArCH_3), 2.09 (s, 3H, ArCH_3), 1.83 – 1.67 (m, 2H, H4'''), 1.61 – 1.20 (m, 26H, H3, H4, H2'', H3'', H2''', H3''', -$C(CH_3)_3$ and -$C(CH_3)_2$), 0.79 (d, *J* = 6.6 Hz, 6H, H4'' and H5''); ^{13}C NMR (101 MHz, $CDCl_3$) δ 170.0 (C6'''), 158.9 (Pbf C_{Ar}), 156.7 (CAr2'), 156.5 (C=O), 156.3 (C=N), 155.9 (CAr2), 145.1 (C4'), 138.5 (Pbf C_{Ar}), 133.1 (Pbf C_{Ar}), 132.4 (Pbf C_{Ar}), 131.9 (CAr6 or CAr6'), 131.7 (CAr6' or CAr6), 128.8 (CAr1), 128.7 (CAr4 or CAr4'), 128.6 (CAr4' or CAr4), 128.2 (CAr1'), 124.8 (Pbf C_{Ar}), 124.0

(C5'), 121.3 (CAr5), 120.3 (CAr5'), 117.7 (Pbf C_{Ar}), 113.5 (CAr3), 112.6 (CAr3'), 86.5 (-$\underline{C}(CH_3)_2$), 79.6 (-$\underline{C}(CH_3)_3$), 67.2 (C1''), 63.4 (C5'''), 63.3 (-OCH_2-C4'), 53.2 (C1), 49.0 (C2), 43.4 ($ArCH_2$-), 40.6 (C5), 40.4 (C1'''), 38.1 (C2''), 31.3 (C4'''), 29.8 (C3), 29.0 (C2'''), 28.7 (-C($\underline{C}H_3)_2$), 28.6 (-C($\underline{C}H_3)_3$), 25.8 (C4), 25.1 (C3''), 22.6 (C4'' and C5''), 22.4 (C3'''), 19.4 ($ArCH_3$), 18.1 ($ArCH_3$), 12.6 ($ArCH_3$); IR (neat) $\bar{\nu}_{max}$ 3328, 2955, 2931, 2876, 2375, 2323, 2104, 1700, 1684, 1653, 1559, 1540, 1507, 1457, 1437, 1419, 1340, 1241, 1164, 1106, 1091, 1052, 1002, 854, 810, 782, 752, 734, 668, 640, 621 cm^{-1}; MS (ESI +ve) *m/z* 1008 ($[M + Na]^+$, 100%), 986 ($[M + H]^+$, 21%); HRMS (ESI +ve TOF) calcd for $C_{50}H_{72}N_{11}O_8S$ 986.5286, found 986.5313 ($[M + H]^+$).

(*R*)-6-Amino-2-(4-benzyl-1*H*-1,2,3-triazol-1-yl)-*N*-((*R*)-5-guanidino-1-(4-(((2'-(isopentyloxy)-[1,1'-biphenyl]-2-yl)oxy)methyl)-1*H*-1,2,3-triazol-1-yl)pentan-2-yl)hexanamide dihydrochloride (69a)

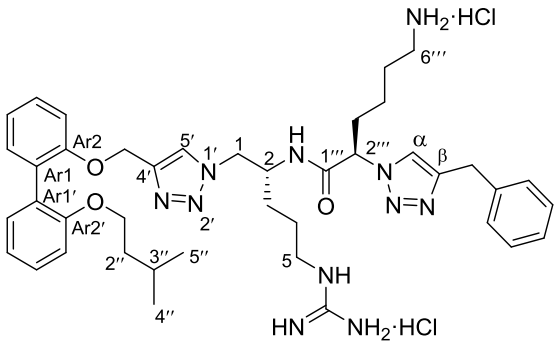

Following **General Procedure A**, azide **67b** (45 mg, 0.05 mmol), 3-phenyl-1-propyne (18 mg, 0.15 mmol), $Cu(OAc)_2 \cdot H_2O$ (2 mg, 0.01 mmol) and sodium ascorbate (4 mg, 0.02 mmol) were stirred in *t*-BuOH (1.0 mL) and H_2O (0.25 mL) for 18 h to give the intermediate triazole as a light tan gum after flash chromatography over SiO_2 gel (EtOAc/P.S. – 10:90 → 100:0). Following **General Procedure C**, the triazole was dissolved in CH_2Cl_2 (1.5 mL) and treated

with H_2O (18 mg, 1.00 mmol) and CF_3CO_2H (1.5 mL) followed by work-up with ethereal HCl to give the amine salt **69a** (37 mg, 97% over two steps) as a light tan powder that rapidly transitioned to a sticky gum. $[\alpha]_D^{23}$ +18.1 (*c* 1.00, MeOH); ^{1}H NMR (400 MHz, CD_3OD) δ 7.82 (s, 1H, H5'), 7.80 (s, 1H, Hα), 7.34 – 7.11 (m, 10H, ArH), 7.03 – 6.89 (m, 3H, ArH), 5.21 (br s, 1H, H2'''), 5.10 (s, 2H, -OC$\underline{H}_2$-C4'), 4.61 – 4.51 (m, 1H, $H1_A$ or $H1_B$), 4.49 – 4.39 (m, 1H, $H1_B$ or $H1_A$), 4.30 (br s, 1H, H2), 4.05 (s, 2H, -C$\underline{H}_2$Ph), 3.90 (t, *J* = 6.0 Hz, 2H, H1''), 3.14 (s, 2H, H5), 2.85 (s, 2H, H6'''), 2.02 – 1.77 (m, 2H, H3'''), 1.76 – 1.26 (m, 9H, H3, H4, H2'', H3'' and H5'''), 1.07 (s, 2H, H4'''), 0.80 (d, *J* = 6.5 Hz, 6H, H4'' and H5''); ^{13}C NMR (101 MHz, CD_3OD) δ 170.1 (C1'''), 158.7 (C=N), 158.1 (CAr2'), 157.5 (CAr2), 148.4 (Cβ – observed by gHMBC), 145.7 (C4' – observed by gHMBC), 140.1 (Phenyl C_{Ar}), 133.1 (CAr6 or CAr6'), 132.7 (CAr6' or CAr6), 130.4 (CAr1), 129.92 (Phenyl C_{Ar})*, 129.89 (CAr4 or CAr4'), 129.86 (Phenyl C_{Ar})*, 129.8 (CAr4' or CAr4), 129.7 (CAr1'), 127.9 (Phenyl C_{Ar}), 126.2 (C5'), 124.0 (Cα), 122.4 (CAr5), 121.5 (CAr5'), 114.7 (CAr3), 113.9 (CAr3'), 68.2 (C1''), 65.0 (C2'''), 63.6 (-CH_2-C4'), 54.7 (C1), 51.1 (C2), 42.1 (C6'''), 40.5 (C5), 39.4 (C2''), 32.61 (C3'''), 32.57 (-$\underline{C}H_2$Ph), 30.1 (C3), 27.8 (C5'''), 26.3 (C4), 26.2 (C3''), 23.5 (C4'''), 23.1 (C4'' and C5''); IR (neat) $\bar{\nu}_{max}$ 3064, 2954, 2928, 2874, 2376, 2350, 2321, 1734, 1700, 1684, 1653, 1623, 1559, 1540, 1507, 1490, 1457, 1437, 1419, 1340, 1218, 1164, 1109, 1087, 1049, 1003, 855, 752, 729, 669, 621 cm^{-1}; MS (ESI +ve) *m*/2 376 ($[M + 2H]^{2+}$, 100%), *m/z* 750 ($[M + H]^+$, 32%), 772 ($[M + Na]^+$, 8%); HRMS (ESI +ve TOF) calcd for $C_{41}H_{56}N_{11}O_3$ 750.4568, found 750.4581 ($[M + H]^+$).

(*R*)-6-Amino-*N*-((*R*)-5-guanidino-1-(4-(((2'-(isopentyloxy)-[1,1'-biphenyl]-2-yl)oxy)methyl)-1*H*-1,2,3-triazol-1-yl)pentan-2-yl)-2-(4-phenethyl-1*H*-1,2,3-triazol-1-yl)hexanamide dihydrochloride (69b)

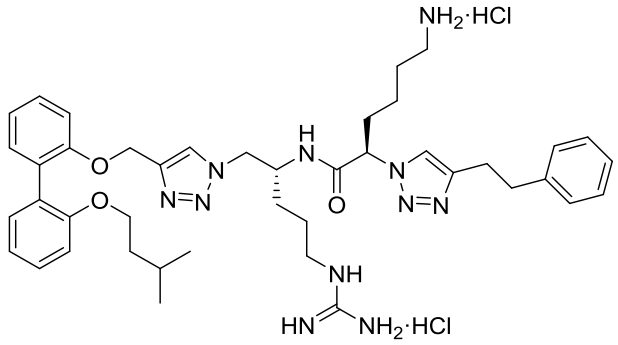

Following **General Procedure A**, azide **67b** (45 mg, 0.05 mmol), 4-phenyl-1-butyne (20 mg, 0.15 mmol), $Cu(OAc)_2 \cdot H_2O$ (2 mg, 0.01 mmol) and sodium ascorbate (4 mg, 0.02 mmol) were stirred in *t*-BuOH (1.0 mL) and H_2O (0.25 mL) for 18 h to give the intermediate triazole as a light tan gum after flash chromatography over SiO_2 gel (EtOAc/P.S. – 10:90 → 100:0). Following **General Procedure C**, the triazole was dissolved in CH_2Cl_2 (1.5 mL) and treated with H_2O (18 mg, 1.00 mmol) and CF_3CO_2H (1.5 mL) followed by work-up with ethereal HCl to give the amine salt **69b** (36 mg, 95% over two steps) as a light tan powder that rapidly transitioned to a sticky gum. $[\alpha]_D^{23}$ +19.4 (*c* 0.40, MeOH); ^{1}H NMR (400 MHz, CD_3OD) δ 7.80 (s, 1H), 7.67 (s, 1H), 7.36 – 7.10 (m, 10H), 7.05 – 6.98 (m, 2H), 6.95 (t, *J* = 7.4 Hz, 1H), 5.17 (t, *J* = 7.4 Hz, 1H), 5.12 (s, 2H), 4.57 (dd, *J* = 13.9, 3.7 Hz, 1H), 4.49 – 4.39 (m, 1H), 4.30 (br s, 1H), 3.92 (t, *J* = 6.3 Hz, 2H), 3.23 – 3.07 (m, 2H), 3.04 – 2.91 (m, 4H), 2.90 – 2.76 (m, 2H), 2.00 – 1.88 (m, 1H), 1.85 – 1.75 (m, 1H), 1.73 – 1.40 (m, 9H), 1.11 – 0.95 (m, 2H), 0.81 (d, *J* = 6.6 Hz, 6H); ^{13}C NMR (101 MHz, CD_3OD) δ 170.2, 158.8, 158.2, 157.5, 148.5 (observed by gHMBC), 145.9 (observed by gHMBC), 142.3, 133.1, 132.7, 130.4, 129.9, 129.81, 129.76, 129.7*, 129.6*, 127.4, 126.1, 123.4, 122.4, 121.5, 114.8, 113.9, 68.2,

64.8, 63.6, 54.7, 51.1, 42.1, 40.5, 39.4, 36.6, 32.7, 30.1, 28.4, 27.8, 26.4, 26.3, 23.5, 23.1*; IR (neat) $\bar{\nu}_{max}$ 3164, 3065, 2953, 2927, 2874, 2375, 2322, 1734, 1700, 1684, 1653, 1623, 1559, 1540, 1507, 1490, 1457, 1437, 1419, 1340, 1218, 1161, 1110, 1085, 1050, 1002, 855, 750, 700, 668, 621 cm^{-1}; MS (ESI +ve) *m*/2 383 ($[M + 2H]^{2+}$, 100%), *m/z* 764 ($[M + H]^+$, 28%), 786 ($[M + Na]^+$, 13%); HRMS (ESI +ve TOF) calcd for $C_{42}H_{58}N_{11}O_3$ 764.4724, found 764.4708 ($[M + H]^+$).

(*R*)-6-Amino-2-(4-cyclohexyl-1*H*-1,2,3-triazol-1-yl)-*N*-((*R*)-5-guanidino-1-(4-(((2'-(isopentyloxy)-[1,1'-biphenyl]-2-yl)oxy)methyl)-1*H*-1,2,3-triazol-1-yl)pentan-2-yl)hexanamide dihydrochloride (69c)

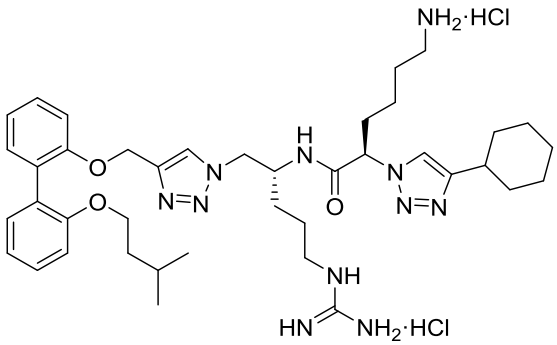

Following **General Procedure A**, azide **67b** (45 mg, 0.05 mmol), cyclohexylacetylene (18 mg, 0.15 mmol), $Cu(OAc)_2 \cdot H_2O$ (2 mg, 0.01 mmol) and sodium ascorbate (4 mg, 0.02 mmol) were stirred in *t*-BuOH (1.0 mL) and H_2O (0.25 mL) for 18 h to give the intermediate triazole as a light tan gum after flash chromatography over SiO_2 gel (EtOAc/P.S. – 10:90 → 100:0). Following **General Procedure C**, the triazole was dissolved in CH_2Cl_2 (1.5 mL) and treated with H_2O (18 mg, 1.00 mmol) and CF_3CO_2H (1.5 mL) followed by work-up with ethereal HCl to give the amine salt **69c** (31 mg, 84% over two steps) as a light tan powder that rapidly transitioned to a sticky gum. $[\alpha]_D^{23}$ +19.3 (*c* 0.60, MeOH); ^1H NMR (400 MHz, CD_3OD)

δ 7.94 (s, 1H), 7.82 (s, 1H), 7.36 – 7.24 (m, 2H), 7.24 – 7.12 (m, 3H), 7.07 – 6.91 (m, 3H), 5.25 (t, *J* = 7.3 Hz, 1H), 5.12 (s, 2H), 4.63 – 4.52 (m, 1H), 4.51 – 4.40 (m, 1H), 4.31 (br s, 1H), 3.99 – 3.84 (m, 2H), 3.24 – 3.07 (m, 2H), 2.87 (br s, 2H), 2.73 (br s, 1H), 2.09 – 1.21 (m, 23H), 1.11 (br s, 2H), 0.81 (d, *J* = 6.6 Hz, 6H); ^{13}C NMR (101 MHz, CD_3OD) δ 169.9, 158.8, 158.2, 157.5, 153.6 (observed by gHMBC), 145.7 (observed by gHMBC), 133.1, 132.7, 130.4, 129.9, 129.8, 129.7, 126.2, 122.8, 122.4, 121.5, 114.8, 113.9, 68.2, 65.4, 63.6, 54.7, 51.2, 42.1, 40.5, 39.4, 36.3, 33.94*, 33.91, 32.5, 30.1, 27.8, 27.3, 27.1, 26.4, 26.3, 23.6, 23.1*; IR (neat) $\bar{\nu}_{max}$ 3329, 3164, 3065, 2954, 2928, 2874, 2375, 2322, 1734, 1700, 1684, 1653, 1623, 1559, 1540, 1507, 1490, 1457, 1437, 1419, 1340, 1212, 1162, 1109, 1087, 1050, 1003, 854, 750, 668, 622 cm^{-1}; MS (ESI +ve) *m*/2 372 ($[M + 2H]^{2+}$, 100%), *m/z* 742 ($[M + H]^+$, 37%), 764 ($[M + Na]^+$, 11%); HRMS (ESI +ve TOF) calcd for $C_{40}H_{59}N_{11}O_3Na$ 764.4700, found 764.4723 ($[M + Na]^+$).

(*R*)-6-Amino-2-azido-*N*-((*R*)-5-guanidino-1-(4-(((2'-(isopentyloxy)-[1,1'-biphenyl]-2-yl)oxy)methyl)-1*H*-1,2,3-triazol-1-yl)pentan-2-yl)hexanamide dihydrochloride (69d)

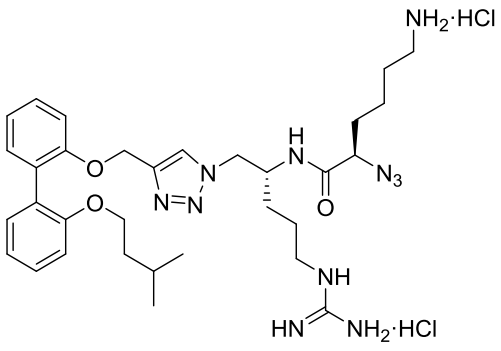

Following **General Procedure C**, azide **67b** (45 mg, 0.05 mmol) was dissolved in CH_2Cl_2 (1.5 mL) and treated with H_2O (18 mg, 1.00 mmol) and CF_3CO_2H (1.5 mL) followed by work-up with ethereal HCl to give the amine salt **69d** (30 mg, 97%) as a light tan powder

that rapidly transitioned to a sticky gum. $[\alpha]_D^{23}$ +43.4 (*c* 0.50, MeOH); ^{1}H NMR (400 MHz, $CDCl_3$) δ 7.75 (s, 1H), 7.34 – 7.23 (m, 2H), 7.22 – 7.12 (m, 3H), 7.05 – 6.90 (m, 3H), 5.10 (s, 2H), 4.55 – 4.41 (m, 2H), 4.31 (br s, 1H), 3.91 (t, *J* = 6.4 Hz, 2H), 3.81 (t, *J* = 6.5 Hz, 1H), 3.28 – 3.07 (m, 2H), 2.89 (br s, 2H), 1.77 – 1.50 (m, 9H), 1.50 – 1.41 (m, 2H), 1.27 (br s, 2H), 0.80 (d, *J* = 6.6 Hz, 6H); ^{13}C NMR (101 MHz, CD_3OD) δ 172.9, 158.9, 158.2, 157.5, 145.8 (observed by gHMBC), 133.0, 132.6, 130.5, 129.9, 129.8, 129.8, 126.0, 122.3, 121.5, 114.8, 113.9, 68.2, 63.7, 63.4, 54.7, 51.1, 42.2, 40.5, 39.4, 31.9, 29.9, 27.7, 26.3, 26.3, 23.3, 23.1*; IR (neat) $\bar{\nu}_{max}$ 3165, 3065, 2955, 2928, 2874, 2368, 2322, 2106, 1734, 1700, 1684, 1653, 1623, 1559, 1540, 1507, 1490, 1457, 1437, 1419, 1340, 1216, 1161, 1106, 1088, 1051, 1003, 855, 750, 668, 611 cm^{-1}; MS (ESI +ve) *m*/2 318 ($[M + 2H]^{2+}$, 100%), *m*/*z* 634 ($[M + H]^+$, 64%), 656 ($[M + Na]^+$, 23%); HRMS (ESI +ve TOF) calcd for $C_{32}H_{48}N_{11}O_3$ 634.3942, found 634.3966 ($[M + H]^+$).

***Tert*-butyl ((*R*)-5-((*R*)-2-azido-5-(2-((2,2,4,6,7-pentamethyl-2,3-dihydrobenzofuran-5-yl)sulfonyl)guanidino)pentanamido)-6-(4-((((*S*)-2'-(isopentyloxy)-[1,1'-binaphthalen]-2-yl)oxy)methyl)-1*H*-1,2,3-triazol-1-yl)hexyl)carbamate (67c)**

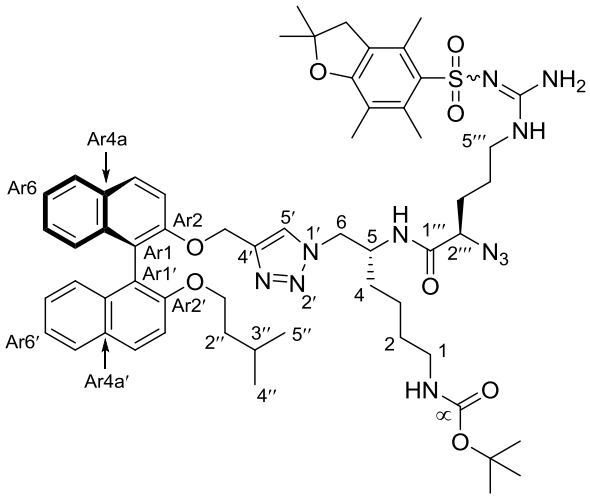

Following **General Procedure B**, amine **63c** (65 mg, 0.10 mmol), acid **28** (54 mg, 0.12 mmol), EDCI (23 mg, 0.12 mmol) and HOBt (18 mg, 0.11 mmol) were stirred in acetonitrile (1.0 mL) for 24 h to give the amide **67c** (105 mg, 96%) as a translucent tan gum. TLC ($MeOH/CH_2Cl_2$ – 5:95): R_f =

0.55; $[\alpha]_D^{23}$ −18.0 (*c* 0.40, MeOH); ^{1}H NMR (400 MHz, $CDCl_3$) δ 7.99 – 7.92 (m, 2H, ArH), 7.90 – 7.84 (m, 2H, ArH), 7.53 (d, *J* = 9.0 Hz, 1H, HAr3), 7.45 (d, *J* = 9.0 Hz, 1H, HAr3'), 7.38 – 7.29 (m, 2H, ArH), 7.25 – 7.16 (m, 3H, N^5-H and ArH), 7.15 – 7.09 (m, 2H, ArH), 7.06 (br s, 1H, H5'), 5.99 (br s, 2H, -$NH_{2\ (guanidine)}$), 5.08 (s, 2H, -OCH_2-C4'), 4.63 (br s, 1H, N^1-H), 4.37 – 4.23 (m, 3H, H5 and H6), 4.06 – 3.96 (m, 1H, H1"$_A$ or H1"$_B$), 3.92 – 3.82 (m, 1H, H1"$_B$ or H1"$_A$), 3.81 – 3.74 (m, 1H, H2'"), 3.32 (br s, 1H, H5'"$_A$ or H5'"$_B$), 3.09 (br s, 2H, H1), 2.95 (s, 2H, $ArCH_2$-), 2.72 (br s, 1H, H5'"$_B$ or H5'"$_A$), 2.55 (s, 3H, $ArCH_3$), 2.49 (s, 3H, $ArCH_3$), 2.08 (s, 3H, $ArCH_3$), 1.57 – 1.03 (m, 28H, H2, H3, H4, H2", H3", H3'", H4'", -$C(CH_3)_2$ and -$C(CH_3)_3$), 0.58 (d, *J* = 6.4 Hz, 3H, H4" or H5"), 0.51 (d, *J* = 6.3 Hz, 3H, H5" or H4"); ^{13}C NMR (101 MHz, $CDCl_3$) δ 170.9 (C1'"), 159.0 (Pbf C_{Ar}), 156.2 (C=N), 155.0 (Cα), 154.7 (CAr2'), 154.5 (CAr2), 144.5 (C4'), 138.4 (Pbf C_{Ar}), 134.1 (CAr8a or CAr8a'), 134.0 (CAr8a' or CAr8a), 132.8 (Pbf C_{Ar}), 132.4 (Pbf C_{Ar}), 130.2 (CAr4a), 130.0 (CAr4), 129.7 (CAr4'), 129.3 (CAr4a'), 128.2 (CAr5), 128.1 (CAr5'), 126.7 (CAr7), 126.6 (CAr7'), 125.7 (CAr8), 125.4 (CAr8'), 124.8 (Pbf C_{Ar}), 124.4 (CAr6), 124.0 (CAr6'), 123.8 (C5' – observed by gHSQC), 121.5 (CAr1), 120.6 (CAr1'), 117.7 (Pbf C_{Ar}), 117.6 (CAr3), 116.3 (CAr3'), 86.6 (-$\underline{C}(CH_3)_2$), 79.0 (-$\underline{C}(CH_3)_3$ – observed by gHMBC), 68.8 (C1"), 65.3 (-OCH_2-C4'), 60.8 (C2'"), 53.5 (C6), 49.3 (C5), 43.4 (C1), 40.3 (C5'"), 38.2 (C2"), 31.7 (C4), 29.6 (C3'"), 28.7 (-C($\underline{C}H_3)_2$), 28.6 (-C($\underline{C}H_3)_3$), 27.3 (C2), 25.3 (C4'"), 24.7 (C3"), 23.1 (C3), 22.5 (C4" or C5"), 22.2 (C5" or C4"), 19.5 ($ArCH_3$), 18.1 ($ArCH_3$), 12.6 ($ArCH_3$); IR (neat) $\overline{\nu}_{max}$ 3320, 2955, 2927, 2868, 2108, 1688, 1617, 1559, 1540, 1507, 1458, 1366, 1244, 1164, 1147, 1105, 1089, 1051, 1013, 903, 854, 808, 783, 748, 663, 640, 614 cm^{-1}; MS (ESI +ve) *m/z* 413 (100%), 1108 ($[M + Na]^+$, 20%), 1086 ($[M + H]^+$, 13%); HRMS (ESI +ve TOF) calcd for $C_{58}H_{75}N_{11}O_8SNa$ 1108.5419, found 1108.5476 ($[M + Na]^+$).

(*R*)-*N*-((*R*)-6-Amino-1-(4-((((*S*)-2'-(isopentyloxy)-[1,1'-binaphthalen]-2-yl)oxy)methyl)-1*H*-1,2,3-triazol-1-yl)hexan-2-yl)-2-(4-benzyl-1*H*-1,2,3-triazol-1-yl)-5-guanidinopentanamide dihydrochloride (70a)

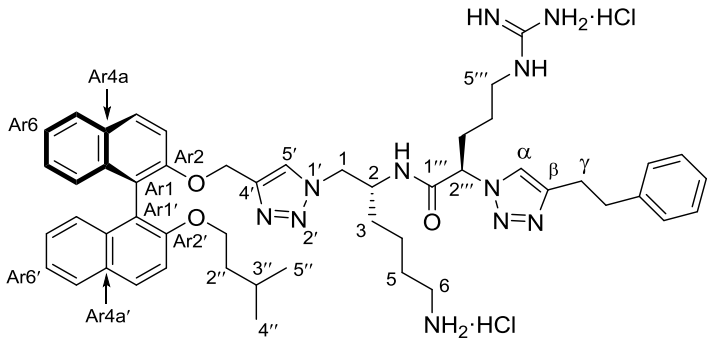

Following **General Procedure A**, azide **67c** (50 mg, 0.05 mmol), 4-phenyl-1-butyne (18 mg, 0.14 mmol), $Cu(OAc)_2 \cdot H_2O$ (2 mg, 0.01 mmol) and sodium ascorbate (4 mg, 0.02 mmol) were stirred in *t*-BuOH (1.0 mL) and H_2O (0.25 mL) for 18 h to give the intermediate triazole as a light tan gum after flash chromatography over SiO_2 gel ($MeOH/CH_2Cl_2$ – 0:100 → 10:90). Following **General Procedure C**, the triazole was dissolved in CH_2Cl_2 (1.5 mL) and treated with H_2O (18 mg, 1.00 mmol) and CF_3CO_2H (1.5 mL) followed by work-up with ethereal HCl to give the amine salt **70a** (25 mg, 58% over two steps) as a light tan powder that rapidly transitioned to a sticky gum. $[\alpha]_D^{23}$ −65.4 (*c* 0.37, MeOH); ^{1}H NMR (400 MHz, CD_3OD) δ 8.05 – 7.96 (m, 2H, ArH), 7.93 – 7.86 (m, 2H, ArH), 7.66 – 7.60 (m, 2H, HAr3 and Hα), 7.53 (d, *J* = 9.0 Hz, 1H, HAr3'), 7.39 (s, 1H, H5'), 7.37 – 7.27 (m, 2H, ArH), 7.27 – 7.10 (m, 7H, ArH), 7.07 – 6.97 (m, 2H, ArH), 5.18 – 5.08 (m, 3H, H2''' and -OCH_2-C4'), 4.48 – 4.40 (m, 1H, $H1_A$ or $H1_B$), 4.35 – 4.26 (m, 1H, $H1_B$ or $H1_A$), 4.25 – 4.16 (m, 1H, H2), 4.09 – 4.00 (m, 1H, $H1''_A$ or $H1''_B$), 3.96 – 3.87 (m, 1H, $H1''_B$ or $H1''_A$), 3.00 – 2.90 (m, 6H, H5''', Hγ and -C$\underline{H}_2$Ph), 2.85 (t, *J* = 7.0 Hz, 2H, H6), 1.97 – 1.87 (m, 1H, $H3_A$ or $H3_B$), 1.85 – 1.03 (m, 12H, $H3_B$ or $H3_A$, H4, H5, H3''', H4''', H2'' and H3''), 0.58 (d, *J* = 6.4 Hz, 3H, H4''

or H5"), 0.52 (d, J = 6.4 Hz, 3H, H5" or H4"); ^{13}C NMR (101 MHz, CD_3OD) δ 170.1 (C=O), 158.7 (C=N), 156.2 (CAr2'), 155.7 (CAr2), 148.5 (Cβ), 145.9 (C4' - observed by gHMBC), 142.4 (Phenyl C_{Ar}), 135.62 (CAr8a or CAr8a'), 135.57 (CAr8a' or CAr8a), 131.7 (CAr4a), 131.0 (CAr4a'), 130.8 (CAr4 and CAr4'), 129.7 (Phenyl C_{Ar})*, 129.6 (Phenyl C_{Ar})*, 129.4 (CAr5 or CAr5'), 129.2 (CAr5' or CAr5), 127.50 (CAr7), 127.46 (Phenyl C_{Ar}), 127.4 (CAr7'), 126.7 (CAr8), 126.4 (CAr8'), 125.9 (Cα), 125.3 (CAr6), 124.8 (CAr6'), 123.2 (CAr1), 123.0 (C5'), 121.5 (CAr1'), 118.3 (CAr3), 117.1 (CAr3'), 69.3 (C1"), 65.2 (-OCH_2-C4'), 64.4 (C2'"), 54.6 (C1), 51.1 (C2), 41.6 (C5'"), 40.6 (C6), 39.6 (C2"), 36.7 (Cγ), 32.2 (C3), 30.5 (C3'"), 28.6 (-C$\underline{H}_2$Ph), 28.2 (C5), 26.0 (C4'"), 25.9 (C3"), 23.8 (C4), 23.0 (C4" or C5"), 22.7 (C5" or C4"); IR (neat) $\bar{\nu}_{max}$ 3318, 3155, 3061, 2952, 2928, 2868, 1669, 1653, 1617, 1591, 1559, 1540, 1507, 1458, 1328, 1242, 1215, 1147, 1133, 1106, 1084, 1040, 1006, 905, 861, 808, 748, 701, 680, 614 cm^{-1}; MS (ESI +ve) $m/2$ 433 ($[M + 2H]^{2+}$, 100%), m/z 864 ($[M + H]^+$, 12%); HRMS (ESI +ve TOF) calcd for $C_{50}H_{62}N_{11}O_3$ 864.5037, found 864.5074 ($[M + H]^+$).

(*R*)-*N*-((*R*)-6-Amino-1-(4-((((*S*)-2'-(isopentyloxy)-[1,1'-binaphthalen]-2-yl)oxy)methyl)-1*H*-1,2,3-triazol-1-yl)hexan-2-yl)-2-(4-(cyclohexylmethyl)-1*H*-1,2,3-triazol-1-yl)-5-guanidinopentanamide dihydrochloride (70b)

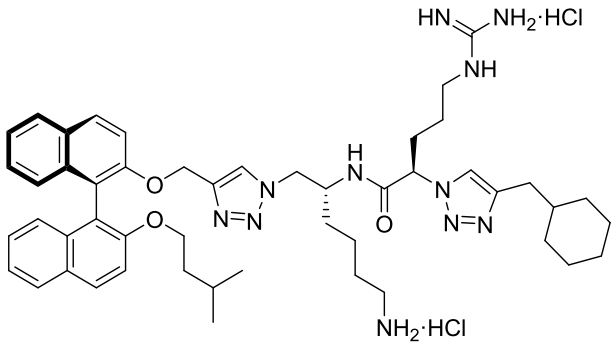

Following **General Procedure A**, azide **67c** (50 mg, 0.05 mmol), 3-cyclohexyl-1-propyne (17 mg, 0.14 mmol), $Cu(OAc)_2 \cdot H_2O$ (2 mg, 0.01 mmol) and sodium ascorbate (4 mg, 0.02 mmol) were stirred in *t*-BuOH (1.0 mL) and H_2O (0.25 mL) for 18 h to give the intermediate triazole as a light tan gum after flash chromatography over SiO_2 gel ($MeOH/CH_2Cl_2$ – 0:100 → 10:90). Following **General Procedure C**, the triazole was dissolved in CH_2Cl_2 (1.5 mL) and treated with H_2O (18 mg, 1.00 mmol) and CF_3CO_2H (1.5 mL) followed by work-up with ethereal HCl to give the amine salt **70b** (32 mg, 74% over two steps) as a light tan powder that rapidly transitioned to a sticky gum. $[\alpha]^2{}_D{}^3$ −42.1 (*c* 0.37, MeOH); ^{1}H NMR (400 MHz, CD_3OD) δ 8.05 – 7.98 (m, 2H), 7.93 – 7.86 (m, 3H), 7.64 (d, *J* = 9.0 Hz, 1H), 7.53 (d, *J* = 9.0 Hz, 1H), 7.44 (s, 1H), 7.38 – 7.27 (m, 2H), 7.24 – 7.12 (m, 2H), 7.04 (d, *J* = 8.5 Hz, 1H), 7.00 (d, *J* = 8.5 Hz, 1H), 5.27 – 5.19 (m, 1H), 5.19 – 5.07 (m, 2H), 4.46 (dd, *J* = 13.8, 3.9 Hz, 1H), 4.33 (dd, *J* = 13.6, 8.8 Hz, 1H), 4.28 – 4.17 (m, 1H), 4.11 – 4.00 (m, 1H), 3.97 – 3.85 (m, 1H), 2.98 (t, *J* = 6.7 Hz, 2H), 2.87 (t, *J* = 6.8 Hz, 2H), 2.56 (d, *J* = 6.9 Hz, 2H), 2.03 – 1.83 (m, 2H), 1.77 – 1.09 (m, 20H), 1.03 – 0.86 (m, 2H), 0.58 (d, *J* = 6.4 Hz, 3H), 0.52 (d, *J* = 6.4 Hz, 3H); ^{13}C NMR (101 MHz, CD_3OD) δ 169.7, 158.6, 156.2, 155.7, 147.1 (observed

by gHMBC), 145.9 (observed by gHMBC), 135.6, 135.6, 131.7, 130.9, 130.8*, 129.4, 129.2, 127.5, 127.4, 126.7, 126.4, 126.1, 125.4, 124.8, 124.6, 123.2, 121.5, 118.4, 117.1, 69.3, 65.2, 65.1, 54.6, 51.2, 41.6, 40.6, 39.6, 39.4, 34.2*, 33.7, 32.2, 30.5, 28.2, 27.6, 27.4*, 26.0, 25.9, 23.8, 23.0, 22.7; IR (neat) $\overline{\nu}_{max}$ 3319, 3158, 3059, 2950, 2926, 2855, 1669, 1653, 1623, 1591, 1559, 1540, 1507, 1458, 1328, 1242, 1213, 1147, 1133, 1106, 1084, 1040, 1007, 903, 861, 808, 746, 613 cm^{-1}; MS (ESI +ve) *m*/2 429 ($[M + 2H]^{2+}$, 100%), *m/z* 856 ($[M + H]^{+}$, 31%); HRMS (ESI +ve TOF) calcd for $C_{49}H_{66}N_{11}O_3$ 856.5350, found 856.5313 ($[M + H]^{+}$).

(*R*)-*N*-((*R*)-6-Amino-1-(4-(((2'-(isopentyloxy)-[1,1'-biphenyl]-2-yl)oxy)methyl)-1*H*-1,2,3-triazol-1-yl)hexan-2-yl)-5-guanidino-2-(2-phenylacetamido)pentanamide dihydrochloride (73)

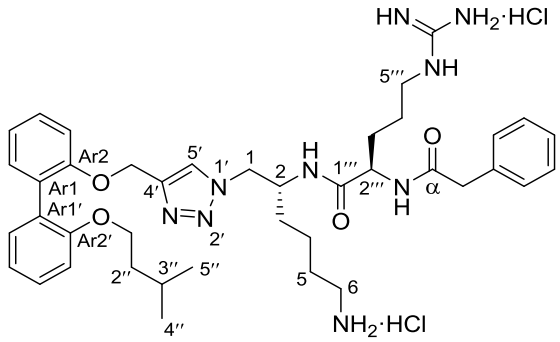

Following **General Procedure B**, amine **63a** (400 mg, 0.73 mmol), Fmoc-(D)-Arg(Pbf)-OH (**61**) (564 mg, 0.87 mmol), EDCI (166 mg, 0.87 mmol) and HOBt (118 mg, 0.79 mmol) were stirred in acetonitrile (7.2 mL) for 24 h to give the intermediate amide **72** (665 mg, 78%) as a translucent tan gum after flash chromatography over SiO_2 gel (MeOH/EtOAc/P.S. – 0:40:60 → 0.5:80:19.5). To a solution of the amide (250 mg, 0.21 mmol) in acetonitrile (2.1 mL) was added tris-(2-aminoethyl)amine (155 mg, 1.06 mmol) and the reaction was stirred vigorously at rt for 90 min. The reaction mixture was diluted with CH_2Cl_2 (100 mL) and

washed successively with phosphate buffer (pH = 5.5) – (3 × 50 mL) and brine (1 × 50 mL). The organic phase was dried (Na_2SO_4), filtered, concentrated and the residue was subjected to flash chromatography over SiO_2 gel ($MeOH/CH_2Cl_2$ – 5:95 → 10:90) to afford the intermediate amine **71** (151 mg, 74%). Following **General Procedure B**, the intermediate amine (53 mg, 0.06 mmol), phenylacetic acid (9 mg, 0.07 mmol), EDCI (13 mg, 0.07 mmol) and HOBt (9 mg, 0.06 mmol) were stirred in acetonitrile (0.6 mL) for 18 h to give the intermediate amide as a translucent tan gum. Following **General Procedure C**, the amide was dissolved in CH_2Cl_2 (1.7 mL) and treated with H_2O (20 mg, 1.10 mmol) and CF_3CO_2H (1.7 mL) followed by work-up with ethereal HCl to give the amine salt **73** (27 mg, 61% over two steps) as a light tan powder that rapidly transitioned to a sticky gum. $[\alpha]_D^{23}$ −6.2 (*c* 0.57, MeOH); ^{1}H NMR (400 MHz, CD_3OD) δ 7.69 (s, 1H, H5'), 7.35 – 7.08 (m, 10H, ArH), 7.02 – 6.86 (m, 3H, ArH), 5.05 (s, 2H, -OCH_2-C4'), 4.48 – 4.30 (m, 2H, H1), 4.23 (s, 1H, H2), 4.15 (br s, 1H, H2'''), 3.93 – 3.84 (m, 2H, H1''), 3.66 – 3.51 (m, 2H, -C$\underline{H}_2$Ph), 3.11 (br s, 2H, H6), 2.85 (br s, 2H, H5'''), 1.75 – 1.27 (m, 13H, H3, H4, H5, H2'', H3'', H3''' and H4'''), 0.79 (d, *J* = 6.6 Hz, 6H, H4'' and H5''); ^{13}C NMR (101 MHz, CD_3OD) δ 174.9 (C1'''), 174.6 (Cα), 158.8 (C=N), 158.1 (CAr2'), 157.5 (CAr2), 145.4 (C4'), 137.3 (Phenyl C_{Ar}), 133.0 (CAr6 or CAr6'), 132.7 (CAr6' or CAr6), 130.6 (Phenyl C_{Ar})*, 130.4 (CAr1 and CAr1'), 129.83 (CAr4 or CAr4'), 129.78 (Phenyl C_{Ar})*, 129.7 (CAr4' or CAr4), 128.1 (Phenyl C_{Ar}), 126.3 (C5'), 122.3 (CAr5), 121.5 (CAr5'), 114.8 (CAr3), 113.8 (CAr3'), 68.2 (C1''), 63.6 (-O$\underline{C}H_2$-C4'), 55.2 (C2'''), 54.7 (C1), 51.1 (C2), 43.7 (-$\underline{C}H_2$Ph), 41.7 (C6), 40.5 (C5'''), 39.4 (C2''), 31.9 (C3), 29.9 (C3'''), 28.1 (C5), 26.3 (C3''), 26.2 (C4'''), 23.6 (C4), 23.1 (C4'' and C5''); IR (neat) $\overline{\nu}_{max}$ 3069, 2955, 2931, 2869, 1663, 1540, 1506, 1473, 1438, 1386, 1260, 1203, 1089, 1053, 1022, 800, 751, 721, 696, 616 cm^{-1}; MS (ESI +ve) *m/z* 726 ([M + H]$^+$, 100%), 748 ([M +

Na]$^+$, 22%); HRMS (ESI +ve TOF) calcd for $C_{40}H_{55}N_9O_4Na$ 748.4275, found 748.4288 ([M + Na]$^+$).

(9*H*-Fluoren-9-yl)methyl ((*R*)-1-(((*R*)-6-amino-1-(4-(((2'-(isopentyloxy)-[1,1'-biphenyl]-2-yl)oxy)methyl)-1*H*-1,2,3-triazol-1-yl)hexan-2-yl)amino)-5-guanidino-1-oxopentan-2-yl)carbamate dihydrochloride (74)

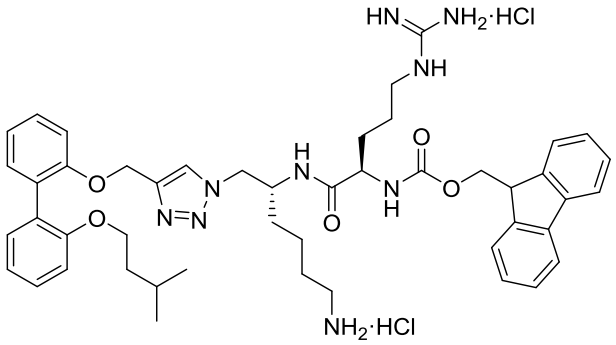

Following **General Procedure C**, the intermediate amide **72** (50 mg, 0.04 mmol) was dissolved in CH_2Cl_2 (1.3 mL) and treated with H_2O (15 mg, 0.85 mmol) and CF_3CO_2H (1.3 mL) followed by work-up with ethereal HCl to give the amine salt **74** (36 mg, 95%) as a light tan powder that rapidly transitioned to a sticky gum. $[\alpha]_D^{23}$ −4.4 (*c* 1.03, MeOH); ^{1}H NMR (400 MHz, CD_3OD) δ 7.82 – 7.51 (m, 5H), 7.42 – 7.08 (m, 9H), 7.04 – 6.83 (m, 3H), 5.05 (s, 2H), 4.53 – 4.22 (m, 6H), 4.00 – 3.83 (m, 3H), 3.15 – 3.04 (m, 2H), 2.98 – 2.84 (m, 2H), 1.75 – 1.25 (m, 13H), 0.79 (d, *J* = 6.6 Hz, 6H); ^{13}C NMR (101 MHz, $CDCl_3$) δ 175.0, 158.8, 158.4, 158.1, 157.5, 147.7, 145.4, 141.3, 136.5*, 133.0, 132.7, 130.6, 130.5, 130.4, 129.84, 129.76, 129.7, 126.0, 125.2*, 122.3, 122.0, 121.5*, 114.8, 113.8, 71.0, 68.2, 63.7, 56.2, 54.7, 50.9, 48.5, 41.9, 40.7, 39.4, 32.1, 30.2, 28.1, 26.3, 26.2, 23.7, 23.1*; IR (neat) $\bar{\nu}_{max}$ 3168, 3067, 2956, 2932, 2871, 1714, 1664, 1526, 1506, 1473, 1438, 1386, 1227, 1150, 1091, 1052, 976, 917, 859, 737, 615 cm^{-1}; MS (ESI +ve) *m*/2 416 ([M + 2H]$^{2+}$, 100%), *m/z* 852 ([M +

Na]$^+$, 8%); HRMS (ESI +ve TOF) calcd for $C_{47}H_{60}N_9O_5$ 830.4717, found 830.4747 ([M + H]$^+$).

6.3.4 – Series B1

(*R*)-6-((*Tert*-butoxycarbonyl)amino)-2-(4-(((2'-(isopentyloxy)-[1,1'-biphenyl]-2-yl)oxy)methyl)-1*H*-1,2,3-triazol-1-yl)hexanoic acid (75a)

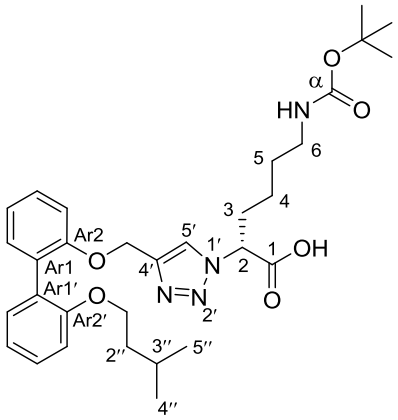

Following **General Procedure A**, azide **24** (400 mg, 1.47 mmol), alkyne **21** (865 mg, 2.94 mmol), $Cu(OAc)_2 \cdot H_2O$ (59 mg, 0.29 mmol) and sodium ascorbate (116 mg, 0.59 mmol) were stirred in *t*-BuOH (29.4 mL) and H_2O (7.4 mL) for 26 h to give the product triazole **75a** (703 mg, 85%) as a translucent tan gum after flash chromatography over SiO_2 gel (EtOAc/P.S. – 10:90 → MeOH/CH_2Cl_2 – 10:90). TLC (MeOH/CH_2Cl_2 – 10:90): R_f = 0.44; $[\alpha]_D^{23}$ +5.0 (*c* 1.27, MeOH); ^{1}H NMR (400 MHz, DMSO) δ 7.89 (s, 1H, H5'), 7.35 – 7.20 (m, 3H, ArH), 7.20 – 7.11 (m, 2H, ArH), 7.05 – 6.88 (m, 3H, ArH), 6.73 (br s, 1H, N^6-H), 5.19 (br s, 1H, H2), 5.09 (s, 2H, -OCH_2-C4'), 3.94 – 3.83 (m, 2H, H1''), 2.89 – 2.77 (m, 2H, H6), 2.19 – 1.92 (m, 2H, H3), 1.61 – 1.50 (m, 1H, H3''), 1.47 – 1.26 (m, 13H, H5, H2'' and -$C(CH_3)_3$), 1.19 – 1.07 (m, 1H, $H4_A$ or $H4_B$), 1.01 – 0.88 (m, 1H, $H4_B$ or $H4_A$), 0.78 (d, *J* = 6.6 Hz, 6H, H4'' and H5''); ^{13}C NMR (101 MHz, DMSO) δ 156.1 (CAr2'), 155.7 (CAr2), 155.6 (C1), 155.5 (Cα), 142.9 (C4'), 131.13 (CAr6 or CAr6'), 131.07 (CAr6' or CAr6), 128.4 (CAr4 or CAr4'), 128.3 (CAr4' or CAr4), 127.9 (CAr1), 127.4 (CAr1'), 123.3 (C5'), 120.4 (CAr5), 119.8 (CAr5'), 113.0 (CAr3), 112.2 (CAr3'), 77.3 (-$\underline{C}(CH_3)_3$), 66.2 (C1''), 63.0 (C2 – observed by gHSQC), 62.2 (-O$\underline{C}H_2$-C4'), 39.4 (C6 –

observed by gHSQC), 37.4 (C2''), 31.4 (C3), 28.8 (C5), 28.2 (-C(<u>C</u>H$_3$)$_3$), 24.4 (C3''), 22.8 (C4), 22.3 (C4'' and C5''); IR (neat) $\bar{\nu}_{max}$ 3345, 2956, 2932, 2869, 2362, 2341, 1734, 1718, 1700, 1684, 1653, 1636, 1594, 1577, 1559, 1540, 1507, 1473, 1457, 1437, 1395, 1367, 1340, 1260, 1238, 1165, 1124, 1109, 1052, 1003, 982, 931, 855, 810, 751, 734 cm^{-1}; MS (ESI −ve) *m/z* 565 ([M − H]$^-$, 100%); HRMS (ESI +ve TOF) calcd for $C_{31}H_{42}N_4O_6Na$ 589.3002, found 589.2993 ([M + Na]$^+$).

(*R*)-6-Amino-*N*-benzyl-2-(4-(((2'-(isopentyloxy)-[1,1'-biphenyl]-2-yl)oxy)methyl)-1*H*-1,2,3-triazol-1-yl)hexanamide hydrochloride (76a)

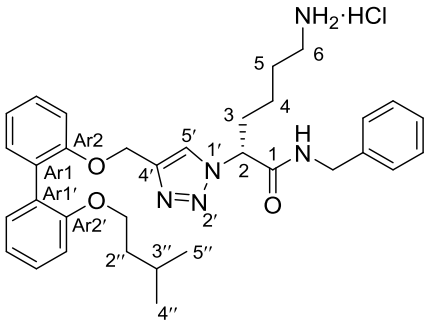

Following **General Procedure B**, acid **75a** (50 mg, 0.09 mmol), benzylamine (11 mg, 0.11 mmol), EDCI (20 mg, 0.11 mmol) and HOBt (14 mg, 0.11 mmol) were stirred in acetonitrile (0.9 mL) for 24 h to give the intermediate amide as a translucent tan gum. Following **General Procedure D**, the amide was dissolved in CH_2Cl_2 (2.7 mL) and treated with CF_3CO_2H (2.7 mL) followed by work-up with ethereal HCl to give the amine salt **76a** (56 mg, 95% over two steps) as a light tan powder that rapidly transitioned to a sticky gum. $[\alpha]_D^{23}$ +7.0 (*c* 1.33, MeOH); ^{1}H NMR (400 MHz, CD_3OD) δ 7.75 (s, 1H, H5'), 7.34 – 7.10 (m, 10H, ArH), 7.05 – 6.97 (m, 2H, ArH), 6.94 (t, *J* = 7.1 Hz, 1H, ArH), 5.29 (t, *J* = 7.6 Hz, 1H, H2), 5.15 – 5.04 (m, 2H, -OC<u>H</u>$_2$-C4'), 4.37 (s, 2H, -C<u>H</u>$_2$Ph), 3.95 – 3.83 (m, 2H, H1''), 2.83 (t, *J* = 6.8 Hz, 2H, H6), 2.23 – 2.01 (m, 2H, H3), 1.72 – 1.50 (m, 3H, H5 and H3''), 1.46 – 1.38 (m, 2H, H2''), 1.34 – 1.11 (m, 2H, H4), 0.77 (d, *J* = 6.6 Hz, 6H, H4'' and H5''); ^{13}C NMR (101 MHz, CD_3OD) δ 169.8 (C1), 158.2 (CAr2'), 157.6 (CAr2), 146.3 (C4'), 139.5 (Phenyl C_{Ar}), 132.8 (CAr6 or

CAr6'), 132.5 (CAr6' or CAr6), 130.7 (CAr1 and CAr1'), 129.9 (CAr4 or CAr4'), 129.84 (Phenyl C_{Ar})*, 129.76 (CAr4' or CAr4), 128.8 (Phenyl C_{Ar})*, 128.7 (Phenyl C_{Ar}), 124.1 (C5'), 122.5 (CAr5), 121.5 (CAr5'), 114.7 (CAr3), 113.7 (CAr3'), 68.2 (C1"), 64.9 (C2), 64.1 (-OCH_2-C4'), 44.6 (-$\underline{C}H_2$Ph), 40.5 (C6), 39.4 (C2"), 33.3 (C3), 28.0 (C5), 26.2 (C3"), 23.8 (C4), 23.10 (C4" or C5"), 23.07 (C5" or C4"); IR (neat) $\bar{\nu}_{max}$ 3276, 3065, 2954, 2934, 2870, 2364, 2318, 1718, 1684, 1669, 1653, 1636, 1594, 1576, 1559, 1540, 1507, 1473, 1457, 1437, 1395, 1340, 1260, 1202, 1180, 1130, 1110, 1052, 1003, 982, 932, 836, 799, 751, 721, 698, 615 cm^{-1}; MS (ESI +ve) *m/z* 578 ($[M + Na]^+$, 100%), 556 ($[M + H]^+$, 91%); HRMS (ESI +ve TOF) calcd for $C_{33}H_{42}N_5O_3$ 556.3288, found 556.3302 ($[M + H]^+$).

(*R*)-6-Amino-2-(4-(((2'-(isopentyloxy)-[1,1'-biphenyl]-2-yl)oxy)methyl)-1*H*-1,2,3-triazol-1-yl)-*N*-phenethylhexanamide hydrochloride (76b)

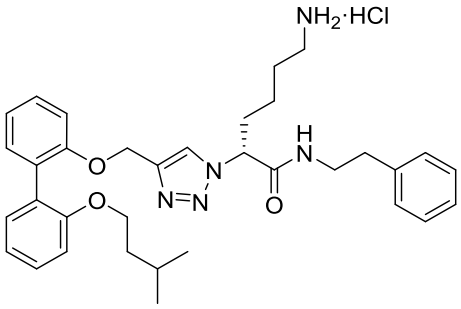

Following **General Procedure B**, acid **75a** (50 mg, 0.09 mmol), β-phenylethylamine (13 mg, 0.11 mmol), EDCI (20 mg, 0.11 mmol) and HOBt (14 mg, 0.11 mmol) were stirred in acetonitrile (0.9 mL) for 24 h to give the intermediate amide as a translucent tan gum. Following **General Procedure D**, the amide was dissolved in CH_2Cl_2 (2.7 mL) and treated with CF_3CO_2H (2.7 mL) followed by work-up with ethereal HCl to give the amine salt **76b** (51 mg, 94% over two steps) as a light tan powder that rapidly transitioned to a sticky gum. $[\alpha]_D^{23}$ +7.9 (*c* 1.20, MeOH); ^{1}H NMR (400 MHz, CD_3OD) δ 7.72 (s, 1H), 7.35 – 7.08 (m, 10H), 7.01 (t, *J* = 7.5 Hz, 2H), 6.94 (t, *J* = 7.4 Hz, 1H), 5.21 (t, *J* = 7.6 Hz, 1H), 5.14 – 5.06 (m, 2H), 3.95 – 3.84 (m, 2H), 3.45 (t, *J* = 7.0 Hz, 2H), 2.83 (t, *J* = 7.2 Hz, 2H), 2.78 (t, *J* =

7.1 Hz, 2H), 2.15 – 1.94 (m, 2H), 1.70 – 1.50 (m, 3H), 1.47 – 1.38 (m, 2H), 1.29 – 1.10 (m, 2H), 0.78 (d, *J* = 6.6 Hz, 6H); ^{13}C NMR (101 MHz, CD_3OD) δ 169.7, 158.2, 157.5, 146.1, 140.3, 132.8, 132.6, 130.6, 130.0*, 129.9, 129.82, 129.76, 129.7*, 127.6, 124.2, 122.5, 121.5, 114.7, 113.7, 68.2, 65.0, 64.0, 42.2, 40.5, 39.4, 36.3, 33.2, 28.0, 26.2, 23.7, 23.11, 23.09; IR (neat) $\bar{\nu}_{max}$ 3242, 3065, 2954, 2934, 2869, 2363, 1684, 1670, 1594, 1555, 1502, 1474, 1438, 1385, 1367, 1261, 1219, 1161, 1123, 1110, 1052, 1002, 933, 852, 799, 749, 700, 616 cm^{-1}; MS (ESI +ve) *m/z* 570 ([M + H]$^+$, 100%), 592 ([M + Na]$^+$, 82%); HRMS (ESI +ve TOF) calcd for $C_{34}H_{44}N_5O_3$ 570.3444, found 570.3448 ([M + H]$^+$).

(*R*)-6-Amino-*N*-cyclohexyl-2-(4-(((2'-(isopentyloxy)-[1,1'-biphenyl]-2-yl)oxy)methyl)-1*H*-1,2,3-triazol-1-yl)hexanamide hydrochloride (76c)

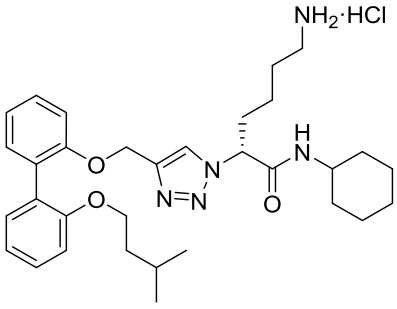

Following **General Procedure B**, acid **75a** (50 mg, 0.09 mmol), cyclohexylamine (11 mg, 0.11 mmol), EDCI (20 mg, 0.11 mmol) and HOBt (14 mg, 0.11 mmol) were stirred in acetonitrile (0.9 mL) for 24 h to give the intermediate amide as a translucent tan gum. Following **General Procedure D**, the amide was dissolved in CH_2Cl_2 (2.7 mL) and treated with CF_3CO_2H (2.7 mL) followed by work-up with ethereal HCl to give the amine salt **76c** (48 mg, 94% over two steps) as a light tan powder that rapidly transitioned to a sticky gum. $[\alpha]_D^{23}$ +5.7 (*c* 1.37, MeOH); ^{1}H NMR (400 MHz, CD_3OD) δ 7.75 (s, 1H), 7.34 – 7.25 (m, 2H), 7.21 – 7.10 (m, 3H), 7.06 – 6.98 (m, 2H), 6.95 (t, *J* = 7.4 Hz, 1H), 5.26 (t, *J* = 7.6 Hz, 1H), 5.14 – 5.04 (m, 2H), 3.98 – 3.84 (m, 2H), 3.68 – 3.56 (m, 1H), 2.87 (t, *J* = 6.6 Hz, 2H), 2.19 – 1.98 (m, 2H), 1.92 – 1.50 (m, 7H), 1.47 – 1.11 (m, 10H), 0.78 (d, *J* = 6.6 Hz, 6H); ^{13}C NMR (101 MHz,

CD_3OD) δ 168.9, 158.2, 157.5, 146.2, 132.7, 132.5, 130.6*, 129.8, 129.7, 123.9, 122.4, 121.5, 114.7, 113.7, 68.2, 64.9, 64.1, 50.4, 40.5, 39.4, 33.8, 33.6, 33.5, 28.1, 26.7, 26.24, 26.20, 26.17, 23.8, 23.11, 23.08; IR (neat) $\bar{\nu}_{max}$ 3265, 3065, 2934, 2855, 2371, 1680, 1665, 1545, 1507, 1472, 1441, 1339, 1261, 1219, 1160, 1023, 892, 854, 805, 750, 616 cm^{-1}; MS (ESI +ve) *m/z* 548 ($[M + H]^+$, 100%), 570 ($[M + Na]^+$, 73%); HRMS (ESI +ve TOF) calcd for $C_{32}H_{46}N_5O_3$ 548.3601, found 548.3602 ($[M + H]^+$).

(*R*)-6-Amino-*N*-(cyclohexylmethyl)-2-(4-(((2'-(isopentyloxy)-[1,1'-biphenyl]-2-yl)oxy)methyl)-1*H*-1,2,3-triazol-1-yl)hexanamide hydrochloride (76d)

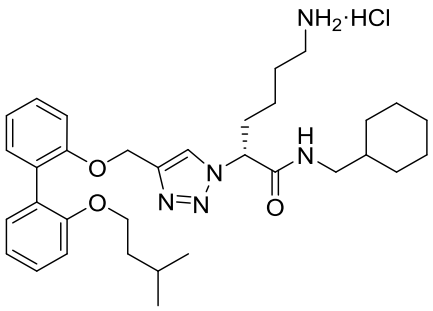

Following **General Procedure B**, acid **75a** (50 mg, 0.09 mmol), cyclohexylmethylamine (12 mg, 0.11 mmol), EDCI (20 mg, 0.11 mmol) and HOBt (14 mg, 0.11 mmol) were stirred in acetonitrile (0.9 mL) for 24 h to give the intermediate amide as a translucent tan gum. Following **General Procedure D**, the amide was dissolved in CH_2Cl_2 (2.7 mL) and treated with CF_3CO_2H (2.7 mL) followed by work-up with ethereal HCl to give the amine salt **76d** (49 mg, 92% over two steps) as a light tan powder that rapidly transitioned to a sticky gum. $[\alpha]_D^{23}$ +4.5 (*c* 1.00, MeOH); ^1H NMR (400 MHz, CD_3OD) δ 7.75 (s, 1H), 7.35 – 7.25 (m, 2H), 7.22 – 7.10 (m, 3H), 7.01 (t, *J* = 7.0 Hz, 2H), 6.95 (t, *J* = 7.4 Hz, 1H), 5.29 (t, *J* = 7.6 Hz, 1H), 5.15 – 5.05 (m, 2H), 3.97 – 3.85 (m, 2H), 3.04 (dd, *J* = 6.7, 2.6 Hz, 2H), 2.93 – 2.79 (m, 2H), 2.21 – 2.00 (m, 2H), 1.76 – 1.40 (m, 10H), 1.35 – 1.10 (m, 6H), 0.97 – 0.83 (m, 2H),

0.78 (d, J = 6.6 Hz, 6H); ^{13}C NMR (101 MHz, CD_3OD) δ 170.1‡, 158.2, 157.6, 146.2, 132.7, 132.6, 130.7*, 129.9, 129.8, 124.0, 122.5, 121.5, 114.7, 113.7, 68.2, 65.0‡, 64.1, 47.2‡, 40.5, 39.4, 39.2, 33.3, 32.08, 32.05, 28.1, 27.7, 27.1*, 26.3, 23.9, 23.12, 23.08; IR (neat) $\bar{\nu}_{max}$ 3241, 3068, 2954, 2925, 2868, 2856, 2362, 1684, 1669, 1594, 1555, 1503, 1474, 1441, 1386, 1368, 1261, 1223, 1161, 1123, 1109, 1052, 1019, 982, 932, 851, 799, 750, 615 cm^{-1}; MS (ESI +ve) *m/z* 584 ([M + Na]$^+$, 100%), 562 ([M + H]$^+$, 81%); HRMS (ESI +ve TOF) calcd for $C_{33}H_{48}N_5O_3$ 562.3757, found 562.3759 ([M + H]$^+$).

(*R*)-6-Amino-2-(4-(((2'-(isopentyloxy)-[1,1'-biphenyl]-2-yl)oxy)methyl)-1*H*-1,2,3-triazol-1-yl)-*N*-(4-(trifluoromethyl)benzyl)hexanamide hydrochloride (76e)

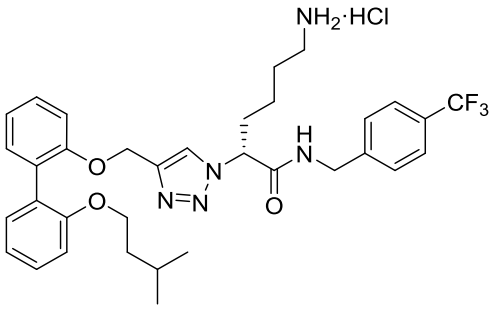

Following **General Procedure B**, acid **75a** (50 mg, 0.09 mmol), 4-(trifluoromethyl)benzylamine (19 mg, 0.11 mmol), EDCI (20 mg, 0.11 mmol) and HOBt (14 mg, 0.11 mmol) were stirred in acetonitrile (0.9 mL) for 24 h to give the intermediate amide as a translucent tan gum. Following **General Procedure D**, the amide was dissolved in CH_2Cl_2 (2.7 mL) and treated with CF_3CO_2H (2.7 mL) followed by work-up with ethereal HCl to give the amine salt **76e** (56 mg, 97% over two steps) as a light tan powder that rapidly transitioned to a sticky gum. $[\alpha]_D^{23}$ +14.2 (*c* 1.50, MeOH); ^{1}H NMR (400

‡ Indicates that the ^{13}C NMR resonance was split into two resonances due to the presence of both amide rotamers (i.e. the *syn*- and *anti*-amide conformations); only the major resonance from each resonance pair is reported for clarity.

MHz, CD_3OD) δ 7.79 (s, 1H), 7.59 (d, J = 8.0 Hz, 2H), 7.42 (d, J = 8.0 Hz, 2H), 7.34 – 7.22 (m, 2H), 7.21 – 7.10 (m, 3H), 7.04 – 6.97 (m, 2H), 6.93 (t, J = 7.3 Hz, 1H), 5.37 (t, J = 7.4 Hz, 1H), 5.16 – 5.04 (m, 2H), 4.52 – 4.40 (m, 2H), 3.95 – 3.82 (m, 2H), 2.86 (br s, 2H), 2.28 – 2.04 (m, 2H), 1.75 – 1.61 (m, 2H), 1.61 – 1.48 (m, 1H), 1.46 – 1.37 (m, 2H), 1.36 – 1.11 (m, 2H), 0.76 (d, J = 6.6 Hz, 6H); ^{13}C NMR (101 MHz, CD_3OD) δ 170.1, 158.2, 157.5, 146.3, 144.2, 132.8, 132.5, 130.9 (q, $^2J_{CF}$ = 32.2 Hz)†, 130.6, 129.9, 129.82, 129.75, 129.3*, 126.7 (q, $^3J_{CF}$ = 3.8 Hz)*, 126.6, 124.5 (q, $^1J_{CF}$ = 270.5 Hz)†, 124.3, 122.5, 121.5, 114.7, 113.7, 68.2, 64.9, 64.0, 44.0, 40.5, 39.4, 33.2, 28.0, 26.2, 23.8, 23.08, 23.05; IR (neat) $\overline{\nu}_{max}$ 3242, 3067, 2955, 2928, 2869, 2361, 1684, 1620, 1594, 1555, 1504, 1474, 1441, 1420, 1387, 1324, 1261, 1223, 1164, 1122, 1112, 1067, 1018, 849, 819, 751, 615 cm^{-1}; MS (ESI +ve) *m/z* 624 ($[M + H]^+$, 100%), 646 ($[M + Na]^+$, 98%); HRMS (ESI +ve TOF) calcd for $C_{34}H_{41}N_5O_3F_3$ 624.3162, found 624.3173 ($[M + H]^+$).

† Incomplete multiplet resonance: the two ^{13}C NMR quartet resonances (assigned to the carbons closest to the fluorine atoms (i.e. -$\underline{C}F_3$ and $\underline{C}$-CF_3)) were each missing one of their outer quartet peaks due to the strong J_{CF} coupling that spread the weak quaternary signals over multiple lines (as quartets) – thus, the signals became even weaker and buried amongst the background noise. Furthermore, quaternary carbons do not experience the large Overhauser enhancement by proton decoupling that is experienced by protonated carbons, hence the weaker signal.

(*R*)-6-Amino-*N*-(4-fluorophenethyl)-2-(4-(((2'-(isopentyloxy)-[1,1'-biphenyl]-2-yl)oxy)methyl)-1*H*-1,2,3-triazol-1-yl)hexanamide hydrochloride (76f)

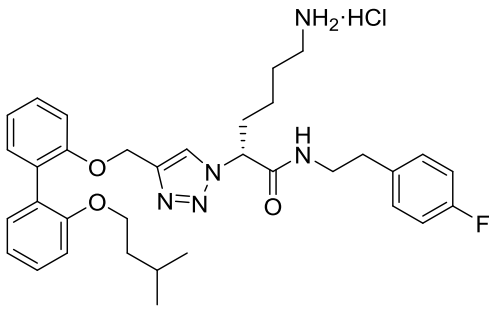

Following **General Procedure B**, acid **75a** (50 mg, 0.09 mmol), 2-(4-fluorophenyl)ethylamine (15 mg, 0.11 mmol), EDCI (20 mg, 0.11 mmol) and HOBt (14 mg, 0.11 mmol) were stirred in acetonitrile (0.9 mL) for 24 h to give the intermediate amide as a translucent tan gum. Following **General Procedure D**, the amide was dissolved in CH_2Cl_2 (2.7 mL) and treated with CF_3CO_2H (2.7 mL) followed by work-up with ethereal HCl to give the amine salt **76f** (51 mg, 93% over two steps) as a light tan powder that rapidly transitioned to a sticky gum. $[\alpha]_D^{23}$ +10.8 (*c* 1.23, MeOH); ^{1}H NMR (400 MHz, CD_3OD) δ 7.70 (s, 1H), 7.34 – 7.23 (m, 2H), 7.21 – 7.06 (m, 5H), 7.05 – 6.88 (m, 5H), 5.20 (t, *J* = 7.6 Hz, 1H), 5.14 – 5.05 (m, 2H), 3.95 – 3.84 (m, 2H), 3.50 – 3.33 (m, 2H), 2.84 (t, *J* = 6.6 Hz, 2H), 2.76 (t, *J* = 6.9 Hz, 2H), 2.14 – 1.94 (m, 2H), 1.71 – 1.50 (m, 3H), 1.47 – 1.39 (m, 2H), 1.28 – 1.09 (m, 2H), 0.78 (d, *J* = 6.6 Hz, 6H); ^{13}C NMR (101 MHz, CD_3OD) δ 169.8, 163.2 (d, $^1J_{CF}$ = 242.8 Hz), 158.2, 157.5, 146.2, 136.2 (d, $^4J_{CF}$ = 3.2 Hz), 132.8, 132.6, 131.7 (d, $^3J_{CF}$ = 7.9 Hz), 130.6*, 129.9, 129.8, 124.0, 122.4, 121.5, 116.2 (d, $^2J_{CF}$ = 21.4 Hz), 114.7, 113.7, 68.2, 64.9, 64.0, 42.1, 40.5, 39.4, 35.4, 33.2, 28.0, 26.2, 23.8, 23.10, 23.08; IR (neat) $\bar{\nu}_{max}$ 3241, 3068, 2954, 2925, 2868, 2362, 1684, 1594, 1555, 1503, 1474, 1441, 1386, 1368, 1261, 1223, 1161, 1123, 1109, 1052, 1019, 982, 932, 851, 805, 750, 615 cm^{-1}; MS (ESI +ve) *m/z* 610 ([M + Na]$^+$, 100%), 588 ([M + H]$^+$, 86%); HRMS (ESI +ve TOF) calcd for $C_{34}H_{43}N_5O_3F$ 588.3350, found 588.3358 ([M + H]$^+$).

(*R*)-2-(4-(((2'-(Isopentyloxy)-[1,1'-biphenyl]-2-yl)oxy)methyl)-1*H*-1,2,3-triazol-1-yl)-5-(2-((2,2,4,6,7-pentamethyl-2,3-dihydrobenzofuran-5-yl)sulfonyl)guanidino)pentanoic acid (75b)

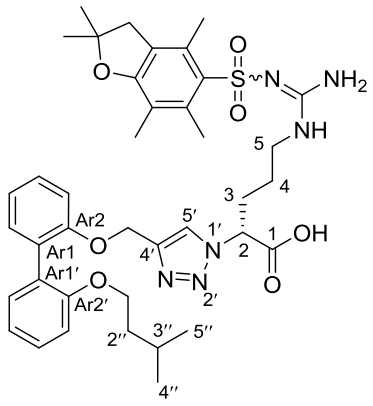

Following **General Procedure A**, azide **28** (1.20 g, 2.65 mmol), alkyne **21** (1.56 g, 5.30 mmol), $Cu(OAc)_2 \cdot H_2O$ (106 mg, 0.53 mmol) and sodium ascorbate (210 mg, 1.06 mmol) were stirred in *t*-BuOH (53 mL) and H_2O (13.3 mL) for 18 h to give the product triazole **75b** (1.63 g, 82%) as a translucent tan gum after flash chromatography over SiO_2 gel (EtOAc/P.S. – 10:90 → $MeOH/CH_2Cl_2$ – 10:90). TLC ($MeOH/CH_2Cl_2$ – 10:90): R_f = 0.40, (EtOAc/P.S. – 80:20): R_f = 0.42; $[\alpha]_D^{23}$ −28.1 (*c* 1.03, MeOH); ^{1}H NMR (400 MHz, DMSO) δ 7.84 (s, 1H, H5'), 7.60 (br s, 1H, N^5-H), 7.33 – 7.18 (m, 3H, ArH), 7.18 – 7.10 (m, 2H, ArH), 7.01 – 6.94 (m, 2H, ArH), 6.88 (t, *J* = 7.3 Hz, 1H, ArH), 6.80 (br s, 2H, $-NH_2$), 5.06 (s, 2H, $-OCH_2$-C4'), 4.91 (br s, 1H, H2), 3.93 – 3.81 (m, 2H, H1''), 3.07 – 2.96 (m, 2H, H5), 2.94 (s, 2H, $ArCH_2$-), 2.47 (s, 3H, $ArCH_3$), 2.41 (s, 3H, $ArCH_3$), 2.22 – 2.07 (m, 1H, $H3_A$ or $H3_B$), 1.99 (s, 3H, $ArCH_3$), 1.91 – 1.77 (m, 1H, $H3_B$ or $H3_A$), 1.54 (td, *J* = 13.2, 6.6 Hz, 1H, H3''), 1.45 – 1.33 (m, 8H, H2'' and $-C(CH_3)_2$), 1.23 (br s, 1H, $H4_A$ or $H4_B$), 1.07 (br s, 1H, $H4_B$ or $H4_A$), 0.76 (d, *J* = 6.6 Hz, 6H, H4'' and H5''); ^{13}C NMR (101 MHz, DMSO) δ 157.4 (Pbf C_{Ar}), 156.32 (C=N), 156.27 (C1), 156.1 (CAr2'), 155.7 (CAr2), 142.6 (C4'), 137.2 (Pbf C_{Ar}), 134.3 (Pbf C_{Ar}), 131.4 (Pbf C_{Ar}), 131.2 (CAr6 or CAr6'), 131.1 (CAr6' or CAr6), 128.5 (CAr4 or CAr4'), 128.4 (CAr4' or CAr4), 127.9 (CAr1), 127.4 (CAr1'), 124.3 (Pbf C_{Ar}), 123.1 (C5'), 120.4 (CAr5), 119.9 (CAr5'), 116.2 (Pbf C_{Ar}), 113.0 (CAr3), 112.2 (CAr3'), 86.2 ($-\underline{C}(CH_3)_2$), 66.2 (C1''), 64.9 (C2), 62.2 ($-OCH_2$-C4'), 42.5 ($ArCH_2$-), 39.5 (C5 – observed by

gHSQC), 37.5 (C2"), 30.2 (C3), 28.3 (-C(<u>C</u>H$_3$)$_2$), 25.9 (C4), 24.5 (C3"), 22.4 (C4" and C5"), 18.9 (ArCH$_3$), 17.6 (ArCH$_3$), 12.3 (ArCH$_3$); IR (neat) $\bar{\nu}_{max}$ 3327, 2946, 2873, 2831, 2363, 2167, 2027, 1617, 1559, 1506, 1442, 1405, 1238, 1108, 1023, 804, 751, 668 cm^{-1}; MS (ESI +ve) *m/z* 747 ([M + H]$^+$, 100%), MS (ESI −ve) *m/z* 745 ([M − H]$^-$, 100%); HRMS (ESI +ve TOF) calcd for $C_{39}H_{51}N_6O_7S$ 747.3540, found 747.3572 ([M + H]$^+$).

(*R*)-*N*-Benzyl-5-guanidino-2-(4-(((2'-(isopentyloxy)-[1,1'-biphenyl]-2-yl)oxy)methyl)-1*H*-1,2,3-triazol-1-yl)pentanamide hydrochloride (77a)

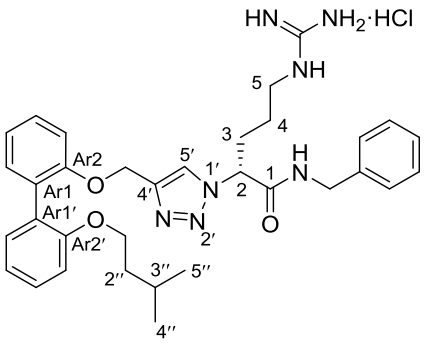

Following **General Procedure B**, acid **75b** (50 mg, 0.07 mmol), benzylamine (9 mg, 0.08 mmol), EDCI (15 mg, 0.08 mmol) and HOBt (11 mg, 0.07 mmol) were stirred in acetonitrile (0.7 mL) for 22 h to give the intermediate amide as a translucent tan gum. Following **General Procedure C**, the amide was dissolved in CH_2Cl_2 (2.0 mL) and treated with H_2O (24 mg, 1.34 mmol) and CF_3CO_2H (2.0 mL) followed by work-up with ethereal HCl to give the amine salt **77a** (39 mg, 94% over two steps) as a light tan powder that rapidly transitioned to a sticky gum. $[\alpha]_D^{23}$ +17.8 (*c* 0.93, MeOH); ^{1}H NMR (400 MHz, CD_3OD) δ 7.77 (s, 1H, H5'), 7.33 – 7.11 (m, 10H, ArH), 7.05 – 6.91 (m, 3H, ArH), 5.34 – 5.27 (m, 1H, H2), 5.13 – 5.06 (m, 2H, -OCH$_2$-C4'), 4.44 – 4.32 (m, 2H, -C<u>H</u>$_2$Ph), 3.95 – 3.82 (m, 2H, H1"), 3.20 – 3.12 (m, 2H, H5), 2.27 – 2.03 (m, 2H, H3), 1.60 – 1.33 (m, 5H, H4, H2" and H3"), 0.77 (d, *J* = 6.9 Hz, 6H, H4" and H5"); ^{13}C NMR (101 MHz, CD_3OD) δ 169.7 (C1), 158.7 (C=N), 158.2 (CAr2'), 157.6 (CAr2), 146.3 (C4'), 139.5 (Phenyl C_{Ar}), 132.8 (CAr6 or CAr6'), 132.5 (CAr6' or CAr6), 130.7 (CAr1), 129.9 (CAr4 or CAr4'), 129.84 (Phenyl C_{Ar})*, 129.82 (CAr1'), 129.76

(CAr4' or CAr4), 128.8 (Phenyl C_{Ar})*, 128.6 (Phenyl C_{Ar}), 124.2 (C5'), 122.5 (CAr5), 121.5 (CAr5'), 114.8 (CAr3), 113.7 (CAr3'), 68.2 (C1"), 64.8 (C2), 64.1 (-OCH_2-C4'), 44.6 (-$\underline{C}H_2$Ph), 41.8 (C5), 39.4 (C2"), 31.0 (C3), 26.4 (C4), 26.2 (C3"), 23.09 (C4" or C5"), 23.07 (C5" or C4"); IR (neat) $\bar{\nu}_{max}$ 3328, 3183, 3065, 2955, 2932, 2871, 2364, 2323, 1669, 1653, 1617, 1559, 1540, 1507, 1473, 1457, 1437, 1387, 1363, 1340, 1213, 1123, 1107, 1082, 1040, 1003, 855, 801, 749, 698, 669 cm^{-1}; MS (ESI +ve) *m/z* 584 ($[M + H]^+$, 100%), 606 ($[M + Na]^+$, 5%); HRMS (ESI +ve TOF) calcd for $C_{33}H_{42}N_7O_3$ 584.3349, found 584.3373 ($[M + H]^+$).

(*R*)-5-Guanidino-2-(4-(((2'-(isopentyloxy)-[1,1'-biphenyl]-2-yl)oxy)methyl)-1*H*-1,2,3-triazol-1-yl)-*N*-phenethylpentanamide hydrochloride (77b)

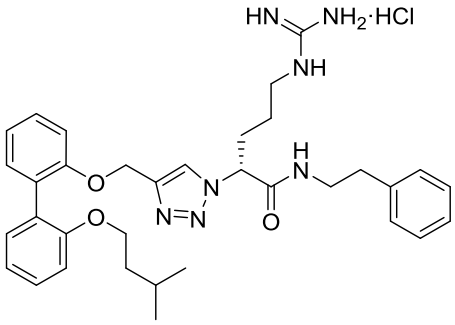

Following **General Procedure B**, acid **75b** (50 mg, 0.07 mmol), β-phenylethylamine (10 mg, 0.08 mmol), EDCI (15 mg, 0.08 mmol) and HOBt (11 mg, 0.07 mmol) were stirred in acetonitrile (0.7 mL) for 22 h to give the intermediate amide as a translucent tan gum. Following **General Procedure C**, the amide was dissolved in CH_2Cl_2 (2.0 mL) and treated with H_2O (24 mg, 1.34 mmol) and CF_3CO_2H (2.0 mL) followed by work-up with ethereal HCl to give the amine salt **77b** (37 mg, 87% over two steps) as a light tan powder that rapidly transitioned to a sticky gum. $[\alpha]_D^{23}$ +33.8 (*c* 0.97, MeOH); ^{1}H NMR (400 MHz, CD_3OD) δ 7.71 (s, 1H), 7.34 – 7.08 (m, 10H), 7.04 – 6.91 (m, 3H), 5.21 (t, *J* = 7.7 Hz, 1H), 5.12 – 5.06 (m, 2H), 3.95 – 3.83 (m, 2H), 3.48 – 3.41 (m, 2H), 3.14 (t, *J* = 7.0 Hz, 2H), 2.78 (t, *J* = 7.1 Hz, 2H), 2.18 – 1.95 (m, 2H), 1.61 – 1.50 (m, 1H), 1.48 – 1.29 (m, 4H), 0.77 (d, *J* = 6.6

Hz, 6H); ^{13}C NMR (101 MHz, CD_3OD) δ 169.6, 158.7, 158.2, 157.5, 146.1, 140.2, 132.8, 132.6, 130.6, 130.0*, 129.9, 129.81, 129.77, 129.7*, 127.6, 124.2, 122.5, 121.5, 114.7, 113.8, 68.2, 64.9, 64.0, 42.2, 41.9, 39.4, 36.3, 30.8, 26.2, 26.2, 23.09, 23.08; IR (neat) $\bar{\nu}_{max}$ 3330, 3185, 3065, 2953, 2930, 2870, 2364, 2322, 1684, 1669, 1653, 1617, 1559, 1540, 1507, 1473, 1457, 1437, 1387, 1363, 1340, 1212, 1123, 1109, 1087, 1040, 1003, 936, 855, 801, 748, 700, 668 cm^{-1}; MS (ESI +ve) *m/z* 598 ([M + H]$^+$, 100%), 620 ([M + Na]$^+$, 22%); HRMS (ESI +ve TOF) calcd for $C_{34}H_{44}N_7O_3$ 598.3506, found 598.3523 ([M + H]$^+$).

(*R*)-*N*-Cyclohexyl-5-guanidino-2-(4-(((2'-(isopentyloxy)-[1,1'-biphenyl]-2-yl)oxy)methyl)-1*H*-1,2,3-triazol-1-yl)pentanamide hydrochloride (77c)

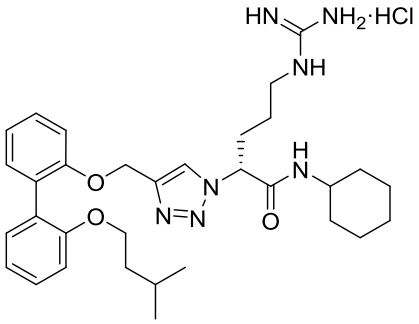

Following **General Procedure B**, acid **75b** (50 mg, 0.07 mmol), cyclohexylamine (8 mg, 0.08 mmol), EDCI (15 mg, 0.08 mmol) and HOBt (11 mg, 0.07 mmol) were stirred in acetonitrile (0.7 mL) for 21 h to give the intermediate amide as a translucent tan gum. Following **General Procedure C**, the amide was dissolved in CH_2Cl_2 (2.0 mL) and treated with H_2O (24 mg, 1.34 mmol) and CF_3CO_2H (2.0 mL) followed by work-up with ethereal HCl to give the amine salt **77c** (39 mg, 95% over two steps) as a light tan powder that rapidly transitioned to a sticky gum. $[\alpha]_D^{23}$ +15.9 (*c* 0.83, MeOH); ^{1}H NMR (400 MHz, CD_3OD) δ 7.77 (s, 1H), 7.34 – 7.24 (m, 2H), 7.23 – 7.09 (m, 3H), 7.05 – 6.98 (m, 2H), 6.95 (t, *J* = 7.4 Hz, 1H), 5.24 (t, *J* = 7.7 Hz, 1H), 5.14 – 5.05 (m, 2H), 3.96 – 3.85 (m, 2H), 3.68 – 3.57 (m, 1H), 3.18 (t, *J* = 7.0 Hz, 2H), 2.22 – 2.00 (m, 2H), 1.92 – 1.12 (m, 15H), 0.77 (d, *J* = 6.6 Hz, 6H); ^{13}C NMR (101 MHz, CD_3OD) δ 168.7, 158.8, 158.2, 157.5, 146.2, 132.7, 132.5, 130.7*, 129.9, 129.7,

124.0, 122.5, 121.5, 114.7, 113.8, 68.2, 64.8, 64.1, 50.4, 41.9, 39.4, 33.7, 33.6, 31.1, 26.7, 26.4, 26.3, 26.20, 26.16, 23.1*; IR (neat) $\bar{\nu}_{max}$ 3329, 3185, 3067, 2953, 2929, 2868, 2364, 2323, 1684, 1669, 1653, 1617, 1559, 1540, 1507, 1473, 1457, 1437, 1387, 1363, 1340, 1213, 1123, 1108, 1088, 1040, 1003, 941, 855, 802, 749, 668 cm^{-1}; MS (ESI +ve) *m/z* 576 ($[M + H]^+$, 100%), 598 ($[M + Na]^+$, 19%); HRMS (ESI +ve TOF) calcd for $C_{32}H_{46}N_7O_3$ 576.3662, found 576.3688 ($[M + H]^+$).

(*R*)-*N*-(Cyclohexylmethyl)-5-guanidino-2-(4-(((2'-(isopentyloxy)-[1,1'-biphenyl]-2-yl)oxy)methyl)-1*H*-1,2,3-triazol-1-yl)pentanamide hydrochloride (77d)

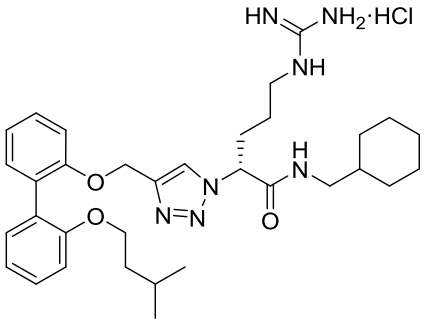

Following **General Procedure B**, acid **75b** (50 mg, 0.07 mmol), cyclohexylmethylamine (9 mg, 0.08 mmol), EDCI (15 mg, 0.08 mmol) and HOBt (11 mg, 0.07 mmol) were stirred in acetonitrile (0.7 mL) for 24 h to give the intermediate amide as a translucent tan gum. Following **General Procedure C**, the amide was dissolved in CH_2Cl_2 (2.0 mL) and treated with H_2O (24 mg, 1.34 mmol) and CF_3CO_2H (2.0 mL) followed by work-up with ethereal HCl to give the amine salt **77d** (25 mg, 60% over two steps) as a light tan powder that rapidly transitioned to a sticky gum. $[\alpha]_D^{23}$ −5.6 (*c* 0.63, MeOH); ^{1}H NMR (400 MHz, CD_3OD) δ 7.76 (s, 1H), 7.34 – 7.24 (m, 2H), 7.22 – 7.10 (m, 3H), 7.05 – 6.98 (m, 2H), 6.95 (t, *J* = 7.4 Hz, 1H), 5.31 (t, *J* = 7.6 Hz, 1H), 5.13 – 5.04 (m, 2H), 3.96 – 3.85 (m, 2H), 3.17 (t, *J* = 6.7 Hz, 2H), 3.07 – 2.99 (m, 2H), 2.26 – 2.01 (m, 2H), 1.77 – 1.36 (m, 11H), 1.33 – 1.12 (m, 3H), 0.96 – 0.82 (m, 2H), 0.78 (d, *J* = 6.6 Hz, 6H); ^{13}C NMR (101 MHz, CD_3OD) δ 169.9, 158.8, 158.2, 157.6, 146.4, 132.8, 132.6, 130.7, 129.9, 129.84, 129.76, 124.2, 122.5, 121.5, 114.8, 113.8, 68.2,

64.8, 64.1, 47.2, 41.8, 39.4, 39.2, 32.08, 32.06, 31.0, 27.7, 27.1*, 26.31, 26.25, 23.11, 23.08; IR (neat) $\bar{\nu}_{max}$ 3330, 3185, 2954, 2926, 2869, 2364, 2322, 1684, 1669, 1653, 1617, 1559, 1540, 1507, 1473, 1457, 1437, 1387, 1363, 1340, 1213, 1123, 1108, 1088, 1049, 854, 801, 749, 668 cm^{-1}; MS (ESI +ve) *m/z* 590 ($[M + H]^+$, 100%), 612 ($[M + Na]^+$, 28%); HRMS (ESI +ve TOF) calcd for $C_{33}H_{48}N_7O_3$ 590.3819, found 590.3829 ($[M + H]^+$).

(*R*)-5-Guanidino-2-(4-(((2'-(isopentyloxy)-[1,1'-biphenyl]-2-yl)oxy)methyl)-1*H*-1,2,3-triazol-1-yl)-*N*-(4-(trifluoromethyl)benzyl)pentanamide hydrochloride (77e)

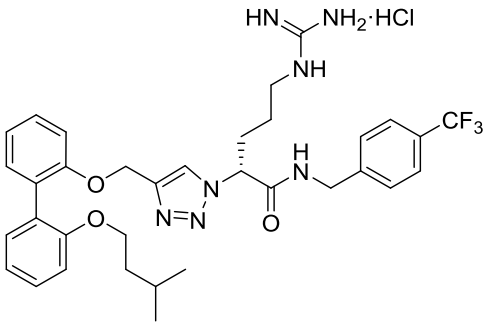

Following **General Procedure B**, acid **75b** (50 mg, 0.07 mmol), 4-(trifluoromethyl)benzylamine (14 mg, 0.08 mmol), EDCI (15 mg, 0.08 mmol) and HOBt (11 mg, 0.07 mmol) were stirred in acetonitrile (0.7 mL) for 24 h to give the intermediate amide as a translucent tan gum. Following **General Procedure C**, the amide was dissolved in CH_2Cl_2 (2.0 mL) and treated with H_2O (24 mg, 1.34 mmol) and CF_3CO_2H (2.0 mL) followed by work-up with ethereal HCl to give the amine salt **77e** (30 mg, 65% over two steps) as a light tan powder that rapidly transitioned to a sticky gum. $[\alpha]_D^{23}$ +17.8 (*c* 1.23, MeOH); ^{1}H NMR (400 MHz, CD_3OD) δ 7.77 (s, 1H), 7.62 – 7.52 (m, 2H), 7.45 – 7.36 (m, 2H), 7.33 – 7.07 (m, 5H), 7.05 – 6.84 (m, 3H), 5.40 – 5.30 (m, 1H), 5.14 – 5.04 (m, 2H), 4.49 – 4.40 (m, 2H), 3.93 – 3.79 (m, 2H), 3.23 – 3.08 (m, 2H), 2.25 – 1.97 (m, 2H), 1.62 –

1.18 (m, 5H), 0.77 – 0.71 (m, 6H); ^{13}C NMR (101 MHz, CD_3OD)† δ 169.9, 158.8, 158.2, 157.6, 149.6, 144.2, 132.8, 132.5, 130.6, 129.9, 129.83, 129.76, 129.3*, 126.7 (q, $^3J_{CF}$ = 3.6 Hz)*, 124.3, 122.5, 121.5, 114.7, 113.7, 68.2, 64.8, 64.1, 44.0, 41.9, 39.4, 30.9, 26.4, 26.2, 23.09, 23.07; IR (neat) $\overline{\nu}_{max}$ 2954, 2926, 2869, 2371, 2349, 2322, 1700, 1684, 1669, 1653, 1617, 1559, 1540, 1507, 1473, 1457, 1437, 1387, 1363, 1340, 1324, 1260, 1223, 1164, 1110, 1067, 1052, 1017, 917, 818, 751, 669 cm^{-1}; MS (ESI +ve) *m/z* 652 ([M + H]$^+$, 100%), 674 ([M + Na]$^+$, 18%); HRMS (ESI +ve TOF) calcd for $C_{34}H_{41}N_7O_3F_3$ 652.3223, found 652.3243 ([M + H]$^+$).

(*R*)-*N*-(4-Fluorophenethyl)-5-guanidino-2-(4-(((2'-(isopentyloxy)-[1,1'-biphenyl]-2-yl)oxy)methyl)-1*H*-1,2,3-triazol-1-yl)pentanamide hydrochloride (77f)

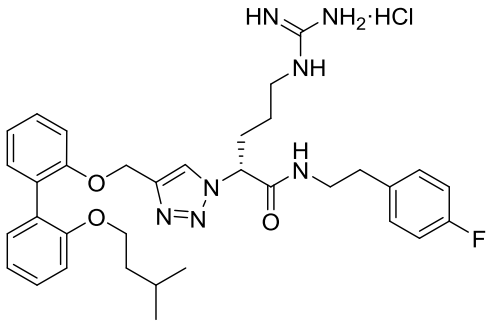

Following **General Procedure B**, acid **75b** (50 mg, 0.07 mmol), 2-(4-fluorophenyl)ethylamine (11 mg, 0.08 mmol), EDCI (15 mg, 0.08 mmol) and HOBt (11 mg, 0.07 mmol) were stirred in acetonitrile (0.7 mL) for 24 h to give the intermediate amide as a translucent tan gum. Following **General Procedure C**, the amide was dissolved in CH_2Cl_2

† Missing resonances: the two carbons closest to the fluorine atoms (i.e. -$\underline{C}F_3$ and $\underline{C}$-CF_3) could not be assigned to resonances in the ^{13}C NMR spectrum due to the strong J_{CF} coupling that spread the weak quaternary resonances over multiple lines (as quartets) – thus, the resonances became even weaker and buried amongst the background noise. Furthermore, quaternary carbons do not experience the large Overhauser enhancement by proton decoupling that is experienced by protonated carbons, thus making the resonances even weaker and more difficult to observe..

(2.0 mL) and treated with H_2O (24 mg, 1.34 mmol) and CF_3CO_2H (2.0 mL) followed by work-up with ethereal HCl to give the amine salt **77f** (37 mg, 84% over two steps) as a light tan powder that rapidly transitioned to a sticky gum. $[\alpha]_D^{23}$ +12.6 (*c* 1.00, MeOH); ^{1}H NMR (400 MHz, CD_3OD) δ 7.72 (s, 1H), 7.34 – 7.05 (m, 7H), 7.04 – 6.85 (m, 5H), 5.20 (t, *J* = 7.6 Hz, 1H), 5.10 (s, 2H), 3.94 – 3.81 (m, 2H), 3.50 – 3.34 (m, 2H), 3.15 (t, *J* = 6.9 Hz, 2H), 2.79 – 2.68 (m, 2H), 2.18 – 1.96 (m, 2H), 1.60 – 1.26 (m, 5H), 0.77 (d, *J* = 6.5 Hz, 6H); ^{13}C NMR (101 MHz, CD_3OD) δ 169.6, 163.2 (d, $^1J_{CF}$ = 242.8 Hz), 158.7, 158.2, 157.5, 146.0 (observed by gHMBC), 136.2 (d, $^4J_{CF}$ = 3.2 Hz), 132.8, 132.6, 131.7 (d, $^3J_{CF}$ = 7.9 Hz)*, 130.6, 129.9, 129.80, 129.76, 124.1, 122.5, 121.5, 116.2 (d, $^2J_{CF}$ = 21.4 Hz)*, 114.7, 113.7, 68.2, 64.8, 64.0, 42.2, 41.9, 39.4, 35.5, 30.8, 26.3, 26.2, 23.09, 23.08; IR (neat) $\bar{\nu}_{max}$ 3330, 3194, 3072, 2954, 2931, 2869, 2370, 2323, 1671, 1669, 1625, 1603, 1573, 1551, 1509, 1473, 1441, 1385, 1364, 1220, 1158, 1108, 1040, 1005, 914, 823, 750, 668 cm^{-1}; MS (ESI +ve) *m/z* 616 ([M + H]$^+$, 100%), 638 ([M + Na]$^+$, 25%); HRMS (ESI +ve TOF) calcd for $C_{34}H_{43}N_7O_3F$ 616.3411, found 616.3428 ([M + H]$^+$).

(*R*)-*N*-(3,5-Difluorobenzyl)-5-guanidino-2-(4-(((2'-(isopentyloxy)-[1,1'-biphenyl]-2-yl)oxy)methyl)-1*H*-1,2,3-triazol-1-yl)pentanamide (77g)

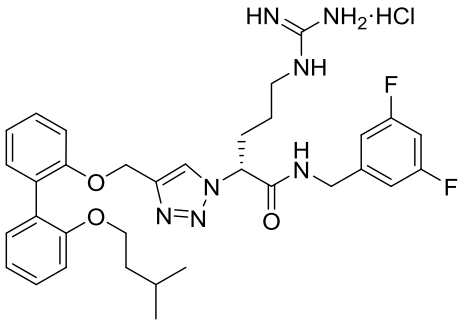

Following **General Procedure B**, acid **75b** (50 mg, 0.07 mmol), 3,5-difluorobenzylamine (12 mg, 0.08 mmol), EDCI (15 mg, 0.08 mmol) and HOBt (11 mg, 0.07 mmol) were stirred in acetonitrile (0.7 mL) for 24 h to give the intermediate amide as a translucent tan gum. Following **General Procedure C**, the amide was dissolved in CH_2Cl_2 (2.0 mL) and

treated with H_2O (24 mg, 1.34 mmol) and CF_3CO_2H (2.0 mL) followed by work-up with ethereal HCl to give the amine salt **77g** (23 mg, 53% over two steps) as a light tan powder that rapidly transitioned to a sticky gum. $[\alpha]_D^{23}$ −13.9 (*c* 0.50, MeOH); ^{1}H NMR (400 MHz, CD_3OD) δ 7.76 (s, 1H), 7.33 – 7.09 (m, 5H), 7.05 – 6.77 (m, 6H), 5.33 (dd, *J* = 8.6, 6.6 Hz, 1H), 5.13 – 5.06 (m, 2H), 4.37 (m, 2H), 3.93 – 3.81 (m, 2H), 3.17 (t, *J* = 7.1 Hz, 2H), 2.21 – 1.98 (m, 2H), 1.59 – 1.25 (m, 5H), 0.79 – 0.71 (m, 6H); ^{13}C NMR (101 MHz, CD_3OD) δ 169.9, 164.8 (dd, $^{1,3}J_{CF}$ = 248.6, 12.0 Hz)*, 158.8, 158.2, 157.6, 146.4, 144.3 (t, $^3J_{CF}$ = 9.1 Hz), 132.8, 132.5, 130.7*, 129.9, 129.8, 124.2, 122.5, 121.5, 114.8, 113.7, 111.5 (d, $^2J_{CF}$ = 25.7 Hz)*, 103.7 (t, $^2J_{CF}$ = 25.8 Hz), 68.2, 64.8, 64.2, 43.7, 41.9, 39.4, 30.9, 26.4, 26.2, 23.1, 23.0; IR (neat) $\bar{\nu}_{max}$ 3329, 3196, 3070, 2955, 2931, 2869, 2369, 2323, 1671, 1625, 1597, 1573, 1550, 1503, 1462, 1441, 1384, 1364, 1317, 1222, 1163, 1117, 1041, 1004, 914, 847, 750, 733, 668 cm^{-1}; MS (ESI +ve) *m/z* 620 ([M + H]$^+$, 100%), 642 ([M + Na]$^+$, 34%); HRMS (ESI +ve TOF) calcd for $C_{33}H_{40}N_7O_3F_2$ 620.3161, found 620.3152 ([M + H]$^+$).

(*R*)-*N*-(3-Fluorophenyl)-5-guanidino-2-(4-(((2'-(isopentyloxy)-[1,1'-biphenyl]-2-yl)oxy)methyl)-1*H*-1,2,3-triazol-1-yl)pentanamide hydrochloride (77h)

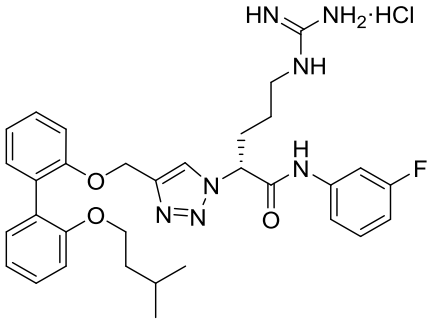

Following **General Procedure B**, acid **75b** (50 mg, 0.07 mmol), 3-fluoroaniline (9 mg, 0.08 mmol), EDCI (15 mg, 0.08 mmol) and HOBt (11 mg, 0.07 mmol) were stirred in acetonitrile (0.7 mL) for 24 h to give the intermediate amide as a translucent tan gum. Following **General Procedure C**, the amide was dissolved in CH_2Cl_2 (2.0 mL) and treated with H_2O (24 mg, 1.34 mmol) and CF_3CO_2H (2.0 mL) followed by work-up with ethereal HCl to give

the amine salt **77h** (33 mg, 79% over two steps) as a light tan powder that rapidly transitioned to a sticky gum. $[\alpha]_D^{23}$ +3.5 (*c* 0.93, MeOH); ^{1}H NMR (400 MHz, CD_3OD) δ 7.70 (s, 1H), 7.65 (d, *J* = 11.3 Hz, 1H), 7.43 – 7.39 (m, 1H), 7.35 – 7.08 (m, 6H), 7.06 – 6.88 (m, 3H), 6.88 – 6.79 (m, 1H), 5.34 (dd, *J* = 9.6, 5.0 Hz, 1H), 5.14 – 5.05 (m, 2H), 3.94 – 3.82 (m, 2H), 3.15 (t, *J* = 7.3 Hz, 2H), 2.41 – 2.24 (m, 1H), 2.21 – 2.06 (m, 1H), 1.65 – 1.24 (m, 5H), 0.80 – 0.72 (m, 6H); ^{13}C NMR (101 MHz, CD_3OD) δ 168.4, 164.4 (d, $^1J_{CF}$ = 242.6 Hz), 158.8, 158.2, 157.6, 146.5, 141.4 (d, $^3J_{CF}$ = 10.8 Hz), 132.8, 132.6, 131.5 (d, $^3J_{CF}$ = 9.4 Hz), 130.7, 129.9, 129.81, 129.76, 124.9, 122.5, 121.5, 117.1 (d, $^4J_{CF}$ = 2.9 Hz), 114.8, 113.7, 112.2 (d, $^2J_{CF}$ = 21.8 Hz), 108.6 (d, $^2J_{CF}$ = 26.7 Hz), 68.1, 65.1, 64.1, 41.7, 39.4, 30.5, 26.6, 26.2, 23.10, 23.08; IR (neat) $\bar{\nu}_{max}$ 3329, 3171, 2955, 2931, 2871, 2369, 2323, 2107, 1672, 1626, 1555, 1503, 1474, 1443, 1387, 1368, 1260, 1223, 1160, 1087, 1049, 1024, 875, 799, 750, 669, 611 cm^{-1}; MS (ESI +ve) *m/z* 588 ([M + H]$^+$, 100%), 610 ([M + Na]$^+$, 9%); HRMS (ESI +ve TOF) calcd for $C_{32}H_{39}N_7O_3F$ 588.3098, found 588.3081 ([M + H]$^+$).

(*R*)-5-Guanidino-2-(4-(((2'-(isopentyloxy)-[1,1'-biphenyl]-2-yl)oxy)methyl)-1*H*-1,2,3-triazol-1-yl)-*N*-phenylpentanamide hydrochloride (77i)

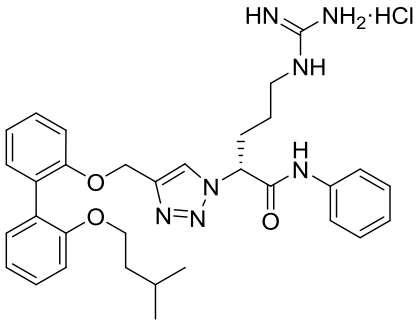

Following **General Procedure B**, acid **75b** (50 mg, 0.07 mmol), aniline (8 mg, 0.08 mmol), EDCI (15 mg, 0.08 mmol) and HOBt (11 mg, 0.07 mmol) were stirred in acetonitrile (0.7 mL) for 24 h to give the intermediate amide as a translucent tan gum. Following **General Procedure C**, the amide was dissolved in CH_2Cl_2 (2.0 mL) and treated with H_2O (24 mg, 1.34 mmol) and CF_3CO_2H (2.0 mL) followed by work-up with ethereal HCl to give the amine

salt **77i** (36 mg, 89% over two steps) as a light tan powder that rapidly transitioned to a sticky gum. $[\alpha]_D^{23}$ +18.3 (*c* 0.83, MeOH); ^{1}H NMR (400 MHz, CD_3OD) δ 7.79 (s, 1H), 7.62 (d, *J* = 7.7 Hz, 2H), 7.38 – 7.09 (m, 8H), 7.04 – 6.89 (m, 3H), 5.48 (dd, *J* = 8.4, 6.8 Hz, 1H), 5.15 – 5.06 (m, 2H), 3.93 – 3.77 (m, 2H), 3.20 (t, *J* = 7.0 Hz, 2H), 2.37 – 2.10 (m, 2H), 1.64 – 1.29 (m, 5H), 0.73 (d, *J* = 6.6 Hz, 6H); ^{13}C NMR (101 MHz, CD_3OD) δ 167.9, 158.8, 158.2, 157.6, 146.5, 139.3, 132.7, 132.5, 130.7, 130.2*, 129.9, 129.82, 129.77, 126.1, 124.0, 122.5, 121.5**, 114.7, 113.7, 68.1, 65.3, 64.2, 41.9, 39.4, 31.1, 26.4, 26.2, 23.1, 23.0; IR (neat) $\overline{\nu}_{max}$ 3346, 3277, 3201, 2954, 2931, 2871, 2370, 2323, 1671, 1625, 1602, 1555, 1501, 1474, 1445, 1386, 1368, 1254, 1215, 1163, 1123, 1109, 1048, 1019, 873, 810, 750, 692 cm^{-1}; MS (ESI +ve) *m/z* 570 ([M + H]$^+$, 100%), 592 ([M + Na]$^+$, 20%); HRMS (ESI +ve TOF) calcd for $C_{32}H_{40}N_7O_3$ 570.3193, found 570.3207 ([M + H]$^+$).

(*R*)-*N*-(3,5-Dimethoxyphenyl)-5-guanidino-2-(4-(((2'-(isopentyloxy)-[1,1'-biphenyl]-2-yl)oxy)methyl)-1*H*-1,2,3-triazol-1-yl)pentanamide hydrochloride (77j)

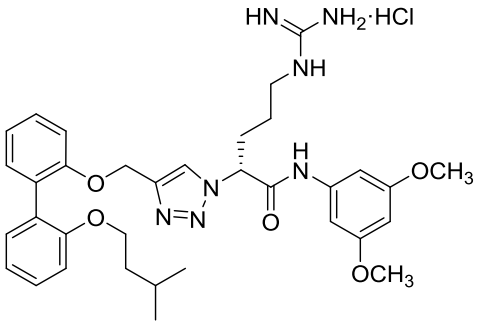

Following **General Procedure B**, acid **75b** (50 mg, 0.07 mmol), 3,5-dimethoxyaniline (12 mg, 0.08 mmol), EDCI (15 mg, 0.08 mmol) and HOBt (11 mg, 0.07 mmol) were stirred in acetonitrile (0.7 mL) for 22 h to give the intermediate amide as a translucent tan gum. Following **General Procedure C**, the amide was dissolved in CH_2Cl_2 (2.0 mL) and treated with H_2O (24 mg, 1.34 mmol) and CF_3CO_2H (2.0 mL) followed by work-up with ethereal HCl to give the amine salt **77j** (36 mg, 81% over two steps) as a light tan powder that rapidly transitioned to a sticky gum. $[\alpha]_D^{23}$ +10.5 (*c* 0.90, MeOH); ^{1}H NMR (400 MHz,

CD_3OD) δ 7.77 (s, 1H), 7.34 – 7.09 (m, 5H), 7.05 – 6.86 (m, 5H), 6.27 (s, 1H), 5.53 – 5.45 (m, 1H), 5.14 – 5.05 (m, 2H), 3.92 – 3.80 (m, 2H), 3.75 (s, 6H), 3.19 (t, *J* = 6.9 Hz, 2H), 2.37 – 2.24 (m, 1H), 2.22 – 2.09 (m, 1H), 1.62 – 1.29 (m, 5H), 0.73 (d, *J* = 6.6 Hz, 6H); ^{13}C NMR (101 MHz, CD_3OD) δ 168.0, 162.7*, 158.8, 158.2, 157.6, 146.4, 141.0, 132.6, 132.5, 130.7, 129.9, 129.79, 129.77, 124.1, 122.5, 121.5, 114.7, 113.7, 99.8*, 98.0, 68.1, 65.3, 64.2, 56.0, 41.8, 39.4, 31.0, 26.3, 26.2, 23.1, 23.0; IR (neat) $\bar{\nu}_{max}$ 3345, 3278, 3199, 2955, 2931, 2870, 2370, 2323, 1672, 1619, 1595, 1555, 1502, 1446, 1386, 1260, 1205, 1154, 1110, 1049, 1019, 844, 750, 669 cm^{-1}; MS (ESI +ve) *m/z* 630 ([M + H]$^+$, 100%), 652 ([M + Na]$^+$, 34%); HRMS (ESI +ve TOF) calcd for $C_{34}H_{44}N_7O_5$ 630.3404, found 630.3404 ([M + H]$^+$).

(*R*)-*N*-Cyclopropyl-5-guanidino-2-(4-(((2'-(isopentyloxy)-[1,1'-biphenyl]-2-yl)oxy)methyl)-1*H*-1,2,3-triazol-1-yl)pentanamide hydrochloride (77k)

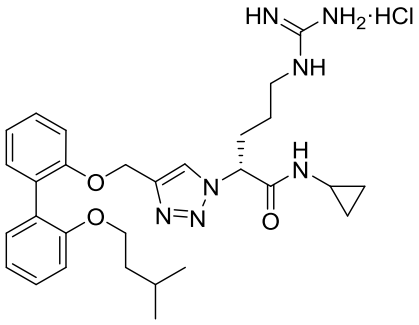

Following **General Procedure B**, acid **75b** (50 mg, 0.07 mmol), cyclopropylamine (5 mg, 0.08 mmol), EDCI (15 mg, 0.08 mmol) and HOBt (11 mg, 0.07 mmol) were stirred in acetonitrile (0.7 mL) for 23 h to give the intermediate amide as a translucent tan gum. Following **General Procedure C**, the amide was dissolved in CH_2Cl_2 (2.0 mL) and treated with H_2O (24 mg, 1.34 mmol) and CF_3CO_2H (2.0 mL) followed by work-up with ethereal HCl to give the amine salt **77k** (34 mg, 89% over two steps) as a light tan powder that rapidly transitioned to a sticky gum. $[\alpha]_D^{23}$ +5.1 (*c* 0.80, MeOH); ^{1}H NMR (400 MHz, CD_3OD) δ 7.77 (s, 1H), 7.36 – 7.25 (m, 2H), 7.23 – 7.10 (m, 3H), 7.04 – 6.99 (m, 2H), 6.96 (td, *J* = 7.4, 0.9 Hz, 1H), 5.20 (dd, *J* = 8.5, 6.9 Hz, 1H), 5.14 – 5.05 (m, 2H), 3.96 – 3.84 (m, 2H), 3.17 (t, *J* = 7.0 Hz,

2H), 2.73 – 2.65 (m, 1H), 2.22 – 2.01 (m, 2H), 1.61 – 1.31 (m, 5H), 0.82 – 0.65 (m, 8H), 0.57 – 0.45 (m, 2H); ^{13}C NMR (101 MHz, CD_3OD) δ 171.1, 158.8, 158.2, 157.5, 146.2, 132.8, 132.5, 130.7, 129.9, 129.83, 129.76, 124.0, 122.5, 121.5, 114.7, 113.7, 68.2, 64.6, 64.0, 41.8, 39.4, 31.0, 26.3, 26.2, 23.8, 23.09, 23.07, 6.7, 6.6; IR (neat) $\overline{\nu}_{max}$ 3344, 3278, 3200, 2955, 2931, 2871, 2369, 2323, 1666, 1626, 1594, 1555, 1503, 1474, 1440, 1387, 1367, 1253, 1212, 1163, 1123, 1109, 1049, 1004, 854, 750, 668 cm^{-1}; MS (ESI +ve) *m/z* 534 ([M + H]$^+$, 100%), 556 ([M + Na]$^+$, 41%); HRMS (ESI +ve TOF) calcd for $C_{29}H_{40}N_7O_3$ 534.3193, found 534.3204 ([M + H]$^+$).

(*R*)-*N*-(Cyclopropylmethyl)-5-guanidino-2-(4-(((2'-(isopentyloxy)-[1,1'-biphenyl]-2-yl)oxy)methyl)-1*H*-1,2,3-triazol-1-yl)-*N*-propylpentanamide hydrochloride (77l)

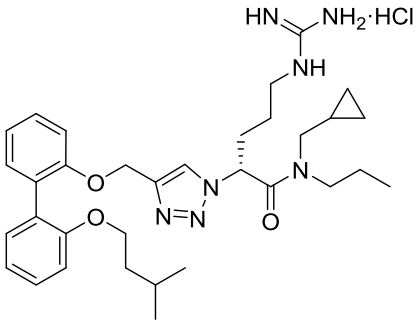

Following **General Procedure B**, acid **75b** (50 mg, 0.07 mmol), *N*-propyl-cyclopropylmethylamine (9 mg, 0.08 mmol), EDCI (15 mg, 0.08 mmol) and HOBt (11 mg, 0.07 mmol) were stirred in acetonitrile (0.7 mL) for 24 h to give the intermediate amide as a translucent tan gum. Following **General Procedure C**, the amide was dissolved in CH_2Cl_2 (2.0 mL) and treated with H_2O (24 mg, 1.34 mmol) and CF_3CO_2H (2.0 mL) followed by work-up with ethereal HCl to give the amine salt **77l** (36 mg, 86% over two steps) as a light tan powder that rapidly transitioned to a sticky gum. $[\alpha]_D^{23}$ +5.2 (*c* 0.70, MeOH); ^{1}H NMR (400 MHz, CD_3OD) : (mixture of rotamers) ‡ δ 7.74 (s, 1H), 7.34 – 7.25 (m, 2H), 7.21 – 7.10 (m, 3H), 7.05 – 6.91

‡ All rotamer resonances are reported.

(m, 3H), 5.86 – 5.73 (m, 1H), 5.18 – 5.02 (m, 2H), 3.98 – 3.83 (m, 2H), 3.54 – 3.24 (m, 4H), 3.23 – 3.11 (m, 2H), 2.22 – 1.99 (m, 2H), 1.66 – 1.28 (m, 7H), 1.06 – 0.93 (m, 1H), 0.92 – 0.80 (m, 3H), 0.78 (d, J = 6.6 Hz, 6H), 0.59 – 0.39 (m, 2H), 0.35 – 0.13 (m, 2H); ^{13}C NMR (101 MHz, CD_3OD) : (mixture of rotamers)‡ δ 169.2, 168.8, 158.8, 158.2, 157.49, 157.45, 146.6, 146.5, 132.8, 132.5, 130.6, 129.88, 129.86, 129.7, 123.74, 123.66, 122.5, 121.5, 114.6, 113.7, 68.2, 64.0, 63.9, 60.9, 53.7, 51.9, 51.0, 49.9, 42.0, 39.4, 31.6, 31.5, 26.3, 26.1, 23.6, 23.10, 23.07, 21.7, 11.8, 11.6, 11.5, 10.6, 5.1, 4.4, 4.2, 4.0; IR (neat) $\overline{\nu}_{max}$ 3345, 3189, 2955, 2931, 2871, 2370, 2323, 1650, 1594, 1503, 1474, 1438, 1385, 1367, 1254, 1214, 1162, 1122, 1109, 1047, 1020, 934, 855, 801, 749, 669 cm^{-1}; MS (ESI +ve) *m/z* 590 ([M + H]$^+$, 100%), 612 ([M + Na]$^+$, 16%); HRMS (ESI +ve TOF) calcd for $C_{33}H_{48}N_7O_3$ 590.3819, found 590.3834 ([M + H]$^+$).

(*R*)-6-((*Tert*-butoxycarbonyl)amino)-2-(4-((((*S*)-2'-(isopentyloxy)-[1,1'-binaphthalen]-2-yl)oxy)methyl)-1*H*-1,2,3-triazol-1-yl)hexanoic acid (75c)

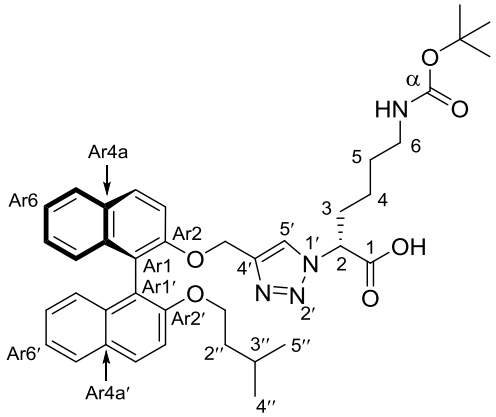

Following **General Procedure A**, azide **24** (253 mg, 0.93 mmol), alkyne **20** (733 mg, 1.86 mmol), $Cu(OAc)_2{\cdot}H_2O$ (37 mg, 0.19 mmol) and sodium ascorbate (74 mg, 0.37 mmol) were stirred in *t*-BuOH (18.6 mL) and H_2O (4.7 mL) at 40 °C for 72 h to give the product triazole **75c** (386 mg, 64%) as a translucent tan gum after flash chromatography over SiO_2 gel (EtOAc/P.S. – 10:90 →

‡ All rotamer resonances are reported.

50:50). TLC (EtOAc/P.S. – 40:60): R_f = 0.50; $[\alpha]_D^{23}$ −11.3 (*c* 0.76, MeOH); ^{1}H NMR (400 MHz, DMSO) δ 8.04 (app. t, *J* = 8.6 Hz, 2H, ArH), 7.93 (app. t, *J* = 8.0 Hz, 2H, ArH), 7.74 (d, *J* = 9.0 Hz, 1H, ArH), 7.57 (d, *J* = 9.0 Hz, 1H, ArH), 7.47 – 7.37 (br s, 1H, H5'), 7.37 – 7.26 (m, 2H, ArH), 7.26 – 7.13 (m, 2H, ArH), 7.00 – 6.89 (m, 2H, ArH), 6.74 (br s, 1H, N^6-H), 5.22 – 5.06 (m, 3H, H2 and -OCH_2-C4'), 4.05 – 3.90 (m, 2H, H1"), 2.87 – 2.74 (m, 2H, H6), 2.04 (br s, 1H, $H3_A$ or $H3_B$), 1.91 (br s, 1H, $H3_B$ or $H3_A$), 1.39 – 1.13 (m, 14H, H5, H2", H3" and -$C(CH_3)_3$), 1.08 (br s, 1H, $H4_A$ or $H4_B$), 0.86 (br s, 1H, $H4_B$ or $H4_A$), 0.57 (d, *J* = 6.3 Hz, 3H, H4" or H5"), 0.55 (d, *J* = 6.2 Hz, 3H, H5" or H4"); ^{13}C NMR (101 MHz, DMSO)† δ 155.5 (Cα), 154.1 (CAr2'), 153.7 (CAr2), 143.5 (C4' – observed by gHMBC), 133.4 (CAr8a or CAr8a'), 133.3 (CAr8a' or CAr8a), 129.2 (CAr4), 129.1 (CAr4'), 129.0 (CAr4a), 128.7 (CAr4a'), 127.9 (CAr5 and CAr5'), 126.2 (CAr7), 126.1 (CAr7'), 124.7 (CAr8), 124.5 (CAr8'), 123.5 (CAr6), 123.3 (CAr6'), 123.0 (C5'), 119.8 (CAr1), 119.1 (CAr1'), 116.2 (CAr3), 115.6 (CAr3'), 77.3 (-$\underline{C}(CH_3)_3$), 67.2 (C1"), 63.0 (-$O\underline{C}H_2$-C4'), 39.4 (C6), 37.6 (C2"), 31.0 (C3), 28.7 (C5), 28.2 (-$C(\underline{C}H_3)_3$), 24.1 (C3"), 22.6 (C4), 22.2 (C4" or C5"), 22.1 (C5" or C4"); IR (neat) $\bar{\nu}_{max}$ 3342, 3061, 2954, 2932, 2869, 2366, 2345, 1734, 1718, 1700, 1684, 1653, 1623, 1591, 1559, 1540, 1507, 1458, 1430, 1395, 1366, 1329, 1263, 1243, 1165, 1147, 1083, 1046, 1015, 915, 862, 809, 747, 668, 610 cm^{-1}; MS (ESI −ve) *m/z* 665 ($[M - H]^-$, 100%); HRMS (ESI −ve TOF) calcd for $C_{39}H_{45}N_4O_6$ 665.3339, found 665.3353 ($[M - H]^-$).

† Missing resonances: two carbons (the carboxyl carbon (C1) and the adjacent methine carbon (C2)) could not be assigned to resonances in the ^{13}C NMR spectrum; the corresponding methine proton (H2) was assigned to a very broad signal in the ^{1}H NMR spectrum (by gCOSY correlation with H3). This ^{1}H NMR signal showed no heterocorrelations in 2-D NMR (i.e. gHSQC and gHMBC).

(*R*)-2-(4-((((*S*)-2'-(Isopentyloxy)-[1,1'-binaphthalen]-2-yl)oxy)methyl)-1*H*-1,2,3-triazol-1-yl)-5-(2-((2,2,4,6,7-pentamethyl-2,3-dihydrobenzofuran-5-yl)sulfonyl)guanidino)pentanoic acid (75d)

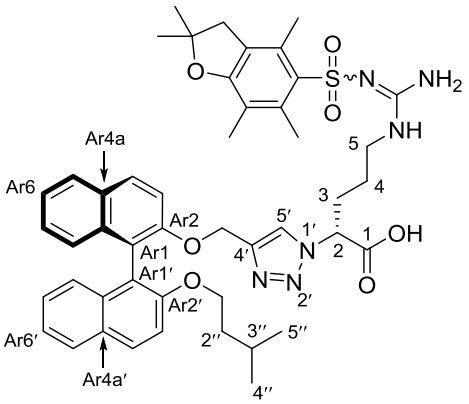

Following **General Procedure A**, azide **28** (152 mg, 0.34 mmol), alkyne **20** (265 mg, 0.67 mmol), $Cu(OAc)_2 \cdot H_2O$ (13 mg, 0.07 mmol) and sodium ascorbate (27 mg, 0.13 mmol) were stirred in *t*-BuOH (6.7 mL) and H_2O (1.7 mL) for 24 h to give the product triazole **75d** (236 mg, 83%) as a translucent tan gum after flash chromatography over SiO_2 gel (EtOAc/P.S. – 10:90 → MeOH/CH_2Cl_2 – 10:90). TLC (EtOAc/P.S. – 80:20): R_f = 0.34; $[\alpha]_D^{23}$ −25.8 (*c* 0.43, MeOH); ^{1}H NMR (400 MHz, DMSO) δ 8.03 (d, *J* = 9.0 Hz, 1H, ArH), 7.98 – 7.88 (m, 2H, ArH), 7.84 (d, *J* = 8.0 Hz, 1H, ArH), 7.73 (d, *J* = 9.1 Hz, 1H, ArH), 7.54 (br s, 1H, N^5-H), 7.52 (d, *J* = 9.0 Hz, 1H, ArH), 7.39 (br s, 1H, H5'), 7.32 (t, *J* = 7.0 Hz, 1H, ArH), 7.28 – 7.18 (m, 2H, ArH), 7.14 (t, *J* = 7.4 Hz, 1H, ArH), 6.94 (d, *J* = 8.5 Hz, 1H, ArH), 6.90 (d, *J* = 8.4 Hz, 1H, ArH), 6.82 (br s, 2H, -NH_2), 5.13 and 5.06 (ABq, *J* = 12.4 Hz, 2H, -OCH_2-C4'), 4.81 (br s, 1H, H2), 4.05 – 3.88 (m, 2H, H1''), 2.96 (br s, 2H, H5), 2.92 (s, 2H, $ArCH_2$-), 2.48 (s, 3H, $ArCH_3$), 2.42 (s, 3H, $ArCH_3$), 2.08 (br s, 1H, $H3_A$ or $H3_B$), 1.98 (s, 3H, $ArCH_3$), 1.73 (br s, 1H, $H3_B$ or $H3_A$), 1.36 (s, 6H, -$C(CH_3)_2$), 1.29 – 0.87 (m, 5H, H4, H2'', H3''), 0.56 (d, *J* = 6.2 Hz, 3H, H4'' or H5''), 0.54 (d, *J* = 6.2 Hz, 3H, H5'' or H4''); ^{13}C NMR (101 MHz, DMSO)† δ 157.4 (Pbf C_{Ar}), 156.3 (C=N), 154.1 (CAr2'), 153.8 (CAr2),

† Missing resonances: two carbons (the carboxyl carbon (C1) and the adjacent methine carbon (C2)) could not be assigned to resonances in the ^{13}C NMR spectrum; the corresponding methine proton (H2) was assigned to a

142.7 (C4'), 137.2 (Pbf C_{Ar}), 134.3 (Pbf C_{Ar}), 133.4 (CAr8a or CAr8a'), 133.3 (CAr8a' or CAr8a), 131.3 (Pbf C_{Ar}), 129.2 (CAr4), 129.1 (CAr4'), 129.0 (CAr4a), 128.6 (CAr4a'), 127.9 (CAr5 and CAr5'), 126.1 (CAr7), 126.0 (CAr7'), 124.7 (CAr8), 124.5 (CAr8'), 124.3 (Pbf C_{Ar}), 123.4 (CAr6), 123.2 (CAr6'), 122.7 (C5'), 119.8 (CAr1), 119.1 (CAr1'), 116.23 (Pbf C_{Ar}), 116.20 (CAr3), 115.5 (CAr3'), 86.2 (-$\underline{C}(CH_3)_2$), 67.2 (C1''), 63.2 (-O$\underline{C}H_2$-C4'), 42.4 ($ArCH_2$-), 39.6 (C5 – observed by gHSQC), 37.6 (C2''), 30.0 (C3), 28.2 (-C($\underline{C}H_3)_2$), 25.8 (C4), 24.1 (C3''), 22.2 (C4'' or C5''), 22.1 (C5'' or C4''), 18.9 ($ArCH_3$), 17.6 ($ArCH_3$), 12.2 ($ArCH_3$); IR (neat) $\overline{\nu}_{max}$ 2961, 2932, 2873, 2362, 2342, 1734, 1700, 1684, 1653, 1623, 1559, 1540, 1507, 1473, 1457, 1437, 1419, 1399, 1260, 1243, 1147, 1109, 1087, 1059, 1016, 907, 852, 808, 784, 746, 734, 668, 641 cm^{-1}; MS (ESI −ve) *m/z* 845 ($[M - H]^-$, 100%); HRMS (ESI −ve TOF) calcd for $C_{47}H_{53}N_6O_7S$ 845.3696, found 845.3710 ($[M - H]^-$).

(*R*)-*N*-Benzyl-5-guanidino-2-(4-((((*S*)-2'-(isopentyloxy)-[1,1'-binaphthalen]-2-yl)oxy)methyl)-1*H*-1,2,3-triazol-1-yl)pentanamide hydrochloride (78a)

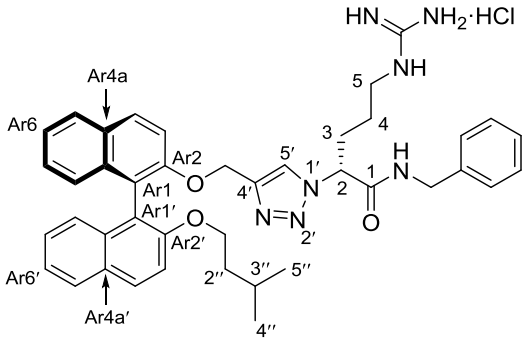

Following **General Procedure B**, acid **75d** (50 mg, 0.06 mmol), benzylamine (8 mg, 0.07 mmol), EDCI (14 mg, 0.07 mmol) and HOBt (10 mg, 0.06 mmol) were stirred in acetonitrile (0.6 mL) for 21 h to give the intermediate amide as a translucent tan gum. Following **General Procedure C**, the amide was dissolved in CH_2Cl_2 (1.8 mL) and treated with H_2O (21 mg, 1.18 mmol) and CF_3CO_2H (1.8 mL) followed by

very broad signal in the ^1H NMR spectrum (by gCOSY correlation with H3). This ^1H NMR signal showed no heterocorrelations in 2-D NMR (i.e. gHSQC and gHMBC).

work-up with ethereal HCl to give the amine salt **78a** (37 mg, 87% over two steps) as a light tan powder that rapidly transitioned to a sticky gum. $[\alpha]_D^{23}$ −15.0 (*c* 0.90, MeOH); ^{1}H NMR (400 MHz, CD_3OD) δ 8.02 – 7.96 (m, 2H, ArH), 7.91 – 7.85 (m, 2H, ArH), 7.58 (d, *J* = 9.0 Hz, 1H, ArH), 7.51 (d, *J* = 9.0 Hz, 1H, ArH), 7.36 – 7.11 (m, 10H, ArH and H5'), 7.08 (d, *J* = 8.6 Hz, 1H, ArH), 7.02 (d, *J* = 8.6 Hz, 1H, ArH), 5.20 (dd, *J* = 8.7, 6.7 Hz, 1H, H2), 5.14 and 5.09 (ABq, *J* = 12.4 Hz, 2H, -OCH_2-C4'), 4.35 (s, 2H, -C$\underline{H}_2$Ph), 4.02 (dt, *J* = 9.6, 6.0 Hz, 1H, H1"$_A$ or H1"$_B$), 3.91 (dt, *J* = 9.6, 6.3 Hz, 1H, H1"$_B$ or H1"$_A$), 3.17 – 3.04 (m, 2H, H5), 2.18 – 2.05 (m, 1H, H3$_A$ or H3$_B$), 2.02 – 1.84 (m, 1H, H3$_B$ or H3$_A$), 1.49 – 1.11 (m, 5H, H4, H2", H3"), 0.55 (d, *J* = 6.4 Hz, 3H, H4" or H5"), 0.52 (d, *J* = 6.3 Hz, 3H, H5" or H4"); ^{13}C NMR (101 MHz, CD_3OD) δ 169.6 (C1), 158.7 (C=N), 156.1 (CAr2'), 155.5 (CAr2), 146.3 (C4' – observed by gHMBC), 139.5 (Phenyl C_{Ar}), 135.6 (CAr8a or CAr8a'), 135.5 (CAr8a' or CAr8a), 131.6 (CAr4a), 130.9 (CAr4a'), 130.8 (CAr4), 130.7 (CAr4'), 129.8 (Phenyl C_{Ar})*, 129.3 (CAr5 or CAr5'), 129.2 (CAr5' or CAr5), 128.8 (Phenyl C_{Ar})*, 128.6 (Phenyl C_{Ar}), 127.5 (CAr7 or CAr7'), 127.4 (CAr7' or CAr7), 126.7 (CAr8), 126.4 (CAr8'), 125.2 (CAr6), 124.8 (CAr6'), 124.0 (C5'), 122.9 (CAr1), 121.4 (CAr1'), 117.7 (CAr3), 117.0 (CAr3'), 69.2 (C1"), 65.1 (-O$\underline{C}H_2$-C4'), 64.7 (C2), 44.5 (-$\underline{C}H_2$Ph), 41.8 (C5), 39.5 (C2"), 30.8 (C3), 26.2 (C4), 25.8 (C3"), 23.0 (C4" or C5"), 22.8 (C5" or C4"); IR (neat) $\bar{\nu}_{max}$ 3335, 3190, 3059, 2959, 2931, 2875, 2364, 2325, 1734, 1700, 1684, 1669, 1653, 1636, 1623, 1590, 1559, 1540, 1507, 1473, 1457, 1437, 1419, 1399, 1340, 1261, 1241, 1212, 1147, 1083, 1040, 1007, 908, 861, 808, 775, 745, 699, 668, 601 cm^{-1}; MS (ESI +ve) *m/z* 684 ($[M + H]^+$, 100%), 706 ($[M + Na]^+$, 8%); HRMS (ESI +ve TOF) calcd for $C_{41}H_{46}N_7O_3$ 684.3662, found 684.3669 ($[M + H]^+$).

(*R*)-5-Guanidino-2-(4-((((*S*)-2'-(isopentyloxy)-[1,1'-binaphthalen]-2-yl)oxy)methyl)-1*H*-1,2,3-triazol-1-yl)-*N*-phenethylpentanamide hydrochloride (78b)

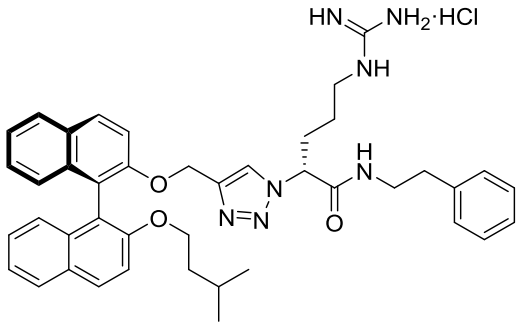

Following **General Procedure B**, acid **75d** (50 mg, 0.06 mmol), β-phenylethylamine (9 mg, 0.07 mmol), EDCI (14 mg, 0.07 mmol) and HOBt (10 mg, 0.06 mmol) were stirred in acetonitrile (0.6 mL) for 21 h to give the intermediate amide as a translucent tan gum. Following **General Procedure C**, the amide was dissolved in CH_2Cl_2 (1.8 mL) and treated with H_2O (21 mg, 1.18 mmol) and CF_3CO_2H (1.8 mL) followed by work-up with ethereal HCl to give the amine salt **78b** (21 mg, 49% over two steps) as a light tan powder that rapidly transitioned to a sticky gum. $[\alpha]_D^{23}$ −20.3 (*c* 0.33, MeOH); ^{1}H NMR (400 MHz, CD_3OD) δ 8.01 (s, 1H), 7.99 (s, 1H), 7.92 – 7.85 (m, 2H), 7.60 (d, *J* = 9.0 Hz, 1H), 7.52 (d, *J* = 9.1 Hz, 1H), 7.37 – 7.00 (m, 12H), 5.16 – 5.06 (m, 3H), 4.07 – 3.98 (m, 1H), 3.96 – 3.88 (m, 1H), 3.49 – 3.34 (m, 2H), 3.08 (t, *J* = 7.1 Hz, 2H), 2.75 (t, *J* = 7.1 Hz, 2H), 2.09 – 1.98 (m, 1H), 1.91 – 1.79 (m, 1H), 1.36 – 1.12 (m, 5H), 0.56 (d, *J* = 6.4 Hz, 3H), 0.52 (d, *J* = 6.3 Hz, 3H); ^{13}C NMR (101 MHz, CD_3OD) δ 169.6, 158.8, 156.2, 155.5, 146.4 (observed by gHMBC), 140.3, 135.61, 135.57, 131.6, 130.9, 130.8, 130.7, 130.0*, 129.7*, 129.3, 129.2, 127.6, 127.5, 127.4, 126.7, 126.4, 125.2, 124.8, 123.9, 122.9, 121.5, 117.7, 117.0, 69.2, 65.2, 64.6, 42.2, 41.8, 39.5, 36.3, 30.7, 26.1, 25.9, 23.0, 22.8; IR (neat) $\overline{\nu}_{max}$ 3335, 3189, 3061, 2960, 2932, 2874, 2364, 2325, 1734, 1700, 1684, 1669, 1653, 1636, 1623, 1591, 1559, 1540, 1507, 1473, 1457, 1437, 1419, 1363, 1340, 1261, 1241, 1213, 1147, 1132, 1083, 1045, 1016, 908, 878, 864, 808, 775, 747, 699, 668, 601 cm^{-1}; MS (ESI +ve) *m/z* 698 ([M +

H]$^+$, 100%), 720 ([M + Na]$^+$, 7%); HRMS (ESI +ve TOF) calcd for $C_{42}H_{48}N_7O_3$ 698.3819, found 698.3837 ([M + H]$^+$).

6.3.5 – Series B2

Tert-butyl ((_R_)-6-(((_R_)-1-azido-5-(2-((2,2,4,6,7-pentamethyl-2,3-dihydrobenzofuran-5-yl)sulfonyl)guanidino)pentan-2-yl)amino)-5-(4-(((2'-(isopentyloxy)-[1,1'-biphenyl]-2-yl)oxy)methyl)-1_H_-1,2,3-triazol-1-yl)-6-oxohexyl)carbamate (79a)

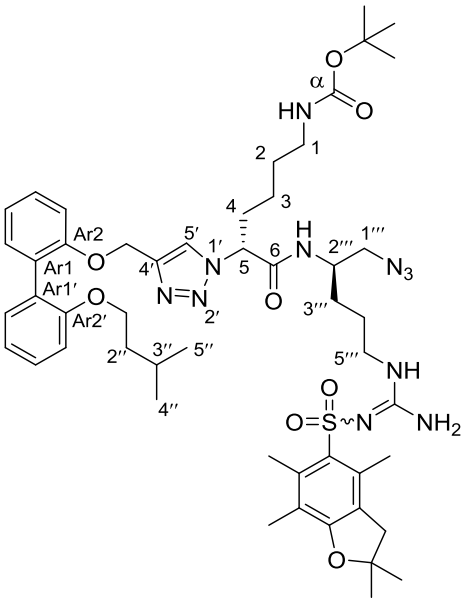

Following **General Procedure B**, acid **75a** (176 mg, 0.31 mmol), amine **25** (143 mg, 0.33 mmol), EDCI (72 mg, 0.37 mmol) and HOBt (50 mg, 0.33 mmol) were stirred in acetonitrile (3.1 mL) for 48 h to give the product amide **79a** (251 mg, 82%) as a translucent tan gum after flash chromatography over SiO_2 gel (EtOAc/P.S. – 60:40 → 80:20). TLC (EtOAc/P.S. – 80:20): R_f = 0.44; $[\alpha]_D^{23}$ −8.0 (*c* 1.23, MeOH); ^{1}H NMR (400 MHz, $CDCl_3$) δ 7.54 (br s, 2H, H5′ and $N^{2'''}$-H), 7.32 – 7.17 (m, 4H, ArH), 7.09 – 6.99 (m, 2H, ArH), 6.99 – 6.90 (m, 2H, ArH), 6.11 (br s, 3H, $N^{5'''}$-H and -NH_2), 5.34 – 5.25 (m, 1H, H5), 5.09 (s, 2H, -OCH_2-C4′), 4.71 (br s, 1H, N^1-H), 3.96 (br s, 1H, H2‴), 3.90 (t, *J* = 6.1 Hz, 2H, H1″), 3.30 (br s, 2H, H1‴), 3.08 – 2.95 (m, 4H, H1 and H5‴), 2.94 (s, 2H, $ArCH_2$-), 2.54 (s, 3H, $ArCH_3$), 2.49 (s, 3H, $ArCH_3$), 2.21 – 2.12 (m, 1H, $H4_A$ or $H4_B$), 2.08 (s, 3H, $ArCH_3$), 2.02 – 1.88 (m, 1H, $H4_B$ or $H4_A$), 1.64 – 1.09 (m, 26H, H2, H3, H2″, H3″, H3‴, H4‴, -$C(CH_3)_2$ and -$C(CH_3)_3$), 0.78 (d, *J* = 6.3 Hz, 6H, H4″ and H5″); ^{13}C NMR (101 MHz, $CDCl_3$) δ 168.5 (C6), 158.9 (Pbf C_{Ar}), 156.6 (CAr2′), 156.3 (CAr2 and C=N), 155.9

(Cα), 145.0 (C4′), 138.4 (Pbf C_{Ar}), 132.9 (Pbf C_{Ar}), 132.3 (Pbf C_{Ar}), 131.8 (CAr6 or CAr6′), 131.6 (CAr6′ or CAr6), 128.9 (CAr1), 128.8 (CAr4), 128.7 (CAr4′), 128.1 (CAr1′), 124.8 (Pbf C_{Ar}), 122.6 (C5′), 121.5 (CAr5), 120.4 (CAr5′), 117.7 (Pbf C_{Ar}), 113.7 (CAr3), 112.6 (CAr3′), 86.6 (-<u>C</u>$(CH_3)_2$), 79.4 (-<u>C</u>$(CH_3)_3$), 67.2 (C1″), 63.8 (C5), 63.5 (-O<u>C</u>H_2-C4′), 54.6 (C1‴), 49.6 (C2‴), 43.4 (ArCH_2-), 40.8 (C1 or C5‴), 40.1 (C5‴ or C1), 38.1 (C2″), 32.3 (C4), 29.3 (C3‴), 29.0 (C2), 28.7 (-C(<u>C</u>$H_3)_2$), 28.5 (-C(<u>C</u>$H_3)_3$), 25.6 (C4‴), 25.1 (C3″), 22.8 (C3), 22.63 (C4″ or C5″), 22.61 (C5″ or C4″), 19.4 (ArCH_3), 18.1 (ArCH_3), 12.6 (ArCH_3); IR (neat) $\overline{\nu}_{max}$ 3443, 3339, 2958, 2926, 2870, 2101, 1700, 1684, 1617, 1559, 1545, 1507, 1457, 1442, 1395, 1368, 1241, 1163, 1106, 1091, 1052, 1028, 905, 853, 808, 784, 751, 734, 668, 659, 640, 620, 615 cm^{-1}; MS (ESI +ve) *m/z* 1009 $([M + Na]^+$, 100%), 987 $([M + H]^+$, 21%); HRMS (ESI +ve TOF) calcd for $C_{50}H_{72}N_{11}O_8S$ 986.5286, found 986.5335 $([M + H]^+$).

(*R*)-6-Amino-*N*-((*R*)-1-(4-benzyl-1*H*-1,2,3-triazol-1-yl)-5-guanidinopentan-2-yl)-2-(4-(((2'-(isopentyloxy)-[1,1'-biphenyl]-2-yl)oxy)methyl)-1*H*-1,2,3-triazol-1-yl)hexanamide dihydrochloride (80a)

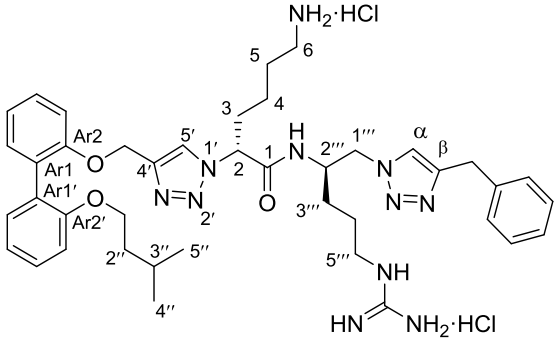

Following **General Procedure A**, azide **79a** (50 mg, 0.05 mmol), 3-phenyl-1-propyne (18 mg, 0.15 mmol), $Cu(OAc)_2 \cdot H_2O$ (2 mg, 0.01 mmol) and sodium ascorbate (4 mg, 0.02 mmol) were stirred in *t*-BuOH (1.0 mL) and H_2O (0.25 mL) for 24 h to give the intermediate triazole

as a light tan gum after flash chromatography over SiO_2 gel ($MeOH/CH_2Cl_2$ – 0:100 → 10:90). Following **General Procedure C**, the triazole was dissolved in CH_2Cl_2 (1.5 mL) and treated with H_2O (18 mg, 1.00 mmol) and CF_3CO_2H (1.5 mL) followed by work-up with ethereal HCl to give the amine salt **80a** (40 mg, 95% over two steps) as a light tan powder that rapidly transitioned to a sticky gum. $[\alpha]_D^{23}$ +6.2 (*c* 1.07, MeOH); ^{1}H NMR (400 MHz, CD_3OD) δ 7.92 (s, 1H, Hα), 7.69 (s, 1H, H5′), 7.36 – 7.09 (m, 10H, ArH), 7.05 – 6.97 (m, 2H, ArH), 6.94 (t, *J* = 7.3 Hz, 1H, ArH), 5.25 (t, *J* = 7.0 Hz, 1H, H2), 5.09 (s, 2H, -OCH_2-C4′), 4.66 – 4.56 (m, 1H, H1‴$_A$ or H1‴$_B$), 4.51 – 4.40 (m, 1H, H1‴$_B$ or H1‴$_A$), 4.32 (br s, 1H, H2‴), 4.14 – 4.02 (m, 2H, -C<u>H</u>$_2$Ph), 3.95 – 3.86 (m, 2H, H1″), 3.12 (br s, 2H, H5‴), 2.83 (br s, 2H, H6), 1.98 – 1.25 (m, 11H, H3, H5, H2″, H3″, H3‴ and H4‴), 1.16 – 0.99 (m, 2H, H4), 0.78 (d, *J* = 6.6 Hz, 6H, H4″ and H5″); ^{13}C NMR (101 MHz, CD_3OD) δ 170.2 (C1), 158.7 (C=N), 158.2 (CAr2′), 157.5 (CAr2), 148.3 (Cβ – observed by gHMBC), 145.9 (C4′ – observed by gHMBC), 140.2 (Phenyl C_{Ar}), 132.9 (CAr6 or CAr6′), 132.6 (CAr6′ or CAr6), 130.5 (CAr1), 129.97 (Phenyl C_{Ar})*, 129.95 (Phenyl C_{Ar})*, 129.9 (CAr4), 129.79 (CAr4′), 129.76 (CAr1′), 127.9 (Phenyl C_{Ar}), 125.7 (Cα), 124.5 (C5′), 122.5 (CAr5), 121.5 (CAr5′), 114.8 (CAr3), 113.8 (CAr3′), 68.2 (C1″), 64.6 (C2), 64.0 (-O<u>C</u>H_2-C4′), 55.2 (C1‴), 51.2 (C2‴), 42.0 (C5‴), 40.5 (C6), 39.4 (C2″), 32.9 (C3), 32.4 (-<u>C</u>H_2Ph), 30.0 (C3‴), 27.7 (C5), 26.3 (C4‴), 26.2 (C3″), 23.6 (C4), 23.11 (C4″ or C5″), 23.10 (C5″ or C4″); IR (neat) $\overline{\nu}_{max}$ 3333, 3166, 3061, 2958, 2934, 2872, 2377, 2324, 1684, 1669, 1653, 1559, 1540, 1507, 1473, 1457, 1437, 1395, 1363, 1340, 1260, 1219, 1162, 1124, 1109, 1049, 1002, 855, 808, 751, 726, 698, 697, 668, 616 cm^{-1}; MS (ESI +ve) *m*/2 376 ($[M + 2H]^{2+}$, 100%), *m/z* 750 ($[M + H]^+$, 27%), 772 ($[M + Na]^+$, 8%); HRMS (ESI +ve TOF) calcd for $C_{41}H_{56}N_{11}O_3$ 750.4568, found 750.4570 ($[M + H]^+$).

(*R*)-6-Amino-*N*-((*R*)-5-guanidino-1-(4-phenethyl-1*H*-1,2,3-triazol-1-yl)pentan-2-yl)-2-(4-(((2'-(isopentyloxy)-[1,1'-biphenyl]-2-yl)oxy)methyl)-1*H*-1,2,3-triazol-1-yl)hexanamide dihydrochloride (80b)

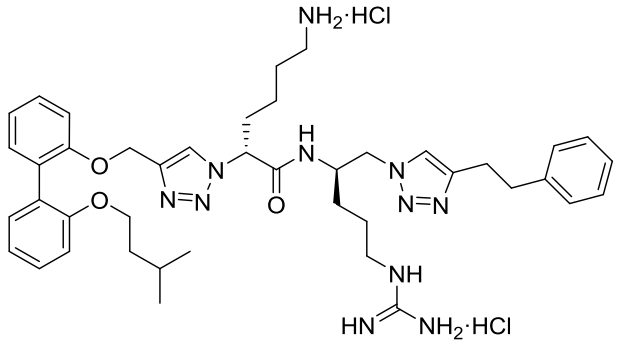

Following **General Procedure A**, azide **79a** (50 mg, 0.05 mmol), 4-phenyl-1-butyne (20 mg, 0.15 mmol), $Cu(OAc)_2 \cdot H_2O$ (2 mg, 0.01 mmol) and sodium ascorbate (4 mg, 0.02 mmol) were stirred in *t*-BuOH (1.0 mL) and H_2O (0.25 mL) for 20 h to give the intermediate triazole as a light tan gum after flash chromatography over SiO_2 gel ($MeOH/CH_2Cl_2$ – 0:100 → 10:90). Following **General Procedure C**, the triazole was dissolved in CH_2Cl_2 (1.5 mL) and treated with H_2O (18 mg, 1.00 mmol) and CF_3CO_2H (1.5 mL) followed by work-up with ethereal HCl to give the amine salt **80b** (36 mg, 85% over two steps) as a light tan powder that rapidly transitioned to a sticky gum. $[\alpha]_D^{23}$ +3.1 (*c* 0.97, MeOH); ^{1}H NMR (400 MHz, CD_3OD) δ 8.07 (s, 1H), 7.79 (s, 1H), 7.35 – 7.07 (m, 10H), 7.05 – 6.96 (m, 2H), 6.93 (t, *J* = 7.4 Hz, 1H), 5.38 – 5.28 (m, 1H), 5.13 – 5.03 (m, 2H), 4.76 – 4.64 (m, 1H), 4.61 – 4.49 (m, 1H), 4.28 (br s, 1H), 3.96 – 3.81 (m, 2H), 3.21 – 3.06 (m, 4H), 3.06 – 2.95 (m, 2H), 2.95 – 2.81 (m, 2H), 2.15 – 1.89 (m, 2H), 1.81 – 1.09 (m, 11H), 0.77 (d, *J* = 6.6 Hz, 6H); ^{13}C NMR (101 MHz, CD_3OD) δ 170.3, 158.7, 158.2, 157.5, 146.1 (observed by gHMBC), 144.2 (observed by gHMBC), 141.7, 132.8, 132.6, 130.5*, 129.9**, 129.8, 129.7*, 127.7, 127.0, 124.7, 122.5, 121.5, 114.8, 113.8, 68.2, 64.7, 64.0, 56.0, 51.3, 42.0, 40.5, 39.4, 36.1, 32.9,

29.7, 27.8, 27.5, 26.4, 26.2, 23.7, 23.1*; IR (neat) $\bar{\nu}_{max}$ 3334, 3165, 3059, 2959, 2934, 2872, 2378, 2324, 1684, 1669, 1653, 1559, 1540, 1507, 1473, 1457, 1437, 1395, 1363, 1340, 1260, 1218, 1162, 1124, 1109, 1048, 1021, 856, 751, 702, 668, 616 cm^{-1}; MS (ESI +ve) *m*/2 383 ($[M + 2H]^{2+}$, 100%), *m/z* 764 ($[M + H]^+$, 24%), 786 ($[M + Na]^+$, 8%); HRMS (ESI +ve TOF) calcd for $C_{42}H_{58}N_{11}O_3$ 764.4724, found 764.4731 ($[M + H]^+$).

(*R*)-6-Amino-*N*-((*R*)-1-(4-cyclohexyl-1*H*-1,2,3-triazol-1-yl)-5-guanidinopentan-2-yl)-2-(4-(((2'-(isopentyloxy)-[1,1'-biphenyl]-2-yl)oxy)methyl)-1*H*-1,2,3-triazol-1-yl)hexanamide dihydrochloride (80c)

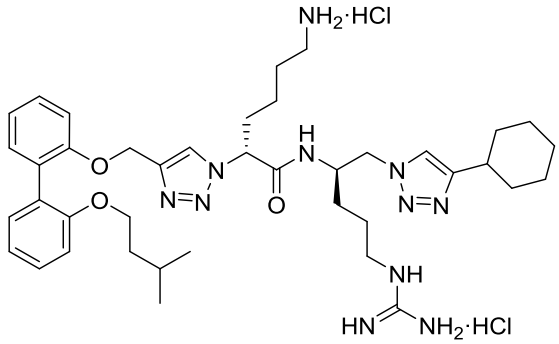

Following **General Procedure A**, azide **79a** (50 mg, 0.05 mmol), cyclohexylacetylene (18 mg, 0.15 mmol), $Cu(OAc)_2 \cdot H_2O$ (2 mg, 0.01 mmol) and sodium ascorbate (4 mg, 0.02 mmol) were stirred in *t*-BuOH (1.0 mL) and H_2O (0.25 mL) for 20 h to give the intermediate triazole as a light tan gum after flash chromatography over SiO_2 gel ($MeOH/CH_2Cl_2$ – 0:100 → 10:90). Following **General Procedure C**, the triazole was dissolved in CH_2Cl_2 (1.5 mL) and treated with H_2O (18 mg, 1.00 mmol) and CF_3CO_2H (1.5 mL) followed by work-up with ethereal HCl to give the amine salt **80c** (39 mg, 94% over two steps) as a light tan powder that rapidly transitioned to a sticky gum. $[\alpha]_D^{23}$ +2.9 (*c* 0.97, MeOH); ^1H NMR (400 MHz, CD_3OD) δ 8.16 (br s, 1H), 7.78 (br s, 1H), 7.36 – 7.23 (m, 2H), 7.22 – 7.09 (m, 3H), 7.05 –

6.90 (m, 3H), 5.31 (br s, 1H), 5.09 (s, 2H), 4.77 – 4.62 (m, 1H), 4.62 – 4.45 (m, 1H), 4.32 (br s, 1H), 3.98 – 3.84 (m, 2H), 3.14 (br s, 2H), 2.90 (br s, 3H), 2.14 – 1.05 (m, 23H), 0.78 (d, *J* = 6.4 Hz, 6H); ^{13}C NMR (101 MHz, CD_3OD) δ 170.3, 158.7, 158.2, 157.5, 152.9 (observed by gHMBC), 146.5 (observed by gHMBC), 132.8, 132.6, 130.5, 129.9, 129.82, 129.77, 126.4, 124.9, 122.5, 121.5, 114.8, 113.8, 68.2, 64.7, 64.0, 56.2, 51.3, 42.1, 40.6, 39.4, 35.8, 33.8*, 33.0, 29.9, 27.9, 27.1*, 27.0, 26.4, 26.2, 23.7, 23.1*; IR (neat) $\overline{\nu}_{max}$ 3338, 3168, 3059, 2953, 2931, 2870, 2371, 2323, 1684, 1669, 1653, 1559, 1540, 1507, 1473, 1457, 1437, 1395, 1363, 1340, 1260, 1218, 1164, 1123, 1108, 1048, 1017, 853, 818, 750, 668, 616 cm^{-1}; MS (ESI +ve) *m*/2 372 ($[M + 2H]^{2+}$, 100%), *m/z* 742 ($[M + H]^+$, 52%), 764 ($[M + Na]^+$, 38%); HRMS (ESI +ve TOF) calcd for $C_{40}H_{60}N_{11}O_3$ 742.4881, found 742.4903 ($[M + H]^+$).

(*R*)-6-Amino-*N*-((*R*)-1-(4-(cyclohexylmethyl)-1*H*-1,2,3-triazol-1-yl)-5-guanidinopentan-2-yl)-2-(4-(((2'-(isopentyloxy)-[1,1'-biphenyl]-2-yl)oxy)methyl)-1*H*-1,2,3-triazol-1-yl)hexanamide dihydrochloride (80d)

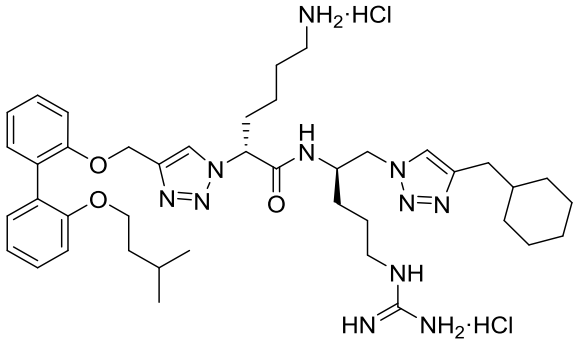

Following **General Procedure A**, azide **79a** (50 mg, 0.05 mmol), 3-cyclohexyl-1-propyne (19 mg, 0.15 mmol), $Cu(OAc)_2{\cdot}H_2O$ (2 mg, 0.01 mmol) and sodium ascorbate (4 mg, 0.02 mmol) were stirred in *t*-BuOH (1.0 mL) and H_2O (0.25 mL) for 20 h to give the intermediate triazole as a light tan gum after flash chromatography over SiO_2 gel ($MeOH/CH_2Cl_2$ – 0:100

→ 10:90). Following **General Procedure C**, the triazole was dissolved in CH_2Cl_2 (1.5 mL) and treated with H_2O (18 mg, 1.00 mmol) and CF_3CO_2H (1.5 mL) followed by work-up with ethereal HCl to give the amine salt **80d** (38 mg, 90% over two steps) as a light tan powder that rapidly transitioned to a sticky gum. $[\alpha]_D^{23}$ +5.2 (*c* 1.00, MeOH); ^{1}H NMR (400 MHz, CD_3OD) δ 8.21 (s, 1H), 7.76 (s, 1H), 7.35 – 7.23 (m, 2H), 7.22 – 7.10 (m, 3H), 7.05 – 6.97 (m, 2H), 6.94 (t, *J* = 7.3 Hz, 1H), 5.37 – 5.27 (m, 1H), 5.11 (s, 2H), 4.79 – 4.68 (m, 1H), 4.61 – 4.50 (m, 1H), 4.29 (br s, 1H), 3.95 – 3.85 (m, 2H), 3.21 – 3.07 (m, 2H), 2.98 – 2.83 (m, 2H), 2.70 (d, *J* = 5.4 Hz, 2H), 2.13 – 1.90 (m, 2H), 1.85 – 0.94 (m, 22H), 0.79 (d, *J* = 6.6 Hz, 6H); ^{13}C NMR (101 MHz, CD_3OD) δ 170.3, 158.7, 158.2, 157.5, 146.2 (observed by gHMBC), 146.0 (observed by gHMBC), 132.9, 132.6, 130.5, 129.9, 129.82, 129.77, 127.5, 124.5, 122.5, 121.5, 114.8, 113.8, 68.2, 64.7, 64.0, 56.5, 51.3, 42.0, 40.6, 39.4, 39.3, 34.02, 33.97, 32.90, 32.87, 29.7, 27.8, 27.5, 27.34, 27.32, 26.4, 26.3, 23.7, 23.1*; IR (neat) $\bar{\nu}_{max}$ 3338, 3169, 3060, 2953, 2925, 2867, 2370, 2323, 1684, 1669, 1653, 1559, 1540, 1507, 1473, 1457, 1437, 1387, 1363, 1340, 1261, 1217, 1162, 1136, 1124, 1109, 1049, 1002, 936, 853, 749, 668, 616 cm^{-1}; MS (ESI +ve) *m*/2 379 ($[M + 2H]^{2+}$, 100%), *m/z* 756 ($[M + H]^+$, 41%), 778 ($[M + Na]^+$, 17%); HRMS (ESI +ve TOF) calcd for $C_{41}H_{62}N_{11}O_3$ 756.5037, found 756.5038 ($[M + H]^+$).

***Tert*-butyl ((*R*)-6-azido-5-((*R*)-2-(4-(((2'-(isopentyloxy)-[1,1'-biphenyl]-2-yl)oxy)methyl)-1*H*-1,2,3-triazol-1-yl)-5-(2-((2,2,4,6,7-pentamethyl-2,3-dihydrobenzofuran-5-yl)sulfonyl)guanidino)pentanamido)hexyl)carbamate (79b)**

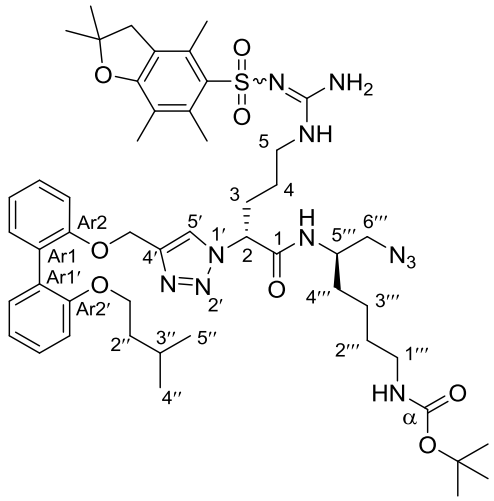

Following **General Procedure B**, acid **75b** (200 mg, 0.27 mmol), amine **22** (69 mg, 0.27 mmol), EDCI (62 mg, 0.32 mmol) and HOBt (43 mg, 0.32 mmol) were stirred in acetonitrile (2.7 mL) for 48 h to give the product amide **79b** (241 mg, 91%) as a translucent tan gum. TLC (EtOAc/P.S. – 60:40): R_f = 0.30, (MeOH/CH_2Cl_2 – 10:90): R_f = 0.38; $[\alpha]_D^{23}$ −9.1 (*c* 1.03, MeOH); ^{1}H NMR (400 MHz, $CDCl_3$) δ 7.89 (br s, 1H, $N^{5'''}$-H), 7.69 (s, 1H, H5′), 7.32 – 7.17 (m, 4H, ArH), 7.10 – 6.97 (m, 2H, ArH), 6.97 – 6.87 (m, 2H, ArH), 6.31 (br s, 2H, -NH_2), 6.03 (br s, 1H, N^5-H), 5.65 (br s, 1H, H2), 5.12 and 5.08 (ABq, *J* = 12.3 Hz, 2H), 4.66 (br s, 1H, $N^{1'''}$-H), 4.04 – 3.93 (m, 1H, H5″), 3.93 – 3.84 (m, 2H, H1″), 3.46 – 3.27 (m, 3H, $H5_A$ or $H5_B$ and H6‴), 3.03 – 2.90 (m, 5H, $H5_B$ or $H5_A$, H1‴ and $ArCH_2$-), 2.60 (s, 3H, $ArCH_3$), 2.52 (s, 3H, $ArCH_3$), 2.21 – 1.98 (m, 5H, H3 and $ArCH_3$), 1.63 – 1.02 (m, 26H, H4, H2″, H3″, H2‴, H3‴, H4‴, -$C(CH_3)_2$ and –$C(CH_3)_3$), 0.78 (d, *J* = 6.6 Hz, 6H, H4″ and H5″); ^{13}C NMR (101 MHz, $CDCl_3$) δ 168.7 (C1), 159.0 (Pbf C_{Ar}), 156.7 (C=N), 156.6 (CAr2′), 156.2 (Cα), 156.0 (CAr2), 145.0 (C4′), 138.5 (Pbf C_{Ar}), 132.7 (Pbf C_{Ar}), 132.4 (Pbf C_{Ar}), 131.8 (CAr6 or CAr6′), 131.6 (CAr6′ or CAr6), 128.9 (CAr1), 128.7 (CAr4), 128.6 (CAr4′), 128.0 (CAr1′), 124.9 (Pbf C_{Ar}), 122.7 (C5′), 121.4 (CAr5), 120.2 (CAr5′), 117.8 (Pbf C_{Ar}), 113.8 (CAr3), 112.5 (CAr3′), 86.6 (-C(CH$_3$)$_2$), 79.2 (-C(CH$_3$)$_3$), 67.1 (C1″), 63.6 (-OCH_2-C4′), 62.7 (C2), 54.4 (C6‴), 50.0 (C5‴), 43.4 ($ArCH_2$-), 40.3 (C1‴), 38.8 (C5), 38.0

(C2″), 31.4 (C4‴), 29.8 (C3), 29.7 (C2‴), 28.7 (-C(<u>C</u>H$_3$)$_2$), 28.5 (-C(<u>C</u>H$_3$)$_3$), 25.6 (C4), 25.1 (C3″), 23.1 (C3‴), 22.63 (C4″ or C5″), 22.61 (C5″ or C4″), 19.5 (ArCH$_3$), 18.2 (ArCH$_3$), 12.6 (ArCH$_3$); IR (neat) $\overline{\nu}_{max}$ 3338, 2956, 2932, 2873, 2356, 2323, 2100, 1718, 1700, 1684, 1653, 1636, 1617, 1559, 1540, 1507, 1457, 1441, 1419, 1395, 1363, 1340, 1250, 1163, 1107, 1091, 1051, 1005, 933, 853, 806, 782, 752, 733, 668, 642, 621 cm^{-1}; MS (ESI +ve) *m/z* 1009 ([M + Na]$^+$, 100%), 987 ([M + H]$^+$, 8%); HRMS (ESI +ve TOF) calcd for $C_{50}H_{72}N_{11}O_8S$ 986.5286, found 986.5322 ([M + H]$^+$).

(*R*)-*N*-((*R*)-6-Amino-1-(4-benzyl-1*H*-1,2,3-triazol-1-yl)hexan-2-yl)-5-guanidino-2-(4-(((2'-(isopentyloxy)-[1,1'-biphenyl]-2-yl)oxy)methyl)-1*H*-1,2,3-triazol-1-yl)pentanamide dihydrochloride (81a)

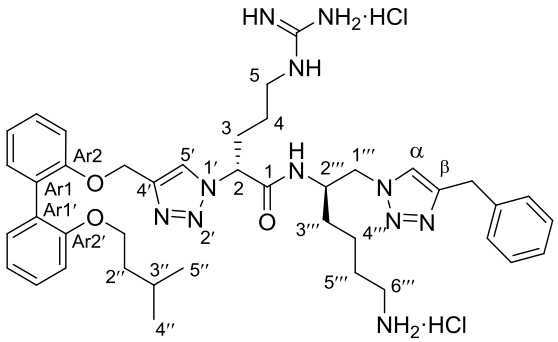

Following **General Procedure A**, azide **79b** (50 mg, 0.05 mmol), 3-phenyl-1-propyne (18 mg, 0.15 mmol), Cu(OAc)$_2$·H$_2$O (2 mg, 0.01 mmol) and sodium ascorbate (4 mg, 0.02 mmol) were stirred in *t*-BuOH (1.0 mL) and H$_2$O (0.25 mL) for 24 h to give the intermediate triazole as a light tan gum after flash chromatography over SiO$_2$ gel (MeOH/CH$_2$Cl$_2$ – 0:100 → 10:90). Following **General Procedure C**, the triazole was dissolved in CH$_2$Cl$_2$ (1.5 mL) and treated with H$_2$O (18 mg, 1.00 mmol) and CF$_3$CO$_2$H (1.5 mL) followed by work-up with ethereal HCl to give the amine salt **81a** (35 mg, 84% over two steps) as a light tan powder

that rapidly transitioned to a sticky gum. $[\alpha]_D^{23}$ +5.1 (*c* 1.00, MeOH); ^{1}H NMR (400 MHz, CD_3OD) δ 7.94 (s, 1H, Hα), 7.70 (s, 1H, H5′), 7.36 – 7.10 (m, 10H, ArH), 7.05 – 6.98 (m, 2H, ArH), 6.95 (t, *J* = 7.1 Hz, 1H, ArH), 5.26 (dd, *J* = 8.9, 6.2 Hz, 1H, H2), 5.09 (s, 2H, -OCH_2-C4′), 4.62 (dd, *J* = 13.8, 3.6 Hz, 1H, H1‴$_A$ or H1‴$_B$), 4.45 (dd, *J* = 13.7, 9.5 Hz, 1H, H1‴$_B$ or H1‴$_A$), 4.35 – 4.23 (m, 1H, H2‴), 4.14 – 4.02 (m, 2H, -C$\underline{H}_2$Ph), 3.96 – 3.85 (m, 2H, H1″), 3.06 (t, *J* = 6.8 Hz, 2H, H5), 2.83 (t, *J* = 7.0 Hz, 2H, H6‴), 2.04 – 1.91 (m, 1H, H3$_A$ or H3$_B$), 1.84 – 1.14 (m, 12H, H3$_B$ or H3$_A$, H4, H2″, H3″, H3‴, H4‴, H5‴), 0.78 (d, *J* = 6.6 Hz, 6H, H4″ and H5″); ^{13}C NMR (101 MHz, CD_3OD) δ 170.0 (C1), 158.7 (C=N), 158.2 (CAr2′), 157.6 (CAr2), 148.2 (Cβ – observed by gHMBC), 146.0 (C4′ – observed by gHMBC), 140.0 (Phenyl C_{Ar}), 132.9 (CAr6 or CAr6′), 132.6 (CAr6′ or CAr6), 130.5 (CAr1), 129.98 (Phenyl C_{Ar})*, 129.96 (Phenyl C_{Ar})*, 129.9 (CAr4), 129.8 (CAr1′), 129.8 (CAr4′), 128.0 (Phenyl C_{Ar}), 125.8 (Cα), 124.4 (C5′), 122.5 (CAr5), 121.5 (CAr5′), 114.8 (CAr3), 113.8 (CAr3′), 68.2 (C1″), 64.4 (C2), 64.0 (-O$\underline{C}H_2$-C4′), 55.2 (C1‴), 51.4 (C2‴), 41.6 (C5), 40.6 (C6‴), 39.4 (C2″), 32.3 (-$\underline{C}H_2$Ph), 32.2 (C3‴), 30.6 (C3), 28.2 (C5‴), 26.3 (C3″), 26.0 (C4), 23.8 (C4‴), 23.1 (C4″ and C5″); IR (neat) $\bar{\nu}_{max}$ 3338, 3186, 3064, 2953, 2935, 2870, 2358, 2323, 1734, 1718, 1700, 1684, 1653, 1636, 1617, 1595, 1559, 1540, 1507, 1473, 1457, 1437, 1419, 1395, 1363, 1340, 1219, 1162, 1108, 1091, 1050, 1021, 937, 853, 751, 721, 697, 669, 620 cm^{-1}; MS (ESI +ve) *m*/2 376 ($[M + 2H]^{2+}$, 100%), *m/z* 750 ($[M + H]^+$, 18%), 772 ($[M + Na]^+$, 7%); HRMS (ESI +ve TOF) calcd for $C_{41}H_{56}N_{11}O_3$ 750.4568, found 750.4572 ($[M + H]^+$).

(*R*)-*N*-((*R*)-6-Amino-1-(4-phenethyl-1*H*-1,2,3-triazol-1-yl)hexan-2-yl)-5-guanidino-2-(4-(((2'-(isopentyloxy)-[1,1'-biphenyl]-2-yl)oxy)methyl)-1*H*-1,2,3-triazol-1-yl)pentanamide dihydrochloride (81b)

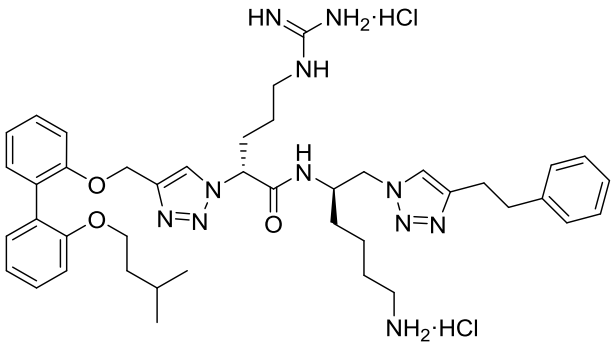

Following **General Procedure A**, azide **79b** (50 mg, 0.05 mmol), 4-phenyl-1-butyne (20 mg, 0.15 mmol), $Cu(OAc)_2 \cdot H_2O$ (2 mg, 0.01 mmol) and sodium ascorbate (4 mg, 0.02 mmol) were stirred in *t*-BuOH (1.0 mL) and H_2O (0.25 mL) for 24 h to give the intermediate triazole as a light tan gum after flash chromatography over SiO_2 gel ($MeOH/CH_2Cl_2$ – 0:100 → 10:90). Following **General Procedure C**, the triazole was dissolved in CH_2Cl_2 (1.5 mL) and treated with H_2O (18 mg, 1.00 mmol) and CF_3CO_2H (1.5 mL) followed by work-up with ethereal HCl to give the amine salt **81b** (40 mg, 94% over two steps) as a light tan powder that rapidly transitioned to a sticky gum. $[\alpha]_D^{23}$ +9.5 (*c* 0.83, MeOH); ^{1}H NMR (400 MHz, CD_3OD) δ 7.96 (s, 1H), 7.78 (s, 1H), 7.34 – 7.09 (m, 10H), 7.06 – 6.96 (m, 2H), 6.93 (t, *J* = 7.4 Hz, 1H), 5.32 (dd, *J* = 9.1, 6.0 Hz, 1H), 5.11 (s, 2H), 4.65 (dd, *J* = 13.8, 3.6 Hz, 1H), 4.49 (dd, *J* = 13.8, 8.9 Hz, 1H), 4.31 – 4.20 (m, 1H), 3.94 – 3.85 (m, 2H), 3.19 (t, *J* = 6.9 Hz, 2H), 3.11 – 2.96 (m, 4H), 2.84 (t, *J* = 7.2 Hz, 2H), 2.20 – 1.92 (m, 2H), 1.75 – 1.23 (m, 11H), 0.78 (d, *J* = 6.6 Hz, 6H); ^{13}C NMR (101 MHz, CD_3OD) δ 170.0, 158.8, 158.2, 157.5, 147.9 (observed by gHMBC), 146.1 (observed by gHMBC), 141.9, 132.9, 132.6, 130.5*, 129.9, 129.82*, 129.79, 129.7*, 127.6, 126.3, 124.5, 122.5, 121.5, 114.8, 113.8, 68.2, 64.5, 64.0,

55.6, 51.5, 41.8, 40.6, 39.4, 36.3, 32.0, 30.6, 28.2, 27.8, 26.2, 26.1, 23.8, 23.1*; IR (neat) $\overline{\nu}_{max}$ 3338, 3140, 3065, 2953, 2925, 2871, 2378, 2324, 1734, 1718, 1700, 1684, 1669, 1653, 1636, 1617, 1559, 1540, 1507, 1473, 1457, 1437, 1419, 1395, 1363, 1340, 1213, 1160, 1136, 1109, 1049, 1003, 937, 853, 751, 699, 669, 620 cm^{-1}; MS (ESI +ve) *m*/2 383 ($[M + 2H]^{2+}$, 100%), *m/z* 786 ($[M + Na]^{+}$, 28%), 764 ($[M + H]^{+}$, 22%); HRMS (ESI +ve TOF) calcd for $C_{42}H_{58}N_{11}O_3$ 764.4724, found 764.4754 ($[M + H]^{+}$).

(*R*)-*N*-((*R*)-6-Amino-1-(4-cyclohexyl-1*H*-1,2,3-triazol-1-yl)hexan-2-yl)-5-guanidino-2-(4-(((2'-(isopentyloxy)-[1,1'-biphenyl]-2-yl)oxy)methyl)-1*H*-1,2,3-triazol-1-yl)pentanamide dihydrochloride (81c)

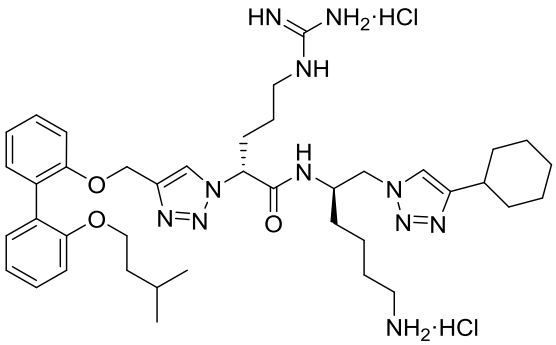

Following **General Procedure A**, azide **79b** (50 mg, 0.05 mmol), cyclohexylacetylene (18 mg, 0.15 mmol), $Cu(OAc)_2 \cdot H_2O$ (2 mg, 0.01 mmol) and sodium ascorbate (4 mg, 0.02 mmol) were stirred in *t*-BuOH (1.0 mL) and H_2O (0.25 mL) for 24 h to give the intermediate triazole as a light tan gum after flash chromatography over SiO_2 gel ($MeOH/CH_2Cl_2$ – 0:100 → 10:90). Following **General Procedure C**, the triazole was dissolved in CH_2Cl_2 (1.5 mL) and treated with H_2O (18 mg, 1.00 mmol) and CF_3CO_2H (1.5 mL) followed by work-up with ethereal HCl to give the amine salt **81c** (40 mg, 97% over two steps) as a light tan powder that rapidly transitioned to a sticky gum. $[\alpha]_D^{23}$ +2.6 (*c* 0.97, MeOH); ^1H NMR (400 MHz,

CD_3OD) δ 7.82 (s, 1H), 7.73 (s, 1H), 7.34 – 7.24 (m, 2H), 7.17 (mp, 3H), 7.05 – 6.97 (m, 2H), 6.94 (t, *J* = 7.2 Hz, 1H), 5.37 – 5.29 (m, 1H), 5.10 (s, 2H), 4.60 – 4.41 (m, 2H), 4.30 (br s, 1H), 3.97 – 3.84 (m, 2H), 3.18 (t, *J* = 6.2 Hz, 2H), 2.89 – 2.79 (m, 2H), 2.79 – 2.67 (m, 1H), 2.13 – 1.21 (m, 23H), 0.78 (d, *J* = 6.6 Hz, 6H); ^{13}C NMR (101 MHz, CD_3OD) δ 170.0, 158.8, 158.2, 157.6, 154.6 (observed by gHMBC), 146.1 (observed by gHMBC), 132.8, 132.6, 130.6*, 129.9, 129.8, 124.4, 123.3, 122.5, 121.5, 114.8, 113.8, 68.2, 64.3, 64.1, 54.5, 51.5, 41.5, 40.6, 39.4, 36.7, 34.40, 34.35, 32.3, 30.8, 28.2, 27.4*, 27.3, 26.3, 25.9, 23.8, 23.1*; IR (neat) $\bar{\nu}_{max}$ 3337, 3139, 3064, 2954, 2927, 2864, 2378, 2324, 1734, 1718, 1700, 1684, 1669, 1653, 1636, 1617, 1559, 1540, 1507, 1473, 1457, 1437, 1419, 1395, 1363, 1340, 1261, 1213, 1159, 1123, 1109, 1049, 1002, 937, 853, 800, 750, 668, 619 cm^{-1}; MS (ESI +ve) *m*/2 372 ($[M + 2H]^{2+}$, 100%), *m/z* 742 ($[M + H]^+$, 58%), 764 ($[M + Na]^+$, 52%); HRMS (ESI +ve TOF) calcd for $C_{40}H_{60}N_{11}O_3$ 742.4881, found 742.4908 ($[M + H]^+$).

(*R*)-*N*-((*R*)-6-Amino-1-(4-(cyclohexylmethyl)-1*H*-1,2,3-triazol-1-yl)hexan-2-yl)-5-guanidino-2-(4-(((2'-(isopentyloxy)-[1,1'-biphenyl]-2-yl)oxy)methyl)-1*H*-1,2,3-triazol-1-yl)pentanamide dihydrochloride (81d)

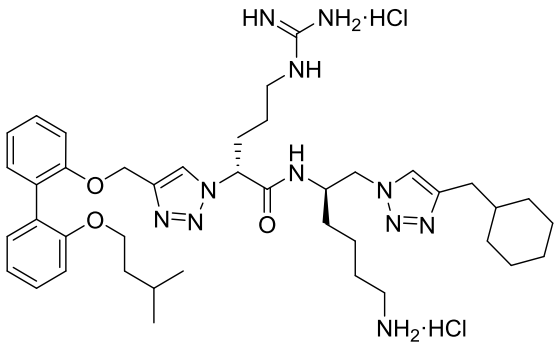

Following **General Procedure A**, azide **79b** (50 mg, 0.05 mmol), 3-cyclohexyl-1-propyne (19 mg, 0.15 mmol), $Cu(OAc)_2 \cdot H_2O$ (2 mg, 0.01 mmol) and sodium ascorbate (4 mg, 0.02

mmol) were stirred in *t*-BuOH (1.0 mL) and H_2O (0.25 mL) for 24 h to give the intermediate triazole as a light tan gum after flash chromatography over SiO_2 gel ($MeOH/CH_2Cl_2$ – 0:100 → 10:90). Following **General Procedure C**, the triazole was dissolved in CH_2Cl_2 (1.5 mL) and treated with H_2O (18 mg, 1.00 mmol) and CF_3CO_2H (1.5 mL) followed by work-up with ethereal HCl to give the amine salt **81d** (38 mg, 90% over two steps) as a light tan powder that rapidly transitioned to a sticky gum. $[\alpha]_D^{23}$ +3.0 (*c* 0.70, MeOH); ^{1}H NMR (400 MHz, CD_3OD) δ 7.98 (s, 1H), 7.75 (s, 1H), 7.35 – 7.24 (m, 2H), 7.23 – 7.09 (m, 3H), 7.05 – 6.98 (m, 2H), 6.94 (t, *J* = 7.4 Hz, 1H), 5.30 (dd, *J* = 8.9, 6.2 Hz, 1H), 5.09 (s, 2H), 4.64 (dd, *J* = 13.8, 3.5 Hz, 1H), 4.47 (dd, *J* = 13.8, 9.3 Hz, 1H), 4.28 (br s, 1H), 3.97 – 3.84 (m, 2H), 3.19 (t, *J* = 6.8 Hz, 2H), 2.83 (t, *J* = 7.1 Hz, 2H), 2.63 (d, *J* = 6.8 Hz, 2H), 2.15 – 1.88 (m, 2H), 1.78 – 1.12 (m, 20H), 1.06 – 0.93 (m, 2H), 0.79 (d, *J* = 6.6 Hz, 6H); ^{13}C NMR (101 MHz, CD_3OD) δ 170.0, 158.8, 158.2, 157.6, 147.1 (observed by gHMBC), 146.2 (observed by gHMBC), 132.9, 132.6, 130.6, 129.88, 129.85, 129.8, 126.2, 124.4, 122.5, 121.5, 114.8, 113.8, 68.2, 64.5, 64.0, 55.4, 51.5, 41.8, 40.6, 39.5, 39.4, 34.2, 34.1, 33.6, 32.2, 30.7, 28.2, 27.6, 27.4*, 26.3, 26.1, 23.8, 23.1*; IR (neat) $\overline{\nu}_{max}$ 3337, 3140, 3064, 2953, 2926, 2866, 2376, 2323, 1734, 1718, 1700, 1684, 1669, 1653, 1636, 1617, 1559, 1540, 1507, 1473, 1457, 1437, 1419, 1395, 1363, 1340, 1260, 1214, 1159, 1123, 1109, 1049, 1003, 937, 870, 852, 750, 669, 620 cm^{-1}; MS (ESI +ve) *m*/2 379 ($[M + 2H]^{2+}$, 100%), *m/z* 778 ($[M + Na]^+$, 38%), 756 ($[M + H]^+$, 18%); HRMS (ESI +ve TOF) calcd for $C_{41}H_{62}N_{11}O_3$ 756.5037, found 756.5062 ($[M + H]^+$).

***Tert*-butyl ((*R*)-6-(((*R*)-1-azido-5-(2-((2,2,4,6,7-pentamethyl-2,3-dihydrobenzofuran-5-yl)sulfonyl)guanidino)pentan-2-yl)amino)-5-(4-((((*S*)-2'-(isopentyloxy)-[1,1'-binaphthalen]-2-yl)oxy)methyl)-1*H*-1,2,3-triazol-1-yl)-6-oxohexyl)carbamate (79c)**

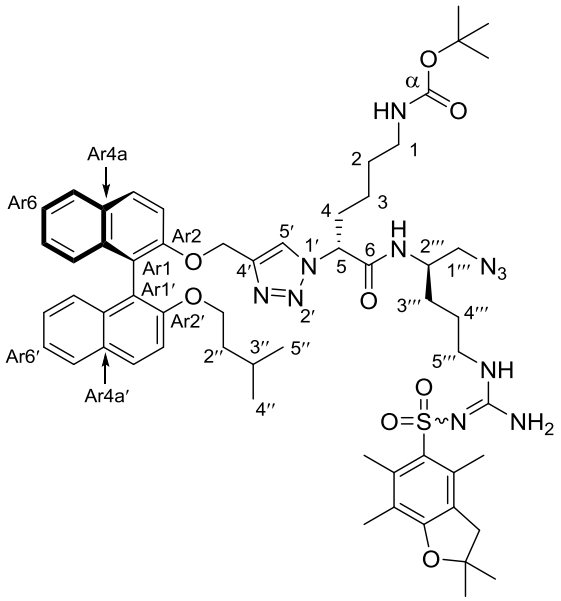

Following **General Procedure B**, acid **75c** (182 mg, 0.27 mmol), amine **25** (131 mg, 0.30 mmol), EDCI (63 mg, 0.33 mmol) and HOBt (44 mg, 0.30 mmol) were stirred in acetonitrile (2.7 mL) for 18 h to give the product amide **79c** (252 mg, 86%) as a translucent tan gum after flash chromatography over SiO_2 gel (EtOAc/P.S. – 80:20). TLC (EtOAc/P.S. – 80:20): R_f = 0.38; $[\alpha]_D^{23}$ −18.3 (*c* 0.43, MeOH); ^{1}H NMR (400 MHz, $CDCl_3$) δ 7.99 – 7.90 (m, 2H, ArH), 7.90 – 7.82 (m, 2H, ArH), 7.45 (d, *J* = 9.0 Hz, 1H, ArH), 7.41 (d, *J* = 9.0 Hz, 1H, ArH), 7.38 – 7.09 (m, 6H, ArH), 6.72 (s, 1H, H5′), 6.04 (br s, 3H, $N^{5'''}$-H and -NH_2), 5.17 – 5.02 (m, 3H, H5 and -OC$\underline{H}_2$-C4′), 4.66 (br s, 1H, N^1-H), 4.02 – 3.80 (m, 3H, H5 and H1″), 3.32 – 3.20 (m, 2H, H1‴), 3.07 – 2.85 (m, 6H, H1, H5‴ and $ArCH_2$-), 2.56 (s, 3H, $ArCH_3$), 2.50 (s, 3H, $ArCH_3$), 2.12 – 1.99 (m, 4H, $ArCH_3$ and $H4_A$ or $H4_B$), 1.83 – 1.72 (m, 1H, $H4_B$ or $H4_A$), 1.50 – 0.98 (m, 26H, H2, H3, H2″, H3″, H3‴, H4‴, -$C(CH_3)_3$ and -$C(CH_3)_2$), 0.55 (d, *J* = 6.3 Hz, 3H, H4″ or H5″), 0.51 (d, *J* = 6.2 Hz, 3H, H5″ or H4″); ^{13}C NMR (101 MHz, CD_3OD) δ 168.3 (C6), 158.9 (Pbf C_{Ar}), 156.2 (Cα), 156.1 (C=N), 154.6 (CAr2′), 153.8 (CAr2), 145.1 (C4′), 138.4 (Pbf C_{Ar}), 134.13 (CAr8a or CAr8a′), 134.10 (CAr8a′ or CAr8a), 133.0 (Pbf C_{Ar}), 132.4 (Pbf C_{Ar}), 130.0 (CAr4a), 129.71 (CAr4), 129.67 (CAr4′), 129.3 (CAr4a′), 128.2 (CAr5), 128.1 (CAr5′),

126.6 (CAr7), 126.5 (CAr7′), 125.7 (CAr8), 125.3 (CAr8′), 124.8 (Pbf C_{Ar}), 124.3 (CAr6), 123.8 (CAr6′), 122.4 (C5′), 121.6 (CAr1), 120.2 (CAr1′), 117.7 (Pbf C_{Ar}), 116.4 (CAr3), 115.9 (CAr3′), 86.5 (-$\underline{C}(CH_3)_2$), 79.3 (-$\underline{C}(CH_3)_3$ – observed by gHMBC), 68.3 (C1‴), 64.6 (-O$\underline{C}H_2$-C4′), 63.8 (C5), 54.7 (C1″), 49.4 (C2‴), 43.4 (ArCH_2-), 40.8 (C5‴), 40.1 (C1), 38.1 (C2″), 31.8 (C4), 29.3 (C3‴), 29.0 (C2), 28.7 (-C($\underline{C}H_3)_2$), 28.6 (-C($\underline{C}H_3)_3$), 25.5 (C4‴), 24.7 (C3″), 22.8 (C3), 22.5 (C4″ or C5″), 22.2 (C5″ or C4″), 19.5 (ArCH_3), 18.1 (ArCH_3), 12.6 (ArCH_3); IR (neat) $\overline{\nu}_{max}$ 3320, 2954, 2928, 2870, 2102, 1718, 1700, 1684, 1653, 1617, 1559, 1540, 1507, 1457, 1363, 1243, 1163, 1147, 1089, 1045, 1014, 908, 852, 807, 782, 749, 734, 661, 641, 621 cm^{-1}; MS (ESI +ve) *m/z* 1109 ($[M + Na]^+$, 100%), 1087 ($[M + H]^+$, 17%); HRMS (ESI +ve TOF) calcd for $C_{58}H_{76}N_{11}O_8S$ 1086.5599, found 1086.5637 ($[M + H]^+$).

(*R*)-6-Amino-*N*-((*R*)-5-guanidino-1-(4-phenethyl-1*H*-1,2,3-triazol-1-yl)pentan-2-yl)-2-(4-((((*S*)-2'-(isopentyloxy)-[1,1'-binaphthalen]-2-yl)oxy)methyl)-1*H*-1,2,3-triazol-1-yl)hexanamide di**hydrochloride (82a)**

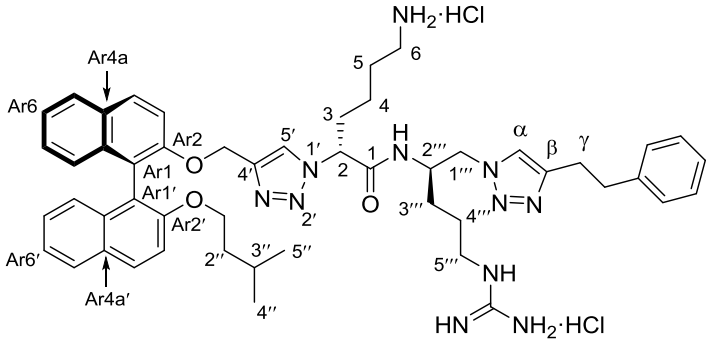

Following **General Procedure A**, azide **79c** (50 mg, 0.05 mmol), 4-phenyl-1-butyne (18 mg, 0.14 mmol), $Cu(OAc)_2 \cdot H_2O$ (2 mg, 0.01 mmol) and sodium ascorbate (4 mg, 0.02 mmol) were stirred in *t*-BuOH (1.0 mL) and H_2O (0.25 mL) for 24 h to give the intermediate triazole as a light tan gum after flash chromatography over SiO_2 gel ($MeOH/CH_2Cl_2$ – 0:100 →

10:90). Following **General Procedure C**, the triazole was dissolved in CH_2Cl_2 (1.4 mL) and treated with H_2O (18 mg, 1.00 mmol) and CF_3CO_2H (1.4 mL) followed by work-up with ethereal HCl to give the amine salt **82a** (24 mg, 56% over two steps) as a light tan powder that rapidly transitioned to a sticky gum. $[\alpha]_D^{23}$ −27.9 (*c* 0.47, MeOH); ^{1}H NMR (400 MHz, CD_3OD) δ 8.05 – 7.94 (m, 2H, ArH), 7.93 – 7.81 (m, 2H, ArH), 7.73 (s, 1H, H5′), 7.58 (d, *J* = 8.9 Hz, 1H, ArH), 7.49 (d, *J* = 8.9 Hz, 1H, ArH), 7.39 – 7.11 (m, 10H, ArH), 7.09 – 6.99 (m, 2H, ArH), 5.11 (m, 3H, H2 and -OC$\underline{H}_2$-C4′), 4.61 – 4.50 (m, 1H, H1‴$_A$ or H1‴$_B$), 4.47 – 4.34 (m, 1H, H1‴$_B$ or H1‴$_A$), 4.25 (br s, 1H, H2‴), 4.08 – 3.96 (m, 1H, H1″$_A$ or H1″$_B$), 3.96 – 3.86 (m, 1H, H1″$_B$ or H1″$_A$), 3.19 – 2.94 (m, 6H, H5‴, Hγ and -C$\underline{H}_2$Ph), 2.86 (br s, 2H, H6), 1.96 – 1.84 (m, 1H, H3$_A$ or H3$_B$), 1.76 – 0.79 (m, 12H, H3$_B$ or H3$_A$, H4, H5, H2″, H3″, H3‴ and H4‴), 0.55 (d, *J* = 6.4 Hz, 3H, H4″ or H5″), 0.51 (d, *J* = 6.3 Hz, 3H, H5″ or H4″); ^{13}C NMR (101 MHz, CD_3OD) δ 170.1 (C1), 158.7 (C=N), 156.1 (CAr2′), 155.4 (CAr2), 148.4 (Cβ – observed by gHMBC), 145.7 (C4′ – observed by gHMBC), 142.4 (Phenyl C_{Ar}), 135.6 (CAr8a or CAr8a′), 135.5 (CAr8a′ or CAr8a), 131.6 (CAr4a), 130.9 (CAr4a′), 130.8 (CAr4), 130.7 (CAr4′), 129.76 (Phenyl C_{Ar})*, 129.75 (Phenyl C_{Ar})*, 129.3 (CAr5), 129.2 (CAr5′), 127.49 (Phenyl C_{Ar}), 127.48 (CAr7 and CAr7′), 126.6 (CAr8), 126.4 (CAr8′), 125.3 (CAr6), 124.8 (CAr6′ and Cα), 124.0 (C5′), 122.9 (CAr1), 121.4 (CAr1′), 117.7 (CAr3), 117.0 (CAr3′), 69.2 (C1″), 65.2 (-O$\underline{C}H_2$-C4′), 64.6 (C2), 54.7 (C1‴), 51.2 (C2‴), 42.1 (C5‴), 40.6 (C6), 39.5 (C2″), 36.8 (Cγ), 32.8 (C3), 30.1 (C3‴), 28.5 (-$\underline{C}H_2$Ph), 27.9 (C5), 26.3 (C4‴), 25.8 (C3″), 23.6 (C4), 23.0 (C4″ or C5″), 22.7 (C5″ or C4″); IR (neat) $\overline{\nu}_{max}$ 3320, 3178, 2954, 2926, 2869, 2375, 2352, 2322, 1734, 1718, 1700, 1684, 1669, 1653, 1617, 1559, 1540, 1507, 1457, 1437, 1363, 1243, 1212, 1147, 1085, 1055, 1040, 1005, 912, 865, 809, 776, 746, 701, 669, 611 cm^{-1}; MS (ESI +ve) *m*/2 433 ([M + 2H]$^{2+}$, 100%), *m/z* 865

([M + H]$^+$, 21%); HRMS (ESI +ve TOF) calcd for $C_{50}H_{62}N_{11}O_3$ 864.5037, found 864.5078 ([M + H]$^+$).

(*R*)-6-Amino-*N*-((*R*)-1-(4-(cyclohexylmethyl)-1*H*-1,2,3-triazol-1-yl)-5-guanidinopentan-2-yl)-2-(4-((((*S*)-2'-(isopentyloxy)-[1,1'-binaphthalen]-2-yl)oxy)methyl)-1*H*-1,2,3-triazol-1-yl)hexanamide dihydrochloride (82b)

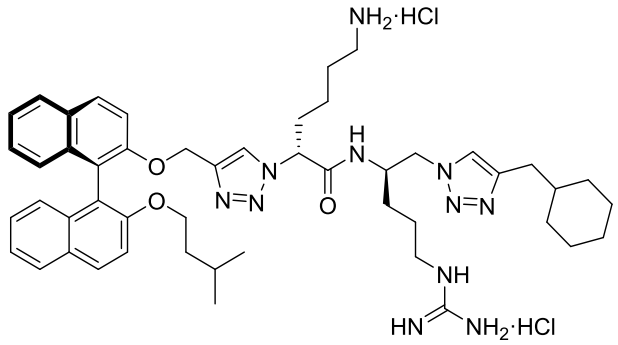

Following **General Procedure A**, azide **79c** (50 mg, 0.05 mmol), 3-cyclohexyl-1-propyne (17 mg, 0.15 mmol), $Cu(OAc)_2{\cdot}H_2O$ (2 mg, 0.01 mmol) and sodium ascorbate (4 mg, 0.02 mmol) were stirred in *t*-BuOH (1.0 mL) and H_2O (0.25 mL) for 24 h to give the intermediate triazole as a light tan gum after flash chromatography over SiO_2 gel ($MeOH/CH_2Cl_2$ – 0:100 → 10:90). Following **General Procedure C**, the triazole was dissolved in CH_2Cl_2 (1.4 mL) and treated with H_2O (18 mg, 1.00 mmol) and CF_3CO_2H (1.4 mL) followed by work-up with ethereal HCl to give the amine salt **82b** (32 mg, 75% over two steps) as a light tan powder that rapidly transitioned to a sticky gum. $[\alpha]_D^{23}$ −10.2 (*c* 0.80, MeOH); ^{1}H NMR (400 MHz, CD_3OD) δ 8.04 – 7.96 (m, 2H), 7.94 (s, 1H), 7.92 – 7.86 (m, 2H), 7.59 (d, *J* = 9.0 Hz, 1H), 7.51 (d, *J* = 9.0 Hz, 1H), 7.37 – 7.27 (m, 2H), 7.25 – 7.14 (m, 3H), 7.06 (d, *J* = 8.4 Hz, 1H), 7.02 (d, *J* = 8.5 Hz, 1H), 5.21 – 5.04 (m, 3H), 4.66 – 4.56 (m, 1H), 4.51 – 4.41 (m, 1H), 4.29 (br s, 1H), 4.08 – 3.99 (m, 1H), 3.97 – 3.87 (m, 1H), 3.16 – 3.03 (m, 2H), 2.95 – 2.81 (m,

2H), 2.63 (d, *J* = 6.5 Hz, 2H), 1.97 – 1.86 (m, 1H), 1.80 – 0.79 (m, 23H), 0.56 (d, *J* = 6.4 Hz, 3H), 0.52 (d, *J* = 6.3 Hz, 3H); ^{13}C NMR (101 MHz, CD_3OD) δ 170.1, 158.7, 156.2, 155.4, 147.5 (observed by gHMBC), 146.0 (observed by gHMBC), 135.6, 135.5, 131.6, 130.9, 130.8, 130.7, 129.3, 129.2, 127.48, 127.46, 126.6, 126.4, 125.8, 125.2, 124.8, 124.2, 122.9, 121.4, 117.8, 117.0, 69.2, 65.1, 64.6, 55.2, 51.2, 42.0, 40.6, 39.6, 39.5, 34.2, 34.2, 33.9, 32.8, 30.0, 27.9, 27.6, 27.5, 27.4, 26.3, 25.8, 23.6, 23.0, 22.8; IR (neat) $\overline{\nu}_{max}$ 3320, 3178, 2953, 2923, 2854, 2376, 2351, 2321, 1734, 1718, 1700, 1684, 1669, 1653, 1617, 1559, 1540, 1507, 1457, 1437, 1374, 1363, 1340, 1261, 1244, 1212, 1147, 1083, 1055, 1040, 1006, 915, 864, 809, 774, 744, 669, 614 cm^{-1}; MS (ESI +ve) *m*/2 429 ([M + 2H]$^{2+}$, 100%), *m/z* 857 ([M + H]$^+$, 22%); HRMS (ESI +ve TOF) calcd for $C_{49}H_{66}N_{11}O_3$ 856.5350, found 856.5377 ([M + H]$^+$).

***Tert*-butyl ((*R*)-6-azido-5-((*R*)-2-(4-((((*S*)-2'-(isopentyloxy)-[1,1'-binaphthalen]-2-yl)oxy)methyl)-1*H*-1,2,3-triazol-1-yl)-5-(2-((2,2,4,6,7-pentamethyl-2,3-dihydrobenzofuran-5-yl)sulfonyl)guanidino)pentanamido)hexyl)carbamate (79d)**

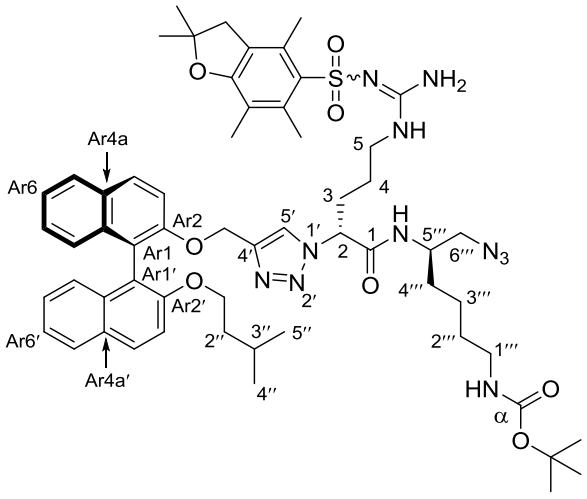

Following **General Procedure B**, acid **75d** (120 mg, 0.14 mmol), amine **22** (37 mg, 0.14 mmol), EDCI (33 mg, 0.17 mmol) and HOBt (23 mg, 0.17 mmol) were stirred in acetonitrile (1.4 mL) for 48 h to give the product amide **79d** (143 mg, 93%) as a translucent tan gum. TLC (EtOAc/P.S. – 80:20): R_f = 0.72; $[\alpha]_D^{23}$ −8.7 (*c* 1.27, MeOH);

^{1}H NMR (400 MHz, $CDCl_3$) δ 7.90 (app. t, *J* = 9.0 Hz, 2H, ArH), 7.85 (d, *J* = 8.2 Hz, 1H, ArH), 7.77 (m, 2H, $N^{5'''}$-H and ArH), 7.48 (d, *J* = 9.0 Hz, 1H, ArH), 7.42 (d, *J* = 9.0 Hz, 1H, ArH), 7.33 (t, *J* = 7.3 Hz, 1H, ArH), 7.24 – 7.04 (m, 6H, H5′ and ArH), 6.27 (br s, 2H, -NH_2), 5.93 (br s, 1H, N^5-H), 5.49 (br s, 1H, H2), 5.11 and 5.07 (ABq, *J* = 12.3 Hz, 2H, -OCH_2-C4′), 4.64 (br s, 1H, $N^{1'''}$-H), 4.05 – 3.84 (m, 3H, H1″ and H5‴), 3.40 – 3.22 (m, 3H, $H5_A$ or $H5_B$ and H6‴), 2.93 (br s, 5H, $H5_B$ or $H5_A$, H1‴ and $ArCH_2$-), 2.61 (s, 3H, $ArCH_3$), 2.52 (s, 3H, $ArCH_3$), 2.13 – 2.01 (m, 4H, $H3_A$ or $H3_B$ and $ArCH_3$), 1.96 – 1.82 (m, 1H, $H3_B$ or $H3_A$), 1.53 – 1.07 (m, 25H, $H4_A$ or $H4_B$, H2″, H3″, H2‴, H3‴, H4‴, -$C(CH_3)_2$ and -$C(CH_3)_3$), 0.93 – 0.77 (m, 1H, $H4_B$ or $H4_A$), 0.57 (d, *J* = 6.3 Hz, 3H, H4″ or H5″), 0.53 (d, *J* = 6.3 Hz, 3H, H5″ or H4″); ^{13}C NMR (101 MHz, CD_3OD) δ 168.5 (C1), 159.0 (Pbf C_{Ar}), 156.6 (C=N), 156.2 (Cα), 154.7 (CAr2′), 154.1 (CAr2), 145.0 (C4′), 138.5 (Pbf C_{Ar}), 134.14 (CAr8a or CAr8a′), 134.10 (CAr8a′ or CAr8a), 132.8 (Pbf C_{Ar}), 132.4 (Pbf C_{Ar}), 130.0 (CAr4a), 129.52 (CAr4), 129.51 (CAr4′), 129.2 (CAr4a′), 128.04 (CAr5), 127.99 (CAr5′), 126.4 (CAr7), 126.3 (CAr7′), 125.7 (CAr8), 125.4 (CAr8′), 124.9 (Pbf C_{Ar}), 124.1 (CAr6), 123.6 (CAr6′), 122.7 (C5′), 121.7 (CAr1), 120.1 (CAr1′), 117.8 (Pbf C_{Ar}), 116.9 (CAr3), 115.9 (CAr3′), 86.6 (-$\underline{C}(CH_3)_2$), 79.2 (-$\underline{C}(CH_3)_3$, 68.3 (C1″), 64.7 (-O$\underline{C}H_2$-C4′), 62.7 (C2), 54.3 (C6‴), 50.0 (C5‴), 43.4 ($ArCH_2$-), 40.3 (C1‴), 38.9 (C5), 38.2 (C2″), 31.4 (C4‴), 29.8 (C3), 29.6 (C5‴), 28.7 (-C($\underline{C}H_3$)$_2$), 28.5 (-C($\underline{C}H_3$)$_3$), 25.5 (C4), 24.7 (C3″), 23.1 (C3‴), 22.5 (C4″ or C5″), 22.3 (C5″ or C4″), 19.6 ($ArCH_3$), 18.2 ($ArCH_3$), 12.6 ($ArCH_3$); IR (neat) $\bar{\nu}_{max}$ 3334, 2958, 2933, 2878, 2377, 2323, 2099, 1751, 1734, 1718, 1700, 1684, 1653, 1636, 1617, 1559, 1540, 1507, 1490, 1473, 1457, 1437, 1419, 1395, 1363, 1340, 1244, 1166, 1154, 1106, 1090, 1048, 1015, 904, 853, 808, 779, 748, 668, 641, 620, 609 cm^{-1}; MS (ESI +ve) *m/z* 1109 ($[M + Na]^+$, 100%),

1087 ([M + H]$^+$, 9%); HRMS (ESI +ve TOF) calcd for $C_{58}H_{75}N_{11}O_8SNa$ 1108.5419, found 1108.5433 ([M + Na]$^+$).

(*R*)-*N*-((*R*)-6-Amino-1-(4-phenethyl-1*H*-1,2,3-triazol-1-yl)hexan-2-yl)-5-guanidino-2-(4-((((*S*)-2'-(isopentyloxy)-[1,1'-binaphthalen]-2-yl)oxy)methyl)-1*H*-1,2,3-triazol-1-yl)pentanamide dihydrochloride (83a)

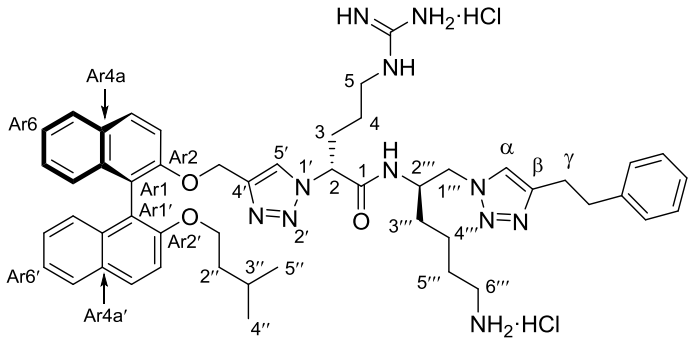

Following **General Procedure A**, azide **79d** (45 mg, 0.04 mmol), 4-phenyl-1-butyne (16 mg, 0.12 mmol), $Cu(OAc)_2·H_2O$ (2 mg, 0.01 mmol) and sodium ascorbate (4 mg, 0.02 mmol) were stirred in *t*-BuOH (0.8 mL) and H_2O (0.2 mL) for 24 h to give the intermediate triazole as a light tan gum after flash chromatography over SiO_2 gel ($MeOH/CH_2Cl_2$ – 0:100 → 10:90). Following **General Procedure C**, the triazole was dissolved in CH_2Cl_2 (1.2 mL) and treated with H_2O (15 mg, 0.83 mmol) and CF_3CO_2H (1.2 mL) followed by work-up with ethereal HCl to give the amine salt **83a** (37 mg, 95% over two steps) as a light tan powder that rapidly transitioned to a sticky gum. $[\alpha]_D^{23}$ −10.3 (*c* 0.90, MeOH); ^{1}H NMR (400 MHz, CD_3OD) δ 8.19 (s, 1H, Hα), 8.03 – 7.94 (m, 2H, ArH), 7.92 – 7.84 (m, 2H, ArH), 7.60 (d, *J* = 9.0 Hz, 1H, ArH), 7.49 (d, *J* = 9.0 Hz, 1H, ArH), 7.37 – 7.13 (m, 10H, H5′ and ArH), 7.08 – 6.99 (m, 2H, ArH), 5.24 (dd, *J* = 9.3, 5.6 Hz, 1H, H2), 5.14 and 5.10 (ABq, *J* = 12.4 Hz, 2H, -OCH_2-C4′), 4.77 – 4.69 (m, 1H, H1‴$_A$ or H1‴$_B$), 4.59 – 4.49 (m, 1H, H1‴$_B$ or H1‴$_A$),

4.22 (br s, 1H, H2‴), 4.07 – 3.97 (m, 1H, H1″$_A$ or H1″$_B$), 3.94 – 3.85 (m, 1H, H1″$_B$ or H1″$_A$), 3.22 – 3.10 (m, 4H, H5 and Hγ), 3.08 – 2.98 (m, 2H, -C<u>H</u>$_2$Ph), 2.84 (t, *J* = 7.2 Hz, 2H, H6‴), 2.16 – 2.01 (m, 1H, H3$_A$ or H3$_B$), 1.93 – 1.81 (m, 1H, H3$_B$ or H3$_A$), 1.78 – 1.07 (m, 11H, H4, H2″, H3″, H3‴, H4‴ and H5‴), 0.55 (d, *J* = 6.4 Hz, 3H, H4″ or H5″), 0.51 (d, *J* = 6.3 Hz, 3H, H5″ or H4″); ^{13}C NMR (101 MHz, CD_3OD) δ 170.0 (C1), 158.8 (C=N), 156.1 (CAr2′), 155.5 (CAr2), 146.4 (Cβ – observed by gHMBC), 146.2 (C4′ – observed by gHMBC), 141.3 (Phenyl C_{Ar}), 135.6 (CAr8a or CAr8a′), 135.5 (CAr8a′ or CAr8a), 131.6 (CAr4a), 130.9 (CAr4a′), 130.80 (CAr4), 130.77 (CAr4′), 129.9 (Phenyl C_{Ar})*, 129.8 (Phenyl C_{Ar})*, 129.3 (CAr5), 129.2 (CAr5′), 128.3 (Cα – observed by gHMBC), 127.9 (Phenyl C_{Ar}), 127.51 (CAr7), 127.46 (CAr7′), 126.6 (CAr8), 126.4 (CAr8′), 125.3 (CAr6), 124.8 (CAr6′), 124.5 (C5′ – observed by gHMBC), 122.9 (CAr1), 121.4 (CAr1′), 117.8 (CAr3), 117.0 (CAr3′), 69.2 (C1″), 65.0 (-O<u>C</u>H$_2$-C4′), 64.5 (C2), 56.6 (C1‴), 51.5 (C2‴), 41.7 (C5), 40.6 (C6‴), 39.5 (C2″), 35.9 (-<u>C</u>H$_2$Ph), 31.8 (C3‴), 30.4 (C3), 28.1 (C5‴), 27.1 (Cγ), 26.0 (C4), 25.8 (C3″), 23.8 (C4‴), 23.0 (C4″ or C5″), 22.7 (C5″ or C4″); IR (neat) $\bar{\nu}_{max}$ 3334, 3147, 3060, 2953, 2933, 2874, 2377, 2324, 1751, 1734, 1718, 1700, 1684, 1653, 1636, 1617, 1559, 1540, 1507, 1490, 1473, 1457, 1437, 1419, 1395, 1363, 1340, 1319, 1243, 1215, 1164, 1147, 1108, 1083, 1047, 1009, 903, 861, 810, 747, 702, 668, 620, 608 cm^{-1}; MS (ESI +ve) *m*/2 433 ([M + 2H]$^{2+}$, 100%), *m/z* 887 ([M + Na]$^+$, 18%), 865 ([M + H]$^+$, 8%); HRMS (ESI +ve TOF) calcd for $C_{50}H_{62}N_{11}O_3$ 864.5037, found 864.5018 ([M + H]$^+$).

(*R*)-*N*-((*R*)-6-Amino-1-(4-(cyclohexylmethyl)-1*H*-1,2,3-triazol-1-yl)hexan-2-yl)-5-guanidino-2-(4-((((*S*)-2'-(isopentyloxy)-[1,1'-binaphthalen]-2-yl)oxy)methyl)-1*H*-1,2,3-triazol-1-yl)pentanamide dihydrochloride (83b)

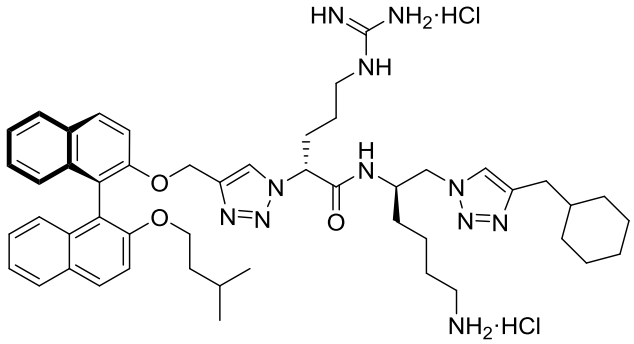

Following **General Procedure A**, azide **79d** (45 mg, 0.04 mmol), 3-cyclohexyl-1-propyne (15 mg, 0.12 mmol), $Cu(OAc)_2 \cdot H_2O$ (2 mg, 0.01 mmol) and sodium ascorbate (4 mg, 0.02 mmol) were stirred in *t*-BuOH (0.8 mL) and H_2O (0.2 mL) for 24 h to give the intermediate triazole as a light tan gum after flash chromatography over SiO_2 gel ($MeOH/CH_2Cl_2$ – 0:100 → 10:90). Following **General Procedure C**, the triazole was dissolved in CH_2Cl_2 (1.2 mL) and treated with H_2O (15 mg, 0.83 mmol) and CF_3CO_2H (1.2 mL) followed by work-up with ethereal HCl to give the amine salt **83b** (26 mg, 68% over two steps) as a light tan powder that rapidly transitioned to a sticky gum. $[\alpha]_D^{23}$ −25.9 (*c* 0.30, MeOH); ^{1}H NMR (400 MHz, CD_3OD) δ 8.03 – 7.96 (m, 2H), 7.93 – 7.82 (m, 3H), 7.57 (d, *J* = 9.0 Hz, 1H), 7.51 (d, *J* = 9.0 Hz, 1H), 7.38 – 7.25 (m, 2H), 7.25 – 7.13 (m, 3H), 7.07 (d, *J* = 8.4 Hz, 1H), 7.02 (d, *J* = 8.4 Hz, 1H), 5.33 – 5.25 (m, 1H), 5.11 and 5.09 (ABq, *J* = 12.3 Hz, 2H), 4.57 – 4.47 (m, 2H), 4.32 – 4.23 (m, 1H), 4.08 – 4.00 (m, 1H), 3.97 – 3.88 (m, 1H), 3.13 (br s, 2H), 2.84 (br s, 2H), 2.63 – 2.51 (m, 2H), 2.00 (s, 1H), 1.78 – 0.84 (m, 23H), 0.57 (d, *J* = 6.4 Hz, 3H), 0.53 (d, *J* = 6.3 Hz, 3H); ^{13}C NMR (101 MHz, CD_3OD) δ 170.1, 158.9, 156.2, 147.5 (observed by gHMBC), 146.3 (observed by gHMBC), 155.5, 135.60, 135.56, 131.6, 130.9, 130.8, 130.7,

129.3, 129.2, 127.5*, 126.7, 126.4, 125.3, 125.2, 124.8, 124.2, 123.0, 121.5, 117.8, 117.0, 69.2, 65.2, 64.1, 54.4, 51.6, 41.2, 40.5, 39.7, 39.5, 34.4, 34.34, 34.28, 32.2, 30.6, 28.2, 27.7, 27.5*, 25.9, 25.7, 23.5, 23.0, 22.8; IR (neat) $\overline{\nu}_{max}$ 3337, 3146, 3059, 2952, 2923, 2853, 2378, 2323, 1751, 1734, 1718, 1700, 1684, 1653, 1636, 1623, 1559, 1540, 1507, 1490, 1473, 1457, 1437, 1419, 1395, 1363, 1340, 1319, 1261, 1244, 1202, 1177, 1131, 1083, 1056, 1017, 916, 862, 808, 775, 748, 721, 669, 620, 609 cm^{-1}; MS (ESI +ve) *m*/2 429 ($[M + 2H]^{2+}$, 100%), *m/z* 857 ($[M + H]^+$, 34%), 879 ($[M + Na]^+$, 16%); HRMS (ESI +ve TOF) calcd for $C_{49}H_{66}N_{11}O_3$ 856.5350, found 856.5376 ($[M + H]^+$).

(*R*)-N^2-((*R*)-6-((*Tert*-butoxycarbonyl)amino)-2-(4-((((*S*)-2'-(isopentyloxy)-[1,1'-binaphthalen]-2-yl)oxy)methyl)-1*H*-1,2,3-triazol-1-yl)hexanoyl)-2-amino-5-(2-((2,2,4,6,7-pentamethyl-2,3-dihydrobenzofuran-5-yl)sulfonyl)guanidino)pentanoic acid (84)

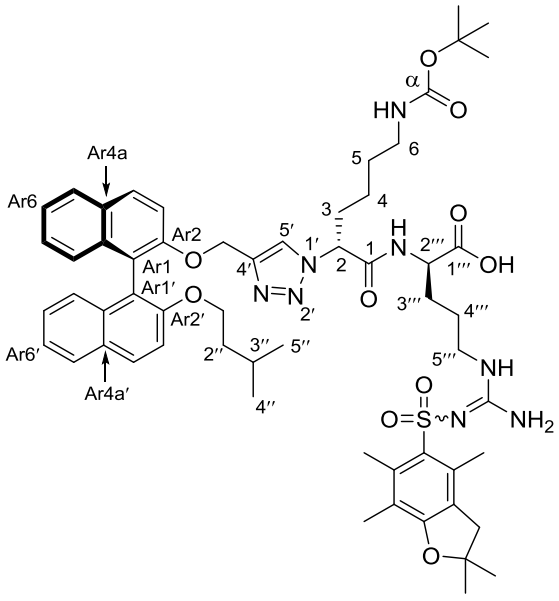

Following **General Procedure B**, acid **75c** (150 mg, 0.23 mmol), amine **29** (109 mg, 0.25 mmol), EDCI (52 mg, 0.27 mmol) and HOBt (37 mg, 0.25 mmol) were stirred in acetonitrile (2.3 mL) for 18 h to give the intermediate ester as a translucent tan gum after flash chromatography over SiO_2 gel (EtOAc). The ester was dissolved in THF (3.0 mL) with stirring, H_2O (2.0 mL) and $LiOH{\cdot}H_2O$ (84 mg, 2.00 mmol) were added and the reaction was stirred vigorously at rt for 24 h. The mixture

was diluted with 1.0 M aqueous HCl (25 mL), extracted with EtOAc (2 × 50 mL) and the combined organic extracts were washed with H_2O (1 × 50 mL), brine (1 × 50 mL), dried ($MgSO_4$), filtered and concentrated to give the acid **84** (205 mg, 86% over two steps) as a light tan gum. TLC (MeOH/CH_2Cl_2 – 5:95): R_f = 0.25; $[\alpha]_D^{23}$ −4.6 (*c* 1.53, MeOH); ^{1}H NMR (400 MHz, CD_3OD) : (mixture of rotamers) δ 8.00 – 7.90 (m, 2H, ArH), 7.90 – 7.81 (m, 2H, ArH), 7.58 – 7.42 (m, 2H, ArH)‡, 7.34 – 7.22 (m, 2H, ArH), 7.22 – 6.98 (m, 5H, H5′ and ArH), 5.21 (t, *J* = 7.0 Hz, 1H, H2), 5.15 – 5.03 (m, 2H, -OCH_2-C4′), 4.36 – 4.26 (m, 1H, H2‴), 4.05 – 3.85 (m, 2H, H1″), 3.17 (br s, 1H, H5‴$_A$ or H5‴$_B$), 3.08 (br s, 1H, H5‴$_B$ or H5‴$_A$), 3.01 – 2.86 (m, 4H, H6 and $ArCH_2$-), 2.60 – 2.52 (m, 3H, $ArCH_3$)‡, 2.52 – 2.44 (m, 3H, $ArCH_3$)‡, 2.08 – 2.00 (m, 4H, H3$_A$ or H3$_B$ and $ArCH_3$)‡, 1.93 – 1.75 (m, 2H, H3$_B$ or H3$_A$ and H3‴$_A$ or H3‴$_B$), 1.73 – 0.80 (m, 25H, H4, H5, H2″, H3″, H3‴$_B$ or H3‴$_A$, H4‴, -$C(CH_3)_2$ and -$C(CH_3)_3$), 0.59 – 0.46 (m, 6H, H4″ and H5″)‡; ^{13}C NMR (101 MHz, CD_3OD) : (mixture of rotamers)† δ 174.8 (C1‴), 170.2 (C1), 160.0 (Pbf C_{Ar}), 158.6 (Cα), 158.2 (C=N), 156.1 (CAr2′), 155.4 (CAr2), 146.1 (C4′), 139.5 (Pbf C_{Ar}), 135.6 (CAr8a or CAr8a′), 135.5 (CAr8a′ or CAr8a), 134.5 (Pbf C_{Ar}), 133.7 (Pbf C_{Ar})$^{\Delta}$, 131.5 (CAr4a), 130.8 (CAr4a′)$^{\Delta}$, 130.7 (CAr4), 130.6 (CAr4′), 129.3 (CAr5), 129.2 (CAr5′), 127.5 (CAr7), 127.4 (CAr7′), 126.7 (CAr8)$^{\Delta}$, 126.3 (CAr8′), 126.2 (Pbf C_{Ar}), 125.1 (CAr6), 124.8 (CAr6′), 123.8 (C5′), 122.8 (CAr1),

‡ Indicates that the ^{1}H NMR resonance was split into two or more signals due to the presence of amide and carbamate rotamers (e.g. the *syn*- and *anti*-amide conformations).

† All ^{13}C NMR resonances (except those denoted with a Δ symbol) were split into two resonances due to the presence of amide and/or carbamate rotamers (e.g. the *syn*- and *anti*-amide conformations); only the major resonance from each resonance pair is reported for clarity.

Δ Indicates that the ^{13}C NMR resonance was **not** split into multiple resonances due to rotamers.

121.3 (CAr1′), 118.6 (Pbf C_{Ar}), 117.6 (CAr3), 116.9 (CAr3′), 87.8 (-$\underline{C}(CH_3)_2$), 80.1 (-$\underline{C}(CH_3)_3$), 69.1 (C1″)$^{\Delta}$, 65.1 (-O$\underline{C}H_2$-C4′), 64.7 (C2), 53.7 (C2‴)$^{\Delta}$, 44.1 (ArCH_2-), 41.6 (C5‴), 41.1 (C6)$^{\Delta}$, 39.5 (C2″)$^{\Delta}$, 33.8 (C3), 30.4 (C3‴), 30.0 (C5), 29.0 (-C($\underline{C}H_3)_2$ or -C($\underline{C}H_3)_3$), 28.9 (-C($\underline{C}H_3)_3$ or -C($\underline{C}H_3)_2$)$^{\Delta}$, 27.2 (C4‴), 25.8 (C3″), 23.9 (C4), 23.0 (C4″ or C5″), 22.8 (C5″ or C4″), 19.8 (ArCH_3), 18.6 (ArCH_3), 12.7 (ArCH_3); IR (neat) $\overline{\nu}_{max}$ 3336, 2967, 2931, 2870, 2369, 2322, 1700, 1684, 1653, 1559, 1540, 1507, 1473, 1457, 1419, 1363, 1340, 1244, 1163, 1147, 1088, 1049, 1016, 906, 852, 808, 783, 747, 669, 614 cm^{-1}; MS (ESI −ve) *m/z* 1074 ([M − H]$^-$, 100%); HRMS (ESI −ve TOF) calcd for $C_{58}H_{73}N_8O_{10}S$ 1073.5170, found 1073.5156 ([M − H]$^-$).

(*R*)-6-Amino-*N*-((*R*)-1-(benzylamino)-5-guanidino-1-oxopentan-2-yl)-2-(4-((((*S*)-2'-(isopentyloxy)-[1,1'-binaphthalen]-2-yl)oxy)methyl)-1*H*-1,2,3-triazol-1-yl)hexanamide dihydrochloride (85a)

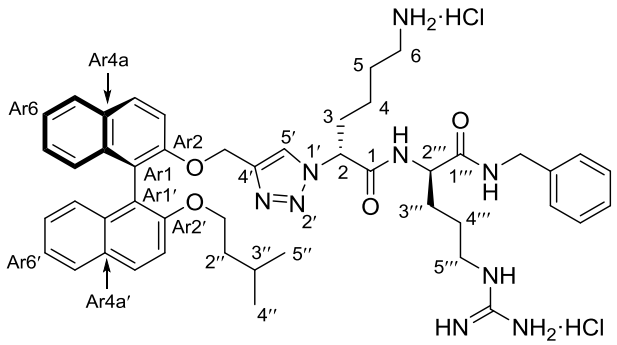

Following **General Procedure B**, acid **84** (50 mg, 0.05 mmol), benzylamine (6 mg, 0.06 mmol), EDCI (11 mg, 0.06 mmol) and HOBt (8 mg, 0.05 mmol) were stirred in acetonitrile (0.5 mL) for 24 h to give the intermediate amide as a translucent tan gum. Following **General Procedure C**, the amide was dissolved in CH_2Cl_2 (1.4 mL) and treated with H_2O (17 mg, 0.94 mmol) and CF_3CO_2H (1.4 mL) followed by work-up with ethereal HCl to give the amine

salt **85a** (33 mg, 79% over two steps) as a light tan powder that rapidly transitioned to a sticky gum. $[\alpha]_D^{23}$ −8.7 (*c* 0.87, MeOH); ^{1}H NMR (400 MHz, CD_3OD) : (mixture of rotamers) δ 8.02 – 7.92 (m, 2H, ArH), 7.91 – 7.81 (m, 2H, ArH), 7.62 – 7.41 (m, 2H, ArH)‡, 7.37 – 6.97 (m, 12H, H5′ and ArH), 5.48 – 5.25 (m, 1H, H2)‡, 5.16 – 5.03 (m, 2H, -OCH_2-C4′)‡, 4.40 – 4.19 (m, 3H, H2‴ and -C$\underline{H}_2$Ph)‡, 4.07 – 3.85 (m, 2H, H1″), 3.24 – 3.05 (m, 2H, H5‴)‡, 2.93 – 2.76 (m, 2H, H6)‡, 2.22 – 2.01 (m, 2H, $H3_A$ or $H3_B$), 1.97 – 1.06 (m, 12H, $H3_B$ or $H3_A$, H4, H5, H2″, H3″, H3‴ and H4‴), 0.60 – 0.46 (m, 6H, H4″ and H5″)‡; ^{13}C NMR (101 MHz, CD_3OD) : (mixture of rotamers)† δ 174.2 (C1‴), 170.6 (C1), 158.9 (C=N), 156.1 (CAr2′), 155.5 (CAr2), 145.8 (C4′ – observed by gHMBC), 139.8 (Phenyl C_{Ar}), 135.6 (CAr8a), 135.5 (CAr8a′), 131.5 (CAr4a), 130.9 (CAr4a′)Δ, 130.8 (CAr4), 130.7 (CAr4′), 129.8 (Phenyl C_{Ar})*, 129.3 (CAr5)Δ, 129.2 (CAr5′)Δ, 128.8 (Phenyl C_{Ar})*, 128.4 (Phenyl C_{Ar}), 127.6 (CAr7), 127.4 (CAr7′), 126.7 (CAr8)Δ, 126.4 (CAr8′), 125.2 (CAr6), 124.8 (CAr6′), 124.2 (C5′ – observed by gHMBC), 122.9 (CAr1), 121.4 (CAr1′), 117.7 (CAr3), 116.9 (CAr3′), 69.2 (C1″), 65.1 (-O$\underline{C}H_2$-C4′), 64.0 (C2), 55.0 (C2‴), 44.2 (-$\underline{C}H_2$Ph), 42.1 (C5‴), 40.5 (C6), 39.5 (C2″)Δ, 32.7 (C3), 30.1 (C3‴), 27.5 (C5), 26.4 (C4‴), 25.8 (C3″)Δ, 23.2 (C4), 23.0 (C4″ or C5″), 22.8 (C5″ or C4″); IR (neat) $\bar{\nu}_{max}$ 3060, 2954, 2932, 2869, 2367, 2319, 1734, 1718, 1700, 1684, 1669, 1653, 1623, 1590, 1559, 1540, 1507, 1490, 1457, 1437, 1419, 1395, 1363,

‡ Indicates that the ^{1}H NMR resonance was split into two or more signals due to the presence of amide and carbamate rotamers (e.g. the *syn*- and *anti*-amide conformations).

† All ^{13}C NMR resonances (except those denoted with a Δ symbol) were split into two resonances due to the presence of amide and/or carbamate rotamers (e.g. the *syn*- and *anti*-amide conformations); only the major resonance from each resonance pair is reported for clarity.

Δ Indicates that the ^{13}C NMR resonance was **not** split into multiple resonances due to rotamers.

1340, 1261, 1242, 1223, 1146, 1109, 1084, 1049, 1014, 914, 861, 809, 746, 668, 608 cm^{-1}; MS (ESI +ve) *m*/2 407 ($[M + 2H]^{2+}$, 100%), *m/z* 812 ($[M + H]^{+}$, 24%); HRMS (ESI +ve TOF) calcd for $C_{47}H_{58}N_9O_4$ 812.4612, found 812.4604 ($[M + H]^{+}$).

(*R*)-6-Amino-*N*-((*R*)-5-guanidino-1-oxo-1-(phenethylamino)pentan-2-yl)-2-(4-((((*S*)-2'-(isopentyloxy)-[1,1'-binaphthalen]-2-yl)oxy)methyl)-1*H*-1,2,3-triazol-1-yl)hexanamide dihydrochloride (85b)

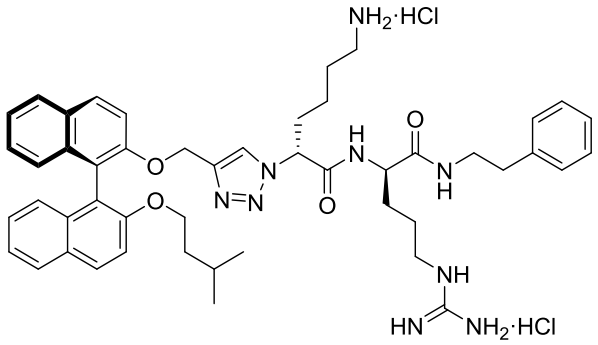

Following **General Procedure B**, acid **84** (50 mg, 0.05 mmol), β-phenylethylamine (7 mg, 0.06 mmol), EDCI (11 mg, 0.06 mmol) and HOBt (8 mg, 0.05 mmol) were stirred in acetonitrile (0.5 mL) for 24 h to give the intermediate amide as a translucent tan gum. Following **General Procedure C**, the amide was dissolved in CH_2Cl_2 (1.4 mL) and treated with H_2O (17 mg, 0.94 mmol) and CF_3CO_2H (1.4 mL) followed by work-up with ethereal HCl to give the amine salt **85b** (39 mg, 92% over two steps) as a light tan powder that rapidly transitioned to a sticky gum. $[\alpha]_D^{23}$ −19.4 (*c* 0.40, MeOH); ^{1}H NMR (400 MHz, CD_3OD) : (mixture of rotamers) δ 8.04 – 7.91 (m, 2H), 7.91 – 7.80 (m, 2H), 7.60 – 7.41 (m, 2H)‡, 7.36

‡ Indicates that the ^{1}H NMR resonance was split into two or more signals due to the presence of amide and carbamate rotamers (e.g. the *syn*- and *anti*-amide conformations).

– 6.97 (m, 12H), 5.50 – 5.24 (m, 1H)‡, 5.16 – 5.03 (m, 2H)‡, 4.26 – 4.10 (m, 1H)‡, 4.07 – 3.83 (m, 2H), 3.57 – 3.31 (m, 2H)‡, 3.24 – 3.02 (m, 2H)‡, 2.97 – 2.74 (m, 4H)‡, 2.22 – 2.02 (m, 1H), 1.97 – 1.02 (m, 12H), 0.55 (d, J = 6.3 Hz, 3H)‡, 0.51 (d, J = 6.3 Hz, 3H)‡; ^{13}C NMR (101 MHz, CD_3OD) : (mixture of rotamers)† δ 174.1, 170.3, 158.8, 156.1, 155.5, 145.8, 140.5, 135.6$^{\Delta}$, 135.5$^{\Delta}$, 131.6, 130.9$^{\Delta}$, 130.8, 130.7, 130.1*, 129.6*, 129.3, 129.2, 127.6, 127.5, 127.4, 126.7$^{\Delta}$, 126.4, 125.2, 124.8, 124.2, 122.9, 121.4$^{\Delta}$, 117.7, 117.0, 69.2, 65.1, 64.1, 55.5, 42.2, 42.1, 40.4, 39.5$^{\Delta}$, 36.7, 32.7, 30.3, 27.5, 26.3, 25.8$^{\Delta}$, 23.3, 23.0, 22.8; IR (neat) $\overline{\nu}_{max}$ 2953, 2926, 2869, 2366, 2322, 1734, 1718, 1700, 1684, 1669, 1653, 1623, 1591, 1559, 1540, 1507, 1490, 1457, 1437, 1419, 1395, 1363, 1340, 1261, 1242, 1223, 1085, 1048, 1016, 915, 861, 809, 748, 698, 668, 613 cm^{-1}; MS (ESI +ve) $m/2$ 414 ([M + 2H]$^{2+}$, 100%), m/z 826 ([M + H]$^{+}$, 28%); HRMS (ESI +ve TOF) calcd for $C_{48}H_{60}N_9O_4$ 826.4768, found 826.4800 ([M + H]$^{+}$).

† All ^{13}C NMR resonances (except those denoted with a Δ symbol) were split into two resonances due to the presence of amide and/or carbamate rotamers (e.g. the *syn*- and *anti*-amide conformations); only the major resonance from each resonance pair is reported for clarity.

Δ Indicates that the ^{13}C NMR resonance was **not** split into multiple resonances due to rotamers.

(*R*)-6-Amino-*N*-((*R*)-5-guanidino-1-oxo-1-(piperidin-1-yl)pentan-2-yl)-2-(4-((((*S*)-2'-(isopentyloxy)-[1,1'-binaphthalen]-2-yl)oxy)methyl)-1*H*-1,2,3-triazol-1-yl)hexanamide dihydrochloride (85c)

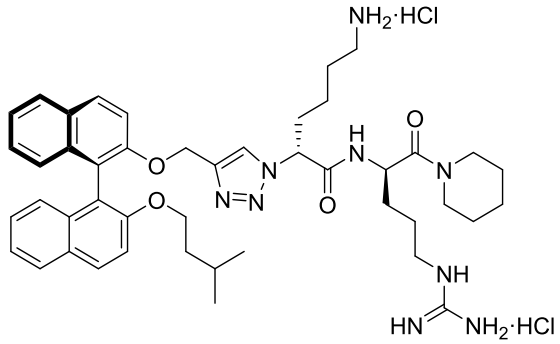

Following **General Procedure B**, acid **84** (50 mg, 0.05 mmol), piperidine (5 mg, 0.06 mmol), EDCI (11 mg, 0.06 mmol) and HOBt (8 mg, 0.05 mmol) were stirred in acetonitrile (0.5 mL) for 24 h to give the intermediate amide as a translucent tan gum. Following **General Procedure C**, the amide was dissolved in CH_2Cl_2 (1.4 mL) and treated with H_2O (17 mg, 0.94 mmol) and CF_3CO_2H (1.4 mL) followed by work-up with ethereal HCl to give the amine salt **85c** (31 mg, 76% over two steps) as a light tan powder that rapidly transitioned to a sticky gum. $[\alpha]_D^{23}$ −18.5 (*c* 0.60, MeOH); ^{1}H NMR (400 MHz, CD_3OD) : (mixture of rotamers) δ 8.05 – 7.93 (m, 2H, ArH), 7.92 – 7.83 (m, 2H, ArH), 7.62 – 7.43 (m, 2H, ArH)‡, 7.37 – 7.11 (m, 5H), 7.10 – 6.98 (m, 2H), 5.45 – 5.26 (m, 1H)‡, 5.18 – 5.03 (m, 2H)‡, 4.75 – 4.66 (m, 1H)‡, 4.08 – 3.87 (m, 2H), 3.67 – 3.36 (m, 2H)‡, 3.28 – 3.06 (m, 4H)‡, 2.89 (m, 2H)‡, 2.22 – 2.05 (m, 1H), 1.99 – 1.08 (m, 18H), 0.56 (d, *J* = 6.4 Hz, 3H)‡, 0.53 (d, *J* = 5.9 Hz, 3H)‡; ^{13}C

‡ Indicates that the ^{1}H NMR resonance was split into two or more signals due to the presence of amide and carbamate rotamers (e.g. the *syn*- and *anti*-amide conformations).

NMR (101 MHz, CD_3OD) : (mixture of rotamers)† δ 170.9, 170.1, 158.9, 156.2, 155.4, 146.0, 135.6$^{\Delta}$, 135.5$^{\Delta}$, 131.6, 130.9, 130.74, 130.71, 129.3, 129.2, 127.5, 127.4, 126.6$^{\Delta}$, 126.4, 125.2, 124.8, 124.2, 122.6, 121.5, 117.7, 117.0, 69.2$^{\Delta}$, 65.1, 64.4, 50.7, 48.1, 44.7, 42.2, 40.6, 39.5, 33.2, 30.2, 27.8, 27.7, 26.8, 26.5, 25.8$^{\Delta}$, 25.6, 23.6, 23.0, 22.8; IR (neat) $\overline{\nu}_{max}$ 2950, 2924, 2869, 2367, 2322, 1734, 1718, 1700, 1684, 1669, 1653, 1636, 1623, 1591, 1559, 1540, 1507, 1490, 1457, 1437, 1419, 1395, 1363, 1340, 1261, 1243, 1222, 1107, 1082, 1048, 1015, 912, 865, 808, 747, 669, 613 cm^{-1}; MS (ESI +ve) *m*/2 396 ($[M + 2H]^{2+}$, 100%), *m/z* 790 ($[M + H]^{+}$, 38%); HRMS (ESI +ve TOF) calcd for $C_{45}H_{60}N_9O_4$ 790.4768, found 790.4802 ($[M + H]^{+}$).

† All ^{13}C NMR resonances (except those denoted with a Δ symbol) were split into two resonances due to the presence of amide and/or carbamate rotamers (e.g. the *syn*- and *anti*-amide conformations); only the major resonance from each resonance pair is reported for clarity.

Δ Indicates that the ^{13}C NMR resonance was **not** split into multiple resonances due to rotamers.

6.3.6 – Series C

(*R*)-2-(2-(((*S*)-2'-(Isopentyloxy)-[1,1'-binaphthalen]-2-yl)oxy)acetamido)-5-(2-((2,2,4,6,7-pentamethyl-2,3-dihydrobenzofuran-5-yl)sulfonyl)guanidino)pentanoic acid (86)

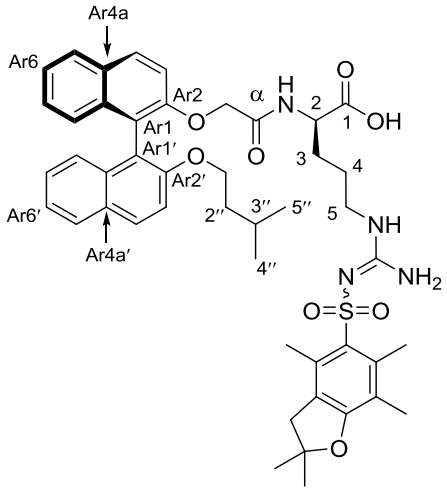

Following **General Procedure B**, acid **42** (246 mg, 0.59 mmol), amine **29** (261 mg, 0.59 mmol), EDCI (136 mg, 0.71 mmol) and HOBt (107 mg, 0.64 mmol) were stirred in acetonitrile (6.0 mL) for 21 h to give the intermediate amide as a translucent tan gum after flash chromatography over SiO_2 gel (EtOAc). To a solution of the amide in THF (5.0 mL) was added $LiOH{\cdot}H_2O$ (210 mg, 5.00 mmol) and H_2O (5.0 mL) followed by vigorous stirring at rt for 18 h. The reaction mixture was diluted with 1.0 M aqueous HCl (50 mL), extracted with EtOAc (3 x 40 mL) and the combined extracts were dried ($MgSO_4$), filtered and concentrated to afford the acid **86** (398 mg, 82% over two steps) as a translucent tan gum after flash chromatography over SiO_2 gel ($MeOH/CH_2Cl_2$ – 10:90). TLC ($MeOH/CH_2Cl_2$ – 5:95) R_F = 0.31; $[\alpha]_D^{23}$ −4.1 (*c* 1.87, MeOH); ^1H NMR (400 MHz, CD_3OD) δ 8.03 – 7.94 (m, 2H, ArH), 7.92 – 7.81 (m, 2H, ArH), 7.75 (br s, 1H, N^2-H), 7.50 – 7.39 (m, 2H, ArH), 7.36 – 7.27 (m, 1H, ArH), 7.23 – 7.14 (m, 2H, ArH), 7.12 – 6.95 (m, 3H, ArH), 4.54 and 4.42 (ABq, *J* = 14.6 Hz, 2H, $-OCH_2-C\alpha$), 4.16 (br s, 1H, H2), 4.12 – 4.04 (m, 1H, $H1''_A$ or $H1''_B$), 3.99 – 3.88 (m, 1H, $H1''_B$ or $H1''_A$), 3.08 – 2.84 (m, 4H, H5 and $ArCH_2$-), 2.60 (s, 3H, $ArCH_3$), 2.53 (s, 3H, $ArCH_3$), 2.11 (s, 3H, $ArCH_3$), 1.56 – 1.44 (m, 1H, $H3_A$ or $H3_B$), 1.41 – 1.12 (m, 11H, H4, H2″, H3″ and $-C(CH_3)_2$), 1.09 – 0.96 (m, 1H, $H3_B$ or $H3_A$), 0.58 (d, *J* = 6.4 Hz, 3H, H4″ or

H5″), 0.52 (d, J = 6.4 Hz, 3H, H5″ or H4″); ^{13}C NMR (101 MHz, CD_3OD)† δ 173.8 (C1), 170.6 (Cα), 160.4 (Pbf C_{Ar} – observed by gHMBC), 156.1 (CAr2′), 154.0 (CAr2), 139.8 (Pbf C_{Ar} – observed by gHMBC), 135.4 (CAr8a or CAr8a′), 135.1 (CAr8a′ or CAr8a), 134.5 (Pbf C_{Ar} – observed by gHMBC), 133.7 (Pbf C_{Ar} – observed by gHMBC), 131.5 (CAr4a), 131.10 (CAr4), 131.06 (CAr4′), 130.8 (CAr4a′), 129.5 (CAr5), 129.3 (CAr5′), 127.74 (CAr7), 127.70 (CAr7′), 126.6 (CAr8), 126.4 (Pbf C_{Ar} – observed by gHMBC), 126.0 (CAr8′), 125.4 (CAr6), 125.0 (CAr6′), 121.9 (CAr1), 120.6 (CAr1′), 118.7 (Pbf C_{Ar} – observed by gHMBC), 117.1 (CAr3), 115.9 (CAr3′), 88.1 (-$\underline{C}(CH_3)_2$ – observed by gHMBC), 69.2 (C1″), 69.2 (-O$\underline{C}H_2$-Cα), 52.4 (C2), 44.1 (ArCH_2-), 41.6 (C5 – observed by gHSQC), 39.4 (C2″), 30.9 (C4), 30.1 (C3), 28.9 (-C($\underline{C}H_3)_2$), 25.8 (C3″), 22.9 (C4″ or C5″), 22.8 (C5″ or C4″), 19.9 (ArCH_3), 18.6 (ArCH_3), 12.8 (ArCH_3); IR (neat) $\bar{\nu}_{max}$ 2953, 2926, 2372, 2324, 1734, 1718, 1700, 1684, 1653, 1636, 1617, 1577, 1559, 1540, 1521, 1507, 1490, 1473, 1457, 1437, 1419, 1395, 1363, 1340, 1271, 1243, 1147, 1092, 852, 808, 779, 748, 668, 619, 609 cm^{-1}; MS (ESI −ve) *m/z* 821 ([M − H]$^-$, 100%); HRMS (ESI +ve TOF) calcd for $C_{46}H_{54}N_4O_8SNa$ 845.3560, found 845.3597 ([M + Na]$^+$).

† The guanidine carbon (C=N) could not be assigned to a resonance in the ^{13}C NMR spectrum. This carbon was easily observed and assigned to resonances in the ^{13}C NMR spectra of the corresponding amide derivatives (as seen below).

(*R*)-*N*-Benzyl-5-guanidino-2-(2-(((*S*)-2'-(isopentyloxy)-[1,1'-binaphthalen]-2-yl)oxy)acetamido)pentanamide hydrochloride (87a)

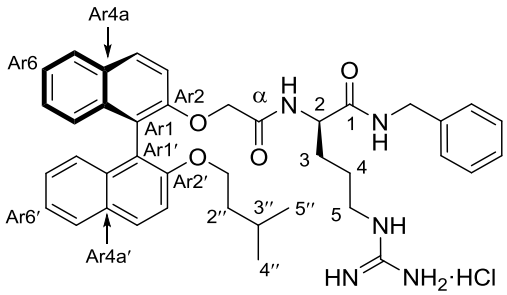

Following **General Procedure B**, acid **86** (50 mg, 0.06 mmol), benzylamine (8 mg, 0.07 mmol), EDCI (14 mg, 0.07 mmol) and HOBt (10 mg, 0.07 mmol) were stirred in acetonitrile (0.6 mL) for 22 h to give the intermediate amide as a translucent tan gum. Following **General Procedure C**, the amide was dissolved in CH_2Cl_2 (1.8 mL) and treated with H_2O (22 mg, 1.21 mmol) and CF_3CO_2H (1.8 mL) followed by work-up with ethereal HCl to give the amine salt **87a** (41 mg, 97% over two steps) as a light tan powder that rapidly transitioned to a sticky gum. $[\alpha]_D^{23}$ −7.5 (*c* 0.83, MeOH); ^{1}H NMR (400 MHz, CD_3OD) δ 8.06 – 7.97 (m, 2H, ArH), 7.95 – 7.86 (m, 2H, ArH), 7.52 (d, *J* = 9.0 Hz, 1H, ArH), 7.46 (d, *J* = 9.0 Hz, 1H, ArH), 7.39 – 7.15 (m, 9H, ArH), 7.10 – 7.02 (m, 2H, ArH), 4.57 and 4.43 (ABq, *J* = 14.7 Hz, 2H, -OCH_2-Cα), 4.37 – 4.25 (m, 2H, -C$\underline{H}_2$Ph), 4.23 (t, *J* = 6.0 Hz, 1H, H2), 4.08 (dt, *J* = 9.7, 6.1 Hz, 1H, H1″$_A$ or H1″$_B$), 3.93 (dt, *J* = 9.6, 6.4 Hz, 1H, H1″$_B$ or H1″$_A$), 3.09 – 2.89 (m, 2H, H5), 1.62 – 1.49 (m, 1H, H3$_A$ or H3$_B$), 1.31 – 1.02 (m, 6H, H3$_B$ or H3$_A$, H4, H2″ and H3″), 0.56 (d, *J* = 6.5 Hz, 3H, H4″ or H5″), 0.50 (d, *J* = 6.4 Hz, 3H, H5″ or H4″); ^{13}C NMR (101 MHz, CD_3OD) δ 172.9 (C1), 171.0 (Cα), 158.7 (C=N), 156.1 (CAr2′), 154.2 (CAr2), 140.0 (Phenyl C_{Ar}), 135.4 (CAr8a or CAr8a′), 135.2 (CAr8a′ or CAr8a), 131.6 (CAr4a), 131.13 (CAr4), 131.09 (CAr4′), 130.9 (CAr4a′), 129.8 (Phenyl C_{Ar})*, 129.5 (CAr5), 129.3 (CAr5′), 128.7 (Phenyl C_{Ar})*, 128.5 (Phenyl C_{Ar}), 127.8 (CAr7), 127.7 (CAr7′), 126.6 (CAr8), 126.1 (CAr8′), 125.4 (CAr6), 125.0 (CAr6′), 122.1 (CAr1), 120.8 (CAr1′), 117.3 (CAr3), 116.3 (CAr3′), 69.6 (C1″), 69.3 (-O$\underline{C}H_2$-Cα), 53.3 (C2), 44.2

(-CH$_2$Ph), 41.9 (C5), 39.5 (C2″), 30.5 (C3), 25.9 (C4), 25.8 (C3″), 23.0 (C4″ or C5″), 22.8 (C5″ or C4″); IR (neat) $\overline{\nu}_{max}$ 3334, 3188, 2954, 2926, 2376, 2323, 1734, 1718, 1700, 1684, 1653, 1636, 1617, 1577, 1559, 1540, 1521, 1507, 1490, 1473, 1457, 1437, 1419, 1395, 1363, 1340, 1329, 1271, 1242, 1215, 1147, 1094, 1073, 1047, 920, 862, 807, 775, 747, 696, 669, 621, 608 cm^{-1}; MS (ESI +ve) *m/z* 660 ([M + H]$^+$, 100%), 682 ([M + Na]$^+$, 16%); HRMS (ESI +ve TOF) calcd for $C_{40}H_{46}N_5O_4$ 660.3550, found 660.3553 ([M + H]$^+$).

(*R*)-5-Guanidino-2-(2-(((*S*)-2'-(isopentyloxy)-[1,1'-binaphthalen]-2-yl)oxy)acetamido)-*N*-phenethylpentanamide hydrochloride (87b)

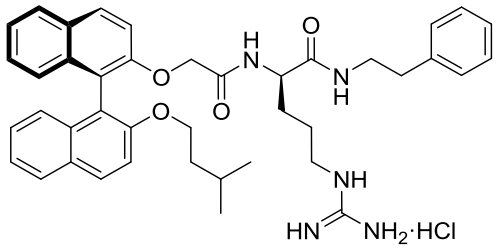

Following **General Procedure B**, acid **86** (50 mg, 0.06 mmol), β-phenylethylamine (9 mg, 0.07 mmol), EDCI (14 mg, 0.07 mmol) and HOBt (10 mg, 0.07 mmol) were stirred in acetonitrile (0.6 mL) for 22 h to give the intermediate amide as a translucent tan gum. Following **General Procedure C**, the amide was dissolved in CH_2Cl_2 (1.8 mL) and treated with H_2O (22 mg, 1.21 mmol) and CF_3CO_2H (1.8 mL) followed by work-up with ethereal HCl to give the amine salt **87b** (42 mg, 97% over two steps) as a light tan powder that rapidly transitioned to a sticky gum. $[\alpha]_D^{23}$ −3.7 (*c* 0.97, MeOH); ^{1}H NMR (400 MHz, CD_3OD) δ 8.05 – 7.98 (m, 2H), 7.94 – 7.86 (m, 2H), 7.56 (d, *J* = 9.1 Hz, 1H), 7.46 (d, *J* = 9.0 Hz, 1H), 7.38 – 7.12 (m, 9H), 7.10 – 7.02 (m, 2H), 4.52 and 4.44 (ABq, *J* = 14.8 Hz, 2H), 4.18 – 4.08 (m, 2H), 3.96 (dt, *J* = 9.5, 6.5 Hz, 1H), 3.42 – 3.32 (m, 2H), 3.02 – 2.89 (m, 2H), 2.79 – 2.67 (m, 2H), 1.53 – 1.41 (m, 1H), 1.34 – 0.96 (m, 6H), 0.57 (d, *J* = 6.5 Hz, 3H), 0.52 (d, *J* = 6.4 Hz, 3H); ^{13}C NMR (101 MHz, CD_3OD) δ 172.8, 170.9, 158.7, 156.1, 154.3, 140.5, 135.4, 135.2, 131.7, 131.14,

131.08, 131.0, 130.1*, 129.7*, 129.5, 129.3, 127.8, 127.7, 127.6, 126.6, 126.1, 125.4, 125.0, 122.2, 120.8, 117.2, 116.3, 69.6, 69.3, 53.2, 42.1, 41.9, 39.5, 36.6, 30.5, 25.9, 25.8, 23.0, 22.8; IR (neat) $\bar{\nu}_{max}$ 3335, 3185, 2953, 2926, 2874, 2376, 2323, 1734, 1718, 1700, 1684, 1653, 1636, 1617, 1577, 1559, 1540, 1521, 1507, 1490, 1473, 1457, 1437, 1419, 1395, 1363, 1340, 1319, 1271, 1244, 1215, 1147, 1094, 1072, 1048, 920, 861, 808, 775, 747, 698, 668, 620, 609 cm^{-1}; MS (ESI +ve) *m/z* 674 ($[M + H]^+$, 100%), 696 ($[M + Na]^+$, 14%); HRMS (ESI +ve TOF) calcd for $C_{41}H_{48}N_5O_4$ 674.3706, found 674.3722 ($[M + H]^+$).

(*R*)-*N*-(4-Fluorophenethyl)-5-guanidino-2-(2-(((*S*)-2'-(isopentyloxy)-[1,1'-binaphthalen]-2-yl)oxy)acetamido)pentanamide hydrochloride (87c)

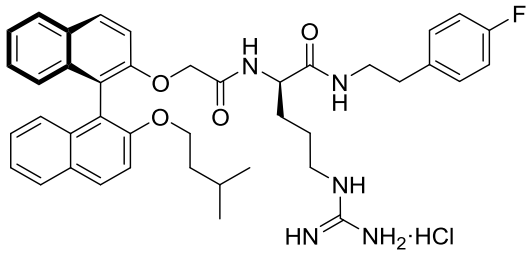

Following **General Procedure B**, acid **86** (40 mg, 0.05 mmol), 2-(4-fluorophenyl)ethylamine (8 mg, 0.06 mmol), EDCI (11 mg, 0.06 mmol) and HOBt (8 mg, 0.06 mmol) were stirred in acetonitrile (0.5 mL) for 22 h to give the intermediate amide as a translucent tan gum. Following **General Procedure C**, the amide was dissolved in CH_2Cl_2 (1.5 mL) and treated with H_2O (18 mg, 1.00 mmol) and CF_3CO_2H (1.5 mL) followed by work-up with ethereal HCl to give the amine salt **87c** (26 mg, 74% over two steps) as a light tan powder that rapidly transitioned to a sticky gum. $[\alpha]_D^{23}$ −9.2 (*c* 0.50, MeOH); ^{1}H NMR (400 MHz, CD_3OD) δ 8.06 – 8.00 (m, 2H), 7.93 – 7.88 (m, 2H), 7.56 (d, *J* = 9.1 Hz, 1H), 7.48 (d, *J* = 9.0 Hz, 1H), 7.39 – 7.29 (m, 2H), 7.26 – 7.14 (m, 4H), 7.10 – 7.03 (m, 2H), 6.98 (app. t, *J* = 8.8 Hz, 2H), 4.49 (ABq, *J* = 14.8 Hz, 2H), 4.18 – 4.08 (m, 2H), 3.97 (dt, *J* = 9.5, 6.6 Hz, 1H), 3.40 – 3.32 (m, 2H), 3.03 – 2.91 (m, 2H), 2.73 (t, *J* = 7.2 Hz, 2H), 1.50 – 1.40 (m, 1H), 1.33 – 0.97 (m, 6H),

0.58 (d, J = 6.5 Hz, 3H), 0.52 (d, J = 6.5 Hz, 3H); ^{13}C NMR (101 MHz, CD_3OD) δ 172.8, 170.9, 163.2 (d, $^1J_{CF}$ = 242.7 Hz), 158.7, 156.1, 154.3, 136.5 (d, $^4J_{CF}$ = 3.2 Hz), 135.5, 135.3, 131.8 (d, $^3J_{CF}$ = 7.9 Hz), 131.7, 131.14, 131.10, 131.0, 129.5, 129.3, 127.8, 127.7, 126.6, 126.1, 125.5, 125.0, 122.2, 120.8, 117.2, 116.3, 116.2 (d, $^2J_{CF}$ = 21.3 Hz), 69.6, 69.3, 53.1, 42.1, 41.9, 39.5, 35.7, 30.5, 25.9, 25.8, 23.0, 22.7; IR (neat) $\bar{\nu}_{max}$ 3335, 3184, 2954, 2927, 2873, 2375, 2323, 1734, 1718, 1700, 1684, 1653, 1636, 1623, 1577, 1559, 1540, 1521, 1507, 1490, 1473, 1457, 1437, 1419, 1395, 1363, 1340, 1319, 1272, 1243, 1219, 1147, 1096, 1074, 1048, 1016, 920, 860, 807, 775, 748, 669, 620, 609 cm^{-1}; MS (ESI +ve) *m/z* 692 ([M + H]$^+$, 100%), 714 ([M + Na]$^+$, 6%); HRMS (ESI +ve TOF) calcd for $C_{41}H_{47}N_5O_4F$ 692.3612, found 692.3634 ([M + H]$^+$).

Tert-butyl ((_R_)-6-azido-5-(2-(((_S_)-2'-(isopentyloxy)-[1,1'-binaphthalen]-2-yl)oxy)acetamido)hexyl)carbamate (88)

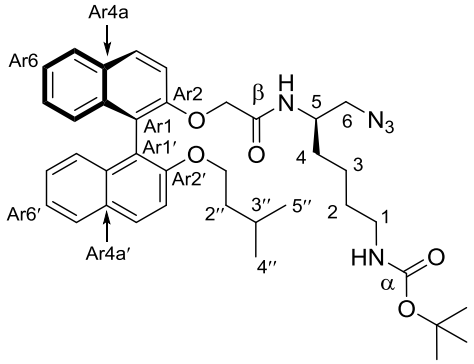

Following **General Procedure B**, acid **42** (207 mg, 0.50 mmol), amine **22** (142 mg, 0.55 mmol), EDCI (115 mg, 0.60 mmol) and HOBt (81 mg, 0.54 mmol) were stirred in acetonitrile (5.0 mL) for 24 h to give the product amide **88** (309 mg, 94%) as a translucent tan gum after flash chromatography over SiO_2 gel (EtOAc). TLC (MeOH/CH_2Cl_2 – 5:95): R_F = 0.45, (EtOAc/P.S. – 30:70) R_f = 0.17; $[\alpha]_D^{23}$ −28.7*c* 0.73, CH_2Cl_2); ^{1}H NMR (500 MHz, $CDCl_3$) δ 8.01 (d, J = 9.1 Hz, 1H, ArH), 7.99 (d, J = 8.9 Hz, 1H, ArH), 7.89 (app. t, J = 6.7 Hz, 2H, ArH), 7.48 (d, J = 9.1 Hz, 1H, ArH), 7.39 – 7.29 (m, 3H, ArH), 7.28 – 7.22 (m, 2H, ArH), 7.18 (app. t, J = 9.2 Hz, 2H, ArH), 5.60 (d,

J = 9.1 Hz, 1H, N^5-H), 4.48 (s, 2H, -OCH_2-Cβ), 4.42 (br s, 1H, N^1-H), 4.01 (dt, *J* = 9.4, 6.3 Hz, 1H, H1″$_A$ or H1″$_B$), 3.94 (dt, *J* = 9.5, 6.4 Hz, 1H, H1″$_B$ or H1″$_A$), 3.79 – 3.72 (m, 1H, H5), 3.06 (dd, *J* = 12.3, 4.7 Hz, 1H, H6$_A$ or H6$_B$), 2.99 – 2.88 (m, 3H, H1 and H6$_B$ or H6$_A$), 1.44 (s, 9H, -$C(CH_3)_3$), 1.33 – 1.15 (m, 6H, H2, H4$_A$ or H4$_B$, H2″ and H3″), 1.11 – 1.02 (m, 1H, H4$_B$ or H4$_A$), 0.86 – 0.76 (m, 2H, H3), 0.60 (d, *J* = 6.5 Hz, 3H, H4″ or H5″), 0.56 (d, *J* = 6.4 Hz, 3H, H5″ or H4″); ^{13}C NMR (125 MHz, $CDCl_3$) δ 167.9 (Cβ), 155.8 (Cα), 154.5 (CAr2′), 151.9 (CAr2), 133.8 (CAr8a or CAr8a′), 133.6 (CAr8a′ or CAr8a), 129.7 (CAr4a), 129.6 (CAr4), 129.4 (CAr4′), 129.1 (CAr4a′), 127.86 (CAr5), 127.92 (CAr5′), 126.6 (CAr7), 126.5 (CAr7′), 125.3 (CAr8), 124.9 (CAr8′), 124.0 (CAr6), 123.8 (CAr6′), 120.1 (CAr1), 119.5 (CAr1′), 115.7 (CAr3), 113.8 (CAr3′), 78.9 (-$\underline{C}(CH_3)_3$), 68.1 (C1″), 67.7 (-O$\underline{C}H_2$-Cβ), 54.2 (C6), 47.6 (C5), 40.1 (C1), 37.9 (C2″), 31.0 (C4), 29.3 (C2), 28.3 (-$C(\underline{C}H_3)_3$), 24.5 (C3″), 22.6 (C3), 22.1 (C4″ or C5″), 22.0 (C5″ or C4″); IR (neat) $\overline{\nu}_{max}$ 3385, 2930, 2101, 1683, 1506, 1457, 1363, 1243, 1168, 1094, 807, 747 cm^{-1}; MS (ESI +ve) *m/z* 676 ($[M + Na]^+$, 100%); HRMS (ESI +ve TOF) calcd for $C_{38}H_{48}N_5O_5$ 654.3655, found 654.3657 ($[M + H]^+$).

_N_-((_R_)-6-Amino-1-(4-benzyl-1_H_-1,2,3-triazol-1-yl)hexan-2-yl)-2-(((_S_)-2'-(isopentyloxy)-[1,1'-binaphthalen]-2-yl)oxy)acetamide hydrochloride (89a)

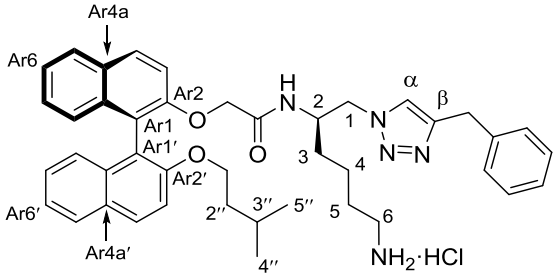

Following **General Procedure A**, azide **88** (50 mg, 0.08 mmol), 3-phenyl-1-propyne (27 mg, 0.23 mmol), $Cu(OAc)_2{\cdot}H_2O$ (3 mg, 0.02 mmol) and sodium ascorbate (6 mg, 0.03 mmol) were stirred in *t*-BuOH (1.6 mL) and H_2O (0.4 mL) for 20 h to give the intermediate triazole as a light tan gum after flash chromatography over SiO_2 gel ($MeOH/CH_2Cl_2$ – 0:100 → 10:90).

Following **General Procedure C**, the triazole was dissolved in CH_2Cl_2 (2.3 mL) and treated with H_2O (27 mg, 1.52 mmol) and CF_3CO_2H (2.3 mL) followed by work-up with ethereal HCl to give the amine salt **89a** (27 mg, 50% over two steps) as a light tan powder that rapidly transitioned to a sticky gum. $[\alpha]_D^{23}$ −14.5 (*c* 0.58, MeOH); ^{1}H NMR (500 MHz, CD_3OD) δ 8.08 (d, *J* = 9.1 Hz, 1H, ArH), 8.04 (d, *J* = 9.1 Hz, 1H, ArH), 7.98 (d, *J* = 8.2 Hz, 1H, ArH), 7.93 (d, *J* = 8.2 Hz, 1H, ArH), 7.59 (d, *J* = 9.0 Hz, 1H, ArH), 7.44 – 7.34 (m, 3H, ArH), 7.31 – 7.22 (m, 2H, ArH), 7.22 – 7.08 (m, 8H, Hα and ArH), 4.38 and 4.11 (ABq, *J* = 14.6 Hz, 2H, -CH_AH_B-C=O), 4.31 (dd, *J* = 14.0, 4.3 Hz, 1H, $H1_A$ or $H1_B$), 4.10 – 3.98 (m, 2H, H2 and $H1''_A$ or $H1''_B$), 3.99 – 3.87 (m, 3H, $H1''_B$ or $H1''_A$ and -C<u>H</u>$_2$Ph), 3.67 (dd, *J* = 14.0, 9.2 Hz, 1H, $H1_B$ or $H1_A$), 2.81 – 2.66 (m, 2H, H6), 1.53 – 1.40 (m, 2H, H5), 1.36 – 1.25 (m, 1H, $H3_A$ or $H3_B$), 1.27 – 1.11 (m, 2H, H2″), 1.14 – 1.02 (m, 1H, H3″), 1.03 – 0.93 (m, 2H, H4), 0.88 – 0.76 (m, 1H, $H3_B$ or $H3_A$), 0.52 (d, *J* = 6.6 Hz, 3H, H4″ or H5″), 0.48 (d, *J* = 6.6 Hz, 3H, H5″ or H4″); ^{13}C NMR (125 MHz, CD_3OD) δ 170.7 (C=O), 156.1 (CAr2′), 153.7 (CAr2), 148.2 (Cβ), 140.4 (Phenyl C_{Ar}), 135.2 (CAr8a or CAr8a′), 135.1 (CAr8a′ or CAr8a), 131.5 (CAr4a), 131.1 (CAr4 and CAr4′), 130.8 (CAr4a′), 129.7 (Phenyl C_{Ar})*, 129.5 (CAr5 and Phenyl C_{Ar})*, 129.2 (CAr5′), 128.0 (Phenyl C_{Ar}), 127.7 (CAr7), 127.5 (CAr7′), 126.3 (CAr8), 126.1 (CAr8′), 125.3 (CAr6), 125.2 (CAr6′), 124.3 (Cα), 121.5 (CAr1), 121.1 (CAr1′), 117.3 (CAr3), 115.7 (CAr3′), 69.4 (C1″), 68.9 (-O<u>C</u>H_2-C=O), 54.3 (C1), 50.0 (C2), 40.5 (C6), 39.3 (C2″), 32.5 (C3), 32.0 (-<u>C</u>H_2Ph), 27.8 (C5), 25.5 (C3″), 23.4 (C4), 22.8 (C4″ or C5″), 22.4 (C5″ or C4″); IR (neat) $\bar{\nu}_{max}$ 3650, 2957, 1734, 1683, 1653, 1558, 1506, 1457, 1244, 1073, 809, 750 cm^{-1}; MS (ESI +ve) *m/z* 670 ($[M + H]^+$, 100%), 692 ($[M + Na]^+$, 10%); HRMS (ESI +ve TOF) calcd for $C_{42}H_{47}N_5O_3Na$ 692.3577, found 692.3611 ($[M + Na]^+$).

***N*-((*R*)-6-Amino-1-(4-phenyl-1*H*-1,2,3-triazol-1-yl)hexan-2-yl)-2-(((*S*)-2'-(isopentyloxy)-[1,1'-binaphthalen]-2-yl)oxy)acetamide hydrochloride (89b)**

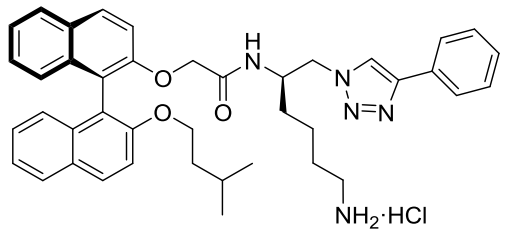

Following **General Procedure A**, azide **88** (50 mg, 0.08 mmol), phenylacetylene (24 mg, 0.23 mmol), $Cu(OAc)_2 \cdot H_2O$ (3 mg, 0.02 mmol) and sodium ascorbate (6 mg, 0.03 mmol) were stirred in *t*-BuOH (1.6 mL) and H_2O (0.4 mL) for 20 h to give the intermediate triazole as a light tan gum after flash chromatography over SiO_2 gel ($MeOH/CH_2Cl_2$ – 0:100 → 10:90). Following **General Procedure C**, the triazole was dissolved in CH_2Cl_2 (2.3 mL) and treated with H_2O (27 mg, 1.52 mmol) and CF_3CO_2H (2.3 mL) followed by work-up with ethereal HCl to give the amine salt **89b** (37 mg, 70% over two steps) as a light tan powder that rapidly transitioned to a sticky gum. $[\alpha]_D^{23}$ −19.7 (*c* 1.22, MeOH); ^{1}H NMR (500 MHz, CD_3OD) δ 8.10 – 7.82 (m, 6H), 7.74 (d, *J* = 7.5 Hz, 2H), 7.51 (d, *J* = 9.0 Hz, 1H), 7.46 – 7.18 (m, 7H), 7.13 (d, *J* = 8.6 Hz, 1H), 7.09 (d, *J* = 8.6 Hz, 1H), 4.54 – 4.29 (m, 3H), 4.12 (br s, 1H), 4.00 – 3.80 (m, 3H), 2.86 – 2.64 (m, 2H), 1.59 – 1.39 (m, 2H), 1.35 – 1.22 (m, 1H), 1.22 – 1.08 (m, 2H), 1.08 – 0.93 (m, 3H), 0.93 – 0.74 (m, 1H), 0.50 (d, *J* = 6.6 Hz, 3H), 0.46 (d, *J* = 6.7 Hz, 3H); ^{13}C NMR (125 MHz, CD_3OD) δ 171.0, 156.1, 153.8, 150.3, 135.2, 135.0, 131.6, 131.4, 131.1, 131.0, 130.0*, 129.44, 129.42, 129.2, 127.9, 127.6, 126.7*, 126.3, 126.1, 125.3, 125.2, 122.7, 121.5, 121.0, 117.3, 115.6, 69.4, 69.0, 54.2, 50.0, 40.5, 39.2, 31.9, 27.9, 25.5, 23.5, 22.7, 22.4; IR (neat) $\overline{\nu}_{max}$ 3373, 2954, 1683, 1653, 1558, 1506, 1244, 1147, 809, 765 cm^{-1}; MS (ESI +ve) *m/z* 656 ($[M + H]^+$, 100%); HRMS (ESI +ve TOF) calcd for $C_{41}H_{45}N_5O_3Na$ 678.3420, found 678.3448 ($[M + Na]^+$).

***N*-((*R*)-6-Amino-1-(4-isopentyl-1*H*-1,2,3-triazol-1-yl)hexan-2-yl)-2-(((*S*)-2'-(isopentyloxy)-[1,1'-binaphthalen]-2-yl)oxy)acetamide hydrochloride (89c)**

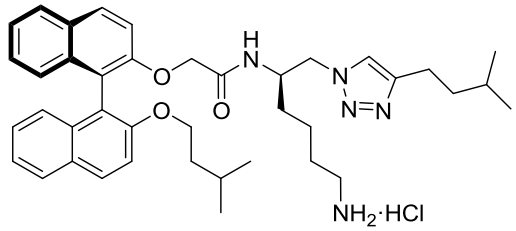

Following **General Procedure A**, azide **88** (50 mg, 0.08 mmol), 5-methyl-1-hexyne (22 mg, 0.23 mmol), $Cu(OAc)_2 \cdot H_2O$ (3 mg, 0.02 mmol) and sodium ascorbate (6 mg, 0.03 mmol) were stirred in *t*-BuOH (1.6 mL) and H_2O (0.4 mL) for 20 h to give the intermediate triazole as a light tan gum after flash chromatography over SiO_2 gel ($MeOH/CH_2Cl_2$ – 0:100 → 10:90). Following **General Procedure C**, the triazole was dissolved in CH_2Cl_2 (2.3 mL) and treated with H_2O (27 mg, 1.52 mmol) and CF_3CO_2H (2.3 mL) followed by work-up with ethereal HCl to give the amine salt **89c** (37 mg, 70% over two steps) as a light tan powder that rapidly transitioned to a sticky gum. ^{1}H NMR (500 MHz, CD_3OD) δ 8.10 (d, *J* = 8.9 Hz, 1H), 8.04 (d, *J* = 9.0 Hz, 1H), 7.98 (d, *J* = 8.3 Hz, 1H), 7.92 (d, *J* = 8.1 Hz, 1H), 7.62 (d, *J* = 9.0 Hz, 1H), 7.44 – 7.33 (m, 3H), 7.27 (m, 2H), 7.20 (s, 1H), 7.15 (d, *J* = 8.6 Hz, 1H), 7.11 (d, *J* = 8.5 Hz, 1H), 4.45 and 4.34 (ABq, *J* = 14.6 Hz, 2H), 4.27 (dd, *J* = 13.9, 4.5 Hz, 1H), 4.13 – 4.01 (m, 2H), 4.01 – 3.90 (m, 1H), 3.74 (dd, *J* = 13.9, 8.7 Hz, 1H), 2.80 – 2.66 (m, 2H), 2.65 – 2.53 (m, 2H), 1.54 – 1.37 (m, 4H), 1.37 – 1.06 (m, 6H), 1.02 – 0.76 (m, 8H), 0.56 (d, *J* = 6.5 Hz, 3H), 0.51 (d, *J* = 6.6 Hz, 3H); ^{13}C NMR (125 MHz, CD_3OD) δ 170.8, 156.1, 153.8, 149.2, 135.2, 135.1, 131.5, 131.09, 131.05, 130.8, 129.5, 129.2, 127.9, 127.7, 126.3, 126.1, 125.3, 125.2, 123.4, 121.6, 121.1, 117.3, 115.8, 69.4, 69.1, 54.2, 49.9, 40.4, 39.7, 39.3, 32.0, 28.6, 27.8, 25.6, 24.2, 23.4, 22.8, 22.7*, 22.5; IR (neat) $\bar{\nu}_{max}$ 3363, 2956, 2361, 1680, 1653, 1507, 1272, 1203, 1136, 810 cm^{-1}; MS (ESI +ve) *m/z* 650 ([M + H]$^+$, 100%); HRMS (ESI +ve TOF) calcd for $C_{40}H_{52}N_5O_3$ 650.4070, found 650.4043 ([M + H]$^+$).

6.4 – Microbiology and pharmacology

6.4.1 – Minimum inhibitory concentration (MIC) and cytotoxicity assays

Primary screening (University of Western Australia)

The following experiments were performed by Dr. Katherine Hammer and/or Dr. Daniel Knight. MIC assays were performed on *Staphylococcus aureus* (ATCC 29213), methicillin-resistant *Staphylococcus aureus* (NCTC 10442), *Enterococcus faecalis* (ATCC 29212) and *Escherichia coli* (ATCC 25922) in Mueller Hinton broth and incubation was performed in ambient air at 35 °C for 24 h. *Streptococcus pneumoniae* (ATCC 49619) was cultivated in Mueller Hinton broth with 2.5% lysed horse blood and incubated with 5% CO_2 at 35 °C for 24 h. MIC studies for *Clostridium difficile* (ATCC 700057) and *Clostridium difficile* (NSW132 - RT027) were conducted in Brucella broth supplemented with haemin and vitamin K and incubation was performed anaerobically at 35 °C for 48 h. Each compound was dissolved in DMSO at 5 mg/mL and then diluted to 512 μg/mL with sterile, distilled water. The compounds were then serially diluted in 100 μL volumes of sterile, distilled water in a 96-well microtitre tray. Each test organism in double strength broth (100 μL) was then added to each well and incubated as described above. Testing concentrations of the compounds ranged from 0.25 μg/mL to 128 μg/mL. Vancomycin and a control well (i.e. no antibacterial compound present) were included in the assays. A DMSO control (5% v/v) was also tested to ensure that the solvent did not inhibit bacterial growth. The assay was performed in triplicate for each organism/compound combination and the modal MIC values were recorded. The MIC was recorded as the lowest concentration that inhibited bacterial growth. The minimum bactericidal concentration (MBC) was also recorded as the lowest concentration that caused cellular death.

Secondary screening (Community for Open Antimicrobial Drug Discovery (CO-ADD))

Samples were provided to CO-ADD for antimicrobial screening by whole cell growth inhibition assays. The inhibition of growth was measured against five bacteria: *Escherichia coli (*ATCC 25922), *Klebsiella pneumoniae* (ATCC 700603), *Acinetobacter baumannii* (ATCC 19606), *Pseudomonas aeruginosa* (ATCC 27853) and *Staphylococcus aureus* (ATCC 43300), and two fungi: *Candida albicans* (ATCC 90028) and *Cryptococcus neoformans* (ATCC 208821). In addition to MIC, compounds were screened for cytotoxicity against a human embryonic kidney cell line (HEK293) by determining their CC_{50} value.

Samples were prepared in DMSO to a final testing concentration of 32 μg/mL and serially diluted 1:2 fold for 8 times. Each sample concentration was prepared in 384-well plates, non-binding surface (NBS) plate (Corning 3640) for each bacterial/fungal strain and tissue-culture treated (Corning 3712/3764) black for mammalian cell types, all in duplicate (n = 2) and keeping the final DMSO concentration to a maximum of 0.5%. All the sample preparation was done using liquid handling robots.

Bacterial Inhibition

All bacteria were cultured in Cation-adjusted Mueller Hinton broth at 37 °C overnight. A sample of each culture was then diluted 40-fold in fresh broth and incubated at 37 °C for 1 – 3.5 h. The resultant mid-log phase cultures were diluted (CFU/mL measured by OD_{600}), then added to each well of the compound-containing plates, giving a cell density of 5×10^5 CFU/mL and a total volume of 50 μL. All plates were covered and incubated at 37 °C for 18 h without shaking. Inhibition of bacterial growth was determined by measuring absorbance at 600 nm (OD_{600}), using a Tecan M1000 Pro monochromator plate reader. The percentage of growth inhibition was calculated for each well, using the negative control

(media only) and positive control (bacteria without inhibitors) on the same plate as references. The MIC was determined as the lowest concentration at which growth was fully inhibited, defined by an inhibition ≥ 80%. Colistin and vancomycin were used as positive bacterial inhibitor standards for Gram-negative and Gram-positive bacteria, respectively. Each antibiotic standard was provided in four concentrations, with two above and two below its MIC value, and plated into the first eight wells of column 23 of the 384-well NBS plates.

Fungal Inhibition

Fungi strains were cultured for three days on Yeast Extract-Peptone Dextrose agar at 30 °C. A yeast suspension of 1×10^6 to 5×10^6 CFU/mL (as determined by OD_{530}) was prepared from five colonies. The suspension was subsequently diluted and added to each well of the compound-containing plates giving a final cell density of fungi suspension of 2.5×10^3 CFU/mL and a total volume of 50 µL. All plates were covered and incubated at 35 °C for 36 h without shaking. Growth inhibition for *C. albicans* was determined by measuring absorbance at 630 nm (OD_{630}), while the growth inhibition of *C. neoformans* was determined measuring the difference in absorbance between 600 and 570 nm ($OD_{600-570}$), after the addition of resazurin (0.001 % final concentration) and incubation at 35 °C for 2 h. The absorbance was measured using a Biotek Multiflo Synergy HTX plate reader. In both cases, the percentage of growth inhibition was calculated for each well, using the negative control (media only) and positive control (fungi without inhibitors) on the same plate. The MIC was determined as the lowest concentration at which the growth was fully inhibited, definied as an inhibition ≥ 80% for *C. albicans* and an inhibition ≥ 70% for *C. neoformans*. Due to the higher variance in growth and inhibition, a lower threshold was applied to the data for *C. neoformans*. Fluconazole was used a positive fungal inhibitor standard for *C. albicans* and

C. neoformans using the same control methodology as the bacterial inhibition assays. The antifungal standard was provided in four concentrations, with two above and two below its MIC value, and plated into the first eight wells of column 23 of the 384-well NBS plates.

Cytotoxicity Assay

HEK293 cells were counted manually in a Neubauer haemocytometer and then plated in the 384-well plates containing the compounds to give a density of 5000 cells/well in a final volume of 50 µL. Dulbecco's modified eagle medium (DMEM) supplemented with 10% fetal bovine serum (FBS) was used as a growth media and the cells were incubated together with the compounds for 20 h at 37 °C in 5% CO_2. Cytotoxicity (cell viability) was measured by fluorescence, ex: 560/10 nm, em: 590/10 nm ($F_{560/590}$), after addition of 5 µL of 25 µg/mL resazurin (2.3 µg/mL final concentration) and after incubation for further 3 h at 37 °C in 5% CO_2. The fluorescence intensity was measured using a Tecan M1000 Pro monochromator plate reader, using automatic gain calculation. CC_{50} (concentration at 50% cytotoxicity) values were calculated by curve-fitting the inhibition values vs. log(concentration) using a sigmoidal dose-response function, with variable fitting values for bottom, top and slope. Tamoxifen was utilized as a positive cytotoxicity standard; it was used in eight concentrations in two-fold serial dilutions with 50 µg/mL as the highest concentration tested.

6.4.2 – *In vivo* CDI mouse model (Monash University)

Study design

The foillowing *in vivo* study was performed by Prof. Dena Lyras, Dr. Melanie Hutton and Dr. Amy King. Mice were pre-treated with an antibiotic cocktail containing kanamycin (0.4 mg/ml; Amresco), gentamicin (0.035 mg/ml; Sigma), colistin (850 U/ml; Sigma), metronidazole (0.215 mg/ml; Sigma), vancomycin (0.045 mg/ml; Sigma) and cefaclor (0.3

mg/ml; Sigma) in the drinking water for seven days, followed by three days of cefaclor alone to disrupt the commensal microbiota and induce susceptibility to infection with *C. difficile*. The mice were switched to plain drinking water and given clean cages on the day of infection. Groups of five mice were infected with 10^5 *C. difficile* spores of the RT027 strain M7404. Six hours post-infection, mice were given 2.5 mg of the selected compounds (in 10% aqueous DMSO) by oral gavage. The mice were then administered fresh compound every 12 hours after the initial dose. The mice were monitored twice daily for weight loss and other physiological signs of infection. Blood was also collected at euthanasia and left to clot at room temperature prior to centrifugation. The serum was collected and frozen at −80 °C. Faeces collected at euthanasia was also frozen −80 °C for subsequent pharmacokinetic analysis. Note that mice were euthanised according to animal ethics guidelines: i.e. if the mice lose ≥ 10 % of their total body weight in the first 24 h or ≥ 15 % at any point after 24 h.

Sample preparation

Each compound was suspended in 100% DMSO to obtain a stock concentration of 250 mg/mL. Twenty minutes prior to administration, the compounds were diluted (1:10) by adding warm water (37 °C) to the compound stock solution to achieve a final concentration of 25 mg/mL. The compounds were vortexed and carried to the animal house floating in warm water in an attempt to maintain a homogeneous solution. They were then vortexed again immediately prior to gavaging the mice. Each mouse received 100 μL of solution containing 2.5 mg of compound – this equates to a dose of 100 mg/kg (based on an average 25 g mouse).

6.4.3 – Pharmacokinetics assay

Mouse blood analysis: procedure

A 200 μL aliquot of the mouse blood was placed into a glass vial and diluted with phosphate buffered saline (PBS) solution (3.3 mL). The solution was vortexed for 20 s and then CH_2Cl_2 (3.5 mL) was added and the mixture was manually swirled to ensure adequate mixing with minimal emulsion formation. The layers were allowed to separate and the CH_2Cl_2 was removed by syringe. The aqueous blood layer was extracted again with another aliquot of CH_2Cl_2 (3.5 mL). The two extracts were combined and evaporated under reduced pressure to obtain an opaque residue. The residue was dissolved in MeOH (2.0 mL) with the aid of ultrasonication (30 s); the solution was filtered through a PTFE membrane (0.45 μm). The obtained solution was then subjected to LRMS analysis.

Mouse blood analysis: procedure verification

To ensure the mouse blood analysis procedure was sufficiently sensitive to detect small amounts of drug absorption, unadulterated mouse blood (i.e. blood from an untreated cohort) was doped with a small quantity of lead compound **2** and then subjected to the analysis procedure. The volume of mouse blood was accounted for to ensure that an accurate concentration representative of a 1% systemic bioavailability was achieved. To dope the blood with the correct concentration, 50 μL of a 0.05 mg/mL solution of compound **2** in 0.1% DMSO in H_2O was added to the PBS diluent prior to extraction with CH_2Cl_2. The corresponding doubly-protonated molecular ion ($m/2 = 421 = [M + 2H]^{2+}$) was found in the LRMS spectrum of the doped blood, verifying the sensitivity of the analysis procedure.

Mouse faeces analysis: procedure

The obtained sample of mouse faeces (from the treated cohort) was added to a glass vial with CH_2Cl_2 (2.0 mL) and the mixture was stirred vigorously for 30 min. The solution was then filtered through a cotton plug and the solvent was removed under reduced pressure. The residue was taken up in MeOH (1.0 mL), sonicated for 30 s and then filtered through a PTFE membrane filter (0.45 μm). The obtained solution was then subjected to LRMS analysis.

6.4.4 – Comparative solubility assay

Procedure

Five milligrams of the target compound was fully dissolved in 50 μL DMSO. Small aliquots (5 μL) of H_2O were added to the DMSO solution with manual agitation in between each addition; additions were continued until a visible turbidity/cloudiness was apparent that did not fade after mixing. The quantity of H_2O required for precipitation of the compound was recorded; this value was then divided by the standard value (i.e. 15 μL = quantity of H_2O required to precipitate lead compound **1**) to obtain a comparative solubility ratio. This ratio helped to approximate the observed change in solubility that was observed for various compounds.

7.0 – References

1. World Health Organization. Antibiotic Resistance Fact Sheet. http://www.who.int/mediacentre/factsheets/antibiotic-resistance/en/ (accessed Oct 12th, 2017).
2. Centers for Disease Control. Antibiotic/Antimicrobial Resistance. https://www.cdc.gov/drugresistance/ (accessed Oct 12th, 2017)
3. Centers for Disease Control. Antibiotic Resistance Threats in the United States. **2013**. https://www.cdc.gov/drugresistance/threat-report-2013/index.html (accessed Oct 12th, 2017).
4. Pourmand, A.; Mazer-Amirshahi, M.; Jasani, G.; May, L. Emerging trends in antibiotic resistance: Implications for emergency medicine. *Am. J. Emerg. Med.* **2017**, *35* (8), 1172-1176.
5. Pendleton, J. N.; Gorman, S. P.; Gilmore, B. F., Clinical relevance of the ESKAPE pathogens. *Expert Rev. Anti-inf.* **2013**, *11* (3), 297-308.
6. Roca, I.; Akova, M.; Baquero, F.; Carlet, J.; Cavaleri, M.; Coenen, S.; Cohen, J.; Findlay, D.; Gyssens, I.; Heure, O. E.; et al. The global threat of antimicrobial resistance: science for intervention. *New Microbes New Infect.* **2015**, *6*, 22-9.
7. Martens, E.; Demain, A. L. The antibiotic resistance crisis, with a focus on the United States. *J. Antibiot.* **2017**, *70* (5), 520-526.
8. World Health Organization. Global Priority List of Antibiotic-Resistant Bacteria to Guide Research, Discovery and Development of New Antibiotics. **2017**. http://www.who.int/medicines/publications/WHO-PPL-Short_Summary_25Feb-ET_NM_WHO.pdf (accessed Oct 12th, 2017).
9. Williams, D. H.; Bardsley, B. The vancomycin group of antibiotics and the fight against resistant bacteria. *Angew. Chem. - Int. Edit.* **1999**, *38* (9), 1173-1193.

10. Ziemska, J.; Rajnisz, A.; Solecka, J. New perspectives on antibacterial drug research. *Cent. Eur. J. Biol.* **2013**, *8* (10), 943-957.

11. Levine, D. P. Vancomycin: Understanding its past and preserving its future. *South. Med. J.* **2008**, *101* (3), 284-291.

12. Hiramatsu, K.; Katayama, Y.; Matsuo, M.; Sasaki, T.; Morimoto, Y.; Sekiguchi, A.; Baba, T. Multi-drug-resistant *Staphylococcus aureus* and future chemotherapy. *J. Infect. Chemother.* **2014**, *20* (9-10), 593-601.

13. O'Neill, A. New antibacterial agents for treating infections caused by multi-drug resistant Gram-negative bacteria. *Expert Opin. Investig. Drugs* **2008**, *17* (3), 297-302.

14. Tazi, A.; Chapron, J.; Touak, G.; Longo, M.; Hubert, D.; Collobert, G.; Dusser, D.; Poyart, C.; Morand, P. C. Rapid Emergence of Resistance to Linezolid and Mutator Phenotypes in *Staphylococcus aureus* Isolates from an Adult Cystic Fibrosis Patient. *Antimicrob. Agents Chemother.* **2013**, *57* (10), 5186-5188.

15. Spellberg, B.; Guidos, R.; Gilbert, D.; Bradley, J.; Boucher, H. W.; Scheld, W. M.; Bartlett, J. G.; Edwards, J. The Epidemic of Antibiotic-Resistant Infections: A Call to Action for the Medical Community from the Infectious Diseases Society of America. *Clin. Infect. Dis.* **2008**, *46* (2), 155-164.

16. World Health Organization. Antimicrobial resistance: global report on surveillance 2014. http://www.who.int/antimicrobial-resistance/publications/surveillancereport/en/ (accessed on Oct 12th, 2017).

17. Leffler, D. A.; Lamont, J. T. Treatment of *Clostridium difficile*-Associated Disease. *Gastroenterology* **2009**, *136* (6), 1899-1912.

18. Eaton, S. R.; Mazuski, J. E. Overview of Severe *Clostridium difficile* Infection. *Crit. Care Clin.* **2013**, *29* (4), 827.

19. Aslam, S.; Hamill, R. J.; Musher, D. M. Treatment of *Clostridium difficile*-associated disease: old therapies and new strategies. *Lancet Infect. Dis.* **2005**, *5* (9), 549-557.

20. Jarrad, A. M.; Karoli, T.; Blaskovich, M. A. T.; Lyras, D.; Cooper, M. A. *Clostridium difficile* Drug Pipeline: Challenges in Discovery and Development of New Agents. *J. Med. Chem.* **2015**, *58* (13), 5164-5185.

21. Stanley, J. D.; Bartlett, J. G.; Dart, B. W.; Ashcraft, J. *Clostridium difficile* infection. *Curr. Probl. Surg.* **2013,** *50* (7), 302-337.

22. Johnson, A. P. New antibiotics for selective treatment of gastrointestinal infection caused by *Clostridium difficile*. *Expert Opin. Ther. Patents* **2010**, *20* (10), 1389-1399.

23. Centers for Disease Control. *Clostridium difficile* Update. **2015**. https://www.cdc.gov/media/releases/2015/p0225-clostridium-difficile.html (accessed Oct 12th, 2017)

24. Joseph, J.; Singhal, S.; Patel, G. M.; Anand, S. *Clostridium difficile* Colitis: Review of the Therapeutic Approach. *Am. J. Ther.* **2014**, *21* (5), 385-394.

25. Ritter, A. S.; Petri, W. A. New developments in chemotherapeutic options for *Clostridium difficile* colitis. *Curr. Opin. Infect. Dis.* **2013**, *26* (5), 461-470.

26. Ackermann, G.; Loffler, B.; Adler, D.; Rodloff, A. C. *In vitro* activity of OPT-80 against *Clostridium difficile*. *Antimicrob. Agents Chemother.* **2004**, *48* (6), 2280-2282.

27. Lofmark, S.; Edlund, C.; Nord, C. E. Metronidazole is Still the Drug of Choice for Treatment of Anaerobic Infections. *Clin. Infect. Dis.* **2010**, *50*, S16-S23.

28. Edwards, D. I. Nitroimidazole Drugs - Action and Resistance Mechanisms: 1. Mechanisms of Action. *J. Antimicrob. Chemother.* **1993**, *31* (1), 9-20.

29. Hostler, C. J.; Chen, L. F. Fidaxomicin for treatment of *Clostridium difficile*-associated diarrhea and its potential role for prophylaxis. *Expert Opin. Pharmacother.* **2013**, *14* (11), 1529-1536.

30. Cornely, O. A.; Miller, M. A.; Louie, T. J.; Crook, D. W.; Gorbach, S. L. Treatment of First Recurrence of *Clostridium difficile* Infection: Fidaxomicin Versus Vancomycin. *Clin. Infect. Dis.* **2012**, *55* (S2), S154-S161.

31. Hecht, D. W.; Galang, M. A.; Sambol, S. P.; Osmolski, J. R.; Johnson, S.; Gerding, D. N. *In Vitro* Activities of 15 Antimicrobial Agents against 110 Toxigenic *Clostridium difficile* Clinical Isolates Collected from 1983 to 2004. *Antimicrob. Agents Chemother.* **2007**, *51* (8), 2716-2719.

32. Kim, M.-S.; Morales, W.; Hani, A. A.; Kim, S.; Kim, G.; Weitsman, S.; Chang, C.; Pimentel, M. The Effect of Rifaximin on Gut Flora and Staphylococcus Resistance. *Dig. Dis. Sci.* **2013,** *58* (6), 1676-1682.

33. Mattila, E.; Arkkila, P.; Mattila, P. S.; Tarkka, E.; Tissari, P.; Anttila, V. J., Rifaximin in the treatment of recurrent Clostridium difficile infection. *Aliment Pharmacol. Ther.* **2013,** *37* (1), 122-128.

34. Brazier, J. S.; Fawley, W.; Freeman, J.; Wilcox, M. H. Reduced susceptibility of *Clostridium difficile* to metronidazole. *J. Antimicrob. Chemother.* **2001**, *48* (5), 741-742.

35. Mascio, C. T. M.; Chesnel, L.; Thorne, G.; Silverman, J. A., Surotomycin Demonstrates Low *In Vitro* Frequency of Resistance and Rapid Bactericidal Activity in *Clostridium difficile*, *Enterococcus faecalis*, and *Enterococcus faecium*. *Antimicrob. Agents Chemother.* **2014**, *58* (7), 3976-3982.

36. Citron, D. M.; Tyrrell, K. L.; Merriam, C. V.; Goldstein, E. J. C. *In Vitro* Activities of CB-183,315, Vancomycin, and Metronidazole against 556 Strains of *Clostridium difficile*, 445 Other Intestinal Anaerobes, and 56 *Enterobacteriaceae* Species. *Antimicrob. Agents Chemother.* **2012**, *56* (3), 1613-1615.

37. Snydman, D. R.; Jacobus, N. V.; McDermott, L. A., Activity of a Novel Cyclic Lipopeptide, CB-183,315, against Resistant *Clostridium difficile* and Other Gram-Positive Aerobic and Anaerobic Intestinal Pathogens. *Antimicrob. Agents Chemother.* **2012**, *56* (6), 3448-3452.

38. Boix, V.; Fedorak, R. N.; Mullane, K. M.; Pesant, Y.; Stoutenburgh, U.; Jin, M.; Adedoyin, A.; Chesnel, L.; Guris, D.; Larson, K. B.; Murata, Y. Primary Outcomes From a Phase 3, Randomized, Double-Blind, Active-Controlled Trial of Surotomycin in Subjects With *Clostridium difficile* Infection. *Open Forum Infect. Dis.* **2017**, *4* (1), 275.

39. Critchley, I. A.; Green, L. S.; Young, C. L.; Bullard, J. M.; Evans, R. J.; Price, M.; Jarvis, T. C.; Guiles, J. W.; Janjic, N.; Ochsner, U. A. Spectrum of activity and mode of action of REP3123, a new antibiotic to treat *Clostridium difficile* infections. *J. Antimicrob. Chemother.* **2009**, *63* (5), 954-963.

40. Nayak, S. U.; Griffiss, J. M.; Blumer, J.; O'Riordan, M. A.; Gray, W.; McKenzie, R.; Jurao, R. A.; An, A. T.; Le, M.; Bell, S. J.; et al. Safety, tolerability, systemic exposure and metabolism of CRS3123, a methionyl-tRNA synthetase inhibitor developed for treatment of *Clostridium difficile* infections, in a Phase I study. *Antimicrob. Agents Chemother.* **2017**, *61* (8), e02760-16.

41. LaMarche, M. J.; Leeds, J. A.; Amaral, A.; Brewer, J. T.; Bushell, S. M.; Deng, G.; Dewhurst, J. M.; Ding, J.; Dzink-Fox, J.; Gamber, G.; et al. Discovery of LFF571: An Investigational Agent for *Clostridium difficile* Infection. *J. Med. Chem.* **2012**, *55* (5), 2376-2387.

42. Trzasko, A.; Leeds, J. A.; Praestgaard, J.; LaMarche, M. J.; McKenney, D. Efficacy of LFF571 in a Hamster Model of *Clostridium difficile* Infection. *Antimicrob. Agents Chemother.* **2012**, *56* (8), 4459-4462.

43. Leeds, J. A.; Sachdeva, M.; Mullin, S.; Dzink-Fox, J.; LaMarche, M. J. Mechanism of action of, and mechanism of reduced susceptibility to the novel anti-*Clostridium difficile* compound LFF571. *Antimicrob. Agents Chemother.* **2012**, *56* (8), 4463-4465.

44. Mullane, K.; Lee, C.; Bressler, A.; Buitrago, M.; Weiss, K.; Dabovic, K.; Praestgaard, J.; Leeds, J. A.; Blais, J.; Pertel, P. Multicenter, Randomized Clinical Trial To

Compare the Safety and Efficacy of LFF571 and Vancomycin for *Clostridium difficile* Infections. *Antimicrob. Agents Chemother.* **2015**, *59* (3), 1435-1440.

45. Musher, D. M.; Logan, N.; Hamill, R. J.; DuPont, H. L.; Lentnek, A.; Gupta, A.; Rossignol, J.-F. Nitazoxanide for the Treatment of *Clostridium difficile* Colitis. *Clin. Infect. Dis.* **2006**, *43* (4), 421-427.

46. Warren, C. A.; van Opstal, E.; Ballard, T. E.; Kennedy, A.; Wang, X.; Riggins, M.; Olekhnovich, I.; Warthan, M.; Kolling, G. L.; Guerrant, R. L.; et al. Amixicile, a Novel Inhibitor of Pyruvate:Ferredoxin Oxidoreductase, Shows Efficacy against *Clostridium difficile* in a Mouse Infection Model. *Antimicrob. Agents Chemother.* **2012**, *56* (8), 4103-4111.

47. Musher, D. M.; Logan, N.; Bressler, A. M.; Johnson, D. P.; Rossignol, J.-F. Nitazoxanide versus Vancomycin in *Clostridium difficile* Infection: A Randomized, Double-Blind Study. *Clin. Infect. Dis.* **2009**, *48* (4), e41-e46.

48. Crowther, G. S.; Baines, S. D.; Todhunter, S. L.; Freeman, J.; Chilton, C. H.; Wilcox, M. H. Evaluation of NVB302 versus vancomycin activity in an *in vitro* human gut model of *Clostridium difficile* infection. *J. Antimicrob. Chemother.* **2013**, *68* (1), 168-176.

49. Mann, J.; Taylor, P. W.; Dorgan, C. R.; Johnson, P. D.; Wilson, F. X.; Vickers, R.; Dale, A. G.; Neidle, S. The discovery of a novel antibiotic for the treatment of *Clostridium difficile* infections: a story of an effective academic–industrial partnership. *Medchemcomm* **2015**, *6* (8), 1420-1426.

50. Vickers, R. J.; Tillotson, G.; Goldstein, E. J. C.; Citron, D. M.; Garey, K. W.; Wilcox, M. H. Ridinilazole: a novel therapy for *Clostridium difficile* infection. *Int. J. Antimicrob. Agents* **2016**, *48* (2), 137-143.

51. Kali, A.; Charles, M. V. P.; Srirangaraj, S. Cadazolid: A new hope in the treatment of *Clostridium difficile* infection. *Med. J. Aust.* **2015**, *8* (8), 253-262.

52. Endres, B. T.; Bassères, E.; Alam, M. J.; Garey, K. W. Cadazolid for the treatment of *Clostridium difficile*. *Expert Opin. Investig. Drugs* **2017**, *26* (4), 509-514.

53. Actelion Ltd. Phase III Clinical Trial Results (News Conference). https://www1.actelion.com/en-rebranded/investors/news-archive.page?newsId=2111437 (accessed Dec 26th, 2017).

54. Dvoskin, S.; Xu, W.-C.; Brown, N. C.; Yanachkov, I. B.; Yanachkova, M.; Wright, G. E. A Novel Agent Effective against *Clostridium difficile* Infection. *Antimicrob. Agents Chemother.* **2012**, *56* (3), 1624-1626.

55. Kirst, H. A.; Toth, J. E.; Debono, M.; Willard, K. E.; Truedell, B. A.; Ott, J. L.; Counter, F. T.; Felty-Duckworth, A. M.; Pekarek, R. S. Synthesis and evaluation of tylosin-related macrolides modified at the aldehyde function: a new series of orally effective antibiotics. *J. Med. Chem.* **1988**, *31* (8), 1631-1641.

56. Ballard, T. E.; Wang, X.; Olekhnovich, I.; Koerner, T.; Seymour, C.; Hoffman, P. S.; Macdonald, T. L. Biological Activity of Modified and Exchanged 2-Amino-5-Nitrothiazole Amide Analogues of Nitazoxanide. *Bioorg. Med. Chem. Lett.* **2010**, *20* (12), 3537-3539.

57. Zhang, S.-J.; Yang, Q.; Xu, L.; Chang, J.; Sun, X. Synthesis and antibacterial activity against *Clostridium difficile* of novel demethylvancomycin derivatives. *Bioorg. Med. Chem. Lett.* **2012**, *22* (15), 4942-4945.

58. Ueda, C.; Tateda, K.; Horikawa, M.; Kimura, S.; Ishii, Y.; Nomura, K.; Yamada, K.; Suematsu, T.; Inoue, Y.; Ishiguro, M.; et al. Anti-*Clostridium difficile* Potential of Tetramic Acid Derivatives from *Pseudomonas aeruginosa* Quorum-Sensing Autoinducers. *Antimicrob. Agents Chemother.* **2010**, *54* (2), 683-688.

59. Wales, S. M.; Hammer, K. A.; King, A. M.; Tague, A. J.; Lyras, D.; Riley, T. V.; Keller, P. A.; Pyne, S. G. Binaphthyl-1,2,3-triazole peptidomimetics with activity against *Clostridium difficile* and other pathogenic bacteria. *Org. Biomol. Chem.* **2015**, *13* (20), 5743-5756.

60. Liu, R.; Suárez, J. M.; Weisblum, B.; Gellman, S. H.; McBride, S. M. Synthetic Polymers Active against *Clostridium difficile* Vegetative Cell Growth and Spore Outgrowth. *J. Am. Chem. Soc.* **2014**, *136* (41), 14498-14504.

61. Butler, M. M.; Williams, J. D.; Peet, N. P.; Moir, D. T.; Panchal, R. G.; Bavari, S.; Shinabarger, D. L.; Bowlin, T. L. Comparative *In Vitro* Activity Profiles of Novel Bis-Indole Antibacterials against Gram-Positive and Gram-Negative Clinical Isolates. *Antimicrob. Agents Chemother.* **2010**, *54* (9), 3974-3977.

62. Lowes, R. FDA Approves Zinplava for Preventing Return of *C. difficile*. https://www.medscape.com/viewarticle/870887 (accessed 21/12/2017).

63. Boyle, T. P.; Bremner, J. B.; Brkic, Z.; Coates, J. A. V.; Dalton, N. K.; Deadman, J.; Keller, P. A.; Morgan, J.; Pyne, S. G.; Rhodes, D. I.; Robertson, M. J. Preparation of biaryl-based peptides for the treatment of infection. WO2006074501A1, **2006**.

64. Bremner, J. B.; Keller, P. A.; Pyne, S. G.; Boyle, T. P.; Brkic, Z.; David, D. M.; Garas, A.; Morgan, J.; Robertson, M.; Somphol, K.; et al. Binaphthyl-Based Dicationic Peptoids with Therapeutic Potential. *Angew. Chem.-Int. Edit.* **2010**, *49* (3), 537-540.

65. Bremner, J. B.; Keller, P. A.; Pyne, S. G.; Boyle, T. P.; Brkic, Z.; David, D. M.; Robertson, M.; Somphol, K.; Baylis, D.; Coates, J. A.; et al. Synthesis and antibacterial studies of binaphthyl-based tripeptoids. Part 1. *Bioorg. Med. Chem.* **2010**, *18* (7), 2611-2620.

66. Bremner, J. B.; Keller, P. A.; Pyne, S. G.; Boyle, T. P.; Brkic, Z.; Morgan, J.; Somphol, K.; Coates, J. A.; Deadman, J.; Rhodes, D. I. Synthesis and antibacterial studies of binaphthyl-based tripeptoids. Part 2. *Bioorg. Med. Chem.* **2010**, *18* (13), 4793-4800.

67. Garas, A.; Bremner, J. B.; Coates, J.; Deadman, J.; Keller, P. A.; Pyne, S. G.; Rhodes, D. I. Binaphthyl scaffolded peptoids *via* ring-closing metathesis reactions and their anti-bacterial activities. *Bioorg. Med. Chem. Lett.* **2009**, *19* (11), 3010-3013.

68. Wales, S. M.; Hammer, K. A.; Somphol, K.; Tague, A. J.; Brkic, Z.; Lyras, D.; Riley, T. V.; Bremner, J. B.; Keller, P. A.; Pyne, S. G.; et al. Synthesis and antimicrobial activity of binaphthyl-based, functionalized oxazole and thiazole peptidomimetics. *Org. Biomol. Chem.* **2015**, *13* (44), 10813-10824.

69. Tague, A. J. Synthesis and Medicinal Chemistry of the Cationic Antibacterial Binaphthyltriazolyl-peptides. B.Sc. (Honours) Thesis, University of Wollongong, June 2014.

70. Goldie, B. New antibacterial compound licensed to Swiss drug development company. https://media.uow.edu.au/news/UOW091521.html (accessed 20/12/2017).

71. Lyras, D.; King, A. M. Unpublished results: *in vivo* mouse model of CDI. Monash University, 2015.

72. Wearley, L. L. Recent Progress in Protein and Peptide Delivery by Noninvasive Routes. *Crit. Rev. Ther. Drug Carr. Syst.* **1991**, *8* (4), 331-394.

73. Angell, Y. L.; Burgess, K. Peptidomimetics *via* copper-catalyzed azide-alkyne cycloadditions. *Chem. Soc. Rev.* **2007**, *36* (10), 1674-1689.

74. Koopmanschap, G.; Ruijter, E.; Orru, R. V. A. Isocyanide-based multicomponent reactions towards cyclic constrained peptidomimetics. *Beilstein J. Org. Chem.* **2014**, *10*, 544-598.

75. Rostovtsev, V. V.; Green, L. G.; Fokin, V. V.; Sharpless, K. B., A stepwise Huisgen cycloaddition process: Copper(I)-catalyzed regioselective "ligation" of azides and terminal alkynes. *Angew. Chem. - Int. Edit.* **2002**, *41* (14), 2596.

76. Pyne, S. G.; Keller, P. A.; Brkic, Z. Unpublished Results: Reversed Peptide Variants of the Binaphthylpeptides. University of Wollongong, 2009.

77. Amblard, M.; Fehrentz, J. A.; Martinez, J.; Subra, G. Methods and Protocols of modern solid phase peptide synthesis. *Mol. Biotechnol.* **2006**, *33* (3), 239-254.

78. Clayden, J.; Greeves, N.; Warren, S. *Organic Chemistry*. 2nd Edition; Oxford University Press: New York, 2012.

79. Wales, S. M. Unpublished results. University of Wollongong, 2014.

80. Vogel, A. I.; Furniss, B. S.; Hannaford, A. J.; Smith, P. W. G.; Tatchell, A. R., *Vogel's Textbook of Practical Organic Chemistry*. 5th Edition; Pearson Education Limited (Prentice Hall): London, England, 1989.

81. Rodriguez, M.; Llinares, M.; Doulut, S.; Heitz, A.; Martinez, J., A Facile Synthesis of Chiral *N*-protected Beta-amino Alcohols. *Tetrahedron Lett.* **1991**, *32* (7), 923-926.

82. Lee, J. Cobalt (III) Complexes as Novel Matrix Metalloproteinase-9 Inhibitors. *Bull. Korean Chem. Soc.* **2012**, *33* (8), 2762-2764.

83. Starks, C. M. Phase-transfer catalysis. I. Heterogeneous reactions involving anion transfer by quaternary ammonium and phosphonium salts. *J. Am. Chem. Soc.* **1971**, *93* (1), 195-199.

84. Chen, C. C.; Rajagopal, B.; Liu, X. Y.; Chen, K. L.; Tyan, Y. C.; Lin, F.; Lin, P. C. A mild removal of Fmoc group using sodium azide. *Amino Acids* **2014**, *46* (2), 367-374.

85. Wendt, M. D.; Shen, W.; Kunzer, A.; McClellan, W. J.; Bruncko, M.; Oost, T. K.; Ding, H.; Joseph, M. K.; Zhang, H.; Nimmer, P. M.; et al. Discovery and Structure−Activity Relationship of Antagonists of B-Cell Lymphoma 2 Family Proteins with Chemopotentiation Activity *in Vitro* and *in Vivo*. *J. Med. Chem.* **2006**, *49* (3), 1165-1181.

86. Pandiakumar, A. K.; Sarma, S. P.; Samuelson, A. G. Mechanistic studies on the diazo transfer reaction. *Tetrahedron Lett.* **2014**, *55* (18), 2917-2920.

87. Ye, H.; Liu, R. H.; Li, D. M.; Liu, Y. H.; Yuan, H. X.; Guo, W. K.; Zhou, L. F.; Cao, X. F.; Tian, H. Q.; Shen, J.; Wang, P. G. A Safe and Facile Route to Imidazole-1-sulfonyl Azide as a Diazotransfer Reagent. *Org. Lett.* **2013**, *15* (1), 18-21.

88. Goddard-Borger, E. D.; Stick, R. V. An Efficient, Inexpensive, and Shelf-Stable Diazotransfer Reagent: Imidazole-1-sulfonyl Azide Hydrochloride. *Org. Lett.* **2011**, *13* (9), 2514-2514.

89. Lundquist; Pelletier, J. C. Improved Solid-Phase Peptide Synthesis Method Utilizing α-Azide-Protected Amino Acids. *Org. Lett.* **2001**, *3* (5), 781-783.

90. Beierle, J. M.; Horne, W. S.; van Maarseveen, J. H.; Waser, B.; Reubi, J. C.; Ghadiri, M. R. Conformationally Homogeneous Heterocyclic Pseudotetra-peptides as Three-Dimensional Scaffolds for Rational Drug Design: Receptor-Selective Somatostatin Analogues. *Angew. Chem. - Int. Edit.* **2009**, *48* (26), 4725-4729.

91. Kocienski, P. J. *Protecting Groups*. Georg Thieme Verlag: 2005.

92. Orwig, K. S.; Lassetter, M. R.; Hadden, M. K.; Dix, T. A. Comparison of N-Terminal Modifications on Neurotensin(8−13) Analogues Correlates Peptide Stability but Not Binding Affinity with in Vivo Efficacy. *J. Med. Chem.* **2009**, *52* (7), 1803-1813.

93. Berg, R.; Straub, B. F. Advancements in the mechanistic understanding of the copper-catalyzed azide-alkyne cycloaddition. *Beilstein J. Org. Chem.* **2013**, *9*, 2715-2750.

94. Meldal, M.; Tornoe, C. W. Cu-catalyzed azide-alkyne cycloaddition. *Chem. Rev.* **2008**, *108* (8), 2952-3015.

95. Rodionov, V. O.; Fokin, V. V.; Finn, M. G. Mechanism of the ligand-free Cu-I-catalyzed azide-alkyne cycloaddition reaction. *Angew. Chem. - Int. Edit.* **2005**, *44* (15), 2210-2215.

96. Rodionov, V. O.; Presolski, S. I.; Díaz Díaz, D.; Fokin, V. V.; Finn, M. G. Ligand-Accelerated Cu-Catalyzed Azide−Alkyne Cycloaddition: A Mechanistic Report. *J. Am. Chem. Soc.* **2007**, *129* (42), 12705-12712.

97. Ziegler, M. S.; Lakshmi, K. V.; Tilley, T. D. Dicopper Cu(I)Cu(I) and Cu(I)Cu(II) Complexes in Copper-Catalyzed Azide–Alkyne Cycloaddition. *J. Am. Chem. Soc.* **2017**, *139* (15), 5378-5386.

98. Palladino, P.; Stetsenko, D. A. New TFA-Free Cleavage and Final Deprotection in Fmoc Solid-Phase Peptide Synthesis: Dilute HCl in Fluoro Alcohol. *Org. Lett.* **2012**, *14* (24), 6346-6349.

99. Stetsenko, D. A.; Apukhtina, V. S.; Chelobanov, B. P.; Palladino, P. Removal of acid-labile protecting or anchoring groups in the presence of polyfluorinated alcohol: Application to solid-phase peptide synthesis. *Russ. J. Bioorgan. Chem.* **2016**, *42* (2), 143-152.

100. Papageorgiou, E. A.; Gaunt, M. J.; Yu, J. Q.; Spencer, J. B. Selective hydrogenolysis of novel benzyl carbamate protecting groups. *Org. Lett.* **2000**, *2* (8), 1049-1051.

101. Gaunt, M. J.; Yu, J.; Spencer, J. B. Rational Design of Benzyl-Type Protecting Groups Allows Sequential Deprotection of Hydroxyl Groups by Catalytic Hydrogenolysis. *J. Org. Chem.* **1998**, *63* (13), 4172-4173.

102. Moynihan, H. A.; Yu, W. P. Alkoxycarbonylation and selective deprotection of *N*-silyl derivatives of L-arginine. *Tetrahedron Lett.* **1998**, *39* (20), 3349-3352.

103. Carpino, L. A.; Shroff, H.; Triolo, S. A.; Mansour, E. M. E.; Wenschuh, H.; Albericio, F. The 2,2,4,6,7-pentamethyldihydrobenzofuran-5-sulfonyl Group (Pbf) as Arginine Side-chain Protectant. *Tetrahedron Lett.* **1993**, *34* (49), 7829-7832.

104. Beck-Sickinger, A. G.; Schnorrenberg, G.; Metzger, J.; Jung, G. Sulfonation of arginine residues as side reaction in Fmoc-peptide synthesis. *Int. J. Pept. Protein Res.* **1991**, *38* (1), 25-31.

105. Ramage, R.; Green, J.; Blake, A. J. An acid labile arginine derivative for peptide synthesis: *N*γ-2,2,5,7,8-pentamethylchroman-6-sulphonyl-L-arginine. *Tetrahedron* **1991**, *47* (32), 6353-6370.

106. Ramage, R.; Green, J. *N*γ-2,2,5,7,8-pentamethylchroman-6-sulfonyl-L-arginine - A New Acid Labeile Derivative for Peptide-Synthesis. *Tetrahedron Lett.* **1987**, *28* (20), 2287-2290.

107. Joullie, M. M.; Lassen, K. M. Evolution of amide bond formation. *Arkivoc* **2010**, 189-250.

108. Montalbetti, C. A. G. N.; Falque, V. Amide bond formation and peptide coupling. *Tetrahedron* **2005**, *61* (46), 10827-10852.

109. Al-Warhi, T. I.; Al-Hazimi, H. M. A.; El-Faham, A. Recent development in peptide coupling reagents. *J. Saudi Chem. Soc.* **2012**, *16* (2), 97-116.

110. El-Faham, A.; Albericio, F. Peptide Coupling Reagents, More than a Letter Soup. *Chem. Rev.* **2011**, *111* (11), 6557-6602.

111. Maegawa, T.; Fujiwara, Y.; Ikawa, T.; Hisashi, H.; Monguchi, Y.; Sajiki, H. Novel deprotection method of Fmoc group under neutral hydrogenation conditions. *Amino Acids* **2009**, *36* (3), 493-499.

112. Fields, G. B. Methods for removing the Fmoc group. *Methods Mol. Biol.* **1994**, *35*, 17-27.

113. Brogden, K. A. Antimicrobial peptides: Pore formers or metabolic inhibitors in bacteria? *Nat. Rev. Microbiol.* **2005**, *3* (3), 238-250.

114. Silverman, J. A.; Perlmutter, N. G.; Shapiro, H. M. Correlation of daptomycin bactericidal activity and membrane depolarization in *Staphylococcus aureus*. *Antimicrob. Agents Chemother.* **2003**, *47* (8), 2538-2544.

115. Ghosh, C.; Manjunath, G. B.; Akkapeddi, P.; Yarlagadda, V.; Hoque, J.; Uppu, D.; Konai, M. M.; Haldar, J. Small Molecular Antibacterial Peptoid Mimics: The Simpler the Better! *J. Med. Chem.* **2014**, *57* (4), 1428-1436.

116. Reddy, K. V. R.; Yedery, R. D.; Aranha, C. Antimicrobial peptides: premises and promises. *Int. J. Antimicrob. Agents* **2004**, *24* (6), 536-547.

117. Marcovici-Mizrahi, D.; Gottlieb, H. E.; Marks, V.; Nudelman, A. On the stabilization of the *syn*-rotamer of amino acid carbamate derivatives by hydrogen bonding. *J. Org. Chem.* **1996**, *61* (24), 8402-8406.

118. Moraczewski, A. L.; Banaszynski, L. A.; From, A. M.; White, C. E.; Smith, B. D. Using Hydrogen Bonding to Control Carbamate C−N Rotamer Equilibria. *J. Org. Chem.* **1998**, *63* (21), 7258-7262.

119. Silverstein, R. M.; Webster, F. X.; Kiemle, D. J. *Spectrometric Identification of Organic Compounds*. 7th Edition; John Wiley & Sons, Inc.: USA, 2005.

120. Ghiviriga, I.; El-Gendy, B. E. D.; Steel, P. J.; Katritzky, A. R. Tautomerization of guanidines studied by ^{15}N-NMR: 2-hydrazono-3-phenylquinazolin-4(3H)-ones. *Org. Bio. Chem.* **2009**, *7*, 4110-4119.

121. Sorg, G., Progress in the preparation of peptide aldehydes via polymer supported IBX oxidation and scavenging by threonyl resin. *J. Pept. Sci.* **2005**, *11* (3), 142-152.

Appendix A – Supplementary figures and schemes

A1 – Additional reaction mechanisms

Mechanism for alkynes 20 and 21

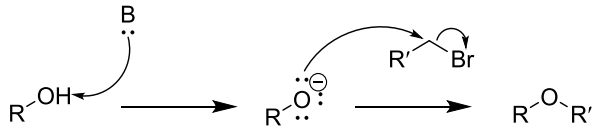

Scheme A1.1 – Mechanism of base-promoted ether synthesis (i.e. Williamson ether synthesis).[78]

Mechanisms for *N*-Cbz and *N*-Boc protecting group installation

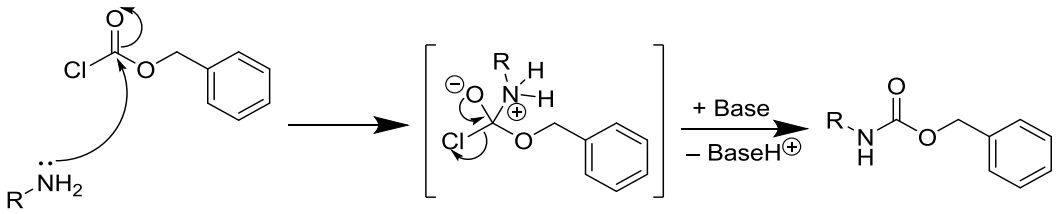

Scheme A1.2 – Mechanism of *N*-Cbz protection *via* nucleophilic substitution at the carbonyl position.[78]

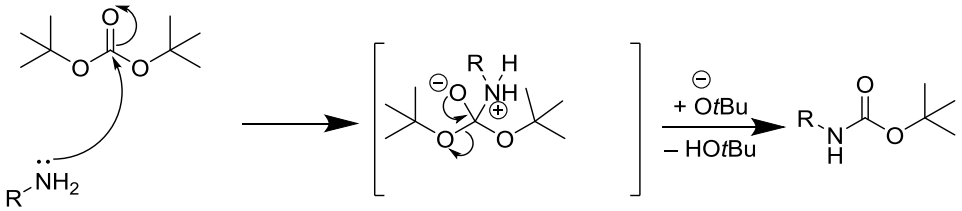

Scheme A1.3 – Mechanism of *N*-Boc protection *via* nucleophilic substitution at the carbonyl position.[78]

Mechanism for the mixed-anhydride reduction reaction

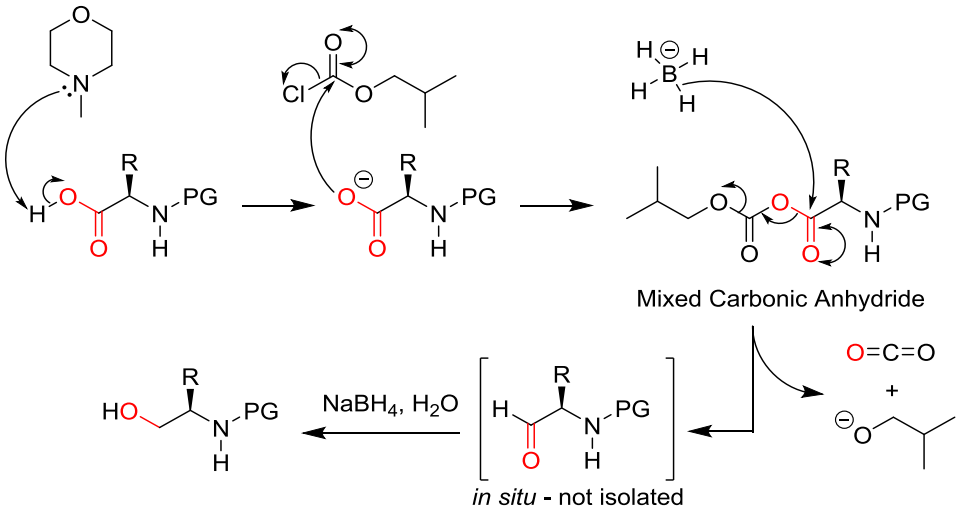

Scheme A1.4 – Mechanism showing formation of the mixed anhydride intermediate followed by borohydride reduction[78] to give the alcohol product. **PG** = Protecting Group = Cbz or Fmoc.

Mechanism for mesylation and S_N2 azidation

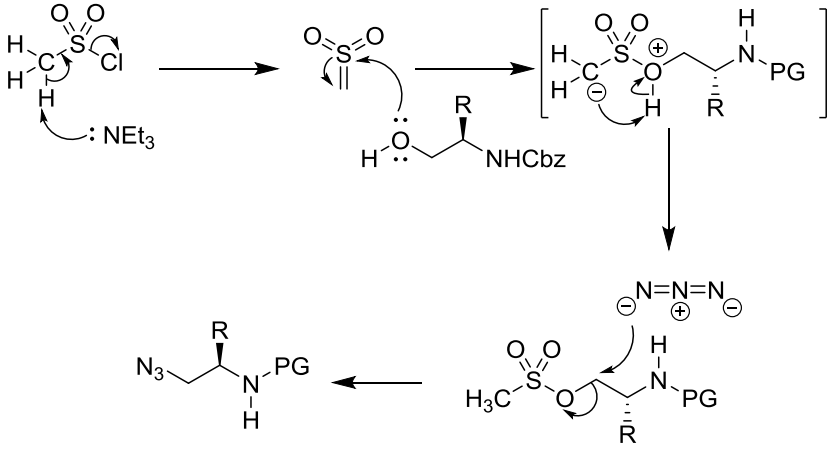

Scheme A1.5 – Mechanism showing the formation of the mesylate followed by S_N2-type displacement of the mesylate leaving group by the azide anion[78] to give the product azide. **PG** = Protecting Group = Cbz or Fmoc.

Mechanism for iodination and oxazolidinone by-product formation

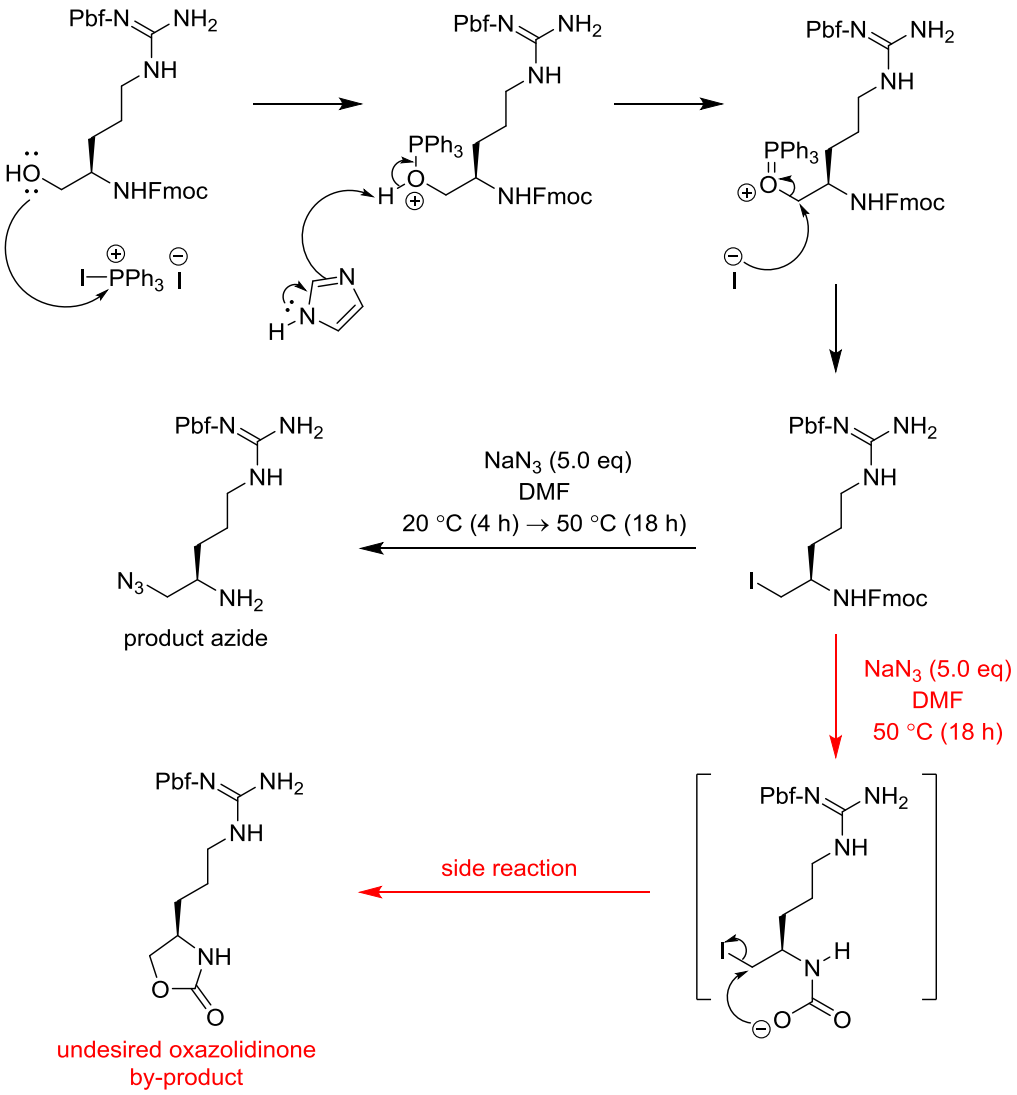

Scheme A1.6 – Mechanism for the formation of azide **25** from the alcohol precursor: iodination followed by azidation/*N*-Fmoc deprotection.[59, 78] The potential oxazolidinone by-product reaction (red pathway) is also displayed.

Mechanism for base-promoted *N*-Fmoc deprotection

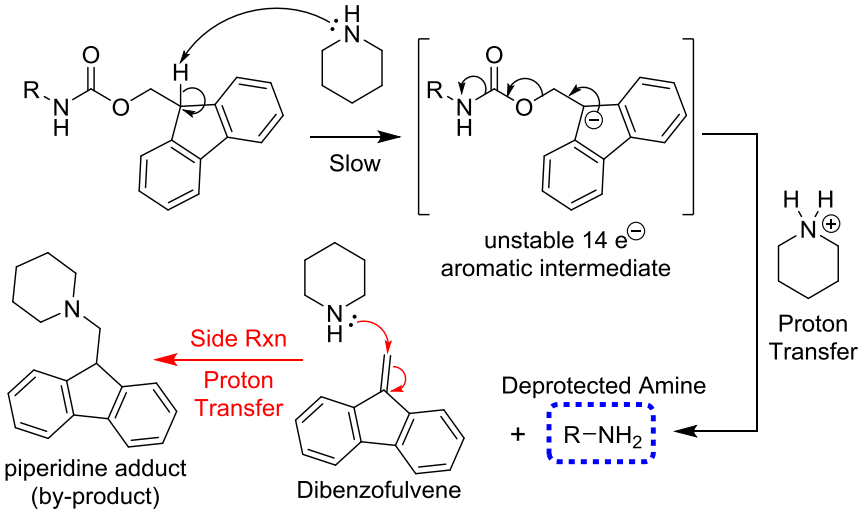

Scheme A1.7 – Mechanism of base-promoted Fmoc cleavage by piperidine with the dibenzofulvene scavenging pathway (red) shown. In DMSO at 50 °C, an azide anion can also function as the catalytic base required for *N*-Fmoc cleavage.[84]

Mechanism for copper-catalysed diazotransfer reaction

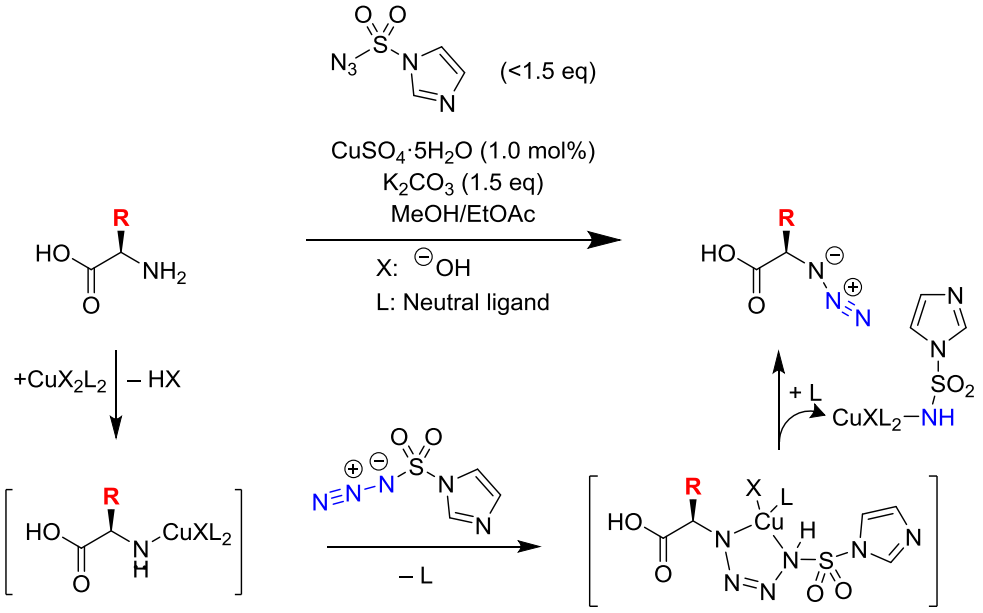

Scheme A1.8 – Diazotransfer reaction mechanism[86] for the formation of the α-azido acid precursors.

A2 – Additional figures and schemes

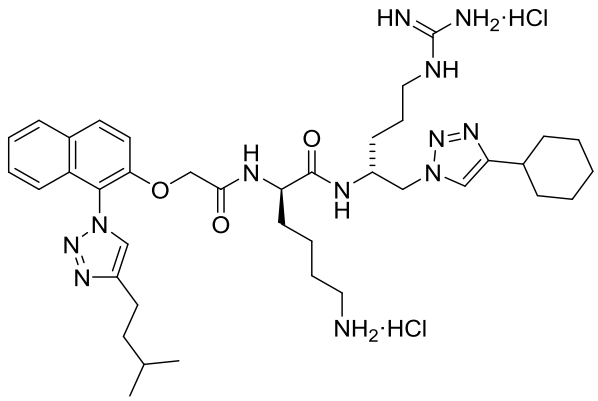

90

Figure A2.1 – Structure for compound **90 (**made by a current PhD student, Muni Kumar Mahadari, who is continuing the biarylpeptide research).

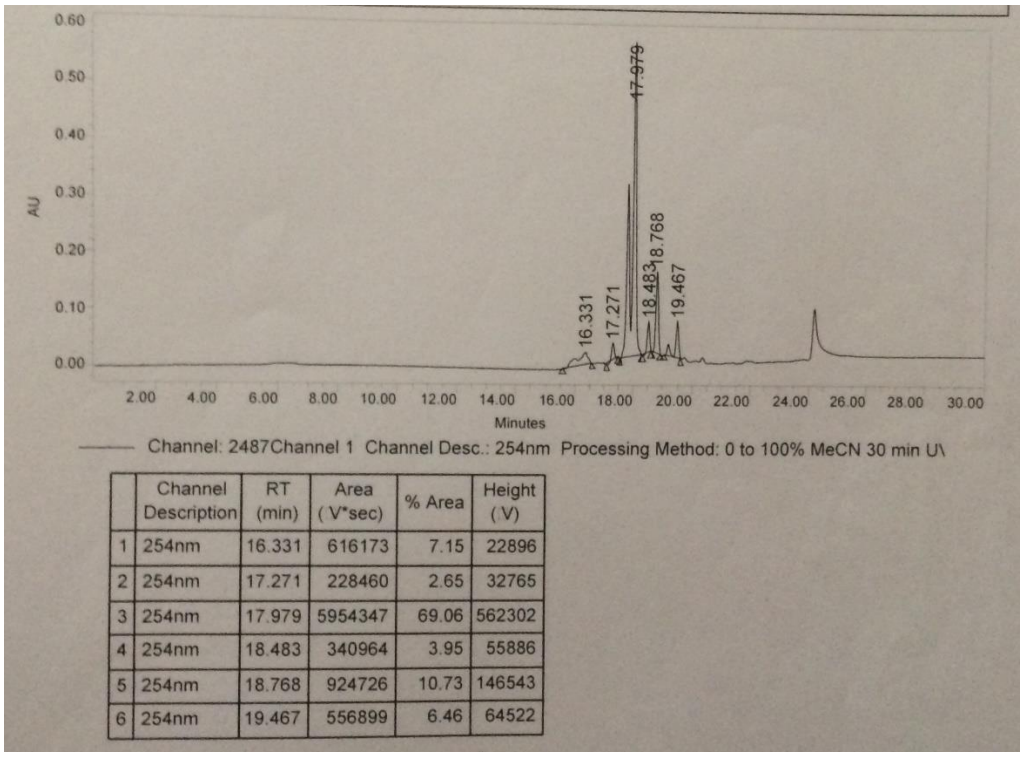

	Channel Description	RT (min)	Area (V*sec)	% Area	Height (V)
1	254nm	16.331	616173	7.15	22896
2	254nm	17.271	228460	2.65	32765
3	254nm	17.979	5954347	69.06	562302
4	254nm	18.483	340964	3.95	55886
5	254nm	18.768	924726	10.73	146543
6	254nm	19.467	556899	6.46	64522

Figure A2.2 – HPLC trace for compound **2** synthesized by *N*-Boc/*N*-Pbf deprotection without H_2O present; large quantities of *N*-sulfonation by-products were observed.

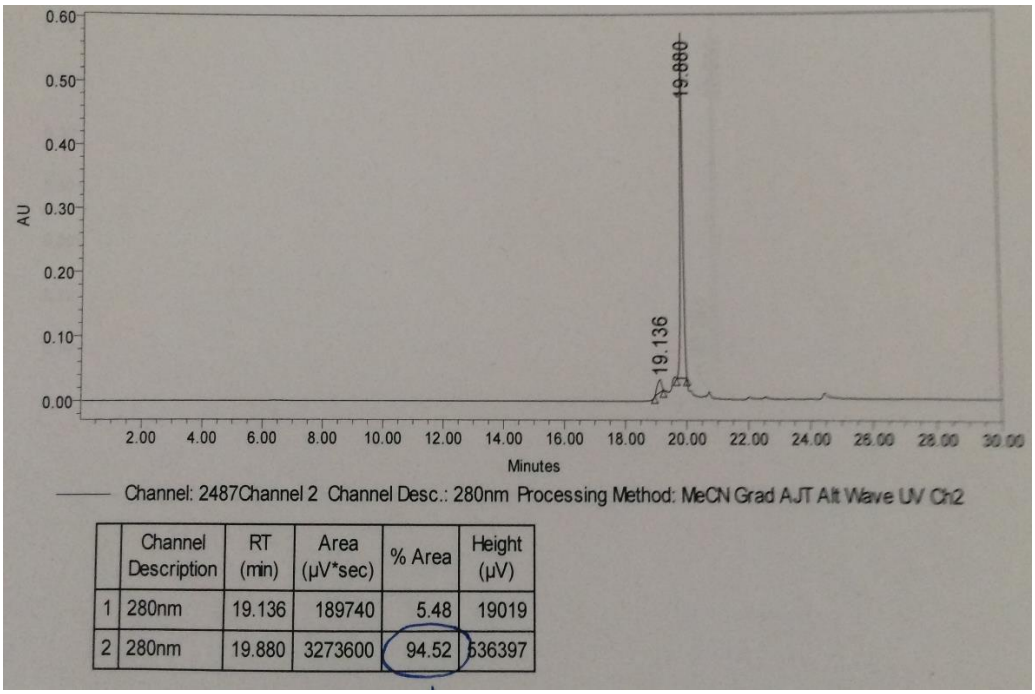

	Channel Description	RT (min)	Area (µV*sec)	% Area	Height (µV)
1	280nm	19.136	189740	5.48	19019
2	280nm	19.880	3273600	94.52	536397

Figure A2.3 – HPLC trace for compound **2** synthesized by *N*-Boc/*N*-Pbf deprotection with H_2O present; minimal impurities were observed (~95% pure).

Figure A2.4 – Recrystallization of compound **68b** by passive evaporation of MeOH/CH_2Cl_2.

Appendix B – **Biological testing data and supplementary information**

This appendix contains a complete set of the *in vitro* antimicrobial testing data acquired for all final compounds – see Tables B1.1 – B2.9 in Sections B1 and B2. The solubility assay data (Tables B3.1 – B3.6 in Section B3) and HPLC purity traces (Figures B4.1 – B4.4 in Section B4) are also included.

B1 – Primary MIC screening data (UWA)

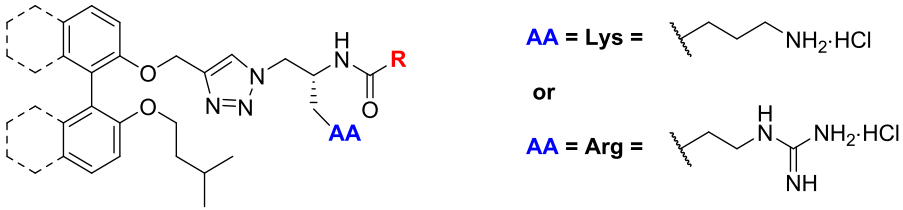

Compound	Aromatic Core	AA	R	*S. aureus* ATCC 29213	*S. aureus* NCTC 10442	*E. faecalis* ATCC 29212	*S. pneumoniae* ATCC 49619	*E. coli* ATCC 25922	*C. difficile* ATCC 700057	*C. difficile* 132 (RT027)
64a	Biphenyl	Lys	Bn	8	8	8	8	32	32	32
64b	Biphenyl	Lys	PhEt	8	4	8	8	16	8	16
64c	Biphenyl	Lys	OBn	16	16	16	32	32	8	32
65a	Biphenyl	Arg	Bn	16	16	16	16	64	64	16
65b	Biphenyl	Arg	PhEt	16	16	16	32	64	128	16
65c	Biphenyl	Arg	OBn	4	4	8	16	32	32	32
66a	Binaphthyl	Arg	Bn	4	4	8	8	32	64	64
66b	Binaphthyl	Arg	PhEt	4	4	8	8	>128	16	16
66c	Binaphthyl	Arg	OBn	4	4	8	8	>128	32	32
Vancomycin				1	1	4	1	>16	0.5	0.5

Table B1.1 – Antibacterial activities of Series A1 derivatives reported as MIC values (μg/mL).

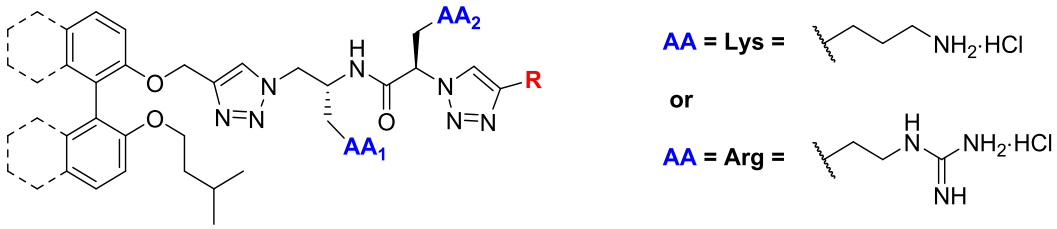

Compound	Aromatic Core	AA_1	AA_2	R	*S. aureus* ATCC 29213	*S. aureus* *MRSA* NCTC 10442	*E. faecalis* ATCC 29212	*S. pneumoniae* ATCC 49619	*E. coli* ATCC 25922	*C. difficile* ATCC 700057	*C. difficile* 132 (RT027)
68a	Biphenyl	Lys	Arg	Bn	8	8	16	4	64	16	16
68b	Biphenyl	Lys	Arg	PhEt	4	4	8	8	64	8	8
68c	Biphenyl	Lys	Arg	Cy	8	4	8	4	64	4	8
68d	Biphenyl	Lys	Arg	CH_2Cy	4	4	4	4	32	4	4
69a	Biphenyl	Arg	Lys	Bn	4	4	8	4	32	64	64
69b	Biphenyl	Arg	Lys	PhEt	4	4	8	4	32	16	16
69c	Biphenyl	Arg	Lys	Cy	4	4	8	4	32	32	32
69d	Biphenyl	Arg	Lys	N/A†	16	16	16	8	64	64	32
70a	Binaphthyl	Lys	Arg	PhEt	4	4	4	4	16	16	16
70b	Binaphthyl	Lys	Arg	CH_2Cy	4	4	4	4	16	8	16
Vancomycin					1	1	4	1	>16	0.5	0.5

Table B1.2 – Antibacterial activities of Series A2 derivatives reported as MIC values (μg/mL). † No terminal triazole – compound **69d** contains an unreacted azide terminus – see Section 2.2.2.2 for compound structure.

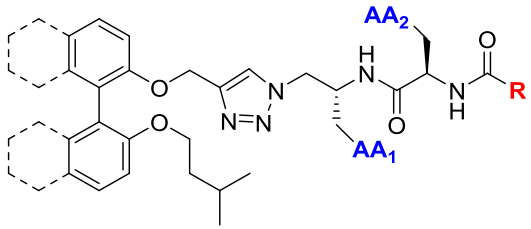

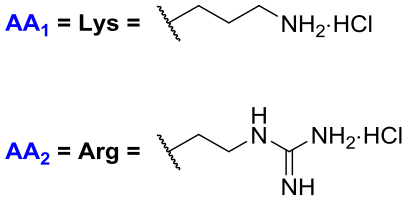

Compound	**Aromatic Core**	**AA1**	**AA2**	**R**	*S. aureus* ATCC 29213	*S. aureus* *MRSA* NCTC 10442	*E. faecalis* ATCC 29212	*S. pneumoniae* ATCC 49619	*E. coli* ATCC 25922	*C. difficile* ATCC 700057	*C. difficile* 132 (RT027)
73	Biphenyl	Lys	Arg	Bn	8	8	8	8	32	16	16
74	Biphenyl	Lys	Arg	Fmo†	4	4	4	4	64	32	32
Vancomycin					1	1	4	1	>16	0.5	0.5

Table B1.3 – Antibacterial activities of Series A2 derivatives reported as MIC values (μg/mL). † Fluorenylmethyloxy (Fmo).

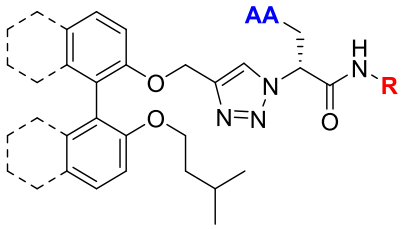

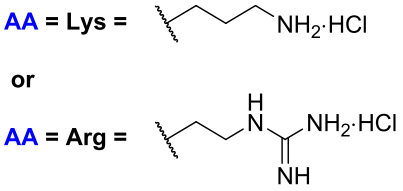

Compound	**Aromatic Core**	**AA**	**R**	*S. aureus* ATCC 29213	*S. aureus* NCTC 10442	*E. faecalis* ATCC 29212	*S. pneumoniae* ATCC 49619	*E. coli* ATCC 25922	*C. difficile* ATCC 700057	*C. difficile* 132 (RT027)
76a	Biphenyl	Lys	Bn	8	16	16	8	32	32	32
76b	Biphenyl	Lys	PhEt	8	8	8	8	16	32	32
76c	Biphenyl	Lys	Cy	8	16	16	8	32	16	32
76d	Biphenyl	Lys	CH_2Cy	8	8	8	8	16	16	32
76e	Biphenyl	Lys	4-CF_3-Bn	4	4	4	8	16	32	32
76f	Biphenyl	Lys	4-F-PhEt	4	8	8	8	16	32	64
77a	Biphenyl	Arg	Bn	4	8	8	4	32	32	64
77b	Biphenyl	Arg	PhEt	2	2	4	4	16	8	32
77c	Biphenyl	Arg	Cy	4	4	4	4	16	8	16
77d	Biphenyl	Arg	CH_2Cy	4	4	8	8	32	32	64
Vancomycin				1	1	4	1	>16	0.5	0.5

Table B1.4 – Antibacterial activities of Series B1 derivatives reported as MIC values (μg/mL).

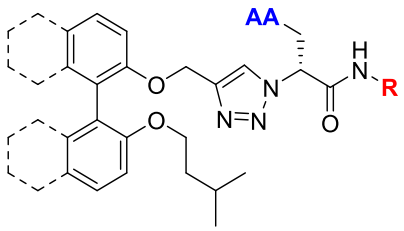

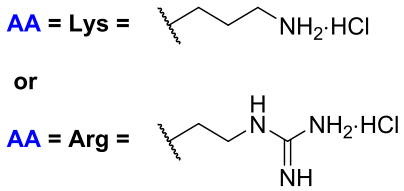

Compound	Aromatic Core	AA	R	*S. aureus* ATCC 29213	*S. aureus* NCTC 10442	*E. faecalis* ATCC 29212	*S. pneumoniae* ATCC 49619	*E. coli* ATCC 25922	*C. difficile* ATCC 700057	*C. difficile* 132 (RT027)
77e	Biphenyl	Arg	4-CF_3-Bn	16	16	16	32	64	128	128
77f	Biphenyl	Arg	4-F-PhEt	4	4	4	4	32	64	64
77g	Biphenyl	Arg	3,5-diF-Bn	8	8	8	16	32	32	32
77h	Biphenyl	Arg	3-F-Ph	4	8	8	8	32	32	64
77i	Biphenyl	Arg	Ph	2	2	2	2	16	16	32
77j	Biphenyl	Arg	3,5-diMeO-Bn	4	4	4	4	32	32	32
77k	Biphenyl	Arg	Cyclopropyl	16	32	32	8	64	64	128
77l	Biphenyl	Arg	Ethyl and Cyclopropylmethyl	4	4	4	2	32	16	16
78a	Binaphthyl	Arg	Bn	4	8	2	8	>128	16	16
78b	Binaphthyl	Arg	PhEt	8	8	4	16	>128	16	64
Vancomycin				1	1	4	1	>16	0.5	0.5

Table B1.5 – Antibacterial activities of Series B1 derivatives reported as MIC values (μg/mL).

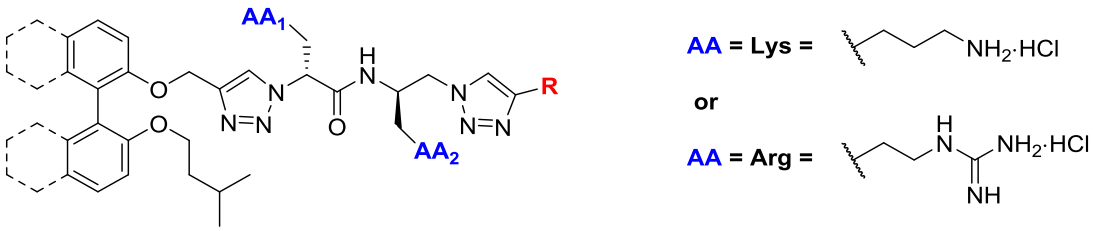

Compound	Aromatic Core	AA_1	AA_2	R	*S. aureus* ATCC 29213	*S. aureus* NCTC 10442	*E. faecalis* ATCC 29212	*S. pneumoniae* ATCC 49619	*E. coli* ATCC 25922	*C. difficile* ATCC 700057	*C. difficile* 132 (RT027)
80a	Biphenyl	Lys	Arg	Bn	4	4	8	4	32	8	16
80b	Biphenyl	Lys	Arg	PhEt	4	4	8	8	16	16	16
80c	Biphenyl	Lys	Arg	Cy	16	16	16	32	64	64	128
80d	Biphenyl	Lys	Arg	CH_2Cy	4	4	4	8	32	16	16
81a	Biphenyl	Arg	Lys	Bn	8	8	8	4	32	32	16
81b	Biphenyl	Arg	Lys	PhEt	4	8	8	2	16	16	16
81c	Biphenyl	Arg	Lys	Cy	8	8	8	2	16	8	16
81d	Biphenyl	Arg	Lys	CH_2Cy	4	4	4	2	16	8	16
Vancomycin					1	1	4	1	>16	0.5	0.5

Table B1.6 – Antibacterial activities of Series B2 derivatives reported as MIC values (μg/mL).

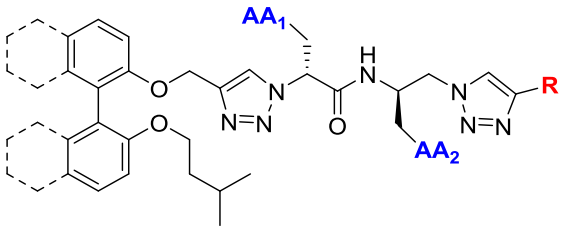

AA = Lys = $NH_2 \cdot HCl$

or

AA = Arg = $NH_2 \cdot HCl$

Compound	Aromatic Core	AA_1	AA_2	R	*S. aureus* ATCC 29213	*S. aureus* NCTC 10442	*E. faecalis* ATCC 29212	*S. pneumoniae* ATCC 49619	*E. coli* ATCC 25922	*C. difficile* ATCC 700057	*C. difficile* 132 (RT027)
82a	Binaphthyl	Lys	Arg	PhEt	4	4	4	4	16	16	16
82b	Binaphthyl	Lys	Arg	CH_2Cy	4	4	4	4	16	16	16
83a	Binaphthyl	Arg	Lys	PhEt	4	4	4	2	8	16	16
83b	Binaphthyl	Arg	Lys	CH_2Cy	4	4	4	2	8	8	8
Vancomycin					1	1	4	1	>16	0.5	0.5

Table B1.7 – Antibacterial activities of Series B2 derivatives reported as MIC values (μg/mL).

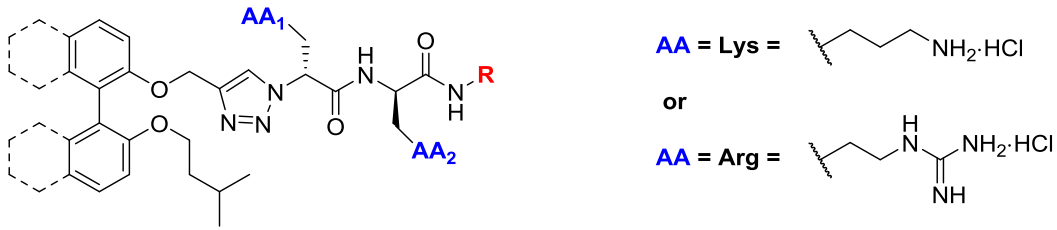

Compound	Aromatic Core	AA_1	AA_2	R	*S. aureus* ATCC 29213	*S. aureus* NCTC 10442	*E. faecalis* ATCC 29212	*S. pneumoniae* ATCC 49619	*E. coli* ATCC 25922	*C. difficile* ATCC 700057	*C. difficile* 132 (RT027)
85a	Binaphthyl	Lys	Arg	Bn	8	8	8	8	32	16	16
85b	Binaphthyl	Lys	Arg	PhEt	8	8	4	8	32	16	32
85c	Binaphthyl	Arg	Lys	Piperidinyl†	8	8	8	8	16	16	32
Vancomycin					1	1	4	1	>16	0.5	0.5

Table B1.8 – Antibacterial activities of Series B2 derivatives reported as MIC values (μg/mL). † Piperidinyl amide – see Section 2.3.2.2 for compound structure.

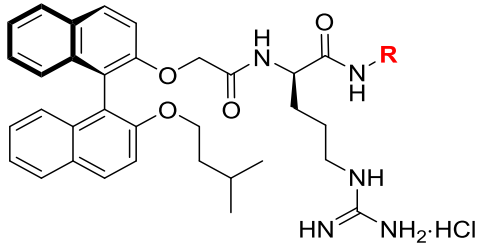

Compound	R	*S. aureus* ATCC 29213	*S. aureus* NCTC 10442	*E. faecalis* ATCC 29212	*S. pneumoniae* ATCC 49619	*E. coli* ATCC 25922	*C. difficile* ATCC 700057	*C. difficile* 132 (RT027)
87a	Bn	2	2	2	2	>128	8†	8†
87b	PhEt	2	2	4	2	>128	32	32
87c	4-F-PhEt	>128	>128	>128	>128	>128	>128	64
Vancomycin		1	1	4	1	>16	0.5	0.5

Table B1.9 – Antibacterial activities of Series C derivatives reported as MIC values (μg/mL). Compound **87a** displayed an MIC value of 2 μg/mL against *C. difficile* (M7404 – RT027) when tested at the Monash University laboratory.

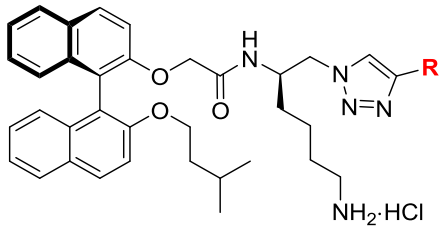

Compound	R	*S. aureus*		*E. faecalis*	*S. pneumoniae*	*E. coli*	*C. difficile*	
		ATCC 29213	NCTC 10442	ATCC 29212	ATCC 49619	ATCC 25922	ATCC 700057	132 (RT027)
89a	Ph	4	8	4	32	>128	16	16
89b	Bn	4	4	4	32	>128	8	8
89c	Isopentyl	8	8	4	32	128	16	16
Vancomycin		1	1	4	1	>16	0.5	0.5

Table B1.10 – Antibacterial activities of Series C derivatives reported as MIC values (μg/mL).

B2 – Secondary MIC screening and cytotoxicity data (CO-ADD)

Control Data

Compound	*S. aureus* ATCC 43300 (*MRSA*)	*P. aeruginosa* ATCC 27853	*K. pneumoniae* ATCC 700603	*A. baumannii* ATCC 19606	*E. coli* ATCC 25922	*C. albicans* ATCC 90028	*C. neoformans* ATCC 208821	Cytotoxicity (CC_{50}) (HEK-293) ATCC CRL-1573
Vancomycin	1	>32	>32	>32	>32	-	-	-
Colistin	>32	0.25	0.25	0.25	0.125	-	-	-
Fluconazole	-	-	-	-	-	0.125	8	-
Tamoxifen	-	-	-	-	-	-	-	13.06

Table B2.1 – MIC or CC_{50} values for the various control inhibitors – reported in μg/mL.

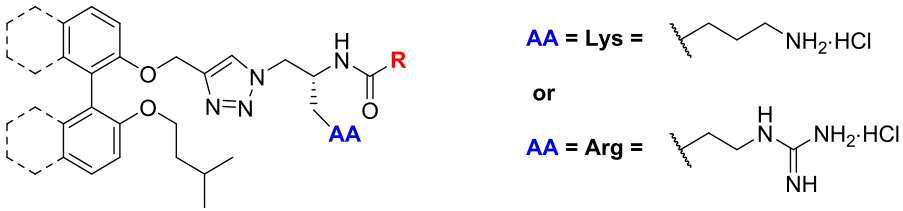

Compound	**Aromatic Core**	**AA**	**R**	*S. aureus* ATCC 43300 (*MRSA*)	*P. aeruginosa* ATCC 27853	*K. pneumoniae* ATCC 700603	*A. baumannii* ATCC 19606	*E. coli* ATCC 25922	*C. albicans* ATCC 90028	*C. neoformans* ATCC 208821	Cytotoxicity (CC_{50}) (HEK-293) ATCC CRL-1573
64a	Biphenyl	Lys	Bn	16	32	>32	32	>32	32	32	14.2
64b	Biphenyl	Lys	PhEt	16	32	32	>32	32	>32	16	4.8
64c	Biphenyl	Lys	OBn	16	32	>32	32	32	16	32	4.7
65a	Biphenyl	Arg	Bn	16	>32	>32	>32	>32	>32	32	29.0
65b	Biphenyl	Arg	PhEt	16	>32	>32	>32	>32	>32	32	>32
65c	Biphenyl	Arg	OBn	8	>32	>32	>32	>32	8	16	>32
66a	Binaphthyl	Arg	Bn	4	>32	>32	>32	>32	32	8	16.5
66b	Binaphthyl	Arg	PhEt	4	>32	>32	>32	>32	32	8	15.9
66c	Binaphthyl	Arg	OBn	4	>32	>32	>32	>32	16	4	13.8

Table B2.2 – Antibacterial activities of Series A1 derivatives reported as MIC values (μg/mL). The cytotoxicity of each compound is also reported as the CC_{50} (μg/mL).

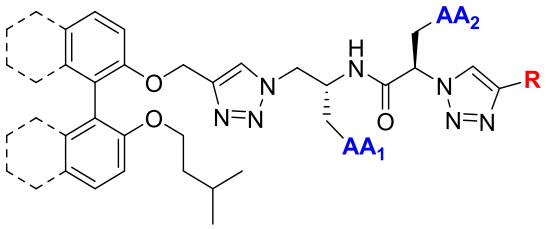

AA = Lys = 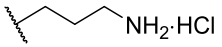

or

AA = Arg = 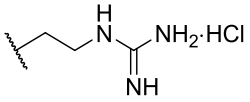

Compound	**Aromatic Core**	**AA$_1$**	**AA$_2$**	**R**	*S. aur.*	*P. aer.*	*K. pneu.*	*A. bau.*	*E. coli*	*C. alb.*	*C. neo.*	Cytotoxicity (CC_{50})
68a	Biphenyl	Lys	Arg	Bn	4	16	16	8	16	32	32	21.9
68b	Biphenyl	Lys	Arg	PhEt	2	8	16	16	8	32	4	>32
68c	Biphenyl	Lys	Arg	Cy	4	8	16	16	8	32	4	14.2
68d	Biphenyl	Lys	Arg	CH_2Cy	2	16	16	8	4	>32	4	>32
69a	Biphenyl	Arg	Lys	Bn	4	16	32	16	8	32	4	17.8
69b	Biphenyl	Arg	Lys	PhEt	2	8	16	16	4	32	2	17.4
69c	Biphenyl	Arg	Lys	Cy	4	8	32	8	8	32	2	15.3
69d	Biphenyl	Arg	Lys	N/A†	8	32	32	16	16	>32	4	>32
70a	Binaphthyl	Lys	Arg	PhEt	4	32	>32	32	>32	8	2	>32
70b	Binaphthyl	Lys	Arg	CH_2Cy	2	32	>32	16	32	4	2	>32

Table B2.3 – Antibacterial activities of Series A2 derivatives reported as MIC values (μg/mL). The cytotoxicity of each compound is also reported as the CC_{50} (μg/mL). † No terminal triazole – compound **69d** contains an unreacted azide terminus – see Section 2.2.2.2 for structure.

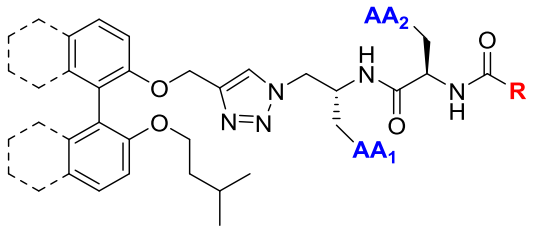

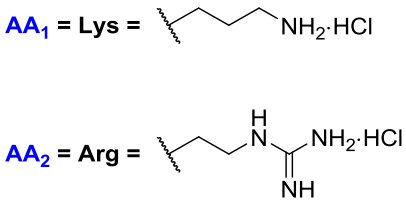

Compound	**Aromatic Core**	**AA1**	**AA2**	**R**	*S. aur.*	*P. aer.*	*K. pneu.*	*A. bau.*	*E. coli*	*C. alb.*	*C. neo.*	Cytotoxicity (CC_{50})
73	Biphenyl	Lys	Arg	Fmo†	4	32	32	32	16	32	2	28.7
74	Biphenyl	Lys	Arg	Bn	4	>32	>32	>32	>32	>32	8	16.5

Table B2.4 – Antibacterial activities of Series A2 derivatives reported as MIC values (μg/mL). The cytotoxicity of each compound is also reported as the CC_{50} (μg/mL). † Fluorenylmethyloxy (Fmo).

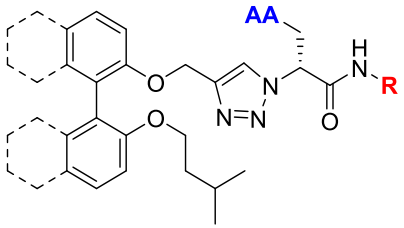

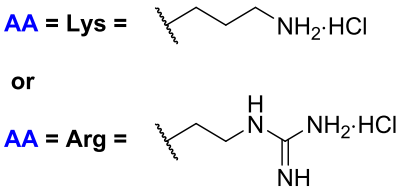

Compound	**Aromatic Core**	**AA**	**R**	*S. aureus* ATCC 43300 (*MRSA*)	*P. aeru.* ATCC 27853	*K. pneum.* ATCC 700603	*A. baumannii* ATCC 19606	*E. coli* ATCC 25922	*C. albicans* ATCC 90028	*C. neoformans* ATCC 208821	Cytotoxicity (CC_{50}) (HEK-293) ATCC CRL-1573
76a	Biphenyl	Lys	Bn	16	32	>32	32	>32	>32	>32*	>32
76b	Biphenyl	Lys	PhEt	8	>32	>32	32	>32	>32	>32*	>32
76c	Biphenyl	Lys	Cy	8	32	>32	32	>32	32	32*	>32
76d	Biphenyl	Lys	CH_2Cy	8	>32	>32	32	>32	32	16*	5.6
76e	Biphenyl	Lys	4-CF_3-Bn	8	>32	>32	32	>32	>32	32*	>32
76f	Biphenyl	Lys	4-F-PhEt	8	>32	>32	16	>32	>32	12*	5.5
77a	Biphenyl	Arg	Bn	8	>32	>32	32	>32	16	16	16.8
77b	Biphenyl	Arg	PhEt	8	>32	>32	32	>32	16	32	17.9
77c	Biphenyl	Arg	Cy	4	>32	>32	32	>32	16	16	19.7
77d	Biphenyl	Arg	CH_2Cy	4	>32	>32	>32	>32	32	32	16.9

Table B2.5 – Antibacterial activities of Series B1 derivatives reported as MIC values (μg/mL). The cytotoxicity of each compound is also reported as the CC_{50} (μg/mL). * *Cryptococcus neoformans* data was not consistent with initial screening data – compounds need to be rescreened.

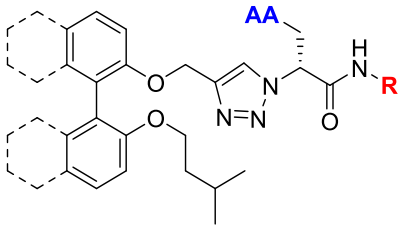

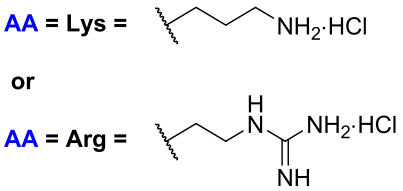

Compound	**Aromatic Core**	**AA**	**R**	*S. aureus* ATCC 43300 (*MRSA*)	*P. aeru.* ATCC 27853	*K. pneum.* ATCC 700603	*A. baum.* ATCC 19606	*E. coli* ATCC 25922	*C. albicans* ATCC 90028	*C. neoformans* ATCC 208821	Cytotoxicity (CC_{50}) (HEK-293) ATCC CRL-1573
77e	Biphenyl	Arg	4-CF_3-Bn	16	>32	>32	>32	>32	>32	32	>32
77f	Biphenyl	Arg	4-F-PhEt	16	>32	>32	>32	>32	>32	32	19.1
77g	Biphenyl	Arg	3,5-diF-Bn	16	>32	>32	>32	>32	>32	>32	22.9
77h	Biphenyl	Arg	3-F-Ph	4	>32	>32	>32	>32	>32	4	>32
77i	Biphenyl	Arg	Ph	8	>32	>32	>32	>32	>32	32	21.6
77j	Biphenyl	Arg	3,5-diMeO-Bn	8	>32	>32	>32	>32	>32	>32	12.2
77k	Biphenyl	Arg	Cyclopropyl	32	>32	>32	>32	>32	>32	>32	20.0
77l	Biphenyl	Arg	Ethyl and cyclopropyl-methyl	8	>32	>32	>32	>32	32	32	19.7
78a	Binaphthyl	Arg	Bn	8	>32	>32	>32	>32	16	8	16.5
78b	Binaphthyl	Arg	PhEt	8	>32	>32	>32	>32	32	16	>32

Table B2.6 – Antibacterial activities of Series B1 derivatives reported as MIC values (μg/mL). The cytotoxicity of each compound is also reported as the CC_{50} (μg/mL).

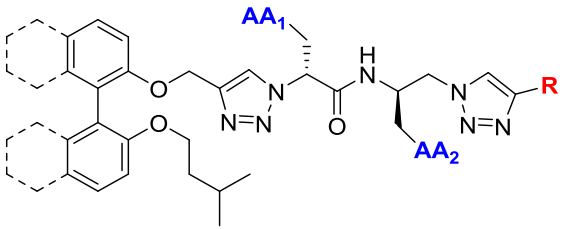

AA = Lys = 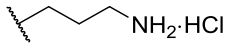

or

AA = Arg = 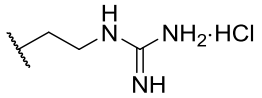

Compound	**Aromatic Core**	**AA 1**	**AA2**	**R**	*S. aur.*	*P. aer.*	*K. pneu.*	*A. bau.*	*E. coli*	*C. alb.*	*C. neo.*	Cytotoxicity (CC_{50})
80a	Biphenyl	Lys	Arg	Bn	4	16	32	16	8	32	4	17.1
80b	Biphenyl	Lys	Arg	PhEt	2	8	16	8	8	32	4	16.4
80c	Biphenyl	Lys	Arg	Cy	4	16	16	8	8	32	4	19.8
80d	Biphenyl	Lys	Arg	CH_2Cy	2	32	16	8	8	16	4	19.1
81a	Biphenyl	Arg	Lys	Bn	8	16	32	32	>32	32	4*	>32
81b	Biphenyl	Arg	Lys	PhEt	4	16	16	32	16	32	2*	>32
81c	Biphenyl	Arg	Lys	Cy	4	8	16	16	16	32	2*	>32
81d	Biphenyl	Arg	Lys	CH_2Cy	8	16	16	16	16	32	2*	>32
82a	Binaphthyl	Lys	Arg	PhEt	2	16	>32	8	>32	4	2	>32
82b	Binaphthyl	Lys	Arg	CH_2Cy	2	32	>32	8	>32	4	1	16.6
83a	Binaphthyl	Arg	Lys	PhEt	4	32	>32	32	>32	32	1*	>32
83b	Binaphthyl	Arg	Lys	CH_2Cy	32	32	>32	32	>32	32	1*	>32

Table B2.7 – Antibacterial activities of Series B2 derivatives reported as MIC values (μg/mL). The cytotoxicity of each compound is also reported as the CC_{50} (μg/mL). ***** *Cryptococcus neoformans* data was not consistent with initial screening data – compounds need to be rescreened.

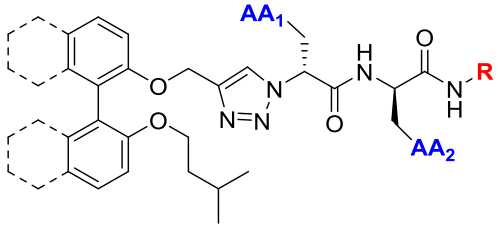

Compound	**Aromatic Core**	**AA$_1$**	**AA$_2$**	**R**	*S. aur.*	*P. aer.*	*K. pneu.*	*A. bau.*	*E. coli*	*C. alb.*	*C. neo.*	Cytotoxicity (CC_{50})
85a	Binaphthyl	Lys	Arg	Bn	4	32	32	32	>32	16	4	17.4
85b	Binaphthyl	Lys	Arg	PhEt	2	32	16	8	>32	16	2	15.2
85c	Binaphthyl	Lys	Arg	Piperid-inyl†	2	16	16	8	32	16	4	16.8

Table B2.8 – Antibacterial activities of Series B2 derivatives reported as MIC values (μg/mL). The cytotoxicity of each compound is also reported as the CC_{50} (μg/mL). † Piperidinyl amide – see Section 2.3.2.2 for compound structure.

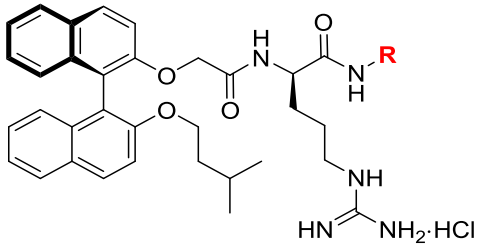

Compound	R	*S. aureus* ATCC 43300 (*MRSA*)	*P. aeru.* ATCC 27853	*K. pneum.* ATCC 700603	*A. baumannii* ATCC 19606	*E. coli* ATCC 25922	*C. albicans* ATCC 90028	*C. neoformans* ATCC 208821	Cytotoxicity (CC_{50}) (HEK-293) ATCC CRL-1573
87a	Bn	4	>32	>32	>32	>32	>32	16*	>32
87b	PhEt	4	>32	>32	>32	>32	32	16*	>32
87c	4-F-PhEt	4	>32	>32	>32	>32	>32	16*	>32

Table B2.9 – Antibacterial activities of Series C derivatives reported as MIC values (μg/mL). The cytotoxicity of each compound is also reported as the CC_{50} (μg/mL).

B3 – Solubility assay data – Series A1

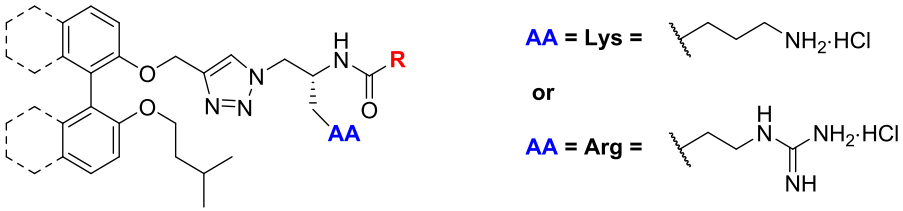

Compound	Aromatic Core	AA	R	H_2O ppt. vol (µL)	Solubility Ratio (Compound : compound **1**)	CLogP
1	Binaphthyl	-	-	15	1	7.47
66c	Binaphthyl	Arg	OBenzyl	20	1.33	6.61
65c	Biphenyl	Arg	OBenzyl	65	4.33	4.26
64a	Biphenyl	Lys	Benzyl	>300 **(NP)**	>20 **(NP)**	4.97

Table B3.1 – Solubility assay data for selected Series A1 derivatives. **NP** = No precipitation observed.

Solubility assay data – Series A2

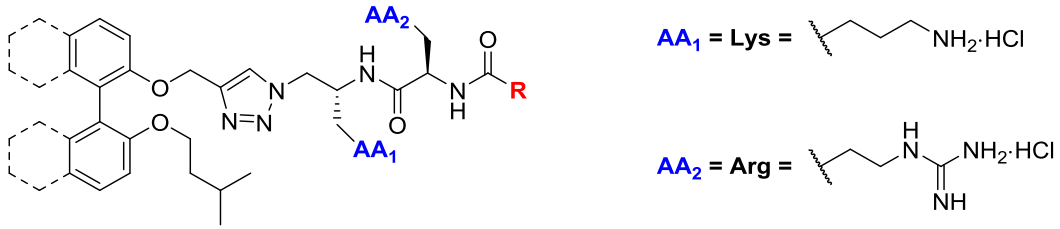

Compound	Aromatic Core	AA	AA	R	H_2O ppt. vol (µL)	Solubility Ratio (Compound : compound **1**)	CLogP
1	Binaphthyl	-	-	-	15	1	7.47
2	Binaphthyl	Lys	Arg	PhEt	45	3	5.76
73	Biphenyl	Lys	Arg	Benzyl	15	1	3.02

Table B3.2 – Solubility assay data for selected Series A2 derivatives.

Solubility assay data – Series A2 (cont.)

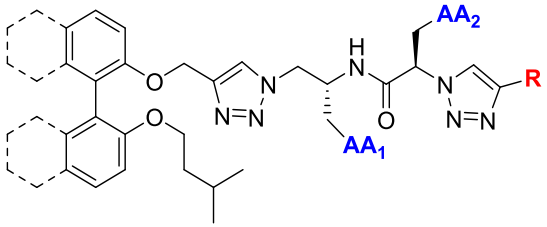

AA = Lys = 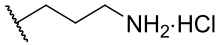

or

AA = Arg = 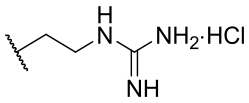

Compound	Aromatic Core	AA	AA	R	H_2O ppt. vol (µL)	Solubility Ratio (Compound : compound **1**)	CLogP
1	Binaphthyl	-	-	-	15	1	7.47
70a	Binaphthyl	Lys	Arg	PhEt	30	2	6.24
68b	Biphenyl	Lys	Arg	PhEt	35	2.33	3.89
68c	Biphenyl	Lys	Arg	Cy	60	4	4.07
68d	Biphenyl	Lys	Arg	CH_2Cy	45	3	4.60
69c	Biphenyl	Arg	Lys	Cy	30	2	4.07

Table B3.3 – Solubility assay data for selected Series A2 derivatives.

Solubility assay data – Series B1

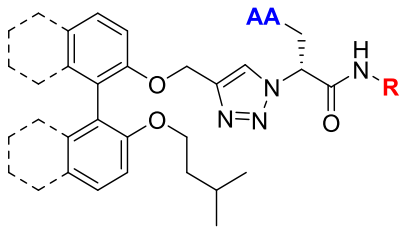

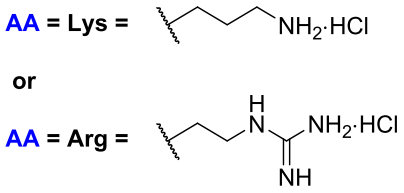

Compound	Aromatic Core	AA	R	H_2O ppt. vol (µL)	Solubility Ratio (Compound : compound **1**)	CLogP
1	Binaphthyl	-	-	15	1	7.47
77c	Biphenyl	Arg	Cy	30	2	3.77
76d	Biphenyl	Lys	CH_2Cy	>200 **(NP)**	>13.3 **(NP)**	5.81

Table B3.4 – Solubility assay data for selected Series B1 derivatives. **NP** = No precipitation observed.

Solubility assay data – Series B2

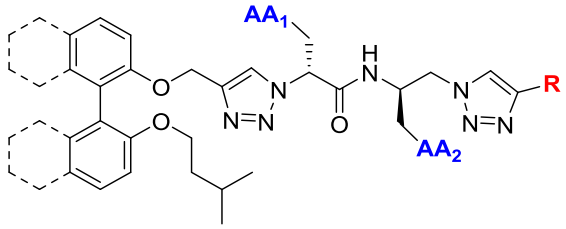

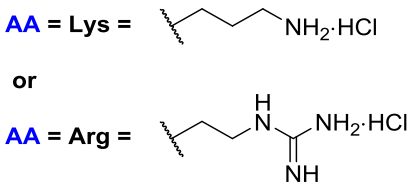

Compound	Aromatic Core	AA	AA	R	H_2O ppt. vol (µL)	Solubility Ratio (Compound : compound **1**)	CLogP
1	Binaphthyl	-	-	-	15	1	7.47
83b	Binaphthyl	Arg	Lys	CH_2Cy	15	1	6.94
81d	Biphenyl	Arg	Lys	CH_2Cy	55	3.67	4.60
80c	Biphenyl	Lys	Arg	Cy	30	2	4.07

Table B3.5 – Solubility assay data for selected Series B2 derivatives.

Solubility assay data – Series C

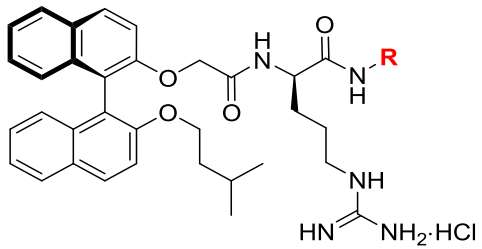

Compound	Aromatic Core	R	H_2O ppt. vol (μL)	Solubility Ratio (Compound : compound **1**)	CLogP
1	Binaphthyl	-	15	1	7.47
87a	Binaphthyl	Benzyl	15	1	5.82

Table B3.6 – Solubility assay data for selected Series C derivatives.

B4 – HPLC purity traces

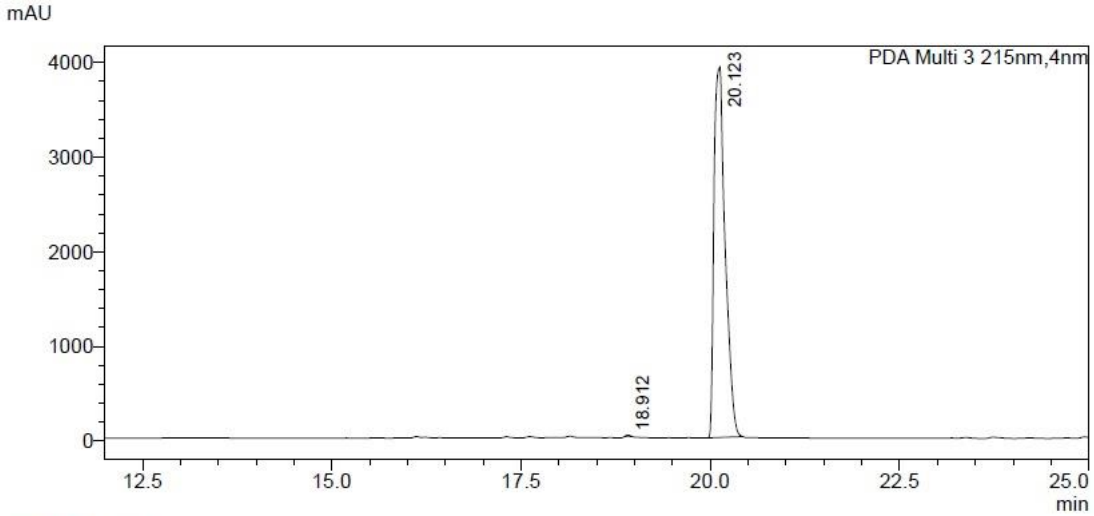

<Peak Table>

PDA Ch3 215nm

Peak#	Ret. Time	Area	Height	Area%
1	18.912	30595	10243	0.077
2	20.123	39790056	3914355	99.923
Total		39820650	3924598	100.000

Figure B4.1 – HPLC trace and peak integration table for compound **77c**.

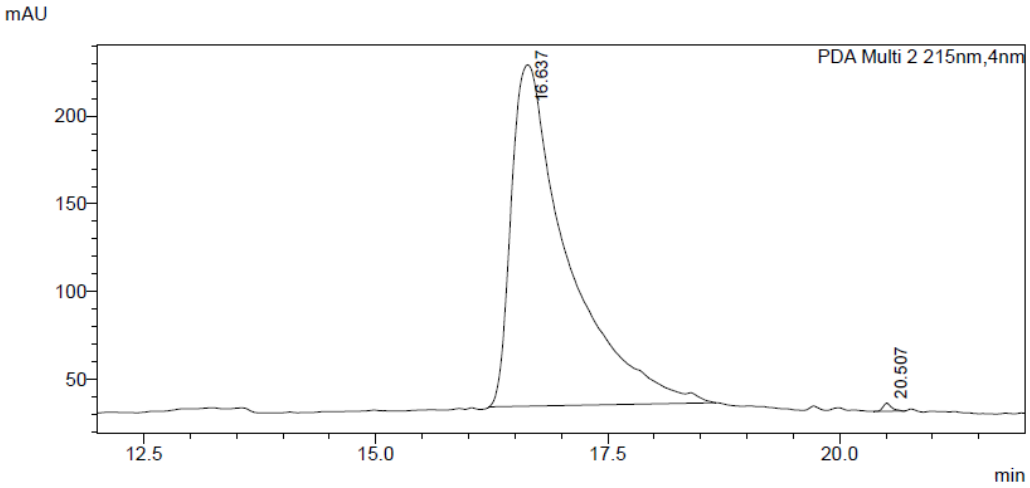

<Peak Table>

PDA Ch2 215nm

Peak#	Ret. Time	Area	Height	Area%
1	16.637	8237117	194155	98.275
2	20.507	29620	4503	0.353
3	23.406	85298	12293	1.018
4	23.842	29628	4570	0.353
Total		8381663	215521	100.000

Figure B4.2 – HPLC trace and peak integration table for compound **87a**.

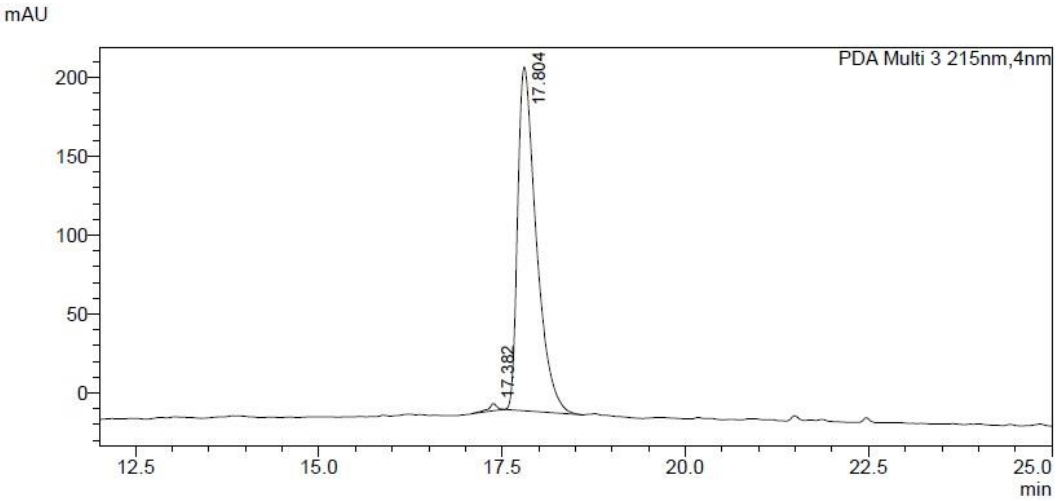

<Peak Table>

PDA Ch3 215nm

Peak#	Ret. Time	Area	Height	Area%
1	17.382	37666	4544	0.970
2	17.804	3846483	217920	99.030
Total		3884149	222464	100.000

Figure B4.3 – HPLC trace and peak integration table for compound **68c**.

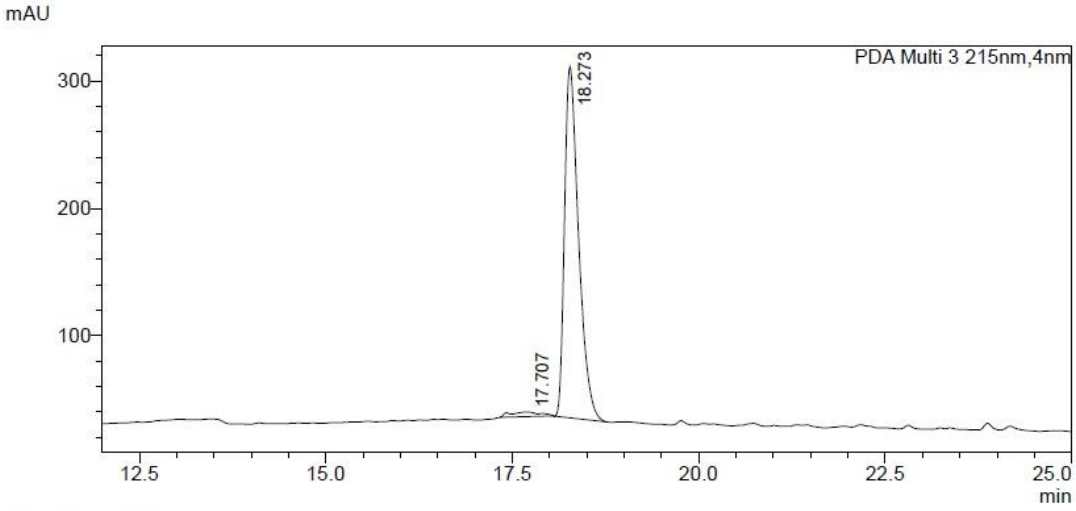

<Peak Table>

PDA Ch3 215nm

Peak#	Ret. Time	Area	Height	Area%
1	17.707	98661	3329	2.671
2	18.273	3594571	275874	97.329
Total		3693232	279203	100.000

Figure B4.4 – HPLC trace and peak integration table for compound **68d**.

Appendix C – Selected ^{1}H, ^{13}C and 2-D NMR spectra

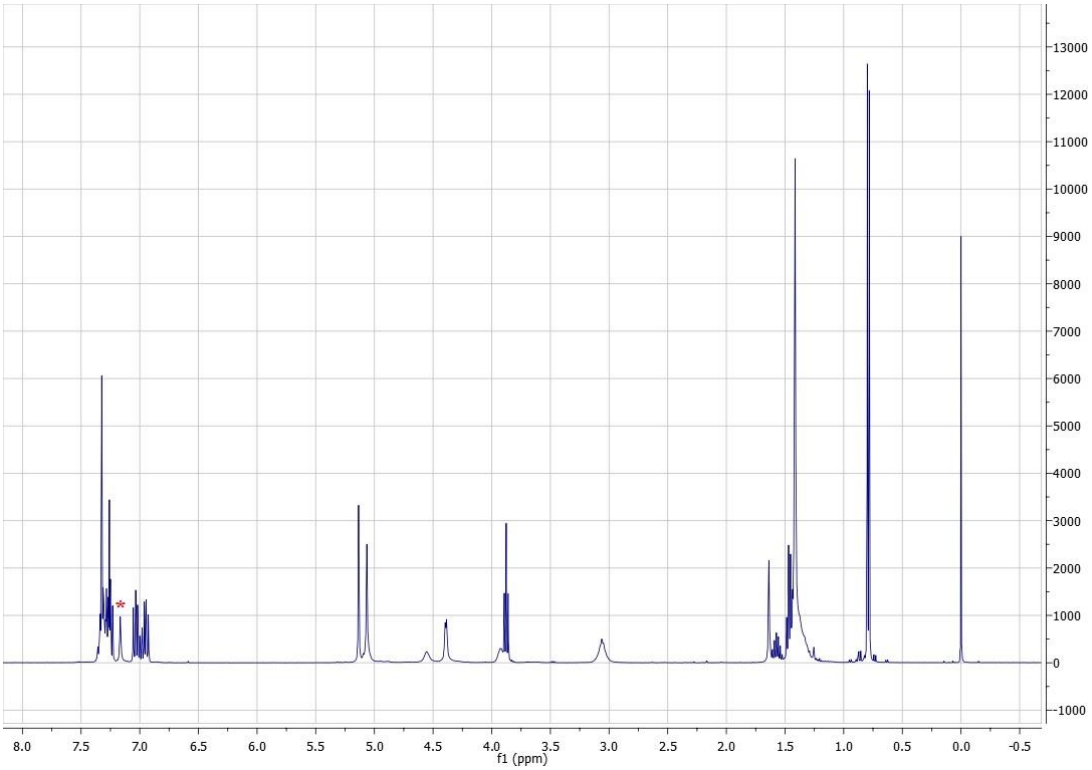

Figure C1.1 – ^{1}H NMR spectrum of compound **62a** (recorded in $CDCl_3$). The new triazole proton is marked with a red asterisk (*****).

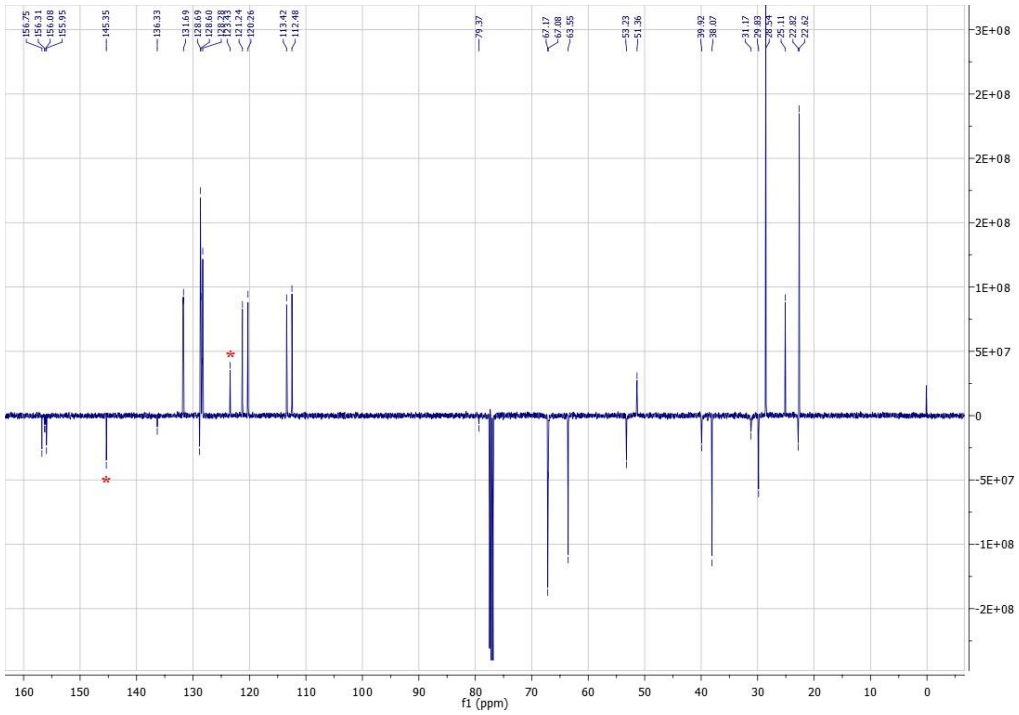

Figure C1.2 – ^{13}C NMR spectrum of compound **62a** (recorded in $CDCl_3$). The new triazole carbons are marked with a red asterisk (*).

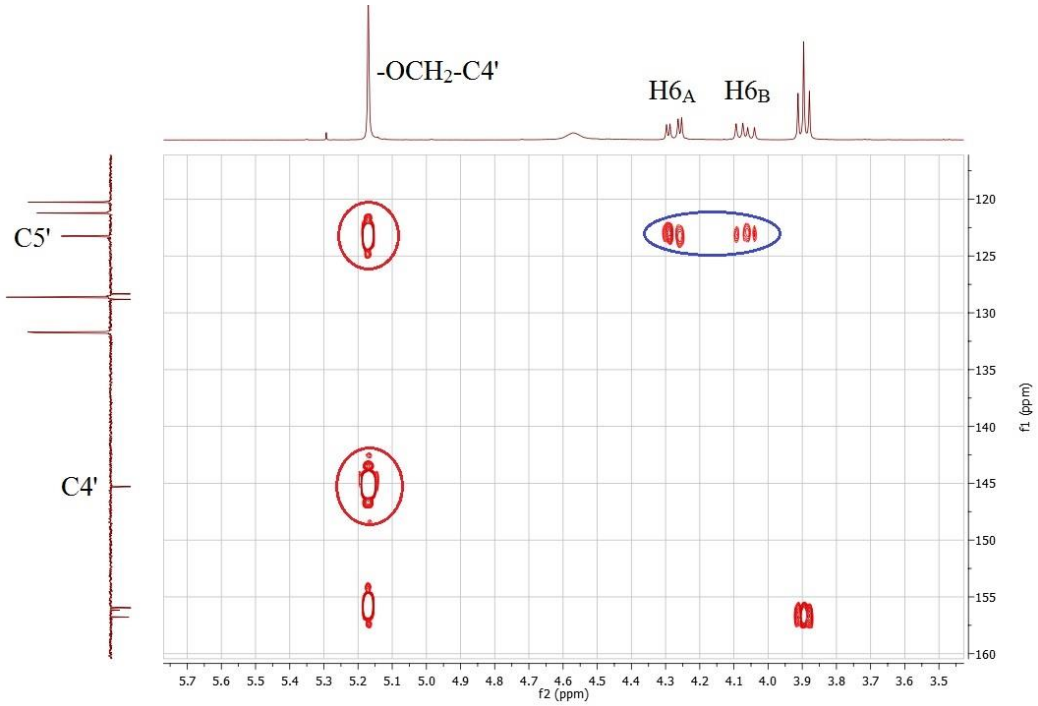

Figure C1.3 – Selected expansion of the gHMBC spectrum of compound **63a** (recorded in $CDCl_3$). The expansion shows the relevant correlations (circled in red and blue) that prove the 1,4-regioselectivity.

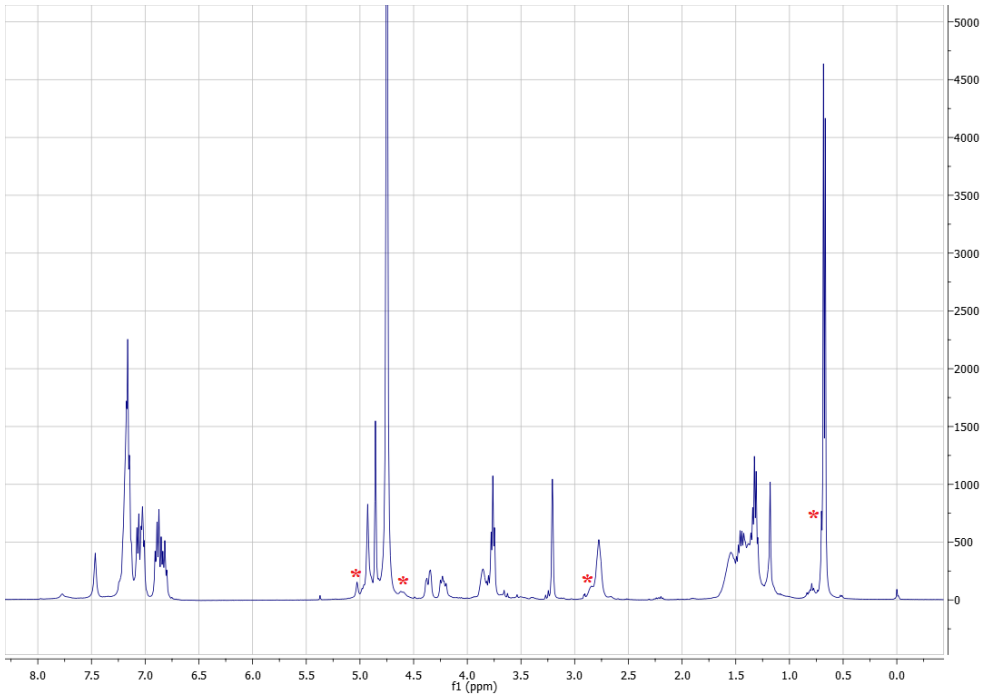

Figure C1.4 – ^{1}H NMR spectrum of compound **64c** (recorded in CD_3OD). Visible rotameric shoulder peaks are marked with a red asterisk (*).

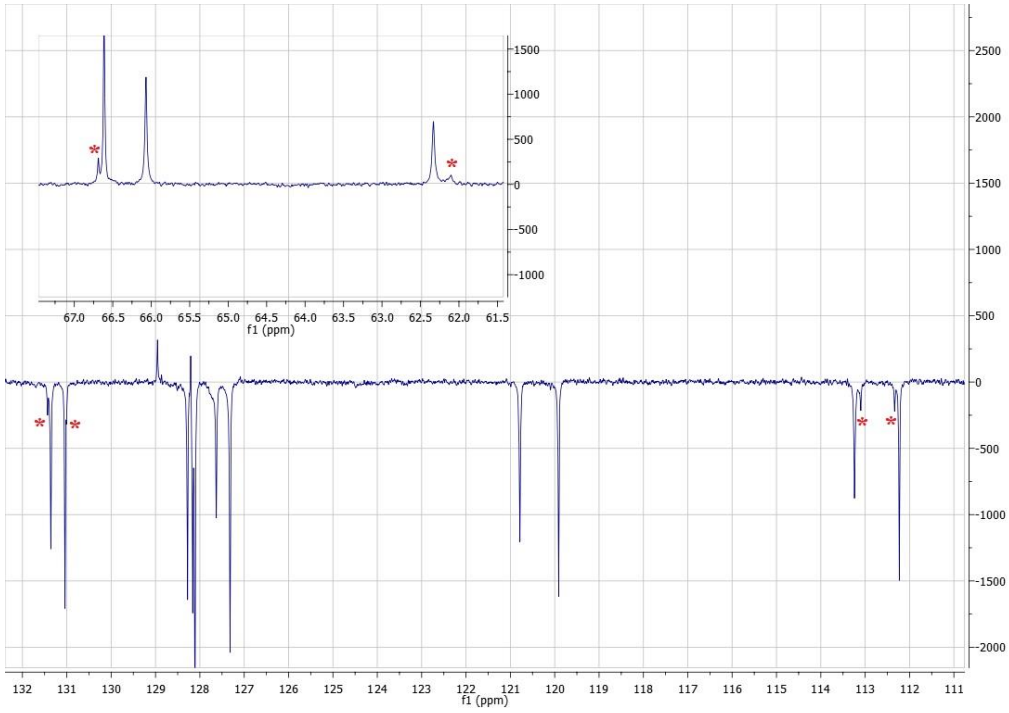

Figure C1.5 – Selected expansion of the ^{13}C NMR spectrum of compound **64c** (recorded in CD_3OD). Clearly visible rotameric shoulder peaks are marked with a red asterisk (*).

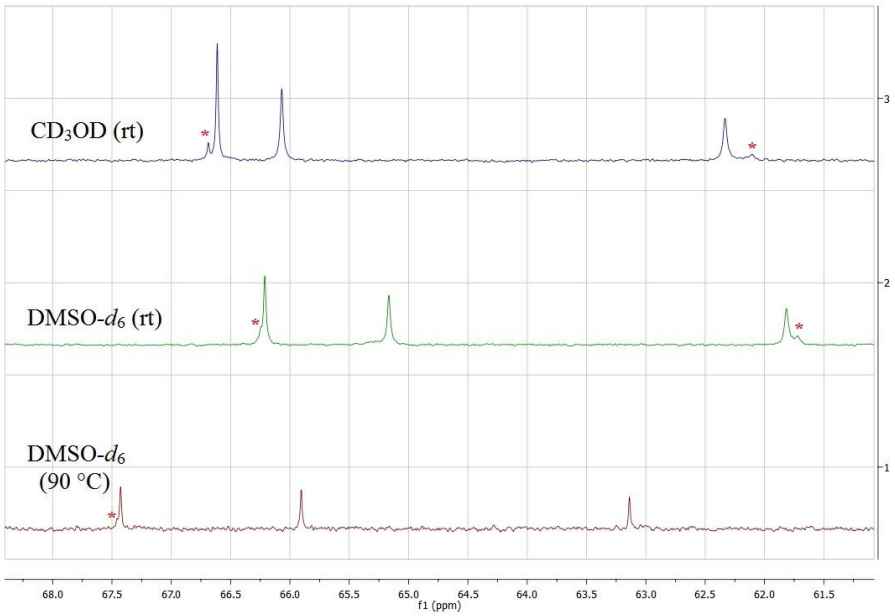

Figure C1.6– Selected expansion of the ^{13}C NMR spectrum of compound **64c** recorded in CD_3OD at rt (blue), DMSO-d_6 at rt (green) and DMSO-d_6 at 90 °C (red). Visible rotameric shoulder peaks are marked with a red asterisk (*). Note the reduced ^{13}C NMR resonance splitting in the sample recorded in DMSO-d_6 at 90 °C.

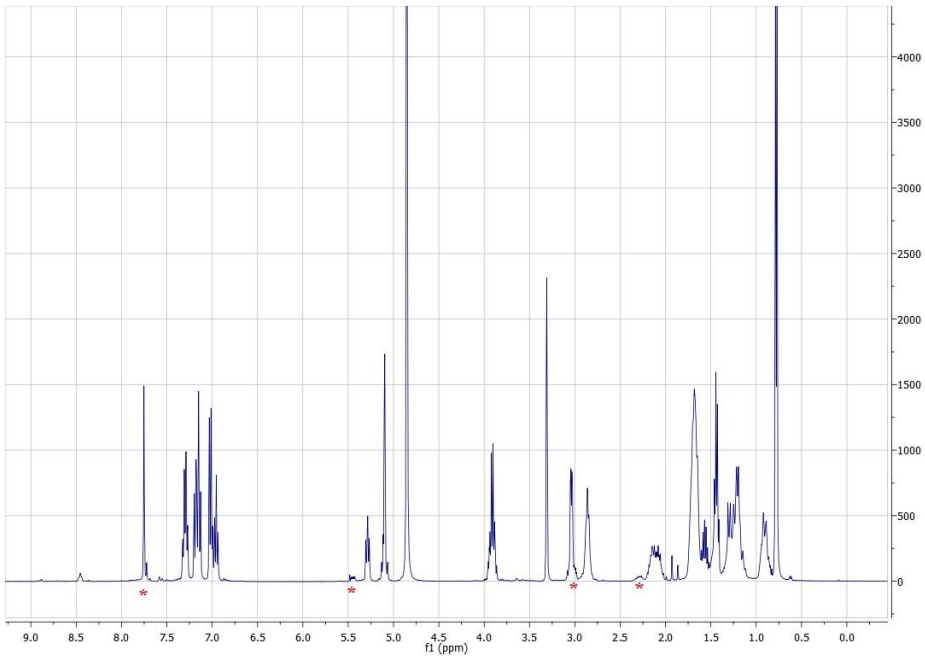

Figure C1.7 – ^{1}H NMR spectrum of compound **76d** recorded in CD_3OD. Visible rotameric shoulder peaks are marked with a red asterisk (*).

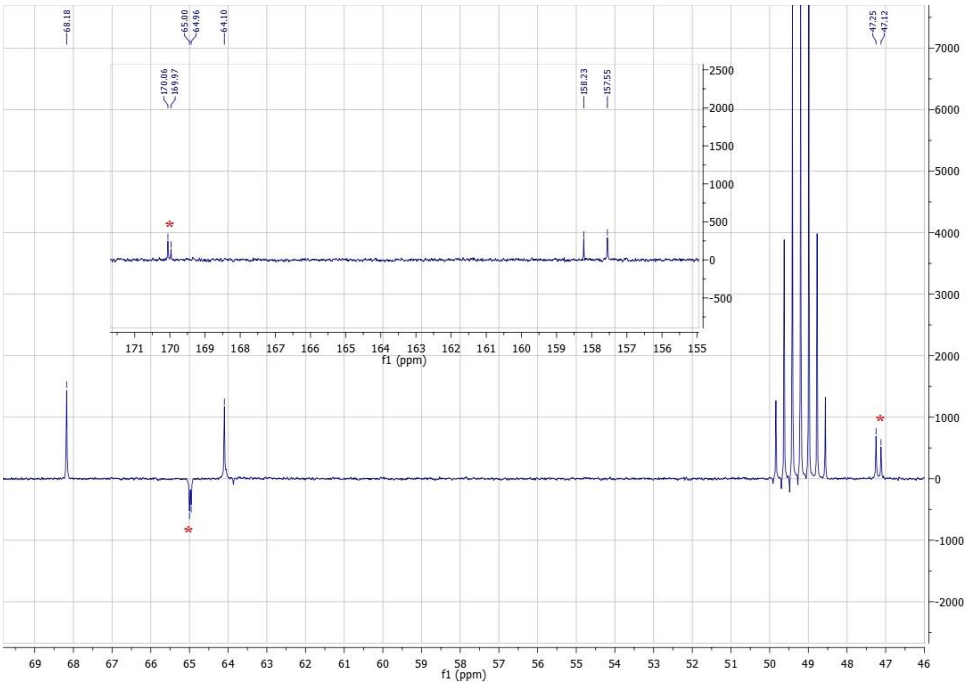

Figure C1.8 – Selected expansions of the ^{13}C NMR spectrum of compound **76d** recorded in CD_3OD. Visible rotameric splitting of ^{13}C NMR resonances is marked with a red asterisk (*).

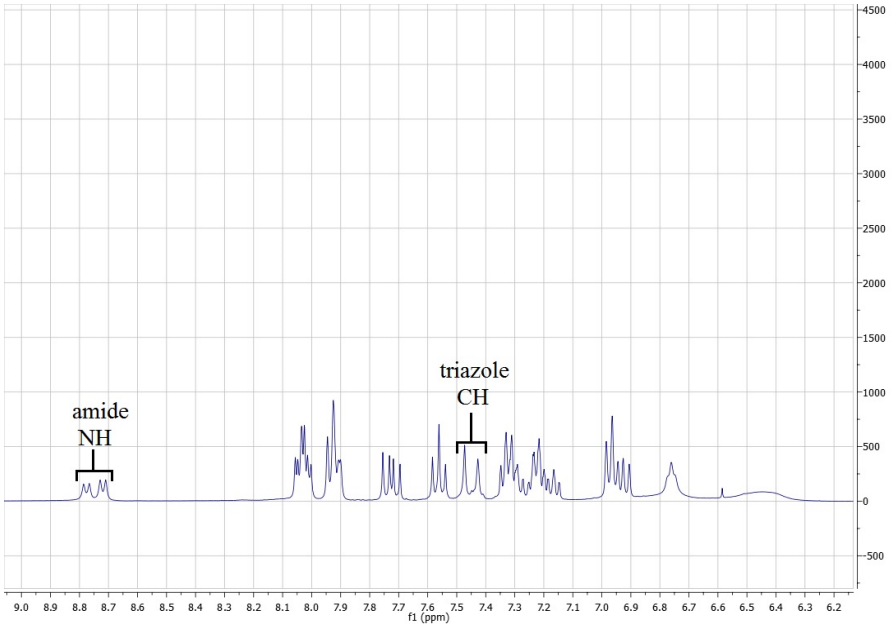

Figure C1.9 – Selected expansion of the ^{1}H NMR spectrum of scaffold acid **84** recorded in DMSO-d_6. The rotameric splitting of ^{1}H NMR resonances assigned to the amide (NH) and triazole (CH) protons are noted.

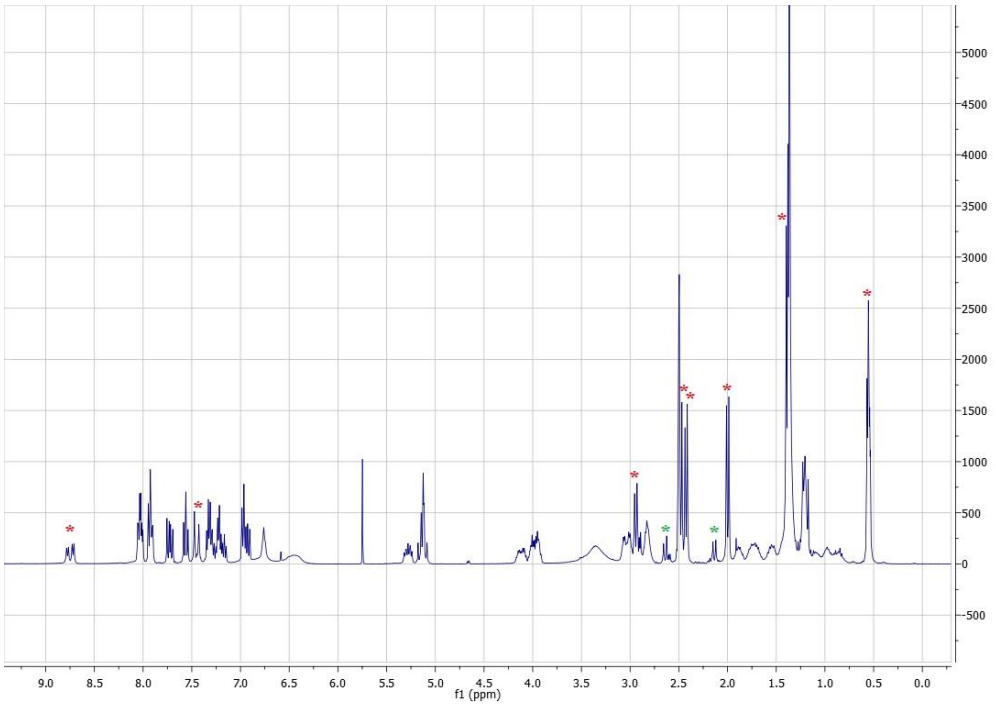

Figure C1.10 – ^{1}H NMR spectrum of scaffold acid **84** recorded in DMSO-d_6. Primary rotameric splitting of ^{1}H NMR resonances is marked with a red asterisk (*). Secondary rotameric splitting of ^{1}H NMR resonances is marked with a green asterisk (*).

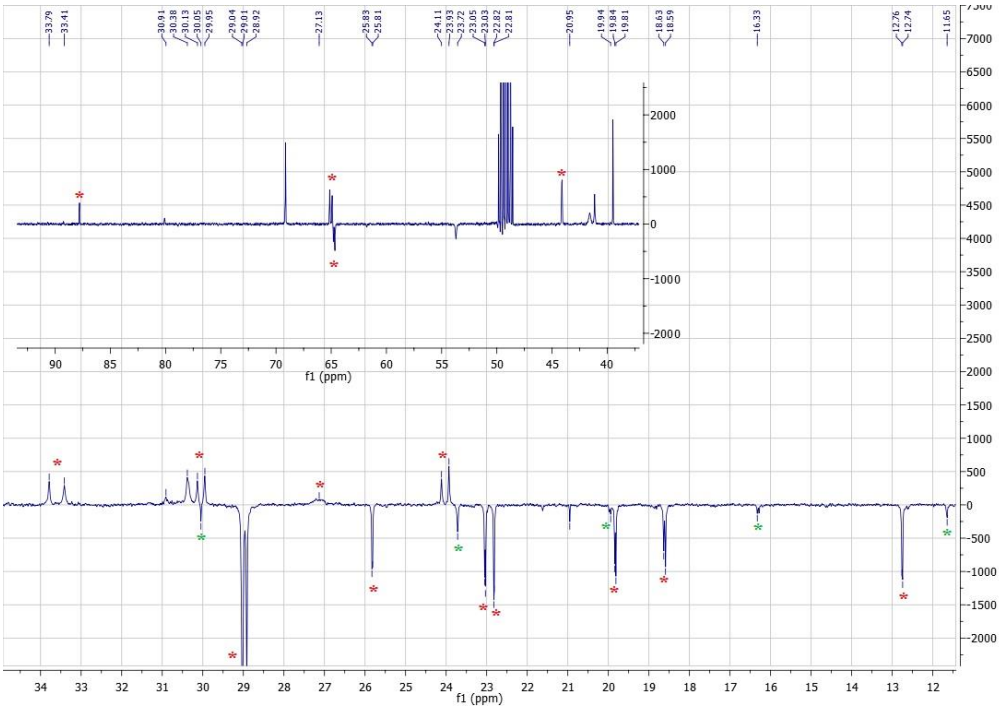

Figure C1.11 – Selected expansions of the alkyl region of the ^{13}C NMR spectrum of scaffold acid **84** recorded in CD_3OD. Primary rotameric splitting of ^{13}C NMR resonances is marked with a red asterisk (*). Secondary rotameric splitting of ^{13}C NMR resonances is marked with a green asterisk (*).

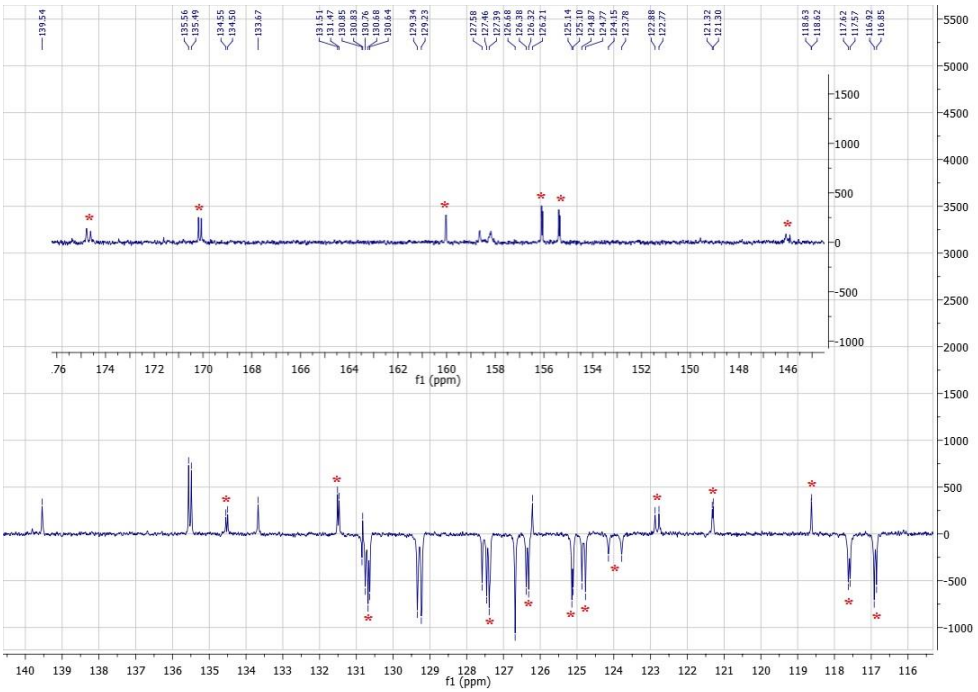

Figure C1.12 – Selected expansions of the aromatic region of the ^{13}C NMR spectrum of scaffold acid **84** recorded in CD_3OD. Rotameric splitting of ^{13}C NMR resonances is marked with a red asterisk (*).

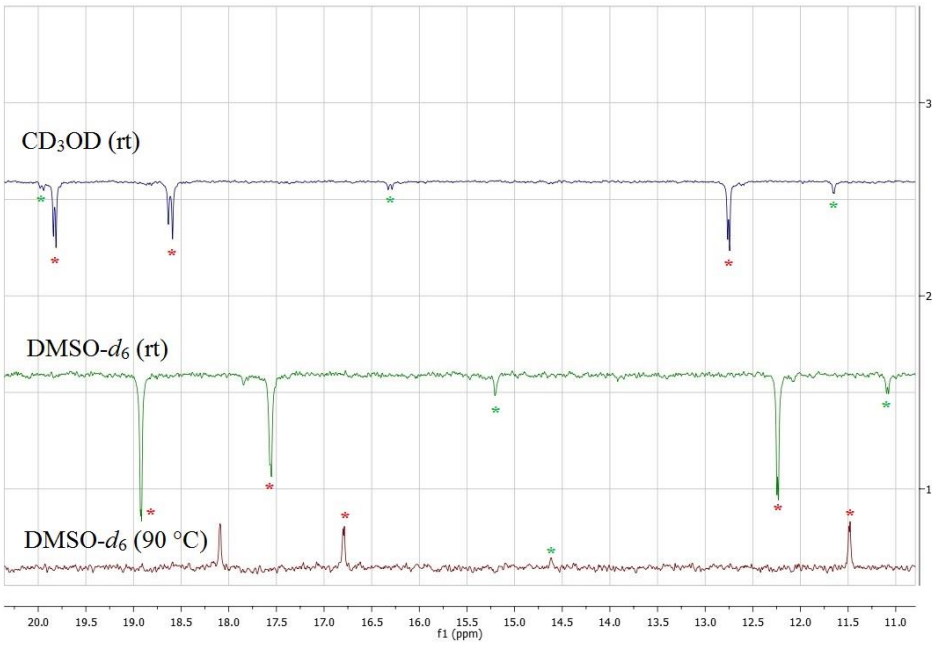

Figure C1.13 – Selected expansion of the ^{13}C NMR spectrum of compound **84** recorded in CD_3OD at rt (blue), DMSO-d_6 at rt (green) and DMSO-d_6 at 90 °C (red). Primary rotameric splitting of ^{13}C NMR resonances is marked with a red asterisk (*). Secondary rotameric splitting of ^{13}C NMR resonances is marked with a green asterisk (*). Note the reduced amount of primary and secondary rotameric splitting of ^{13}C NMR resonances in the sample recorded in DMSO-d_6 at 90 °C.

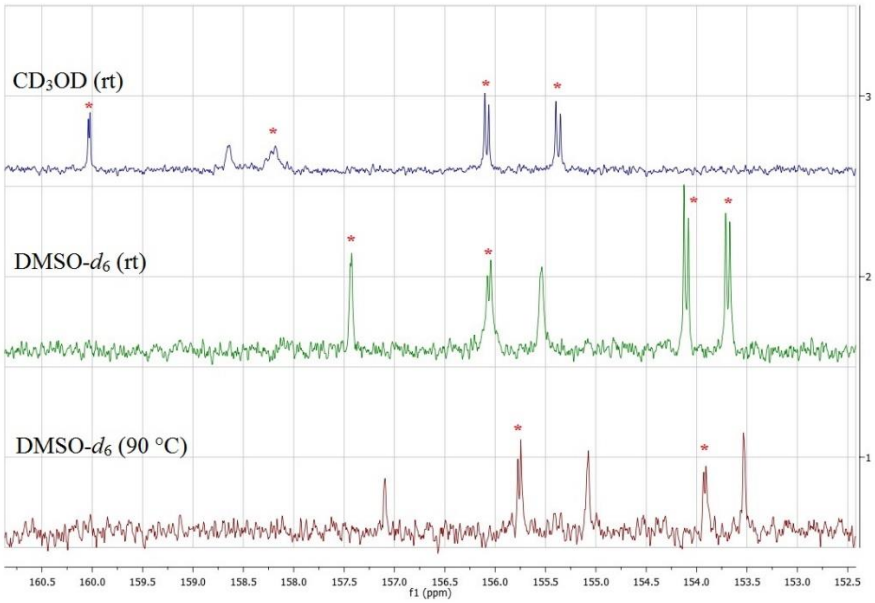

Figure C1.14 – Selected expansion of the ^{13}C NMR spectrum of compound **84** recorded in CD_3OD at rt (blue), DMSO-d_6 at rt (green) and DMSO-d_6 at 90 °C (red). Visible rotameric splitting of ^{13}C NMR resonances is marked with a red asterisk (*). Note the reduced number of split ^{13}C NMR resonances in the sample recorded in DMSO-d_6 at 90 °C.

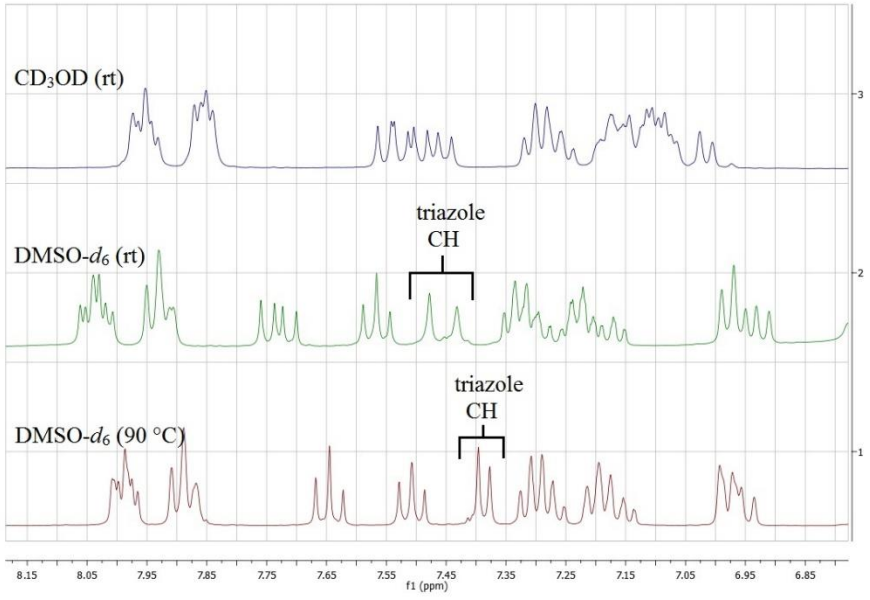

Figure C1.15– Selected expansion of the ^{1}H NMR spectrum of compound **84** recorded in CD_3OD at rt (blue), DMSO-d_6 at rt (green) and DMSO-d_6 at 90 °C (red). Visible rotameric splitting of the resonance assigned to the triazole methine proton is marked on the two ^{1}H NMR spectra that were recorded in DMSO-d_6 (middle and bottom spectra). Note the observed change in the splitting pattern and resolution.

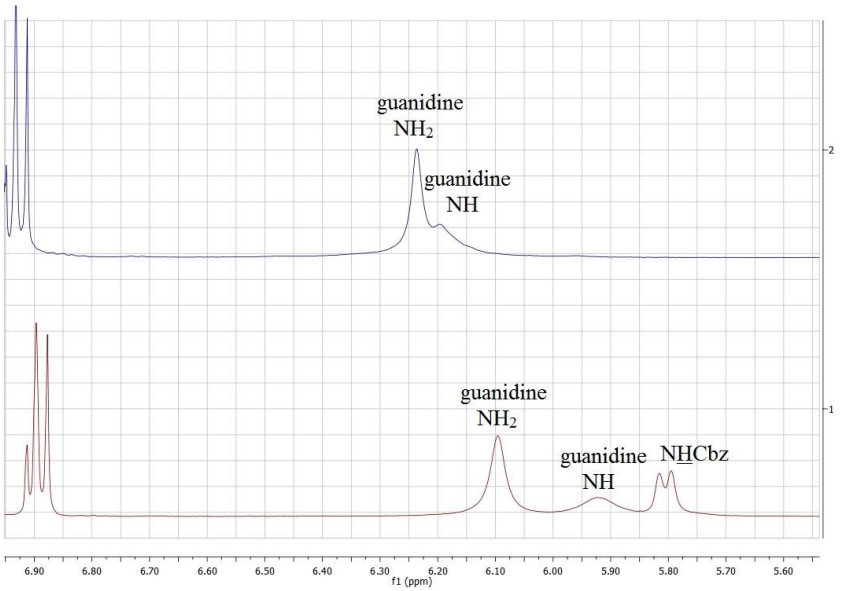

Figure C1.16 – Selected expansion of the ^{1}H NMR spectra compound **63b** (top spectra in blue - recorded in $CDCl_3$) and compound **62b** (bottom spectra in red – recorded in $CDCl_3$). The expansion shows the various resonance patterns that are exhibited by the exchangeable protons on the *N*-Pbf protected guanidine.

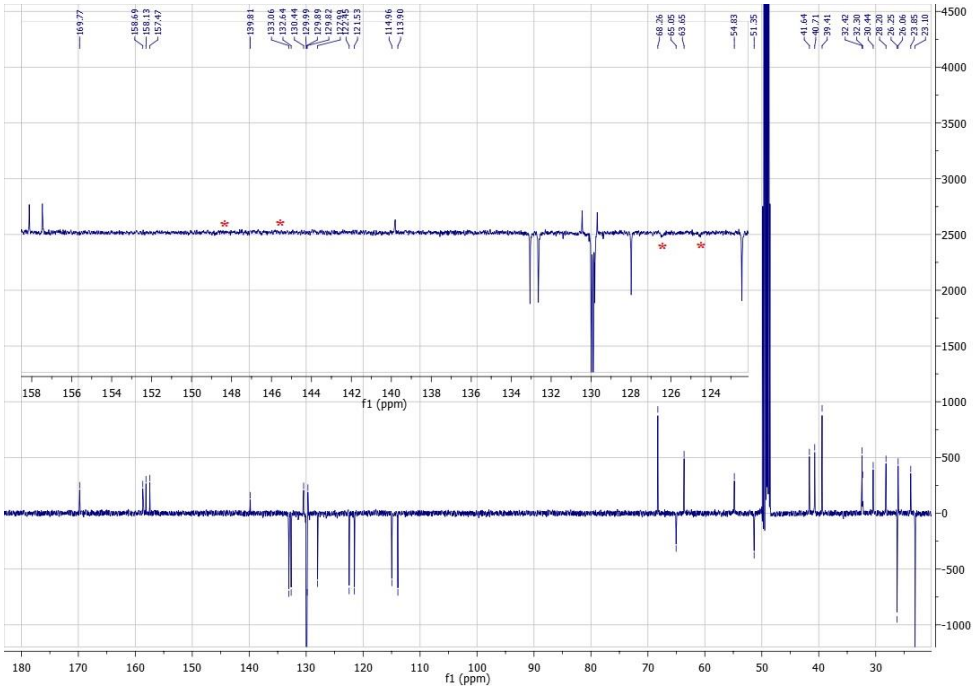

Figure C1.17 – ^{13}C NMR spectrum of bis-triazole compound **68a** recorded in CD_3OD. The locations of the missing ^{13}C NMR resonances (as determined by gHSQC and gHMBC) are marked with a red asterisk (*).

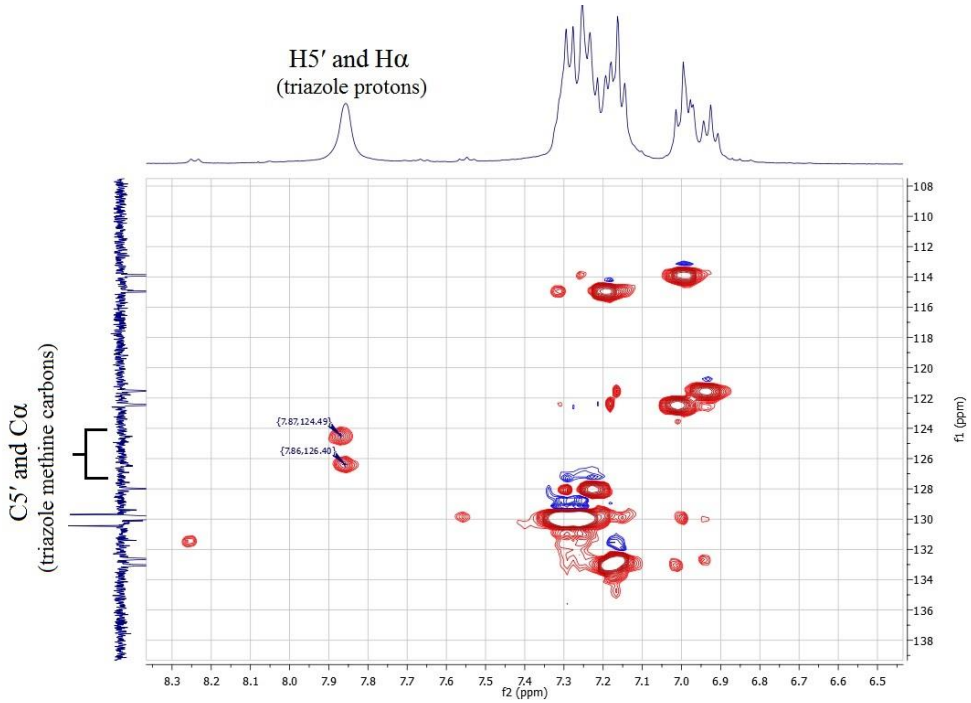

Figure C1.18 – Selected expansion of the gHSQC NMR spectrum of bis-triazole compound **68a** recorded in CD_3OD. The relevant correlations that allowed for assignment of the triazole methine carbons are marked.

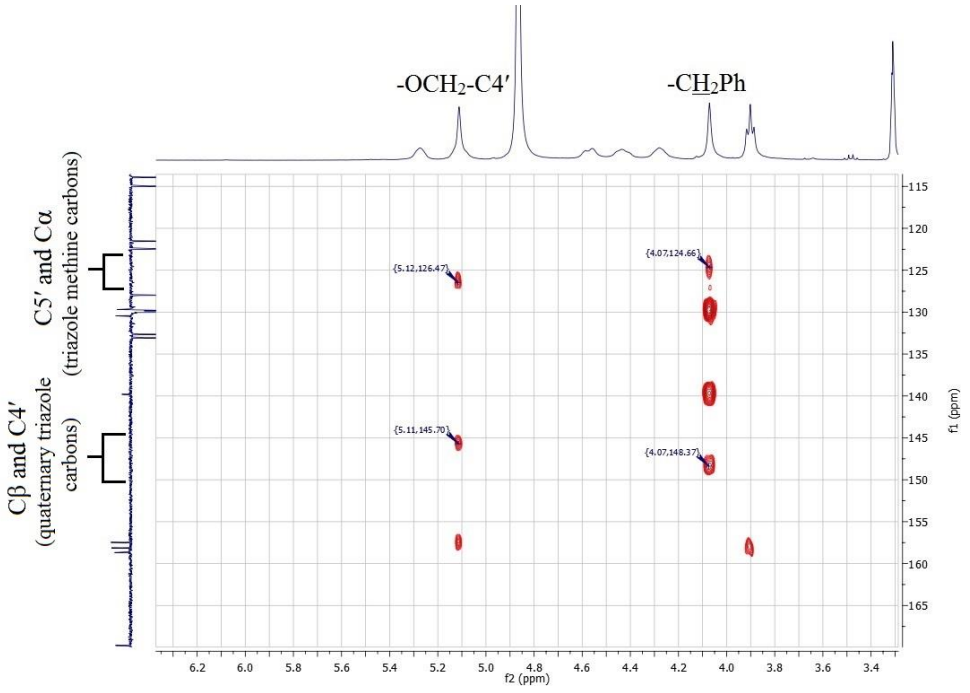

Figure C1.19 – Selected expansion of the gHMBC NMR spectrum of bis-triazole compound **68a** recorded in CD_3OD. The relevant correlations that allowed for assignment of the both the methine and quaternary triazole carbons are marked.

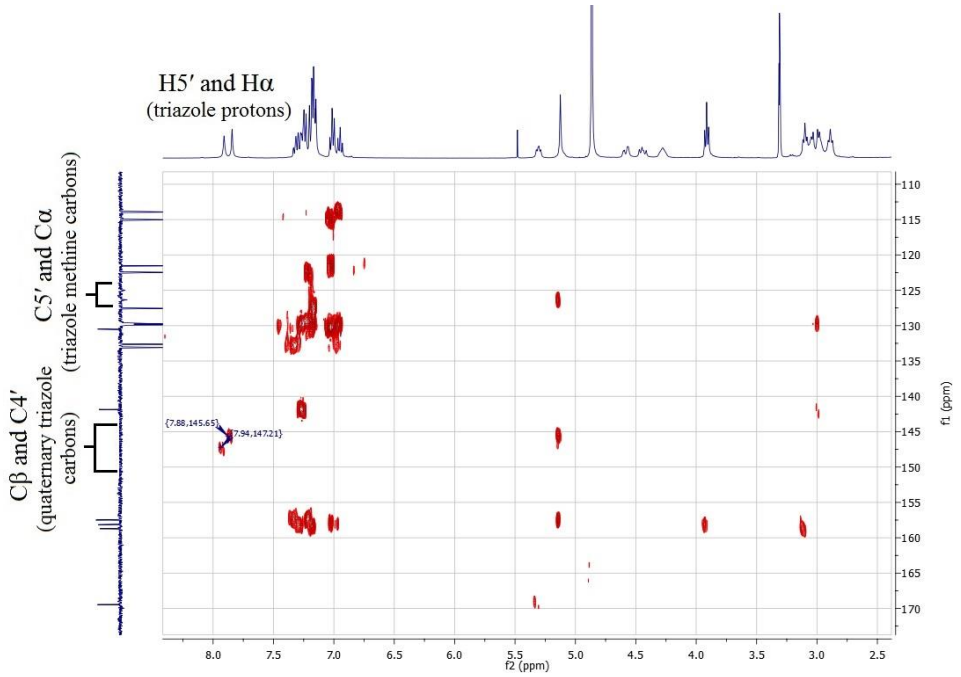

Figure C1.20 – Selected expansion of the gHMBC NMR spectrum of bis-triazole compound **68b** recorded in CD_3OD. The relevant correlations that allowed for assignment of the quaternary triazole carbons are marked.

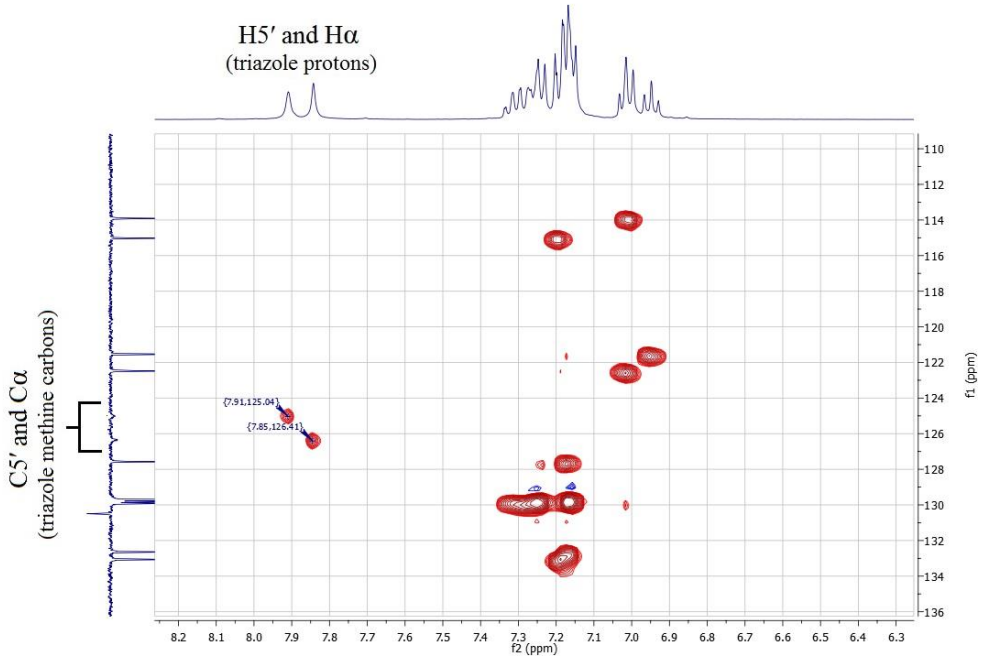

Figure C1.21 – Selected expansion of the gHSQC NMR spectrum of bis-triazole compound **68b** recorded in CD_3OD. The relevant correlations that allowed for assignment of the triazole methine carbons are marked.

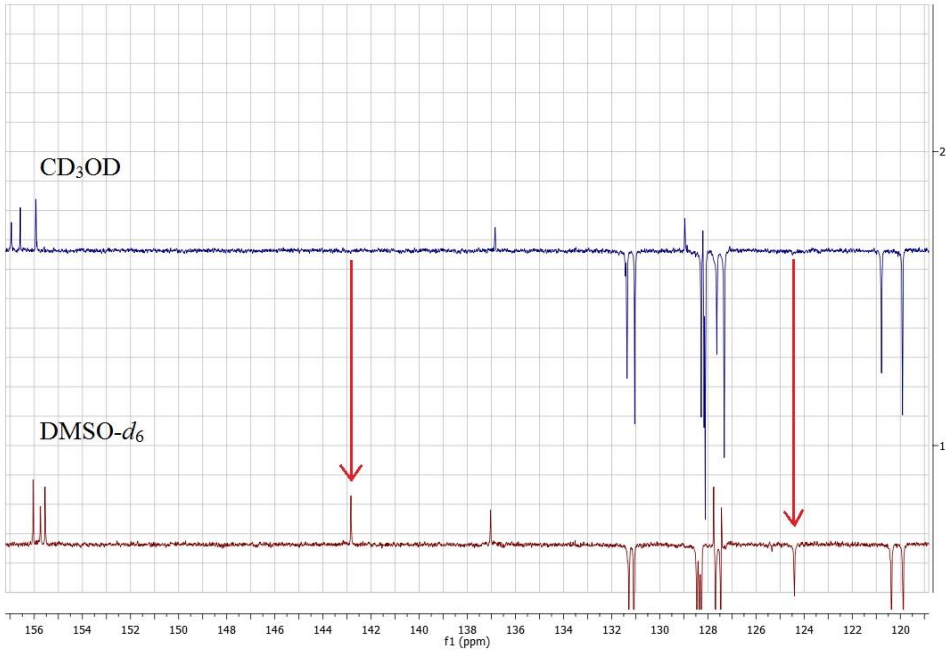

Figure C1.22 – Selected expansion of the ^{13}C NMR spectra of compound **64c** recorded in CD_3OD (blue) and DMSO-d_6 (red). Note the new ^{13}C NMR resonances that are observed with the use of DMSO-d_6 (marked with red arrows →).

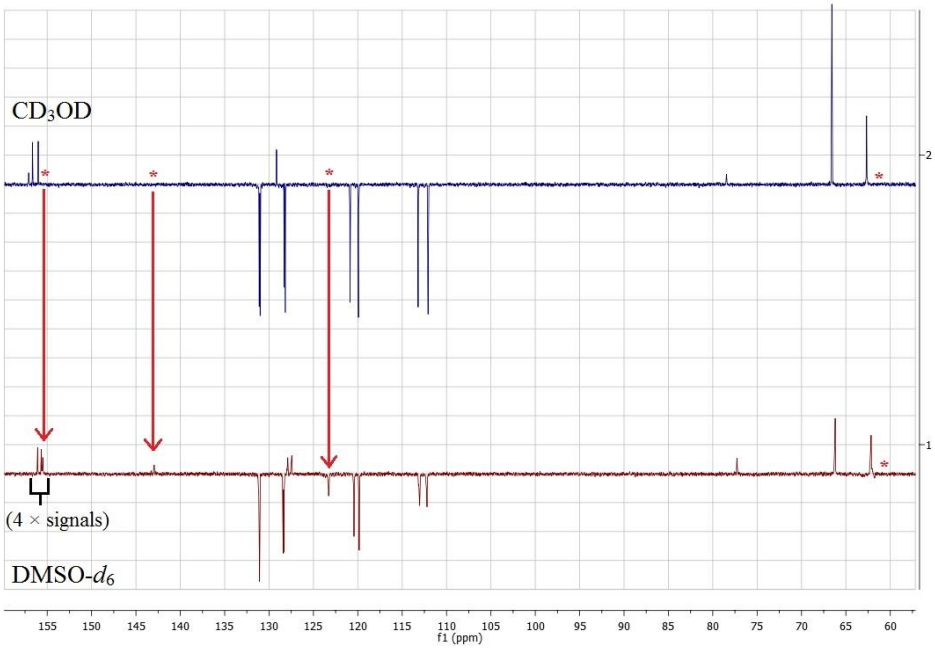

Figure C1.23 – Selected expansion of the ^{13}C NMR spectra of compound **75a** recorded in CD_3OD (blue) and DMSO-d_6 (red). Note the new ^{13}C NMR resonances that are observed with the use of DMSO-d_6 (marked with red arrows →). Missing resonances are marked with a red asterisk (*); note the missing methine (C2) resonance in the spectrum acquired in DMSO-d_6.

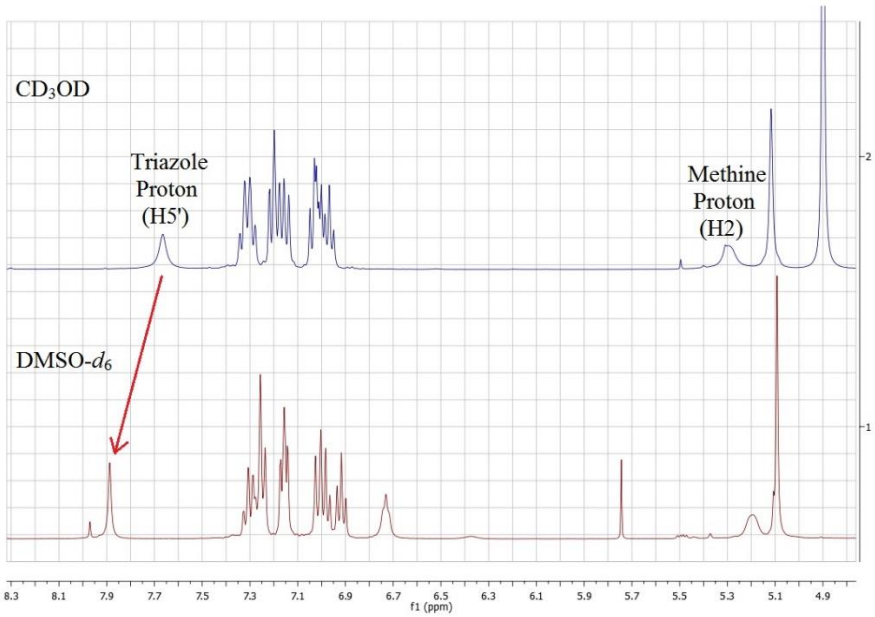

Figure C1.24 – Selected expansion of the ^{1}H NMR spectrum of compound **75a** recorded in CD_3OD (blue) and DMSO-d_6 (red). Note the broadening of the labelled resonances (assigned to the triazole and methine protons) in the spectrum acquired in CD_3OD; reduced broadening was observed for the resonance assigned to the triazole proton (H5′) in the spectrum acquired in DMSO-d_6 (red arrow →).

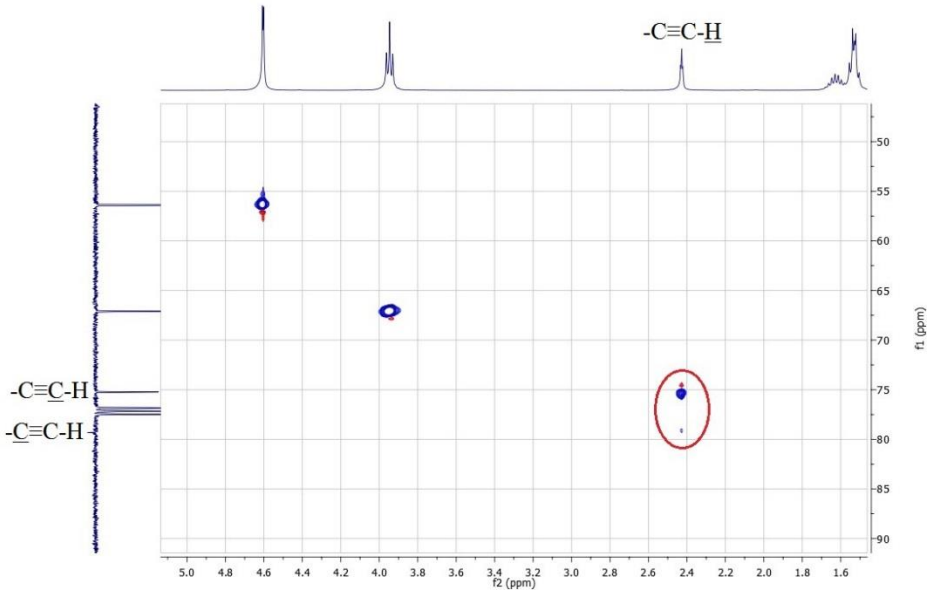

Figure C1.25 – Selected expansion of the gHSQC NMR spectrum of alkyne **21** recorded in $CDCl_3$. The anomalous correlation is circled in red; note the reversed polarity of the DEPT Q ^{13}C resonances assigned to the alkyne carbons.